

LONDON
SCHOOL of
HYGIENE
& TROPICAL
MEDICINE



**CHARACTERISATION OF B CELL AND T FOLLICULAR HELPER CELL RESPONSES
TO HPV VACCINATION: THE EFFECT OF AGE AND DOSE NUMBER ON THE VACCINE
IMMUNOGENICITY**

EUNICE WAVINYA KIAMBA

BSc, PGDip, MSc

**Thesis submitted in accordance with the requirements for the
degree of Doctor of Philosophy of the University of London**

January 2025

Department of Clinical Research

Faculty of Infectious and Tropical Diseases

LONDON SCHOOL OF HYGIENE & TROPICAL MEDICINE

Funded by:

- Medical Research Council Unit The Gambia at London School of Hygiene and Tropical Medicine Doctoral Training Programme
- Merck Sharp & Dorne Corp.
- Wellcome Institutional strategic Support Fund 3 partnership grants

Research group affiliation(s):

- Vaccines and Immunity Theme, MRC Unit The Gambia at London School of Hygiene and Tropical Medicine (MRCG at LSHTM)
- The Vaccine Centre
- Clinical Research Department

Supervisory team**Lead supervisor:**

Professor Ed Clarke

Professor of Paediatric Infection, Immunity and Global Health

Vaccines and Immunity Theme Lead

MRCG at LSHTM

Co supervisors:

Professor Martin Holland

Professor of Microbial Immunity

London School of Hygiene and Tropical Medicine

Assistant Professor Martin Goodier

Assistant Professor in Immunology

Flow cytometry and immunology facility manager

MRCG at LSHTM

DECLARATION OF OWN WORK

I, Eunice Wavinya Kiamba, confirm that the work presented in this thesis is my own. Where information has been derived from other sources, I confirm that this has been indicated in the thesis.

Eunice Wavinya Kiamba

Date: 03 January 2025

ABSTRACT

Introduction

This thesis investigates B cell and T follicular helper cell (Tfh) responses elicited by Gardasil 9 HPV vaccination as key drivers of long-term antibody-mediated protection and hence vaccine efficacy. The research was performed within a randomised clinical trial that aimed to compare antibody responses between one and two doses of Gardasil 9 given to 4 to 8- and 9 to 14-year-old females with reference to three doses given to 15 to 26-year-olds.

Methods

ELISpot and FluoroSpot assays were used to enumerate HPV 16 and HPV 18 specific IgG memory B cells and IgG and IgM plasma cells, respectively. An activation-induced marker flow cytometry assay was used to identify HPV 16 and HPV 18 specific Tfh cells following in-vitro stimulation with respective virus-like particles. The frequencies of total IgG and IgM plasma cells, and ex vivo activated Tfh cells in circulation were measured using flow cytometry. HPV 16 specific B cell repertoire was mapped by first sorting single HPV 16 specific memory B cells using fluorescently labelled HPV 16 virus-like particles and subsequently sequencing the naturally paired B cell receptor heavy and light chains using arm-iPair technology. HPV specific antibody titers were measured commercially using a Competitive Luminex Inhibition assay. The effects of age and dose number on vaccine-induced immune responses were evaluated.

Results

Frequencies of HPV 16 and HPV 18 specific plasma cells, memory B cells and Tfh cells were generally low after the first vaccination dose across all three age groups. A robust boosting of all responses was observed following the second or third vaccination dose which tended to be higher in the younger age groups, except the in vitro activated Tfh cell response which increased modestly in the youngest age group. Both 2- and 3-dose vaccination schedules induced high HPV 16 and HPV 18 specific IgG antibody titers which

increased with decreasing age. There was a strong positive correlation between antibody titers and plasma cells which was not observed upon comparing the antibody titers with memory B cells and Tfh cells. HPV 16 specific B cell repertoire was enriched for diverse germline heavy and light chain variable and junctional gene variants and utilized unique complimentary determining region 3 (CDR3) of variable amino acid lengths.

Conclusion

The B cell and Tfh cell responses induced by HPV vaccination at variable magnitudes by age and dose may be responsible for the similar trends observed on subsequent antibody responses. This study provides insights on the possible roles played by these cell responses in shaping short- and long-term vaccine protection. Additionally, the low cellular response induced from the first vaccination dose may indicate a potential impact of single dose vaccination that should vaccine immunogenicity wane, low responders may be at risk of acquiring new infections and developing cancer, hence, the immunogenicity induced by single dose vaccination requires keen monitoring. The higher immunogenicity observed in the youngest age group highlights a need to further explore vaccination of children aged below 9 years in which HPV vaccination has not been tested previously.

ACKNOWLEDGEMENTS

My PhD journey has been a transformative experience, through numerous learning experiences, challenges and triumphs. I am grateful to many people who made it a success.

First and foremost, I wish to express my deepest gratitude to my supervisors, Prof. Ed Clarke, Prof. Martin Holland and Dr. Martin Goodier. Your unwavering support, insightful feedback, and constant encouragement have been the bedrock of my academic journey. Your expertise and dedication have not only shaped my research but have also significantly contributed to my growth as a scholar. Thank you for believing in my potential and for providing me with the guidance and support necessary to navigate the complexities of this research, especially through the COVID-19 pandemic, getting this PhD completed is like a miracle. Many thanks to the Research Training and Career Development department in MRCG at LSHTM for the PhD scholarship and the continued mentorship and guidance from Prof. Assan Jaye. Great thanks to Dr. Anne Segonds, Michael Ooko and Miriam Wathuo for the statistical advice.

I would like to thank the Clinical Research Department, the Doctoral College and LSHTM at large for the support and guidance accorded to me as a research degree student at the school. Thanks to my Research Degree Coordinator Dr. Helen White for being very supportive any time I needed your help and the heads of Doctoral College Profs. Sam and Alex for information/discussions during Doctoral College seminars and student rep meetings and of course the prompt email replies whenever I asked anything.

I am deeply appreciative of the support from the entire HPV study team led by Drs. Adedapo Bashorun and Dolapo Obayemi for all the effort you put into seeing the success of this trial through all the challenges faced during the COVID-19 pandemic. Thank you to the members of the Vaccines and Immunity Theme at MRCG at LSHTM. Your collective invaluable insights, constructive criticism, and thoughtful suggestions have enriched my work. Great thanks to Dr. Sophie Roetynck for initial supervision and training on various immunoassays, Sanneh Bakary for help in the flow cytometry facility, Tijan Jobarteh, Francis Kanu, Anna Harte, Mohammed Jagana and Biran Gaye for the support you offered in different ways. Thank you to my colleagues and friends in the Infant Immunology Laboratory at MRCG at LSHTM. Your intellectual discussions, and moral support have been a source of strength throughout this journey. Special thanks to Mrs. Elishia Roberts for your concern and support in many ways. I lack words to thank my best sister, Dr. Ya Jankey Jagne for all the encouragement and for being a sounding board for ideas and frustrations alike not only with

the PhD journey but also ensuring we created some balance to keep on providing the critical support our young children need from us.

Outside work, I greatly thank the Abiding Word Ministries in The Gambia under the leadership of Pastor Forbes and all Pastors, Ministers as well as all Gatekeepers for the great familyhood full of love, spiritual guidance, encouragement and support. I have not only grown professionally but also spiritually, and I am grateful that God led me here.

Special appreciation to my sister-in-law Phylis Michael Mutisya and father-in-law Julius Maithya Muia for kind support back home in many ways. To my late brother, Michael Mutisya Kiamba (whom we lost on the first year into my PhD), It has never been easy without you around, I wish you were here to see me achieve this milestone. Thank you for stepping in the huge shoes of our late parents and being there for us in the time that God gave you. I am sorry you are not here.

To my husband, Jacob Maithya, your love, patience, and steadfast support have been my anchor throughout this journey, thanks for proofreading too. Thank you for making sure our children Adley and Vidette were always well taken care of even when I got intensively engaged in my PhD work. Immeasurable gratefulness to our wonderful, blessed children, Adley and vidette for always being the most amazingly understanding children.

This accomplishment would not have been possible without all that support, and I am deeply thankful and forever indebted to you all.

I finally acknowledge MRCG at LSHTM Doctoral Training Programme, Merck Sharp & Dorne and Wellcome Trust for funding this studentship and research work as well as all study participants without whom this work would not have been possible.

Dear GOD, I am eternally grateful to you for this milestone, only YOU know what this means. I dedicate this PhD to you, that it may open more opportunities for my career development and all be used to make impact for YOUR kingdom through making the lives of others better. Thank YOU for always assuring me that I can do all things in YOU that gives me strength.

Philippians 4:13

Career development small grant to characterise innate immunity to HPV vaccination

2024 British Society of Immunology

Travel grants/conferences where this or related work was presented

2023 Co-organizer of a cancer research symposium and presenter, Nairobi, Kenya

Oral presentation on cervical cancer vaccines

2023 International Union of Immunological Societies congress, Cape Town, South Africa

Oral presentation on B cell and Tfh cell responses to HPV vaccination

2023 Immuno-Morocco cancer immunology course, Marrakech, Morocco

Poster on cellular immunity to HPV vaccination

2023 LSHTM clinical research department workshop, virtual

Oral presentation on cellular immunity to HPV vaccines, best presenter prize

2022 British Society of Immunology Congress (virtual)

Poster on the role of cellular immunity in vaccine protection

2022 African flow cytometry workshop, HVTN lab, Cape Town, South Africa

2021 British Society of Immunology Congress (virtual)

Poster on B cell and T cell immunity to HPV vaccination

2021 West African College of Physicians meeting (virtual)

Recorded presentation on cervical cancer protection by HPV vaccines

2021 African immunobiology of parasites, pathogens and pathogenesis course (virtual)

Recorded video on potential mechanisms for HPV vaccine protection, best presenter prize

Voluntary leadership responsibilities undertaken during PhD

Co-organised an immunology course for pre-doctoral staff and students, MRCG at LSHTM

Chaired PhD and post-doc fellows representative committee, MRCG at LSHTM (2021-2024)

Representative of MRCG-based PhD students at the LSHTM doctoral college (2022 - 2024)

Member of MRCG at LSHTM staff and students EDI and well-being committee (2022 - 2024)

Table of Contents

DECLARATION OF OWN WORK	3
ABSTRACT	4
ACKNOWLEDGEMENTS	6
LIST OF TABLES	14
TABLE OF FIGURES	15
ABBREVIATIONS	17
1. INTRODUCTION.....	20
1.1 HPV AND CERVICAL CANCER EPIDEMIOLOGY	23
1.2 HPV BIOLOGY AND PATHOGENICITY	26
1.3 IMMUNE RESPONSES TO HPV INFECTIONS.....	32
1.3.1 <i>Innate immunity</i>	32
1.3.2 <i>Adaptive immunity</i>	37
1.3.2.1 Antigen presentation	37
1.3.2.2 T cell responses	39
1.3.2.2.1 CD4+ T cell response	39
1.3.2.2.2 Cytotoxic T lymphocytes (CD8+ T cells) response	40
1.3.2.3 Humoral responses	41
1.4 HPV VACCINES.....	46
1.4.1 <i>Immune activation by HPV vaccines</i>	48
1.4.2 <i>Vaccine protection and immunogenicity</i>	48
1.4.3 <i>Humoral responses to HPV vaccines</i>	51
1.5 MECHANISMS UNDERLYING SEROLOGICAL PROTECTION	55
1.5.1 <i>An overview of B cell biology</i>	56
1.5.1.1 B cell development and subsets based on differentiation status	61
1.5.1.1.1 Precursor B cells	61
1.5.1.1.2 Peripheral B cells.....	63
1.5.1.2 Subsets based on localization in B follicle compartments	65
1.5.1.2.1 Germinal centre B cells	65
1.5.1.2.2 Lymphocytic corona B cells	67
1.5.1.2.3 Marginal zone B cells.....	68
1.5.1.3 Subsets based on B cell developmental origin.....	69
1.5.1.3.1 B-1 B cells	69
1.5.1.3.2 B-2 B cells	70
1.5.2 <i>Maintenance of long-term antibodies by LLPCs and memory B cells</i>	71
1.5.3 <i>Tfh cell biology</i>	75
1.5.3.1 Models of Tfh cells development	77
1.5.3.1.1 Direct Tfh cell differentiation via cytokines.....	77
1.5.3.1.2 B cell-dependent direct Tfh cell differentiation	77
1.5.3.1.3 Secondary program of Tfh cells development	78
1.5.3.1.4 Multistage multifactorial model of Tfh cells differentiation	80
1.5.4 <i>B cells and Tfh cells interaction to generate memory B cells and long-lived plasma cells</i>	84
1.5.5 <i>HPV vaccine induced-cellular immunity</i>	87
1.6 GENERAL PROJECT AIM	90
1.6.1 <i>Specific objectives</i>	90
2. MATERIALS AND METHODS.....	92
2.1 STUDY DESIGN AND SUBJECTS	92
2.2 STUDY VACCINE FORMULATION AND ADMINISTRATION	92
2.3 LABORATORY METHODS	96
2.3.1 <i>Isolation of peripheral blood mononuclear cells (PBMC)</i>	96
2.3.2 <i>ELISpot</i>	97

2.3.2.1 In-vitro stimulation of memory B cells.....	97
2.3.2.2 Enumeration of HPV specific antibody secreting cells	98
2.3.3 <i>FluoroSpot</i>	101
2.3.4 <i>Flow cytometry</i>	103
2.3.4.1 Whole blood staining for plasma cell immunophenotyping	104
2.3.4.2 PBMC thawing and staining for plasma cell immunophenotyping	104
2.3.4.3 Whole blood staining for immunophenotyping of total Tfh cells ex vivo	105
2.3.4.4 PBMC staining for immunophenotyping of total Tfh cells ex vivo	106
2.3.4.5 Whole blood T cell stimulation and staining for identification of HPV 16 and HPV 18 specific Tfh cells.....	106
2.3.4.6 PBMC stimulation and staining for immunophenotyping of HPV 16 and 18 specific Tfh cells	106
2.3.4.7 Data acquisition on LSR Fortessa III cytometer	107
2.3.4.8 Measurement of antibody response using Competitive Luminex immunoassay	107
2.3.4.9 Single cell sorting of HPV 16 specific memory B cells	109
2.3.4.10 Heavy and light chains Arm-PCR amplification	110
2.3.4.11 iPair sequencing of paired B cell heavy and light chains.....	110
2.4 STATISTICAL ANALYSIS	112
2.4.1 <i>Sample size and statistical power considerations</i>	114
3. ASSAY DEVELOPMENT.....	116
3.1 ELISPOT AND FLUOROSPOT	116
3.1.1 <i>Introduction</i>	116
3.1.2 <i>Aims</i>	117
3.1.3 <i>Results and discussion</i>	117
3.1.3.1 Optimal cell numbers in total IgG and total IgM wells.....	117
3.1.3.2 HPV VLP plate coating concentrations	120
3.1.3.3 Plasma cell and memory B cell kinetics after first dose of Gardasil 9 vaccine	122
3.2 FLOW CYTOMETRY	124
3.2.1 <i>Introduction</i>	124
3.2.2 <i>Aims</i>	124
3.2.3 <i>Results and discussion</i>	124
3.2.3.1 Designing of plasma cell and Tfh cell multicolour antibody panels	124
3.2.3.2 Preliminary antibody testing	132
3.2.3.3 Antibody titration.....	134
3.2.3.4 Plasma cell antibody panel optimisation	136
3.2.3.4.1 Effect of TE on immunoglobulin surface staining.....	136
3.2.3.4.2 IgA staining and effect of TE.....	139
3.2.3.4.3 Effect of BSBP on multiple BV dye staining	140
3.2.3.4.4 Complete plasma cell panel evaluation	142
3.2.3.5 Tfh cell AIM antibody panel	148
3.2.3.5.1 Evaluation of Tfh cell culture stimulation using a mitogen stimulus.....	149
3.2.3.5.2 Titration of HPV 16 and 18 VLPs for Tfh cell culture stimulation	151
3.2.3.5.3 Evaluation of complete Tfh cell AIM panel	153
3.2.3.5.4 Evaluation of AIM panel for identification of HPV specific Tfh cells after vaccination	156
3.2.3.6 Tfh cell ex vivo antibody panel.....	158
3.2.3.6.1 Optimisation of Tfh cell ex vivo panel	158
3.3 CONCLUSION AND DISCUSSION	162
4. PLASMA CELL AND MEMORY B CELL RESPONSES AFTER GARDASIL 9 VACCINATION	164
4.1 AIMS	164
4.2 RESULTS	164
4.2.1 PLASMA CELL RESPONSES AFTER HPV VACCINATION	164
4.2.1.1 HPV 16 and HPV 18 specific IgG plasma cell response.....	166
4.2.1.2 HPV 16 and HPV 18 specific IgM plasma cell response.....	170
4.2.1.3 Total IgG and IgM plasma cell frequencies	174
4.2.2 MEMORY B CELL RESPONSES AFTER HPV VACCINATION	183
4.3 DISCUSSION AND FUTURE WORK.....	195

5. T FOLLICULAR HELPER CELL RESPONSE AFTER GARDASIL 9 VACCINATION	204
5.1 AIMS	204
5.2 RESULTS	204
5.2.1 HPV 16 and HPV 18 specific Tfh cell AIM response after Gardasil 9 vaccination	205
5.2.2 Comparison of HPV 16 and HPV 18 specific Tfh cell AIM frequencies with plasma cell numbers	219
5.2.3 Frequencies of total ex vivo activated Tfh cells after Gardasil 9 vaccination	220
5.3 DISCUSSION AND FUTURE WORK	231
6. SERUM IGG ANTIBODY RESPONSES AFTER HPV VACCINATION	237
6.1 AIMS	238
6.2 RESULTS	238
6.2.1 HPV 16 AND HPV 18 ANTIBODY TITRES	238
6.2.2 Correlations between plasma cells, memory B cells and Tfh cells with antibody titres	240
6.3 DISCUSSION AND FUTURE WORK	242
7. SINGLE CELL SORTING OF HPV 16 SPECIFIC MEMORY B CELLS AND B CELL REPERTOIRE MAPPING	245
7.1 INTRODUCTION	245
7.2 AIMS.....	250
7.3 RESULTS	250
7.3.1 Titration of HPV 16-AF488 and HPV 18-AF647 VLP.....	250
7.3.2 Confirmation of HPV 16+ memory B cell staining on fresh PBMC.....	253
7.3.3 Confirmation of HPV 16+ memory B cells staining in young age groups	255
7.3.4 B cell enrichment using magnetic activated cell sorting and staining	257
7.3.5 Validation of single sorting on FACS Melody.....	258
7.3.6 Single cell sorting of HPV 16+IgG+ memory B cells for B cell repertoire mapping	260
7.3.7 PCR-amplification of B cell heavy and light chains of HPV 16 specific memory B cells	262
7.3.8 Sequencing of naturally paired B cell heavy and light chains	264
7.3.9 Usage of germline IGHV, IGKV/LV, IGHJ, and IGKV/LJ gene variants and unique CDR3 amino acid length	270
7.3.10 Single cell sorting of HPV 16+ memory B cells from different study age groups.....	274
7.4 DISCUSSION AND FUTURE WORK	279
8. FINAL DISCUSSION	282
8.1 RESEARCH AIMS AND BACKGROUND	282
8.2 SUMMARY OF RESULTS	283
8.3 FUTURE WORK	288
REFERENCES	291
APPENDICES	328
Appendix 1. Preliminary testing of antibodies in the plasma cell panel at manufacturer’s recommended dilutions.....	328
Appendix 2. Preliminary testing of antibodies in the Tfh cell AIM panel at manufacturers’ recommended dilutions.....	331
Appendix 3. Antibody titration for initial plasma cell panel.....	333
Appendix 4. Antibody titration for initial Tfh cell AIM panel	337
Appendix 5. Antibody titration for initial Tfh cell ex vivo panel	340
Appendix 6. Antibody titration for re-designed plasma cell panel.....	342
Appendix 7. Antibody titration for re-designed Tfh cell AIM panel	344
Appendix 8: Antibody titration for re-designed Tfh cell ex vivo panel.....	346
Appendix 9. Tfh cell responses in negative and positive controls used in the AIM assay.....	348
Appendix 10. Total Tfh cell frequencies after Gardasil 9 vaccination	350
Appendix 11. Gating strategy for identification of HPV 16+IgG+, HPV 16+IgG-IgM- and HPV 16+IgM+ memory B cell for single cell sorting.....	351
Appendix 12. Gel image for PCR amplification of B cell receptor; A - plate 1, B - plate 2.....	352
Appendix 13. The Gambia Government/MRC Joint ethical approval	354

Appendix 14. London School of Hygiene and Tropical Medicine Ethical approval 356

List of tables

TABLE 1.1. HPV VACCINES' INFORMATION	47
TABLE 1.2. MARKERS FOR PHENOTYPIC IDENTIFICATION OF T _{fh} CELL STAGES IN MICE AND HUMANS	82
TABLE 2.1. GARDASIL 9 VACCINE FORMULATION.	93
TABLE 2.2. VACCINATION AND BLOOD SAMPLING SCHEDULE FOR MAIN STUDY AND SUB-STUDY	95
TABLE 2.3. STATISTICAL COMPARISONS	113
TABLE 2.4. NUMBER OF SAMPLES ANALYSED BY AGE AND DOSE NUMBER.....	114
TABLE 3.1. PLASMA CELL ANTIBODY PANEL MARKERS, BIOLOGICAL FUNCTIONS, AND ROLES IN THE PANEL	126
TABLE 3.2. T FOLLICULAR HELPER CELL PANEL MARKERS, BIOLOGICAL FUNCTIONS, AND ROLES IN THE PANEL.....	127
TABLE 3.3. INITIAL PLASMA CELL (B CELL) AND T FOLLICULAR HELPER CELL ANTIBODY PANELS	130
TABLE 3.4. SI CALCULATIONS FOR CD4-PERCPY5.5 AND CD19-BV786	136
TABLE 4.1. NUMBER OF HPV 16 AND HPV 18 SPECIFIC IGG SECRETING CELLS PER 10 ⁶ PBMC	167
TABLE 4.2. NUMBER OF HPV 16 AND HPV 18 SPECIFIC IGM SECRETING CELLS PER 10 ⁶ PBMC.....	171
TABLE 4.3. NUMBER OF TOTAL IGG AND IGM SECRETING CELLS PER 10 ⁶ PBMC.....	175
TABLE 4.4. FREQUENCIES OF IGG+ AND IGM+ CELLS IN TOTAL PLASMA CELLS.....	180
TABLE 4.5. NUMBER OF HPV 16 AND HPV 18 SPECIFIC AND TOTAL IGG MEMORY B CELLS PER 10 ⁶ STIMULATED PBMC (BACKGROUND NOT SUBTRACTED).....	185
TABLE 4.6. NUMBER OF HPV 16 AND HPV 18 SPECIFIC AND TOTAL IGG MEMORY B CELLS PER 10 ⁶ STIMULATED PBMC (BACKGROUND-SUBTRACTED).....	187
TABLE 4.7. FREQUENCIES OF HPV 16 AND HPV 18 SPECIFIC IGG MEMORY B CELLS.....	191
TABLE 5.1. NUMBER OF SAMPLES USED TO EVALUATE ACTIVATED T _{fh} CELL FREQUENCIES PER TIMEPOINT	205
TABLE 5.2. HPV 16 SPECIFIC T _{fh} CELL AIM RESPONSES AFTER GARDASIL 9 VACCINATION	208
TABLE 5.3. HPV 18 SPECIFIC T _{fh} CELL AIM RESPONSES AFTER GARDASIL 9 VACCINATION	213
TABLE 5.4. FREQUENCIES OF TOTAL EX VIVO ACTIVATED T _{fh} CELLS AFTER GARDASIL 9 VACCINATION	222
TABLE 5.5. FREQUENCIES OF EX VIVO ACTIVATED T _{fh} CELL SUBSETS AFTER GARDASIL 9 VACCINATION	225
TABLE 6.1. HPV 16 AND HPV 18 SPECIFIC ANTIBODY TITRES AFTER GARDASIL 9 VACCINATION	239
TABLE 7.1. EXAMPLES OF SEQUENCE DATA FOR IGH AND IGK/L CHAINS FROM IPAIR ANALYZER SOFTWARE.....	266

Table of Figures

FIGURE 1.1. EVOLUTIONARY RELATIONSHIP BETWEEN HUMAN PAPILLOMAVIRUSES	25
FIGURE 1.2. HPV GENOMIC STRUCTURE	27
FIGURE 1.3. MECHANISM OF HPV ATTACHMENT AND INFECTION.....	30
FIGURE 1.4. ASSEMBLY OF L1 AND L2 MONOMERS IN VIRUS-LIKE PARTICLE AND NATIVE VIRUS	46
FIGURE 1.5. SCHEMATIC REPRESENTATION OF B CELL DEVELOPMENT	65
FIGURE 2.1. HANDS TRIAL SUB-STUDY VACCINATION AND BLOOD SAMPLING TIMEPOINTS	96
FIGURE 2.2. B CELL STIMULATION BY R848 AND IL-2 IN A 6-DAY CULTURE	98
FIGURE 2.3. STEPWISE ELISPOT PROCEDURE	100
FIGURE 2.4. STEPWISE FLUOROSPOT PROCEDURE.....	102
FIGURE 2.5. IPAIR B CELL SEQUENCING STEPS	111
FIGURE 3.1. TOTAL IgG AND IgM PLASMA CELL RESPONSES DETECTED USING DIFFERENT CELL NUMBERS PER WELL IN THE FIRST TWO WEEKS AFTER FIRST DOSE OF GARDASIL 9 VACCINATION	118
FIGURE 3.2. TOTAL IgG PLASMA CELL RESPONSES AT DAY 7 POST-FIRST DOSE OF GARDASIL 9 VACCINE.....	119
FIGURE 3.3. HPV SPECIFIC IgG AND IgM ANTIBODY SECRETING CELLS ACROSS DIFFERENT VLP PLATE COATING CONCENTRATIONS	121
FIGURE 3.4. PLASMA CELL AND MEMORY B CELL KINETICS AFTER GARDASIL 9 VACCINATION	123
FIGURE 3.5. PRELIMINARY TESTING OF ANTIBODIES IN THE Tfh CELL EX VIVO PANEL AT MANUFACTURERS' RECOMMENDED ANTIBODY DILUTIONS	133
FIGURE 3.6. TITRATION OF CD4-PERCPy5.5 AND CD19-BV786 ANTIBODIES.....	135
FIGURE 3.7. EFFECT OF TANDEM SIGNAL ENHANCER (TE) ON IgG AND IgM STAINING.....	138
FIGURE 3.8. IGA STAINING AND EFFECT OF TE.....	139
FIGURE 3.9. BRILLIANT STAIN BUFFER PLUS IMPROVES RESOLUTION IN MULTICOLOUR STAINING WITH MULTIPLE BV DYES.....	141
FIGURE 3.10. INITIAL COMPLETE PLASMA CELL PANEL TESTING FAILED TO IDENTIFY CLEAR PLASMA CELL POPULATION	143
FIGURE 3.11. RE-DESIGNED PANEL IDENTIFIED CLEAR PLASMA CELL POPULATION WHICH WAS REDUCED BY INTRACELLULAR STAINING OF IgG AND IgM.....	145
FIGURE 3.12. CD138 STAINING WAS LOST ON FROZEN PBMC	146
FIGURE 3.13. FINAL PLASMA CELL PANEL IDENTIFIED CLEAR PLASMA CELL POPULATIONS BEFORE AND AFTER VACCINATION	148
FIGURE 3.14. IDENTIFICATION OF POLYCLONALLY ACTIVATED Tfh CELLS USING AIM ANTIBODY PANEL.....	150
FIGURE 3.15. TITRATION OF HPV 16 AND HPV 18 VLPs FOR IDENTIFICATION OF VACCINE-INDUCED ANTIGEN SPECIFIC Tfh CELLS	152
FIGURE 3.16. INITIAL COMPLETE AIM PANEL FAILED TO IDENTIFY EXPECTED PROFILES OF POLYCLONALLY ACTIVATED Tfh CELLS.	154
FIGURE 3.17. RE-DESIGNED AIM PANEL IDENTIFIED EXPECTED PROFILES OF POLYCLONALLY ACTIVATED Tfh CELLS	155
FIGURE 3.18. AIM PANEL IDENTIFIED HPV 16 AND HPV 18 SPECIFIC Tfh CELLS AFTER VACCINATION.....	157
FIGURE 3.19. INITIAL EX VIVO PANEL FAILED TO IDENTIFY CLEAR ACTIVATED Tfh CELLS	159
FIGURE 3.20. RE-DESIGNED Tfh CELL EX VIVO PANEL CLEARLY IDENTIFIED TOTAL ACTIVATED POOL OF Tfh CELLS AFTER VACCINATION.....	161
FIGURE 4.1. FLUOROSPOT READOUT FROM ONE PARTICIPANT IN THE 15-26-YEAR-OLDS GROUP	165
FIGURE 4.2. HPV 16 AND HPV 18 SPECIFIC IgG PLASMA CELL RESPONSE AFTER GARDASIL 9 VACCINATION.....	169
FIGURE 4.3. HPV 16 AND HPV 18 SPECIFIC IgG PLASMA CELL RESPONSE AFTER GARDASIL 9 VACCINATION, COMPARISONS PER TIMEPOINT	170
FIGURE 4.4. HPV 16 AND HPV 18 SPECIFIC IgM PLASMA CELL RESPONSE AFTER GARDASIL 9 VACCINATION	173
FIGURE 4.5. HPV 16 AND HPV 18 SPECIFIC IgM PLASMA CELL RESPONSE AFTER GARDASIL 9 VACCINATION, COMPARISONS PER TIMEPOINT	174
FIGURE 4.6. TOTAL IgG AND IgM PLASMA CELL RESPONSE AFTER GARDASIL 9 VACCINATION.....	177
FIGURE 4.7. GATING STRATEGY FOR IDENTIFICATION OF TOTAL IgG+ AND IgM+ PLASMA CELL FREQUENCIES AFTER GARDASIL 9 VACCINATION.....	179
FIGURE 4.8. FREQUENCIES OF TOTAL IgG+ AND IgM+ PLASMA CELLS AFTER GARDASIL 9 VACCINATION	182
FIGURE 4.9. HPV 16 AND HPV 18 SPECIFIC AND TOTAL IgG MEMORY B CELL RESPONSE AFTER GARDASIL 9 VACCINATION	184
FIGURE 4.10. HPV 16 AND HPV 18 SPECIFIC IgG MEMORY B CELL RESPONSE AFTER GARDASIL 9 VACCINATION	189
FIGURE 4.11. TOTAL IgG MEMORY B CELL RESPONSE AFTER GARDASIL 9 VACCINATION	190

FIGURE 4.12. HPV 16 AND HPV 18 SPECIFIC IgG MEMORY B CELL RESPONSE AFTER GARDASIL 9 VACCINATION, COMPARISONS PER TIMEPOINT	193
FIGURE 4.13. FREQUENCIES OF HPV 16 AND HPV 18 SPECIFIC IgG MEMORY B CELLS AFTER GARDASIL 9 VACCINATION, COMPARISONS PER TIMEPOINT	194
FIGURE 5.1. GATING STRATEGY FOR IDENTIFICATION OF HPV 16 AND HPV 18 Tfh CELLS	207
FIGURE 5.2. HPV 16 SPECIFIC Tfh CELL AIM RESPONSES AFTER GARDASIL 9 VACCINATION	211
FIGURE 5.3. HPV 18 SPECIFIC Tfh CELL AIM RESPONSES AFTER GARDASIL 9 VACCINATION	216
FIGURE 5.4. IMPACT OF AGE ON HPV 16 AND HPV 18 SPECIFIC Tfh CELL RESPONSES AFTER GARDASIL 9 VACCINATION	218
FIGURE 5.5. CORRELATION OF HPV 16 (A) AND HPV 18 (B) SPECIFIC Tfh CELL FREQUENCIES WITH PLASMA CELL NUMBERS ...	219
FIGURE 5.6. GATING STRATEGY FOR IDENTIFICATION OF EX VIVO ACTIVATED Tfh CELLS	221
FIGURE 5.7. FREQUENCIES OF TOTAL EX VIVO ACTIVATED Tfh CELLS AFTER GARDASIL 9 VACCINATION	223
FIGURE 5.8. FREQUENCIES OF EX VIVO ACTIVATED Tfh CELL SUBSETS AFTER GARDASIL 9 VACCINATION	228
FIGURE 5.9. COMPARISONS OF EX VIVO Tfh CELL ACTIVATION IN DIFFERENT AGE GROUPS AFTER GARDASIL 9 VACCINATION	230
FIGURE 6.1. HPV 16 AND HPV 18 SPECIFIC ANTIBODY TITRES AFTER GARDASIL 9 VACCINATION	240
FIGURE 6.2. COMPARISONS BETWEEN HPV 16 AND HPV 18 SPECIFIC IgG ANTIBODY TITRES WITH PLASMA CELLS, MEMORY B CELLS AND Tfh CELLS	241
FIGURE 7.1. B CELL RECEPTOR STRUCTURE	246
FIGURE 7.2. VDJ RECOMBINATION DURING B CELL DEVELOPMENT STAGES	248
FIGURE 7.3. TITRATION OF HPV 16-AF488 AND HPV 18-AF647 VLP	252
FIGURE 7.4. HPV 16+ MEMORY B CELL FREQUENCY ON FRESH PBMC BEFORE AND AFTER GARDASIL 9 VACCINATION	254
FIGURE 7.5. HPV 16+ FREQUENCIES BEFORE AND AFTER GARDASIL 9 VACCINATION	255
FIGURE 7.6. B CELL FREQUENCIES AFTER ENRICHMENT BY MAGNETIC ACTIVATED CELL SORTING	258
FIGURE 7.7. VALIDATION OF SINGLE CELL SORTING OF RAJI CELL LINE BY IPAIR ARM-PCR-AMPLIFICATION	260
FIGURE 7.8. HPV 16+ MEMORY B CELL FREQUENCY AFTER DOSE 3 OF GARDASIL 9 VACCINATION	263
FIGURE 7.9. SEQUENCE QUALITY DISTRIBUTION, HEAVY (IGH) AND LIGHT CHAIN (IGK/L) PAIRING ON PLATES 1 AND 2	265
FIGURE 7.10. CONFIRMATION OF ISOTYPE, HEAVY-LIGHT (GH-IGK/L) CHAIN PAIRING AND UNIQUE CDR3S	269
FIGURE 7.11. USAGE OF GERMLINE HEAVY AND LIGHT CHAIN GENE VARIANTS AND DISTRIBUTION OF CDR3 AMINO ACID LENGTH	272
FIGURE 7.12. IDENTIFICATION OF VACCINE-INDUCED HPV 16+ MEMORY B CELL FOR SINGLE CELL SORTING	275
FIGURE 7.13. IDENTIFICATION OF BASELINE HPV 16- MEMORY B CELLS FOR SINGLE CELL SORTING	277

ABBREVIATIONS

AF	AlexaFluor
AIM	Activation Induced Markers
ALP	Alkaline Phosphatase
ALUM	Aluminium Hydroxyphosphate Sulfate
ANOVA	Analysis of variance
APC	Allophycocyanin
AS04	Adjuvant System 04
ASC	Antibody Secreting Cells
BCR	B Cell Receptor
BV	Brilliant Violet
CCR	Chemokine Receptor
CD	Cluster of Differentiation
CI	Confidence interval
CXCL	CXC Chemokine Ligand
CXCR	CXC Chemokine Receptor
DC	Dendritic Cells
DMSO	Dimethyl Sulfoxide
DNA	Deoxyribonucleic Acid
ELISpot	Enzyme-linked Immunosorbent Spot
FACS	Fluorescence Activated Cell Sorting
FcR	Fragment Crystallizable Receptor
FMO	Fluorescence Minus One
FSC	Forward Scatter
GC	Germinal Centre
GM CSF	Granulocyte/Macrophage Colony Stimulating Factor
HANDS	HPV Vaccination in Africa- New Delivery Schedules
HPV	Human Papillomavirus
HSIL	High-grade Squamous Intraepithelial Lesions

IC	Isotype Control
ICOS	Inducible T cell Costimulator
ICOS-L	Inducible T cell Costimulator-Ligand
IFN	Interferon
Ig	Immunoglobulin
IL	Interleukin
Kb	Kilobase Pairs
LC	Langerhans Cells
LCR	Long Control Region
LLPC	Long-Lived Plasma Cells
LMIC	Low- and Middle-Income Countries
LSIL	Low-grade Squamous Intraepithelial Lesions
MHC II	Major Histocompatibility Complex Class II
mL	Millilitre
mM	Millimolar
MPL	Monophosphoryl Lipid A
NK	Natural Killer
ON	Overnight
ORF	Open Reading Frame
PBMC	Peripheral Blood Mononuclear Cells
PBS	Phosphate Buffered Saline
PD	Programmed Cell Death Protein 1
PD-L1	Programmed Cell Death Protein 1-Ligand
PE	Phycoerythrin
PerCP	Peridinin Chlorophyll Protein Complex
PFA	Paraformaldehyde
PMT	Photomultiplier Tube
pRB	Retinoblastoma Protein
PVDF	Polyvinylidene Difluoride
RB	Retinoblastoma Gene
RBC	Red Blood Cells
RPMI	Roswell Park Memorial Institute
RT	Room Temperature
SD	Standard deviation

SEB	Staphylococcus Enterotoxin B
SI	Separation Index
SSC	Side Scatter
SSM	Spillover Spreading Matrix
TE	Tandem Signal Enhancer
Tfh	T Follicular Helper
Th	T Helper
TLR	Toll-like Receptor
TNF	Tumor Necrosis Factor
TNTC	Too Numerous To Count
VLP	Virus-Like Particles
µg	Microgram
µL	Microlitre

1. INTRODUCTION

The global public health benefits of vaccination in controlling disease and saving lives cannot be overemphasized. Indeed, recent estimations from modelling 50 years of the Expanded Programme on Immunization (EPI) show that vaccines have averted 154 million deaths.(Shattock et al., 2024) Out of these, 146 million were children younger than five years, including 101 million infants.(Shattock et al., 2024) Such benefits would not have been achieved without continued interdisciplinary research in the areas of pathogen biology, epidemiology, immunology and vaccine development.(Pollard and Bijker, 2021) Vaccine immunology is highly dynamic warranting vaccines to be continually monitored for immunogenicity and efficacy in their target populations.(Adam et al., 2021) Additionally, since vaccine development and dosing recommendations have mainly been empirical, new vaccines need to be monitored and optimised as necessary for factors such as the actual vaccine composition, dose schedules and target age based on their initial effectiveness and other factors including cost and availability as well as delivery logistics. Some vaccines may be highly potent to induce sufficiently high immunogenicity and protection from fewer doses than recommended, warranting revision of the dose schedules to ensure the optimal schedules are utilised at lowest cost. Indeed, *Haemophilus influenzae* type b and *Neisseria meningitidis* serogroup C dosage schedules were changed based on their capacity to provide long-term protection. HPV vaccination dose schedules have been revised twice, initially from 3 doses to 2 doses and recently from 2 doses to a single dose for the primary age target.(WHO, 2022)

Currently licensed HPV vaccines are based on virus-like particles (VLPs) containing the major viral capsid protein (L1) and provide robust durable antibody-mediated protection from HPV infection as well as HPV-associated disease.(De Vincenzo et al., 2014) The long-term plateau of antibody titres induced by HPV vaccines even after a single dose is more typically associated with live-attenuated vaccines than sub-unit vaccines.(Minor, 2015) Most studies

evaluating HPV vaccine immunogenicity have focused on antibody responses demonstrating that the vaccines induce similarly robust and durable antibody protection.(Whitworth et al., 2024, Hoes et al., 2022) This may be attributable to the fact that HPV vaccines generate highly effective antibody protection, and seems to have overshadowed research on the actual cellular and molecular immunological mechanisms underlying maintenance of the long-term antibody protection observed even after a single dose. However, characterisation of both cellular and antibody immunogenicity is important in this study exploring single dose HPV vaccine immunogenicity in younger age groups in whom HPV vaccination has not been tested before.

While the repetitive structure of the HPV VLP antigens is thought to enhance B cell activation through cross-linking B cell receptors (BCRs) which has been shown to increase BCR-related downstream signalling, this has not been investigated.(Schiller and Lowy, 2018a, Stanley, 2010d) Various studies demonstrated sustained antibody titres after a single vaccine dose and higher immunogenicity in younger age groups even with extended dosing intervals.(Dobson et al., 2013, Iversen et al., 2016, Puthanakit et al., 2016, Whitworth et al., 2024, Hoes et al., 2022) Such data raised interest to investigate the optimal dosing schedules and best target age group for HPV vaccination. Although a single dose was recently recommended for HPV vaccination, this was mainly based on evidence from observational studies and data from the only single-dose randomised study to have reported then, covering the first 18 months of a planned longer-term follow up.(Barnabas et al., 2022, Porras et al., 2020, Whitworth et al., 2020). Data from longer follow up of randomised single dose trials will contribute to the more reliable evidence of immunogenicity and protection from the single dose schedule.

It is well-documented that the longevity of vaccine- or infection-induced serological responses relies either on sustained antibody production by long-lived plasma cells (LLPC) and memory B cell recall responses.(Ionescu and Urschel, 2019, Sallusto et al., 2010) The studies conducted on HPV-vaccine induced cellular immunity to date have reported that

HPV vaccines generate HPV specific memory B cells with viral neutralisation capacity(Pasmans et al., 2022, Scherer et al., 2014a, Scherer et al., 2016, Scherer et al., 2018), but their role in sustenance of vaccine-induced antibodies is not clear.(Nicoli et al., 2020a, Schiller and Lowy, 2018a) No studies have provided evidence for LLPC responses following HPV vaccination except by inference from the profiles of long-term antibody titres, suggested to indicate the presence of LLPCs.(Schiller and Lowy, 2018a, Stanley, 2010d) The only study characterising HPV specific vaccine-induced plasmablasts/plasma cells was conducted in young women and reported plasma cell expansion in only 1 out of 4 participants at one week after completion of 3 dose schedule (at 0, 2 and 6 months), and were expended in all 4 participants at one week following a 4th booster dose (given at 24 months).(Scherer et al., 2018) While these studies provided early insights, and that cellular responses are required for maintenance of long term antibody protection, further research to improve understanding on the cellular mechanisms driving long-term HPV vaccine protection is needed.

This PhD research work formed a sub-study component within a larger phase 3 non-inferiority clinical trial comparing early and long-term antibody responses to different dose schedules of the nine-valent HPV vaccine (Gardasil 9) in different age groups. The sub-study investigates vaccine-induced cellular immunity with a particular focus on plasma cells, memory B cells and T follicular helper (Tfh) cells and their influence on vaccine-induced antibody responses.

Relevant literature to this subject will be discussed starting with HPV and cervical cancer epidemiology, HPV biology, pathogenicity and immunogenicity - highlighting mechanisms that enhance persistent infection which is a prerequisite for development of HPV-associated cancers. Following this, HPV vaccines will be introduced and data on the vaccine efficacy and humoral immunity reviewed. Next, the mechanisms for generation of long-term serological protection will be discussed. This will discuss B cell and Tfh cell biology including the various subsets and functions based on different classification approaches and the

interaction between these two cell populations to generate short-lived plasma cells, memory B cells and LLPCs. Finally, data on HPV vaccine-induced cellular immunity will be reviewed before the research aims and objectives.

1.1 HPV and cervical cancer epidemiology

Cervical cancer is a major cause of morbidity and mortality in women worldwide, being the fourth most common type of cancer affecting women globally and either first or second most common type of cancer in women in Sub-Saharan Africa.(Bray et al., 2024) About 660,000 new cervical cancer cases and 350,000 deaths were reported globally in 2022 with most of these deaths occurring in Sub-Saharan Africa.(Bray et al., 2024) Global age-standardized data showed that Eastern, Southern and Middle African regions registered the highest incidence/mortality rates at 40.4/28.9, 34.9/20.4 and 28.3/21.1 cases per 100,000 women, respectively.(Bray et al., 2024) On the other hand, Western Asia, Australia-New Zealand and Northern America reported the lowest incidence rates at 4.1, 5.2 and 6.3 per 100,000 women, respectively, and were among regions with lowest mortality rates ranging between 1.4 and 2.2 cases per 100,000.(Bray et al., 2024) Cervical cancer is the most commonly diagnosed type of cancer in the Gambia accounting for 48.1% of cancer cases in women and 27.2% of all cancer cases reported in 2022.(Bray et al., 2024)

HPV, the most common sexually transmitted pathogen worldwide, is associated with a range of diseases from benign lesions such as genital warts to anogenital (cervical, anal, penile, vaginal) and oropharyngeal cancers.(zur Hausen, 2002) Various factors including certain co-infections with *Chlamydia trachomatis*, *Neisseria gonorrhoea* and common *Mycoplasmataceae* species, immunosuppression and others increase the risk of cervical cancer development in the context of high-risk HPV infection which is the confirmed causative agent for cervical cancer, discussed later.(Walboomers et al., 1999, Ghebre et al., 2017, Roura et al., 2014, Tantengco et al., 2022, Noma et al., 2021, Klein et al., 2020) Immunocompromised women are at increased risk-of HPV infection and faster progression to cervical cancer.(Reusser et al., 2015) The role of human immunodeficiency virus (HIV)

infection as a risk factor for HPV infection has been suggested to be due to its direct impairment of CD4 T cell responses.(Strickler et al., 2005, Wang et al., 2011) Additionally, some studies reported that HPV and herpes simplex virus (HSV) and other sexually transmitted infections may also increase the risk of HIV infection.(Houlihan et al., 2012, Joag et al., 2016)

There are more than 200 known HPV genotypes classified into five genera; Alpha, Beta, Gamma, Nu and Mu (Figure 1.1).(Egawa et al., 2015) The alpha genus is responsible for most mucosal and skin epithelial infections. Based on their potential to cause cancer, HPV types in this genus are epidemiologically classified as either high-risk (carcinogenic), low risk (non-carcinogenic) or probable carcinogens.(Moeinzadeh et al., 2020) About 99% of cervical cancer cases are attributable to infection with high-risk HPV types. Of these, two HPV types (HPV 16 and HPV 18) are responsible for approximately 70%, while 10 others (HPV 31, 33, 35, 39, 45, 51, 52, 56, 58 and 59) are responsible for about 27% of the cervical cancer cases diagnosed globally.(WHO, 2023) Additionally, two low risk HPV types (HPV 6 and HPV 11) are responsible for the highest global burden of genital warts.(WHO, 2023)

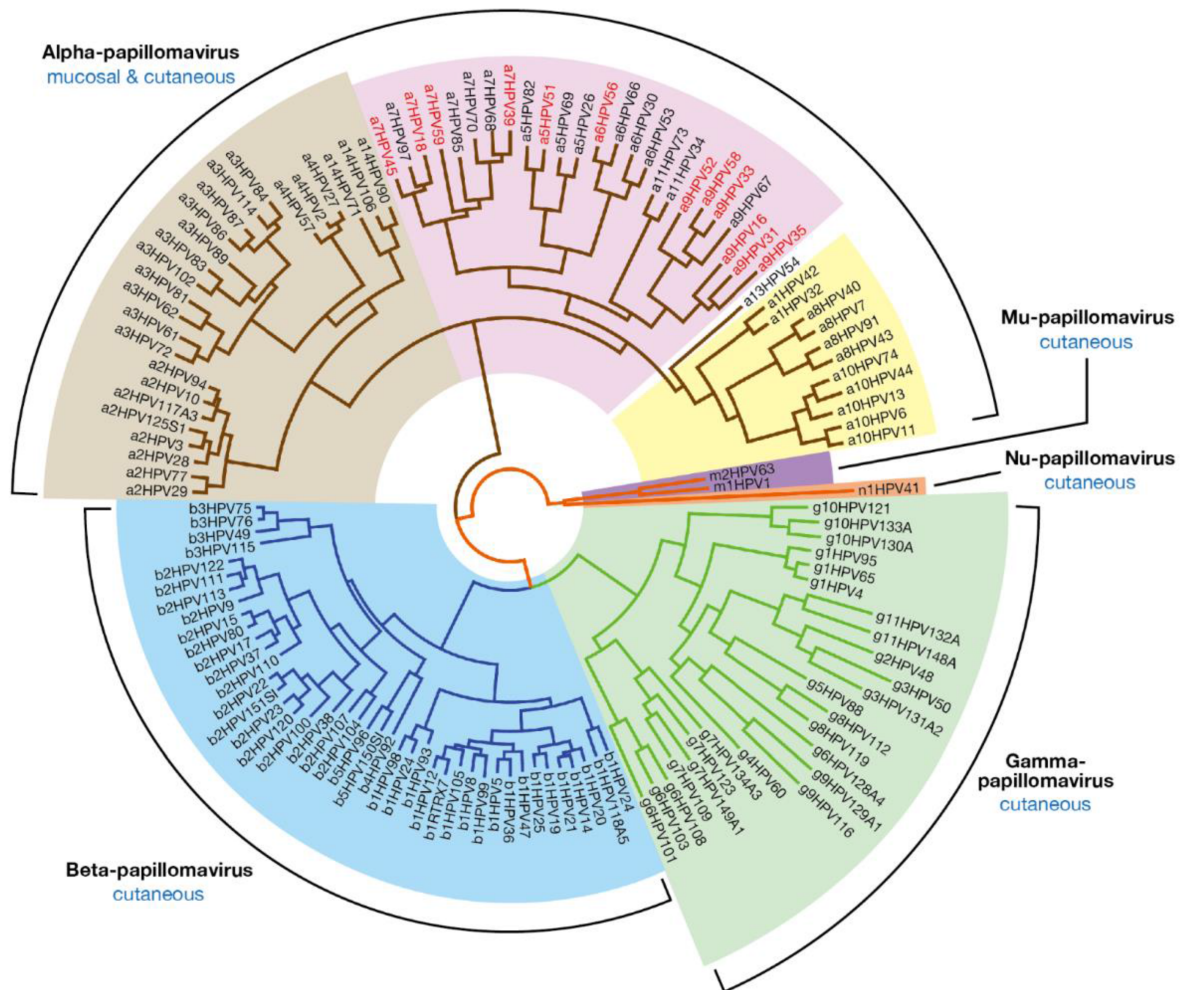


Figure 1.1. Evolutionary relationship between Human Papillomaviruses

Human papillomaviruses are classified into five genera including Alpha-, Beta- and Gamma-papillomavirus representing the largest groups. Alpha papillomavirus genus is often classified as low-risk cutaneous (light brown); low-risk mucosal (yellow); or high-risk (pink) based on their potential to cause development of cancer. The high-risk types highlighted in red text are confirmed as “human carcinogens” from epidemiological studies. The other high-risk types are “probable” or “possible” carcinogens. Although the predominant tissue associations of each genus are listed as either cutaneous or mucosal, these designations do not necessarily hold true for every member of the genus.

The evolutionary tree was reproduced from (Egawa et al., 2015) who developed it by alignment of the E1, E2, L1 and L2 genes from online available sequence data from PaVE. <http://pave.niaid.nih.gov/>

Although there are no data on age of HPV acquisition in the Gambia, data from other West African countries show that typical age at sexual debut in females is 15-25 years.(Clifford et al., 2005, Nejo et al., 2018, Wall et al., 2005) A study conducted in a rural Gambian setting reported HPV prevalence to be about 13% (95/710) with HPV 16 being the most prevalent

and most strongly associated with development of squamous intra-epithelial lesions (SIL) and pre-cervical cancer disease in middle aged women (25 to 44-year-olds).(Wall et al., 2005) Other common high risk HPV types reported in the Gambia included HPV 18, 33 and 58.(Wall et al., 2005) A more recent study conducted in a Gambian urban setting reported HPV prevalence of 12% (28/232), with HPV 52 being the most prevalent.(Bah Camara et al., 2018) In that study, half (14/28) of the HPV cases were co-infected with *Ureaplasma parvum*, a urinary or genital tract bacterial infection known to increase progression to cervical cancer.(Noma et al., 2021, Biernat-Sudolska et al., 2011, Bah Camara et al., 2018) These two are the only HPV prevalence studies conducted in Gambia to date and both noted ethnicity-related differences with the Fula having the highest prevalence of high-risk HPV types followed by Madinka and Wollof ethnic groups.(Bah Camara et al., 2018, Wall et al., 2005)

The host immunity plays a vital role in clearing over 90% of HPV infections and regression of HPV related lesions.(Giuliano et al., 2011) However, the high-risk HPV types employ complex immune evasion mechanisms that enhance their persistence for years and may get integrated into the host genome leading to cancer development.(Zhou et al., 2019a, zur Hausen, 1996)

Next, I discuss HPV biology with a focus on the high-risk types and their complex lifecycle that drives pathogenicity to cancer development.

1.2 HPV biology and pathogenicity

HPV is a small non-enveloped double-stranded DNA virus, approximately 55 nanometres in diameter with a complete genome length of about 8 kilobasepairs.(Doorbar et al., 2012) Figure 1.2 illustrates a general genomic structure of HPV represented by HPV 16. The genome contains a long control region (LCR) and genes encoding six early (E1, E2, E4, E5, E6 and E7) and two late (L1 and L2) proteins named according to their time of expression in the viral life cycle.(Doorbar et al., 2012) The early genes are important in viral replication and transcription as well as dysregulation of host cell processes to enhance the viral survival for

example through: interfering with proliferation and differentiation, cell cycle deregulation, controlling cell signalling, inhibiting apoptosis, chromatin remodelling, silencing of tumour suppressor genes, modulation of host immunity and structural modification of the infected cells.(Graham, 2010, Bossler et al., 2019, Wang et al., 2020) The structural proteins L1 and L2 are important for the viral assembly.(Doorbar et al., 2012, Doorbar, 2007) The major capsid protein, L1 is mostly key for viral assembly while the minor capsid protein, L2 also plays key roles in establishment and persistence of infection.(Doorbar, 2007, Doorbar et al., 2012, Kimbauer et al., 1992)

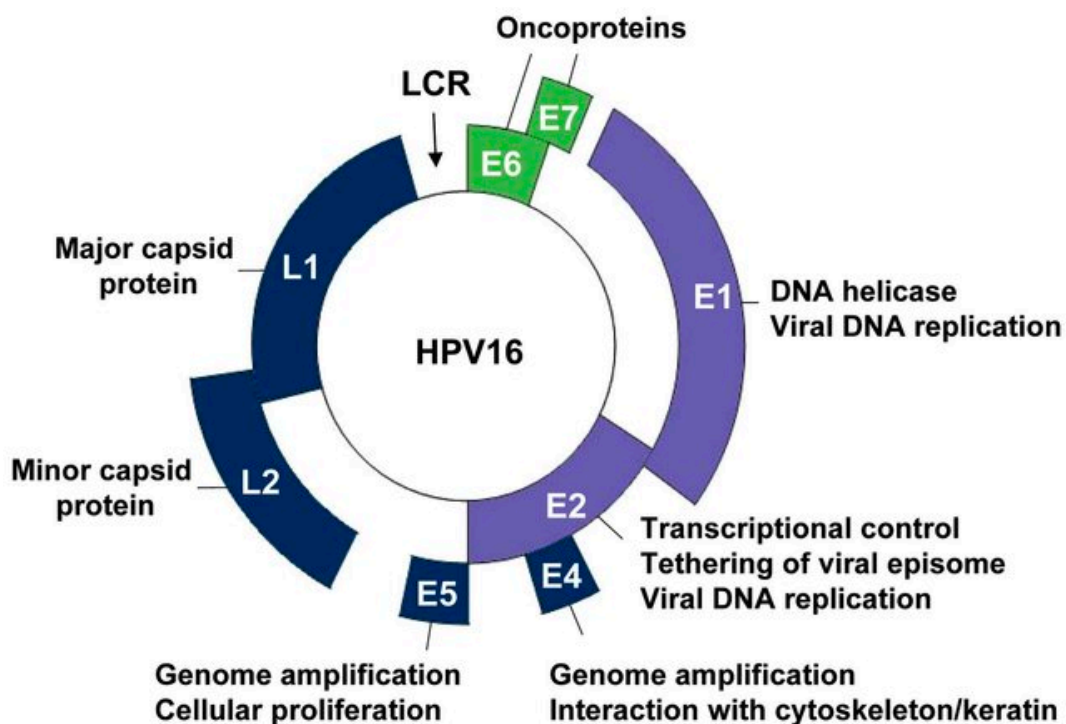


Figure 1.2. HPV genomic structure

Schematic representation of the circular HPV genome structure represented by HPV 16. The location of early (E1, E2, E4 and E5) and late (L1 and L2) genes, and the long control region (LCR) is shown. Functions of the eight well-characterized proteins encoded by the HPV genome are indicated. Replication proteins (E1 and E2) and viral oncogenes (E6 and E7) are shown in violet and green, respectively while capsid proteins (L1 and L2) are shown in dark blue. (C M D'Abramo, figure available via [Creative Commons Attribution-NonCommercial 3.0 Unported](https://creativecommons.org/licenses/by-nc/3.0/))

Differences reported in initial HPV binding to host cells between in vivo and in vitro studies may suggest that the mechanisms may not be entirely analogous for example; binding of laminin 5 is important for infection of cultured keratinocytes in vivo but less important in HPV attachment and infection in murine genital tract.(Selinka et al., 2007, Johnson et al., 2009) Notably, in vitro studies lack various in vivo components such as wound signalling pathways that have been reported to play a key role in establishing HPV infection.(Ozbun, 2019)

Keratinocytes are the main cells infected by HPV at the cervix.(Stanley, 2009) During the initial infection stages, in vitro studies suggest that the viral antigens L1 and L2 bind to keratinocytes surface receptors or the extracellular matrix (ECM) and can infect intact cultured epithelial tissues in various epithelial cell lines which contradicts in vivo studies.(Kirnbauer et al., 1992, Roberts et al., 2007) Mice studies showed that HPV binds exclusively to the cervical basement membrane which must first be exposed by a microtrauma on the epithelium.(Roberts et al., 2007) Several studies suggested Heparan sulfate proteoglycans (HSPG) to be the primary cell surface binding receptors for HPV infection.(Surviladze et al., 2012, Shafti-Keramat et al., 2003, Giroglou et al., 2001, Joyce et al., 1999) HPV infection was blocked by a drug (N,N'-biseteryl derivative of dispirotripiperazine, DSTP27) or antibodies that bound HSPG, in a process thought to have inhibited viral binding to secondary receptors on cultured human keratinocytes and blocked viral cell entry.(Selinka et al., 2007) Digestion of cell surface-bound heparan surface (HS) with heparinase I has been shown to suppress pseudo infection of HPV 16 and HPV 33 on cultured human keratinocytes.(Giroglou et al., 2001) Chinese hamster ovary cells deficient of HSPG were inefficiently infected by HPV as the virus could not bind stably to their surface.(Lugemwa and Esko, 1991) This indicates there may be another receptor(s) mediating some level of infection in the absence of HSPG which remain to be investigated.

Binding of HSPG both in cell culture and in vivo triggers a conformational change on the viral capsid, which exposes the N-terminus of the L2 protein for cleavage by furin or proprotein convertase 5/6.(Richards et al., 2006, Kines et al., 2009) This cleavage exposes a basal keratinocyte secondary receptor binding site on L1 protein and that has been shown to be a critical step for most viral infections.(Richards et al., 2006) The secondary receptor for HPV is not known. Some in vitro studies suggest a cell surface adhesion molecule, α 6-integrin but infection has been shown to take place in cells lacking this molecule.(Richards et al., 2006, Schiller et al., 2010, Kines et al., 2009) It therefore remains to be elucidated if there is a universal secondary receptor or if different HPV types use different receptors. HSPG-independent cellular binding has been reported in HPV 16 with furin pre-cleaved L2.(Day et al., 2008) This supports the main role of HSPG binding, suggested to be furin cleavage of L2 and conformational changes to expose an occluded L1 binding site for the secondary receptor(s).(Johnson et al., 2009) Figure 1.3 outlines the mechanisms involved in the attachment of HPV to host cells and subsequent infection.

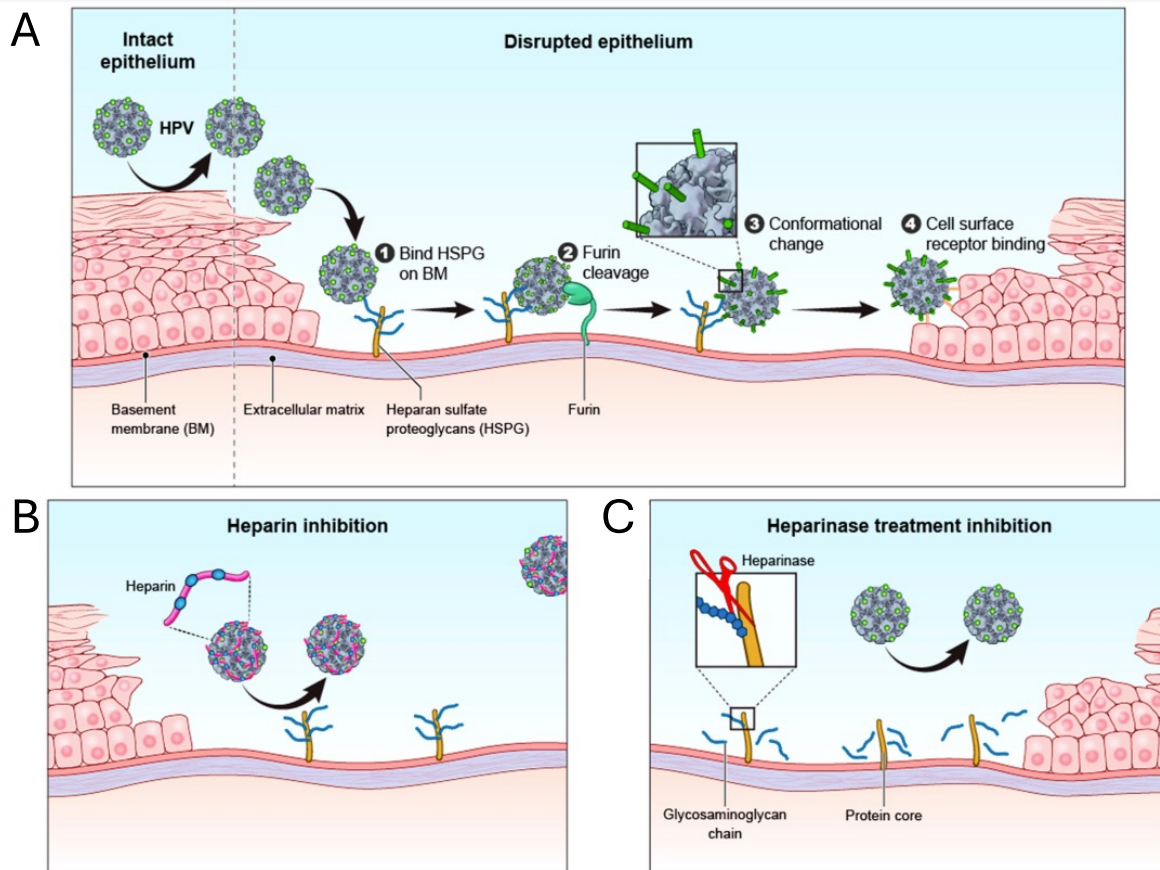


Figure 1.3. Mechanism of HPV attachment and infection

(A) HPV attaches to HSPG on the exposed basement membrane (1). The L2 protein is then cleaved by furin (2) and the virion undergoes a conformational change (3) before attaching to a cell surface receptor (4). (B) depicts heparin inhibition of VLP attachment to basement membrane HSPG and (C) illustrates heparinase cleavage of glycosaminoglycan chains prevents HPV attachment. Human papillomavirus (HPV); heparan sulfate proteoglycan (HSPG); basement membrane (BM) (Kines and Schiller, 2022)

After HPV attachment to keratinocytes, clathrin-mediated receptor endocytosis has been implicated in internalisation of papillomaviruses including HPV 16 and bovine papillomavirus (BPV).(Selinka et al., 2002, Day et al., 2003) Other endocytic pathways have been reported for different or even same HPV types.(Horvath et al., 2010) This may be as a result of different factors such as usage of different pathways by different genotypes, maturation stage and nature of capsid (whether VLP or pseudovirion) used, different experimental manipulations and study end-points.(Schiller et al., 2010) Therefore despite the extensive

literature on HPV internalization, there is no consensus on a universal internalisation pathway for studied genotypes.

Internalised viral particles employ a complex mechanism to escape endosomes after initial trafficking, become uncoated and gain entry to the host cell nucleus where they can exploit the host machinery for their reproduction.(Kämper et al., 2006) Cell cycle progression is required for the viral genome entry into host cell nucleus during the nuclear membrane breakdown in mitosis.(Pyeon et al., 2009) Then the viral genome initially replicates slowly and establishes itself in the nucleus by attachment to host cell chromatin and is maintained at constant copy numbers during cell division.(Pyeon et al., 2009) The viral genome replication is tightly linked to the differentiation of the cervical epithelium.(Graham, 2017) Basal cells divide both symmetrically, into the basal layer and asymmetrically to enable epidermal stratification.(Poulson and Lechler, 2012, Lechler and Fuchs, 2005) The cells moving up through the epithelium differentiate by acquiring various characteristics until they reach the epithelial surface from where they are shed off and this self-renewing process goes on.(Poulson and Lechler, 2012, Lechler and Fuchs, 2005) As the cells differentiate, viral DNA replication and transcription increase as regulated by host cell transcription factors which first interact with the viral LCR, followed by expression of the early viral proteins.(Ozbun, 2002) As cells mature and move towards the epithelial surface, viral capsid proteins are expressed and virions assembled to produce high copy numbers at the terminally differentiated cells at the uppermost epithelial layer which is then shed off.(Kasukawa et al., 1998, Doorbar, 2007)

In most cases, HPV infection is transient and non-cytolytic and does not commonly cause oncogenic transformation, but a few cases of persistent infection with the high-risk HPV types can lead to viral DNA integration into host genome, in a process involving a random breakage between E1 and E2 region and subsequent loss of E2.(Hopman et al., 2006, Pirami et al., 1997, Cullen et al., 1991) Protein E2 is critical for regulation of the expression and activity of E6 and E7 and therefore, its loss interferes with controlled expression of these

proteins and they are consequently actively expressed modifying the cell cycle to ensure the viral genome is favourably amplified throughout the differentiation process, while escaping host immunity.(Hopman et al., 2006) The oncogenes E6 and E7 target two host proteins required for cell cycle regulation (tumor suppressor protein (p53) and the retinoblastoma gene product (pRB)).(Narisawa-Saito and Kiyono, 2007) Protein E6 causes degradation of p53 through the ubiquitin-proteasome pathway, interfering with DNA repair, G1 arrest and apoptosis processes normally regulated by p53.(Narisawa-Saito and Kiyono, 2007) Protein E7 binds to pRB and blocks its interaction with Transcription Factor E2F6.(Chen et al., 2009) Interaction between pRB and E2F6, a transcriptional repressor is a critical regulatory step required to activate E2F6 expression in S phase providing a negative feedback mechanism to slow down progression of S phase or exit when other E2F transcription factors are activated.(Chen et al., 2009) Blocking this step therefore disrupts normal cell cycle transition to S-phase and activates E2F and other proteins that keep the cell cycle continuous resulting to uncontrolled growth, increased proliferation, genomic instability and eventual accumulation of irreparable damaged DNA and mutations that may develop to fully transformed cancerous cells.(Longworth and Laimins, 2004, Chen, 2010)

1.3 Immune responses to HPV infections

Although the focus for this research is immunity generated by HPV vaccines, highlighting differences between immunity to infection and vaccination is deemed relevant. Understanding immunity to natural infections provides a critical background necessary for consideration of vaccine development strategies, that for example in HPV should be able to circumnavigate the complex immune evasion mechanisms employed by the native virus.

1.3.1 Innate immunity

Continuous autorenewal of basal epithelial layer, mainly made of keratinocytes, leads to the formation of keratinized upper layers from partial activation of apoptosis by cell degradative mechanisms, and these keratinized layers act as a barrier to attacks by pathogens and other

threats.(Richmond and Harris, 2014) Integrins maintain the integrity of epidermis by mediating adhesion between cytoskeleton and ECM and regulate wound healing process.(Wang et al., 2010) HPV infection takes place through a wound or abrasion from sexual intercourse which enables α -integrin to conjugate with the viral capsid protein enabling introduction of the virus into the host cell.(Yoon et al., 2001)

Early anti-viral immunity is principally mediated by Type I interferons (IFN-I) including interferon alpha (IFN- α) and interferon beta (IFN- β) which induce antimicrobial states in infected cells to limit infection spread, moderate secretion of pro-inflammatory cytokines, balance innate responses to enhance natural killer cell (NK cell) response and promote antigen presentation to activate adaptive immunity.(Teijaro, 2016) However, HPV uses various intrinsic mechanisms preventing viral protein expression in the initial infection stages, as well as limiting viraemia and cytolysis in the infectious cycle.(Zhou et al., 2019b) The viral replication and assembly occur in cells pre-destined for anoikis, a cell death mechanism which occurs when the integrin-mediated interaction between a cell and the ECM is disrupted, preventing cell anchorage to the ECM, and apoptosis is triggered.(Frisch and Francis, 1994) This reduces inflammation and other danger signals required to activate the immune system greatly.(Stanley, 2010b)

Antigen presenting cells (APCs) including dendritic cells (DCs), Langerhans cells (LCs), macrophages and keratinocytes as well as NK cells play a sentinel role recognizing pathogen associated molecular patterns (PAMPs) via specialized receptors, mainly the Toll like receptor (TLR) family, to promote innate immunity and initiate adaptive immunity.(Scott et al., 2001, Manickam and Sivanandham, 2011) Keratinocytes constitute 95% of cervical epithelium and are the primary cells infected by HPV at the basal layer.(Handisurya et al., 2014, Sterling et al., 1993) They therefore play a key role in initiation of HPV infection and activation of adaptive immunity as non-professional APCs.(Black et al., 2007) Additionally, keratinocytes are triggered by infections to synthesize several signalling and regulatory molecules including IFN-I, intercellular adhesion molecule-I (ICAM-I), antimicrobial peptides,

increase secretion of pro-inflammatory cytokines, growth factors and chemokines, all necessary for activation and recruitment of immune cells.(Stadnyk, 1994, Wang et al., 1999, Woodworth and Simpson, 1993, Bashaw et al., 2017) They express various extracellular and intracellular TLRs, notably TLR9 critical for recognition of double stranded DNA viruses.(Lester and Li, 2014, Lebre et al., 2007, Miller and Modlin, 2007, Yang et al., 2005) Immortalized human keratinocyte (HaCaT) cells express high levels of TLR9 and upregulate key pro-inflammatory cytokines, TNF- α and Interleukin 1 (IL-1).(Manjgaladze et al., 2019) Several studies on cervical and genital HaCaT cells have demonstrated the ability of transforming growth factor-beta (TGF- β), tumor necrosis factor-alpha (TNF- α) and IFN- α to inhibit proliferation of the HPV infected cells and suppress expression of E6 and E7 proteins.(Woodworth et al., 1992, Woodworth et al., 1990)

Effective evasion of recognition by innate immunity is thought to be the hallmark of persistent high-risk HPV infections.(Amador-Molina et al., 2013) HPV 16 E6 and E7 interact directly with components of IFN-I signalling pathways, specifically interfering with IFN- α and IFN- β mediated signalling.(Park et al., 2000, Ronco et al., 1998) A direct correlation between expression of TLR9 and cervical cancer progression was attributed to altered signalling pathways, with suspected upregulation of unknown TLR9 ligands in the tumour microenvironment.(Hao et al., 2014)

The NK cells, as effector lymphocytes of the innate immune system are critical for clearance of virally infected and tumour cells.(Prager and Watzl, 2019, Paul and Lal, 2017) The NK cells strongly recognize altered protein expression including the downregulation or loss of Major Histocompatibility Complex class I (MHC I) on physiologically stressed cells (such as virally infected or cancerous cells). Virally infected or tumor cells release stress-associated chemicals that act as ligands for NK activating receptors, for example Human MHC I chain-related proteins A and B (MICA/B) are ligands for the NK activating receptor, activating natural killer group 2 member D (NKG2D).(Chitadze et al., 2013) NK cells are then activated through engagement of various activating receptors to produce lytic granules containing

perforin and granzyme which destroy the target cells.(Prager and Watzl, 2019, Paul and Lal, 2017) Activated NK cells may also upregulate cell death receptor ligands (Fas ligand (FasL) or Tumor Necrosis Factor-Related Apoptosis Inducing Ligand (TRAIL)) which bind to death receptors on target cells and induce death via death receptor-mediated apoptosis.(Prager and Watzl, 2019)

NK cells were reported to eliminate HPV infected cells resulting to regression of HPV-induced neoplasia in women.(Garzetti et al., 1995, Stentella et al., 1998) A study assessing immune system in patients with either recurrent HPV infection alone or recurrent HPV infection with genital intraepithelial neoplasia reported a strong positive correlation between reduced NK cells and HPV infection associated with intraepithelial neoplasia.(Stentella et al., 1998) High-risk HPV types are able to suppress the cytolytic activity of NK cells to evade early clearance, promoting infection persistence. One study assessed cytotoxic activity of NK cells from the peripheral blood of patients with different cervical cancer stages and reported the cytotoxic activity of NK cells from patients with localised early stage carcinoma to be similar to that of healthy women, while the cytotoxic activity was decreased in patients with advanced metastatic stage.(Vaquer et al., 1990) A study looking at NK cell activity in patients with HPV-induced precancerous and cancerous anogenital lesions reported abrogated NK cell lysis in keratinocytes bearing HPV 16.(Malejczyk et al., 1989) Altered phenotype and function of NK cells were reported in HIV positive women with genital warts, a possible reason as to why HIV positive individuals are less likely to clear genital warts.(Bere et al., 2014) Down-regulation of NK cells-activating receptors, NKp30 and NKp46 was reported in cervical cancer and high grade squamous intraepithelial lesion (HGSIL) patients and this was found to correlate with HPV 16 detection, low NK cells cytolytic activity and disease stage.(Garcia-Iglesias et al., 2009)

From the foregoing, while the function of NK cells in clearance of virally infected cells is well established, they seem to be able to clear persistent high-risk HPV infections in some

individuals. The viral and host factors that make them not as effective in other individuals are not well understood.

Macrophages are key tissue resident immune cells central for maintaining of tissue homeostasis, repair and maintenance, elimination of abnormal cells, phagocytosis and regulation of inflammation via cytokine production, but may also promote tumour development and spread in malignancy.(Gordon and Plüddemann, 2017, Kitamura et al., 2015) Macrophage migration inhibitory factor (MIF) is a pro-inflammatory cytokine that has been implicated in pathogenesis of inflammation and cancer development via p53 inhibition.(Balogh et al., 2018) Higher MIF secretion was observed in HPV positive than in HPV negative human head and neck squamous cell carcinoma cell lines, with similar results observed in murine squamous cell carcinoma cell lines expressing E6 and E7, whereby the suppressive ability of MIF on p53 was observed.(Kindt et al., 2019, Mitchell et al., 2002) Tumour associated macrophages in cervical cancer display different phenotypes at different cancer stages and can inhibit phagocytosis and tumour immunity.(Gordon et al., 2017, Ding et al., 2014) Similar to other viruses such as HIV, hepatitis B and C viruses, human cytomegalovirus, and poliovirus, HPV is thought to infect macrophages to evade immune recognition.(Cao et al., 2017, Tay et al., 1987a) Most literature present macrophages as immune contributors to cervical cancer development enhanced by HPV modulation, but have also been reported to have either a direct antiviral or non-specific phagocytotic effect to HPV cervical infections in women, thus may play a dual role.(Tay et al., 1987b)

Innate immunity to HPV infection is complex with controversies and lack of clarity on the actual mechanisms inhibiting or promoting HPV clearance. A better understanding of these mechanisms may guide development of better interventions for prevention and disease control.

1.3.2 Adaptive immunity

1.3.2.1 Antigen presentation

Expression of major histocompatibility complex (MHC) molecules and costimulatory molecules as well as cytokine milieu from keratinocytes and LCs are critical for activation of HPV specific T cells in the cervical microenvironment.(Cumberbatch and Kimber, 1995, Enk et al., 1993) A study on women with abnormal cervical cytology (low- and high-grade cervical intraepithelial neoplasia (CIN), or normal squamous epithelium, looked at the antigen presenting environment in terms of expression of MHC II (human leucocyte antigen (HLA)-DR and -DQ), costimulatory molecules (CD11a/18, CD50, CD54 (ICAM-1), CD58 and CD86) and the cytokines TNF- α and IL-10.(Mota et al., 1999) De novo expression of HLA-DR was shown to be associated with CIN progression and increased CD58 expression on keratinocytes.(Mota et al., 1999) LCs did not express any costimulatory molecules in both normal and abnormal biopsies.(Mota et al., 1999) 100% of normal biopsies (12/12) showed constitutive expression of TNF- α , a strong stimulator of LCs which was lacking in a substantial number of abnormal biopsies including 87% (20/23) of low-grade CIN and 67% (12/18) of high-grade CIN.(Mota et al., 1999) Upregulation of IL-10 was observed in abnormal biopsies including 52% (12/23) of low-grade CIN and 44% (8/18) of high-grade CIN but this was not observed in normal epithelium (0/12). The expression of costimulatory molecules and the immune suppressive IL-10 may have played a role in suppressing host immunity to promote disease progression.(Mota et al., 1999) This expression of HLA-DR in CIN was similarly reported with majority (83%) of HPV 16-induced cervical carcinomas expressing MHC II in part or whole tumour cells.(Glew et al., 1992)

HPV proteins E6 and E7 suppress TLR9 expression, minimise recognition by most APCs and prevent antigen presentation.(Zhou et al., 2019b) LCs are highly specialized APCs resident in the epithelium and have been shown to access HPV proteins at the epidermis.(Cumberbatch and Kimber, 1995) They play an important role in presentation of HPV antigens to naïve CD4⁺ T cells with contribution from IL-1 α and TNF- α from

keratinocytes and IL-1 β from LCs themselves.(Cumberbatch and Kimber, 1995) Granulocyte-macrophage colony-stimulating factor (GM-CSF), from keratinocytes, promotes LCs maturation to DCs and enhances antigen presentation.(Lappin et al., 1996, Wang et al., 1999) A comparison of lymphokine secretion by cultured human cervical keratinocytes, HPV-immortalized cervical and carcinoma cell lines reported a decrease in IL-1 α , TNF- α , IL-1 β and GM-CSF to be associated with persistent HPV infection.(Woodworth and Simpson, 1993) Altered levels of these cytokines suppress antigen presentation environment in cervical lesions.(Woodworth and Simpson, 1993) Other studies have reported decreased density of LCs in epidermal tissues infected with HPV, postulated to be due to normal egress of activated LCs migrating into draining lymph nodes to present antigens to naïve T cells.(Memar et al., 1995) Calcium-dependent adhesion between keratinocytes and LCs mediated by E-cadherin is required for retention of LCs in the basal epidermal layers.(Jakob and Udey, 1998, Tang et al., 1993)

An investigation undertaken on biopsy samples from patients with cervical lesions showed that expression of E6 protein in HPV 16-infected basal keratinocytes reduces cell surface E-cadherin, hence interfering with the E-cadherin mediated adhesion.(Matthews et al., 2003) This lowers LCs numbers at the basal epidermal layer and consequently limits antigen presentation.(Matthews et al., 2003) Other studies reported reduction of LCs and depletion of specific LCs subpopulations by HPV which further impairs local immune capacity in intraepithelial tissues.(Tay et al., 1987a, Matthews et al., 2003) Despite such interference with the antigen presenting environment by HPV, keratinocytes and LCs are still able to present some HPV E6 and E7 antigens to T cells activating them to mount appropriate antiviral immunity in immunocompetent individuals.(Coleman et al., 1994)

1.3.2.2 T cell responses

1.3.2.2.1 CD4+ T cell response

Assessment of immune events in genital warts patients infected with HPV 6 and HPV 11 showed active cell mediated immune response in those with regressing warts, with predominant CD4+ T cell response in the wart stroma and surface epithelium.(Coleman et al., 1994) Activated CD4+ T cells have been reported to promote HPV clearance by cytotoxic lymphocytes (CTL) preventing persistent infection in immunocompetent individuals.(Coleman et al., 1994)

During HPV 16 infection, T helper 1 (Th1) cytokines IL-2, IL-12, and IFN- γ have been shown to activate CTL to destroy cervical lesions or cancerous cells expressing HPV antigens.(Dillon et al., 2007, Nakagawa et al., 1997) One study reported HPV 18 E6 specific CD4+ T cell response in the blood of 50% of patients with high-grade cervical lesions regardless of the HPV type associated with the lesions.(Seresini et al., 2007) Since only about 15 to 18% of cervical lesions are attributable to HPV 18, the authors hypothesised that HPV 18 infects a higher percentage and that some of the E6 responsive HPV 18 negative patients may have cleared the infection and CD4+ T cell memory remained.(Seresini et al., 2010) HPV 18 E7 specific CD4+ T cell response was evaluated in patients with CIN or low-grade cervical cancer, before Loop Electrosurgical Excision Procedure (LEEP) (for CIN) and radical hysterectomy (for cervical cancer) treatment, and compared with age-matched healthy controls.(Seresini et al., 2010) Upon in vitro stimulation of peripheral blood mononuclear cells (PBMC) with E7 peptides, the study reported a robust Th response, Th1 interferon gamma (IFN- γ) and Th2 (IL-4 and either IL-5 or IL-10 or both) cytokine production from HPV 18 negative patients, while the HPV 18 positive patients produced little or none of these cytokines, instead preferentially secreting IL-5.(Seresini et al., 2010) The suppression of CD4+ T cell response was E7 specific since no difference between the HPV 18 negative and HPV 18 positive patients was observed for E6 specific responses.(Seresini et al., 2010) For the healthy controls, 20% showed E7 specific Th1 and Th2 response as observed in the HPV 18 negative patients, while 16% was observed for E6 specific response.(Seresini et al.,

2010, Seresini et al., 2007) Protein E7 and not E6 specific CD4+ T cell response may have played a protective role.

Women living with HIV are more likely to acquire and less likely to clear HPV infection, thus persistent HPV co-infection increases their risk of developing cervical cancer.(Clifford et al., 2016a, Strickler et al., 2005) Indeed, a recent systematic review reported that about 5.8% (95% confidence interval (CI) 4.6 - 7.3) of global new cervical cancer cases diagnosed in 2018 (33,000/570,00) were attributable to HIV infection.(Stelzle et al., 2021) Suppression of CD4+ T cell response by HIV is thought to create a conducive environment for HPV infection, persistence and cancer development.(Clifford et al., 2016b) Less than 200 CD4+ T cell count per mm³ or HIV RNA level of more than 100,000 copies per mL were reported to increase the risk of cervical incident HPV detection and prevalence of squamous intraepithelial lesions.(Strickler et al., 2005) A nested case control study within a Swiss HIV cohort reported a significant association between the risk of developing CIN2 and CIN3 with low CD4+ T cell counts, whether measured as nadir (odds ratio (OR) 1.15; 95% CI 1.08 - 1.22) per 100 cells/ μ L or at CIN2 and CIN3 diagnosis (OR 1.10; 95% CI 1.04 - 1.16).(Clifford et al., 2016a) A study looking at long-term (8 years) cumulative detection of HPV among HIV seropositive women reported an increase (58% at baseline to 92% at 8 years) in HIV positive women compared to (22% at baseline to 66% at 8 years) in HIV negative women.(Massad et al., 2014)

1.3.2.2.2 Cytotoxic T lymphocytes (CD8+ T cells) response

The CTL, like NK cells hold cytotoxic granules required for clearance of virally infected and cancerous cells, hence are thought to be essential immunotherapeutic targets for cancer treatment.(Watzl, 2014, Yang, 2015) Mice immunization with non-tumour fibroblast-like cells transfected with HPV 16 E6 and E7 genes conferred CTL-mediated anti-tumor protection against cells transplanted from HPV 16 E6 and E7 positive tumour cells.(Chen et al., 1992, Chen et al., 1991) HPV 16 specific CTL are reported in immunohistochemical examination of cervical cancer patients.(Bontkes et al., 1997) Mice knock-out studies demonstrated a

crucial role of Granzyme B in CTL (and NK cells)-mediated target cell apoptosis.(Bontkes et al., 1997) Women with regressing lesions have significantly higher number of Granzyme B+ CTL than those with persistent or progressing lesions.(Woo et al., 2008) The presence of HPV 16 specific CTL with an ability to lyse HPV 16 infected cells in tumours and lymph nodes of cervical cancer patients, and in HPV infections that have not progressed to lesions was reported.(Evans et al., 1996, Evans et al., 1997, Nakagawa et al., 1997, Nakagawa et al., 1999) Studies of persistent HPV 16 infections have shown that E6 but not E7 targeted CTL may be important in HPV 16 clearance.(Nakagawa et al., 2000) Significant loss of MHC I has been reported in cervical biopsies and cutaneous warts while mild losses were observed in condylomas and laryngeal papillomas.(Connor and Stern, 1990, Viac et al., 1993) Other studies have shown a positive correlation between such MHC I loss and HPV-related disease grade and invasiveness which is thought to be a viral suppressive effect on the MHC I to evade presentation.(Torres et al., 1993, Vambutas et al., 2000)

From the foregoing HPV specific CTLs have been reported in different stages of HPV disease, with ability to clear HPV infections resulting to regression of HPV-associated lesions in some patients. On the other hand, although the CTL response may be detectable during HPV infection and or HPV-associated disease, it may be insufficient to clear the infection or disease in some cases. Similar to other cell populations already discussed, the factors determining CTL efficiency in HPV clearance are not well understood and warrant further investigations.

1.3.2.3 Humoral responses

The multi-step infection process of HPV described earlier is very slow. After cell entry, the highly immunogenic L1 antigen is only briefly exposed to the host immune system thus it can trigger some immune response before translocation to the nucleus.(Zhou et al., 2019b, DiGiuseppe et al., 2016, Steinbach and Riemer, 2018) The subsequent intraepithelial lifecycle further delays expression of L1 and L2 antigens, until a later stage characterised by shedding of high viral copy numbers at the upper epithelial layers.(Kajitani et al., 2012) This

limits immune cells accessibility to these antigens at this very critical stage of infection and leads to early antiviral immunity being targeted to early HPV antigens, mainly E6 and E7 that are less immunogenic.(Chen et al., 1991) Assessment of the relationship between HPV DNA in genital mucosa and serum IgG response to HPV 6, 16, and 18 among women with incident HPV infections reported delayed seroconversion occurring at between 8 to 18 months after detection of corresponding HPV DNA.(Carter et al., 2000) Additionally, the seroconversion rates for HPV 6, 16 and 18 were generally low at 59.5%, 54.1% and 68.8% respectively.(Carter et al., 2000) Detection of transient HPV DNA was associated with failure to seroconvert, although even some of those with persistent HPV DNA did not seroconvert.(Carter et al., 2000) This may indicate that transient infections may have been cleared by early cellular immunity before induction of detectable antibody response. A similar delay in seroconversion was reported in another study that assessed the relationship between seroconversion and presence of HPV DNA in 3 anatomical sites (anal canal, genital and oral cavity) in men.(Giuliano et al., 2015) Seroconversion rates to single or multiple HPV types HPV 6, 11, 16 and 18 were low and variable at 6.3%, 18.9% and 0.0% for anal, genital and oral sites, respectively, with an inverse correlation between seroconversion rates and persistence.(Giuliano et al., 2015)

Several studies have reported HPV infection-induced specific IgG and IgA response in cervicovaginal secretions (CVS) to be of low concentration, transient and highly variable.(Pattyn et al., 2019a) One longitudinal study detected very infrequent CVS antibody response against HPV 16 to an extent it was not possible to do a detailed kinetics of the local humoral immunity.(Hagensee et al., 2000) Antibodies IgG, IgA and mucosal IgA associated with the secretory fragment to HPV 16 were detected in 12%, 6%, and 8%, respectively, of CVS samples collected at 4 monthly intervals from college-aged women.(Hagensee et al., 2000) Cervical IgG antibodies associated strongly with HPV 16 detection within the preceding 12 months (OR, 3.3; 95% CI 1.4 - 7.8), while mucosal IgA associated with the secretory fragment associated strongly with detection of SIL within the

last 4 to 8 months (OR, 6.4; 95% CI 1.9-21.8).(Hagensee et al., 2000) Like HPV seroconversion, this study reported several months delay between initial HPV infection and detection of cervical antibodies, with persistent cervical IgG and transient IgA preceding a decline in circulation.(Hagensee et al., 2000)

Most literature on HPV humoral immunity at the cervix is limited to HPV 16, and reports delayed infection-induced HPV specific antibodies to be predominantly targeted to L1 and L2 proteins, and to a less extent to non-structural disease-associated early proteins E2, E4, E5, E6 and E7.(Lopez et al., 2008, Bierl et al., 2005) Infection-induced HPV type specific anti-L1 neutralising antibodies in circulation correlate better to protection than antibodies in the CVS.(Stanley and Sterling, 2014, Stanley, 2010a) Several studies have reported HPV type specific IgA, IgG and IgM responses in individuals with HPV infection, intraepithelial lesions and cervical cancer.(Sasagawa et al., 1998, Sasagawa et al., 1996, Carter et al., 2000) Pooled analysis of data from various studies evaluating natural immunity against anogenital HPV infections in male and female subjects reported that naturally acquired anti-HPV antibodies provided modest protection against subsequent infections in women.(Beachler et al., 2016) This study involved 24 000 individuals from 18 countries and results showed significant protection in women subjects against subsequent HPV 16 (pooled Relative risk (RR), 0.65; 95% CI 0.50 - 0.80 and HPV 18 (pooled RR, 0.70; 95% CI 0.43 - 0.98) infection which was not observed in male subjects (HPV 16: 1.22; 0.6-01.77 and HPV 18: 1.50; 0.46-2.55).(Beachler et al., 2016)

Another recent analysis of pooled data from the unvaccinated control arms of two large phase 3 HPV vaccine trials; PATRICIA trial (NCT001226810) and Costa Rica Vaccine trial (NCT00128661) showed an association between high level of HPV 18 infection-induced serum antibodies in subjects seropositive at enrolment, with reduced risk of subsequent HPV 18 detection (P trend = 0.001; RR = 0.69; 95% CI 0.47-1.01; RR = 0.63; 95% CI 0.43-0.94 for 3rd and 4th quartiles, respectively), compared to those seronegative at enrolment.(Safaeian et al., 2018) The risk of 12 months persistent infection decreased with

increasing antibodies levels (P trend = 0.06; RR = 0.72; 95% CI 0.29-1.77; RR = 0.42; 95% CI 0.13-1.32 for 3rd and 4th quartiles, respectively).(Safaeian et al., 2018) Analysis for comparison of HPV 18-associated atypical squamous cells between seronegative and seropositive subjects showed a significantly decreased risk of having such atypical cells in individuals with increasing antibodies (P trend = 0.01; RR = 0.46; 95% CI 0.21-0.97 for 4th quartile). Similarly, increasing HPV 16 antibody level led to a significantly decreased risk of HPV 16 infection, persistent infection and HPV 16 associated atypical squamous cells.(Safaeian et al., 2018) From the foregoing, although infection-induced HPV specific antibody levels are generally low, they are able to provide some modest level of protection.

Poor concordance is generally reported between detection of HPV specific antibody responses in CVS and serum after infection.(Bontkes et al., 1999) Systemic but not cervical IgA correlated with HPV 16 clearance.(Bontkes et al., 1999) A relatively strong positive correlation has been reported between HPV specific cervical and systemic IgG antibodies. Systemic IgG is believed to transudate to be able to provide protection at the mucosal surface.(Bontkes et al., 1999) No clear relationship has been demonstrated between infection-induced HPV specific antibody response in the genital tract and systemic circulation.(Passmore et al., 2007, Mbulawa et al., 2008, Bontkes et al., 1999) Mucosal anti-HPV 16 antibodies were reported to neutralise HPV 16 virus suggesting such antibodies may be protective against infections.(Lopez et al., 2008, Bierl et al., 2005) However, HPV specific IgG and IgA response in cervical infections neither correlate with viral clearance nor regression of HPV- associated lesions.(Veress et al., 1994, Bontkes et al., 1999) The role of mucosal antibody response to HPV infections therefore remains to be understood with one challenge being methods used in CVS sampling which are not standardized, challenging comparability of results between studies.

As will be discussed later, HPV vaccination generates between 10 and 100-fold higher antibody levels than natural infection, with a moderate to strong correlation between vaccine-induced antibodies in CVS and serum, unlike in infection.(Olsson et al., 2009,

Muñoz et al., 2009, Stanley, 2010b, Pattyn et al., 2019a) Further, vaccine-induced antibodies have higher viral neutralisation capacity and their avidity is 3 times higher than infection-induced antibodies.(Scherpenisse et al., 2013b, Scherer et al., 2016)

In summary, despite the complex immune evasive strategies employed by HPV, both innate and adaptive immunity play an important role in controlling HPV infection and disease as demonstrated from the discussed studies. Future studies aimed at providing better understanding of the natural immunity against high-risk HPV may be useful in guiding development of therapeutic vaccines, an area that is currently faced with numerous challenges.

Next, I will introduce and discuss various aspects of HPV vaccination.

1.4 HPV vaccines

There are currently six nationally licenced HPV vaccines, 4 of which are WHO pre-qualified and two under review for WHO pre-qualification. A 7th more recent HPV vaccine has shown non-inferior immunogenicity compared to the licensed ones, with high potential to advance to WHO pre-qualification.(Zhu et al., 2023) This development of more HPV vaccines is important in increasing vaccine availability which has been a major challenge globally.

HPV vaccines contain non-infectious VLPs self-assembled from 72 L1 pentameric capsomeres of the HPV types they protect against (Figure 1.4).(WHO, 2017b, WHO, 2017a, Inglis et al., 2006, Zhu et al., 2023)

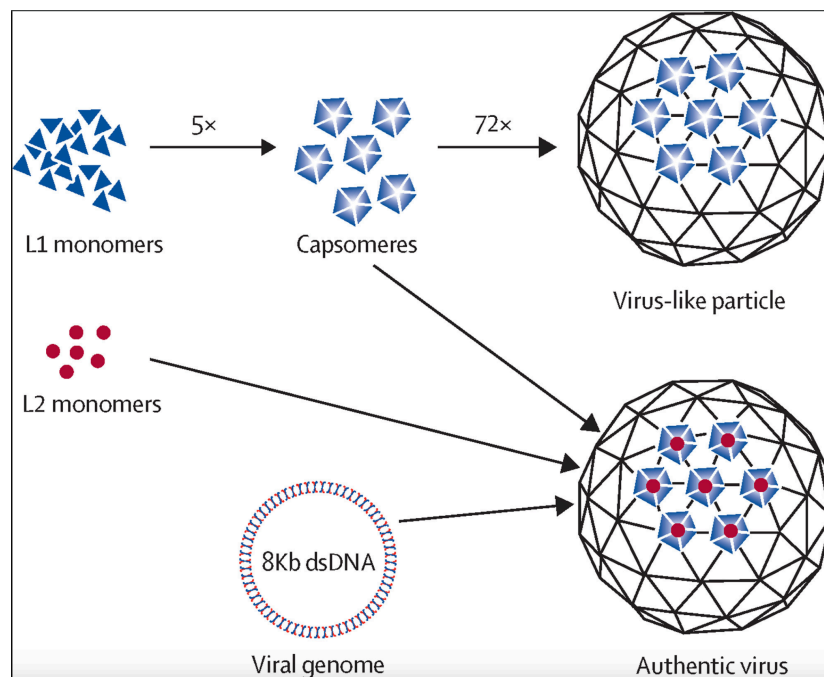


Figure 1.4. Assembly of L1 and L2 monomers in virus-like particle and native virus

x - times, ds - double stranded, L1 - the human papillomavirus major capsid protein, L2 - the human papillomavirus minor capsid protein.(Schiller and Müller, 2015)

Information on the licensure year, valency and HPV types, adjuvant, expression systems and manufactures of currently licensed HPV vaccines is shown (Table 1.1).

Table 1.1. HPV vaccines' information

Licensure year (WHO pre-qualification status)	Valency VLP types	Adjuvant	Expression system	Manufacturer
Cervarix (2009) (WHO pre-qualified)	Bivalent (HPV 16 and 18)	ASO4 (aluminium hydroxide, 3-deacetylated- 4-monophosphoryl lipid A)	<i>Baculovirus expression vector in Trichoplusia ni</i> (Hi 5), insect cells	GlaxoSmithKline Biologicals SA
Gardasil (2006) (WHO pre-qualified)	Quadrivalent (HPV 6, 11, 16 and 18)	Aluminium hydroxyphosphate sulfate (Alum)	<i>Saccharomyces Cerevisiae</i> , baker's yeast	Merck Vaccines
Gardasil 9 (2014) (WHO pre-qualified)	Nonavalent (HPV 6, 11, 16, 18, 31, 33, 45, 52 and 58)	Aluminium hydroxyphosphate sulfate (Alum)	<i>Saccharomyces Cerevisiae</i> , baker's yeast	Merck Vaccines
Cecolin (2019) (WHO pre-qualified)	Bivalent (HPV 16 and 18)	Aluminium hydroxide	<i>Escherichia coli</i> , Bacterial cells	Xiamen Innovax Biotech Co. Ltd
Walrinvax (2022) (submitted to WHO)	Bivalent (HPV 16 and 18)	Aluminium phosphate	<i>Pichia pastoris</i>	Walvax Biotechnology Co.Ltd.
Cervavac (2023) (submitted to WHO)	Quadrivalent (HPV 6, 11, 16 and 18)	Aluminium Hydroxide	<i>Hansenula</i>	Serum Institute of India Pvt. Ltd. (SII)

Current HPV vaccination recommendation by WHO includes one or two doses for girls aged 9 to 14 years as the primary target and secondary targets based on vaccine availability and feasibility including one or two doses for girls and women aged 15 to 20 years and two doses with a 6-month interval for women older than 21 years.(WHO, 2022) Vaccination of boys is also included as a secondary target.

The scope of this work is immunogenicity of Gardasil 9 vaccine. Most literature reviewed here will focus on the first three HPV vaccines (Cervarix, Gardasil and Gardasil 9) for which substantial immunogenicity and efficacy data is available. The progress made with development of therapeutic vaccines and the challenges thereof will be briefly discussed.

1.4.1 Immune activation by HPV vaccines

Immune activation by genital HPV infection is slow due to poor antigen access and presentation to lymphatics and draining lymph nodes for B cell and T cell activation.(Scott et al., 2001) In contrast, HPV vaccines are delivered intramuscularly enabling immediate antigen access to vasculature and lymphatics.(Schiller and Lowy, 2012, Stanley, 2010d) This induces inflammation with VLP antigens readily accessible to stromal DCs which get strongly activated and migrate transferring the antigens to draining lymph nodes to prime B- and T-cells, thereby initiating a strong overall immune activation, further thought to be enhanced by the VLP structure.(Stanley, 2010d) The aluminium salt adjuvants contribute to strong activation of innate immunity and cause slow antigen release for sustained immune activation.(Didierlaurent et al., 2009) ASO4 is considered more potent and responsible for induction of higher immunogenicity observed from Cervarix compared to other HPV vaccines as will be discussed later.(Roy et al., 2023, Pinto et al., 2018) Immune activation by HPV vaccines is therefore reported to be rapid, potent and sustained as indicated by the profile of antibody titres.(Villa et al., 2006a, Naud et al., 2014)

1.4.2 Vaccine protection and immunogenicity

Efficacy of HPV vaccines in humans was first demonstrated against HPV 16 in a randomized controlled trial of HPV 16 vaccine involving 2392 young women.(Koutsky et al., 2002) The vaccine or a placebo was administered in a three-dose regimen (0, 2 and 6 months) and thereafter participants negative for HPV 16 infection at baseline followed up for a median time of 17.4 months. During follow up, they were tested for persistent HPV 16 infection and CIN at one month after the third dose and every 6 months thereafter. The incidence of persistent HPV 16 infection was found to be 3.8 and 0.0 per 100 women-years at risk in the placebo and vaccinated groups, respectively, translating to 100% efficacy (95% CI 90 - 100).(Koutsky et al., 2002) Later studies on different licensed HPV vaccines confirmed this high efficacy against new infections and disease caused by HPV vaccine types as well as some cross-protection against related non-vaccine types.(De Vincenzo et al., 2014, Group,

2007, Joura et al., 2015, Paavonen et al., 2007, Arbyn and Xu, 2018, Group et al., 2010, Giuliano et al., 2019a, Harder et al., 2018, Muñoz et al., 2009, Pinto et al., 2018, Villa et al., 2006b, Akhatova et al., 2022, Villa et al., 2020) The effectiveness of HPV vaccines is broadly documented to be highest when given at younger ages. A recent systematic review including 21 studies found that 17 of them had reported highest vaccine effectiveness in the youngest age group, with estimated effectiveness ranging from 74% to 93% for younger adolescents aged 9 to 14 years and from 12% to 90% for adolescents aged 15 to 18 years.(Ellingson et al., 2023)

Based on global HPV and cervical cancer epidemiology discussed in section 1.1, all HPV vaccines provide at least 70% protection against cervical cancer, plus 90% protection against genital warts in the vaccines containing HPV 6 and HPV 11 and additional 20% cervical cancer protection from the nine-valent vaccine.(Schiller and Müller, 2015) The efficacy of Cervarix, Gardasil and Gardasil 9 vaccines is reported to be about 99% (ranging between 82% to 100%) against the HPV types they contain when given to HPV-naïve women aged below 26 years.(Kamolratanakul and Pitisuttithum, 2021) Gardasil and Gardasil 9 have similar efficacy in protecting against new infections and disease associated with the 4 HPV types that they both contain. Gardasil 9 efficacy was evaluated against infection with the 5 additional HPV types (HPV 31, 33, 45, 52 and 58) that are not included in Gardasil) and development of their related intraepithelial neoplasia.(Joura et al., 2015) The efficacy was 96.7% (95% CI 80.9 - 99.8) against high-grade cervical, vulvar or vaginal disease associated with the 5 HPV types tested.(Joura et al., 2015) Gardasil 9 was also evaluated for efficacy against infection with all the 9 HPV types it contains, their related diseases and definitive therapy.(Giuliano et al., 2019b) Vaccination reduced incidence of high-grade cervical disease and cervical surgery related to the 9 HPV types by 98.2% (95% CI 93.6 - 99.7) and 97.8% (95% CI 93.4 - 99.4), respectively, when given to HPV-naïve women aged between 16 to 26 years.(Giuliano et al., 2019b)

While there were initially no randomised trials planned to evaluate a single dose schedule for HPV vaccination, striking data from females who ultimately only received a single dose suggested high level of stably sustained antibody protection.(Kreimer et al., 2015) The Costa Rica HPV Vaccine Trial (NCT00128661) reported Cervarix vaccine efficacy against HPV 16 and 18 infection in 18 to 25-year-old women to be 80.2% (95% CI 70.7 - 87.0) for three-doses, 83.8% (95% CI 19.5 - 99.2) for two-doses and 82.1% (95% CI 40.2 - 97.0) for single-dose at 10 years post-vaccination.(Kreimer et al., 2020) Recent data from an immunogenicity trial of Gardasil vaccine in India reported a similar ability of a single dose to generate high antibody titres that were stably maintained without waning between 1 and 11 years follow up.(Joshi et al., 2023) The study evaluated vaccine immunogenicity in girls aged between 10 and 18 years. The Geometric mean titre (GMT) of HPV 16 at 1 year was 9.72 International Units per mL (IU/mL), 95% (CI 8.30 - 11.37) and at 12 years was 9.90 IU/mL (95% CI 8.76 - 11.19), with similar antibody profiles for HPV 6, 11 and 18 and overall 96% seroconversion.(Joshi et al., 2023)

Several randomized trials are ongoing to confirm the single dose vaccine protection. The KEN SHE (NCT03675256) trial of Cervarix and Gardasil 9 in 3 Kenyan study sites was the first single-dose randomized study to report high efficacy against HPV 16 and 18 infection from a single dose of either vaccine given to 15 to 20-year-old-women, over 18 months of follow.(Barnabas Ruanne et al., 2022) Compared to a control group that received meningococcal vaccine, efficacy against incident persistent infection with each HPV vaccine types was reported to be 97.5% (95% CI 81.6 - 99.7%) for Cervarix and 97.5% (95% CI 81.7 - 99.7% for Gardasil 9.(Barnabas Ruanne et al., 2022) Another one dose randomized immunobridging trial of Gardasil 9 comparing antibody responses in Tanzanian girls (9 to 14-year-olds) with those observed from the earlier discussed observational single dose from the Costa Rica and Indian trials, recently confirmed non-inferiority of HPV 16 and 18 IgG response from a single dose compared to 2 and 3 doses of Gardasil 9.(Baisley et al., 2022) An immunobridging analysis comparing the proportions of HPV 16 and HPV 18

seroconverting and antibody geometric mean concentrations (GMCs) between the single dose studies in Kenya (KEN SHE) and Tanzania (DoRIS) two years after vaccination was recently published.(Baisley et al., 2024) Findings from this analysis showed that in DoRIS, HPV 16 and HPV 18 antibody GMCs were similar or higher than those in KEN SHE. Cervarix GMC ratios were 0.90 (95% CI 0.72 - 1.14) for HPV 16 and 1.02 (0.78 - 1.33) for HPV 18, while Gardasil 9 GMC ratios were 1.44 (95% CI 1.14 - 1.82) and 1.47 (1.13 - 1.90), respectively. HPV 16 and HPV 18 antibody GMCs and seropositivity were non-inferior for both vaccines. Such data further support the recent recommendation of single dose vaccination, though there is need for data from long-term follow ups and more studies to monitor durability of protection from the single dose schedule.

1.4.3 Humoral responses to HPV vaccines

Early studies showed immunization with cottontail rabbit papillomavirus (CRPV) VLPs protected domestic rabbits against papillomas caused by CRPV, and that passive transfer of IgG or serum from immunized rabbits protected against CRPV challenge, demonstrating antibody mediated protection by VLP-based papillomavirus vaccines.(Breitburd et al., 1995) Further studies in animals and humans have widely documented induction of HPV type specific neutralising antibodies following vaccination and it is presumed that HPV vaccines offer protection via these neutralising antibodies.(Herrin et al., 2014)

HPV vaccine-induced antibody response at the cervix and in serum is broadly documented.(Pattyn et al., 2019a) The vaccines generate predominantly IgG antibodies as the main likely source of protection that is detectable in both CVS and serum.(Scherpenisse et al., 2013a, Gonçalves et al., 2016) Initial experimental studies of HPV 16 L1 vaccine in healthy women reported high level of vaccine-induced anti-HPV 16 IgG antibodies in their CVS during the menstrual proliferative phase, decreased about 9-fold at ovulation and rose about 3-fold at luteal phase, although it is not clear what the implications of such differences are.(Nardelli-Haeffliger et al., 2003) A dose escalation study detected anti-HPV 11 and 16 IgG antibodies induced by HPV 16 L1 and HPV 11 L1 vaccines in a smaller proportion of

women receiving 3 doses.(Fife et al., 2004) The low proportion of participants with detectable antibodies was thought to have resulted from a dilution factor from the lavage procedure used in the study.(Pattyn et al., 2019a, Fife et al., 2004) Unlike in mice, mucosal vaccination via nasal, aerosol or sublingual routes in humans was poorly immunogenic in inducing anti-HPV antibodies in CVS, hence, intramuscular vaccination was studied subsequently.(Nardelli-Haefliger et al., 2005, Huo et al., 2012, Cho et al., 2010)

Majority of data available on vaccine-induced antibody responses in CVS came from Cervarix studies.(Scherpenisse et al., 2013a, Kemp et al., 2008, Schwarz et al., 2010) Cervarix vaccination of females aged 14 - 25 years was reported to induce HPV 16 and 18 specific antibodies detectable in CVS, suggesting vaccine protection at the cervix.(Scherpenisse et al., 2013a, Kemp et al., 2008, Schwarz et al., 2010)

Pooled analysis of data from 4 clinical trials involving girls and women showed CVS positivity of anti-HPV 16 and 18 antibodies to be 95% and 92%, respectively at 7 months post-vaccination, and ranged between 71 - 100% and 55 - 100%, respectively, between 12 to 36 months post-vaccination.(Schwarz et al., 2010) Ten years follow up reported anti-HPV 16 and 18 antibodies to be detectable in 54 - 70% and 35 - 45% of CVS samples respectively, with anti-HPV 16 and 18 antibody titres in serum and CVS showing a mild to strong correlation (correlation coefficients; 0.64 and 0.38), respectively.(Schwarz et al., 2010) Seropositivity for anti-HPV 16 remained high (above 96.3%) in all age groups, while anti-HPV 18 seropositivity ranged from 99.2% in 15-25-year-olds to 93.7% and 83.8%, in 26-45- and 45-55-year olds, respectively.(Schwarz et al., 2010) From the findings of that study, persistence of vaccine-induced anti-HPV 16 and 18 antibodies above infection-induced levels was predicted to last more than 30 years in all age groups after primary vaccination, an indication of long-term protection.(Schwarz et al., 2010) However, this remains to be confirmed practically from long-term post-vaccination follow up studies.

Many studies report low levels of detectable vaccine-induced antibodies in CVS that show moderate to strong correlation with the corresponding vaccine-induced antibodies in

serum.(Pattyn et al., 2019b, Scherpenisse et al., 2013a, Petäjä et al., 2011) This is similar to the correlation reported between diphtheria and tetanus toxoid specific antibodies in CVS and serum where the vaccine does not induce antibody response at the mucosa.(Scherpenisse et al., 2013a) The antibodies are thus believed to reach the cervix through transudation and exudation to provide protection at the mucosal site of infection.(Bouvet et al., 1994)

Data from randomised trials in different populations demonstrated almost 100% seroconversion to vaccine HPV types within the first month of vaccination.(Sow et al., 2013, Mugo et al., 2015, Pinto et al., 2018) Cross reactivity has also been reported against certain non-vaccine HPV types.(Saccucci et al., 2018, Toft et al., 2014) A population-level assessment of the effect of HPV vaccination on infection with non-vaccine HPV types showed cross-protection against HPV 31 and interestingly, slight increases in non-vaccine high-risk HPV 39 and HPV 52 without sufficient evidence to infer replacement.(Mesher et al., 2016). Vaccination generates antibody titres that are 10 to 100-fold higher than in natural infection.(Muñoz et al., 2009, Olsson et al., 2009, Villa et al., 2005)

The antibody profiles induced by Cervarix, Gardasil and Gardasil 9 vaccines show similar patterns peaking at one month after completion of vaccination schedule, followed by an initial rapid decline and plateau at around two years onwards with titres well above pre-vaccination levels.(Pinto et al., 2018, Olsson et al., 2020) Although Cervarix induces higher HPV 16 and 18 antibody titres than Gardasil and Gardasil 9 mainly attributed to a more potent adjuvant used in Cervarix, the high titres from all vaccines are similarly maintained stably without waning.(Einstein et al., 2009, Hernández-Ávila et al., 2016, Leung et al., 2015, Puthanakit et al., 2016) Available data on the longest follow up studies over 10 years for the three vaccines show similar antibody persistence.(Kjaer et al., 2020b, Ferris et al., 2017, Olsson et al., 2020, Kreimer et al., 2020)

The long-term observational follow ups for single dose vaccination showed antibody titres to be significantly lower than in 2 or 3 doses but remained higher than those observed in

unvaccinated subjects. After 10 years follow up, the immunogenicity study in India reported anti-HPV 16 titres from a Gardasil single dose to be 2.05 times (95% CI 1.34 - 3.16) higher than unvaccinated subjects, with similar levels for anti-HPV 18 titers.(Joshi et al., 2023) The longest single dose follow up to date is the Costa Rica 11-years follow up that reported a single dose of Cervarix to have generated antibody titres that were 9 times above those generated by natural infection after the 11 years.(Kreimer et al., 2020) Although this study was not single-dose randomised, it demonstrates that regardless of the number of doses administered, the vaccine induced antibody titres that were sustained for years at higher than infection-induced levels. However, given the higher immunogenicity of Cervarix than the other HPV vaccines and that the study in India showed about only 2 times vaccine induced titers above infection-induced levels after 10 years, the implications of the long-term larger differences in immunogenicity between the vaccines need to be evaluated.

While current prophylactic HPV vaccines are highly immunogenic and effective in preventing new HPV infections, they are only useful when administered to HPV-naïve individuals, and do not have an effect on existent HPV infections or HPV-associated disease. More research on development of therapeutic vaccines is therefore needed, in addition to the current significant efforts in progress. Persistent HPV infection and disease is more common in immunosuppressed individuals; hence, therapeutic vaccines need to be targeted to enhance antiviral immunity. Promising results have been obtained from HPV therapeutic vaccines developed to date and those still in development but are faced with several limitations including: The earliest therapeutic HPV protein-based vaccines targeting E6 and E7 proteins induced desired immune responses correlating with clearance of HPV infection and regression of HPV-induced lesions but it was unclear if this was due to the vaccine effect or by natural immunity.(Khallouf et al., 2014) A placebo controlled PHASE II/III trial showed no effect of HPV 6 L2 and E7 fusion protein on HPV 6-induced warts.(Vandepapeliere et al., 2005) DC-based therapeutic vaccines can induce tumour regression, but are personalised requiring preparation of autologous DCs from individual patients.(Mastelic-Gavillet et al.,

2019) The process is intensive and costly thereby limiting large scale production.(Mastelic-Gavillet et al., 2019) Additionally, DCs based immunity may not be long-lasting since they do not proliferate.(Chen and Wang, 2010) The use of tumour cell-based vaccines in humans is faced with safety concerns and hence not considered for treatment of HPV-precancerous lesions.(Chang et al., 2000, Khallouf et al., 2014) More therapeutic vaccines are under trials, with none licenced to date. Consequently, surgery, chemotherapy, and radiotherapy remain the only standard treatment for cervical cancer treatment, with increased risk of relapse if treatment is performed at advanced stages. Improved understanding of host immunity to HPV infection may help to fast-track development of effective therapeutic vaccines.

1.5 Mechanisms underlying serological protection

Early immunological studies in the 1960s and 1970s demonstrated a primary role of B and T lymphocytes in the basic production of antibodies and cell mediated immune responses respectively.(Cooper and Alder, 2006) Later, a rich body of literature continued to develop understanding on this subject detailing key functional characteristics and the critical role of these cellular responses in generation of long-term antibody protection from various antigens.(Herrin et al., 2014) Early infection triggers proinflammatory signals that recruit various innate immunity components including APCs that constantly survey the body for invading pathogens, as well as adaptive immunity for extrafollicular B cell activation and differentiation to short-lived plasma cells for early antigen clearance. Subsequently, APCs process and present antigens to naïve T cells in secondary lymphoid organs triggering further adaptive immunity via CD4 and CD8 activation depending on the antigen.(Hwang et al., 2020) Upon activation, CD4 T cells can differentiate to a subset called T follicular helper (Tfh) cells that interact directly with cognate B cells and provide them with the help required for production of potent antigen specific long-term antibody protection.

Before discussing the critical interaction between B cells and Tfh cells, each of them is discussed separately to provide a background necessary for ultimate understanding of not only the very important serological protection they generate but also the developmental stages including activation of the cells, their localisation and key characteristic markers used in their phenotypic characterisation.

1.5.1 An overview of B cell biology

B lymphocytes develop from pluripotent hematopoietic stem cells in the liver during fetal development and in the bone marrow after birth.(Cooper and Alder, 2006, Osmond, 1986) The order of early B cell developmental stages in primary lymphoid organs include; stem cell, early pro-B cell, late pro-B cell, pre-B cell, large pre-B cell, small pre-B cell and immature B cell (with several subsets based on IgM and IgD expression) and transitional B cell.(Cooper and Alder, 2006, Osmond, 1986)

From the primary lymphoid organs, transitional B cells move to the secondary lymphoid organs including the spleen and lymph nodes where their maturation continues through a highly regulated and ordered selection process.(Jerne, 1955) Upon antigen encounter, mature naïve B cells finally differentiate into plasma cells (terminally differentiated B cells) that produce antibodies released to peripheral circulation for antigen clearance or to memory B cells for future rapid response against encountered antigens.(Borghesi and Milcarek, 2006, Williams and Nossal, 1966)

The current understanding of B cell biology is mainly based on mouse studies. While they may not be a true representation of human B cell function, they nonetheless provide important insights. Most human B cell studies have been on PBMC which may not adequately represent the cell populations present in primary and secondary lymphoid tissues where long-term serological immunity is generated. Therefore, peripheral blood is only used to give an indication about immunological activities occurring in different parts of

the human body. Functional and phenotypic characterization of B cells can be performed in peripheral whole blood or in isolated PBMC using various techniques including multicolour flow cytometry, Enzyme-Linked Immunosorbent Assay (ELISpot) and FluoroSpot.(Martínez Gómez et al., 2016) Flow cytometry characterization is based on differential expression of antigenic surface and intracellular markers at the different stages of B cell development. Next follows a description of the antigenic markers used in B cell characterisation, highlighting populations in which they are expressed as well as their functions in cell development and B cell-mediated immunity.

Firstly, CD19 and CD20 are pan B cell markers used to identify almost all B cell populations.(LeBien and Tedder, 2008a) To narrow down to a particular B cell sub-population of interest, these markers are used in combination with other B cell antigenic markers to characterise B cell immunity induced by either infection or vaccination or to study other aspects of basic B cell biology. CD20 is expressed in all B cell developmental stages from pro-B cells to memory B cells except the first (early pro-B cells) and the last (plasmablast/plasma cell) stages. This molecule has no known receptor and is thought to play a role in optimal B cell responses specific to T cell-dependent antigens as it also acts as a calcium channel in the cell membrane.(Pavlasova and Mraz, 2020) CD19 is a transmembrane glycoprotein and member of immunoglobulin super-family. It is expressed on follicular dendritic cells (FDCs) and B cells. In B cells, this marker is expressed in all B cell developmental stages from the earliest pro-B cells to maturity. CD19 plays a role in B lymphocytes proliferation and differentiation in response to exposure to different antigens and is a co-receptor that synergizes with the B cell receptor (BCR), CD21 and CD81 to decrease the threshold for antigen receptor-dependent stimulation.(Tedder and Schlossman,

1988) Due to its upregulated expression on early stages of B cell populations, CD19 is mainly used to identify these populations while CD20 is preferred for mature and memory B cell stages.(LeBien and Tedder, 2008b) Both CD20 and CD19 can be used together if targeting all B cell populations.(Tedder and Schlossman, 1988) The choice of additional B lymphocyte markers used to fully characterise B cell phenotypes depend on B cell populations of interest. Earliest transitional B cells translocating from bone marrow to peripheral circulation can be identified based on their differential expression of several markers as;

CD19+CD20+CD10+CD38++CD24++CD23++/lowCD21++/lowIgM++/IgD++/low while naïve mature B cells and their immediate precursors (late transitional B cells) are identified as CD19+CD20+CD10-CD38+CD24++, CD23++CD21++IgM++IgD++ for main surface markers.(LeBien and Tedder, 2008b) Additional discriminatory markers may be used together with these markers to further define smaller B cell subpopulations. CD10 is a cell surface enzyme normally expressed on the surface of early B cells as well as on several other types of normal cells.(Mishra et al., 2016) It is thought to play a role in B lymphoid cell development and is mainly used to identify transitional B cell populations. The CD23 or fragment crystallizable (Fc) receptor II can be expressed as a membrane bound or as a soluble molecule and has been proposed to have multiple functions including growth and differentiation of B cells and a role in the effector phase of IgE mediated immunity.(Veneri et al., 2009) CD38 is expressed on almost all B cell stages with highest expression in transitional and plasma cell stages. This molecule has been implicated in a signalling role that contributes to B cell activation and proliferation and is an inducer of calcium mobilization from cytoplasmic stores.(Camponeschi et al., 2022) Contradictory findings about the role of CD38 in different cell populations in humans show that it is an apoptotic inducer in early B cell stages while it promotes survival in germinal centre derived B cells.(Romero-Ramírez et

al., 2015) This molecule is useful in phenotyping of plasma cells as they express it highly and lack expression of pan B cell markers. CD24 is a cell surface protein anchored on the cell membrane by glycosylphosphatidylinositol where it localizes on lipid rafts.(Ayre et al., 2017) It is expressed in almost all stages in B cell development but highest in pro- and pre-B cell stages where it is thought to play a role in B cell receptor-mediated selection by mediating apoptosis. CD24 is used as a lineage marker for identification of hematopoietic stem cells.

Engagement of the B cell receptor by a cognate antigen and co-stimulation through cell-surface CD19 and CD21 on mature naïve B cells stimulates B cell activation.(Mongini et al., 2003) CD21 is strongly expressed in mature B cells and FDCs and weakly in immature thymocytes and T cells.(Barrington et al., 2009) In B cells, its expression decreases after activation. It functions as a receptor for C3 complement components hence can engage the complement system for pathogen clearance via membrane attack complexes. CD21 is a co-receptor of the BCR that forms an important component of a large signal transduction complex comprising CD19, CD23 and CD81 necessary for B cell activation.(Mongini et al., 2003) This molecule is therefore used in identification of activated B cells.

In the secondary lymphoid tissues mainly the spleen and lymph nodes, activated B cells receive T cell help and form germinal centres (GCs) within which they proliferate and undergo immunoglobulin (ig) isotype class switching or class switch recombination (CSR) from IgM and IgD to IgG, IgA and IgE, (the BCR and isotype CSR is discussed in chapter 7). IgM and IgD are the earliest ig classes to be expressed on the mature B cell surface. They are therefore used in combination with other immunoglobulin markers to discriminate between class-switched and non-switched memory B cell populations following an infection or vaccination. Activated B cells upregulate cell surface markers including CD40, CD80, CD86, and CD69 and these are used as B cell activation markers.(Mongini et al., 2003)

Human in vitro activated naïve, GC and memory B cells express cell surface CD27.(Agematsu, 2000) These populations are very limited in circulation and very few

circulating CD27⁺ B cells show evidence of ongoing proliferation, hence mainly tend to be memory B cells. Most memory B cells in humans are class-switched (IgD⁻) but a few may be non-switched (IgD⁺/IgM⁺). A very small proportion of class switched memory B cell population (less than 5% of the CD19⁺ in healthy individuals) has been shown to be double negative (IgD⁻CD27⁻). (Wei et al., 2011) This minor population is reported to express either IgM or other switched isotypes. (Franz et al., 2011)

Antigen-activated B cells can differentiate into short-lived and long-lived antibody secreting cells (ASC) or memory B cells. (Courey-Ghaouzi et al., 2022) Although rare in the blood of healthy unchallenged individuals, peripheral blood ASCs rapidly and transiently increase within one week following antigen challenge. The long-lived ASCs home in the bone marrow and maintain long-term antibody secretion to the systemic circulation. (Amanna and Slifka, 2010b, Halliley et al., 2015). Most human blood CD19⁺CD27⁺⁺CD38⁺⁺ B cells are considered plasmablasts due to evidence suggesting ongoing cell division. (Nutt et al., 2015b) Plasmablasts can be distinguished from plasma cells which are the terminally differentiated ASC. Plasma cell characteristics such as large size, little to no surface immunoglobulin, and non-proliferation correspond with expression of the adhesion molecule CD138⁺ (syndecan-1) on CD38⁺⁺. (Nutt et al., 2015) Expression of CD138 on more CD38⁺⁺ B cells compared with CD38⁺ B cells suggest that plasmablasts are the plasma cell precursors. Previous studies have shown that less than half of blood plasma cells express CD138, and nearly all bone marrow plasma cells express this molecule hence mainly used as a marker for long lived plasma cells (LLPCs). (Nutt et al., 2015) Differential expression of human CD38, CD138 and other markers including HLA-DR, chemokine receptor 4 (CXCR4), chemokine receptor 3 (CXCR3), B-lymphocyte-induced maturation protein-1 (Blimp-1), X box binding protein-1 (XBI-1) and B cell maturation antigen (BCMA) may alternatively or additionally represent ASC subsets that derive from independent differentiation pathways in blood, bone marrow and other tissues. (Sanz et al., 2019)

Knowledge on B cell subsets and their development in humans and animal models is useful for a better understanding of their function and identification of other immune components necessary for their activation.(LeBien and Tedder, 2008b) Various studies in mouse models and humans have classified B cells into various subsets based on their differentiation status, anatomical localisation and developmental lineage as described next.(Agematsu et al., 2000, Velounias and Tull, 2022, Vale et al., 2015)

1.5.1.1 B cell development and subsets based on differentiation status

Based on their developmental stage and status of differentiation, B cells can be classified into either precursor or peripheral subsets.(Allman and Pillai, 2008, Sagaert and De Wolf-Peeters, 2003) This is particularly important in classifying B cell abnormalities and autoimmunity based on their putative B cell origin mainly useful in the medical field for diagnosis and better treatment of B cell autoimmune diseases.(Jaffe et al., 2008)

1.5.1.1.1 Precursor B cells

The precursor B cell subsets include early B cell developmental stages in the bone marrow that undergo various maturation steps assembling a functional BCR that upon entry to secondary lymphoid organs will be able to distinguish between self and foreign antigens and respond appropriately. The precursor B cell subset consists of early and late pro-B cells, early and late pre-B cells, immature B cells and naïve mature B cells.(Osmond et al., 1988) They originate from the hematopoietic stem cells in the bone marrow and form the primary B cell repertoire before the newly formed B cells are exposed to foreign antigens.(Granato et al., 2015) Commitment of pluripotent stem cells to B cell lineage is a highly regulated process involving extensive rearrangements of the BCR or Ig containing two identical heavy and light chain genes. This gene rearrangement also known as VDJ (for variable, diversity and joining genes) recombination is a process that takes place for both B cells and T cells and involves different factors mediating assembly of heavy and light chain gene segments to produce a functional BCR.(Roth, 2014) VDJ recombination is largely dependent on

activation of the recombination activating proteins (RAG1 and RAG2) that regulate the process.(Chen et al., 2000) Successful VDJ recombination results in formation of the primary B cell repertoire which is characterised by surface expression of a functional BCR.(Tonegawa, 1983)

For assembly of the BCR, progenitor or pro-B cells differentiating from hematopoietic stem cells are able to initiate rearrangement of Ig gene locus.(Chen and Alt, 1993) Recombination of the V and D gene segments of the heavy chain into DJ transforms pro- B cells to early pre-B cells. Further attachment of the V segment to DJ forms late pre-B cells containing a fully rearranged VDJ chain. The light chain locus is subsequently rearranged and contains only DJ genes. Notably, the BCR is initially formed with a surrogate light chain containing an IgM-like complex on the surface of pre-B cells. This signals the successful rearrangement of the heavy chain and signals subsequent rearrangement of the light chain.(Mak and Saunders, 2006) Early B cells with self-reactive pre-BCRs are eliminated by apoptosis while the pre-BCRs on non-self-reactive B cells proceed to rearrangement of the DJ genes on their light chain locus to form a mature functional BCR with surface IgM being the first to be formed and this stage is now called immature B cell stage.(Alt et al., 1992) The primary mRNA transcript containing rearranged VDJ exons contain exons (C μ and C δ) for the constant (C) region. Immature B cells develop into mature B cells in which alternative splicing of the recombined VDJ exons allows expression of IgM from the first C μ exon and IgD from the first C δ exon.(Geisberger et al., 2006) B cell tolerance to autoantigens is maintained by BCR editing which involves replacement of the variable region genes of the heavy and light chains of productively rearranged BCRs to avoid autoreactivity.(Luning Prak et al., 2011)

After successful selection of mature B cells, they leave the bone marrow and migrate to peripheral lymphoid organs, becoming peripheral B cells. The precursor B cell developmental stages are illustrated (Figure 1.5A).

1.5.1.1.2 Peripheral B cells

Newly formed naïve B cells from the precursor stage migrate from bone marrow into secondary lymphoid organs initially homing in the spleen and lymph nodes.(Osmond, 1986) They form primary B follicles in these organs and upon antigen encounter, naïve B cells move into extrafollicular area in the lymph nodes and the periarteriolar lymphocyte sheath in the spleen.(Garraud et al., 2012)

Most antigens are T cell-dependent requiring integration between Th cells and APCs for provision of signals for potent B cell activation, while a few antigens are T cell-independent as they can bind directly to their specific BCRs on naïve B cells and activate them without the need of further help from Th cells.(Turner et al., 2017, McHeyzer-Williams et al., 1993, Mond et al., 1995)

Within secondary lymphoid organs, naïve B cells are activated by encountering an antigen in the extrafollicular or interfollicular space. From extrafollicular activation, B cells differentiate into short-lived plasma cells that produce early antibodies, mainly IgM for early antigen clearance.(Askonas, 1975, Nutt et al., 2015b) B cell activation within the follicle involves interaction between cognate B cells and Tfh cells to form the GC where the activated B cells receive strong co-stimulatory signals and differentiate to memory B cells and LLPCs.(Hentges, 1994, Mesin et al., 2016, Victora and Nussenzweig, 2012a) In the primary follicles, the naïve B cells that have not been exposed to an antigen move aside to form the mantle zone also known as the follicle mantle. The follicle now becomes secondary as it contains a GC and a mantle. Proliferating GC B cells are called centroblasts and transition to the selection stage called centrocytes.(Bannard et al., 2013) Survival of GC B cells is maintained by signals from their continued interaction with antigen specific FDCs and Tfh cells.(Liu et al., 1992, Mesin et al., 2016)

In GCs, B cells undergo random somatic hypermutation (SHM) within the ig variable region that encodes the antigen binding site. The SHM is regulated by activation-induced cytidine

deaminase (AID) enzyme and is a competitive process between mutated B cell receptors whereby those with the highest affinity for the antigen are rescued from apoptosis by survival signals from FDCs and Tfh cells.(Chen and Alt, 1993, Duy et al., 2010) The GC B cells producing high affinity antibodies are positively selected and they induce CD40 ligand expression and secretion of IL-4 and IL-10 cytokines from T cells. This induces expansion and isotype CSR from IgM to IgG, IgA or IgE.(Stavnezer and Schrader, 2014) Some GC B cells may undergo further proliferation, hypermutation and selection. After CSR and affinity maturation, B cells are said to be post-GC and differentiate into plasma cells or memory B cells.(Yoshida et al., 2010, van Rooijen, 1990)

Following differentiation, plasma cells move to different effector tissues with the help of chemokines and tissue specific adhesion molecules. Chemokines therefore determine the character and efficiency of antibody responses in various body tissues to which they direct homing of plasma cells. These effector tissues are directly exposed to foreign antigens and include mucosal surfaces targeted by IgA producing plasma cells and sites of tissue inflammation targeted by IgG producing plasma cells. Both IgA and IgG producing plasma cells also home in special survival niches in the bone marrow which is an important site for serum antibody production for long-term protection.(Kunkel and Butcher, 2003) Memory B cells reside in the follicle mantle or circulate freely to survey for secondary antigenic exposure. They can survive for decades without the need for further antigenic stimulation and proliferation.(Agematsu et al., 2000, Yoshida et al., 2010) The peripheral B cell developmental stages are illustrated (Figure 1.5B).

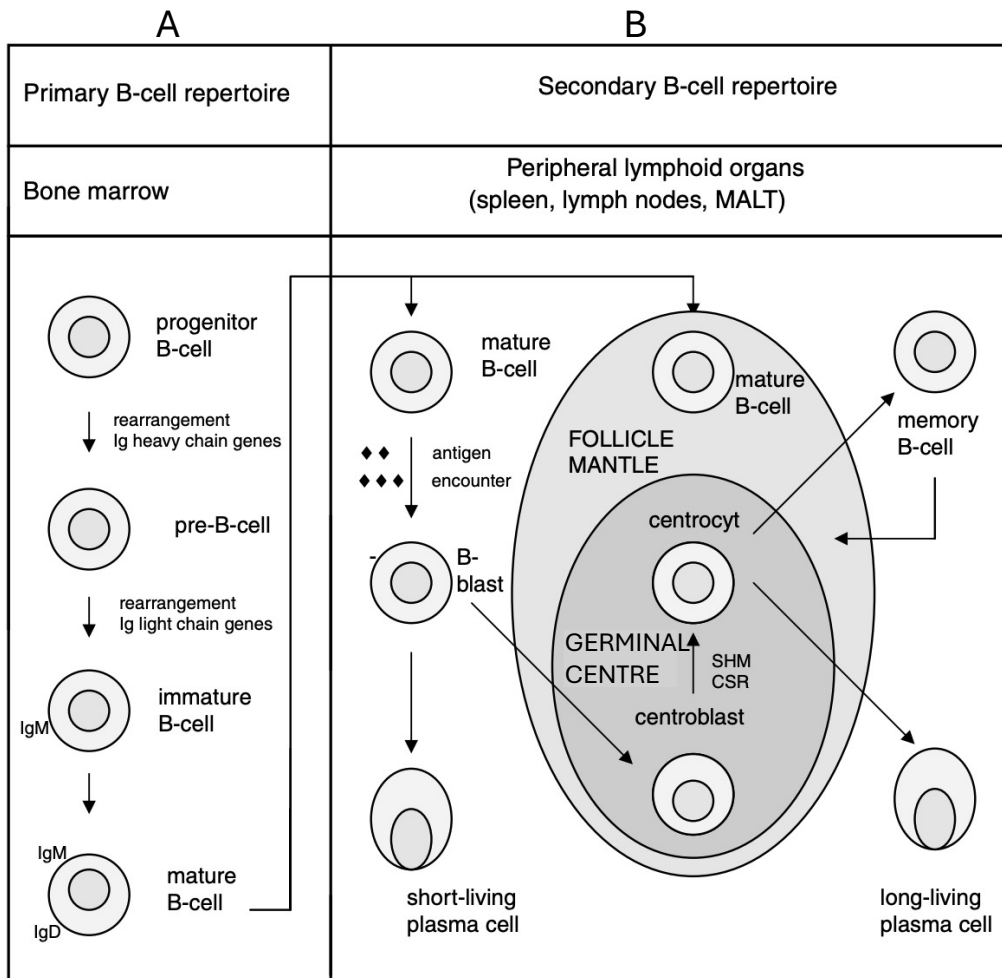


Figure 1.5. Schematic representation of B cell development

Primary repertoire development (A) and secondary repertoire development (B)

CSR - class switch recombination or isotype switching, SHM - somatic hypermutation, MALT - mucosal associated lymphoid tissue

(Sagaert and De Wolf-Peeters, 2003)

1.5.1.2 Subsets based on localization in B follicle compartments

The peripheral or secondary B cell repertoire can further be classified based on their specific anatomical localization in the B follicle into the following subsets.

1.5.1.2.1 Germinal centre B cells

GCs are found in the B cell follicle where activated B cells proliferate, differentiate, and undergo SHM. Follicle centre B cells consist of centroblasts and centrocytes. (Boulianne and

Gommerman, 2016) Centroblasts are large and proliferating, containing a round vesicular nucleus, a narrow basophilic cytoplasm and lack surface expression of ig. Lack of B-cell lymphoma 6 (Bcl-2) expression on centroblasts makes them susceptible to death by apoptosis and are therefore negatively selected.(Cutrona et al., 1997) Most surface molecules expressed by centroblasts are those involved in their interaction with T cells such as CD23, CD27, CD40 and CD86, as well as those involved in their adhesion to FDCs including CD11a/18 and CD29/49a and their natural ligand intercellular adhesion molecule 1 (ICAM 1 or CD54).(Young and Al-Saleem, 2008) They also express other molecules at low levels including surface IgD (sIgD), MHC II, CD19, CD10 and CD38, but lack IgM expression.(Young and Al-Saleem, 2008) GC polarization to dark and light zones is widely documented although the distinctive functional roles between these zones are not well understood. Centroblasts are found mainly in the dark zone where they upregulate expression of markers necessary for their continued interaction with Tfh cells as they undergo SHM in a timed program enabling them to differentiate into centrocytes and transitioning to the light zone.(Bannard et al., 2013) They are medium in size with an irregular nucleus and a scanty cytoplasm, and they do not proliferate. They undergo clonal selection where those with low antigen affinity are negatively selected and eliminated via apoptosis and the high affinity ones are positively selected to undergo subsequent differentiation.(Bannard et al., 2013, Ke et al., 2024)

Follicle centre B cells upregulate B-cell lymphoma 6 (Bcl-6).(Kitano et al., 2011) Bcl-6 is a transcription factor important for GC formation and maintenance during T cell-dependent immune responses. It modulates signals that are essential for B cell responses including IL-4, BCR, CD40 ligand and signals that are important for development of normal B cells.(Duy et al., 2010) Bcl-6 inhibits expression of Blimp-1, a transcription factor that is a major regulator of plasma cell differentiation together with XBP-1. Blimp-1 represses transcription of proteins necessary for MHC II expression and cell proliferation, while activating genes involved in ig secretion. XBP-1 on the other hand controls the final steps of plasma cell

differentiation. Finally, positively selected centrocytes that have undergone isotype switching differentiates into either memory B cells or LLPCs.(Mak and Saunders, 2006) Differentiation to either memory B cells or LLPCs is a complex process influenced by various factors such as transcription factors whereby broad complex-tramtrack-bric a brac and Cap'n'collar homology 2 (Bach2) promotes memory B cell formation while the interferon regulatory factor 4 (IRF4) and Blimp-1 promotes LLPCs differentiation.(Klein and Dalla-Favera, 2008b, Nutt et al., 2015a) Additionally, positively selected B cells with higher affinity for an antigen differentiate to LLPCs while those with lower affinity form memory B cells.(Shinnakasu and Kurosaki, 2017) Interaction between surface molecules also play a role in this process whereby CD40-CD40L interaction with Tfh cells promotes memory B cell development,(Kawabe et al., 1994, Weller et al., 2001) while interaction with CD23 on FDCs promotes the LLPC pathway.(Elgueta et al., 2009) Differentiation of GC B cells into either memory B cells or LLPCs is a subject of ongoing research as our understanding of the immune system continue to evolve.

1.5.1.2.2 Lymphocytic corona B cells

During formation of the follicle centre, mature naïve B cells move towards the inner part of the mantle zone known as the lymphocytic corona.(Martin and Kearney, 2002) Mantle zone is a ring of small, resting B cells that surround the GC. Lymphocytic corona cells are characterised by rearranged but unmutated Ig genes and thus show a high expression of surface IgM and IgD as well as other B cell lineage markers such as CD19 and CD20 and they lack CD10 expression.(Martin and Kearney, 2002)

Lymphocytic corona also contains memory B cells especially in the lymphoid tissues whose marginal zones are poorly developed. The outer part of the mantle corresponds to the marginal zone.

1.5.1.2.3 Marginal zone B cells

Due to their anatomical locations, secondary lymphoid organs encounter high influx of antigens and therefore have well-developed marginal zones.(Martin and Kearney, 2002) Marginal zone refers to the area separating the lymphoid follicle from the surrounding tissue that often contains specialized macrophages and B cells. The marginal zone is well recognizable in the white pulp of the spleen and in Peyer's patches of the intestines and the tonsils as opposed to lymph nodes where there is relatively less antigen exposure.(Cesta, 2006) Marginal zone B cells contain a clear cytoplasm and an irregular central nucleus. These cells express Pan B cell markers and Bcl-2 antigens but lack the expression of CD5, CD10 and CD43. Their IgD expression pattern has been shown to be either negative or weak and this distinguish them from lymphocytic corona B cells that usually have a high expression of IgD.(Martin and Kearney, 2002) The GC B cells strongly express alkaline phosphatase and complement receptors including CR1 (CD35), CR2 (CD21) and CR3 (CD18/11b) important for activation of the complement system to regulate humoral responses and aid in antigen elimination.(Carroll and Isenman, 2012, Perrin-Cocon et al., 2004)

Reactive lymph nodes have subcapsular and cortical sinuses that show adjacent clusters of monocytoïd B cells that closely resemble marginal zone B cells.(Stein et al., 1999) The immunophenotype of marginal zone and monocytoïd B cells are similar except for the varied expression of IgM in both and absence of Bcl-2 expression in monocytoïd B cells.(Stein et al., 1999) Marginal zone B cell population is heterogeneous consisting of naïve and memory B cells as has been shown via mutation analysis of the Ig genes.(Martin and Kearney, 2002) Marginal zone B cells have been shown to play a role in T cell-independent type 2 antigens such as bacterial capsular polysaccharide antigens.(Fagarasan and Honjo, 2000) This role is evident in infants as they remain susceptible to capsulated bacteria until two years of age when the marginal zone B cells are fully developed to provide protection from these

infections.(Klein and Dalla-Favera, 2008a) Marginal zone also plays an important role as a first line of defence for many blood-borne infections.(Fagarasan and Honjo, 2000)

1.5.1.3 Subsets based on B cell developmental origin

This approach is based on functional features as well as expression of surface markers and classifies B cells into two subsets; B-1 and B-2 B cells irrespective of their homing properties.(Sagaert and De Wolf-Peeters, 2003) This classification was initially based on surface expression of CD5 on B-1 B cells and its absence on B-2 B cells. The B-1 subset has different characteristics from B-2 subset, which form the conventional B cell pool.

1.5.1.3.1 B-1 B cells

Initial B-1 subset cells in mice were defined by their surface expression of CD5+, IgM++, IgDlow, CD19++, B220low, CD23+ and CD43+. Later on, an additional B-1 subset was discovered that showed all B-1 characteristics but lacked CD5 surface expression.(Kantor et al., 1992) These two B-1 cell populations were then split into B-1a (CD5+) and B-2b (CD5-) cells. B-1 cell populations are mainly located in the peritoneal and pleural cavities but they are absent or few in the peripheral blood, lymph nodes and Peyer's patches.(Rothstein et al., 2013) Their preferential homing to cavities has been shown to be facilitated by the chemokine receptor CXCL13 from peritoneal macrophages and cells of the omentum.(Cinamon et al., 2004, Montecino-Rodriguez and Dorshkind, 2016) B-1 B cells develop from foetal liver and are thought to be the source of the first line natural antibody (IgM) produced within the first 48 hours following an infection. Their ability to produce antibodies without T cell help helps in mounting a quick response following an infection.(Martin et al., 2001) B-1 B cells were initially thought to be involved in mounting antibody responses to T cell-independent antigens only. However, later studies confirmed B-1 to participate in T cell-dependent activation as well.(Popi et al., 2016) B-1 cells were shown to mount immunity against bacterial, parasitic and viral infections.(Montecino-Rodriguez and Dorshkind, 2016, Haas et al., 2005) These findings have rendered the B-1 classification to be controversial and outdated concept in humans.

1.5.1.3.2 B-2 B cells

B-2 cells develop from precursors in the bone marrow. They include B cell populations of the marginal zone and the follicular zone and are the main populations that are activated upon antigen encounter to form GCs. These cells are therefore long-term responders whose response is desirable for long-term protection. B-2 cell populations are the majority of total B lymphocytes in the host and are found in all lymphoid tissues unlike B-1 cells. Marginal zone B cells in mice are restricted to the splenic marginal zone, while their human counterparts are present in both marginal zones and in blood circulation.(Jorge Ismael et al., 2017) The differences between B-1 and B-2 subsets are not widely studied, hence there may be more complex differences between the two subsets. A recent study profiled cytosine modifications in B-1a and B-2 cells and their precursors and reported that both subsets exhibited distinct 5'-C-phosphate-G-3' (CpG) modification states at DNA (cytosine-5)-methyltransferase 3A, an enzyme involved in DNA methylation.(Mahajan et al., 2021) As a key regulator of gene expression, DNA methylation may therefore play a key role in defining the developmental pathway into either B-1 or B 2.

Despite a lot of advances that continue to improve understanding on B cell immunity, there is still more to be learnt considering the complexities in the B cell development, subsets and function. Additionally, since B cells do not work in isolation but have to interact with different components of the more complex wider immune system for an effective immune response, this makes the subject even more intricate not only for B cells but also the entire immune system.

1.5.2 Maintenance of long-term antibodies by LLPCs and memory B cells

The generation of long-term humoral immunity after infection or vaccination is critical in protecting against microbial pathogens.(Chen et al., 2022) The immunological mechanisms underlying long-term protection are not well understood. It was conventionally believed that maintenance of long-term antibody titres in circulation is mainly dependent on secretion of antibodies from proliferation and differentiation of memory B cells following re-exposure to their specific antigen.(Szakal et al., 1989, Gray et al., 1996) This was supported by the belief that plasma cells are short-lived, and since the half-life of a circulating immunoglobulin is less than three weeks, there must be a mechanism for replenishing the antibody-secreting cells.(Vieira and Rajewsky, 1988) However, it later become clear that some plasma cells can be long-lived with ability to continuously secrete antibodies to systemic circulation for many years or even over a lifetime.(Slifka et al., 1998a, Lightman et al., 2019)

Antigen specific plasma cells are not detectable in circulation at a steady state as they only appear soon after their generation in GCs.(Blanchard-Rohner et al., 2009) Following their generation, short-lived plasma cells secrete antibodies and die off early whilst the LLPCs move to survival niches in the bone marrow from where they continue to secrete antigen specific antibodies into circulation.(Aaron and Fooksman, 2022) The timelines within which plasma cell responses are transiently detectable in circulation are conserved across many pathogens. An early appearance of plasma cells in circulation, around 7 to 13 days following primary vaccination compared to 5 to 10 days after secondary vaccination is consistently reported (Figure 1.6).(Carter et al., 2017b) The exact peak time after secondary vaccination may vary slightly between antigens, with a median peak timepoint across various antigens reported to be 7 days.(Carter et al., 2017b) Genetic factors, mainly the HLA system responsible for antigen presentation, and environmental factors may result to variations in cellular and antibody profiles between individuals.(Manuck et al., 1991, Mangino et al., 2017)

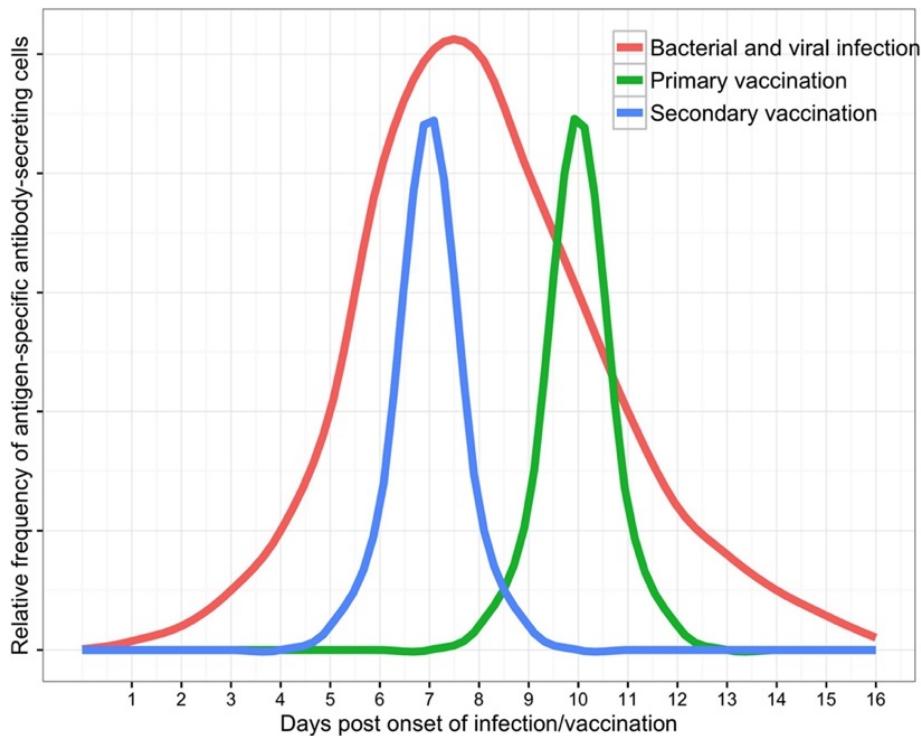


Figure 1.6. Plasma cell response kinetics after infection and vaccination

Schematic representation of time within which antibody secreting cells are detectable in circulation following bacterial and viral infections or primary and secondary vaccination.(Carter et al., 2017b)

Although LLPCs can also be generated from memory B cells upon reactivation, they are considered as an independent B cell population that can survive without the need for repopulation from memory B cells. This was reported in studies including tritium or bromouridine incorporation to demonstrate long-term survival of plasma cells without cell division.(Miller, 1964, Manz et al., 1997) A number of models have been proposed to explain potential sources of long-term antibody responses including chronic infection or cross-reactivity to environmental or self-antigens, memory B cell reactivation by repeated infection or booster vaccination, continued activation of memory B cells by persistent antigens, polyclonal activation of memory B cells, competition of plasma cells for special niches in the bone marrow and plasma cell imprinted lifespan.(Amanna and Slifka, 2010b) Figure 1.7 shows representation of the expected profiles of antibody titres from these models.

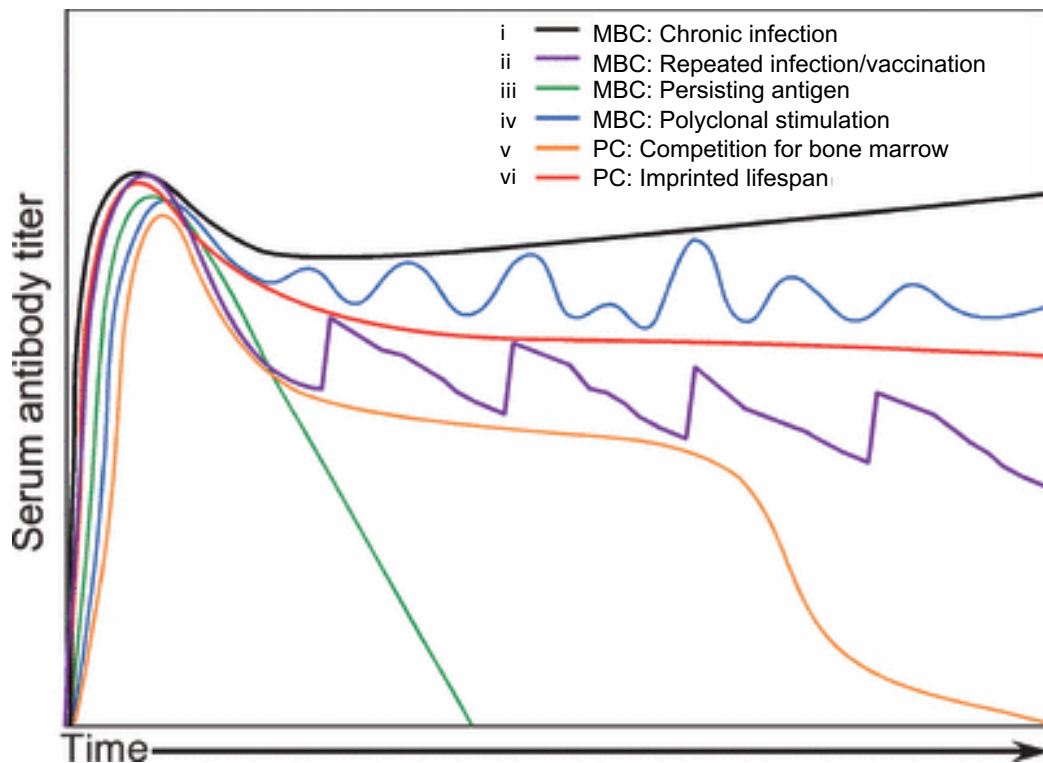


Figure 1.7. Profiles of long-term antibody maintenance from different models

Serum antibodies are maintained by i) continuous re-activation of memory B cells (MBC) through chronic infection or MBC cross reactivity to environmental and self-antigens, ii) MBC re-activation following repeated infection or vaccination, iii) MBC re-activation by antigens persisting in B cell follicles as complexes with follicular dendritic cells, iv) MBC re-activation by bystander T cells or TLR agonists such as CpG oligonucleotides in combination with cytokines, v) competition for special survival niches in the bone marrow where newly generated LLPCs replace the earlier generated ones making them unable to re-occupy the bone marrow niches, vi) Plasma cells (PC) are imprinted with a pre-defined lifespan based on the immune environment at the time of their induction such that LLPCs are generated from B cells receiving CD4 T cell help while the T cell-independent B cell activation generate short lived PC. MBC - memory B cells, TLR - Toll like receptor CpG - 5'-C-phosphate-G-3' (CpG), LLPCs - long-lived plasma cells, PC - plasma cells (Amanna and Slifka, 2010a)

Most of these models have been reviewed as having various shortcomings of not being able to exclusively explain certain aspects of long-term antibody responses to different antigens as described next.(Amanna and Slifka, 2010a) On the first proposed model, not all antigens are able to sustain chronic infections. Additionally, the aspect of cross-reactivity to other environmental or self-antigens to sustain humoral memory in a chronic infection-like manner does not align with antigen specificity required to drive affinity maturation to specific

antigens. The fact that some antigens induce long-term, and others short-term antibody protection does not support the cross-reactivity model which assumes that antibody response to all antigens is equally maintained. Repeated infection or vaccination booster have been demonstrated to trigger increase in antibody titres and this model presents a stronger explanation for maintenance of long-term antibody response than chronic and/or repeated infection model. Antigen specific antibody titres to non-replicating subunit antigens such as tetanus and diphtheria wane within about 10 to 20 years while antibody titres to live-attenuated antigens such as measles, mumps and rubella are maintained for decades in the absence of antigen re-exposure excluding repetitive antigenic exposure as an absolute requirement for maintenance of long-term antibodies. On the model on persisting antigen, not all antigens persist in the host system after an infection or vaccination due to the limitations on antigen binding to FDCs to form complexes and the FDCs are short-lived.

Polyclonal stimulation model contradicts antigen specificity as a critical requirement for maintenance of long-term antibodies. The model on competition for special survival niches in the bone marrow between 'new' and 'old' antibody secreting cells means that exposure to new antigens will lead to the loss earlier generated LLPCs from unrelated antigens. However, this does not happen since despite the constant exposure to various antigens, antigen-specific antibodies are still detectable to antigens that individuals were exposed to long time ago. The last model describes antibodies as imprinted with a lifespan determined by characteristics of antigens for example, generation of more durable antibodies from memory B cell and long-term plasma cells from T cell-dependent compared to T-independent antigens.

While there may not be a single one of these models absolutely describing maintenance of long-term antibody protection for all antigens, the models provide useful insights contributing to the understanding of immunity to various antigens. In most cases, the durability of antibodies induced by certain antigens may be explained by more than one of the described models.

While memory B cells may not be required to maintain LLPCs, they play a vital role in generating secondary responses following re-exposure to their specific antigen. Memory B cells maintain surface expression of antigen specific BCR, and upon re-encountering their cognate antigen, they are reactivated to differentiate to ASCs. Studies have shown that when memory B cells are stimulated by other antigens other than their cognate one, they remain dormant but are able to rapidly expand and repopulate plasma cell numbers upon a booster vaccination with their cognate antigen.(Hebeis et al., 2004)

1.5.3 Tfh cell biology

This CD4 T cell subset was first identified in the tonsils and play a vital role in the GC reaction supporting B cell activation, generation of plasma cells and memory B cells for subsequent antibody response that mediates clearance and protection from pathogens.(Crotty, 2019) Following antigen encounter, naive CD4 T cells can differentiate into a number of distinct functional subsets, one of them being Tfh cells. The expression of CXCR5 (a core Tfh cell lineage marker) on Tfh cells attracts them to the B cell follicles via gradients of the chemokine CXCL13 where they interact with B cells.(Breitfeld et al., 2000)

Within the GC, antigen-specific B cell clones interact with cognate Tfh cells and are repeatedly selected and expanded with increasing antigen affinity. Provision of activation signals from Tfh cells to GC B cells thus generates high-affinity, class-switched LLPCs and memory B cells.(Victoria and Nussenzweig, 2012a) Indeed, activated B cells lacking cognate Tfh cells help are unable to generate and maintain the GC response critical for SHM of igs and other selective processes facilitating affinity maturation.(Crotty, 2011c) Outside the follicles, B cells can differentiate in a GC-independent manner allowing for more rapid clonal expansion of antigen-specific B cells soon after exposure to an antigen. This generates short-lived plasma cells and memory B cells that can be supported by Tfh cells acting outside the B cell follicle.(Lee et al., 2011) During the B cell-Tfh cell interaction, interleukin-2 (IL-2) produced by Tfh cells promotes maturation of B cells and antibody production. Production of different Ig classes is promoted by a combination of cytokines secreted by

different Tfh subsets as follows: IL-21 and IFN- γ from Tfh1 promote IgG1 and IgG2; IL-21, IL-4, IL-5 and IL-13 from Tfh2 promote IgG4, IgE and IgA while IL-21, IL-17 and IL-22 from Tfh17 promote IgA production. Viral infections and vaccine antigens cause secretion of large quantities of interferons. This activates the type 1 immune response predominantly and leads to expansion of Tfh1 cell population which promotes IgG1 and IgG2 production by GC B cells.(Perreau et al., 2013) The reaction of IgG1 to protein antigens from viruses and vaccines makes it very desirable in vaccine induced immune responses. On the other hand IgG2 reacts to encapsulated bacteria making them critical for generation of humoral response to polysaccharide antigens.(Batten et al., 2010) IgG1 is the most abundant IgG subclass followed by IgG2 and they account for 60-70% and 20-30% of the total IgG, respectively.(Batten et al., 2010) Tfh2 promote IgG4 and IgE secretion. The IgG4 and IgE leads to mast cell and basophil activation and results in crosslinking of allergens culminating to release of allergy mediators. Both Tfh2 and the associated Ig responses could mediate type II immune response.(Ballesteros-Tato et al., 2016) Tfh cells are detectable in low frequencies in circulation, mainly within the CD4 T cell central memory population that express CD45RO and have been reported to provide a more rapid and robust B cell help upon reactivation by secondary antigen exposure.(Sage et al., 2014)

The development of this cell subset from naïve CD4 T cell precursors is mainly associated with the interaction between antigen presenting cells such as DCs and B cells at the border of T cell zone and follicles. While DCs-restricted antigen presentation is thought to be required to initiate the development of committed Tfh cells, antigen presentation by B cells is responsible for their complete effector differentiation.(Goenka et al., 2011, Ballesteros-Tato et al., 2013) There are three main Tfh subsets identified classified based on their surface expression of chemokine receptors CCR6 and CXCR3 (i.e CCR6-CXCR3⁺ Tfh1, CCR6-CXCR3⁻ Tfh2 and CCR6⁺CXCR3⁻ Tfh17) as well as the cytokine profiles driving their functions.(Schmitt and Ueno, 2013) Four models have been proposed to describe the development of Tfh cells as discussed next.

1.5.3.1 Models of Tfh cells development

1.5.3.1.1 Direct Tfh cell differentiation via cytokines

The first model is derived from experiments that showed that CD4 T cells cultured in the presence of spleen APCs and IL-21 express CXCR5 and Bcl-6 mRNA and have a better capability to provide enhanced B cell help when transferred to host mice than the uncommitted CD4 T cells (Th0), when the Th1, Th2, Th17 and regulatory T cell pathways are inhibited.(Nurieva et al., 2008) This is supported by studies that showed that the cytokines IL-6 or IL-21 induced Bcl-6 and CXCR5 in vitro. These two cytokines signal through signal transducer and activator of transcription 3 (STAT3) pathway that when deficient in CD4 T cells, they are unable to differentiate to Tfh cells. This model proposes that a single cytokine, either IL-6 or IL-21 causes independent differentiation of naïve CD4 T cells into Tfh cells (Figure 1.8A). However, there are controversies on the specificity of the mentioned cytokines and transcription factors to drive only Tfh cell differentiation as for example IL-21 is also produced by other CD4 T cell subsets such as Th2 and Th17.(Poholek et al., 2010, Eddahri et al., 2009) Additionally, mice deficient of IL-6 can produce normal Tfh cell levels and mice with STAT3-deficient CD4 T cells do not show loss of CD4 T cells.(Poholek et al., 2010, Eddahri et al., 2009) This model does not indicate any requirement of B cells in Tfh cell differentiation.

1.5.3.1.2 B cell-dependent direct Tfh cell differentiation

This second model proposes the Tfh cells to be a distinct subset whose direct differentiation depends on interaction between activated CD4 T cells with B cells enabling CD4 T cells to differentiate independent of the other (Th1, Th2 and Th2) CD4 T cell subsets. This is supported by studies in mice that showed that Tfh cells are not observed in the absence of B cell following immunization and infection with different antigens.(Haynes et al., 2007, Johnston et al., 2009) Further studies demonstrated that not only do Tfh cells require B cells for their differentiation but also that the function of both Tfh and B cells in GCs is interdependent. Sustained differentiation of both Tfh and B cells during the GC reaction

depends on the induction of the same master regulator, Bcl-6, a key process in sustaining antigen specific antibody protection. This model proposes that Tfh cells development starts with extrafollicular interaction between DCs and naïve CD4 T cells expressing low levels of the chemokine receptor CXCR5 and the transcriptional factor Bcl-6 (Figure 1.8B). These CD4 T cells are termed pre-Tfh and their interaction with APCs causes them to migrate to the area between the B cell follicle and T zones. Here, they encounter cognate B cells presenting the same antigen to them on MHC class II and this generates signals for the Tfh specific differentiation and survival necessary to complete differentiation, generation and sustenance of GC Tfh and B cell responses.(Crotty, 2011a) Increased expression of CXCR5 in mature Tfh cells localises them in the follicles where its ligand, CXCL13 is produced by stromal DCs and FDCs.(Bürkle et al., 2007) While B cell and Tfh cell interaction is critical for maintenance of Tfh cells, the unique requirement of B cells for Tfh cells differentiation as indicated in this model is challenged by studies showing that mice lacking MHC II are capable of developing Tfh cells following repeated antigen injection.(Deenick et al., 2010)

1.5.3.1.3 Secondary program of Tfh cells development

This model proposes that Tfh cells develop in a secondary program similar to central versus effector memory differentiation as opposed to being a distinct CD4 T cell subset.(Zaretsky et al., 2009) This secondary program is thought to result in a phenotypic state (Tfh cells) of CD4 T cell differentiation after first differentiating to Th1, Tfh2 or Th17 alongside regulatory T cells (Treg) (Figure 1.8C). The model argues that the overlapping attributes of Tfh cells with other CD4 T cell subsets do not support distinct independent development programs.(Johnston et al., 2009, Hsu et al., 2008) It also implies that the Tfh cell subsets would not antagonize other CD4 T cell subsets.(Awasthi and Kuchroo, 2009) This model is challenged by the fact that during Tfh cells development, there are extensive gene expression changes similar to those that distinguish other CD4 T cell subsets and that Tfh cells undergo more surface receptor changes believed to be necessary for their interaction

with B cells, which are not observed in the other CD4 T cell subsets.(Kim et al., 2004, Rasheed et al., 2006, Chtanova et al., 2004)

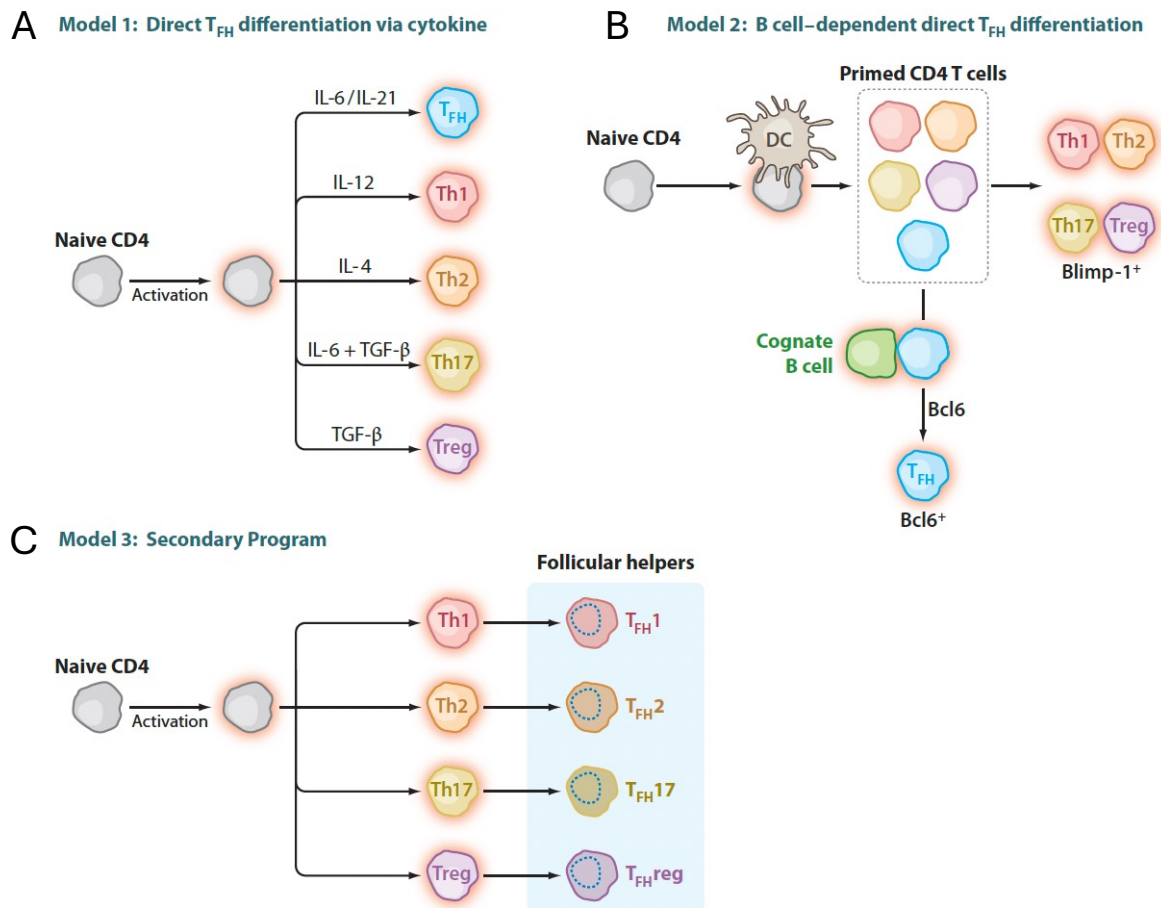


Figure 1.8. Three early models of follicular helper CD4 T Cells (T_{FH})

Model 1: Direct Tfh differentiation (A), Model 2: B cell dependent direct Tfh differentiation (B) and Model 3; Secondary program of Tfh differentiation (C). The figure shows different cells and cytokines or transcription factors involved in each mode. Th - helper T cell subset, IL - interleukin, T reg - regulatory T cell subset, DC - dendritic cells, Bcl6 - B cell lymphoma 6, TGF - transforming growth factor.(Haynes et al., 2007, Johnston et al., 2009, Nurieva, 2008, Zaretsky et al., 2009)

1.5.3.1.4 Multistage multifactorial model of Tfh cells differentiation

This is the latest model combining possible explanations from the earlier three models and addresses some of their controversies.(Crotty, 2011b) This model is based on studies investigating the timing and determinants of induction of Bcl-6, the transcriptional regulator of Tfh cells differentiation whose role is also implicated in the earlier models.(Nurieva et al., 2009, Johnston et al., 2009, Allman et al., 1996) This model is more comprehensive and combines evidence from studies across the entire developmental stages of Tfh cells. It describes the differentiation of Tfh cells to be independent of Th1, Th2 and Th17 differentiation (Figure 1.9). Development of CD4 T cells expressing Bcl-6 and CXCR5 proteins can occur as early as 2 days following an acute viral infection, which is the time DC priming is expected to take place. Further increases in Bcl-6 protein expression levels and cell frequency was observed as the adaptive immune response matured without showing any dependence on CD4 T cells first becoming a Th1, Th2 or Th17 cells. However, in the absence of B cells, this differentiation was lost by day 8 in vivo, supporting the role of DCs in initial priming of Tfh cells differentiation through transient signals and the requirement of B cells in a second stage of rapid antigen presentation to CD4 T cells to sustain and complete differentiation of the Tfh cell subset.(Johnston et al., 2009)

The multi-stage multifactorial model argues that the Tfh cell subset differentiation is neither solely dependent nor exclusive of the differentiation of other CD4 T cell subsets and is best considered an overlaid program, either on top of, or parallel to the differentiation of those other subsets. In line with this, pre-GC and GC Tfh cells can express the transcription factors T-box transcription factor TBX21 (T-bet) or GATA3 or retinoic acid-related orphan receptor gamma t (ROR γ t) enabling them to secrete moderate levels of other CD4 subset (Th1, Th2, or Th17) cytokines required for B cell isotype switching. This lack of exclusivity is a central feature of the Tfh cells differentiation, and they are capable of antagonizing non-Tfh effector CD4 T cell differentiation by Bcl-6 antagonism of Blimp-1. This model also defines pre-GC and GC Tfh cells based on the different levels of expression of not only Bcl-6 but

also other markers whereby increased expression of Bcl-6, IL-21, CXCR5 and inducible T-cell co-stimulator (ICOS or CD278) are believed to stabilise GC Tfh cells (Table 1.2).(Crotty, 2011b) These markers are used in the phenotypic identification of Tfh cells at the different stages.

Table 1.2. Markers for phenotypic identification of Tfh cell stages in mice and humans

Marker	Human		Mouse		CD4 T cell	Activated non-Tfh CD4
	Tfh	GC Tfh	Tfh	GC Tfh		
CXCR5	+	++	+	++	-	-
Bcl-6	+	++	+	++	-	-
PD-1	+	++	+	++	-	variable
ICOS	+	++	+	+	-	variable
SAP	normal	high	normal	High	normal	normal
IL-21	+	++	+	++	-	variable
CXCR4	normal	high	high mRNA	high mRNA	normal	normal
CXCL13	low	high	-	-	-	-
BTLA	normal	high	high	high	normal	low
SLAM	unknown	unknown	normal	normal	normal	variable
CCR7	low	low	low	low	high	variable
CD200	-/+	+	+	+	-	-
IL-4	-	+	-	-	-	Th2+

The table shows markers expressed at various differentiation stages of Tfh cells in mice and humans. Tfh - T follicular helper cells, GC - germinal centre, Bcl-6 - B cell lymphoma 6, PD-1 - programmed cell death 1, ICOS - inducible T-cell co-stimulator, SAP - signaling lymphocyte activation molecule associated protein, IL - interleukin, BTLA - B and T lymphocyte attenuator, SLAM - signaling lymphocytic activation molecule, CXCR - chemokine receptor - CXCL - chemokine ligand, CCR - chemokine receptor, Th2 - T helper 2.(Crotty, 2011b)

Integrated model of T_{FH} differentiation: multistage and multifactorial

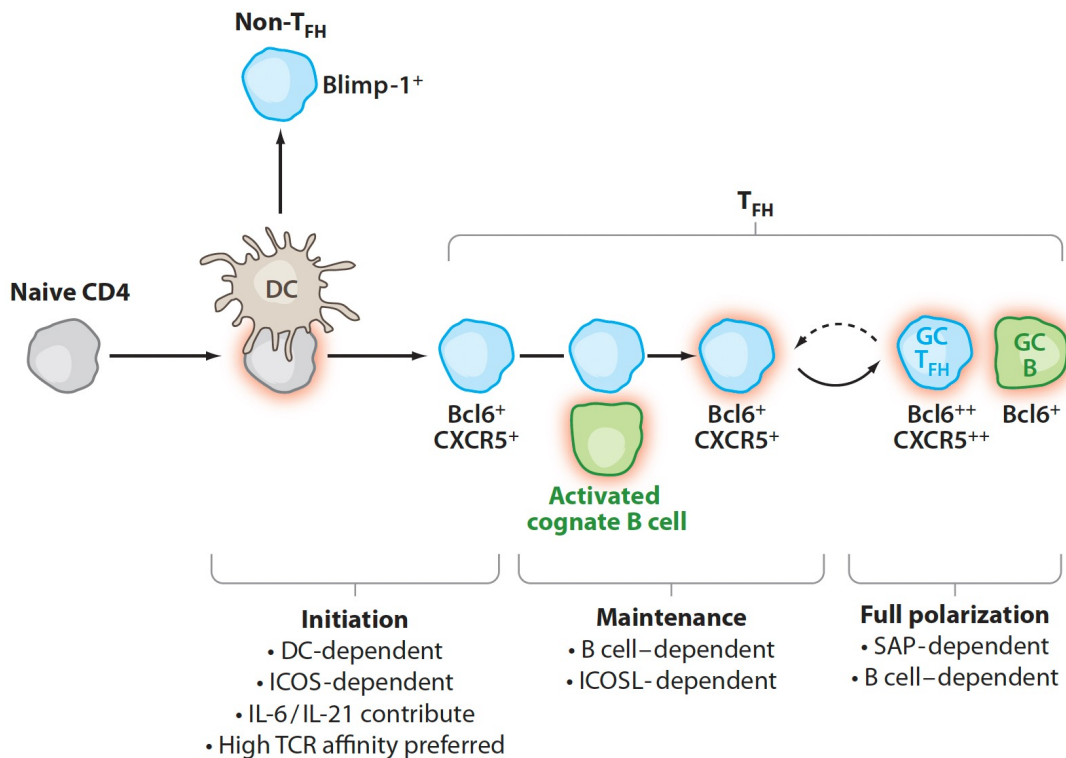


Figure 1.9. Fourth and latest model of Tfh cells differentiation; multistage and multifactorial

This model summarizes possible explanations for Tfh differentiation from the three earlier models. Blimp-1 - B-lymphocyte-induced maturation protein-1, DC - dendritic cell, ICOS - inducible T-cell co-stimulator, IL - interleukin, ICOS - ICOS ligand, SAP - SLAM-associated protein.(Crotty, 2011b)

In summarising these models, the differentiation of Tfh cell subset from naïve CD4 T cells is seen to be initiated by antigen encounter and requires APCs at the priming stage. Whether the antigen presentation at this initial stage is by conventional APCs such as DCs or B cells may depend on the nature of antigen. While it is widely thought that conventional APCs, mainly DCs are the primary T cell priming cells, studies have demonstrated the capability of B cells to prime dominant Tfh cell response in the absence of DCs.(Rodriguez-Pinto et al., 2014, Arroyo and Pepper, 2020, Kroeger et al., 2013) Perhaps, depending on antigen characteristics, both DCs and B cells may present antigens in synergy to prime a robust Tfh

cell response, an area that warrants further research especially for multimeric antigens like HPV that can rapidly cross-link BCRs and induce a robust immune response early on following infection or vaccination.(Pone et al., 2022) The classification of antigens as either T cell-dependent or T cell-independent only may be leaving out antigens with capabilities to employ both mechanisms in priming the immune system. Future studies on the mechanisms employed by various types of antigens in activating the immune system may help to identify antigens able to use both pathways and the extent to which each activation pathway contributes to long-term humoral immunity.

The GC interaction between antigen specific B cells and Tfh cells is extensively demonstrated to be critical for generation of potent and long-term antibody protection via memory B cells or LLPCs. This process is described next.

1.5.4 B cells and Tfh cells interaction to generate memory B cells and long-lived plasma cells

As earlier introduced in the various peripheral B cell subsets, naïve B cells recognize native antigens by their BCR, become activated, proliferate, and differentiate into short-lived antibody secreting plasma cells in the extrafollicular space.(Stanley, 2010d) Antibodies (mainly IgM) generated at this stage are important for early pathogen clearance.(Sathe A, Updated 2021 December) Some activated B cells enter B cell follicles and form GCs where they interact with Tfh cells, leading to clonal expansion, CSR and selection for affinity maturation through SHM.(Sathe A, Updated 2021 December).

Activated B cells in GCs differentiate to LLPCs, that migrate to survival niches in the bone marrow and continue to release high affinity antibodies to peripheral circulation for years, and memory B cells that re-circulate and persist as resting cells and are able to undergo rapid expansion following antigen re-encounter or booster vaccination.(Mesin et al., 2016, Tokoyoda et al., 2009) Additionally, FDCs retain antigens in follicles via linkages to the complement system and immune complexes and present them to GC B cells to initiate a secondary immune response, help to rescue bound B cells from apoptosis and induce

differentiation of B cells into memory B cells and LLPCs (Figure 1.10).(Amanna and Slifka, 2010b) Long-term antibody protection comes from memory B cells and LLPCs.(Hardy and Hayakawa, 2001, Amanna and Slifka, 2010b) Various factors determine whether activated B cells become LLPCs or memory B cells. To understand mechanisms underlying plasma cell lifespan and durability of humoral immunity, one study analysed serum antibody response against eight different viruses and vaccine antigens in human subjects followed up for 26 years, and suggested a model based on the magnitude of B cell signalling generated by the primary antigen specific immune activation.(Amanna and Slifka, 2010b, Amanna et al., 2007) Following generation of an initial high antibody response from the high numbers of short-lived plasma cells, the short-lived plasma cells die off leading to some decline in the antibody levels that are then sustained by LLPCs and memory B cells. T cell-dependent protein antigens generate a more durable B cell progeny that produce more antibodies per cell than non-protein T cell-independent antigens.(Taillardet et al., 2009, Slifka and Ahmed, 1996)

Polyvalent antigens, such as VLP antigens are known to crosslink BCRs strongly which stabilizes B cell signalling by increasing protein tyrosine kinase phosphorylation. (Thyagarajan et al., 2003) This process has been described to induce potent and long-term antibodies with little or no T cell dependency even for protein antigens that are conventionally believed to be T cell-dependent.

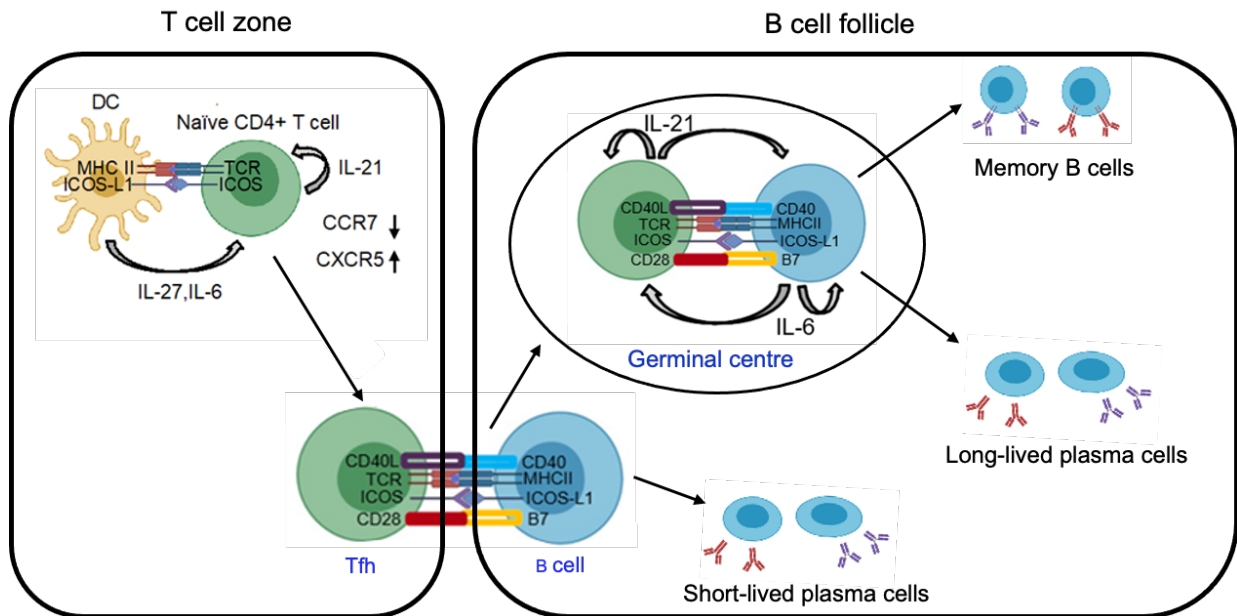


Figure 1.10. Activation of naïve CD4+ T and B cells to generate short-lived plasma cells, long-lived plasma cells (LLPCs) and memory B cells

Activated dendritic cell (DC) presents antigen to naïve CD4+ T cell that differentiates into pre-T follicular helper cells (pre-Tfh) down regulating expression of CCR7 and upregulating CXCR5 expression enabling it to move towards the T-B-cell zone. Pre-Tfh is presented with the same antigen on MHC II by B cell that is in turn activated to differentiate into short lived plasma cells in a reaction involving co-stimulatory signals via ICOS-ICOS ligand and CD40-CD40 ligand interactions. Tfh matures and enters the GC where similar continued interaction with GC B cells leads to differentiation of B cells into memory B cells and long-lived plasma cells with additional co-stimulation from the cytokines IL-6 and IL-21.

MHC II - major histocompatibility complex II, ICOS - inducible T-cell co-stimulator, IL- interleukin, CCR/CXCR chemokine receptors, TCR- T cell receptor

(Created with Biorender.com)

Before introducing the research aims, current literature on cellular responses induced by HPV vaccination will be discussed.

1.5.5 HPV vaccine induced-cellular immunity

Few studies have reported cellular immune responses including T and B cells, generated by HPV vaccination. HPV 16 L1 vaccine induced a broad spectrum of both innate and adaptive cytokines including inflammatory (IL-1b and IL 8), Th1 (IFN γ , TNF- α , IL-12 and GM CSF) and Th2 (IL- 4, IL-5, IL-6 and IL-10) responses which played an important role in robust activation of B cells to produce the desired high titres of HPV neutralising antibodies and Th responses.(Pinto et al., 2005, Pinto et al., 2003, Pinto et al., 2006) HPV specific memory B cells are detectable in circulation after vaccination and can mount a fast recall response upon HPV re-encounter.(Siegrist, 2008, Scherer et al., 2014a, Scherer et al., 2016, Scherer et al., 2018, Nicoli et al., 2020a, Smolen et al., 2012)

A single HPV vaccine dose is able to boost recall response and improve the quality of memory B cells in previously infected subjects.(Scherer et al., 2016) Vaccination boosted memory B cell numbers 3- to 27-fold (median 6-fold) with neutralizing capacity of vaccine-induced antibodies significantly higher than those induced by natural infection and led to increased antibody responses.(Scherer et al., 2016) Characterisation of HPV 16 specific memory B cells elicited by vaccination in female adolescents and young women without pre-existing immunity using fluorescently labelled HPV 16 pseudovirions identified HPV 16 specific memory B cells by flow cytometry.(Scherer et al., 2014a) Ig transcriptomic data showed that antibodies cloned from HPV specific memory B cells were mainly of the IgG isotype, followed by IgA and IgM isotypes and used diverse heavy chain genes.(Scherer et al., 2014a) The cloned antibodies potently neutralized HPV 16 in vitro despite low levels of SHM.(Scherer et al., 2014a)

An exploratory study evaluated Tfh cell response to Gardasil and Cervarix vaccines and reported higher Tfh1 responses at day 7 post the first dose than post the third dose.(Matsui et al., 2015) The first Cervarix dose also induced Tfh17 which were not observed in response to Gardasil vaccination.(Matsui et al., 2015) The ASO4 adjuvant used in Cervarix induces potent pro-inflammatory response which may be responsible for secretion of IL-17

promoting differentiation of CD4 T cells to Tfh17. Another study comparing CD4+ T cell cytokine responses between Cervarix and Gardasil, 12 months post-vaccination showed increased IL-2 and TNF- α in the Cervarix group unlike the Gardasil group and this was consistent across all 4 tested HPV types (HPV 16, 18, 33 and 45). (Herrin et al., 2014) Elevated levels of circulating plasma cytokines and chemokines were observed after the first vaccination dose in Gardasil recipients and proinflammatory cytokines were elevated following first and third doses of Cervarix vaccination. (Herrin et al., 2014) Higher CD4+ T cell responses were achieved with Cervarix after 3 doses, but despite these differences, similar affinity maturation was measured for both vaccines. (Herrin et al., 2014) These vaccine-induced cellular differences may explain the differences in antibody titres discussed earlier, and while clinical implications for these differences are unknown, importantly, both vaccines show equal protection against HPV 16 and 18 infection. (Toft et al., 2014)

No studies reported LLPCs from HPV vaccination, obvious challenge being their homing in the bone marrow. (Schiller and Lowy, 2018b) Additionally, mouse models do not live long enough and are therefore not considered reliable for characterisation of LLPCs. (Schiller and Lowy, 2018b) However, antibody profiles generated from HPV vaccination suggest that LLPCs may be the key mediators of the vaccine protection. (Stanley, 2010b, Schiller and Lowy, 2018b) While memory B cells may be important in long-term HPV vaccine protection, antibody titres are maintained at very high levels presumed to be able to neutralise new invading HPV virus before binding to the host cells to activate immune memory.

LLPCs last long and continue to secrete antibodies in the absence of memory B cells in the absence of further antigenic stimulation. (Miller, 1964, Manz et al., 1997) Memory B cells are also long-lived but to be considered as a source of long-term protection, a direct correlation between their numbers and antibody levels in circulation may be expected, with possible increases in both memory and antibody levels in cases of antigen re-encounter. One observational study compared memory B cells and antibody responses induced by the Cervarix and Gardasil vaccines and reported no correlation between these responses at 4 to

6 years following completion of the vaccination schedule in adolescents and adult women.(Nicoli et al., 2020b) This lack of correlation between vaccine-induced memory B cells and antibody titres indicated these immune responses were independently generated, suggesting LLPCs to be the source of long-term HPV vaccine induced antibody titres.(Nicoli et al., 2020b).

Several potential mechanisms for maintenance of long-term antibody protection by HPV vaccines have been suggested.(Stanley, 2010d, Schiller and Lowy, 2018b) These include; the polyvalent VLP with particulate 55nm structure and repetitive array of epitopes on their surface that binds strongly to innate cells (monocytes, macrophages and DCs), activating them to release cytokines required for strong initial immune activation.(Lenz et al., 2003) The VLP small size is efficiently processed by these phagocytic cells and presented for T cell activation to generate potent Th responses.(Bachmann and Jennings, 2010) The small VLP size can traffic to lymph nodes efficiently to activate naïve B cells and the close surface arrangement of the VLP molecules can bind low avidity natural IgM to activate the complement system, promoting VLP acquisition by FDCs in the lymph nodes.(Reddy et al., 2006, Link et al., 2012) Additionally, the repetitive HPV VLP epitopes are believed to be able to strongly crosslink BCRs generating strong activation signals.(Stanley, 2010d, Schiller and Lowy, 2018b)

The antigen specific plasma cell population identifiable in circulation at its peak following vaccination could constitute both short-lived plasma cells and LLPCs transitioning from the secondary lymphoid organs to the bone marrow. Indeed, murine studies on viral infections such as lymphocytic choriomeningitis virus reported that antigen specific plasma cells peak at the spleen around 8 days after primary vaccination and during this time, they were not detectable in the bone marrow. Subsequently, as they started to decline in the spleen and lymph nodes, they started to appear and accumulate in the bone marrow.(Slifka et al., 1995, Bachmann et al., 1994, Hyland et al., 1994, Smith et al., 1997)

1.6 General project aim

This PhD project aimed to characterise B cell and Tfh cell responses to HPV vaccination and to evaluate the effect of age and dose number on the vaccine immunogenicity. This was performed by analysing samples collected in a randomised phase III clinical Trial of the nine-valent HPV vaccine (Gardasil 9) and the data generated here was compared with antibody responses data from the main trial. The specific objectives of this work are as follows:

1.6.1 Specific objectives

- i) To enumerate HPV 16 and HPV 18 specific IgG and IgM plasma cells and determine the phenotype and frequency of total IgG and IgM plasma cells in peripheral blood before and after 1- or 2/3*-doses of Gardasil 9 in females aged 4 to 26 years.
- ii) To determine the frequency of HPV 16 and HPV 18 specific IgG memory B cells in peripheral blood before and after 1- or 2/3*-doses of Gardasil 9 in females aged 4 to 26 years.
- iii) To determine the phenotype, frequency and immunoglobulin heavy and light chain repertoire of HPV 16 specific memory B cells in peripheral blood before and after 1- or 2/3*-doses of Gardasil 9 in females aged 4 to 26 years.
- iv) To determine the phenotype and frequency of total and HPV 16 and HPV 18 specific Tfh cells in peripheral blood before and after 1- or 2/3*-doses of Gardasil 9 in females aged 4 to 26 years.
- v) To compare early HPV 16 and HPV 18 specific plasma cell, memory B cell and Tfh cell responses with antibody responses measured at one month after 2/3*-doses of Gardasil 9
- vi) To evaluate the effects of age and dose number on the vaccine-induced immune responses

* 4- to 14-year-olds received 1 or 2 doses, 15- to 26-year-olds received 1 or 3 doses and the PhD work analysed samples from those who received either 2 or 3 doses.

The simultaneous characterisation of the three cell populations; plasma cells, memory B cells and Tfh cells in this research allows for a broader understanding of the cellular drivers of the excellent long-term protection observed from HPV vaccination. Such extensive characterisation of cellular immunity following HPV vaccination has not been performed before.

Additionally, the head-to-head comparison of immunity following HPV vaccination has not been performed previously between the three age groups targeted in this study. The fact that HPV vaccination has not been previously tested in the 4 to 8-year-olds means that this study will be the first to report immunity of HPV vaccines in this age group and will give insights as to whether there is a need to further investigate vaccinating this age group in the future.

2. MATERIALS AND METHODS

2.1 Study design and subjects

This PhD project was a sub-study nested within the HANDS (HPV Vaccination in Africa – New Delivery Schedules) trial, (NCT03832049), a randomized, open-label, single-centre, phase 3 non-inferiority clinical trial evaluating reduced dose HPV vaccination schedules in young females. The trial's primary objective was to demonstrate non-inferiority of the antibody titres induced by one dose compared to two doses of Gardasil 9 vaccine in young females (4-14-year-olds). Three doses already recommended in older ages (15-26-year-olds) was used as a reference for definition of non-inferiority threshold. In the entire trial, a total of 1720 participants were enrolled across three age groups and randomised to receive different dose schedules as follows: 4-8-year-olds; n = 688 to receive one (and a second delayed dose), 9-14-year-olds; n = 688 to receive one or two doses and 15-26; n = 344 to receive three doses. The study site was Soma, a rural setting in The Gambia.

The trial received ethical approval from The Gambia Government and MRC Unit The Gambia (MRCG) Joint Ethics Committee (SCC1597) (Appendix 13) and the London School of Hygiene and Tropical Medicine (LSHTM) Research Ethics Committee (LEO 16076) (Appendix 14). It also received regulatory approval from the Medicines Control Agency of the Government of The Gambia. The sub-study assays were optimised using samples collected from non-study volunteers in accordance with MRCG at LSHTM approved SOP-LAB-023_V1.0_28Nov2018.

2.2 Study vaccine formulation and administration

Gardasil 9 is a recombinant L1 VLP vaccine containing HPV types 6, 11, 16, 18, 31, 33, 45, 52 and 58 VLP. The vaccine is administered intramuscularly into the left upper arm using a 23G x 25mm needle. One dose containing 0.5 mL of the vaccine contains approximate quantities of each HPV serotype as shown (Table 2.1).

Table 2.1. Gardasil 9 vaccine formulation.

HPV serotype	Quantity of L1 protein in a 0.5 mL dose
HPV 6	30 µgs
HPV 11	40 µgs
HPV 16	60 µgs
HPV 18	20 µgs
HPV 31	20 µgs
HPV 33	20 µgs
HPV 45	20 µgs
HPV 52	20 µgs
HPV 58	20 µgs

L1 proteins are in the form of VLP produced in yeast cells (*Saccharomyces cerevisiae* CANADE 3C-5 (Strain 1985)) by recombinant DNA technology and absorbed onto amorphous aluminum hydroxyphosphate sulphate adjuvant (0.5mg aluminium).

The vaccine is licensed in both the European Union where it is marketed by Sanofi Pasteur MSD, and in the United States where it is marketed by Merck and CO., Inc. The Gambia introduced HPV national vaccination in 2019 primarily targeting girls aged 9 to 14 years to receive two vaccination doses as per the WHO recommendations at that time. The vaccine is indicated for protection against pre-malignant lesions and cancers affecting the cervix, vulva, vagina and anus caused by vaccine high-risk HPV types as well as genital warts caused mainly by HPV 6 and HPV 11.

Initially, the trial vaccination dose schedule was planned to be 0 and 6 months for the two doses given to 4-14-year-olds and 0, 2 and 6 months for the three doses given to 15-26-year-olds while a delayed second dose would be given at 36 months to the 4-8-year-olds scheduled for one dose. From this initial plan, the sub-study would include 360 participants from the main trial, with 120 participants from each of the three age groups. However,

substantial interruptions on the trial by COVID-19 pandemic warranted amendments on the entire study protocol leading to changes in the vaccination schedules: 0 and 12 months for the two doses given to 4-14-year-olds and 0, 2 and 12 months for the three doses given to 15-26-year-olds and no delayed second dose was given to the single dose 4-8-year-olds. The sub-study sample size was also adjusted downwards to 180, with 60 participants from each of the three age groups.

For the sub-study analyses, participants from the two-dose- and three-dose-schedules were randomised into three groups: A (n = 20), B (n = 20) or C (n = 20) to reduce frequency of blood sampling. The participants were bled at baseline, just before vaccination, and then at either day 2 (group A), day 7 (group B) or day 14 (group C) after the first and second dose for the two younger age groups or after first and third dose in the older age group. Group A samples were preserved for future analysis of innate immune responses which is out of the scope of this PhD work. This work analysed a total of 120 samples from groups B and C whereby group B samples were analysed for plasma cell and Tfh cell responses while group C samples were analysed for memory B cell responses as shown (Figure 2.1). All sub-study participants had their antibody responses data generated as part of the main trial. Therefore, only cellular data was generated in the PhD work and serology data obtained from the main trial for statistical comparisons with the cellular data. Table 2.2 shows the schedules for vaccination and blood sampling for both main trial and sub-study objectives.

Table 2.2. Vaccination and blood sampling schedule for main study and sub-study

Age (years)	Dose numbers	Baseline	+2, 7, 14 days	+28 Days	2 months	12 months	+2, 7, 14 days	+28 Days	18 months	36 months	+28 Days
4 to 8	1 dose	S 	S	S	-	S	S	S	S	S	S
	2 doses	S, C 	S, C	S	-	S, C 	S, C	S	S	S	S
9 to 14	1 dose	S 	S	S	-	S	-	S	S	S	S
	2 doses	S, C 	S, C	S	-	S, C 	S, C	S	S	S	S
15 to 26	3 doses	S, C 	S, C	S		S, C 	S, C	S	S	S	S

Timepoints are shown at which immunization is done and blood samples collected for serology (S) and cellular (C) assays. Serology data was used for both main and sub-study objectives while cellular data was for sub-study objectives only. Cellular responses were measured alongside serology at baseline just before vaccination and subsequently on either days 2 (frozen for future evaluation of innate responses), 7 (analysed for plasma cells and T follicular helper cell responses) or 14 (analysed for memory B cell responses). The cellular analyses performed in this study included plasma cell and T follicular helper cells at baseline (just before vaccination) and at day 7, and memory B cells at baseline (just before vaccination) and at day 14 following each vaccination dose as shown.

 - vaccination

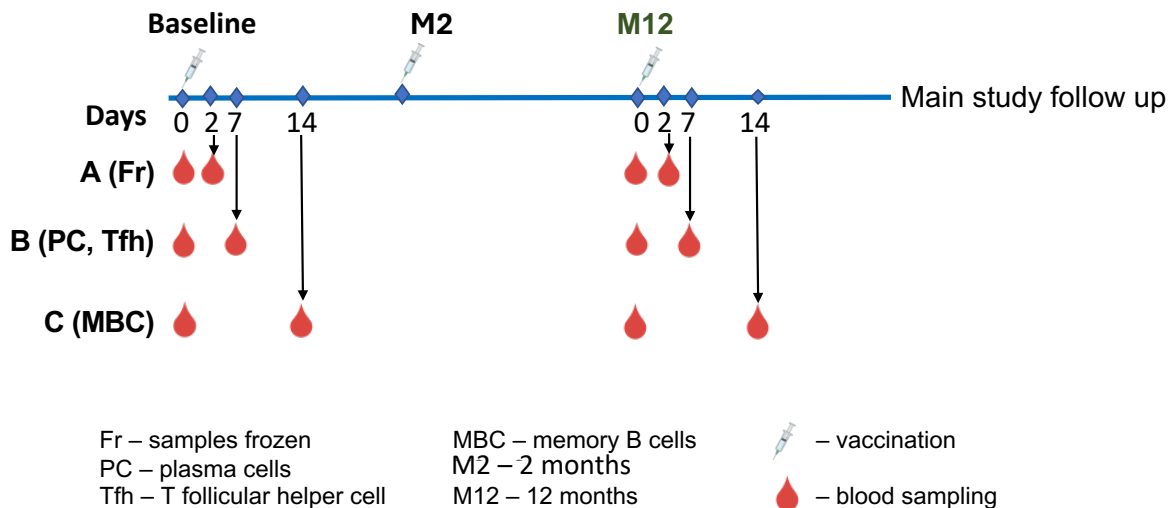


Figure 2.1. HANDS trial sub-study vaccination and blood sampling timepoints

Samples from group **B** were analysed for plasma cell and T follicular helper cell responses, group **C** was analysed for memory B cell responses at the timepoints shown. Group **A** samples were frozen for future analysis of early innate vaccine immunity. The vaccination schedule indicated (baseline, 2, 12 months) was administered to participants aged 15 to 26 years while participants aged 4 to 14 years received two doses (baseline, 12 months).

2.3 Laboratory methods

At the assays' optimisation stage, plasma cell and memory B cell responses were measured for five HPV types contained in the vaccine as part of training. However, the actual study analyses were performed for HPV 16 and HPV 18 specific responses only.

2.3.1 Isolation of peripheral blood mononuclear cells (PBMC)

Blood samples collected in sodium heparin tubes (BD Biosciences., New Jersey, US) were transported to the laboratory at room temperature (RT) within 3 to 6 hours for processing. Plasma was first separated by centrifugation at 700 g at room RT for 10 minutes and stored at -80°C. The PBMC were then isolated from the anticoagulated whole blood by density gradient centrifugation. To do this, the volume of separated plasma was first replaced with Roswell Park Memorial Institute (RPMI) medium (Sigma-Aldrich., St. Louis, US) and the blood was further diluted in RPMI medium at a 1:1 ratio before layering onto Lymphoprep (Axis-Shield., Dundee, UK) at a ratio Lymphoprep:diluted blood of 1:2. The density

centrifugation was done at 2400 revolutions per minute (RPM), with no centrifuge brake for 20 minutes at RT. The PBMC layer was then carefully aspirated and washed twice with complete culture medium (RPMI medium containing 2 mM L-glutamine, 100 U/mL penicillin, 100 µg/mL streptomycin, 10% Fetal Bovine serum (FBS) and 6mM hepes buffer (all supplied by Sigma Aldrich). Cells were finally resuspended in an appropriate volume of complete medium based on the cell pellet size to facilitate counting. Light microscopy at 40x magnification and Trypan blue exclusion method was used for cell counting.

The amount of fresh PBMC required for analysis of plasma cell and Tfh cell responses (Group B) and memory B cells (Group C) was aliquoted, and the remainder was frozen in freezing medium (10% Dimethyl Sulfoxide (DMSO) (Sigma Aldrich) in FBS for later immunophenotyping analysis. One million or at least half a million PBMC were resuspended per mL of freezing medium and frozen at -80°C.

2.3.2 ELISpot

Enzyme-Linked Immunosorbent Spot Assay (ELISpot) was used in enumeration of HPV specific IgG memory B cells. During assay optimisation, ELISpot was also used to optimise plate coating and detection conditions for enumeration of IgG and IgM plasma cell responses by FluoroSpot. Both ELISpot and FluoroSpot assays were performed using freshly isolated PBMC. (All ELISpot and FluoroSpot kit reagents were supplied by Mabtech AB, Stockholm, Sweden except where specified)

2.3.2.1 In-vitro stimulation of memory B cells

The cells to be used in ELISpot assay for enumeration of memory B cells were first stimulated in culture for 6 days using a commercial kit following manufacturer's instructions (StimPack: memory B cells, human). Following cell counting, the number of cells required for the ELISpot assay were resuspended in complete culture medium, further supplemented with sodium pyruvate (Sigma Aldrich) at a concentration of 10^6 cells per mL. Each sample was distributed into two wells of a flat-bottomed 24-well cell culture plate (Thermo Fisher Scientific., Massachusetts, USA). One well was stimulated with 10 ng/mL of R848 and 1

µg/mL of recombinant human IL-2. Cells in the second well were cultured in culture medium only without stimulation to be used as ELISpot negative controls. Figure 2.2 below illustrates memory B cell stimulation with R848 and IL-2.

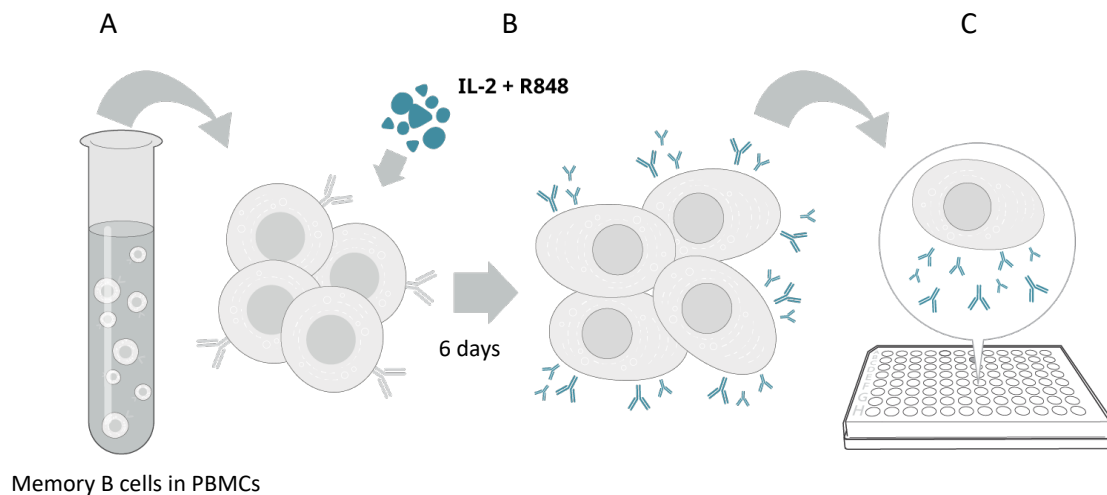


Figure 2.2. B cell stimulation by R848 and IL-2 in a 6-day culture

Polyclonal stimulation of memory B cells in PBMC leads to their differentiation into antibody secreting cells (A and B) and the antigen specific (for example HPV specific) antibodies are detected after binding to their pre-coated antigen in the plate. In this study, the plate was pre-coated with HPV virus-like particles. (Mabtech.com 2024)

<https://www.mabtech.com/knowledge-hub/step-step-guide-elispot> (accessed in May 2024)

2.3.2.2 Enumeration of HPV specific antibody secreting cells

To enumerate HPV specific IgG memory B cell (after 6-days PBMC stimulation) or HPV specific IgG and IgM PC (on freshly isolated PBMC), 96-well clear polyvinylidene fluoride (PVDF) ELISpot plates were activated with 15 µL of 35% ethanol per well for 1 minute, washed 4 times with sterile water and coated with a pre-optimised concentration (10 µg/mL) of HPV VLP (Merck Sharp and Dohme Corp., Kenilworth, USA). Positive control wells were coated with a standard concentration (15 µg/mL) of purified anti-human IgG (clone MT91/145) or anti-human IgM (clone MT22) monoclonal antibodies following manufacturer's recommendations. All antigen and antibody plate coating were performed in 100 µL of PBS and incubated overnight at -4°C. Plates were washed 5 times with sterile PBS before cells incubation. In 200 µL complete medium per well, antigen specific wells were seeded with

2.5x10⁵ cells from the 6-day culture for measurement of memory B cells or freshly isolated cells for measurement of plasma cells. 2.5 x 10⁴ cells per well were seeded in the total IgG and IgM positive control wells. Negative control wells were treated the same way as the antigen specific wells at all steps except that they were seeded with unstimulated cells from the 6-day culture. Plates were then incubated at 37°C in a humidified incubator with 5% CO₂ for 20 hours after which cells were removed and the plate washed. The detection biotinylated anti-human IgG (clone MT78/145) or IgM (clone MT22) monoclonal antibodies were added to the corresponding wells at 1 µg/mL in 100 µL of 0.5% FBS in PBS per well and incubated for 2 hours at RT. The plate was washed, and alkaline phosphatase (ALP)-conjugated streptavidin added at 1:500 dilution in 100 µL of 0.5% FBS in PBS per well and incubated for 1 hour at RT. The plate was washed, ALP substrate (nitro-blue tetrazolium chloride/5-bromo-4-chloro-3'-indolyphosphate p-toluidine salt - NBT/BCIP) was added and incubated at RT protected from light until spots formed. The plate was finally washed thoroughly in running tap water and left to air-dry protected from light before counting the spots on AID ELISpot reader (AID Autoimmun Diagnostika GMBH., Straßberg, Germany). Figure 2.3 illustrates stepwise ELISpot procedure.

Raw data for each participant was analysed as the mean spot counts from triplicate wells (R848/IL-2-stimulated antigen specific and positive control wells) or duplicate wells (unstimulated negative control wells) to reduce variation in final dataset. Since a mitogen stimulation was used for identification of the antigen specific cells, the memory B cell data was first presented alongside the signal in the negative control unstimulated cells. Subsequently, to allow objective quantification and comparisons of vaccine-induced antigen specific memory B cells, the background responses in the negative control wells were subtracted from the response in antigen specific and positive control wells. The background-subtracted antigen specific IgG memory B cell data was then analysed and presented as; (i) IgG secreting cells per million stimulated PBMC and (ii) as a percentage of total IgG secreting cells (by dividing the number of antigen specific by the total IgG secreting cells and

multiplying by 100). Reporting antigen specific memory B cells as a percentage of total IgG secreting cells adjusts for the varying proportion of B cells present in PBMC in different individuals and at different timepoints.

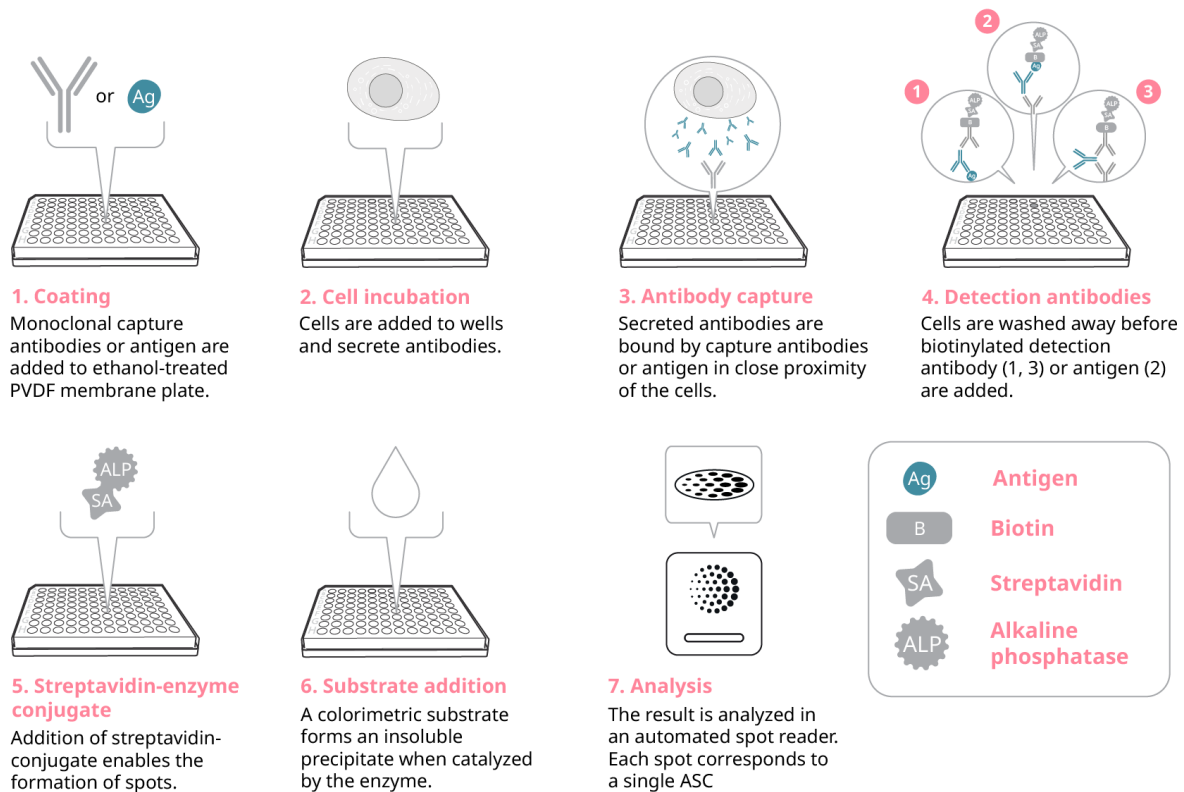


Figure 2.3. Stepwise ELISpot procedure

Vaccine-induced antibodies secreted by the cells are captured by their specific antigen coating the well (for example in this case the antigens are different HPV VLP types), and the cells are removed after incubation period. The secreted antibodies are then detected using a biotinylated detection antibody, streptavidin-enzyme conjugate, and the enzyme substrate. The enzyme-substrate reaction yields a precipitating product detected in form of spots representing individual antigen secreting cells (ASCs). (Mabtech.com)

<https://www.mabtech.com/knowledge-hub/step-step-guide-elispot> (accessed in May 2024)

2.3.3 FluoroSpot

FluoroSpot assay was used for enumeration of IgG and IgM plasma cells using conditions optimised in ELISpot as earlier indicated. Unlike memory B cells that need prior cells stimulation, plasma cells can be detected in freshly isolated cells.

To identify and enumerate HPV specific IgG and IgM antibody secreting cells IgG/IgM FluoroSpot FLEX kit was used following manufacturer's instructions. FluoroSpot plates were coated with the VLP types as described in ELISpot procedure. 2.5×10^4 cells per well for positive control wells and 2.5×10^5 cells per well for antigen-specific wells were tested for identification of IgG and IgM plasma cell responses. Positive control wells were dual coated with purified anti-human IgG (clone MT91/145) and anti-human IgM (clone MT22) monoclonal antibodies and negative control wells with PBS. The coated plates were incubated overnight and the following day the plates washed and incubated for 20 hours with freshly isolated cells. Plates were washed and fluorophore-conjugated anti-human IgG (MT78/145-550-Cy3) and IgM (MT22-490-FITC) monoclonal detection antibodies added and incubated for 2 hours. The plates were washed and incubated for 30 minutes with a fluorescence enhancer. Last wash was performed, plate air-dried and protected from light for spots reading withing 7 days. AID ELISpot reader was used to read FluoroSpot plates applying appropriate settings. Figure 2.4 illustrates stepwise FluoroSpot procedure. Due to the robust boosting of memory B cell responses, cell numbers used in antigen specific and control wells were reduced following secondary vaccination to avoid spots cluttering in the wells and to allow for their clear identification and counting.

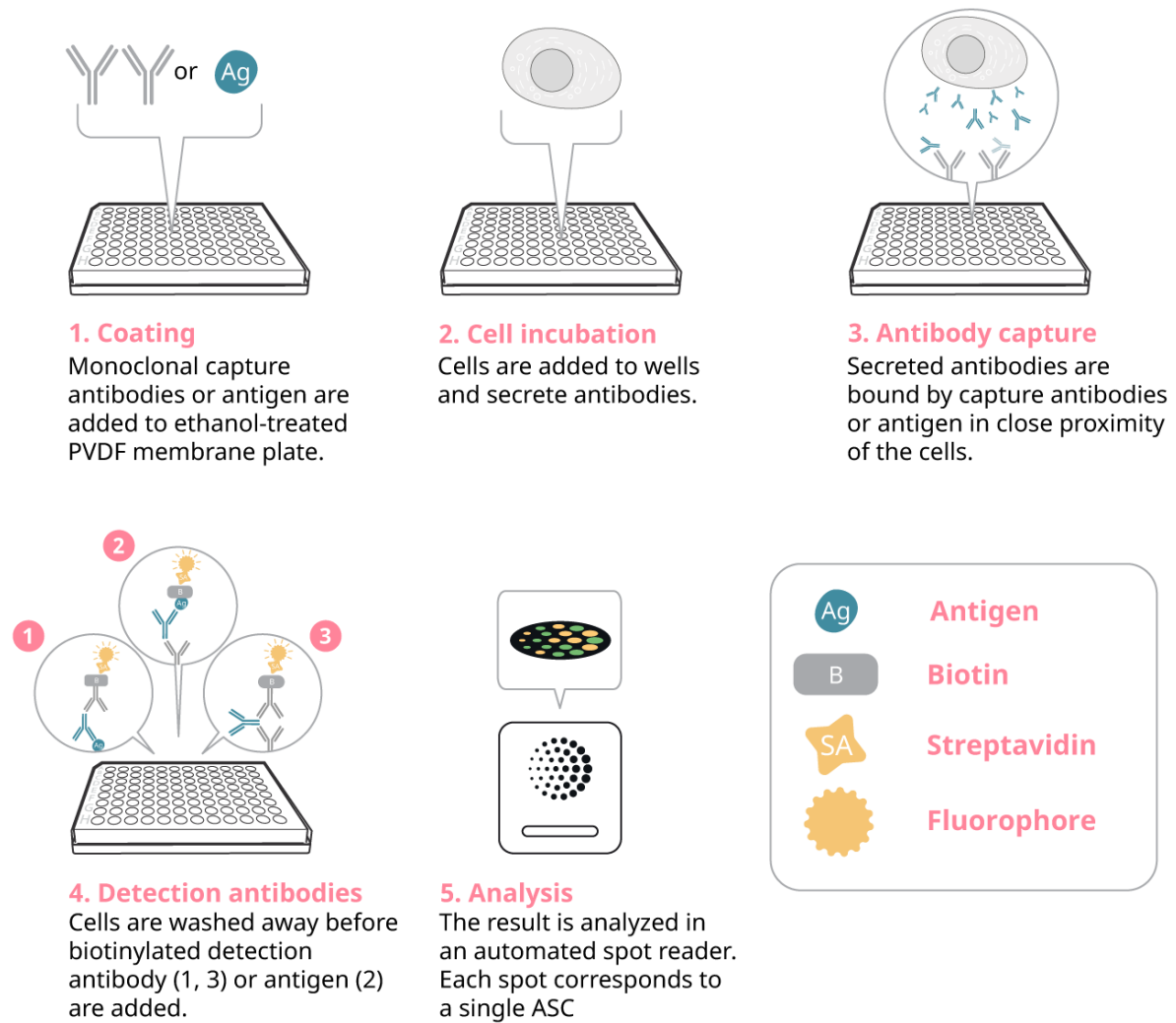


Figure 2.4. Stepwise FluoroSpot procedure

Vaccine-induced antibodies secreted by the cells are captured by their specific antigen coating the well (for example in this case the antigens are different HPV VLP types), and the cells are removed after incubation period. The secreted antibodies are then detected using fluorophore-conjugated anti-human IgG (MT78/145-550-Cy3) and IgM (MT22-490-FITC) monoclonal antibodies and incubated with fluorescence enhancer. The spots are then detected in different fluorescent colours representing individual antigen secreting cells (ASCs). For example, this study used the fluorophores Cy3 for IgG detection as red spots and FITC for detection of IgM as green spots. (Mabtech.com)

<https://www.mabtech.com/knowledge-hub/step-step-guide-fluorospot> (accessed in May 2024)

For both ELISpot and FluoroSpot, assay success was defined by detection of 5 or more spots in the positive control wells. Raw data for each participant was analysed as the mean spot counts from triplicate wells (for antigen specific and positive control wells) or duplicate wells (for negative control wells) to reduce variation in final dataset. Background (spot numbers from negative control wells) was subtracted from the antigen specific or positive control wells before statistical analysis. Plasma cell response was reported as antibody secreting cells per million analysed PBMC.

2.3.4 Flow cytometry

Flow cytometry was used to immunophenotype and determine the frequencies of circulating plasma cells and Tfh cells before and after Gardasil 9 vaccination and for single cell sorting of memory B cells. Four antibody panels were developed to identify the frequencies of different circulating cell populations as follows:

- i) Plasma cell panel: Total IgG plasma cells
- ii) Tfh cell activation-induced-marker (AIM) panel: HPV 16 and HPV 18 specific in vitro stimulated Tfh cell frequencies
- iii) Tfh cell ex vivo panel: Frequencies of total pool of ex vivo stimulated Tfh cells
- iv) Memory B cell single cell sorting panel: sorting of single HPV 16 specific memory B cells

Suppliers for all antibodies used in these panels are listed in chapter 2.

Initial optimisation of the flow cytometry assays was performed on fresh whole blood as was the plan on the study protocol. However, following COVID-19 interruptions, it became necessary to adapt the assays for staining frozen PBMC. This allowed for fast recruitment into the study (when this became possible), with only ELISpot and FluoroSpot analysis performed on fresh PBMC.

Both staining of whole blood and PBMC will be considered in the step-by-step procedures described next highlighting adjustments made to the whole blood staining protocol to adapt it

for staining frozen PBMC. Analysis of frozen samples provided an advantage to control for day-to-day assay variability by analysing both baseline and post-vaccination samples in the same experiment.

2.3.4.1 Whole blood staining for plasma cell immunophenotyping

One hundred microlitres of heparinised blood was aliquoted into 5 mL FACS tubes (BD Biosciences., New Jersey, US) and diluted in 100 μ L of complete culture medium without FBS. Red blood cells (RBC) were lysed at RT for 15 minutes using 3.5 mL of 1X Pharm Lyse buffer (BD Biosciences) and cells washed twice with FACS staining buffer (1x PBS, 2% FBS, 0.1% EDTA and 0.05% sodium azide (all supplied from Thermo Fisher Scientific., Massachusetts, US) followed by two more washes with PBS.

After RBC lysis, cells were stained with Zombie Aqua viability (BD Biosciences) dye for 20 minutes at RT followed by surface staining with a cocktail of antibodies at pre-optimised dilutions for 20 minutes. Normal mouse serum (NMS) was added to the antibody cocktail to prevent non-specific binding, and brilliant stain buffer plus to improve resolution between brilliant violet fluorochromes. A dump channel V500 was used to exclude T cells (CD3+), monocytes (CD14+) and dead cells by the Zombie Aqua viability dye.

After surface staining, cells were washed twice with FACS buffer (then fixed and permeabilized using the BD transcription factor buffer set (BD Biosciences) following manufacturer's instructions for subsequent Blimp-1 intracellular staining (ICS). After Blimp-1 staining, cells were washed twice in Perm/Wash buffer before resuspension in PBS for acquisition.

2.3.4.2 PBMC thawing and staining for plasma cell immunophenotyping

To prepare for the PBMC thawing, both an incubator with 5% CO₂ supply and a clean water bath were set at 37°C. Two 10 mL aliquots of thawing medium (complete culture medium) at 37°C were prepared in 15 mL falcon tubes for each sample. The thawing medium was kept in the incubator until use to maintain it at 37°C. One of the aliquots was supplemented with benzonase nuclease (Merck Millipore., Massachusetts, US) at 50 units per mL of thawing

medium to minimise cell clumping during thawing. PBMC samples to be analysed for the day were retrieved from -80°C and kept on dry ice briefly before thawing. Two 1 mL vials of PBMC were thawed at a time in the water bath for two minutes and vials wiped dry using 70% ethanol before transferring them to a sterile safety hood. The cells were transferred into a sterile 15 mL falcon tube where the benzonase-supplemented thawing medium was added immediately in a dropwise manner. The cells were then centrifuged at 400 g for 8 minutes, thawing medium discarded and the non-supplemented thawing medium used to wash them by centrifugation at the same conditions. Finally, the wash medium was discarded, and cells resuspended at 10^6 cells per mL of complete culture medium and incubated in the 37°C incubator for 2 hours before staining. Trypan blue exclusion was then used to count the cells. Counted cells were distributed in one million cells per well into three 96-well plates for staining with three antibody panels including plasma cell, Tfh ex vivo and Tfh AIM panels. The number of wells stained for each assay depended on the conditions to be tested. Details of the antibodies used in the three antibody panels are presented in chapter 3.

One million PBMC in 100 μL of PBS per well were stained in 96-well plates first with Zombie Aqua viability dye as described earlier and washed twice in PBS before surface staining with antibody cocktail at dilutions optimised on whole blood. The only difference between plasma cell staining in whole blood and PBMC was the staining of PBMC in 96-well plates and whole blood in 4 mL FACS tubes.

2.3.4.3 Whole blood staining for immunophenotyping of total Tfh cells ex vivo

Unlike in the plasma cell panel, ex vivo staining of Tfh cells in whole blood was performed before RBC lysis. 200 μL of heparinised blood was first stained with Zombie Aqua viability dye for 20 minutes at RT. Cells were stained for CXCR5 at 37°C in a humidified incubator with 5% CO_2 for 15 minutes. The cocktail of surface staining antibodies was added and incubated further at RT for 20 minutes. Lysis of RBC was then performed as earlier described followed by three washes and resuspension in 300 μL FACS buffer for acquisition.

2.3.4.4 PBMC staining for immunophenotyping of total Tfh cells ex vivo

PBMC thawing and viability staining were performed as earlier described. CXCR5 was then stained for 15 minutes at 37°C in a humidified incubator with 5% CO₂. A cocktail of antibodies for all other surface markers was then added and incubated further for 20 minutes at RT. Fully stained cells were washed twice and resuspended in 300 µL of FACS buffer for acquisition.

2.3.4.5 Whole blood T cell stimulation and staining for identification of HPV 16 and HPV 18 specific Tfh cells

Four 5 mL FACS tubes each containing heparinised blood were analysed for different stimulation conditions. The whole blood was diluted in complete medium without FBS as described in whole blood plasma cell staining. Cells in three tubes were then stimulated with either 15 µg/mL of HPV 16, 15 µg/mL of HPV 18 VLP or 1 µg/mL (Merck Sharp Corp.) of Staphylococcus Enterotoxin B (SEB) (Sigma Aldrich) for 18 hours at 37°C in a humidified incubator with 5% CO₂. Cells in the fourth tube were cultured in complete medium without stimulation. The mitogen SEB was used as a positive control while cells cultured without stimulation were used as a negative control. Expression of the Tfh cell marker, CXCR5 can be downregulated in culture stimulation and was therefore stained at two levels, first during the 18-hour stimulation and secondly just before surface staining of all other markers as has been described for the ex vivo panel. After stimulation, cells were directly stained with Zombie Aqua viability dye followed by CXCR5 and surface staining antibody cocktail. Lysis of RBC was then performed. Cells were washed twice with FACS buffer before fixation and permeabilization using human FoxP3 staining kit (BD Biosciences) following manufacturer's instructions before FoxP3 ICS staining. Lastly, fully stained cells were washed and resuspended in 300 µL of FACS buffer for acquisition.

2.3.4.6 PBMC stimulation and staining for immunophenotyping of HPV 16 and 18 specific Tfh cells

Very minimal adjustments were made on the whole blood Tfh cell staining protocol to adapt it to PBMC staining. PBMC thawing and viability staining, T cell stimulation and both surface

and intracellular staining were performed as described earlier. Fully stained cells were then washed and resuspended in 300 μ L of FACS buffer for acquisition.

2.3.4.7 Data acquisition on LSR Fortessa III cytometer

Data acquisition for the plasma cell and Tfh cell antibody panels was performed using a 4-laser (2-3-3-6) configuration of the LSR III Fortessa flow cytometer (BD Biosciences). The cytometer can measure 14 fluorescent parameters simultaneously. Photomultiplier tubes (PMT) voltages were initially optimized using the 2.5x rSD_{EN} rule using RBC-lysed unstained blood, and later using PBMC. These optimized parameters were saved as application settings and were applied in subsequent experiments for analysis of all samples in the longitudinal study. Using application settings standardizes flow cytometry assays by updating the optimized PMT voltages to account for changes in cytometer's daily performance. The target values for each antibody panel were set and updated using Rainbow beads (BD Biosciences) after every six months new cytometer baseline. FACS Diva software was used for initial analysis during acquisition to confirm that cell population profiles looked as expected. A minimum of 100,000 total live events and 10,000 lymphocytes were acquired for each sample to allow for robustness in identification of target cell populations. FCS files exported from FACS Diva were further analysed on FlowJo v10.10.0 Software (BD Life Sciences). FlowJo-identified cell frequencies were exported in CSV formats for subsequent statistical analyses.

2.3.4.8 Measurement of antibody response using Competitive Luminex immunoassay

Antibody responses were measured commercially as part of the main trial thus this procedure was not performed as part of this PhD. This is included to provide information on the principle of Competitive Luminex immunoassay applied commercially.

Blood samples were collected in BD Vacutainer Venous Blood Collection Tubes: SST Serum Separation Tubes (BD Biosciences) and transported to the lab. Serum was separated by centrifugation at 1000 g for 10 minutes at room temperature. Separated serum was then distributed into individual cryovials of 400 μ L aliquots to minimize any requirement for

unnecessary freeze-thaw cycles. The serum samples were shipped to an external laboratory where antibody responses were measured using an established competitive Luminex immunoassay for measurement of HPV specific antibody responses.(Roberts et al., 2014) The assay uses yeast-derived VLPs for the nine HPV types (HPV 6, 11, 16, 18, 31, 33, 45, 52, and 58) contained in the 9- valent vaccine and measures the specific antibodies to neutralizing epitopes on the VLPs from serum samples. The VLPs are coupled to a distinct fluorescent Luminex microsphere. Antibody concentrations are determined in a multiplexed direct binding format by measuring the amount of VLP-specific IgG bound to the VLP-microspheres.

To measure anti-VLP specific IgG titres after Gardasil 9 vaccination, the assay was performed in a 96 well microtiter filter plate including a 12-point standard reference serum pool from adult females who received the vaccine, four controls (high, medium, low and negative) and 16 samples in duplicate. Samples were tested at 1:100 and 1:10,000 dilutions. To each well was added the VLP microspheres for the nine HPV types included in the assay. The plates were sealed, covered with foil and incubated for 15 to 60 minutes. The contents of the filter plate were washed and incubated with the mouse anti-human IgG 1 to 4 monoclonal antibody conjugated to PE. The plates were covered with foil and incubated for an additional 30 to 60 minutes. Following the second incubation period, the plates were washed 3 times, and the samples analysed on a Luminex instrument. A fluorescent signal from an anti-human IgG detection antibody that binds directly to serum IgG and equally to each IgG subclass (1 to 4), was directly measured on the Luminex instrument. The fluorescent signal from the IgG-bound fluorescent detection antibody is proportional to the individual's anti-VLP IgG antibody levels. The results are expressed in arbitrary milli-Merck Units per millilitre (mMU/mL).

The antibody data from baseline (month 0) and post-completion of vaccination schedule (12 months plus 4 weeks) was available for statistical analysis and comparison with cellular responses as part of the PhD work. The HPV 16 and HPV 18 specific IgG GMTs were

presented per age groups. Antibody titres were compared with plasma cell, memory B cell and Tfh cell responses.

2.3.4.9 Single cell sorting of HPV 16 specific memory B cells

The plasma cell antibody panel was adapted to the FACS Melody cell sorter (BD Biosciences) configuration by leaving out some of the antibodies and using only those able to target memory B cell markers. Fluorescently labelled HPV 16 and HPV 18 VLPs (Fred Hutchison Cancer Centre) were included in the panel for identification and single cell sorting of antigen specific memory B cells. Anti human-IgD antibody was included in the panel to exclude naïve B cells, allowing for better identification of memory B cell population. Staining of memory B cells initially on PBMC was performed as earlier described for the plasma cell panel except for the different antibodies included in the surface staining cocktail. From the assay optimisation experiments, HPV 18 VLP binding was highly non-specific producing very high staining background, hence was excluded from subsequent analyses. The protocol was later improved by including a B cell isolation step prior to staining to minimise cell deaths during the single cell sorting procedure. PBMC were thawed as earlier described and B cells isolated using magnetic activated cell sorting (MACS) B cell isolation kit (Miltenyi Biotec Inc., Auburn, US) before staining. Isolated B cells were counted and stained for viability using zombie Aqua. Surface staining was then performed at 4°C using a cocktail of antibodies at pre-optimised dilutions including the fluorescently labelled HPV VLPs. Fully stained B cells were washed twice and resuspended in 3 to 4 mL of PBS for sorting.

HPV 16 specific memory B cells were singly sorted into 96-well plates for sequencing of paired IGH and IGK/L chains using iPair technology (iRepertoire Inc. Huntsville, AL, USA) Annotated sequence data was exported in CSV formats for subsequent statistical analyses.

After single cell sorting, subsequent analysis for B cell repertoire mapping was performed commercially (iRepertoire Inc.,) and therefore this section discusses the principle of the repertoire mapping technology applied.

2.3.4.10 Heavy and light chains Arm-PCR amplification

The singly sorted HPV 16 memory B cells were shipped to an external laboratory where iPair arm-PCR was then performed in two steps as follows:

- i) Highly sensitive PCR1: Real Time-PCR1 (RT-PCR1) and PCR1 rescue steps are performed directly on each well without the need for RNA extraction. This uses nested inside and outside primers to selectively amplify all V and C genes and to incorporate communal adaptors.
- ii) Highly specific PCR2: PCR2 is performed using the iDual PCR Plate which allows for tagging of individual wells with Illumina indices to allow for pooled sequencing and subsequent demultiplexing for data analysis. Only target amplicons containing 5' and 3' communal adapters following rescue are exponentially amplified in PCR2.

The multiplex primer mixes used are designed to balance the amplification of both IGH and IGL loci simultaneously in the same PCR well in a low reaction volume. The PCR amplicons are then sequenced using the Illumina MiSeq (Illumina., California, US) platform with more than 500 cycle sequencing kits to allow for calling of the variable region sequences and a segment of the C region for isotype inference.

2.3.4.11 iPair sequencing of paired B cell heavy and light chains

PCR products were cleaned up and quality control performed to confirm expected amplicon sizes were present for sequencing. Amplicon sequencing was performed on the Illumina MiSeq Nano kit covering complementarity-determining (CDR) regions 1, 2 and 3 (CDR1, CDR2, and CDR3). iPair sequencing steps are outlined (Figure 2.5).

The raw sequence data was analysed on iPair 2.4.4.0 Analyzer software (iRepertoire Inc.)



Figure 2.5. iPair B cell sequencing steps

Step 1: FACS Melody cell sorter was used to singly sort HPV 16 specific memory B cells into 96-well plates. Step 2: Arm-PCR was used to amplify the light and heavy chain regions and to index the samples as earlier described. Step 3: Illumina MiSeq sequencing was used for amplicon sequencing of complementarity-determining regions 1, 2 and 3. Step 4 – Sequence data is displayed in a plate format using iPair analysis software. Sequence information in each well can be displayed by clicking on it and can be retrieved for further analysis. (Adapted from iRepertoire, Inc.)

2.4 Statistical analysis

All datasets analysed in this work were first collated in CSV formats for statistical analyses on GraphPad Prism V10.2.2 for Mac. Non-normal data was log-transformed to restore normality. For datasets with many 0 'zero' values at pre-vaccination timepoints, a constant (+1) was added to the absolute values before log-transformation.

For plasma cell, memory B cell and Tfh cell analyses, the data was first pooled for the three age groups to evaluate the overall effect of vaccination dose number using One-way ANOVA with Dunnett's corrected multiple comparisons. Two-way ANOVA was then used to compare responses by age and dose in the age-stratified dataset with Tukey corrected multiple comparisons.

One way ANOVA with Dunnett's corrected multiple comparisons was used to compare antibody responses by age.

Pearson correlation analysis was performed to compare antigen specific plasma cells with corresponding Tfh cell responses. It was also used to compare antigen specific antibody titres with corresponding plasma cell, memory B cell and Tfh cell responses. The specific statistical comparisons performed are detailed in table 2.3.

HPV 16 and HPV 18 specific responses were considered independently and analysed separately to address distinct questions as outlined in the objectives. For all tests, a p value of ≤ 0.05 is used to indicate statistical significance.

Table 2.3. Statistical comparisons

Specific comparisons
<p>Number of HPV 16 and HPV 18 specific and total IgG and IgM plasma cells: Analysed as pooled and age-stratified</p> <ul style="list-style-type: none"> - Baseline versus 7 days after dose 1 (All age groups) - Baseline versus 7 days after dose 2 (4-8- and 9-14-year-olds) - Baseline versus 7 days after dose 3 (15-26-year-olds)
<p>Number of HPV 16 and HPV 18 specific and total IgG memory B cells: Analysed as pooled and age-stratified</p> <ul style="list-style-type: none"> - Baseline versus 14 days after dose 1 (All age groups) - Baseline versus 14 days after dose 2 (4-8- and 9-14-year-olds) - Baseline versus 14 days after dose 3 (15-26-year-olds)
<p>Frequencies of total IgG+ and IgM+ plasma cells: Analysed as pooled and age-stratified</p> <ul style="list-style-type: none"> - Baseline versus 7 days after dose 1 (All age groups) - Baseline versus 7 days after dose 2 (4-8- and 9-14-year-olds) - Baseline versus 7 days after dose 3 (15-26-year-olds)
<p>Frequencies of HPV 16 and HPV 18 specific in vitro stimulated Tfh cells: Analysed as pooled and age-stratified</p> <ul style="list-style-type: none"> - Baseline versus 7 days after dose 1 (All age groups) - Baseline versus 7 days after dose 2 (4-8- and 9-14-year-olds) - Baseline versus 7 days after dose 3 (15-26-year-olds)
<p>Frequencies of ex vivo stimulated Tfh cells: Analysed as pooled and age-stratified</p> <ul style="list-style-type: none"> - Baseline versus 7 days after dose 1 (All age groups) - Baseline versus 7 days after dose 2 (4-8- and 9-14-year-olds) - Baseline versus 7 days after dose 3 (15-26-year-olds)
<p>Pearson correlation between number of HPV 16 and HPV 18 specific IgG plasma cells and frequencies of HPV 16 and HPV 18 specific Tfh cell frequencies, 7 days after complete vaccination schedule</p>
<p>Pearson correlation between HPV 16 and HPV 18 specific GMTs, 4 weeks after completion of vaccination schedule and:</p> <ul style="list-style-type: none"> - HPV 16 and HPV 18 specific plasma cells, 7 days after complete vaccination schedule - HPV 16 and HPV 18 specific memory B cells, 14 days after complete vaccination schedule - HPV 16 and HPV 18 specific Tfh cells, 7 days after complete vaccination schedule
<p>Effect of age and vaccination dose numbers on all measured immune responses were evaluated</p>

Statistical correction for multiple comparisons was incorporated in the analysis models used as appropriate. Statistical significance was defined by a p value ≤ 0.05 .

2.4.1 Sample size and statistical power considerations

This was an exploratory study whose sample size was determined based on feasibility and availability of resources and was initially planned to include 120 participants per age group which would allow randomisation of 40 participants in each of groups A, B and C for evaluation of the different cell responses as earlier indicated. Following COVID-19 pandemic interruptions, adjusting the sample size downwards to 60 participants per age group allowed for randomisation of 20 participants in each of groups A, B and C. The sample size analysed per age group was therefore as shown in table 2.4 below.

Table 2.4. Number of samples analysed by age and dose number

Age group (years)	Number of doses	Samples analysed for plasma cell and Tfh cell responses	Samples analysed for memory B cell responses
4 to 8	2	n = 20	n =20
9 to 14	2	n = 20	n = 20
15 to 26	3	n = 20	n = 20

Previous exploratory studies using similar sample sizes or even less have been able to detect the responses targeted in this study after vaccination. For example a previous influenza vaccination study (n = 14) was able to identify antigen specific IgG and IgM antigen secreting cells using ELISpot assay.(Cox et al., 1994) A previous study (n =10) using the T cell AIM assay was able to identify antigen specific T cell frequencies in circulation after primary and secondary pertussis vaccination.(Dan et al., 2016) This was based on co-expression of OX40 and CD25, and CD25 and PD-L1 AIM markers also used in this work. Another small study (n = 29) was able to identify vaccine-induced HPV 16 and HPV 18 specific antibody titres as well as Tfh cells and memory B cell responses after vaccination with Cervarix and Gardasil vaccines.(Matsui et al., 2015)

The sample size used in this PhD work was therefore believed to be sufficient for identification of vaccine-induced immune responses. Additionally, since the same responses were measured across the three age groups, the pooled analysis for all age groups allowed more sample size power to evaluate the effect of dose number.

3. ASSAY DEVELOPMENT

This chapter describes comprehensive optimisation of all the assays (ELISpot, FluoroSpot, B cell and Tfh cell flow cytometry panels) used to generate the presented data except for the single cell sorting of HPV 16 specific memory B cells which will be discussed in chapter 7. Application of optimised assays in generating the data presented in this thesis was important to ensure:

- The ELISpot and FluoroSpot assays identified ASC accurately by using optimal plate coating and detection conditions as well as optimal automated reader settings.
- The flow cytometry panels allowed for optimal resolution to identify targeted cell populations.
- Efficiency, save time (since at least two assays were performed on the same day) and to reduce cost. ELISpot was used to optimise plate coating conditions that were also applied in FluoroSpot, saving time and cost.
- Reproducibility across different experiments was maintained as this is a longitudinal study. Optimised ELISpot reader settings and flow cytometry acquisition application settings for all panels needed to be set up before the study started to be applied throughout the study. This allowed for automatic updating of the settings based on daily flow cytometer changes.

3.1 ELISPot and FluoroSpot

3.1.1 Introduction

ELISpot and FluoroSpot assays use the same principle and can be used to identify and enumerate cells secreting antibodies against a specific antigen after infection or vaccination. Plasma cells are readily detectable in systemic circulation around day 5 to 10 after vaccination while memory B cells are quiescent and need to be stimulated in culture to differentiate into ASCs for detection. Using ELISpot, cells secreting only one antibody isotype can be identified and enumerated. The FluoroSpot assay on the other hand is a

modification of ELISpot detection system that utilizes fluorophore conjugated detection antibodies enabling simultaneous identification of cells secreting up to 4 different antibody sub-classes or isotypes. This chapter describes results obtained from the development and optimisation of the ELISpot and FluoroSpot assays highlighting decisions made at each step towards a final combination of experimental conditions for objective identification of vaccine-induced immune responses. Given the similarity between ELISpot and FluoroSpot, ELISpot optimisation was used to determine optimal cell numbers and HPV VLP concentrations to be used subsequently in both assays. This minimised the number of cells required at the assay development stage. To optimise ELISpot and FluoroSpot assay conditions, one adult healthy volunteer was vaccinated with Gardasil 9 vaccine and cellular responses measured to achieve the specific aims below.

3.1.2 Aims

- i) Determine optimal cell numbers to be used in positive control total IgG and total IgM wells
- ii) Determine optimal plate coating concentrations for HPV 6, 16, 18, 33, and 52 VLP antigens
- iii) Determine the kinetics of HPV specific plasma cell and memory B cell responses in the first two weeks after primary vaccination with Gardasil 9

3.1.3 Results and discussion

3.1.3.1 Optimal cell numbers in total IgG and total IgM wells

To determine optimal cell numbers to be used in the ELISpot and FluoroSpot positive control wells, total IgG and IgM plasma cell responses were measured across 6 timepoints within the first two weeks of vaccination. Four cell dilutions (2.5×10^5 , 1.0×10^5 , 2.5×10^4 and 1.0×10^4 cells in 200 μ L of culture medium per well) were tested across these timepoints. The number of total IgG and IgM plasma cells were detected at increasing trends with increasing cell numbers and peaked at day 7 after vaccination (Figure 3.1).

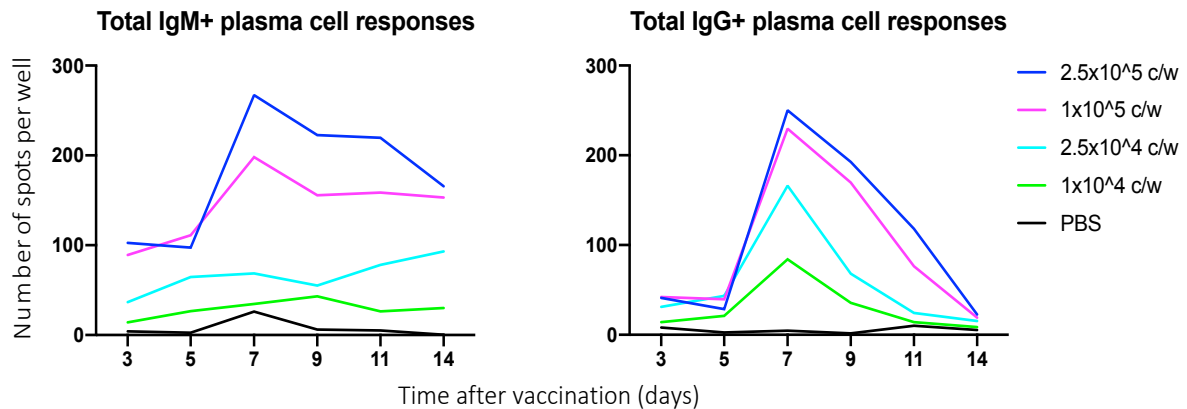


Figure 3.1. Total IgG and IgM plasma cell responses detected using different cell numbers per well in the first two weeks after first dose of Gardasil 9 vaccination

ELISpot plates were pre-coated with either anti-human IgG, anti-human IgM antibody or PBS. The total IgG and IgM wells were then seeded with freshly isolated PBMC in duplicates of 4 different cell numbers/well while PBS wells were seeded with 2.5×10^5 cells/well and cultured for 20 hours. After culture, the number of spots (representing antibody secreting cells) were detected and enumerated using an automated ELISpot reader. Data are shown as mean spot counts from duplicate wells of total IgG and IgM from day 3 to day 14 after Gardasil 9 vaccination of one donor.

Highly reproducible spot numbers were detected in duplicate wells with PBS-precoated wells showing very low background as shown for day 7 (Figure 3.2A & B). Accurate spot counts were verified using the spots reader function to highlight actual counted spots with small red stars (Figure 3.2C). For accurate counts, a single star sits on every clearly observable spot. Where the counting was inaccurate, some spots are left out without any stars on them, so they are not counted (undercounting) and is usually the case when the spots are too numerous to count (TNTC), beyond the maximum reader counting threshold. At day 7, accurate spot counts were observed from 1.0×10^4 and 2.5×10^4 cells, and they became TNTC at 2.5×10^5 and 1.0×10^5 with cells cluttering to partial blackout on the wells. Estimated calculation of spot counts in the undercounted wells was done from wells with countable number of spots. Based on day 7 responses, 2.5×10^4 cells per well was selected as optimal for subsequent use. Total IgM profiles did not show a clear peak over the two weeks period and were generally below total IgG at the optimal cell numbers. This may

indicate prior HPV exposure having generated IgM response at its peak as an early response and later switched to other immunoglobulin isotypes, mainly IgG that is observed at high numbers as a recall response in this case.

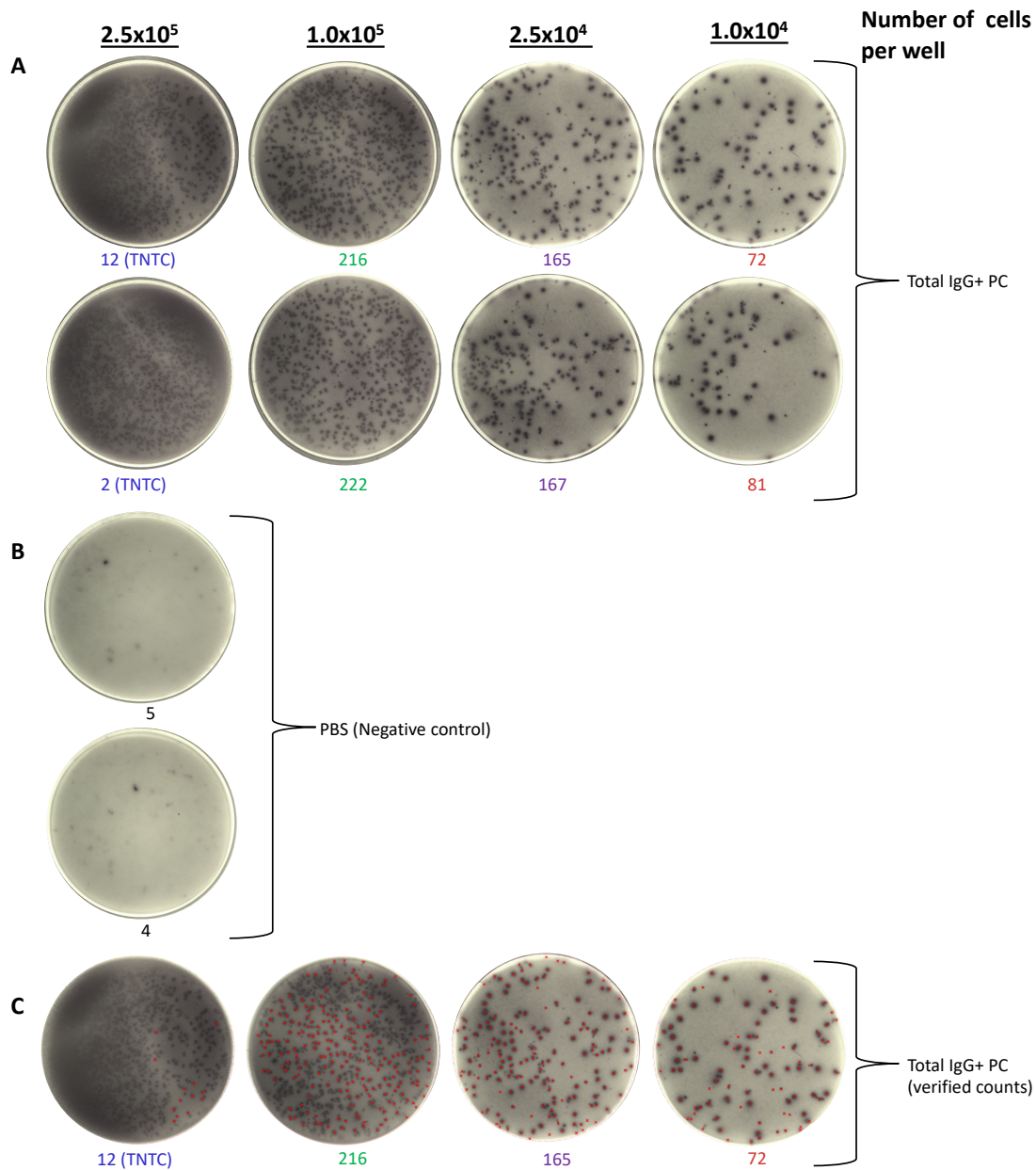


Figure 3.2. Total IgG plasma cell responses at day 7 post-first dose of Gardasil 9 vaccine

A: Responses in duplicate wells, **B:** Responses in negative control wells, **C:** verified spot counts (each red star shows a single spot counted by the reader). Spot counts for different cell numbers per well are shown in different colours (blue: 2.5×10^5 , green: 1.0×10^5 , purple: 2.5×10^4 and red: 1.0×10^4 , respectively). PC - plasma cell, TNTC - Too numerous to count

3.1.3.2 HPV VLP plate coating concentrations

Three plate coating concentrations of HPV 6, 16, 18, 33 and 52 VLP were tested to determine the optimal concentration to be used for analysis of study samples. The spot count results showed an overall increase in the number of detectable antigen specific IgM and IgG plasma cell spots with increasing VLP concentration for all 5 HPV types and were highest for HPV 6 (Figure 3.3A & B). IgM and IgG plasma cell spot numbers peaked at day 7 after vaccination for all tested HPV types except HPV 52 whose IgM numbers peaked at day 9. Though at variable magnitudes, the overall profiles of IgM plasma cells were similar for HPV 6, 16 and 18 with considerable differences between the VLP concentrations used for each one of them (Figure 3.3A). On the other hand, very little differences were observed between the IgM plasma cell spot numbers from different concentrations of HPV 33 and 52. At day 7 post-vaccination, IgG plasma cell profiles were similar for HPV 6, 16 and 52 but at variable magnitudes (Figure 3.3B). HPV 18 IgG spot numbers were equal (and highest) at 10 and 15 µg/mL while the highest HPV 33 IgG spot numbers were detected at 10 µg/mL.

Overall, VLP concentrations of 10 and 15 µg/mL consistently gave the highest IgM and IgG spot numbers for all tested HPV types except HPV 33 whose IgM plasma cell spot numbers were highest at 5 µg/mL but very close to the respective IgM numbers observed at 10 and 15 µg/mL. IgM and IgG numbers at 10 µg/mL VLP were clearly detectable and generally close to those detected at 15 µg/mL VLP for most HPV types and there seemed to be no additional benefit from the higher concentration. A VLP coating concentration of 10 µg/mL was therefore selected for subsequent use.

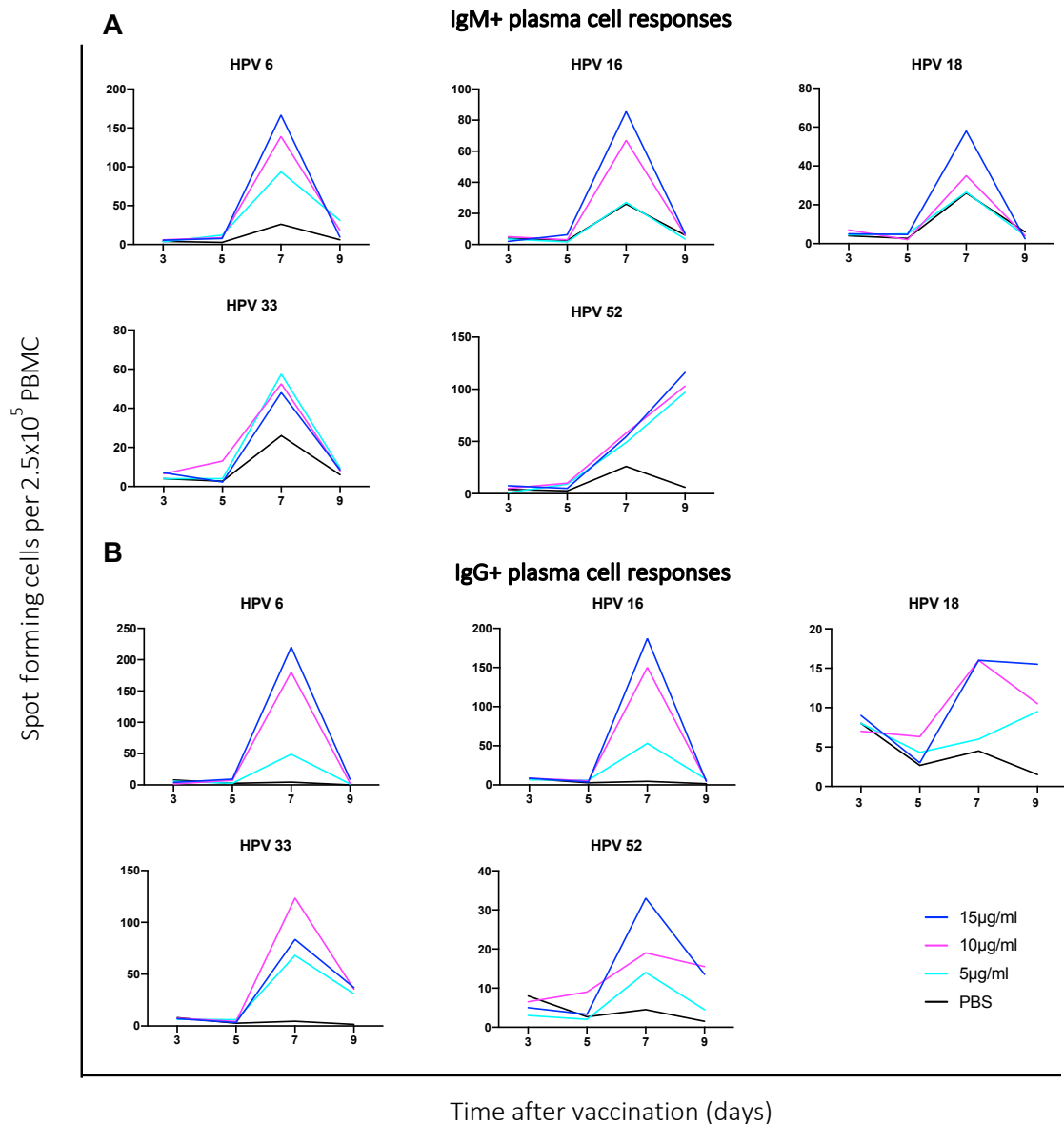


Figure 3.3. HPV specific IgG and IgM antibody secreting cells across different VLP plate coating concentrations

ELISpot plates were pre-coated with 5 HPV types (6, 16, 18, 33 and 52) at 3 different concentrations (5, 10 and 15 µg/mL) or PBS. The plates were then seeded with freshly isolated PBMC (2.5×10^5 cells/well) and cultured for 20 hours. After culture, the spots were detected and enumerated using an automated ELISpot reader. Responses are shown for each HPV type following one dose of Gardasil 9 over the follow up period for one donor. Data are shown as mean spot counts of duplicate HPV specific IgM (A) and IgG (B) for each HPV VLP from day 3 to day 9 after Gardasil 9 vaccination.

The optimised ELISpot plate coating conditions were successfully applied in identification of HPV specific IgG and IgM plasma cell responses by FluoroSpot.

3.1.3.3 Plasma cell and memory B cell kinetics after first dose of Gardasil 9 vaccine

The optimised conditions for ELISpot were used to determine the kinetics of HPV specific IgG and IgM plasma cell and memory B cell response after vaccination. These cell responses started to appear in circulation after day 5 post-vaccination for all 5 HPV types tested. Plasma cell responses peaked at day 7 for both isotypes except HPV 52 whose IgM plasma cell response peaked at day 9 (Figure 3.4). By day 14, antigen specific plasma cells were undetectable. IgM memory B cell responses peaked around day 7 after which they decreased slightly and plateaued from day 9 to 14. IgG memory B cells also increased by day 7, decreased slightly by day 9 and day 14. Most HPV types showed similar profiles for both plasma cell and memory B cell responses though at varying magnitudes.

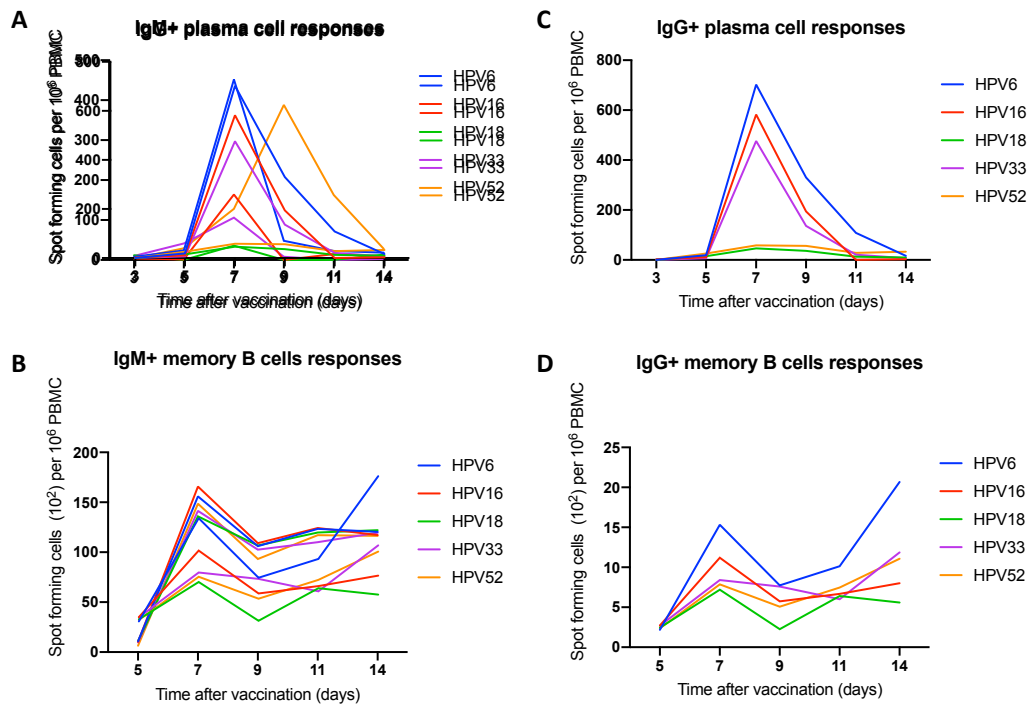


Figure 3.4. Plasma cell and memory B cell kinetics after Gardasil 9 vaccination

Plasma cells were detected on fresh PBMC (A & C) while PBMC were pre-cultured with R848 and recombinant human IL-2 stimulation for 6 days to detect memory B cell (B & D). ELISpot plates were pre-coated with 5 HPV types (6, 16, 18, 33 and 52) at 10 $\mu\text{g}/\text{mL}$. The plates were then seeded with PBMC (2.5×10^5 cells/well) and cultured for 20 hours. After culture, spots were detected and enumerated using an automated ELISpot reader. Data are shown as duplicates mean antibody secreting cells per million PBMC after background subtraction, from day 3 to day 14 after Gardasil 9 vaccination. Data is shown from a single donor.

This assay optimisation step gave an insight to the kinetics of plasma cell and memory B cell response after HPV vaccination about which little is known. However, it is important to note that this data is based on a single donor and a large sample size is needed to draw confident conclusions. While using samples from the study participants to optimise the assays would have been the optimal approach, this was not feasible because there were small sample volumes available. Additionally, there was limited availability of other donors vaccinated against HPV as the vaccine is not routinely administered to adults in the Gambia. The ability to detect antigen specific plasma cells and memory B cells at the timepoints targeted in the actual study confirmed the applicability of the assays to analyse study

samples although there could be individual and age-related differences among study participants that may need slight adjustments on the optimised assay conditions.

3.2 Flow cytometry

3.2.1 Introduction

Flow cytometry is a technique used for identification and characterisation of various cell subsets in heterogeneous cell populations based on their expression of specific surface or intracellular markers. The markers are targeted using fluorochrome-conjugated antibodies and their presence or absence is determined by fluorescent detection in a flow cytometer. Initial analytical plan was to perform flow cytometry analysis on fresh whole blood, but this was changed to analyse frozen PBMC as per study protocol amendment to mitigate COVID-19 interruptions. This section discusses the development and optimisation of flow cytometry antibody panels used for detection immunophenotyping of plasma cells and Tfh cells with considerations for initial work on whole blood and later frozen PBMC.

3.2.2 Aims

- i) To design and optimise a plasma cells multicolour antibody panel for immunophenotyping of total IgG and IgM plasma cell responses.
- ii) To design and optimise a Tfh cell AIM multicolour antibody panel for immunophenotyping of HPV 16 and HPV 18 specific Tfh cells upon in-vitro antigen stimulation.
- iii) To design and optimise a Tfh cell ex vivo multicolour antibody panel for immunophenotyping of total activated pool of Tfh cells.

3.2.3 Results and discussion

3.2.3.1 Designing of plasma cell and Tfh cell multicolour antibody panels

Multicolour antibody panels are developed in several sequential design-evaluation-redesign rounds. First, different extracellular and intracellular markers are selected based on their

known expression patterns and functions in the cell types to be analysed. Each panel combines two groups of markers: backbone (including lineage) markers to identify distinct cell populations in a sample and markers for characterization of specific cell differentiation stages, including functional and activation markers. Three antibody panels were designed; plasma cell panel for identification of total plasma cells, Tfh cell AIM panel for identification of HPV 16 and HPV 18 specific Tfh cell responses after in vitro antigen stimulation and Tfh cell ex vivo panel for identification of overall activated pool of Tfh cell population without in vitro stimulation. Main plasma cell markers included CD19, CD38, CD27 and CD138 while for both Tfh cell AIM and ex vivo panels, the main markers included CD4, CD45RO and CXCR5 for initial identification of total Tfh cell population. Additional markers were then added to each panel based on their expected expression in the cell activation. Expression of the markers at different cell developmental, differential or activation status is also determined by their functions. Tables 3.1 and 3.2 show the selected markers, their biological functions, and roles in the respective panels.

Table 3.1. Plasma cell antibody panel markers, biological functions, and roles in the panel

Marker	Biological function	Where expressed (role in panel)
CD19	Recruitment of cytoplasmic signalling proteins to cell membrane and interacts with CD19 and CD21 to decrease the threshold for B cell receptor signalling pathways	All B cells except plasma cells (B cell lineage marker)
CD27	T dependent B cell activation, plasma cell differentiation and immunoglobulin synthesis	Memory B cells and plasma cells (identification of plasma cells)
CD10	Differentiation of lymphoid progenitors	Immature B cells (exclusion of immature B cells)
CD21	B cell activation and maturation, forms the B cell co-receptor complex with CD19 and CD81 to induce B cell inflammatory responses	Mature B cells (identification of plasma cells)
CD38	Cell adhesion and regulation of intracellular calcium, important for signal transduction	Plasma cells (identification of plasma cells)
CD138	Cell proliferation, migration and cell-matrix interactions, selective survival of mature plasma cells	Plasma cells (identification of plasma cells)
BCMA	B cell maturation antigen, interacts with B cell activation factor receptor (BAFF-R) and transmembrane activator and calcium modulator and cyclophilin ligand interactor (TACI) to regulate B cell proliferation, maturation, differentiation, and survival	Plasma cells and some memory B cells (identification of plasma cells)
Blimp-1	B lymphocyte-induced maturation protein 1, a transcriptional repressor essential for plasma cell differentiation	Plasma cells (identification of plasma cells)
CD95	Elimination of non-specific and autoreactive B cells in germinal centres by apoptosis, and enhancing selection of antigen-specific B cells	Activated and memory B cells (identification of plasma cells)
CXCR4	Chemokine for CXCL12, important for chemotactic homing and retention of plasma cells to the bone marrow	B cells, upregulated on plasma cells (identification of plasma cells)
HLA-DR	MHC II molecule, stimulates B cell proliferation. Marker of cell activation, decreased during PC differentiation.	B cells, downregulated on plasma cells (identification of plasma cells)
IgG	Class switched B cell receptor/immunoglobulin in primary and secondary responses, low in primary response, upregulated in secondary response	Isotype-switched B cells, upregulated on plasma cells (identification of plasma cells)
IgM	B cell receptor/immunoglobulin in both primary and secondary responses, early and upregulated in primary response	Non-isotype-switched B cells, upregulated on plasma cells (identification of plasma cells)

IgA	Class switched B cell receptor/immunoglobulin in primary and secondary responses, low in primary response, upregulated in secondary response	Non-isotype-switched B cells, upregulated on plasma cells (identification of plasma cells)
CD3	T cell co-receptor important in activation of naïve T cells	All T cells (T cell exclusion)
CD14	Monocytes lineage marker	All monocytes (monocytes exclusion)

BCMA - B cell maturation antigen, Blimp-1 - B-lymphocyte-induced maturation protein-1, CXCR4 - chemokine receptor, HLA-DR - Human Leucocyte antigen, CD - cluster of differentiation, Ig - immunoglobulin, CXCL - chemokine ligand, MHC II - Major histocompatibility complex II

Table 3.2. T follicular helper cell panel markers, biological functions, and roles in the panel

Marker	Biological function	Where expressed (role in panel)
CD4	Interaction with MHC class II molecules-antigen complex on antigen presenting cells for T cell activation	All T helper cells (identification of Tfh cells)
CXCR5	Guides migration of Tfh cells toward B cell follicles to provide help for B cell differentiation into plasma and memory B cells	Mainly Tfh cells (identification of Tfh cells)
CD45RO	Essential for T cell activation and memory	Memory T cells (identification of Tfh cells)
CCR6	Play a role in dendritic and T cells recruitment and antigen-driven B cell differentiation.	Expressed by Tfh17 (identification of Tfh17 cells)
CXCR3	Migration of T cells to peripheral tissues and lymphoid compartments, facilitate interaction of T cells with antigen presenting cells and subsequent generation of effector and memory cells.	Upregulated on activated Tfh1 cells (identification of Tfh1 cells)
ICOS	Inducible T cell costimulatory molecule plays a role in generation, survival and reactivation of CD4 T cells and B cells. Directs effector T cell differentiation and signalling in the differentiation and maintenance of Tfh cells.	Expressed on activated Tfh (identification of activated Tfh cells)
PD-1	Programmed cell death receptor 1, can be pro-apoptotic or anti-apoptotic depending on the nature of stimulation to promote antigen specific T cell response	Upregulated on activated Tfh cells (identification of activated Tfh cells)

PD-L1	Ligand for PD1 on antigen presenting cells and a bidirectional membrane protein acting as a ligand to induce anergy in PD-1-positive T cells or induce anti-apoptotic genes in PD-L1-positive target cells depending on the nature of stimulation.	Expressed on activated Tfh cells (identification of activated antigen specific Tfh cells)
CD25	The α -chain of IL-2 receptor. α - and β -chain expression on the receptor leads to high affinity for IL-2 which play a role in regulation of Tfh cell development and immunoregulatory functions of T regulatory cells.	Expressed on activated antigen-specific Tfh cells (identification of activated antigen specific Tfh cells)
OX40 (CD134)	Costimulatory signals from OX40 to a conventional T cell promote division and survival, augmenting the clonal expansion of antigen specific effector and memory populations. OX40 additionally suppresses the differentiation and activity of regulatory T cells	Expressed on activated antigen -specific Tfh cells (identification of activated antigen specific Tfh cells)
FoxP3	Suppress the function of NFAT and NF kappa B leading to suppression of many genes including IL-2 and effector T-cell cytokines to regulate T cell responses.	Expressed on Tregs (Tregs exclusion)
CD14	Co-receptor for several TLRs on the cell surface and in the endosomal compartment that recognise bacterial lipopolysaccharides	All monocytes (monocytes exclusion)

The markers were categorised into primary (high density with either on and off expression), secondary (relatively high density with continuous expression) and tertiary (uncharacterized or expressed at low levels). Fluorochrome-marker combinations were then defined based on factors such as the expected fluorochrome stain index or relative brightness on the cytometer to be used at MRCG at LSHTM immunology laboratory, resolution ranking and antibody availability from manufacturers. Bright fluorochromes were assigned to tertiary markers and dim fluorochromes to primary and secondary markers. Spillover Spreading Matrix (SSM) of the cytometer was used to assess antibody-fluorochrome matching for co-expressed markers to minimize spectral overlaps. This maximises resolution of co-expressed markers and allows for clear identification of target cell populations by multicolour staining. SSM provides a quick visual tool to help assess potential problems with spread of fluorochromes on co-expressed markers. A viability dye (Zombie Aqua) was included in the panels to exclude dead cells to avoid auto-fluorescence and non-specific antibody staining.

A single fluorochrome or dye can be conjugated to different markers for their intended exclusion (dumping) from the analysis if not needed. V500 was used as the dump channel in both plasma cell and Tfh cell AIM panels. Table 3.3 shows a summary of the initial antibody panels developed for whole blood staining. The staining protocol for each antibody panel was developed considering instructions from manufacturers of all included antibodies with adjustments where necessary to suit multicolour staining for identification of target cell populations.

Table 3.3. Initial plasma cell (B cell) and T follicular helper cell antibody panels

Antibody/dye	Site of marker expression	Fluorochrome	Clone	Isotype	Supplier	Catalogue number
B cell panel						
anti-human IgA	Extracellular/intracellular	APC-Vio770	REA1014	Recombinant human IgG1	Miltenyi Biotec	130-116-884
anti-human IgG	Extracellular/intracellular	APC-H7	G18-145	mIgG1	BD Biosciences	561297
anti-human IgG	Extracellular/intracellular	PE-Cy7	G18-145	mIgG1	BD Biosciences	561298
anti-human IgM	Extracellular/intracellular	PE-Cy7	MHM-88	mIgG1	BioLegend	314532
anti-human CD184 (CXCR4)	Extracellular	BV650	12G5	mIgG2a	BD Biosciences	740599
anti-human Blimp-1/PRDM1	Intracellular	PE	646702	mIgG1	Fisher Scientific	13437765
anti-human CD269 (BCMA)	Extracellular	BV421	19F2	mIgG2a	BioLegend	357520
anti-human CD38	Extracellular	BV605	HB7	mIgG1	BD Biosciences	562665
anti-human CD27	Extracellular	APC	M-T271	mIgG1	BD Biosciences	558664
anti-human CD21	Extracellular	BB700	B-Ly4	mIgG1	BD Biosciences	566569
anti-human CD19	Extracellular	BV786	SJ25C1	mIgG1	BD Biosciences	563325
anti-human CD138	Extracellular	APC-R700	MI15	mIgG1	BD Biosciences	566050
anti-human CD10	Extracellular	PE-CF594	HI10a	mIgG1	BD Biosciences	562396
anti-human CD95	Extracellular	BV711	DX2	mIgG1	BD Biosciences	563132
anti-human HLA-DR	Extracellular	BV421	L243	mIgG2a	BioLegend	307636
anti-human CD3	Extracellular	V500	SP34-2	mIgG1	BD Biosciences	560770
anti-human CD14	Extracellular	V500	M5E2	mIgG2a	BD Biosciences	561391
Zombie Aqua™ Fixable Viability dye	-	V500	-	-	BioLegend	423102

Tfh AIM panel						
anti-human ICOS (CD278)	Extracellular	PE	DX29	mIgG1	BD Biosciences	557802
anti-human CD4	Extracellular	PerCP-Cy5.5	RPA-T4	mIgG1	BioLegend	300530
anti-human OX40 (CD134)	Extracellular	APC	Ber-ACT35 (ACT35)	mIgG1	BioLegend	350008
anti-human CXCR3 (CD183)	Extracellular	APC-Cy7	GO25H7	mIgG1	BioLegend	353722
anti-human CXCR5 (CD185)	Extracellular	AF700	J252D4	mIgG1	BioLegend	356916
anti-human CD45RO	Extracellular	BV605	UCHL1	mIgG1	BioLegend	304238
anti-human CD25	Extracellular	PE-Cy7	M-A251	mIgG1	BioLegend	356108
anti-human PD-L1 (CD274)	Extracellular	FITC	MIH1	mIgG1	BD Biosciences	558065
anti-human CCR6 (CD196)	Extracellular	BV421	11A9	mIgG1	BD Biosciences	562515
anti-human FoxP3	Intracellular	PE-CF594	236A/E7	mIgG1	BD Biosciences	563955
Zombie Aqua™ Fixable Viability dye	-	V500	-	-	BioLegend	423102
Tfh Ex vivo panel						
anti-human PD1 (CD279)	Extracellular	PE-Cy7	EH12.2H7	mIgG1	BioLegend	329918
anti-human ICOS (CD278)	Extracellular	PE	DX29	mIgG1	BD Biosciences	557802
anti-human CD4	Extracellular	PerCP-Cy5.5	RPA-T4	mIgG1	BioLegend	300530
anti-human CXCR3 (CD183)	Extracellular	APC-Cy7	G025H7	mIgG1	BioLegend	353722
anti-human CXCR5 (CD185)	Extracellular	AF700	J252D4	mIgG1	BioLegend	356916
anti-human CCR6 (CD196)	Extracellular	BV421	11A9	mIgG1	BD Biosciences	562515
anti-human CD45RO	Extracellular	BV605	UCHL1	mIgG1	BioLegend	304238
Zombie Aqua™ Fixable Viability dye	-	V500	-	-	BioLegend	423102

Each antibody panel was optimized through several steps from preliminary testing and antibody titration in single colour staining (SCS) to determine optimal antibody dilutions, to final evaluation of complete panel in multicolour staining to check for any spectral overlap or spillover that may affect resolution. Adjustments were made to the panels as necessary to clearly identify target cell populations. The same samples used to optimise ELISpot and FluoroSpot assays were used for flow cytometry assays optimisation.

These steps are discussed in subsequent parts of this chapter.

3.2.3.2 Preliminary antibody testing

SCS was first performed on fresh whole blood for all antibodies at manufacturers' recommended dilutions to confirm detection of negative and positive populations for each marker. Unstained cells were used as a control to define background auto-fluorescence of the negative population during the SCS. All antibodies worked well showing clearly identifiable negative and positive populations except BV650-CXCR4 which had unexpected positive population profile. Results of this preliminary antibody testing at manufacturers' recommended dilutions are shown in Figure 3.5 for the Tfh cell ex vivo panel. Similar results for plasma cell and Tfh cell AIM panels are shown in Appendices 1 and 2, respectively.

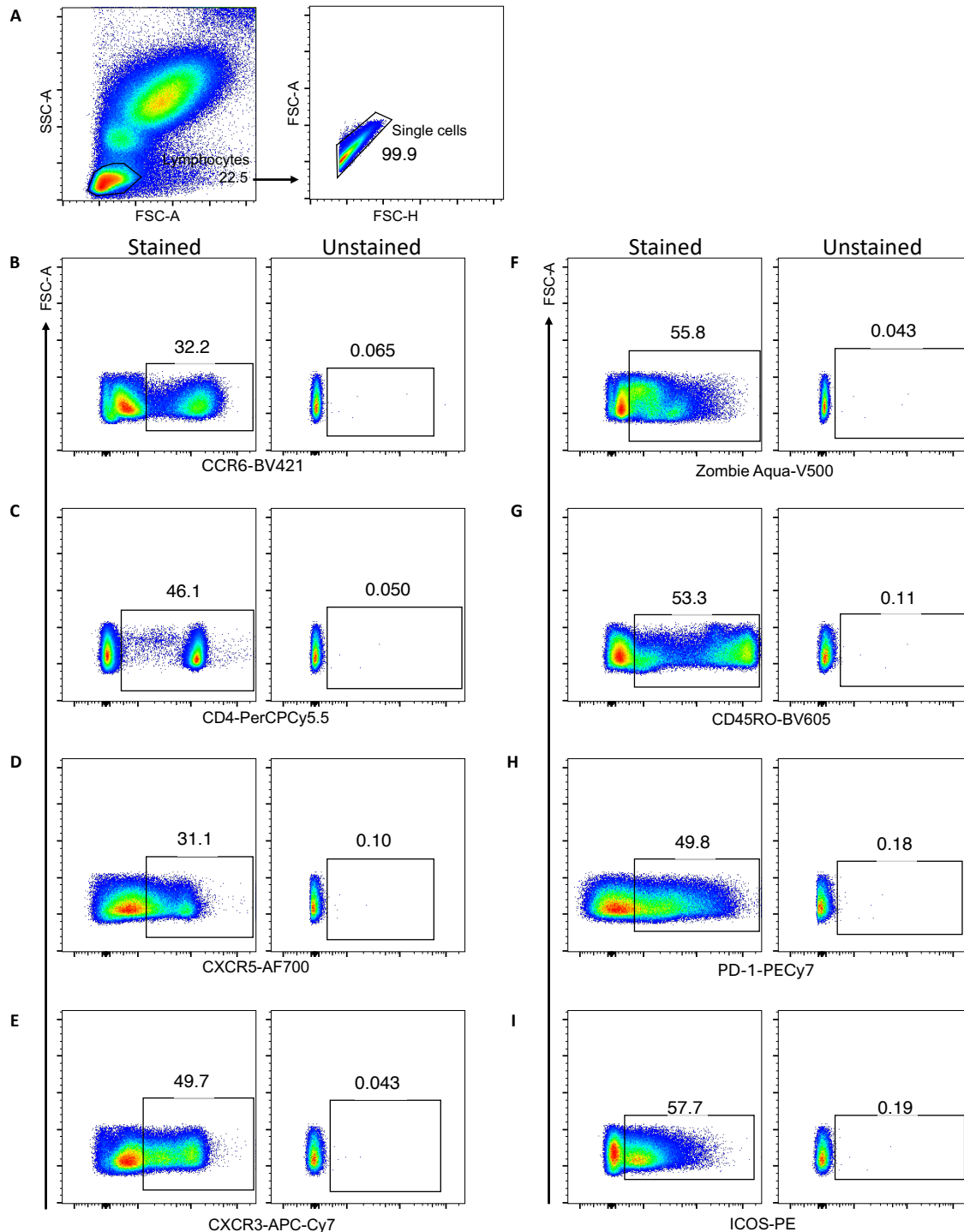


Figure 3.5. Preliminary testing of antibodies in the Tfh cell ex vivo panel at manufacturers' recommended antibody dilutions

Whole blood was single colour stained for eight markers and Zombie Aqua viability dye at the manufacturers' recommended dilutions using the Tfh cell ex vivo staining procedure. Cells were first gated on lymphocytes and single cells (**A**). From the single cells, the positive population was defined for each marker or viability on stained cells using unstained cells as a negative control. **B**: CCR6-BV421, **C**: CD4-PerCPCy5.5, **D**: CXCR5-AF700, **E**: CXCR3-APC-Cy7-CXCR3, **F**: Zombie Aqua-V500, **G**: CD45RO-BV605, **H**: PD-1-PE-Cy7, **I**: ICOS-PE

3.2.3.3 Antibody titration

Upon confirming identification of a positive population for each antibody, the antibodies were titrated down in five dilutions starting from manufacturer's recommendation to determine the optimal dilution with best staining resolution. Separation index (SI), based on mean fluorescent intensity of each antibody and calculated using the formula below was used to determine optimal dilutions for all antibodies.(Bigos, 2007)

$$\text{Separation Index (SI)} = \frac{\text{Median of Positive} - \text{Median of Negative population}}{(\text{84th percentile of Negative} - \text{Median of Negative population})/0.995}$$

The higher the SI value, the better the resolution, hence the dilution with the highest SI value for each antibody was selected as optimal. Examples of gating strategy (Figure 3.6) and statistics (Table 3.4) for calculation of SI values are shown for anti-human CD4-PerCPCy5.5 antibody used in both Tfh cell panels and anti-human CD19-BV786 antibody in the plasma panel. Appendices 3, 4 & 5 show titration results of all other antibodies in the three panels.

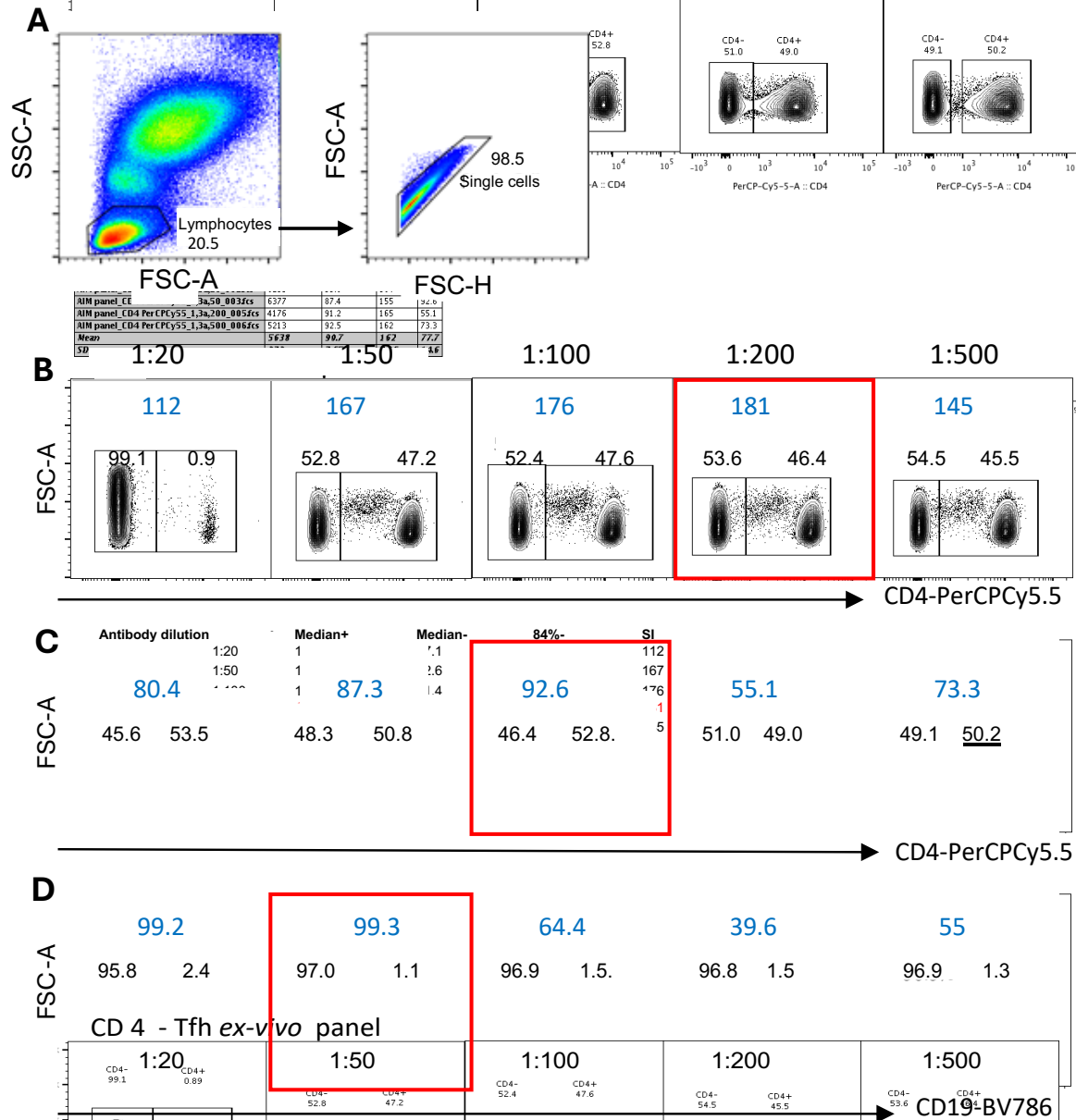


Figure 3.6. Titration of CD4-PerCPCy5.5 and CD19-BV786 antibodies

Each antibody was titrated in single colour-stained whole blood using five dilutions starting from manufacturers' recommendation. Cells were first gated on lymphocytes and single cells (**A**). From the single cells, positive and negative populations were defined for each marker and SI values calculated for each dilution. Frequencies of positive and negative populations are shown above each respective gate. Blue numbers indicate staining index (SI) values and red boxes show the gating for optimal dilutions with highest SI. **B**: CD4-PerCPCy5.5 (Tfh activation induced marker panel), **C**: CD4-PerCPCy5.5 (Tfh ex vivo panel), **D**: CD19-BV786 (B cell panel).

Table 3.4. SI calculations for CD4-PerCPCy5.5 and CD19-BV786

Antibody dilution	Median of positive population	Median of negative population	84% of negative population	SI
Tfh ex vivo panel: CD4-PerCPCy5.5				
1:20	12352	77.1	186	112
1:50	12904	52.6	129	167
1:100	13083	51.4	125	176
1:200	12640	48.8	118	181
1:500	9795	44.9	112	145
Tfh AIM panel: CD4-PerCPCy5.5				
1:20	6173	88.7	164	80.4
1:50	6253	93.8	164	87.3
1:100	6377	87.4	155	92.6
1:200	4176	91.2	165	55.1
1:500	5213	92.5	162	73.3
B cell panel: CD19-BV786				
1:20	9795	79.6	177	99.2
1:50	9449	77.1	171	99.3
1:100	6028	77.1	169	64.4
1:200	3678	74.5	165	39.6
1:500	5169	75.8	168	55

Statistics used for SI values calculation are shown for CD4-PerCPCy 5.5 and CD19-BV786 antibodies. Highlighted in red are optimal dilutions and respective statistics for SI calculations.

3.2.3.4 Plasma cell antibody panel optimisation

Before complete panel testing, conditions recommended by some antibody manufacturers were evaluated for potential interference or benefit when used in multicolour staining. These include the effect of Tandem Signal Enhancer (TE) on immunoglobulin staining and effect of Brilliant stain buffer plus (BSBP) on multiple Brilliant Violet (BV) staining as described next.

3.2.3.4.1 Effect of TE on immunoglobulin surface staining

Tandem dye conjugates can bind to cells non-specifically via their interaction with Fc receptors (FcRs) especially on monocytes. TE is an Fc blocking reagent that minimises this

non-specific binding thereby reducing background staining signals. It is recommended in multicolour staining with multiple tandem dye conjugates. Since the designed plasma cell panel included 6 such conjugates, TE could potentially improve their staining quality. However, Fc blocking reagents often contain polyclonal serum immunoglobulins and can interfere with staining of immunoglobulin markers. The effect of TE on SI values of IgG, IgM and IgA markers was therefore assessed by staining cells with the respective monoclonal antibodies in the presence or absence of TE. A strong interference on IgG surface staining was observed in the presence of TE unlike with IgM surface staining as indicated by loss of staining and low SI values (Figure 3.7), suggesting that TE may contain serum IgG which may have competed for the anti-human IgG antibody binding in the sample. NMS was alternatively used as an Fc block and such interference was not observed leading to its use as an Fc block in subsequent multicolour staining of all panels.

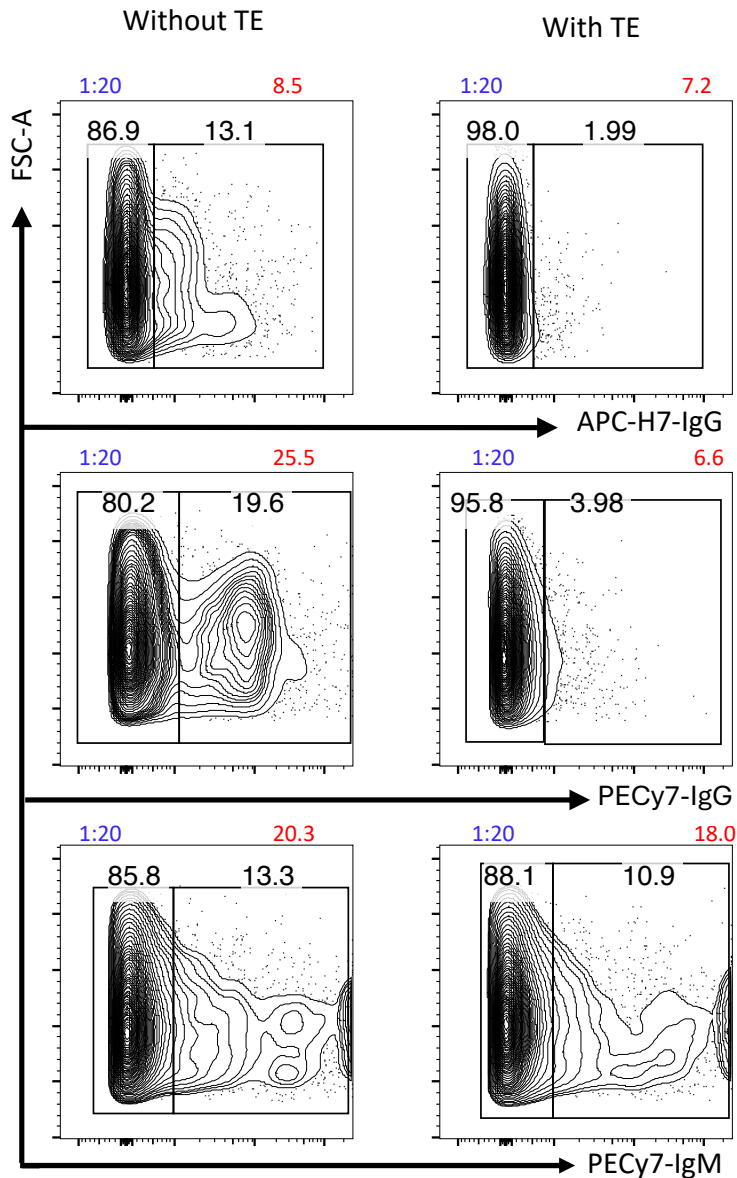


Figure 3.7. Effect of Tandem signal enhancer (TE) on IgG and IgM staining

Human whole blood was single-colour stained with mouse anti-human IgG-APC-H7, IgG-PECy7 or IgM-PECy7 in presence or absence of TE using the plasma cell panel protocol. Gating was first performed on lymphocytes and single live cells. From the single live cells, positive and negative populations were identified. Purple numbers indicate antibody dilution and red numbers indicate SI values for immunoglobulin staining.

3.2.3.4.2 IgA staining and effect of TE

Very few fluorescently labelled anti-human IgA antibodies were commercially available during the antibody panel development. The IgA antibody tested in this panel is a recombinant human IgG1, likely to give high background due to non-specific binding to FcR. Its staining was assessed with or without TE and a high background staining was observed even in the IC control. This led to shifting the positive population gate to the right and detected very low IgA+ frequencies (0.87% without TE and 0.77% with TE against the IC 0.21% and 0.10%, respectively) (Figure 3.8). Additionally, TE did not improve the staining quality of IgA. IgA staining was excluded from complete panel testing due to the high background observed from the IC.

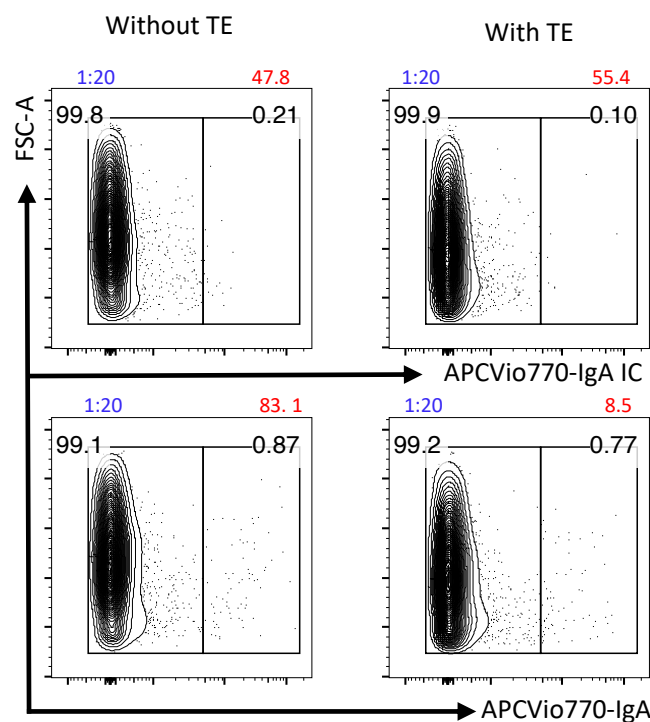


Figure 3.8. IgA staining and effect of TE

Human whole blood was single-colour stained with APCVio770-IgA or its isotype control (IC) in presence or absence of TE using the plasma cell panel protocol. Gating was first done on lymphocytes and single live cells. From the single live cells, positive and negative populations were identified using the IC control gate. Black numbers indicate frequencies (%) of positive and negative populations, respectively; purple numbers indicate antibody dilution and red numbers indicate staining index values.

3.2.3.4.3 Effect of BSBP on multiple BV dye staining

The BSBP is recommended to reduce non-specific interactions between BV dyes when two or more of them are used in the same panel. This improves staining quality of the BV dyes. This panel included 6 BV dyes (Table 3.3). The effect of BSBP on BV dyes staining quality was assessed by staining cells with a dump channel (to exclude T cells (CD3+), monocytes (CD14+) and dead cells) and both BV786-CD19 and BV605-CD38. The SI values for the BV-stained cells were compared between staining in presence or absence of BSBP. Respective fluorescence minus one control (FMO) were used to set gates for BV786-CD19 and BV605-CD38. The SI values for both BV786-CD19 and BV605-CD38 staining with BSBP were higher (18.4 and 29.2) than without it (10.9 and 23.3), respectively (Figure 3.9). BSBP was therefore used subsequently in the complete plasma cell panel.

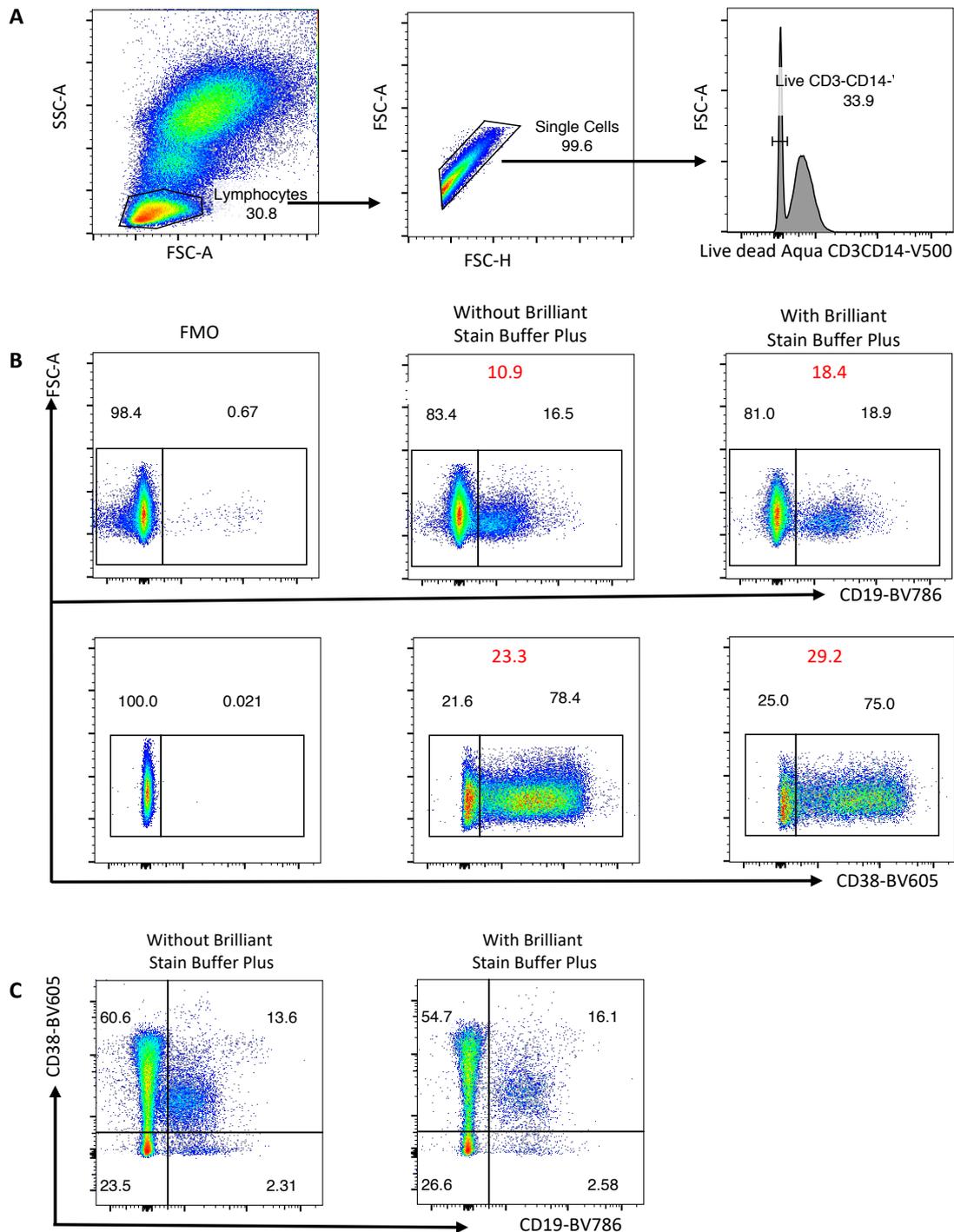


Figure 3.9. Brilliant Stain Buffer Plus improves resolution in multicolour staining with multiple BV dyes

Whole blood was stained with a 13-colour B cell antibody panel containing 5 BV-conjugated antibodies, without and with Brilliant Stain Buffer Plus. Cells were first gated on lymphocytes and single cells and dead cells, CD3⁺ T cells and CD14⁺ monocytes were excluded (**A**). Positive and negative populations are then determined for each marker using FMO. Single (**B**) and double (**C**) colour gating plots show CD19 and CD38 staining without and with Brilliant Stain Plus. SI values in the single colour gating plots are shown in red.

3.2.3.4.4 Complete plasma cell panel evaluation

The earlier described steps identified optimal conditions for testing the complete plasma cell panel. Two antibodies were excluded from the panel at this stage including BV650-CXCR4 due to unclear staining profile observed from SCS preliminary testing and APCVio770-IgA due to high background staining observed in its IC. To evaluate the panel, fresh whole blood in one tube was stained with a mixture of all included antibodies alongside the necessary controls including unstained cells, FMOs and SCS anti-mouse Ig, κ/Negative control compensation particles set (BD Biosciences). Unstained cells were analysed first with standardised application settings to confirm that the negative population for each marker was at the expected position. Compensation particles were then analysed to remove spectral overlaps between detectors before analysing the fully stained and FMO tubes.

To evaluate the panel for the identification of the target cell populations, the compensation matrix and resolution of double and positive populations were checked for presence of spillover spreading errors between detectors. FMOs were used to confirm minimal spread on co-expressed markers and to define positive populations for dim markers. Detection of signal from a given fluorochrome by multiple detectors due to fluorochrome's emission spectral overlap results to errors that interfere with resolution and hinders identification of target cell populations. This complete panel testing is therefore a critical step to confirm that the antibody panel is able to identify the populations of interest before applying it to analyse the study samples.

Next, the fully stained tube was analysed for identification of plasma cell phenotype as CD10-CD19+CD38++CD138+CD27+CD21-/low, from which the frequencies of IgG+ and IgM+ plasma cells would be determined. Staining for plasma cell survival and activation markers BCMA (or HLA-DR), CD95 and Blimp-1 would also be identified.

From checking the double positive populations for all markers, high spectral overlaps between PE-CF594-CD10 and BV605-CD38, APC-R700-CD138 and PECy7-IgM staining were observed. To gate for the complete panel, lymphocytes were gated for singly analysed

cells and CD3+ T cells, CD14+ monocytes and dead cells excluded. CD10-CD19+B cells were identified but subsequent gating for CD138 and CD38 double positive cells was not possible due to poor resolution (Figure 3.10), although some CD38++CD138+ cells were observed. The spreading of CD138- population and sub-optimal resolution for CD38 expression (CD38-, CD38+ and CD38++) necessitated re-designing of this panel.

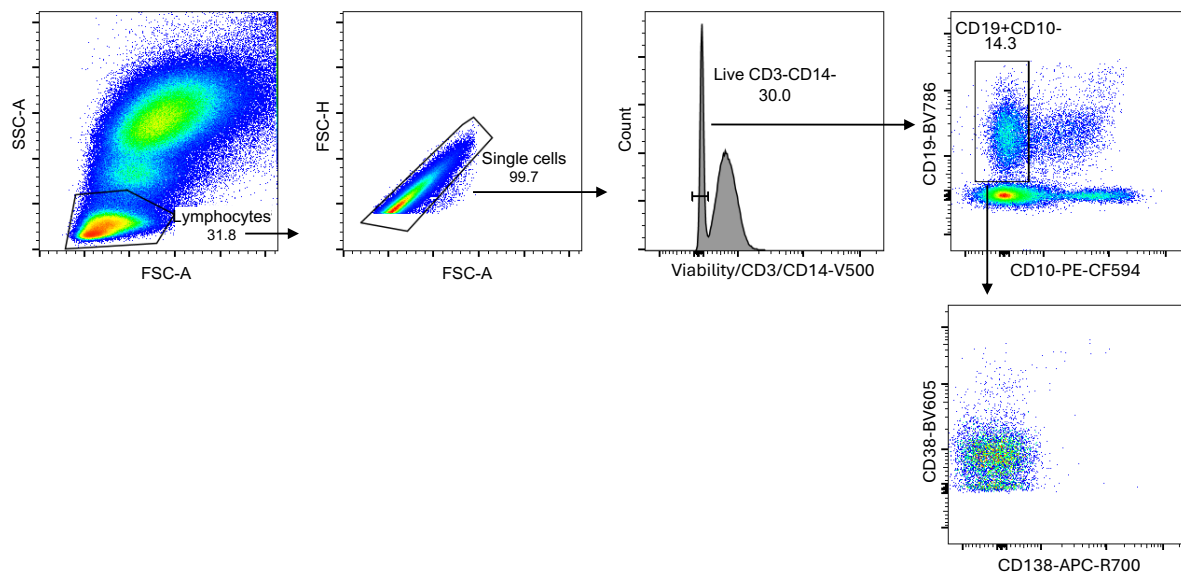


Figure 3.10. Initial complete plasma cell panel testing failed to identify clear plasma cell population

Whole blood was stained with a 13-colour B cell antibody panel. Cells were first gated on lymphocytes and single cells, then CD3+ T cells, CD14+ monocytes and dead cells excluded using a dump channel. CD10-CD19+ B cells were identified after which CD138+CD38++ plasma cell staining was found to be sub-optimal due to poor resolution.

The panel was therefore re-designed to correct the observed spectral overlap problems and to adapt it to staining frozen PBMC. Changes in the new panel included first excluding some markers such as BCMA, CD95 and Blimp-1 that are expressed at very low levels in circulation and would be even more difficult to detect in frozen PBMC. Changed antibodies in the new panel included BV421-CD10, APC-R700-CD38, BV650-CD138, PECF-594-IgM and PECy7-IgG (Appendix 6 shows their titration results). The re-designed panel was first tested for identification of plasma cells in fresh PBMC, exploring three staining approaches

for immunoglobulin markers IgG and IgM, i.e. cell surface staining only (SS), intracellular staining only (ICS) or both surface and intracellular staining (SS + ICS). First, CD10-CD19+CD38++CD138+CD27+CD21-/low plasma cell population was identified successfully using the new panel (Figure 3.11A). However, very few events for CD138 staining were observed in SS only and was completely lost in ICS and SS+ICS, hence plasma cells were gated as CD38++, CD27+CD21-/low (Figure 3.11B & C). The CD38++ population was greatly reduced from 1.48% in SS to 0.28% and 0.26% in ICS and SS+ICS, respectively. The observed loss of CD138 may have been caused by cell loss and disruptions during ICS since CD138 is a rare marker. Higher frequencies of total IgG+ (15.7% SS, 22.1 ICS % and 14.1% SS+ICS) than IgM+ (8.18% SS, 4.81% ICS and 10.9% SS+ICS) plasma cells were observed (Figure 3.11D). This was the expected immunoglobulin profile.

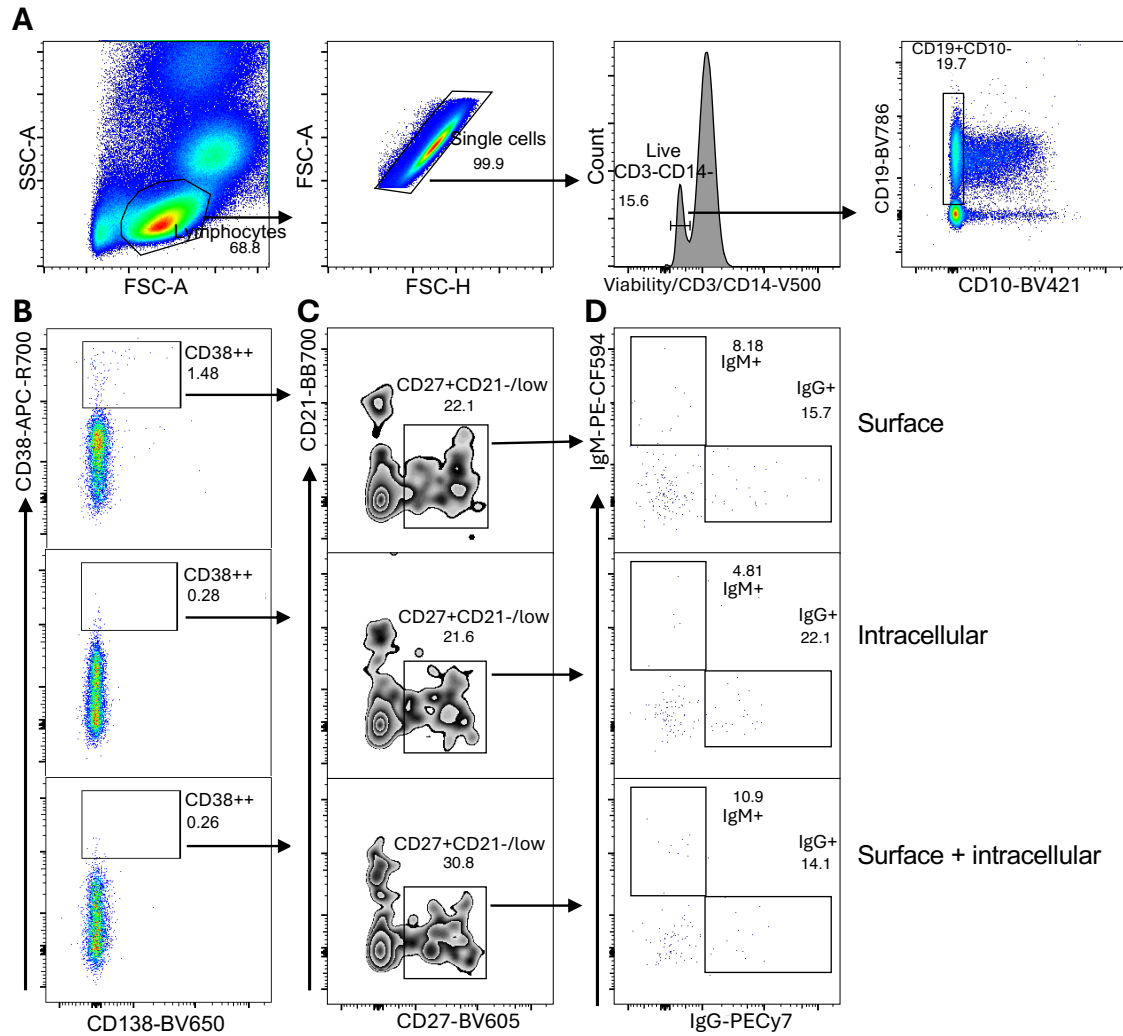


Figure 3.11. Re-designed panel identified clear plasma cell population which was reduced by intracellular staining of IgG and IgM

Fresh PBMC were stained with a 9-colour plasma cell antibody panel and compared for IgG and IgM staining using surface only, intracellular only or both surface and intracellular approaches. Cells were first gated on lymphocytes, single cells and dead cells, CD3+ T cells and CD14+ monocytes excluded in a dump channel, then CD10-CD19+ B cells were identified as shown in panel (A). CD38++ cells were identified from the CD10-CD19+ population (B) before gating for CD27+CD21-/low total plasma cells (C) from which the IgG+ and IgM+ frequencies were identified (D). Gating is shown for surface, intracellular and surface plus intracellular staining.

Next, the successful panel was compared for SS of freshly isolated and frozen PBMC since the final analysis of study samples would be performed on frozen PBMC. This comparison would allow for identification of any staining changes that may arise from freezing. The results showed that CD138 staining in fresh PBMC were clearer than previously observed, which could be attributable to staining more cells in this experiment (Figure 3.12). On the other hand, CD138 staining was completely lost, and IgM staining was very low in frozen PBMC, possibly due to freezing (Figure 3.12). Therefore, subsequent plasma cell staining excluded CD138 from the panel.

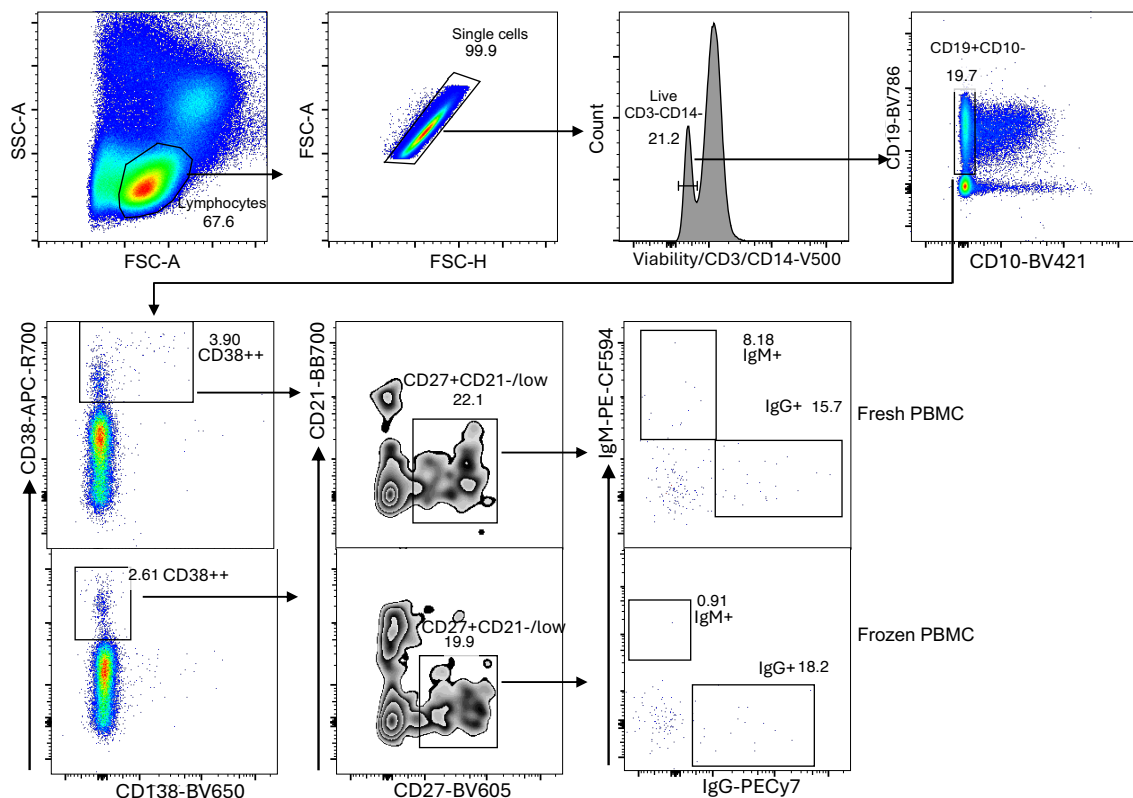


Figure 3.12. CD138 staining was lost on frozen PBMC

Fresh and frozen PBMC were stained with a 9-colour plasma cell antibody panel. Cells were first gated on lymphocytes and single cells, then CD3+ T cells, CD14+ monocytes and dead cells excluded using a dump channel. CD10-CD19+ B cells were identified followed by CD38++, CD27+CD21-/low total plasma cell population since there was no detectable CD138 events in the frozen PBMC sample. The IgG+ and IgM+ frequencies were then identified.

In conclusion, CD138 was excluded from the panel and the SS approach used for IgG and IgM subsequently. The gating strategy was changed based on the final markers to be included; to first identify all CD19+ B cells, followed by CD10-CD38⁺⁺, CD27+CD21-/low, and finally the immunoglobulin IgG⁺ and IgM⁺ populations. This strategy was applied to analyse frozen PBMC samples from the same donor collected before and after Gardasil 9 vaccination and showed very clear staining for all intermediate and final target populations (Figure 3.13). The complete phenotypes of CD19+CD10-CD38⁺⁺CD27+CD21-/lowIgG⁺ and CD19+CD10-CD38⁺⁺CD27+CD21-/lowIgM⁺ populations were identified at frequencies of 27.7% and 28.3% before vaccination and 24.1% and 15.1% after vaccination, respectively. The reduced IgM⁺ frequencies after vaccination may have been as a result of CSR into other isotypes. It is important to note that this was evaluation of total plasma cell population and although the vaccine may have induced antigen specific IgG⁺ plasma cells, this may not reflect an increase in the total IgG plasma cells.

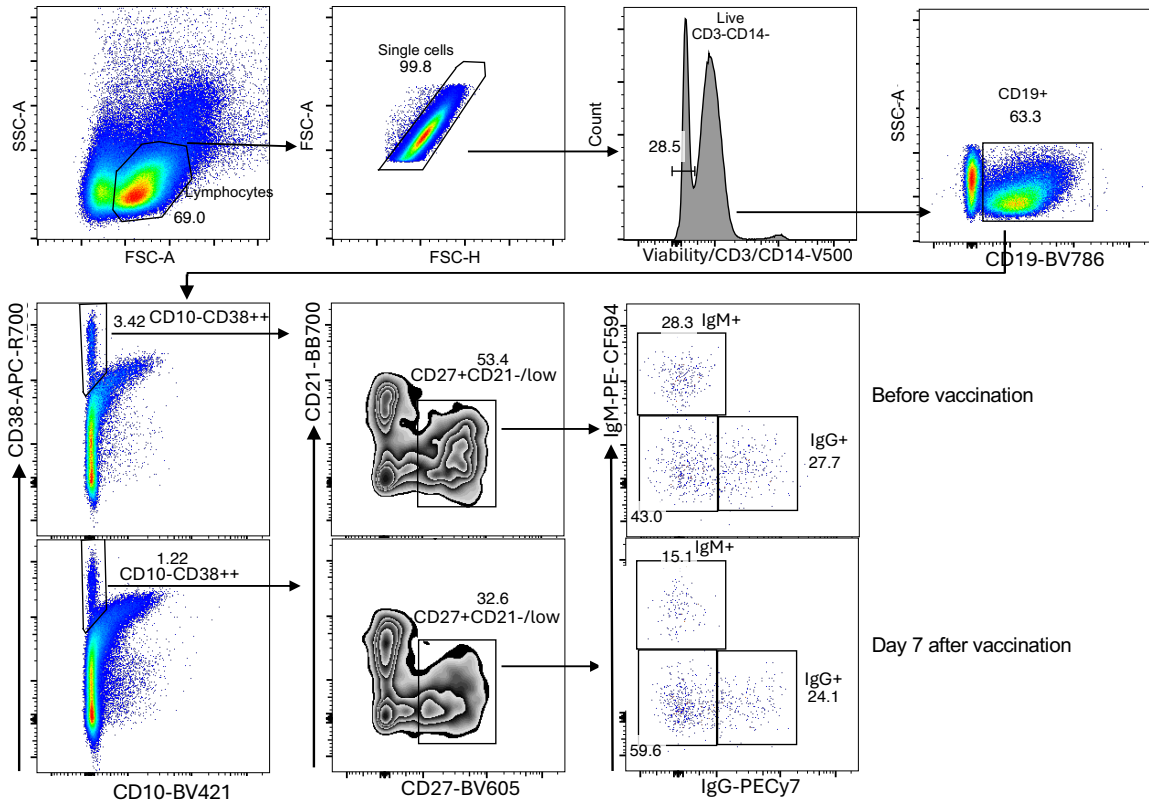


Figure 3.13. Final plasma cell panel identified clear plasma cell populations before and after vaccination

Frozen PBMC collected before and after Gardasil 9 vaccination were stained with 8-colour plasma cell antibody panel. Cells were first gated on lymphocytes and single cells, then CD3+ T cells, CD14+ monocytes and dead cells excluded using a dump channel. CD19+ total B cells were identified followed by CD10-CD38⁺⁺, CD27+CD21^{-/low} total plasma cells and finally IgG⁺ and IgM⁺ frequencies were identified.

3.2.3.5 Tfh cell AIM antibody panel

This panel was developed for identification of vaccine-induced antigen specific Tfh cells after 18 hours in vitro stimulation of PBMC with the HPV VLP antigens. Initial steps therefore involved optimising conditions for antigen stimulation before testing the complete panel staining. Next follows a description of these steps.

3.2.3.5.1 Evaluation of Tfh cell culture stimulation using a mitogen stimulus

Staphylococcus enterotoxin B (SEB) (1 µg/mL), a positive control mitogen stimulus was first used to test the culture stimulation conditions. Total Tfh cell population was identified as CD4+CXCR5+CD45RO+, from which the polyclonally activated OX40+CD25+ frequency was 17.6% (Figure 3.14). Antibodies for other markers in the panel (FITC-PD-L1, PE-ICOS, APC-Cy7-CXCR3, BV421-CCR6 and PE-CF594-FoxP3) were not included at this step as it was mainly aimed at detecting activated Tfh cells for which the use of two AIM markers was sufficient.

Although SEB stimulation worked well based on the gating strategy applied, CXCR5 FMO was required to identify CD4+CXCR5+ cells due to high spread and poor resolution between PerCP-Cy5.5 (CD4) and AF700 (CXCR5). Previous AIM studies looking at total CD4+ and CD8+ activated T cells identified higher SEB-activated T cell frequencies than observed here. (Reiss et al., 2017b, Bowyer et al., 2018) The low frequency (17.6%) of SEB-activated Tfh cells may have been attributable to this panel being sub-optimal. Although the frequency of activated population identified in this study is low, it is important to acknowledge that comparing this frequency between studies requires consideration of the parent population from which the activated cells were gated as this may lead to substantial variations. For example, gating of CD25+OX40+ from total CD4+ T cells may be expected to give a different frequency compared to gating from the Tfh cell population. Although it was clear that the AIM panel was sub-optimal from the observed CD4+CXCR5+ spread, the target activated population was successfully identified after SEB stimulation allowing for optimisation of other stimulation conditions. The anti-CD4 and anti-CXCR5 antibodies were not changed at this early stage to identify any other antibodies in the panel that would need to be changed in the final re-designed panel.

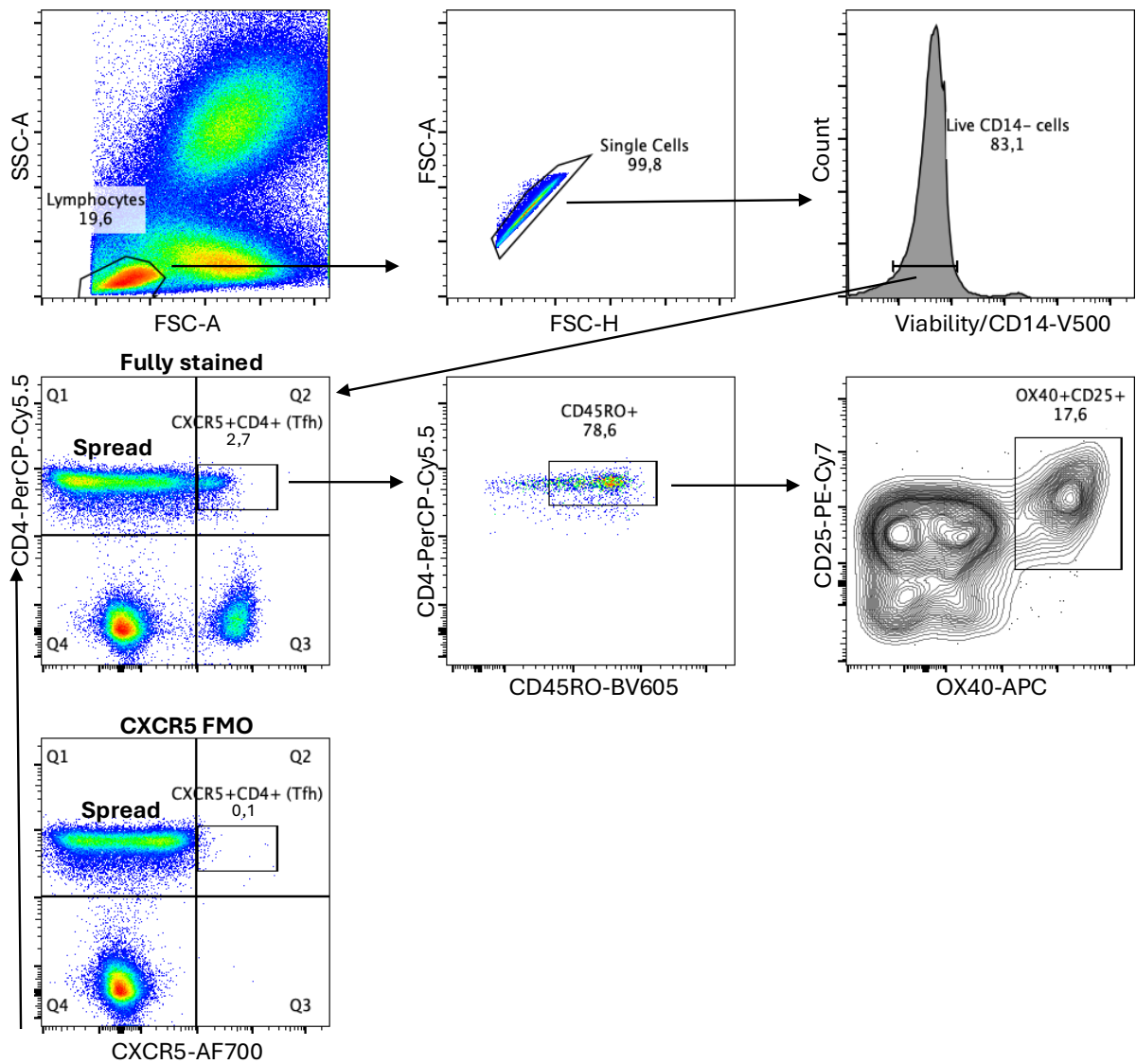


Figure 3.14. Identification of polyclonally activated Tfh cells using AIM antibody panel

A fresh whole blood sample collected at day 7 post-first dose of Gardasil 9 vaccination was stimulated with SEB for 18 hours before staining with a Tfh cell AIM antibody panel. Cells were first gated on lymphocytes and single cells. Dead cells and CD14+ monocytes were excluded and Tfh cells defined as CD4+CXCR5+CD45RO+ from which activated cells are identified as OX40+CD25+. Spillover spreading (**spread**) of CD4 and CXCR5 staining is shown on the fully stained and CXCR5 FMO gates.

3.2.3.5.2 Titration of HPV 16 and 18 VLPs for Tfh cell culture stimulation

Aware of the spread issue between AF700-CXCR5 and PerCpCy5.5-CD4 that did not hinder identification of Tfh cells, HPV 16 and 18 VLPs were titrated to 5, 10, 15 and 20 µg/mL and used to stimulate cells alongside the SEB positive control and negative control (culture medium without stimulus). This would determine optimal VLP concentrations to be used in Tfh cell stimulation for identification of vaccine-induced Tfh cells. Total Tfh cell population (CD4+CXCR5+CD45RO+) was identified as earlier described and the frequencies of activated OX40+CD25+ population identified from the negative control, positive control and the different concentrations of HPV 16 and HPV 18 (Figure 3.15A). The positive and negative control activated frequencies were 15.1% and 0.0%, respectively, an indication that the assay worked as expected, while for antigen specific response, the highest Tfh cell activation was observed at a VLP concentration of 15 µg/mL (HPV 16; 3.51% and HPV 18; 1.07%) (Figure 3.15B). This concentration was therefore selected to be used in subsequent complete panel testing.

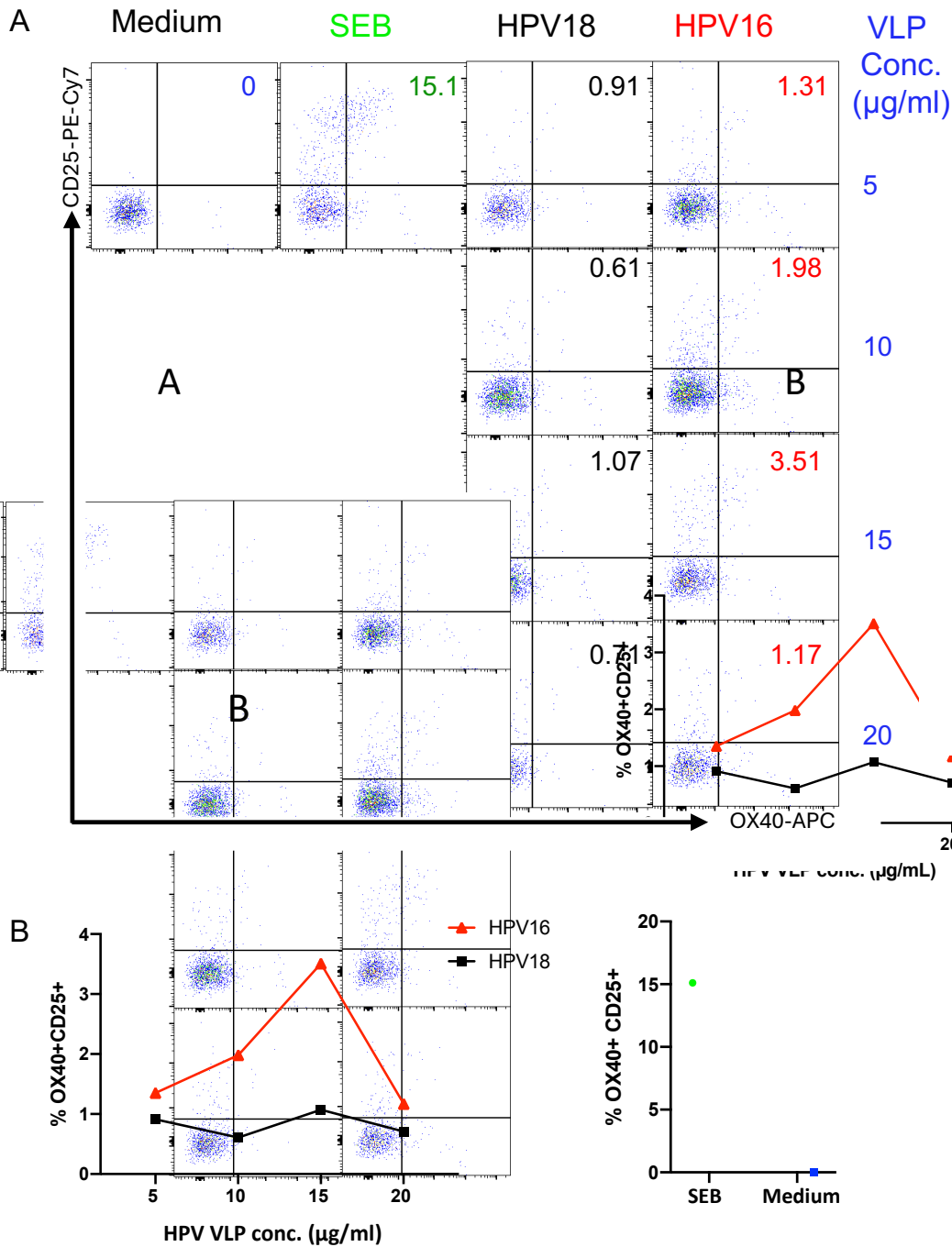


Figure 3.15. Titration of HPV 16 and HPV 18 VLPs for identification of vaccine-induced antigen specific Tfh cells

A fresh whole blood collected at day 9 post-first dose of Gardasil 9 vaccination was stimulated for 18 hours with HPV 16 or 18 VLPs at 4 different concentrations (5,10,15 and 20 µg/mL), SEB as a positive control and culture medium without stimulus as a negative control. The cells were then stained using Tfh cell AIM panel. Lymphocytes and single cell live cells were gated first and total Tfh cells identified from which frequencies of activated OX40+CD25+ Tfh cells were identified for the different stimulation conditions (A) and plotted on a line graph (B).

3.2.3.5.3 Evaluation of complete Tfh cell AIM panel

To evaluate the complete Tfh cell panel, whole blood was stimulated with SEB and stained with all antibodies in the panel including those excluded when optimising for stimulation conditions (FITC-PD-L1, PE-ICOS, APC-Cy7-CXCR3, BV421-CCR6 and PE-CF594-FoxP3). The staining of each antibody in the complete panel was evaluated using respective FMO. The gating strategy for identification of target cell population was adjusted to accommodate all markers in the panel with initial dumping of dead and CD14⁺ cells, followed by identification of total Tfh cells in viable cells as CD4⁺FoxP3⁻CD45RO⁺CXCR5⁺. Activated Tfh cell frequencies were then identified based on different combinations of three AIM markers (OX40, CD25 and PD-L1) and ICOS (non-specific activation marker). The frequency of total Tfh cells (CD45RO⁺CXCR5⁺) in CD4⁺FoxP3⁻ cells was 3.7% (Figure 3.16). Out of six possible combinations of the activation markers used (ICOS⁺OX40⁺, PD-L1⁺OX40⁺, PD-L1⁺ICOS⁺, PD-L1⁺CD25⁺, OX40⁺CD25⁺ and ICOS⁺CD25⁺), a clear population of activated Tfh cells was only observed for OX40⁺CD25⁺ with a frequency of 32.3% while resolution was poor in the other five cases with no clearly identifiable double positive populations (Figure 3.16).

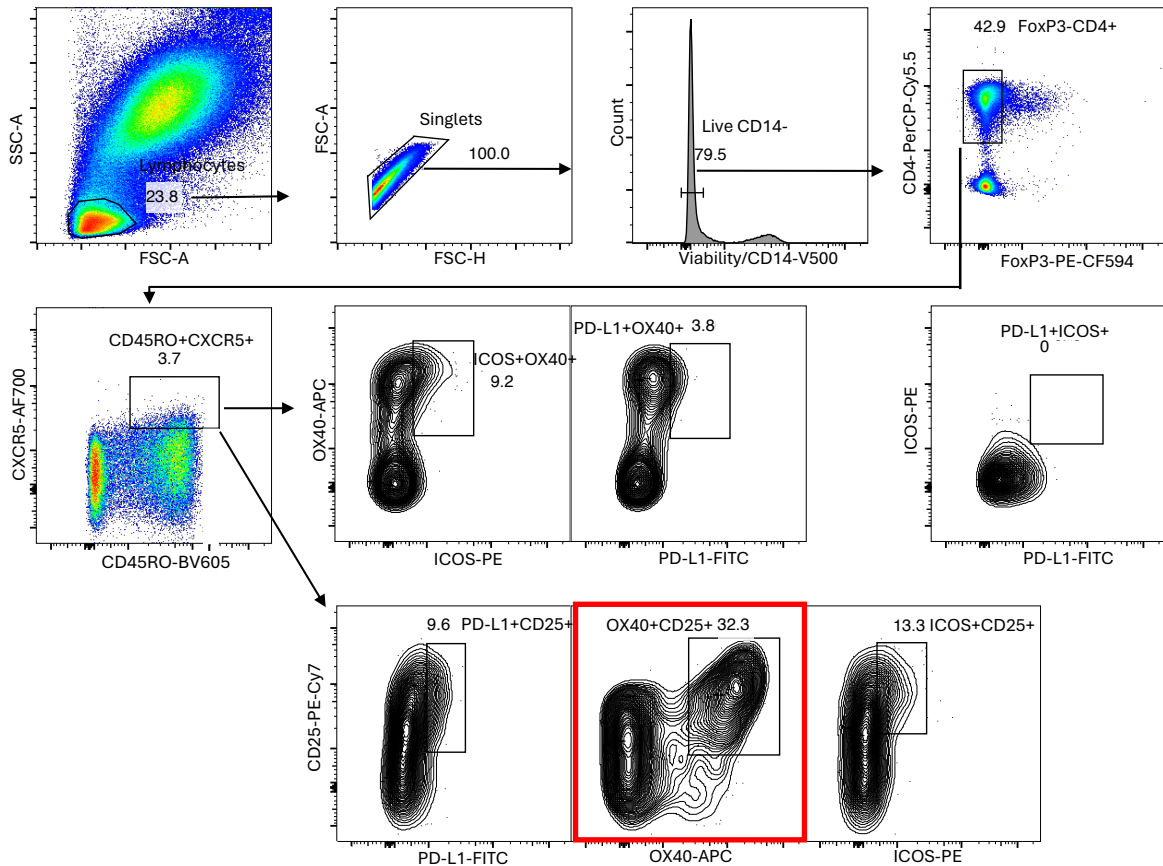


Figure 3.16. Initial complete AIM panel failed to identify expected profiles of polyclonally activated Tfh cells

Fresh whole blood was stimulated for 18 hours with SEB and stained using the initially designed complete Tfh AIM panel. Lymphocytes and single live CD14⁻ cells were gated first and total Tfh cells identified as CD4⁺FoxP3⁻, CD45RO⁺CXCR5⁺ before identification of activated cell populations in six possible combinations of the activation markers used including ICOS⁺OX40⁺, PD-L1⁺OX40⁺, PD-L1⁺ICOS⁺, PD-L1⁺CD25⁺, OX40⁺CD25⁺ and ICOS⁺CD25⁺. OX40⁺CD25⁺ gate in a red box was the only clearly resolved activated population.

The AIM panel was re-designed to resolve the resolution issues identified. Changed antibodies in the new panel included: CD4-AF700, CXCR5-PerCP-Cy5.5, CD25-BV786, OX40-BV650, PD-L1-PE and ICOS-PECy7 (see Appendix 7 for their titration results). The new panel was tested again using SEB stimulation and gating performed the same way described earlier.

Activated Tfh cells were clearly identified using the six combinations of activation markers and showed the expected profiles at higher frequencies than observed earlier (68.8% ICOS+OX40+, 52.5% PD-L1+OX40+, 61.9% PD-L1+ICOS+, 69.5% PD-L1+CD25+, 67.2% OX40+CD25+ and 60.9% ICOS+CD25+) (Figure 3.17). Activation induced markers have been reported to identify similar profiles of overlapping activated T cells and this was expected to confirm the assay was working well.(Reiss et al., 2017a)

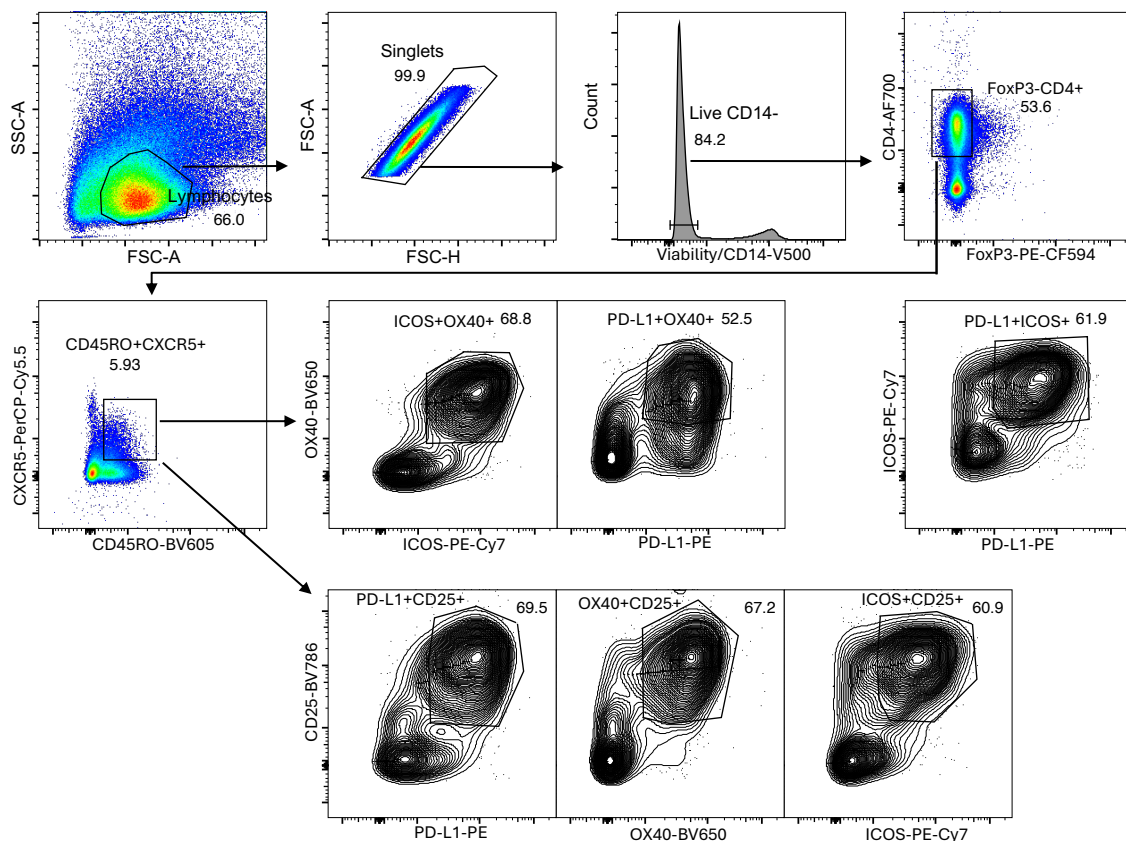


Figure 3.17. Re-designed AIM panel identified expected profiles of polyclonally activated Tfh cells

Fresh whole blood was stimulated for 18 hours with SEB and stained using the complete re-designed Tfh AIM panel. Lymphocytes and single live cells were gated first. After exclusion of dead and CD14+ cells in a dump channel, regulatory T cells were excluded by gating CD4+FoxP3- and total Tfh cells identified as CD45RO+CXCR5+ from which frequencies of activated antigen specific cells were identified by six possible combinations of the activation markers used including ICOS+OX40+, PD-L1+OX40+, PD-L1+ICOS+, PD-L1+CD25+, OX40+CD25+ and ICOS+CD25+. Expected profiles of activated cells were clearly identified.

3.2.3.5.4 Evaluation of AIM panel for identification of HPV specific Tfh cells after vaccination

After confirming successful identification of activated Tfh cell profiles from SEB stimulation the panel was then applied to identify HPV 16 and 18 specific Tfh cells after Gardasil 9 vaccination. Changes were made from this point on to stain frozen PBMC samples using the conditions optimised on whole blood. PBMC were stimulated with HPV 16 and HPV 18 alongside SEB positive control and culture medium without stimulation as negative control. Total Tfh cell population was identified as earlier described with a phenotype of CD4+FoxP3-CD45RO+CXCR5+ from which frequencies of antigen specific cells were identified based on AIM expression. From this point on, expression of only the AIM markers (OX40, CD25 and PD-L1) was considered, bringing the possible combinations down to three (OX40+CD25+, PD-L1+CD25+ and OX40+PD-L1+) while ICOS was excluded to be evaluated in the ex vivo panel only. Both HPV 16 and 18 specific Tfh cell frequencies were clearly identified using the different AIM combinations compared to the controls (Figure 3.18). Additionally, the detected AIM frequencies showed the expected overlapping profiles of OX40+CD25+, PD-L1+CD25+ and OX40+PD-L1+ for HPV 16; 6.70%, 6.97% and 6.97%, and HPV 18; 8.23%, 8.88% and 9.04%, respectively (Figure 3.18). The frequencies of activated cells were very high with SEB stimulation and very low background in the unstimulated cells (Figure 3.18).

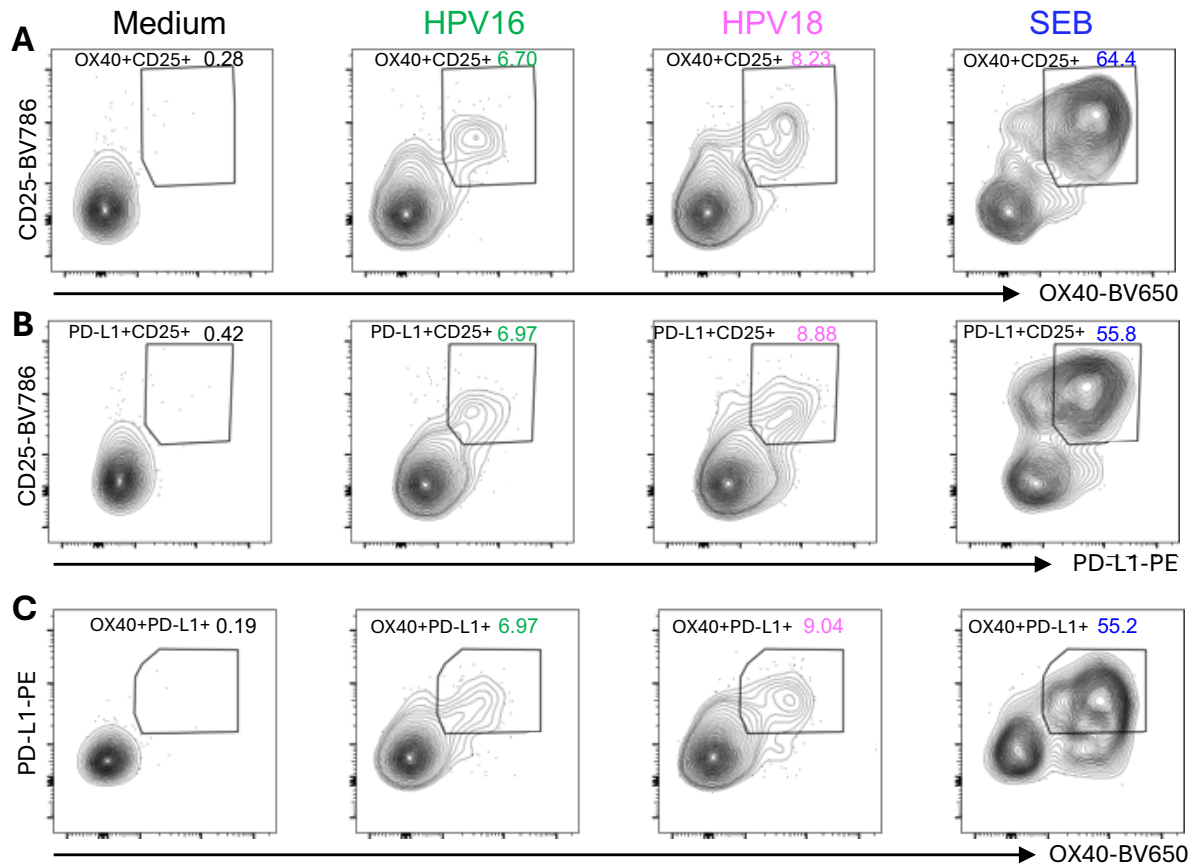


Figure 3.18. AIM panel identified HPV 16 and HPV 18 specific Tfh cells after vaccination

Frozen PBMC collected at day 7 post-second dose of Gardasil 9 vaccination were stimulated in culture for 18 hours using either HPV 16, HPV 18, SEB or cultured in medium without stimulation. Gating was first performed for lymphocytes and single cells. After exclusion of dead and CD14+ cells in a dump channel, regulatory T cells were excluded by gating CD4+FoxP3- and total Tfh cells identified as CD45RO+CXCR5+ from which frequencies of activated antigen specific cells were identified as **(A)** OX40+CD25+, **(B)** PD-L1+CD25+ and **(C)** OX40+PD-L1+ in all stimulation conditions.

3.2.3.6 Tfh cell ex vivo antibody panel

Both Tfh cells ex vivo and AIM panels used the same antibodies for identification of the total Tfh pool in addition to which the ex vivo panel included only two activation markers (ICOS and PD-1) for identification of overall non-specific Tfh cell activation. This panel was simple, with no requirement for cell stimulation before optimising the staining conditions.

3.2.3.6.1 Optimisation of Tfh cell ex vivo panel

Initial complete panel testing was performed on fresh whole blood with FMO controls. The resolution problem between PerCP-Cy5.5-CD4 and AF700-CXCR5 observed in this panel was less than what had been observed in the AIM panel, and the CD4+CXCR5+ population was identified at a lower frequency (1.8%) than in the AIM panel (Figure 3.19A). Total Tfh cells were identified as CD4+CXCR5+CD45RO+ from which the frequency of activated ICOS+PD-1++ was identified in the fully stained sample and compared to all FMOs. Activated cells were not clearly detectable in the fully stained sample (0.4%) and in the FMOs except in the CXCR3 FMO (1.6%) (Figure 3.19A). This was attributed to a spectral overlap between PE (ICOS) and PECy7 (PD-1), as depicted by the respective FMOs, warranting re-designing of the panel (Figure 3.19A).

The three Tfh cell subsets were identified based on expression of CXCR3 and CCR6 as Tfh1; CXCR3+CCR6- (19.1%), Tfh2; CXCR3-CCR6- (20.2%) and Tfh17; CXCR3-CCR6+ (47.5%), with no clearly identifiable activated cells in either of the Tfh cell subsets (Figure 3.19B).

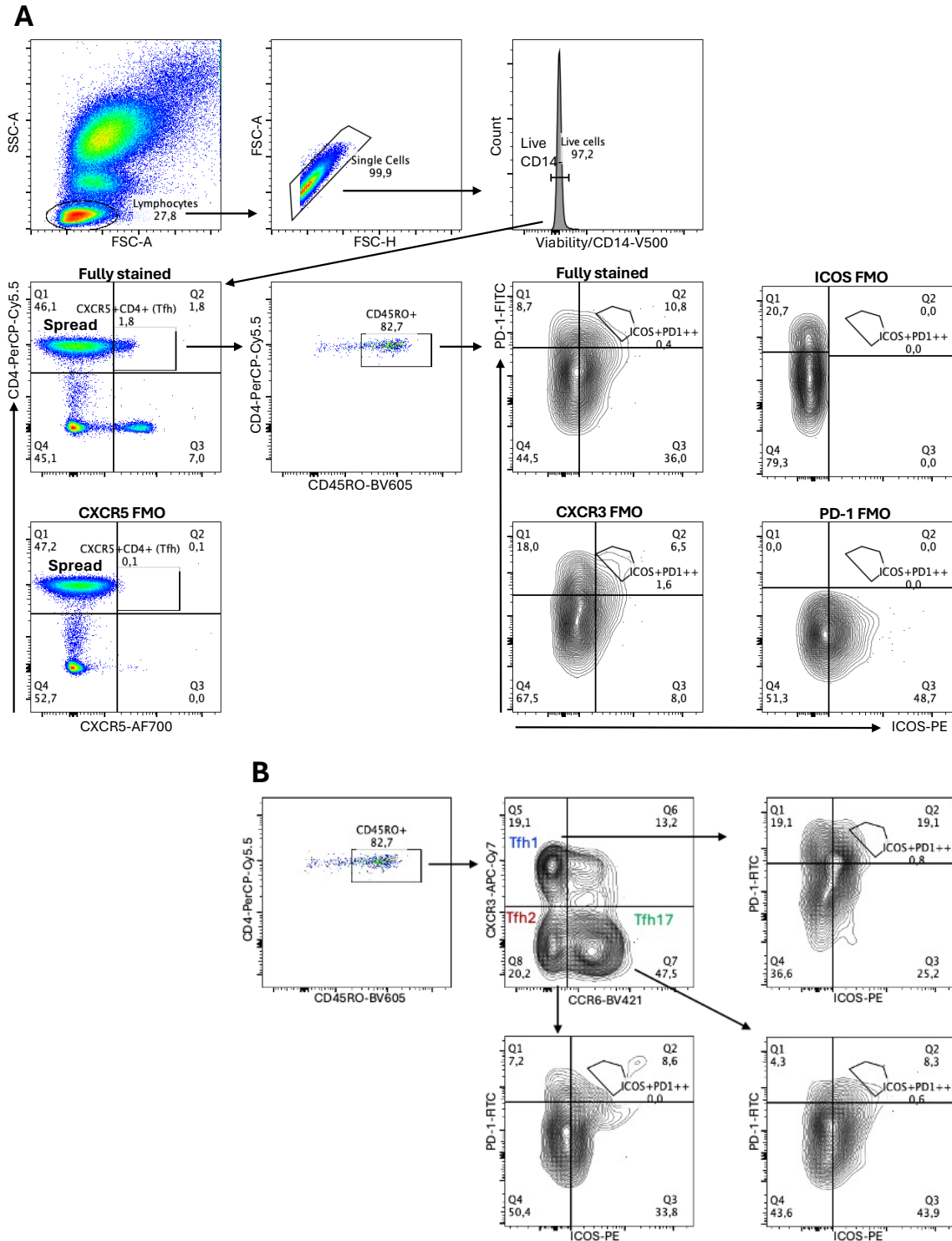


Figure 3.19. Initial ex vivo panel failed to identify clear activated Tfh cells

Whole blood was stained with Tfh cell ex vivo panel. **A:** Gating was first performed for lymphocytes and single cells. Dead cells were excluded and Tfh cells defined as CD4+CXCR5+CD45RO+ from which activated cells were then gated as ICOS+PD-1++. **B:** Three Tfh cell subsets were identified as Tfh1 (CXCR3+CCR6-), Tfh2 (CXCR3-CCR6-) and Tfh17 (CXCR3- CCR6+) and activated Tfh cells (ICOS+PD-1++) gated in each subset.

The ex vivo Tfh panel was re-designed with few adjustments to improve resolution between CD4 and CXCR5 and ICOS and PD-1 identified to have spillover spread errors. The re-designed Tfh cell panel included AF700-CD4, PerCP-Cy5.5-CXCR5, PECy7-ICOS (as changed in the AIM panel) and PE-PD-1. In keeping consistency with the AIM panel, the gating strategy was changed to first identify CD4⁺ T cells before identification of Tfh cell population based on co-expression of CD45RO and CXCR5 markers. FoxP3 was not used in this panel because Tregs contamination was mainly a concern in the AIM panel due to in-vitro stimulation that causes them to upregulate CXCR5. The re-designed panel was tested on PBMC collected after Gardasil 9 vaccination, and target cell populations were identified clearly. Total Tfh cells with a phenotype of CD4⁺CD45RO⁺CXCR5⁺ constituted 2.4% of CD4⁺ T cells, out of which, the frequency of total activated ICOS⁺PD-1⁺⁺ cells was 4.18% (Figure 3.20). Tfh cell subsets were identified at frequencies of Tfh1; 21.2%, Tfh2; 55.3% and Tfh17; 18.3% with frequencies of activated ICOS⁺PD-1⁺⁺ cells in the subsets being Tfh1; 6.64%, Tfh2; 3.63% and Tfh17; 3.38% (Figure 3.20). Overall, activated Tfh cells were detectable at high frequencies with the re-designed panel.

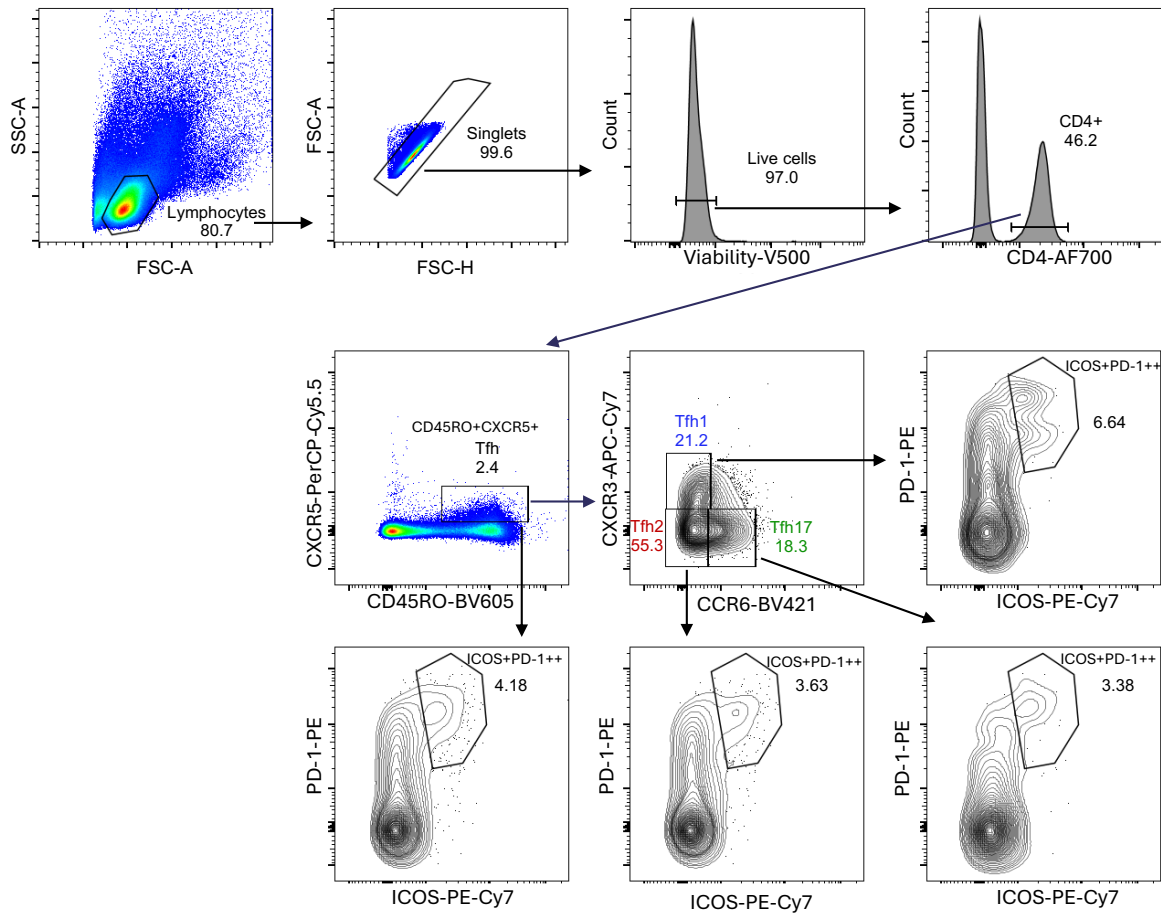


Figure 3.20. Re-designed Tfh cell ex vivo panel clearly identified total activated pool of Tfh cells after vaccination

Frozen PBMC from a donor vaccinated with Gardasil 9 was stained with re-designed Tfh cell ex vivo panel. Gating was first performed for lymphocytes and single cells. Dead cells were excluded and Tfh cells defined as CD4+CXCR5+CD45RO+. Activated Tfh cells were identified as ICOS+PD-1++. The three Tfh cell subsets were then defined as Tfh1 (CXCR3+CCR6-), Tfh2 (CXCR3-CCR6-) and Tfh17 (CXCR3- CCR6+). Activated Tfh cell frequencies (ICOS+PD-1++) within each subset were also identified.

3.3 Conclusion and discussion

ELISpot and FluoroSpot are established sensitive methods for enumeration of antigen specific B cell and T cell responses and have been widely applied in research with few applications and ongoing evaluations for diagnostics use on various diseases.(Essone et al., 2014, Mangsbo et al., 2021). In this work, these assays were successfully optimised for reliable enumeration of cells secreting HPV specific antibodies. Optimal plate coating concentrations of HPV VLP and cell numbers to be analysed were determined. The ELISpot assay identified vaccine-induced HPV type specific IgG and IgM memory B cells and plasma cells while the FluoroSpot assay identified vaccine-induced HPV type specific IgG and IgM plasma cells. Subsequently, ELISpot would be applied to enumerate HPV 16 and HPV 18 specific IgG memory B cells and FluoroSpot to identify IgG and IgM plasma cells.

Flow cytometry is an established technique widely used to characterise cells or particles based on their physical and chemical characteristics and is widely used in immunology research. It allows precise identification and classification of cell populations and sub-populations based on their immunophenotype and can be fitted with cell sorting systems for bulk or single cell sorting for subsequent detailed analysis of the target cells.(Robinson et al., 2023) Development of the flow cytometry assays was intensive involving antibody panel design and re-designing process to ensure the B cell- and two Tfh cell panels allowed clear identification of the target cell populations. Total plasma cell phenotype was identified as CD19+CD38++CD27+CD21+/-low from which IgG+ and IgM+ plasma cell frequencies were identified.

The AIM Tfh cell panel identified in-vitro stimulated HPV 16 and HPV 18 specific Tfh cells after re-designing it by changing some fluorochrome-marker combinations. The phenotype of total Tfh cells was identified as CD4+CXCR5+CD45RO+ from which three combinations of the AIM markers CD40, CD25 and PD-L1 were used to identify the activated cell as CD40+CD25+, CD40+PD-L1+ and PD-L1+CD25+. To maximise on detecting antigen specific Tfh cells, FoxP3-based exclusion of Tregs was used since they also upregulate

CD25.(Reiss et al., 2017a) This strategy is considered to be the most robust way to detect antigen specific T cells of interest using the AIM assay.(Reiss et al., 2017a) Similarly, after re-designing which involved changing some fluorochrome-marker combinations, the Tfh ex vivo panel identified total Tfh cells ex vivo as CD4+CXCR5+CD45RO+ from which total activated cells were identified as ICOS+PD-1++. The three Tfh subsets Tfh1 (CXCR3+CCR6-), Tfh2 (CXCR3-CCR6-) and Tfh17 (CXCR3-CCR6+) were also identified from the total Tfh cells population and activated ICOS+PD-L1++ frequencies identified.

The limitations of this assay development work are acknowledged. First the ideal samples for optimising the assays would have been the study samples which was not feasible due to availability of small sample volumes. Additionally, HPV vaccination is not commonly administered to adults in The Gambia hence only one vaccinated donor provided blood samples for optimising all assays. This contributed to the limitation observed in some optimisation results especially in the flow cytometry assays where few cells were available for analysis leading to acquisition of few events. To address these limitations, results from the first study samples were checked for indications that would warrant adjustments on the pre-optimised assay conditions.

Further limitations were occasioned by COVID-19 pandemic interruptions on the entire clinical trial that started just after all the assays had been optimised for analysis of fresh whole blood samples. To mitigate such interruptions, the flow cytometry assays were adapted to staining frozen PBMC. The exclusion of CD138, a survival marker from the plasma cell panel after losing its staining signal in frozen PBMC limited the capability of the panel to define the likely lifespan of the identified plasma cells.

4. PLASMA CELL AND MEMORY B CELL RESPONSES AFTER GARDASIL 9 VACCINATION

This chapter discusses the results from enumeration of plasma cell and memory B cell responses under the specific objectives listed below.

4.1 Aims

- i) To enumerate HPV 16 and HPV 18 specific and IgG and IgM plasma cells induced by the first and second or third vaccination doses of Gardasil 9 vaccine.
- ii) To immunophenotype and determine the frequencies of total IgG and IgM plasma cells following the first and second or third doses of Gardasil 9 vaccine.
- iii) To enumerate HPV 16 and HPV 18 specific and IgG memory B cells induced by the first and second or third vaccination doses of Gardasil 9 vaccine.
- iv) To evaluate the effect of age and vaccination dose numbers on Gardasil 9-induced plasma cell and memory B cell responses.

4.2 Results

4.2.1 Plasma cell responses after HPV vaccination

A total of 60 females across the 3 age groups (4-8-, 9-14- and 15-26-year-olds) were randomised to group B as outlined in figure 2.1 in chapter 2, for enumeration of vaccine-induced HPV 16 and HPV 18 specific IgG and IgM plasma cells. The participants were vaccinated with two different dose schedules depending on their age. Those aged 4-8 years received two doses at a 12-month interval while those aged 15-26 years received three doses at 0, 2 and 12 months. The HPV 16 and HPV 18 specific IgG and IgM plasma cells were enumerated using dual-colour FluoroSpot assay at 4 timepoints: Baseline (before first dose), seven days post-dose 1, pre-dose 2- and seven-days post-dose 2 (4-14-year-olds) or pre-dose 3- and seven-days post-dose 3 (15-26-year-olds). The HPV specific IgG and IgM secreting cells enumerated by FluoroSpot were expressed per million input PBMC. More

details on the materials, methods and statistical comparisons applied here have been described in chapters 2 and 3

Figure 4.1 shows FluoroSpot data from one individual in the 15-26-year-old group. From this example, total IgG and total IgM plasma cells in the positive control wells were detected across all timepoints while the PBS-coated negative control wells had none or few spots where present. Antigen specific IgG plasma cells were detected at 7 days after both vaccination doses while IgM plasma cells were mainly detected after the first vaccination dose at lower numbers than IgG plasma cells.

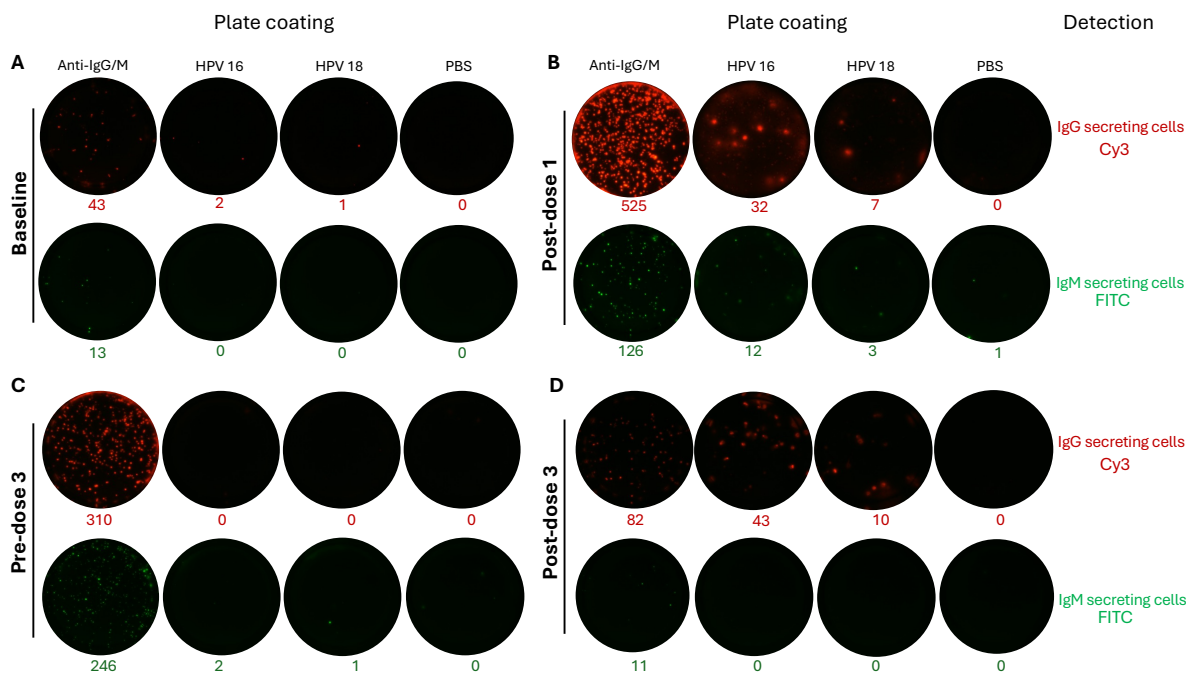


Figure 4.1. FluoroSpot readout from one participant in the 15-26-year-olds group

Wells for detection of IgG and IgM secreting cells are shown for the four test conditions (total IgG and total IgM (positive control), HPV 16 and HPV 18 (antigen specific) and PBS (negative control) across four timepoints; baseline (A), after dose 1 (B), before (C) and after dose 3 (D). Data shown here is from only single well tests, final analysis was based on mean spot counts of triplicate wells for antigen specific tests and duplicate wells for the control tests. IgG and IgM secreting cells were detected in cyanine3 (Cy3) (shown in red), and fluorescein (FITC) (shown in green) fluorescent detectors respectively, in an automated ELISpot reader. Spot counts are indicated below each well.

The plasma cell results described here are for 55 participants (4-8-year-olds; n = 20, 9-14-year-olds; n = 19 and 15-26-year-olds; n = 16) from whom complete paired FluoroSpot data was generated for all four targeted timepoints before and after vaccination. Data analysis was performed after subtraction of ASC counts in the negative control wells as outlined in methods section 2.3.3. Due to presence of many zero values at baseline and overall skewedness after vaccination, a constant (+1) was added to the final FluoroSpot dataset before \log_{10} transformation. The absolute antigen specific cell numbers were tabulated as median counts per million input PBMC and 25th and 75th percentiles and the log-transformed data visualized in box and whisker plots.

4.2.1.1 HPV 16 and HPV 18 specific IgG plasma cell response

From the pooled analysis, although a number of participants generated high IgG plasma cell responses following dose 1, there was overall no significant increase in HPV 16 specific IgG secreting cell numbers (median; 25th - 75th percentiles: baseline = 1; 0 - 4, post-dose 1 = 3; 1- 7, p = 0.0975) (Table 4.1A, Figure 4.2A). There was a significant increase in HPV 18 specific IgG secreting cell numbers (baseline = 1; 0 - 4, post-dose 1 = 3; 1 - 8, p = 0.0175 (Table 4.1B, Figure 4.2B). Doses 2 and 3 generated high IgG secreting cell numbers for both HPV 16 (median; 25th - 75th percentiles: post-dose 2 or 3 = 325;157 - 691, p < 0.0001) (Table 4.1A, Figure 4.2A) and HPV 18 (127; 60 - 271, p < 0.0001) (Table 4.1B, Figure 4.2 B).

The age stratified analysis showed similar overall profiles of IgG plasma cell numbers across the three age groups. Following dose 1, there was an increase in IgG secreting cell numbers in a number of individuals but no significant increase overall and a robust boosting was observed after dose 2 or 3. In the 4-8-year-olds group, HPV 16 and HPV 18 specific IgG secreting cell numbers were: (median; 25th - 75th percentiles: baseline = 0; 0 - 1, post-dose 1 = 2; 0 - 6, p = 0.0553, post-dose 2 = 310; 108 - 636, p < 0.0001 for HPV 16, and baseline = 0; 0 - 1, post-dose 1 = 1; 0 - 8, p = 0.0581, post-dose 2 = 128; 47 - 347, p < 0.0001 for HPV 18) (Table 4.1C & D, Figure 4.2C & D). In the 9-14-year-olds group, HPV 16 and HPV 18

specific IgG secreting cell numbers were: (median; 25th - 75th percentiles: baseline = 3; 0 - 4, post-dose 1 = 3; 1 - 4, p = 0.9748, post-dose 2 = 432; 243 - 827, p < 0.0001 for HPV 16, and baseline = 3; 1 - 4, post-dose 1 = 3; 1 - 7, p = 0.6707, post-dose 2 = 159; 93 - 292, p < 0.0001 for HPV 18) (Table 4.1C & D, Figure 4.2C & D). In the 15-26-year-olds group, HPV 16 and HPV 18 specific IgG secreting cell numbers were: (median; 25th - 75th percentiles: baseline = 5; 2 - 5, post-dose 1 = 2; 0 - 61, p = 0.7740, post-dose 3 = 165; 90 - 361, p < 0.0001 for HPV 16, and baseline = 3; 0 - 5, post-dose 1 = 3; 1 - 11, p = 0.6111, post-dose 3 = 91; 57 - 160, p < 0.0001 for HPV 18) (Table 4.1C & D, Figure 4.2C & D).

Simple main effects ANOVA analysis for effect of age showed that overall antigen specific IgG plasma cell response was higher in younger age groups, p = 0.0393 for HPV 16, and p = 0.0218 for HPV 18. (Table 4.1C & D, Figure 4.3A & B).

Table 4.1. Number of HPV 16 and HPV 18 specific IgG secreting cells per 10⁶ PBMC

A: HPV 16 pooled

	All ages	4 to 26 years; n = 55			
	Sampling timepoint	Baseline	Post-dose 1	Pre-dose 2/3	Post-dose 2/3
No. of IgG secreting cells per 10 ⁶ PBMC	25% Percentile	0	1	0	157
	Median	1	3	0	325
	75% Percentile	4	7	3	691

B: HPV 18 pooled

	All ages	4 to 26 years; n = 55			
	Sampling timepoint	Baseline	Post-dose 1	Pre-dose 2/3	Post-dose 2/3
No. of IgG secreting cells per 10 ⁶ PBMC	25% Percentile	0	1	0	60
	Median	1	3	0	127
	75% Percentile	4	8	1	271

Continued on next page

C: HPV 16 age-stratified

	Age stratified	4 to 8 years; n = 20				9 to 14 years; n = 19				15 to 26 years; n = 16			
	Sampling timepoint	Baseline	Post-dose 1	Pre-dose 2	Post-dose 2	Baseline	Post-dose 1	Pre-dose 2	Post-dose 2	Baseline	Post-dose 1	Pre-dose 3	Post-dose 3
No. of IgG secreting cells per 10 ⁶ PBMC	25% Percentile	0	0	0	108	0	1	0	243	2	0	0	90
	Median	0	2	0	310	3	3	1	432	5	2	0	165
	75% Percentile	1	6	3	636	4	4	3	827	5	61	3	361

D: HPV 18 age-stratified

	Age stratified	4 to 8 years; n = 17				9 to 14 years; n = 20				15 to 26 years; n = 18			
	Sampling timepoint	Baseline	Post-dose 1	Pre-dose 2	Post-dose 2	Baseline	Post-dose 1	Pre-dose 2	Post-dose 2	Baseline	Post-dose 1	Pre-dose 3	Post-dose 3
No. of IgG secreting cells per 10 ⁶ PBMC	25% Percentile	0	0	0	47	1	1	0	93	0	1	0	57
	Median	0	1	0	128	3	3	1	159	3	3	0	91
	75% Percentile	1	8	1	347	4	7	1	292	5	11	1	160

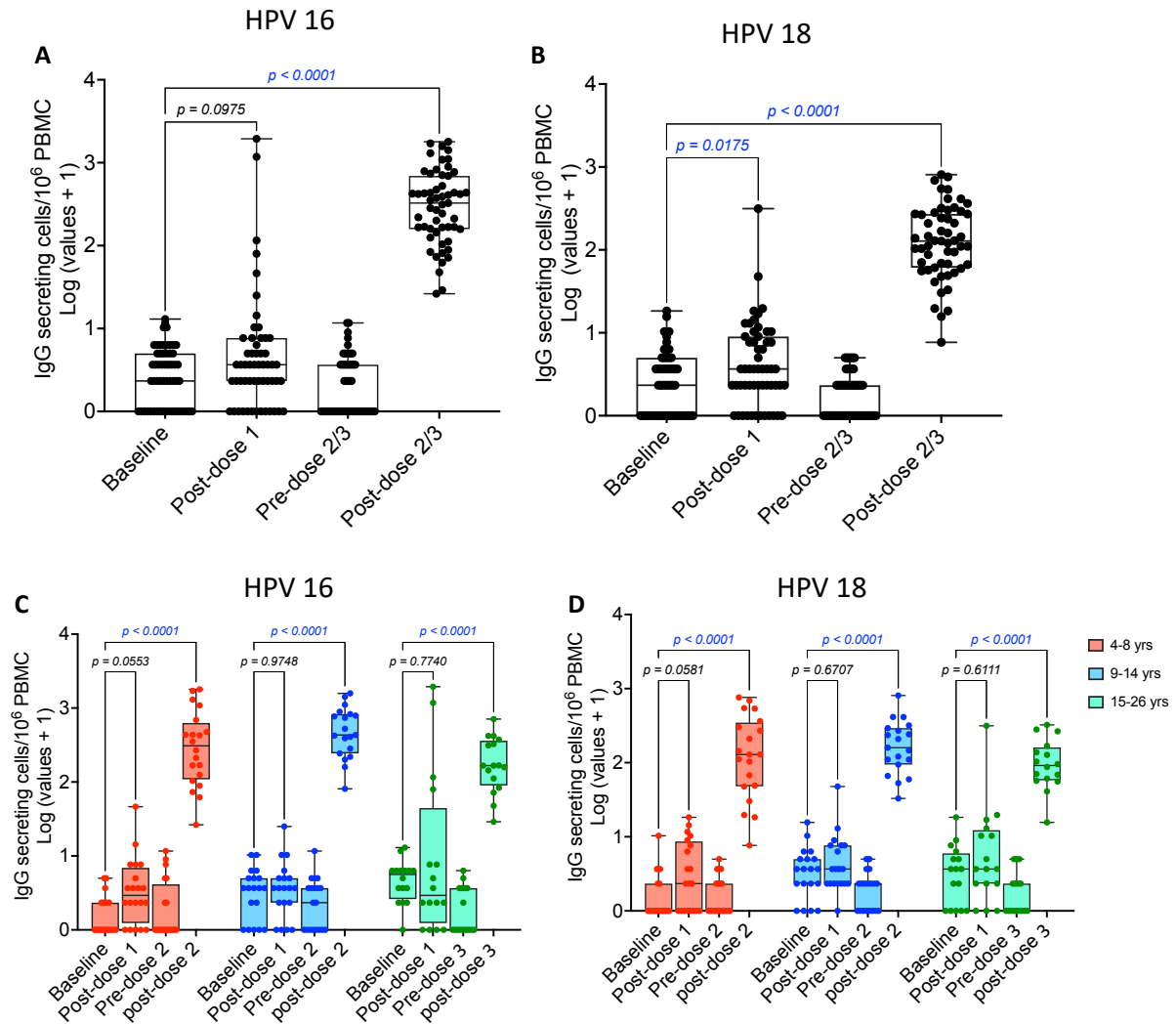


Figure 4.2. HPV 16 and HPV 18 specific IgG plasma cell response after Gardasil 9 vaccination

Fresh PBMC from baseline, day 7 post-dose 1, pre- and day 7 post-dose 2 or 3 of Gardasil 9 vaccination were analysed by FluoroSpot. **A & B:** Pooled data for the 3 age groups ($n = 55$), **C & D:** Age stratified data for 3 age groups (4-8-year-olds; $n = 20$, 9-14-year-olds; $n = 19$ and 15-26-year-olds; $n = 16$) at baseline (before vaccination), post-dose 1, pre- and post-dose 2 or 3 in the respective groups. IgG plasma cell numbers at baseline were compared to those measured after dose 1 and dose 2 or 3 in respective age groups as shown. Pooled (all age groups) and age-stratified analyses were performed. One-way ANOVA followed by Dunnett's adjusted multiple comparison tests were performed for the pooled data and Two-way ANOVA followed by Tukey adjusted multiple comparison tests were performed for age-stratified data. The three age groups are shown in different colours. Each dot represents an individual. The box and whisker plots represent response distribution with the lower, central and upper lines denoting minimum, median and maximum values, respectively. Statistically significant p values ($p < 0.05$) are highlighted in blue.

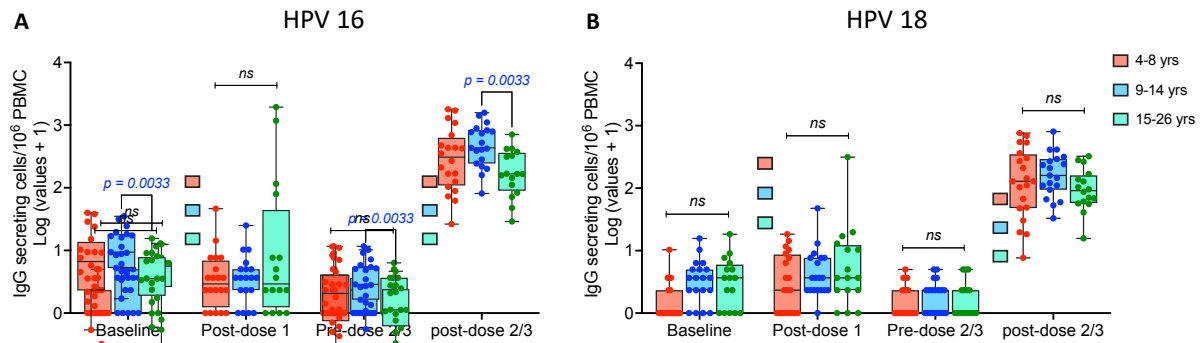


Figure 4.3. HPV 16 and HPV 18 specific IgG plasma cell response after Gardasil 9 vaccination, comparisons per timepoint

Fresh PBMC from baseline, day 7 post-dose 1, pre- and day 7 post-dose 2 or 3 of Gardasil 9 vaccination were analysed for HPV 16 (A) and HPV 18 (B) specific IgG plasma cells by FluoroSpot. Data shown for 3 age groups (4-8-year-olds; $n = 20$, 9-14-year-olds; $n = 19$ and 15-26-year-olds; $n = 16$) at baseline (before vaccination), post-dose 1, pre- and post-dose 2 or 3 in the respective groups. Two-way ANOVA followed by Tukey adjusted multiple comparison tests were performed to compare plasma cell numbers between the three age groups at different timepoints. The three age groups are shown in different colours. Simple main effects analysis showed overall higher response in younger age groups ($p = 0.0393$ and 0.0218 for HPV 16 and HPV 18, respectively). Each dot represents an individual. The box and whisker plots represent response distribution with the lower, central and upper lines denoting minimum, median and maximum values, respectively. Only statistically significant p values ($p < 0.05$) are shown in blue. (ns): non-significant.

4.2.1.2 HPV 16 and HPV 18 specific IgM plasma cell response

From the pooled analysis, there was a slight overall increase in numbers of HPV 16 and HPV 18 specific IgM secreting cells after dose 1, and a decrease on subsequent timepoints with no apparent differences: (median; 25th - 75th percentiles: baseline = 1; 0 - 1, post-dose 1 = 3; 1 - 5, $p = 0.0007$, post-dose 2 or 3 = 1; 0 - 3, $p = 0.9110$ for HPV 16, and baseline = 0; 0 - 1, post-dose 1 = 1; 1 - 4, $p < 0.0001$, post-dose 2 or 3 = 0; 0 - 1, $p = 0.9040$ for HPV 18) (Table 4.2A & B, Figure 4.4A & B).

The age stratified analysis showed similar overall profiles of IgM plasma cell numbers across the three age groups. After dose 1, there was a slight increase in IgM secreting cell numbers followed by a decrease before and after dose 2 or 3. In the 4-8-year-olds group, HPV 16 and HPV 18 specific IgM secreting cell numbers were: (median; 25th - 75th percentiles: baseline = 1; 0 - 3, post-dose 1 = 4; 1 - 10, $p = 0.0344$, post-dose 2 = 1; 0 - 3, $p = 0.9993$ for HPV 16,

and baseline = 0; 0 - 1, post-dose 1 = 1; 0 - 2, p = 0.2754, post-dose 2 = 0; 0 - 1, p >0.9999 for HPV 18) (Table 4.2C & D, Figure 4.4C & D). In the 9-14-year-olds group, HPV 16 and HPV 18 specific IgM secreting cell numbers were: (median; 25th - 75th percentiles: baseline = 0; 0 - 1, post-dose 1 = 1; 0 - 3, p = 0.1702, post-dose 2 = 1; 0 - 4, p = 0.2898 for HPV 16, and baseline = 0; 0 - 1, post-dose 1 = 3; 1 - 4, p = 0.0020, post-dose 2 = 0; 0 - 3, p = 0.9623 for HPV 18) (Table 4.2C & D, Figure 4.4C & D). In the 15-26-year-olds group, HPV 16 and HPV 18 specific IgM secreting cell numbers were: (median; 25th - 75th percentiles: baseline = 1; 0 - 2, post-dose 1 = 2; 0 - 5, p = 0.3467, post-dose 3 = 0; 0 - 1, p = 0.3374 for HPV 16, and baseline = 1; 0 - 2, post-dose 1 = 2; 1 - 4, p = 0.1103, post-dose 3 = 0; 0 - 1 for HPV 18) (Table 4.2C & D, Figure 4.4C & D).

There was no significant age effect on vaccine-induced antigen specific IgM plasma cell response (Table 4.2C & D, Figure 4.5A & B).

Table 4.2. Number of HPV 16 and HPV 18 specific IgM secreting cells per 10⁶ PBMC

A: HPV 16 pooled

	All ages	4 to 26 years; n = 55			
	Sampling timepoint	Baseline	Post-dose 1	Pre-dose 2/3	Post-dose 2/3
No. of IgM secreting cells per 10 ⁶ PBMC	25% Percentile	0	1	0	0
	Median	1	3	0	1
	75% Percentile	1	5	0	3

B: HPV 18 pooled

	All ages	4 to 26 years; n = 55			
	Sampling timepoint	Baseline	Post-dose 1	Pre-dose 2/3	Post-dose 2/3
No. of IgM secreting cells per 10 ⁶ PBMC	25% Percentile	0	1	0	0
	Median	0	1	0	0
	75% Percentile	1	4	1	1

Continued on next page

C: HPV 16 age stratified

	Age stratified	4 to 8 years; n = 17				9 to 14 years; n = 20				15 to 26 years; n = 18			
	Sampling timepoint	Baseline	Post-dose 1	Pre-dose 2	Post-dose 2	Baseline	Post-dose 1	Pre-dose 2	Post-dose 2	Baseline	Post-dose 1	Pre-dose 3	Post-dose 3
No. of IgM secreting cells per 10 ⁶ PBMC	25% Percentile	0	1	0	0	0	0	0	0	0	0	0	0
	Median	1	4	0	1	0	1	0	1	1	2	0	0
	75% Percentile	3	10	1	3	1	3	0	4	2	5	0	1

D: HPV 18 age-stratified

	Age stratified	4 to 8 years; n = 17				9 to 14 years; n = 20				15 to 26 years; n = 18			
	Sampling timepoint	Baseline	Post-dose 1	Pre-dose 2	Post-dose 2	Baseline	Post-dose 1	Pre-dose 2	Post-dose 2	Baseline	Post-dose 1	Pre-dose 3	Post-dose 3
No. of IgM secreting cells per 10 ⁶ PBMC	25% Percentile	0	0	0	0	0	1	0	0	0	1	0	0
	Median	0	1	0	0	0	3	0	0	1	2	0	0
	75% Percentile	1	2	1	1	1	4	1	3	2	4	1	1

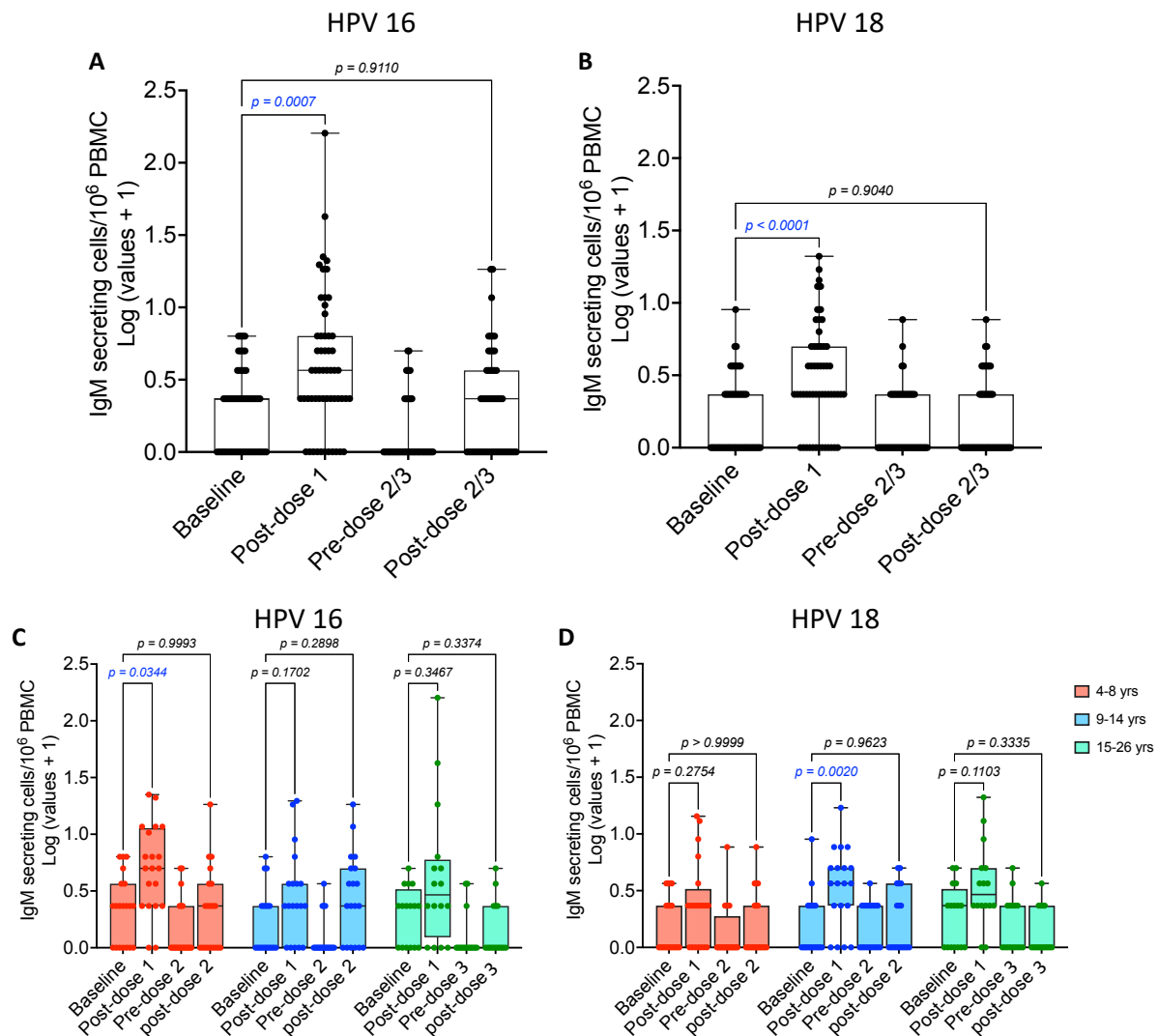


Figure 4.4. HPV 16 and HPV 18 specific IgM plasma cell response after Gardasil 9 vaccination

Fresh PBMC from baseline, day 7 post-dose 1, pre- and day 7 post-dose 2 or 3 of Gardasil 9 vaccination were analysed by FluoroSpot. **A & B:** Pooled data for the 3 age groups ($n = 55$), **C & D:** Age stratified data for 3 age groups (4-8-year-olds; $n = 17$, 9-14-year-olds; $n = 20$ and 15-26-year-olds; $n = 18$) at baseline (before vaccination), post-dose 1, pre- and post-dose 2 or 3 in the respective groups. IgM plasma cell numbers at baseline were compared to those measured after dose 1 and dose 2 or 3 in respective age groups as shown. Pooled (all age groups) and age-stratified analyses were performed. One-way ANOVA followed by Dunnett's adjusted multiple comparison tests were performed for the pooled data and Two-way ANOVA followed by Tukey adjusted multiple comparison tests were performed for age-stratified data. The three age groups are shown in different colours. Each dot represents an individual. The box and whisker plots represent response distribution with the lower, central and upper lines denoting minimum, median and maximum values, respectively. Statistically significant p values ($p < 0.05$) are highlighted in blue.

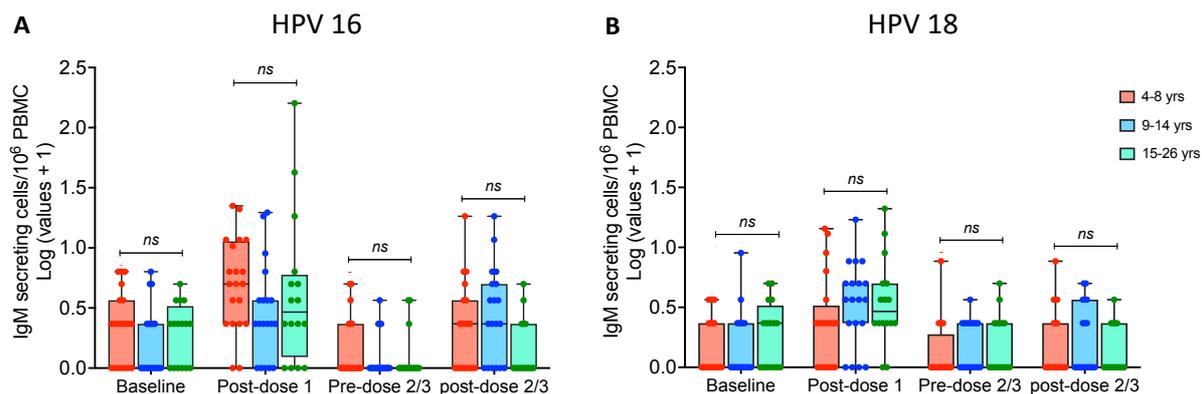


Figure 4.5. HPV 16 and HPV 18 specific IgM plasma cell response after Gardasil 9 vaccination, comparisons per timepoint

Fresh PBMC from baseline, day 7 post-dose 1, pre- and day 7 post-dose 2 or 3 of Gardasil 9 vaccination were analysed for HPV 16 (A) and HPV 18 (B) specific IgM plasma cells by FluoroSpot. Data shown for 3 age groups (4-8-year-olds; $n = 20$, 9-14-year-olds; $n = 19$ and 15-26-year-olds; $n = 16$) at baseline (before vaccination), post-dose 1, pre- and post-dose 2 or 3 in the respective groups. Two-way ANOVA followed by Tukey adjusted multiple comparison tests were performed to compare plasma cell numbers between the three age groups at different timepoints. The three age groups are shown in different colours. Simple main effects analysis showed no significant age effect on vaccine-induced IgM plasma cell response. Each dot represents an individual. The box and whisker plots represent response distribution with the lower, central and upper lines denoting minimum, median and maximum values, respectively. (ns): non-significant.

4.2.1.3 Total IgG and IgM plasma cell frequencies

The total IgG and IgM frequencies in circulation were measured by both FluoroSpot, as a positive control and by flow cytometry to determine their immunophenotype. Total IgG and IgM secreting cells enumerated by FluoroSpot were expressed per million input PBMC. Similar to the antigen specific plasma cell responses, there was high variability in the total IgG and IgM secreting cell numbers and the data was normalised by \log_{10} transformation before analysis. The results are presented for 57 participants (4-8-year-olds; $n = 20$, 9-14-year-olds; $n = 20$ and 15-26-year-olds; $n = 17$) who had complete paired data for the 4 targeted timepoints.

The pooled analysis showed an increase in the number of total IgG secreting cells after the first dose which further increased following dose 2 or dose 3 (median; 25th - 75th percentiles; Baseline = 1290; 615 - 2260, post-dose 1 = 1720; 1025 - 2722, $p = 0.0754$, post-dose 2 or 3 = 2230; 1330 - 3430, $p < 0.0001p$) (Table 4.3A, Figure 4.6A). The number of total IgM secreting cells increased slightly after dose 1 and decreased after dose 2 or 3 (median; 25th - 75th percentiles; Baseline = 250; 125 - 625, post-dose 1 = 330; 220 - 557, $p = 0.5573$, post-dose 2 or 3 = 180; 105 - 350, $p = 0.0522$) (Table 4.3B, Figure 4.6B).

From the age-stratified analysis, profiles of total IgG secreting cells across all age groups were similar to those observed in the pooled analysis with significant increase observed in the 9-14-year-olds after dose 2: (median; 25th - 75th percentiles; Baseline = 1020; 630 - 2161, post-dose 2 = 2900; 1773 - 3905, $p = 0.0017$) and in the 15-26-year-olds after dose 3: (median; 25th - 75th percentiles; Baseline = 640; 400 - 1425, post-dose 3 = 2220; 1110 - 2775, $p = 0.0004$) (Table 4.3C, Figure 4.6C). Total IgM secreting cells tended to decrease after both doses 1 and 2 in the 4-8-year-olds and the profiles were variable in the other two age groups, with no significant changes in all groups (Table 4.3D, Figure 4.6D).

Table 4.3. Number of total IgG and IgM secreting cells per 10⁶ PBMC

A: Total IgG pooled

	All ages	4 to 26 years; n = 57			
	Sampling timepoint	Baseline	Post-dose 1	Pre-dose 2/3	Post-dose 2/3
No. of IgG secreting cells per 10 ⁶ PBMC	25% Percentile	615	1025	700	1330
	Median	1290	1720	1120	2230
	75% Percentile	2260	2722	2240	3430

B: Total IgM pooled

	All ages	4 to 26 years; n = 57			
	Sampling timepoint	Baseline	Post-dose 1	Pre-dose 2/3	Post-dose 2/3
No. of IgM secreting cells per 10 ⁶ PBMC	25% Percentile	125	220	130	105
	Median	250	330	290	180
	75% Percentile	625	557	445	350

Continued on next page

C: Total IgG age-stratified

	Age stratified	4 to 8 years; n = 20				9 to 14 years; n = 20				15 to 26 years; n = 17			
	Sampling timepoint	Baseline	Post-dose 1	Pre-dose 2	Post-dose 2	Baseline	Post-dose 1	Pre-dose 2	Post-dose 2	Baseline	Post-dose 1	Pre-dose 3	Post-dose 3
No. of IgG secreting cells per 10 ⁶ PBMC	25% Percentile	1061	1215	713	1245	630	963	665	1773	400	1065	675	1110
	Median	1820	2280	1130	1825	1020	1235	895	2900	640	1720	1320	2220
	75% Percentile	2977	3123	1868	3420	2161	2058	2033	3905	1425	2495	2755	2775

D: Total IgM age-stratified

	Age stratified	4 to 8 years; n = 20				9 to 14 years; n = 20				15 to 26 years; n = 17			
	Sampling timepoint	Baseline	Post-dose 1	Pre-dose 2	Post-dose 2	Baseline	Post-dose 1	Pre-dose 2	Post-dose 2	Baseline	Post-dose 1	Pre-dose 3	Post-dose 3
No. of IgM secreting cells per 10 ⁶ PBMC	25% Percentile	215	258	115	130	133	173	135	90	95	165	145	100
	Median	440	415	255	195	225	305	225	235	120	320	440	180
	75% Percentile	908	552	415	358	458	570	340	338	358	535	570	390

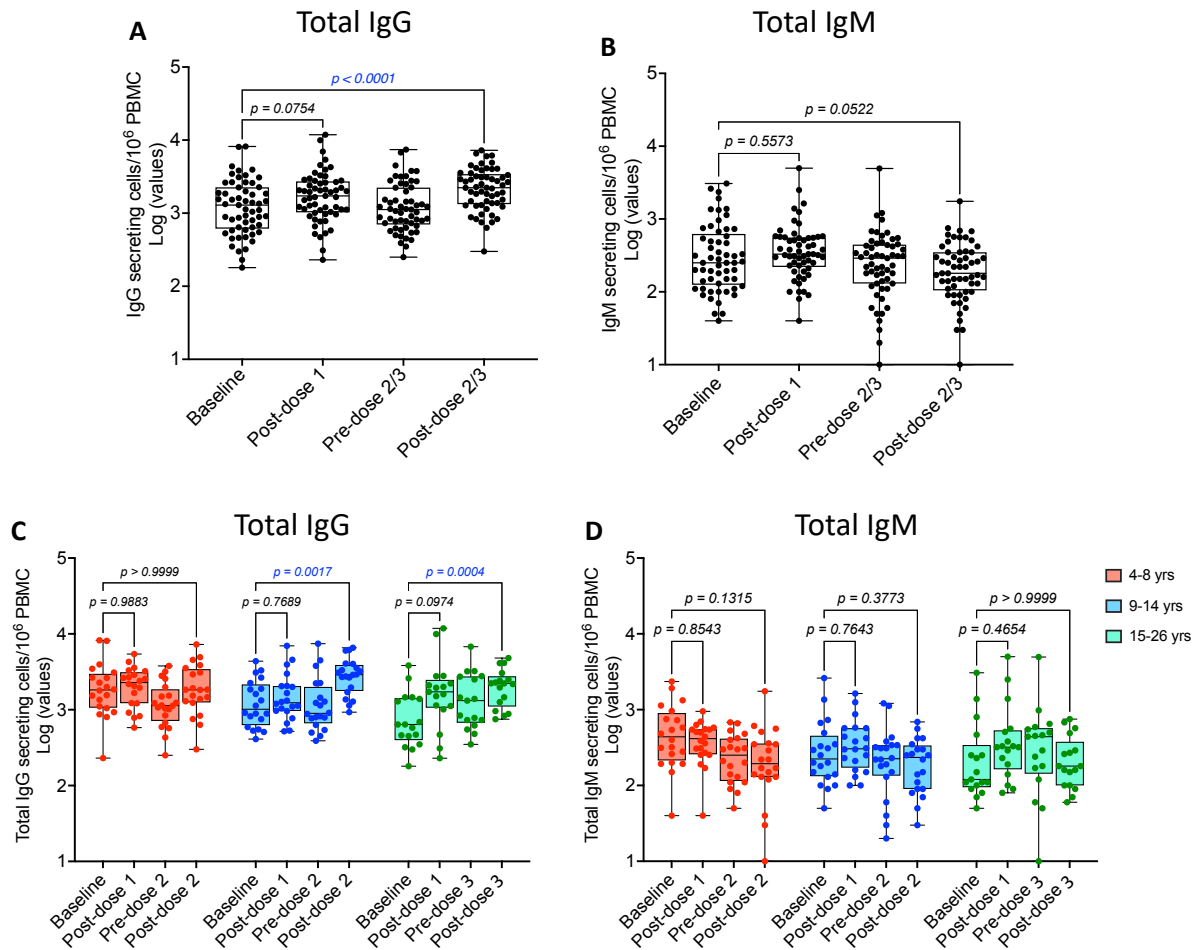


Figure 4.6. Total IgG and IgM plasma cell response after Gardasil 9 vaccination

Fresh PBMC from baseline, day 7 post-dose 1, pre- and day 7 post-dose 2 or 3 of Gardasil 9 vaccination were analysed by FluoroSpot. **A & B**: Pooled data for the 3 age groups ($n = 57$), **C & D**: Age stratified data for 3 age groups (4-8-year-olds; $n = 20$, 9-14-year-olds; $n = 20$ and 15-26-year-olds; $n = 17$) at baseline (before vaccination), post-dose 1, pre- and post-dose 2 or 3 in the respective groups. Total IgG plasma cell numbers at baseline were compared to those measured after dose 1 and dose 2 or 3 in respective age groups as shown. Pooled (all age groups) and age-stratified analyses were performed. One-way ANOVA followed by Dunnett's adjusted multiple comparison tests were performed for the pooled data and Two-way ANOVA followed by Tukey adjusted multiple comparison tests were performed for age-stratified data. The three age groups are shown in different colours. Each dot represents an individual. The box and whisker plots represent response distribution with the lower, central and upper lines denoting minimum, median and maximum values, respectively. Statistically significant p values ($p < 0.05$) are highlighted in blue.

The flow cytometry immunophenotyping of total IgG+ and IgM+ was performed on the same samples analysed by FluoroSpot for HPV 16 and HPV 18 specific and total IgG and IgM secreting cells. For consistency, all plasma cell immunophenotyping was analysed together on frozen PBMC. Paired immunophenotype data was generated from 56 participants (4-8-year-olds; n = 20, 9-14-year-olds; n = 20 and 15-26-year-olds; n = 16). Immunophenotyping of total IgG+ plasma cells with a complete phenotype of CD19+CD10-CD38++CD27+CD21-/lowIgG+ and total IgM+ plasma cells with a complete phenotype of CD19+CD10-CD38++CD27+CD21-/lowIgM+ was performed from the same samples analysed by FluoroSpot. The gating strategy used to identify total IgG+ and IgM+ plasma cells is outlined from a participant in the 15-26-year-olds group (Figure 4.7).

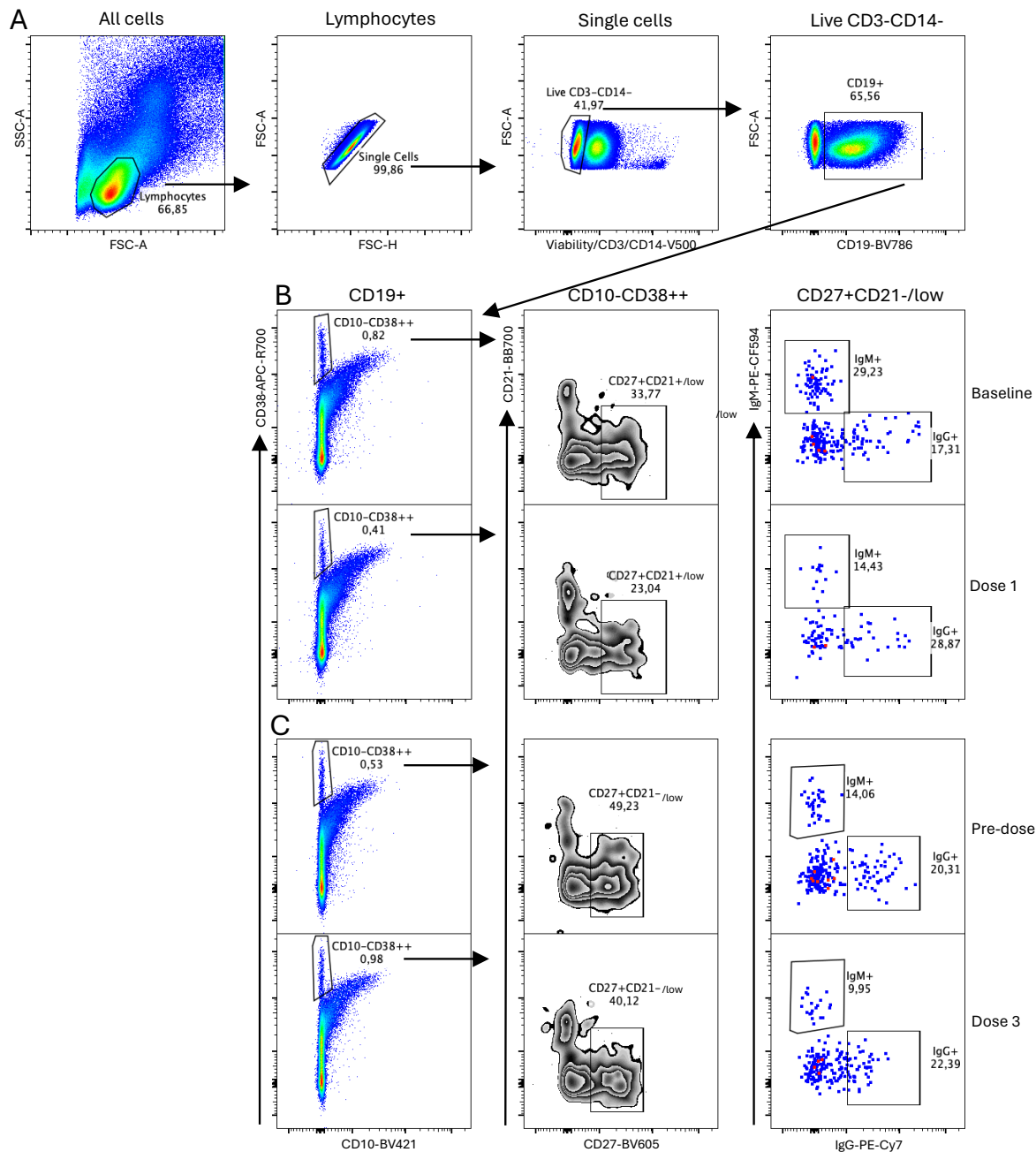


Figure 4.7. Gating strategy for identification of total IgG+ and IgM+ plasma cell frequencies after Gardasil 9 vaccination

Frozen PBMC were thawed, stained with the plasma cell panel and data acquired on LSR Fortessa III. Gating was performed on FlowJo software to first identify lymphocytes and single cells. CD3+ T cells, CD14+ monocytes and dead cells were excluded using a dump channel and CD19+ B cells identified as CD19+ (A). Total plasma plasma cells were identified as CD10-CD38++, CD27+CD21-/low out of which the IgG+ and IgM+ frequencies were identified. Data is shown from one individual in the 15-26-year-olds group across the different timepoints; Baseline and after dose 1 (B) and before and after dose 3 (C).

The dataset of total IgG+ and IgM+ plasma cell frequencies was log₁₀-transformed to restore normality before analysis. There was no significant change observed in IgG+ cell plasma cell frequencies after vaccination from both pooled and age-stratified analyses (Table 4.5A - D, Figure 4.8A - D). The pooled analysis showed a decreasing trend in frequencies of total IgM+ plasma cells after both doses 1 and 2 or 3: (mean; 25th - 75th percentiles; Baseline = 10.75%; 6.85 - 16.30%, post-dose 1 = 8.40%; 5.87 - 14.55%, p = 0.0932, post-dose 2 or 3 = 6.48%; 4.38 - 10.88%, p = 0.0004) (Table 4.4B, Figure 4.8B). From the age-stratified analysis, frequencies of IgM+ plasma cells tended to decrease following both doses 1 and 2 or 3 across all age groups. The decrease was significant in the 9-14-year-olds after both doses 1 and 2: (mean; 25th - 75th percentiles; baseline = 8.45%; 6.30 - 14.88%, post-dose 1 = 6.16%; 5.07 - 8.99%, p = 0.0293, post-dose 2 = 6.10%; 4.36 - 10.44%, p = 0.0475), and in the 4-8-year-olds after dose 2 (baseline = 15.10%; 9.52 - 24.95%, post-dose 2 = 5.83%; 4.67 - 14.43%, p = 0.0057) (Table 4.4D, Figure 4.8D).

Table 4.4. Frequencies of IgG+ and IgM+ cells in total plasma cells

A: IgG+ pooled

	All ages	4 to 26 years; n = 56			
	Sampling timepoint	Baseline	Post-dose 1	Pre-dose 2/3	Post-dose 2/3
% IgG+ in total plasma cells	25% Percentile	12.13	12.83	9.67	11.48
	Median	17.55	18.65	14.80	17.25
	75% Percentile	25.33	25.08	20.35	24.30

B: IgM+ pooled

	All ages	4 to 26 years; n = 56			
	Sampling timepoint	Baseline	Post-dose 1	Pre-dose 2/3	Post-dose 2/3
% IgM+ in total plasma cells	25% Percentile	6.85	5.87	5.91	4.38
	Median	10.75	8.40	8.78	6.48
	75% Percentile	16.30	14.55	13.70	10.88

Continued on next page

C: IgG+ age-stratified

	Age stratified	4 to 8 years; n = 20				9 to 14 years; n = 20				15 to 26 years; n = 16			
	Sampling timepoint	Baseline	Post-dose 1	Pre-dose 2	Post-dose 2	Baseline	Post-dose 1	Pre-dose 2	Post-dose 2	Baseline	Post-dose 1	Pre-dose 3	Post-dose 3
% IgG+ in total plasma cells	25% Percentile	11.48	9.59	9.12	11.15	9.618	12.88	13.70	16.70	17.43	17.38	8.84	8.34
	Median	15.15	16.75	13.15	13.75	15.50	17.90	16.00	20.75	20.65	21.20	11.30	13.65
	75% Percentile	22.23	21.88	20.60	20.78	27.50	26.35	20.15	27.60	25.48	28.33	22.80	28.28

D: IgM+ age-stratified

	Age stratified	4 to 8 years; n = 20				9 to 14 years; n = 20				15 to 26 years; n = 16			
	Sampling timepoint	Baseline	Post-dose 1	Pre-dose 2	Post-dose 2	Baseline	Post-dose 1	Pre-dose 2	Post-dose 2	Baseline	Post-dose 1	Pre-dose 3	Post-dose 3
% IgM+ in total plasma cells	25% Percentile	9.52	7.91	7.61	4.67	6.30	5.07	5.33	4.36	7.62	5.96	5.78	3.85
	Median	15.10	11.59	9.50	5.83	8.45	6.16	7.80	6.10	10.75	8.83	12.15	7.24
	75% Percentile	24.95	24.25	13.58	14.43	14.88	8.99	10.70	10.44	11.45	13.85	17.60	10.45

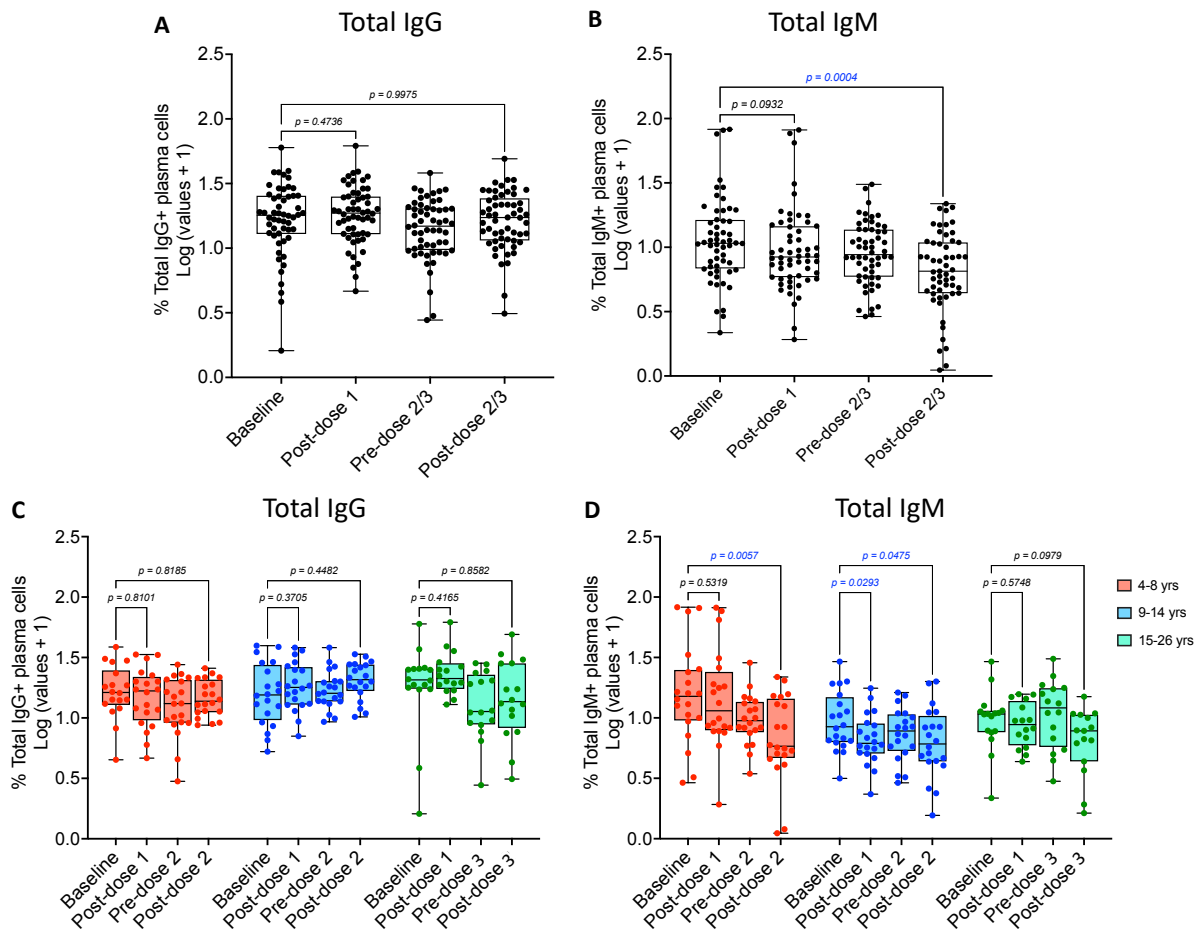


Figure 4.8. Frequencies of total IgG+ and IgM+ plasma cells after Gardasil 9 vaccination

Frozen PBMC were thawed, stained with the plasma cell panel and data acquired on LSR Fortessa III. **A & B:** Pooled data for the 3 age groups ($n = 56$), **C & D:** Age stratified data for 3 age groups (4-8-year-olds; $n = 20$, 9-14-year-olds; $n = 20$ and 15-26-year-olds; $n = 16$) at baseline (before vaccination), post-dose 1, pre- and post-dose 2 or 3 in the respective groups. Frequencies of total IgG+ and total IgM+ plasma cells at baseline were compared to those measured after dose 1 and dose 2 or 3 in respective age groups as shown. Pooled (all age groups) and age-stratified analyses were performed. One-way ANOVA followed by Dunnett's adjusted multiple comparison tests were performed for the pooled data and Two-way ANOVA followed by Tukey adjusted multiple comparison tests were performed for age-stratified data. The three age groups are shown in different colours. Each dot represents an individual. The box and whisker plots represent response distribution with the lower, central and upper lines denoting minimum, median and maximum values, respectively. Statistically significant p values ($p < 0.05$) are highlighted in blue.

4.2.2 Memory B cell responses after HPV vaccination

For enumeration of HPV vaccine-induced IgG memory B cells, a total of 60 participants across 3 age groups were randomised to group C and vaccinated with the same dose schedules of Gardasil 9 vaccine as outlined in the plasma cell results section 4.2.1, with further details on the blood sampling and analysis outlined in figure 2.1 in chapter 2. The materials, methods and statistical comparisons applied here have been described in chapters 2 and 3. The HPV 16 and HPV 18 specific IgG memory B cells were enumerated using ELISpot assay at 4 timepoints: Baseline (before first dose), fourteen days post-dose 1, pre- and fourteen days post-dose 2 (4-14-year-olds) or pre- and fourteen days post-dose 3 (15-26-year-olds). Unlike antigen specific plasma cells that peak in circulation within a week after vaccination, memory B cells are expected at their highest numbers within two weeks of vaccination hence the choice for these timepoints. Figure 4.9A - D shows ELISpot data from one individual in the 4-8-year-olds group. In this example, total IgG memory B cells (positive controls) were detected at high numbers while unstimulated negative control wells had none or few spots across all timepoints. Antigen specific IgG memory B cells were detected at low numbers at baseline and after the first vaccination dose and were higher at pre- and post-dose 2 timepoints.

The memory B cell results described here are for 53 participants from whom complete paired ELISpot data was generated for all targeted timepoints before and after vaccination. The dataset was \log_{10} -transformed to restore normality before analysis. The pooled data was first presented as IgG secreting cells per million stimulated PBMC for HPV 16 and HPV 18 specific, and total IgG memory B cells alongside respective unstimulated negative controls to visualize the level of background responses. The median numbers of antigen specific and total IgG memory B cells in the stimulated wells were significantly above their respective unstimulated negative control wells across all timepoints. (Figure 4.9E - G, Table 4.5A - C).

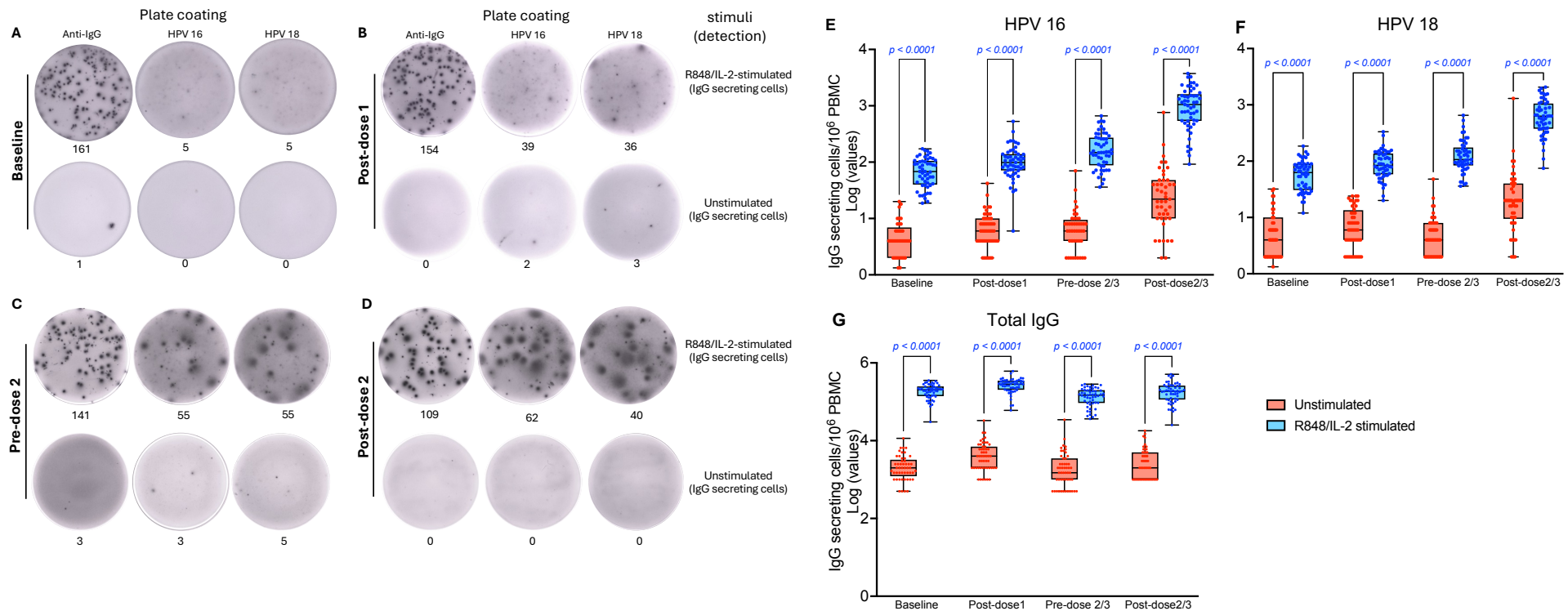


Figure 4.9. HPV 16 and HPV 18 specific and total IgG memory B cell response after Gardasil 9 vaccination

Freshly isolated PBMC at the shown timepoints before and after HPV vaccination were stimulated for 6 days using the mitogen R848 and recombinant human IL-2 alongside unstimulated cells as negative controls. HPV 16 and HPV 18 specific IgG memory B cells, and total IgG memory B cells (positive control) were enumerated from both stimulated and unstimulated cells using ELISpot. Representative data in ELISpot wells is shown from one individual from the 4-8-year-olds group (**A - D**). Single well tests are shown out of triplicate and duplicate wells run for stimulated and unstimulated tests, respectively. Spot counts are indicated below each well. Overall antigen specific and total IgG-secreting cells enumerated using this strategy are presented per million stimulated PBMC (background not subtracted), alongside the response in unstimulated negative controls ($n = 53$) (**E - G**). Two-way ANOVA with Tukey adjusted multiple comparisons was performed to compare cell numbers in R848/IL-2-stimulated and unstimulated wells. Stimulation status is colour-coded. Each dot represents an individual. The box and whisker plots represent response distribution with the lower, central and upper lines denoting minimum, median and maximum values, respectively. Statistically significant p values ($p < 0.05$) are highlighted in blue

Table 4.5. Number of HPV 16 and HPV 18 specific and total IgG memory B cells per 10⁶ stimulated PBMC (background not subtracted)

A: HPV 16 pooled (background not subtracted)

	All ages	4 to 26 years; n = 53							
	Sampling timepoint	Baseline		Post-dose 1		Pre-dose 2/3		Post-dose 2/3	
	Stim status	Unstim	Stim	Unstim	Stim	Unstim	Stim	Unstim	Stim
No. of IgG secreting cells per 10 ⁶ stimulated PBMC	25% Percentile	0	40	4	71	2	88	4	539
	Median	4	68	6	99	6	148	16	1051
	75% Percentile	6	105	10	139	8	271	40	1612

B: HPV 18 pooled (background not subtracted)

	All ages	4 to 26 years; n = 53							
	Sampling timepoint	Baseline		Post-dose 1		Pre-dose 2/3		Post-dose 2/3	
	Stim status	Unstim	Stim	Unstim	Stim	Unstim	Stim	Unstim	Stim
No. of IgG secreting cells per 10 ⁶ stimulated PBMC	25% Percentile	2	31	2	58	2	84	4	376
	Median	4	63	6	84	4	107	16	629
	75% Percentile	7	89	12	137	8	175	34	1055

C: Total IgG pooled (background not subtracted)

	All ages	4 to 26 years; n = 53							
	Sampling timepoint	Baseline		Post-dose 1		Pre-dose 2/3		Post-dose 2/3	
	Stim status	Unstim	Stim	Unstim	Stim	Unstim	Stim	Unstim	Stim
No. of IgG secreting cells per 10 ⁶ stimulated PBMC	25% Percentile	1000	139667	2000	204000	500	93333	1000	114000
	Median	2000	204000	4000	281333	1500	147667	2000	186000
	75% Percentile	3000	247833	7000	347667	3000	198333	5000	260333

unstim - unstimulated, stim - stimulated

Following subtraction of background responses, memory B cell data was analysed as pooled (all 53 participants) or age-stratified (4-8-year-olds; n = 18, 9-14-year-olds; n = 19 and 15-26-year-olds; n = 16). From the pooled analysis of the data presented as antigen secreting cells per million stimulated PBMC, an increase in HPV 16 specific IgG memory B cell numbers was observed after dose 1 and dose 2 or 3 (median; 25th - 75th percentiles: baseline = 64; 39 - 102, post-dose 1 = 93; 61 - 133, p = 0.0420, post dose 2 or 3 = 1027;

513 - 1599, $p < 0.0001$ for HPV 16, and baseline = 57; 29 - 82, post-dose 1 = 77; 51 - 124, $p = 0.0099$, post-dose 2 or 3 = 573; 358 - 961, $p < 0.0001$ for HPV 18) (Table 4.6A & B, Figure 4.10A & B)

After age stratification, significant increase in IgG memory B cell numbers after the first dose was only observed in the 4-8-year-olds (median; 25th - 75th percentiles: baseline = 47; 36 - 84, post-dose 1 = 105; 64 - 132, $p = 0.0077$ for HPV 16, and baseline = 53; 24 - 96, post-dose 1 = 76; 51 - 199, $p = 0.0174$ for HPV 18) (Table 4.6D & E, Figure 4.10C & D). Dose 2 or 3 boosted antigen specific IgG memory B cell numbers robustly across the three age groups (Table 4.6D & E, Figure 4.10C & D).

From the pooled analysis of total IgG memory B cell response, a significant increase was observed after dose 1 followed by a decrease to below pre-vaccination level. (Table 4.6C, Figure 4.11A) Although dose 2 or 3 induced an increase, the total IgG memory response increased to about the pre-vaccination levels.

On the age-stratified analysis, the trend of total IgG memory B cell response in the younger age groups was similar to that observed in the pooled analysis, compared to the older age group where the response increased after the first dose, had increased further pre-dose 3 (possibly due to the second dose not analysed for this group) and decreased post-dose 3 (Table 4.6F, Figure 4.11B).

Simple main effects analysis showed no significant effect of age on vaccine-induced memory B cell response.

Table 4.6. Number of HPV 16 and HPV 18 specific and total IgG memory B cells per 10⁶ stimulated PBMC (background-subtracted)

A: HPV 16 pooled (background-subtracted)

	All ages	4 to 26 years; n = 53			
	Sampling timepoint	Baseline	Post-dose 1	Pre-dose 2/3	Post-dose 2/3
No. of IgG secreting cells per 10 ⁶ stimulated PBMC	25% Percentile	39	61	85	513
	Median	64	93	139	1027
	75% Percentile	102	133	265	1599

B: HPV 18 pooled (background-subtracted)

	All ages	4 to 26 years; n = 53			
	Sampling timepoint	Baseline	Post-dose 1	Pre-dose 2/3	Post-dose 2/3
No. of IgG secreting cells per 10 ⁶ stimulated PBMC	25% Percentile	29	51	77	358
	Median	57	77	106	573
	75% Percentile	82	124	168	961

C: Total IgG pooled (background-subtracted)

	All ages	4 to 26 years; n = 53			
	Sampling timepoint	Baseline	Post-dose 1	Pre-dose 2/3	Post-dose 2/3
No. of IgG secreting cells per 10 ⁶ stimulated PBMC	25% Percentile	143417	199500	92667	109500
	Median	202500	276333	151500	185000
	75% Percentile	255500	338000	266833	256833

Continued on next page

D: HPV 16 age-stratified (background-subtracted)

	Age stratified	4 to 8 years; n = 18				9 to 14 years; n = 19				15 to 26 years; n = 16			
	Sampling timepoint	Baseline	Post-dose 1	Pre-dose 2	Post-dose 2	Baseline	Post-dose 1	Pre-dose 2	Post-dose 2	Baseline	Post-dose 1	Pre-dose 3	Post-dose 3
No. of IgG secreting cells per 10 ⁶ stimulated PBMC	25% Percentile	36	64	81	538	55	69	65	292	24	51	146	644
	Median	47	105	143	886	93	86	115	960	53	76	260	1094
	75% Percentile	84	132	258	1373	120	123	138	2240	96	199	323	2067

E: HPV 18 age-stratified (background-subtracted)

	Age stratified	4 to 8 years; n = 18				9 to 14 years; n = 19				15 to 26 years; n = 16			
	Sampling timepoint	Baseline	Post-dose 1	Pre-dose 2	Post-dose 2	Baseline	Post-dose 1	Pre-dose 2	Post-dose 2	Baseline	Post-dose 1	Pre-dose 3	Post-dose 3
No. of IgG secreting cells per 10 ⁶ stimulated PBMC	25% Percentile	24	71	66	362	59	48	66	291	18	40	88	310
	Median	38	107	104	511	79	61	97	627	40	74	152	605
	75% Percentile	74	133	155	717	98	109	141	1320	63	135	249	895

F: Total IgG age-stratified (background-subtracted)

	Age stratified	4 to 8 years; n = 18				9 to 14 years; n = 19				15 to 26 years; n = 16			
	Sampling timepoint	Baseline	Post-dose 1	Pre-dose 2	Post-dose 2	Baseline	Post-dose 1	Pre-dose 2	Post-dose 2	Baseline	Post-dose 1	Pre-dose 3	Post-dose 3
No. of IgG secreting cells per 10 ⁶ stimulated PBMC	25% Percentile	134500	176833	56708	89750	171000	225000	92167	100667	171708	204250	271833	182500
	Median	170250	263833	124917	137833	204667	284000	141833	179667	209000	283167	383000	212000
	75% Percentile	219042	323000	152208	212250	269000	345000	193167	253333	299250	341417	472167	385583

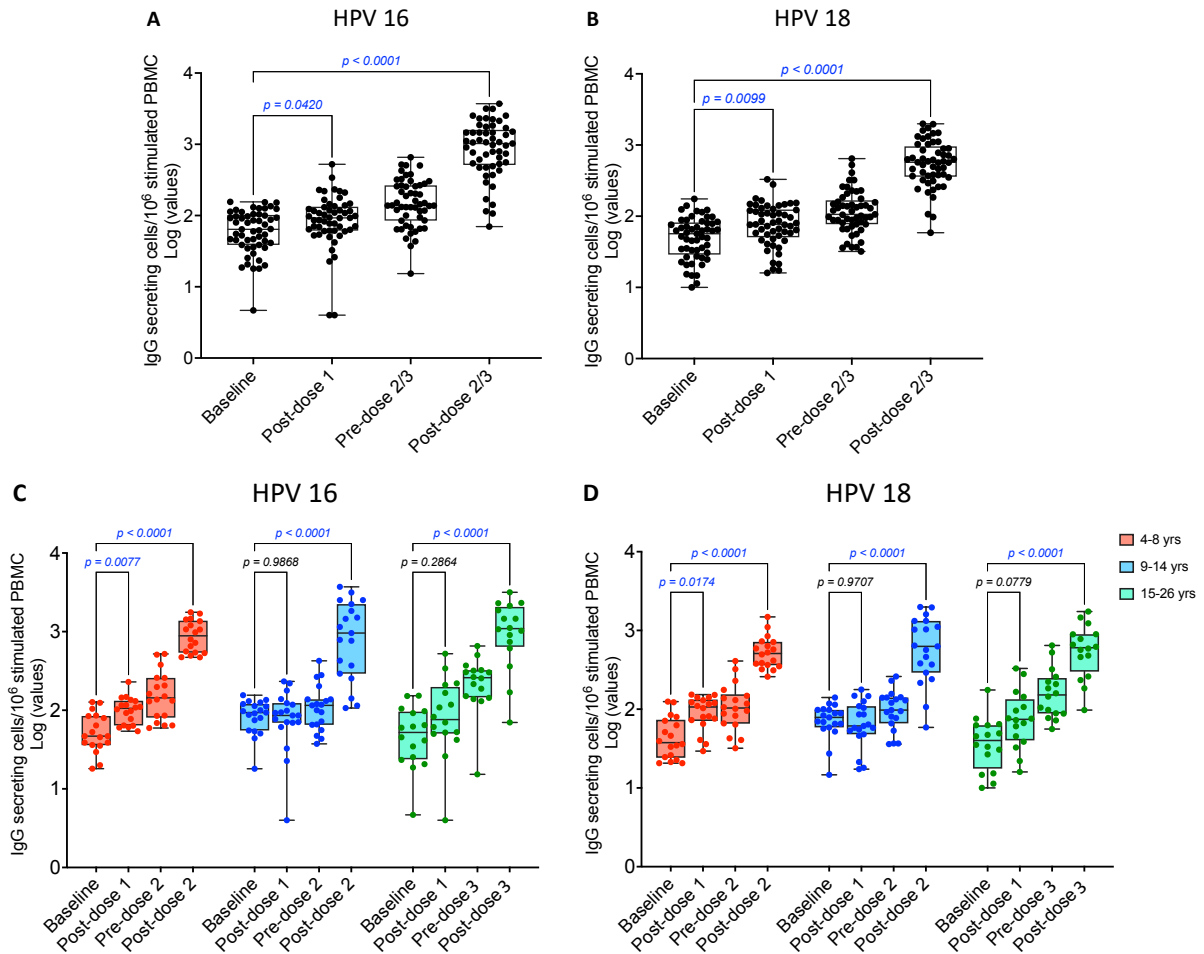


Figure 4.10. HPV 16 and HPV 18 specific IgG memory B cell response after Gardasil 9 vaccination

Fresh PBMC from baseline, day 14 post-dose 1, pre- and day 14 post-dose 2 or 3 of Gardasil 9 vaccination were analysed by ELISpot. **A & B:** pooled data from the 3 age groups ($n = 53$), **C & D:** Age stratified data (4-8-year-olds; $n = 18$, 9-14-year-olds; $n = 19$ and 15-26-year-olds; $n = 16$) at baseline (before vaccination), post-dose 1, pre- and post-dose 2 or 3 in the respective groups. IgG memory B cell numbers at baseline were compared to those measured after dose 1 and dose 2 or 3 in respective age groups as shown. Pooled (all age groups) and age-stratified analyses were performed. One-way ANOVA followed by Dunnett's adjusted multiple comparisons test was performed for the pooled data and Two-way ANOVA followed by Tukey adjusted multiple comparisons test was performed for age-stratified data. The three age groups are shown in different colours. Each dot represents an individual. The box and whisker plots represent response distribution with the lower, central and upper lines denoting minimum, median and maximum values, respectively. Antigen specific IgG-secreting cells presented per million stimulated PBMC (background-subtracted). Statistically significant p values ($p < 0.05$) are highlighted in blue

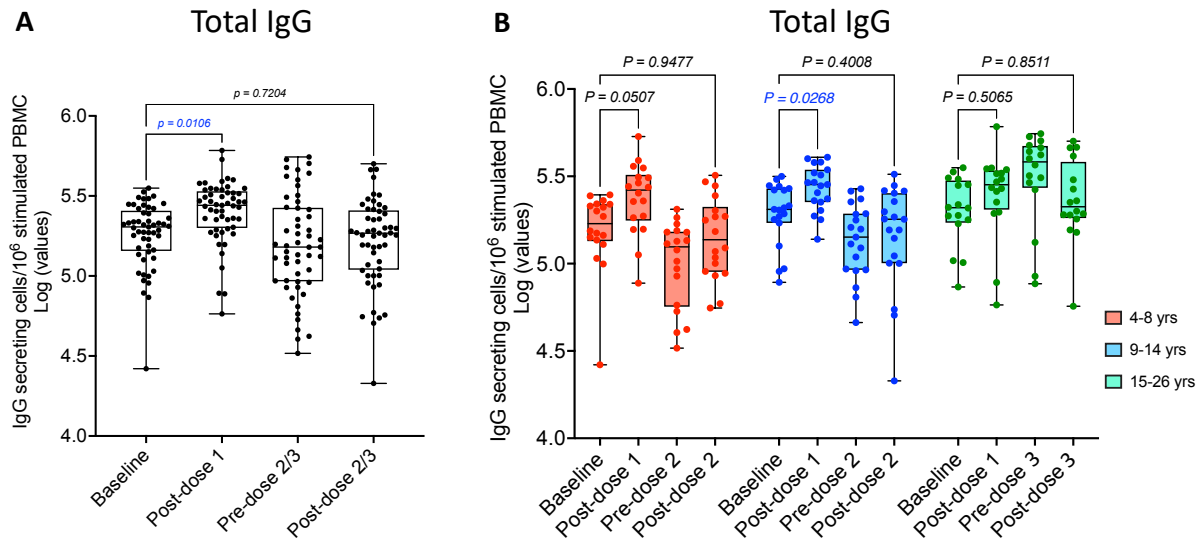


Figure 4.11. Total IgG memory B cell response after Gardasil 9 vaccination

Fresh PBMC from baseline, day 14 post-dose 1, pre- and day 14 post-dose 2 or 3 of Gardasil 9 vaccination were analysed by ELISpot. **A:** pooled data from the 3 age groups ($n = 53$), **B:** Age stratified data (4-8-year-olds; $n = 18$, 9-14-year-olds; $n = 19$ and 15-26-year-olds; $n = 16$) at baseline (before vaccination), post-dose 1, pre- and post-dose 2 or 3 in the respective groups. Total IgG memory B cell numbers at baseline were compared to those measured after dose 1 and dose 2 or 3 in respective age groups as shown. Pooled (all age groups) and age-stratified analyses were performed. One-way ANOVA followed by Dunnett's adjusted multiple comparisons test was performed for the pooled data and Two-way ANOVA followed by Tukey adjusted multiple comparisons test was performed for age-stratified data. The three age groups are shown in different colours. Each dot represents an individual. The box and whisker plots represent response distribution with the lower, central and upper lines denoting minimum, median and maximum values, respectively. Total IgG-secreting cells presented per million stimulated PBMC (background-subtracted). Statistically significant p values ($p < 0.05$) are highlighted in blue

When the antigen specific IgG memory B cell numbers were expressed as a percentage of total IgG memory B cells in circulation, a slightly different overall profile was observed at baseline and after the first vaccination dose. No significant increases were observed after the first dose in both pooled (Table 4.7A & B, Figure 4.12A & B) and age-stratified analyses (Table 4.7C & D, Figure 4.12C & D). These profiles reflect the increase in the total IgG memory B cells observed after the first vaccination dose. The increase observed in the antigen specific memory B cell numbers was therefore normalised for the corresponding change in the overall total memory B cell pool. As observed in the earlier analysis, both pooled and age-stratified analysis showed that dose 2 or 3 induced robust boosting of the

memory B cell response across all age groups. Simple main effects ANOVA analysis showed no effect of age on vaccine-induced memory B cell response.

Similar to the plasma cell response, although there was no significant age effect on vaccine-induced memory B cell response, the overall response tended to be higher in the younger age groups (Table 4.7C & D, Figure 4.13A & B).

Table 4.7. Frequencies of HPV 16 and HPV 18 specific IgG memory B cells

A: HPV 16 pooled (background-subtracted)

	All ages	4 to 26 years; n = 53			
	Sampling timepoint	Baseline	Post-dose 1	Pre-dose 2/3	Post-dose 2/3
% in total IgG memory B cells	25% Percentile	0.02	0.02	0.06	0.30
	Median	0.03	0.03	0.09	0.58
	75% Percentile	0.06	0.06	0.15	1.22

B: HPV 18 pooled (background-subtracted)

	All ages	4 to 26 years; n = 53			
	Sampling timepoint	Baseline	Post-dose 1	Pre-dose 2/3	Post-dose 2/3
% in total IgG memory B cells	25% Percentile	0.01	0.02	0.04	0.20
	Median	0.03	0.03	0.07	0.34
	75% Percentile	0.05	0.05	0.13	0.75

Continued on next page

C: HPV 16 age-stratified (background-subtracted)

	Age stratified	4 to 8 years; n = 18				9 to 14 years; n = 19				15 to 26 years; n = 16			
	Sampling timepoint	Baseline	Post-dose 1	Pre-dose 2	Post-dose 2	Baseline	Post-dose 1	Pre-dose 2	Post-dose 2	Baseline	Post-dose 1	Pre-dose 3	Post-dose 3
% in total IgG memory B cells	25% Percentile	0.02	0.02	0.09	0.39	0.03	0.02	0.04	0.30	0.01	0.02	0.05	0.21
	Median	0.03	0.04	0.14	0.68	0.04	0.03	0.08	0.58	0.03	0.03	0.07	0.46
	75% Percentile	0.06	0.06	0.16	0.99	0.06	0.05	0.15	1.62	0.05	0.08	0.10	1.21

D: HPV 18 age-stratified (background subtracted)

	Age stratified	4 to 8 years; n = 18				9 to 14 years; n = 19				15 to 26 years; n = 16			
	Sampling timepoint	Baseline	Post-dose 1	Pre-dose 2	Post-dose 2	Baseline	Post-dose 1	Pre-dose 2	Post-dose 2	Baseline	Post-dose 1	Pre-dose 3	Post-dose 3
% in total IgG memory B cells	25% Percentile	0.02	0.02	0.06	0.27	0.03	0.02	0.04	0.21	0.01	0.01	0.03	0.14
	Median	0.03	0.04	0.10	0.34	0.04	0.02	0.07	0.57	0.02	0.03	0.05	0.20
	75% Percentile	0.05	0.07	0.16	0.53	0.06	0.04	0.10	0.86	0.04	0.08	0.07	0.57

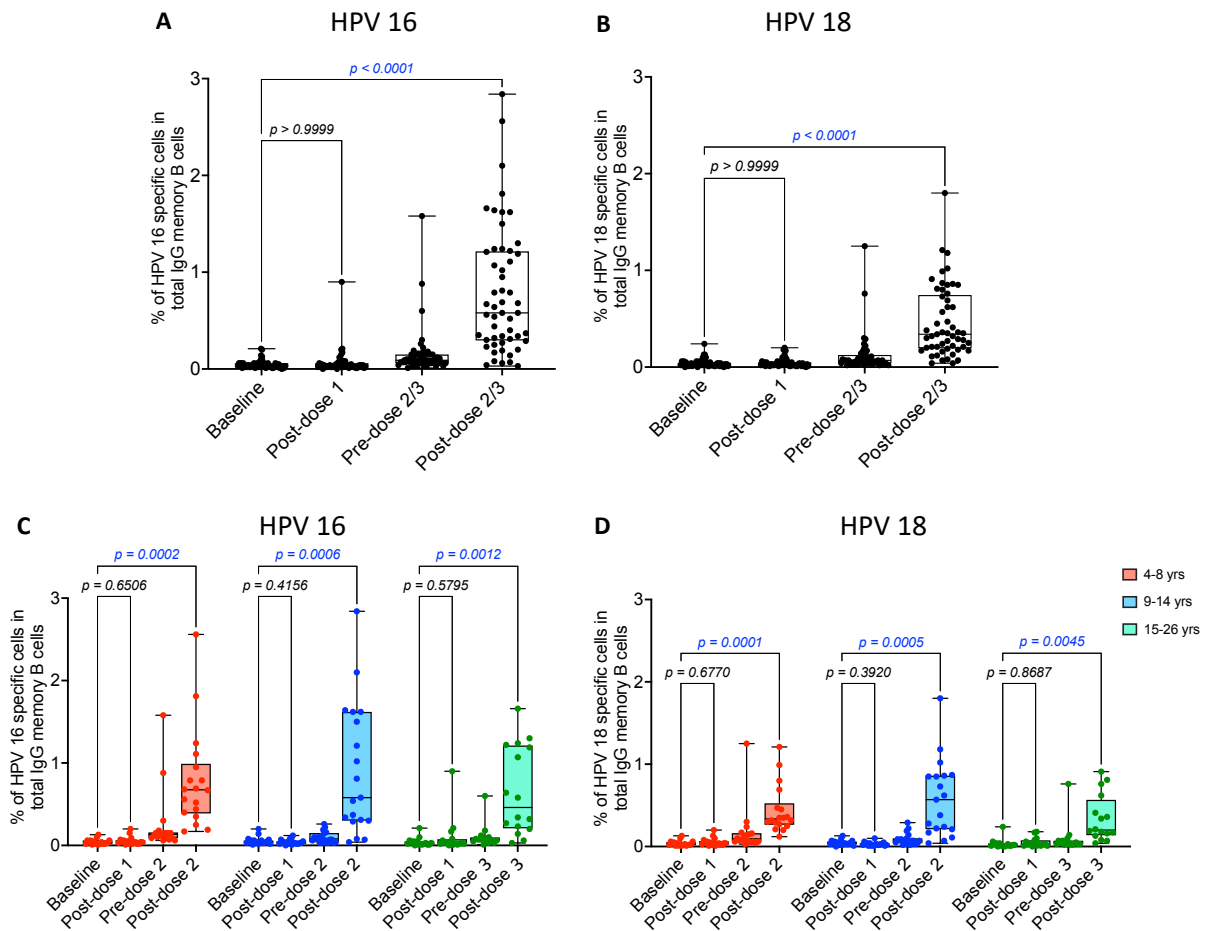


Figure 4.12. HPV 16 and HPV 18 specific IgG memory B cell response after Gardasil 9 vaccination, comparisons per timepoint

Fresh PBMC from baseline, day 14 post-dose 1, pre- and day 14 post-dose 2 or 3 of Gardasil 9 vaccination were analysed by ELISpot. **A & B:** pooled data from the 3 age groups ($n = 53$), **C & D:** Age stratified data (4-8-year-olds; $n = 18$, 9-14-year-olds; $n = 19$ and 15-26-year-olds; $n = 16$) at baseline (before vaccination), post-dose 1, pre- and post-dose 2 or 3 in the respective groups. The IgG memory B cell numbers at baseline were compared to those measured after dose 1 and dose 2 or 3 in respective age groups as shown. Pooled (all age groups) and age-stratified analyses were performed. One-way ANOVA followed by Dunnett's adjusted multiple comparisons test was performed for the pooled data and Two-way ANOVA followed by Tukey adjusted multiple comparisons test was performed for age-stratified data. The three age groups are shown in different colours. Each dot represents an individual. The box and whisker plots represent response distribution with the lower, central and upper lines denoting minimum, median and maximum values, respectively. Statistically significant p values ($p < 0.05$) are highlighted in blue. Antigen specific IgG-secreting cells presented as a percentage of total IgG memory B cells.

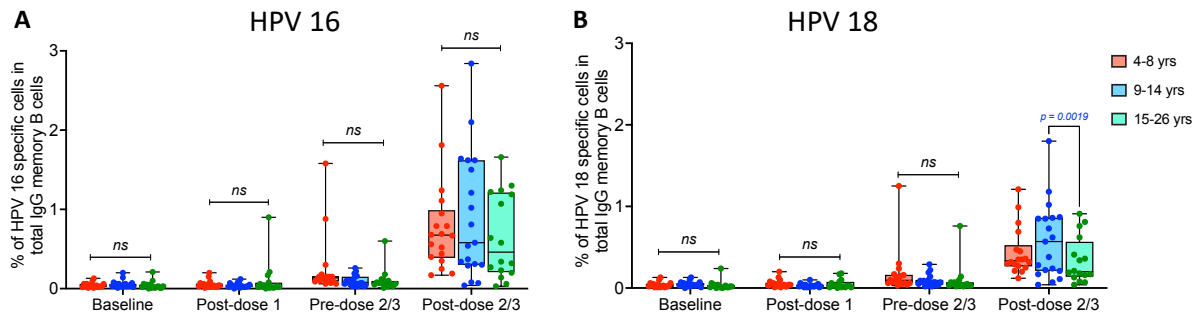


Figure 4.13. Frequencies of HPV 16 and HPV 18 specific IgG memory B cells after Gardasil 9 vaccination, comparisons per timepoint

Fresh PBMC from baseline, day 14 post-dose 1, pre- and day 14 post-dose 2 or 3 of Gardasil 9 vaccination were analysed for HPV 16 (**A**) and HPV 18 (**B**) specific IgG memory B cells by ELISpot. Data shown for 3 age groups (4-8-year-olds; $n = 18$, 9-14-year-olds; $n = 19$ and 15-26-year-olds; $n = 16$) at baseline (before vaccination), post-dose 1, pre- and post-dose 2 or 3 in the respective groups. Two-way ANOVA followed by Tukey adjusted multiple comparison tests were performed to compare memory B cell frequencies between the three age groups at different timepoints. The three age groups are shown in different colours. Simple main effects analysis showed no significant age effect on vaccine-induced memory B cell response. Each dot represents an individual. The box and whisker plots represent response distribution with the lower, central and upper lines denoting minimum, median and maximum values, respectively. Only statistically significant p values ($p < 0.05$) are shown in blue. (ns): non-significant.

4.3 Discussion and future work

This is a discussion of results from enumeration of HPV 16 and HPV 18 specific plasma cells and memory B cells in blood circulation following intramuscular vaccination with the nine-valent HPV vaccine. The effect of age at vaccination and number of vaccination doses on the vaccine-induced cellular responses is also discussed. The 4-8- and 9-14-year-olds received two vaccination doses (at baseline and at 12 months) while the 15-26-year-olds received three doses (at baseline, 2 months and 12 months). Prior to this study, the participants had not been vaccinated against HPV.

Investigations of plasma cells and memory B cells in peripheral circulation are used only as an indication but may not be a true reflection of what is happening in their actual site of generation within GCs in secondary lymphoid organs. Since these cells are predominantly located in secondary lymphoid organs and the bone marrow and are not detectable in circulation in a steady state (Palm and Henry, 2019), their characterisation in peripheral blood including the timing of their appearance, numbers and phenotype should be interpreted with caution. Nevertheless, characterisation of these cell populations in peripheral blood have contributed immensely to our understanding of immunity to natural infections and vaccination.

Before vaccination, overall median IgG and IgM plasma cell numbers were 0 or 1 per million PBMC. Although the participants had not been vaccinated against HPV and that most of them may have been HPV naïve, especially the younger age groups, it is possible that some in the older age groups had been exposed to HPV. However, whether the participants were naïve or primed, plasma cells do not recirculate and therefore no HPV specific plasma cells were expected to be detected at baseline.

Following the first vaccination dose, HPV specific plasma cells started appearing in circulation and although detected at very low numbers overall, some older participants had high plasma cell responses which was indicative of a recall response. The enumeration of these cells at one timepoint may have led to missing their later peak time suggested to be

around 10 days after primary vaccination.(Blanchard-Rohner et al., 2009, Carter et al., 2017a)

Before the second or third vaccinations, antigen specific plasma cells had disappeared from circulation. The long-term maintenance of antibody titres after one, two or three vaccination doses are presumed to be generated from LLPCs, (Kurosawa et al., 2022) hence the absence of plasma cells in circulation after vaccination may indicate they had homed to the bone marrow or died off by apoptosis. Viral infections such as mumps, measles, influenza, as well as tetanus vaccination have been shown to generate decades-long antibody protection via LLPCs in the bone marrow.(Amanna et al., 2007, Halliley et al., 2015, Yu et al., 2008) On the other hand, vaccines generating short-term antibodies such as the COVID-19 mRNA vaccine failed to generate LLPCs.(Nguyen et al., 2024, Tehrani et al., 2024), However, immunogenicity to the COVID-19 vaccines is still not well understood and there are contradictory reports that the vaccines are able to generate LLPCs.(Schulz et al., 2023)

The anamnestic HPV specific plasma cell responses observed following the second and third vaccination doses is consistent with high plasma cell response reported from other vaccines after secondary or tertiary vaccinations.(Frölich et al., 2010, Blanchard-Rohner et al., 2009) This sharp increase in plasma cell response indicates reactivation of immune memory generated from primary vaccination in the younger age groups or from both primary and secondary vaccinations in the older age group.

A previous study documenting detailed kinetics of plasma cells in circulation after rabies vaccination of rabies naïve and immune volunteers showed that antigen specific plasma cells were detectable at day 7, peaked at day 10 and were still detectable at lower numbers by 14 days after primary vaccination of rabies naïve volunteers.(Blanchard-Rohner et al., 2009) On the other hand, the plasma cell response peaked at 7 days following secondary immunization or primary immunization of the rabies immune volunteers. The profiles of plasma cell numbers at the timepoints targeted in this study are consistent with what was observed in the rabies vaccination study. The plasma cell peak at 7 days after primary

vaccination of the rabies immune volunteers is comparable to the high plasma cell response observed at the same time in a few individuals in older age group who may have been naturally primed.

The kinetics of plasma cell isotypes differ. IgM, the earliest isotype generated following primary antigen challenge is expected to appear first in circulation and decreases following secondary and tertiary vaccinations as CSR and affinity maturation takes place.(Duarte, 2016) This profile was observed for both HPV specific and total IgM plasma cells. Importantly, although the FluoroSpot enumeration of total IgG and total IgM secreting cells identified them as a proportion of total PBMC and the flow cytometry immunophenotyping as a proportion of the plasma cell population, the overall profiles by either assay looked very similar. The variable levels of significance in the changes observed in either case may be attributable to the different parent populations from which the plasma cells were identified. Two previous studies using flow cytometry assay reported a rapid increase in the total plasma cell population in circulation one week after a single dose in women previously infected with HPV, or a fourth delayed dose following a 3 dose-schedule of Gardasil vaccine.(Scherer et al., 2016, Scherer et al., 2018) Another recent study also using flow cytometry reported rapid increase in the total plasma cell population a week after 3 dose-schedules of both Cervarix and Gardasil 9 in young women.(Pasmans et al., 2022) Although these studies looked at the overall plasma cell response by flow cytometry which may not be directly comparable to the isotype specific plasma cell populations identified in this study, they provided evidence for induction of plasma cell responses by HPV vaccines.

It may be expected that both short-lived plasma cells as well as plasma cells destined to be long-lived form the population identifiable in circulation shortly after antigen challenge. Most plasma cells identifiable in circulation shortly after antigen challenge are short-lived and die by apoptosis and only a few transition to be long-lived.(Nguyen et al., 2019) The time plasma cells appear in circulation may indicate a migratory period for those destined to be long-lived moving from their site of generation in GCs to other tissues such as the mucosa or

bone marrow where they reside for years and continue to secrete antibodies for long-term humoral protection.(Ulbricht et al., 2023) Various cellular and molecular determinants of plasma cell survival have been identified including increased expression of the chemokine receptor 12 (CXCL12) on the migratory plasma cells which is attracted to CXCL12 ligand (CXCL12) produced by modulatory fibroblastic reticular cells.(Tangye, 2011) These stromal cells form LLPC survival niches in the bone marrow.(Tangye, 2011) The reticular cells also produce plasma cell survival factors including IL-6, B cell activating factor (BAFF) and a proliferation-inducing ligand (APRIL) and are believed to synergize with myeloid cells in promoting plasma cell survival in the bone marrow.(Zehentmeier et al., 2014, Lindquist et al., 2019) Both BAFF and APRIL bind to a common receptor, BCMA to promote plasma cell survival through induction of an anti-apoptotic molecule myeloid cell leukemia-1 (Mcl-1) of the B cell lymphoma 2 (Bcl-2) family.(Khodadadi et al., 2019) The plasma cells identifiable in circulation shortly after antigen exposure do not express longevity markers such as BCMA, Blimp-1 and CD138 hence, their longevity cannot be inferred from their phenotypes.(Nguyen et al., 2021)

Studies in murine models reported GCs to last between 2 to 5 weeks after immunization and were maintained by continuous interaction between the antigen cognate B cells and Tfh cells.(Matz et al., 2023b, Arulraj et al., 2021) In this line of thought, it may be expected that this continuous B cell-Tfh cell interaction continuously replenish the long-term affinity matured B cells of which the plasma cells would be expected to be moving to the bone marrow and possibly be detectable in circulation. However, this does not align with the fact that plasma cells are detectable in circulation within a few days window following antigen challenge. Further, recent studies have reported long-primed GCs persisting for more than 6 months after priming immunization in both mice and non-human primates and while such persistent GCs are expected to be generating plasma cells (as well as memory B cells), they still do not recirculate.(Matz et al., 2023a, Lee et al., 2022)

Within the pool of plasma cells generated following antigen challenge, there is no clear distinction between the short-lived and long-lived subsets with some studies suggesting that the long-lived characteristics are acquired during maturation in the bone marrow while others suggest maturation of the long-lived population take place in the GCs.(Slifka et al., 1998b, Ellyard et al., 2004) This therefore remains a subject for continued research.

The memory B cell response detected before vaccination may be interpreted to be partly due to polyspecificity arising from polyclonal B cell stimulation in culture, especially in the young participants who may not have been exposed to HPV naturally. The mitogen stimulus used in this study which is a combination of the TLR8 agonist, R848 and IL-2 have been shown to induce polyspecific memory B cells with ability to bind to multiple antigens.(Pinna et al., 2009) The initial study to test this stimulus detected polyspecific memory B cells that could bind to tetanus toxoid, measles virus antigens and Varicella Zoster virus antigens, and could even react to uncoated ELISpot wells.(Pinna et al., 2009) However, despite this polyspecificity which may be expected from culture stimulation also with other mitogens, antigen specific memory B cells with ability to neutralise their cognate antigen were clearly identified.

Application of the same stimulation conditions throughout the analysis of all samples at all timepoints is expected to have kept the non-specific signal standardised to be able to identify vaccine induced changes in the numbers of memory B cells. Additionally, the identified antigen specific cells in this study were also expressed as a proportion of the total IgG memory B cells in circulation, which is considered the current best measure to correct for mitogen culture effects as well as any other changes in the total PBMC.(Scholzen et al., 2014) The discussion of the IgG memory B cell response is therefore based on the results corrected in this manner.

Similar to the plasma cell response following the first vaccination dose, the small or no increase in memory B cell response detected in circulation should be interpreted with caution as the timepoint may not have been optimal. The highest memory B cell response

after the first vaccination dose was identified in some participants in the oldest age group. This may indicate presence of infection-induced memory B cells being rapidly reactivated allowing their detection at the 14 days-timepoint targeted in the study. Consistent with this finding in the older age group, a single HPV vaccine dose was demonstrated to improve the magnitude of memory B cell response in women previously infected with HPV 16.(Scherer et al., 2016) Failure to identify an overall significant increase in the HPV specific B cell memory response at 14 days following the first vaccination dose indicate that as a primary response in most of the participants, the cell numbers may have peaked in the subsequent days not included in the study timepoints. In line with this explanation, the numbers of memory B cells generated from the first dose continued to increase and were detectable before administration of the second dose (at 12 months following the first dose) at a higher level than the initial 14 days timepoint.

Before the third dose at 12 months in the older age group, the memory response was generally lower than before dose 2 in the younger age groups. Immunogenicity of HPV vaccines is extensively reported to be higher in younger age groups.(Whitworth et al., 2024) As such, this finding may indicate that the first dose of Gardasil 9 vaccine may have induced a higher B cell memory response than the two doses that the older age group had received before 12 months. The continued increase after the first vaccination dose and robust response after second or third doses is consistent with memory B cell response reported following secondary or tertiary vaccination for other antigens. Studies have shown that memory B cell response is variable between antigens and can appear in circulation within two weeks after vaccination and continue to increase peaking peak at about 4 weeks after which it decreases but remain detectable at low frequencies.(Palm and Henry, 2019)

Following their generation in GCs, high affinity, somatically mutated and class-switched memory B cells home to antigen draining sites or join the recirculating pool of lymphocytes from where they can be rapidly reactivated upon antigen re-encounter to differentiate to plasma cells generating humoral immunity.(Shah et al., 2019) Non-switched somatically

mutated IgM memory B cells have also been reported for T cell-independent antigens such as Pneumococcal polysaccharides.(Lucas et al., 2001) However, this PhD research evaluated only IgG memory B cell response as would be expected from viral antigens, with serological studies also having demonstrated that HPV vaccines induce mainly IgG antibodies that provide protective immunity against HPV by viral neutralisation.(Pinto et al., 2018, Costa et al., 2020) Memory B cells are therefore detectable in circulation for longer durations of time than plasma cells, though they decline to low frequencies after reaching their peak levels.(Syeda et al., 2024) Indeed, HPV specific memory B cells induced by the Cervarix, Gardasil and Gardasil 9 vaccines were identified in circulation by ELISpot or flow cytometry a month after vaccination in studies conducted in both male and female study participants.(Miller et al., 2021, Pasmans et al., 2022, Scherer et al., 2016, Scherer et al., 2014b) Additionally, even in the long-term memory phase, about 4 to 6 years following a three-dose HPV vaccination schedule, HPV vaccine type specific memory B cells were identified in circulation.(Nicoli et al., 2020a) Further, the anamnestic antibody response usually observed following HPV booster vaccinations indicate reactivation of memory B cells.(Safaeian et al., 2013, Guevara et al., 2017)

A recent study in 20 HPV naïve post-menopausal women assessed various early cellular responses after Cervarix (n = 10) and Gardasil 9 (n = 10) vaccination. Slightly higher HPV 16 and HPV 18 specific memory B cell response from Cervarix vaccine than from Gardasil 9 vaccine were reported at one month after three vaccination doses which is consistent with previous studies that reported higher immunogenicity of Cervarix vaccine compared to Gardasil vaccine (reviewed in chapter 1).(Toft et al., 2014) Despite the different study timepoints, the study used ELISpot to demonstrate that Gardasil 9 vaccine is able to generate HPV specific B cell memory which is consistent with the findings in this PhD work.

Overall, no significant changes above baseline were identified in both plasma cell and memory B cell numbers at one week and two weeks, respectively after the first dose. The timing for identification of antigen specific plasma cells in circulation is very critical since they

only appear and peak within a short time before homing to their long-term survival niches in the bone marrow after which they do not recirculate. This study was limited in that the cell responses were identified in circulation which in the first place is not their main location. Additionally, using only one timepoint following all the evaluated vaccination doses is limiting as the kinetics of immune responses to primary, secondary and tertiary vaccinations may be different, compounded by the influence of prior antigen exposure. The inability to detect CD138, a LLPC marker limited the basis for assessment of the likely longevity of the plasma cell population identified in this study.

Consistent with the finding of this research, studies comparing the level of HPV 16 memory B cell response induced by Gardasil vaccination in adolescent girls and young women reported no age associated differences.(Smolen et al., 2012, Nicoli et al., 2022) However, some age associated differences in the level of vaccine-induced HPV 18 specific memory B cell response has been reported which was not observed in this work. The studies looking at antibody responses showed that a single dose induced lower antibody titres than two or three doses with the vaccine-induced titres being lower with a single dose but stably maintained regardless of the regimen.(Joshi et al., 2023, Watson-Jones et al., 2022, Kreimer et al., 2020) The generation of similar HPV 16 and HPV 18 specific plasma cells and memory B cells across the three age groups after two or three doses may indicate the vaccine is similarly immunogenic across the investigated age groups although long-term data will provide a better understanding.

Importantly, both HPV specific IgG plasma cell and memory B cell responses identified in this study tended to be higher in the young age groups in line with previous findings of higher IgG antibody titres when the HPV vaccines were administered to young adolescents compared to young women.(Nicoli et al., 2022) A recent systematic review reported effectiveness of HPV vaccination to be approximately 74% to 93% when given to younger adolescents aged 9-14 years and from 12% to 90% when given to ages 15-18 years.(Ellingson et al., 2023) The findings from this work therefore further contributes to

demonstrating higher immunogenicity of HPV vaccines in young ages including in girls aged 4 to 8 years in whom HPV vaccination has not been tested before.

Long-term antibody protection is thought to be mediated by LLPCs, which if insufficient for immediate antigen neutralisation and elimination requires reactivation of the memory B cells.(Palm and Henry, 2019) With most HPV vaccine efficacy trials reporting no breakthrough infections in HPV naïve vaccinated individuals (reviewed in chapter 1), the role of HPV memory response in maintaining long-term protection remains to be elucidated. To evaluate the short-term influence of cellular responses presented in this chapter, plasma cell and memory B cell responses identified after two or three vaccination doses are compared to antibody responses in chapter 6.

The vaccine-induced Tfh cell responses are discussed next in chapter 5 and are also compared with both plasma cell and antibody responses.

Future studies aimed at improving understanding of B cell responses after HPV vaccination should aim to:

- Evaluate HPV vaccine-induced plasma cell and memory B cell responses over a range of days during which they are expected to peak in circulation after vaccination. This will ensure that responses appearing early or later after vaccination are identified.
- Characterise LLPCs based on their survival markers such as CD138, Blimp-1 and BCMA on bone marrow aspirates where feasible or freshly isolated PBMC.
- Use large enough sample sizes that allow availability of sufficient number of cells for multiple assay testing. Plasma cell survival markers are usually expressed at low levels, thus requiring acquisition of more events than highly and moderately expressed markers for confident identification by flow cytometry.

5. T FOLLICULAR HELPER CELL RESPONSE AFTER GARDASIL 9 VACCINATION

This chapter discusses Tfh cell responses identified in blood circulation following Gardasil 9 vaccination. The vaccination schedules in the age groups studied have been described in chapter 2. In vitro stimulated Tfh cell responses were evaluated using AIM flow cytometry assay based on co-expression of the AIM markers OX40, CD25 and PD-L1 while ex vivo stimulated Tfh cell frequencies were identified based on co-expression of the activation markers ICOS and PD-1.

5.1 Aims

- i) To determine the frequencies of in vitro stimulated Tfh cells induced by the first and second or third vaccination doses of Gardasil 9 vaccine.
- ii) To determine the frequencies of ex vivo stimulated Tfh cells induced by the first and second or third vaccination doses of Gardasil 9 vaccine.
- iii) To evaluate the effect of age and vaccination dose numbers on Gardasil 9-induced Tfh cell responses.

5.2 Results

Activated Tfh cell frequencies were measured from the same samples analysed for plasma cell response owing to the expected similar peak time in circulation for both populations. Due to limited cell numbers, paired data were not available for the analysis of Tfh cell responses and therefore for the samples available, unpaired analyses were performed. The number of samples analysed for the AIM and ex vivo Tfh cell assays are shown in table 5.1.

Table 5.1. Number of samples used to evaluate activated Tfh cell frequencies per timepoint

Age groups (years)	Assay	Baseline	post-dose 1	pre-dose 2/3	post-dose 2/3
4 to 8	Tfh AIM	n = 15	n = 15	n = 15	n = 15
	Tfh ex vivo	n = 20	n = 20	n = 19	n = 19
9 to 14	Tfh AIM	n = 12	n = 12	n = 12	n = 12
	Tfh ex vivo	n = 16	n = 16	n = 16	n = 16
15 to 26	Tfh AIM	n = 13	n = 13	n = 14	n = 14
	Tfh ex vivo	n = 8	n = 8	n = 16	n = 16

The number of samples analysed per timepoint is shown for respective Tfh cell assays in each age group. Overall, most of the samples used were paired for the four target timepoints and a few were paired for at least two timepoints (either baseline and post-dose 1 or pre- and post-dose 2/3).

5.2.1 HPV 16 and HPV 18 specific Tfh cell AIM response after Gardasil 9 vaccination

Samples were analysed for both HPV 16 and HPV 18 specific Tfh cell responses using the AIM assay. Three combinations of activation markers were used to identify activated antigen specific Tfh cell frequencies as follows: OX40+CD25+, OX40+PD-L1+ and PD-L1+CD25+. The gating strategy used to identify antigen specific Tfh cell frequencies is outlined in figure 5.1. The total Tfh cell population was first gated as CD14-CD4+FoxP3-CD45RO+CXCR5+ (Figure 5.1A). Frequencies of activated antigen specific Tfh cells were then identified from the total Tfh cell population based on co-expression of the three AIM combinations as OX40+CD25+, OX40+PD-L1+ and PD-L1+CD25+ (Figure 5.1B). Statistical comparisons were performed on the dataset as pooled, and age stratified as described earlier for plasma cell and memory B cell responses.

Overall, the three combinations of AIM markers, OX40+CD25+, OX40+PD-L1+ and PD-L1+CD25+ used in this project showed comparable signal detection capabilities (Figure 5.1B). From the pooled analysis of HPV 16 specific responses, there was no significant

difference in activated AIM frequencies between baseline and after dose 1 although the post-dose 1 responses tended to be higher (Table 5.2A - C, Figure 5.2A, C & E). After dose 2 or 3, significant increase in HPV 16 specific Tfh cell frequencies was detected using all AIM combinations as OX40+CD25+ (median; 25th - 75th percentiles; baseline = 0.03%; 0.00 - 0.14%, post-dose 2 or 3 = 0.38%; 0.14 - 1.45%, $p = 0.0005$), OX40+PD-L1+ (baseline = 0.00%; 0.00 - 0.08%, post-dose 2 or 3 = 0.42%; 0.08 - 1.70%, $p < 0.0001$) and PD-L1+CD25+ (baseline = 0.12%, 0.00 - 0.47%, post-dose 2 or 3 = 0.81%; 0.24 - 2.34%, $p < 0.0001$) in the pooled analysis (Table 5.2A - C, Figure 5.2A, C & E). Notably, the pre- and post-dose 2 or 3 Tfh cell frequencies were generally high, at almost similar levels in some cases.

In the age-stratified analysis, overall, higher Tfh cell responses were observed in the older age groups (Table 5.2D - F, Figure 5.2B, D & F). As observed in the pooled analysis, there were no significant increases detected post-dose 1 across all age groups. Following dose 2 or 3, significant increases were only detected in the two older age groups as follows: OX40+CD25+ (median; 25th - 75th percentiles; baseline = 0.01%; 0.00 - 0.13%, post-dose 2 = 0.52%; 0.21 - 1.57%, $p = 0.0102$), OX40+PD-L1+ (baseline = 0.00%; 0.00 - 0.14%, post-dose 2 = 1.27%; 0.04 - 1.98%, $p = 0.0062$) and PD-L1+CD25+ (baseline = 0.22%; 0.05 - 0.64%, post-dose2 = 1.65%; 0.78 - 4.21%, $p = 0.0003$) for 9-14-year-olds and OX40+PD-L1+ (baseline = 0.05%; 0.00 - 0.51%, post-dose 3 = 1.12%; 0.30 -1.97%, $p = 0.0101$) and PD-L1+CD25+ (baseline = 0.15%; 0.00 - 1.11%, post-dose 3 = 1.59%; 0.41 - 4.64%, $p = 0.0018$) for 15-26-year-olds. (Table 5.2D - F, Figure 5.2B, D & F). There was a trend towards increase in all AIM combinations in the 4-8-year-olds, but this was not significant. Generally, HPV 16 specific pre- and post-dose 2 or 3 AIM frequencies within each group were almost similar.

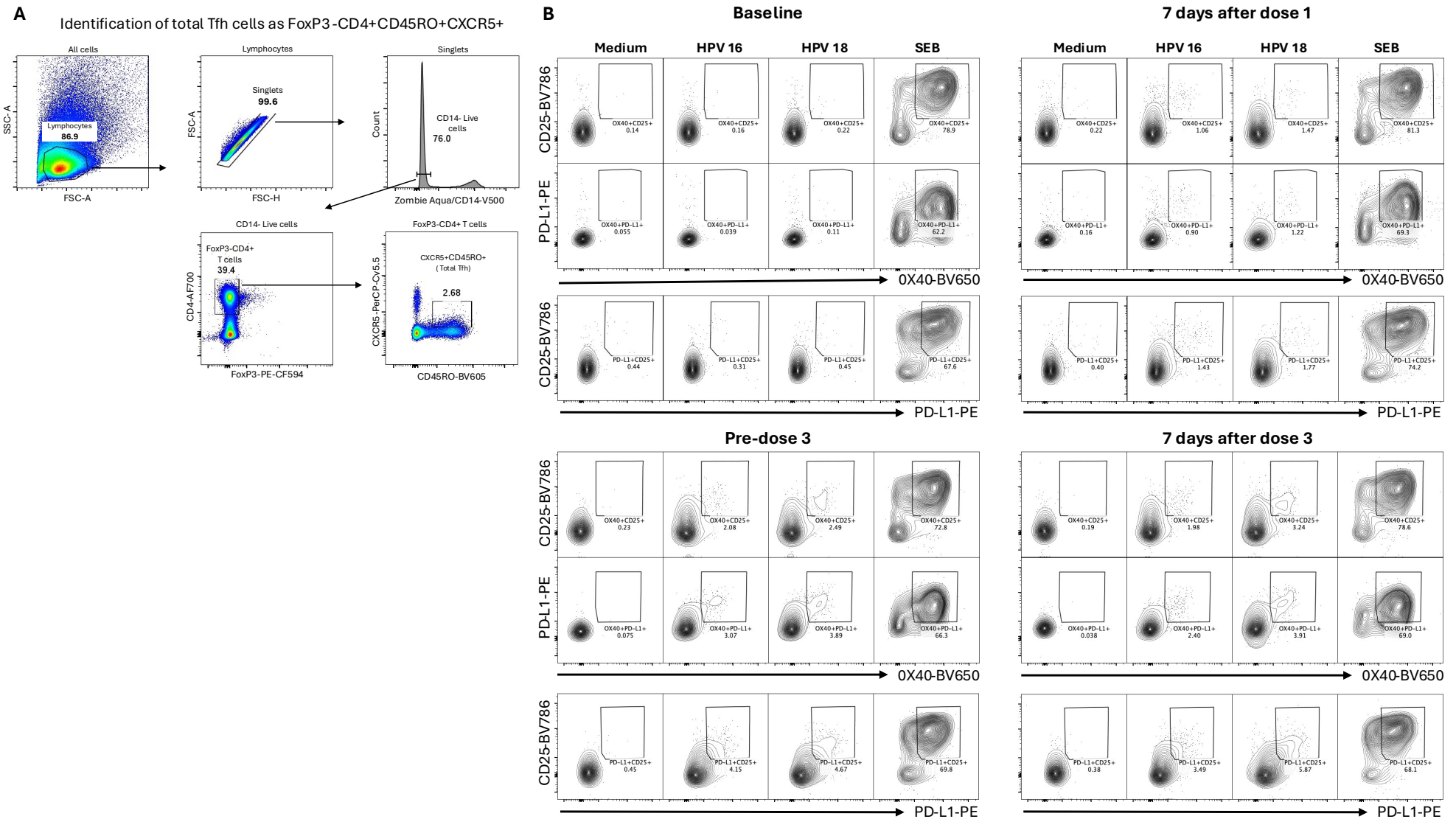


Figure 5.1. Gating strategy for identification of HPV 16 and HPV 18 Tfh cells

Frozen PBMC from baseline, day 7 post-dose 1, pre- and day 7 post-dose 3 of Gardasil 9 vaccination were thawed and stimulated in culture for 18 hours using HPV 16 virus like particles. Stimulated cells were stained with activation induced marker (AIM) flow cytometry panel. Gating was first done on lymphocytes and single cells, dead and CD14+ cells excluded in a dump channel and then total Tfh cells were identified as FoxP3-CD4+CD45RO+CXCR5+ (**A**) and AIM frequencies identified as OX40+CD25+, OX40+PD-L1+ and PD-L1+CD25+ (**B**). Activated frequencies are shown for the negative control (Medium), HPV 16, HPV 18 and the positive control (SEB – staphylococcus enterotoxin). The contour plots show examples of activated frequencies at the four targeted timepoints from one study participant in the 15-26-year-old group.

Table 5.2. HPV 16 specific Tfh cell AIM responses after Gardasil 9 vaccination

A: OX40+CD25+ pooled

	All ages	4 to 26 years			
		n = 40	n = 40	n = 41	n = 41
	Sampling timepoint	Baseline	Post-dose 1	Pre-dose 2/3	Post-dose 2/3
% OX40+CD25+ in total Tfh cells	25% Percentile	0.00	0.00	0.10	0.14
	Median	0.03	0.10	0.48	0.38
	75% Percentile	0.14	0.40	1.27	1.45

B: OX40+PD-L1+ pooled

	All ages	4 to 26 years			
		n = 40	n = 40	n = 41	n = 41
	Sampling timepoint	Baseline	Post-dose 1	Pre-dose 2/3	Post-dose 2/3
% OX40+PD-L1+ in total Tfh cells	25% Percentile	0.00	0.00	0.05	0.08
	Median	0.00	0.04	0.51	0.42
	75% Percentile	0.08	0.13	2.28	1.70

C: PD-L1+CD25+ pooled

	All ages	4 to 26 years			
		n = 40	n = 40	n = 41	n = 41
	Sampling timepoint	Baseline	Post-dose 1	Pre-dose 2/3	Post-dose 2/3
% PD-L1+CD25+ in total Tfh cells	25% Percentile	0.00	0.02	0.12	0.24
	Median	0.12	0.29	0.45	0.81
	75% Percentile	0.47	1.03	1.97	2.34

Continued on next page

D: OX40+CD25+ age-stratified

	Age stratified	4 to 8 years; n = 18				9 to 14 years; n = 19				15 to 26 years; n = 16			
		n = 15	n = 15	n = 15	n = 15	n = 12	n = 12	n = 12	n = 12	n = 13	n = 13	n = 14	n = 14
	Sampling timepoint	Baseline	Post-dose 1	Pre-dose 2	Post-dose 2	Baseline	Post-dose 1	Pre-dose 2	Post-dose 2	Baseline	Post-dose 1	Pre-dose 3	Post-dose 3
% OX40+CD25+ in total Tfh cells	25% Percentile	0.00	0.02	0.05	0.10	0.00	0.00	0.18	0.21	0.03	0.00	0.21	0.21
	Median	0.00	0.07	0.16	0.17	0.01	0.13	0.76	0.52	0.12	0.15	0.77	0.78
	75% Percentile	0.06	0.32	0.67	0.52	0.13	0.63	3.54	1.57	0.66	0.52	2.21	1.85

E: OX40+PD-L1+ age-stratified

	Age stratified	4 to 8 years; n = 18				9 to 14 years; n = 19				15 to 26 years; n = 16			
		n = 15	n = 15	n = 15	n = 15	n = 12	n = 12	n = 12	n = 12	n = 13	n = 13	n = 14	n = 14
	Sampling timepoint	Baseline	Post-dose 1	Pre-dose 2	Post-dose 2	Baseline	Post-dose 1	Pre-dose 2	Post-dose 2	Baseline	Post-dose 1	Pre-dose 3	Post-dose 3
% OX40+PD-L1+ in total Tfh cells	25% Percentile	0.00	0.00	0.00	0.00	0.00	0.01	0.06	0.04	0.00	0.01	0.12	0.30
	Median	0.00	0.00	0.07	0.23	0.00	0.07	1.10	1.27	0.05	0.11	1.39	1.12
	75% Percentile	0.05	0.05	0.51	0.53	0.04	0.18	4.31	1.98	0.51	0.37	3.95	1.97

Continued on next page

F: PD-L1+CD25+ age-stratified

	Age stratified	4 to 8 years; n = 18				9 to 14 years; n = 19				15 to 26 years; n = 16			
		n = 15	n = 15	n = 15	n = 15	n = 12	n = 12	n = 12	n = 12	n = 13	n = 13	n = 14	n = 14
	Sampling timepoint	Baseline	Post-dose 1	Pre-dose 2	Post-dose 2	Baseline	Post-dose 1	Pre-dose 2	Post-dose 2	Baseline	Post-dose 1	Pre-dose 3	Post-dose 3
% PD-L1+CD25+ in total Tfh cells	25% Percentile	0.00	0.00	0.00	0.09	0.05	0.13	0.04	0.78	0.00	0.17	0.40	0.41
	Median	0.00	0.21	0.15	0.27	0.22	0.34	0.90	1.65	0.15	0.30	1.51	1.59
	75% Percentile	0.23	0.41	0.35	0.81	0.64	1.23	5.26	4.21	1.11	1.12	3.53	4.64

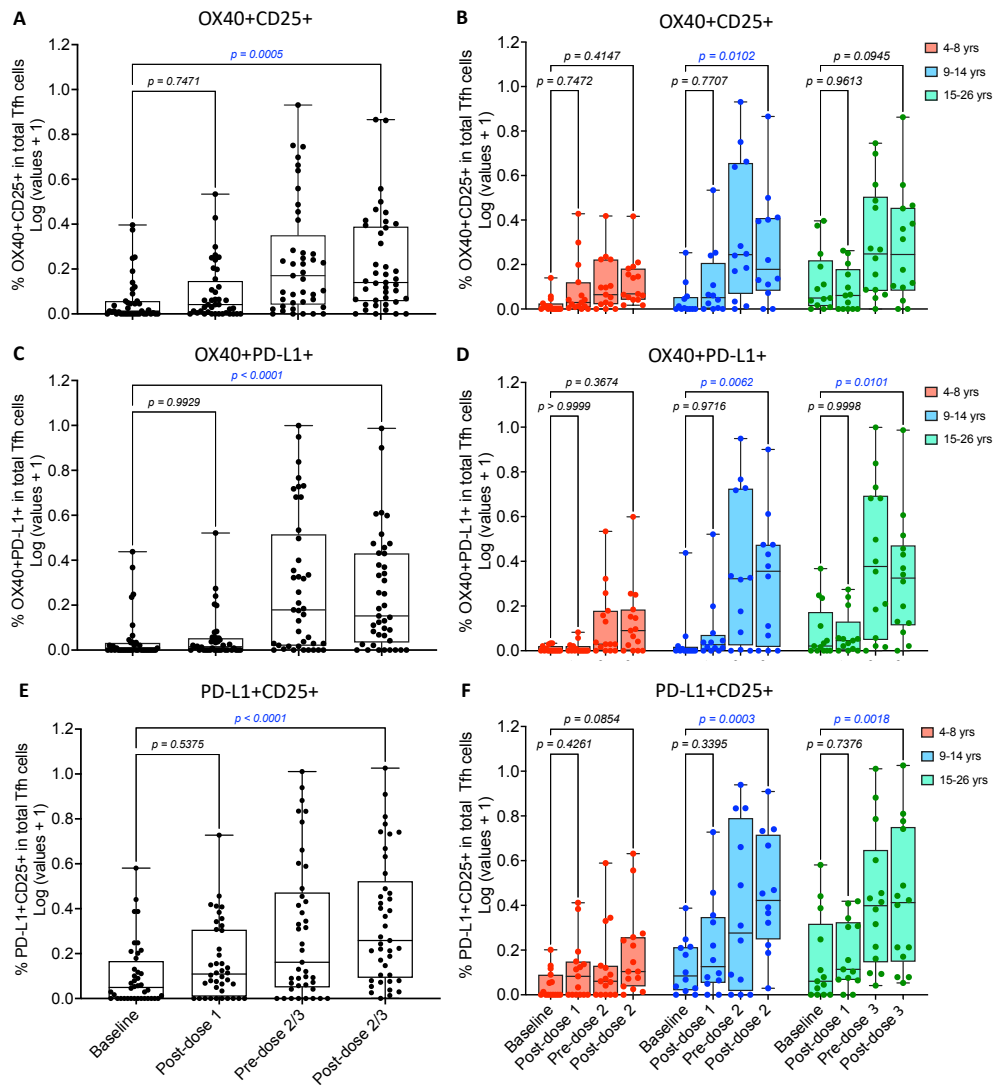


Figure 5.2. HPV 16 specific Tfh cell AIM responses after Gardasil 9 vaccination

Frozen PBMC from baseline, day 7 post-dose 1, pre- and day 7 post-dose 2 or 3 of Gardasil 9 vaccination were thawed and stimulated in culture for 18 hours using HPV 16 virus like particles. Stimulated cells were stained with activation induced marker (AIM) flow cytometry panel and data acquired on LSR Fortessa III. Gating was first performed on lymphocytes and single cells, then dead and CD14+ cells excluded in a dump channel. Total Tfh cells were identified as CD4+FoxP3-CD45RO+CXCR5+ and AIM frequencies identified as OX40+CD25+, OX40+PD-L1+ and PD-L1+CD25+. Data is presented comparing frequencies of OX40+CD25+, OX40+PD-L1+ and PD-L1+CD25+ Tfh cells in the pooled (**A, C & E**) and age-stratified (**B, D & F**) analysis at baseline and post dose 2 or 3 in the respective age groups as shown. One-way ANOVA followed by Dunnett's adjusted multiple comparison tests were performed for the pooled data and Two-way ANOVA followed by Tukey adjusted multiple comparison tests were performed for age-stratified data. The three age groups are shown in different colours. Each dot represents an individual. The box and whisker plots represent response distribution with the lower, central and upper lines denoting minimum, median and maximum values, respectively. Statistically significant p values ($p < 0.05$) are highlighted in blue.

From the pooled analysis of HPV 18 specific AIM frequencies, there was no significant difference between baseline and post-dose 1 although the post-dose 1 response tended to be higher (Table 5.3A - C, Figure 5.3A, C & E). After dose 2 or 3, a significant increase was observed in frequencies of all AIM combinations as OX40+CD25+ (median; 25th -75th percentiles: baseline = 0.08%; 0.00 - 0.22%, post-dose 2 or 3 = 0.34%; 0.02 - 1.30%, p = 0.0014), OX40+PD-L1+ (baseline = 0.04; 0.00 - 0.09%, post-dose 2 or 3 = 0.53%; 0.12 - 1.71%, p < 0001) and PD-L1+CD25+ (baseline = 0.05%; 0.00 - 0.47%, post-dose 2 or 3 = 1.09%; 0.34 - 3.93%, p < 0.0001) (Table 5.3A - C, Figure 5.3A, C & E).

In the age-stratified analysis, there was no significant increase observed in the Tfh frequencies after the first dose across all ages, although the post-dose 1 response tended to be higher. After dose 2 or 3, significant increases were detected in the two older age groups for two AIM combinations as follows: OX40+PD-L1+ (median; 25th - 75th percentiles: baseline = 0.05%; 0.00 - 0.10, post-dose 2 = 1.17%; 0.12 - 1.99%, p = 0.0049) and PD-L1+CD25+ (baseline = 0.09; 0.01 - 0.45%, post-does 2 = 1.63%; 0.38 - 4.47%, p = 0.0033) for 9-14-year-olds and OX40+PD-L1+ (baseline = 0.04%; 0.00 - 0.18%, post-dose 3 = 0.60%; 0.19 - 1.86%, p = 0.0167) and PD-L1+CD25+ (baseline = 0.09; 0.01 - 0.45%, post-dose 3 = 1.26%; 0.40 - 4.33%, p = 0.0039) for 15-26-year-olds (Table 5.3D - F, Figure 5.3B, D & F). Similar to HPV 16 specific response, there was a trend towards increase in all AIM combinations in the 4-8-year-olds, but it was not significant. HPV 18 specific pre- and post-dose 2 or 3 AIM frequencies within each group were variable.

There were no significant changes observed in the AIM frequencies from negative and positive control tests across time and age (Appendix 9).

Table 5.3. HPV 18 specific Tfh cell AIM responses after Gardasil 9 vaccination

A: OX40+CD25+ pooled

	All ages	4 to 26 years			
		n = 39	n = 39	n = 40	n = 40
	Sampling timepoint	Baseline	Post-dose 1	Pre-dose 2/3	Post-dose 2/3
% OX40+CD25+ in total Tfh cells	25% Percentile	0.00	0.07	0.00	0.02
	Median	0.08	0.15	0.42	0.34
	75% Percentile	0.22	0.89	0.89	1.30

B: OX40+PD-L1+ pooled

	All ages	4 to 26 years			
		n = 40	n = 40	n = 41	n = 41
	Sampling timepoint	Baseline	Post-dose 1	Pre-dose 2/3	Post-dose 2/3
% OX40+PD-L1+ in total Tfh cells	25% Percentile	0.00	0.00	0.05	0.12
	Median	0.04	0.14	0.42	0.53
	75% Percentile	0.09	0.33	1.84	1.71

C: PD-L1+CD25+ pooled

	All ages	4 to 26 years			
		n = 39	n = 39	n = 40	n = 40
	Sampling timepoint	Baseline	Post-dose 1	Pre-dose 2/3	Post-dose 2/3
% PD-L1+CD25+ in total Tfh cells	25% Percentile	0.00	0.19	0.02	0.34
	Median	0.05	0.47	0.35	1.09
	75% Percentile	0.47	1.67	1.04	3.93

Continued on next page

D: OX40+CD25+ age-stratified

	Age stratified	4 to 8 years; n = 18				9 to 14 years; n = 19				15 to 26 years; n = 16			
		n = 15	n = 15	n = 15	n = 15	n = 12	n = 12	n = 12	n = 12	n = 12	n = 12	n = 13	n = 13
	Sampling timepoint	Baseline	Post-dose 1	Pre-dose 2	Post-dose 2	Baseline	Post-dose 1	Pre-dose 2	Post-dose 2	Baseline	Post-dose 1	Pre-dose 3	Post-dose 3
% OX40+CD25+ in total Tfh cells	25% Percentile	0.00	0.00	0.00	0.00	0.00	0.08	0.00	0.05	0.00	0.08	0.00	0.11
	Median	0.08	0.08	0.22	0.19	0.06	0.15	0.70	0.69	0.06	0.15	0.74	0.43
	75% Percentile	0.27	0.98	0.47	1.16	0.22	0.81	1.19	1.75	0.22	0.81	1.63	1.61

E: OX40+PD-L1+ age-stratified

	Age stratified	4 to 8 years; n = 18				9 to 14 years; n = 19				15 to 26 years; n = 16			
		n = 15	n = 15	n = 15	n = 15	n = 12	n = 12	n = 12	n = 12	n = 12	n = 12	n = 14	n = 14
	Sampling timepoint	Baseline	Post-dose 1	Pre-dose 2	Post-dose 2	Baseline	Post-dose 1	Pre-dose 2	Post-dose 2	Baseline	Post-dose 1	Pre-dose 3	Post-dose 3
% OX40+PD-L1+ in total Tfh cells	25% Percentile	0.00	0.00	0.01	0.07	0.00	0.05	0.00	0.12	0.00	0.00	0.24	0.19
	Median	0.00	0.00	0.20	0.23	0.05	0.16	0.70	1.17	0.04	0.29	1.48	0.60
	75% Percentile	0.09	0.18	0.42	1.12	0.10	0.62	1.80	1.99	0.18	0.40	4.36	1.86

Continued on next page

F: PD-L1+CD25+ age-stratified

	Age stratified	4 to 8 years; n = 18				9 to 14 years; n = 19				15 to 26 years; n = 16			
		n = 15	n = 15	n = 15	n = 15	n = 12	n = 12	n = 12	n = 12	n = 12	n = 12	n = 13	n = 13
	Sampling timepoint	Baseline	Post-dose 1	Pre-dose 2	Post-dose 2	Baseline	Post-dose 1	Pre-dose 2	Post-dose 2	Baseline	Post-dose 1	Pre-dose 3	Post-dose 3
% PD-L1+CD25+ in total Tfh cells	25% Percentile	0.00	0.05	0.00	0.07	0.01	0.32	0.11	0.38	0.01	0.32	0.15	0.40
	Median	0.00	0.34	0.11	0.39	0.09	0.60	0.86	1.63	0.09	0.60	0.86	1.26
	75% Percentile	0.50	1.73	0.34	1.52	0.45	1.49	1.67	4.47	0.45	1.49	1.74	4.33

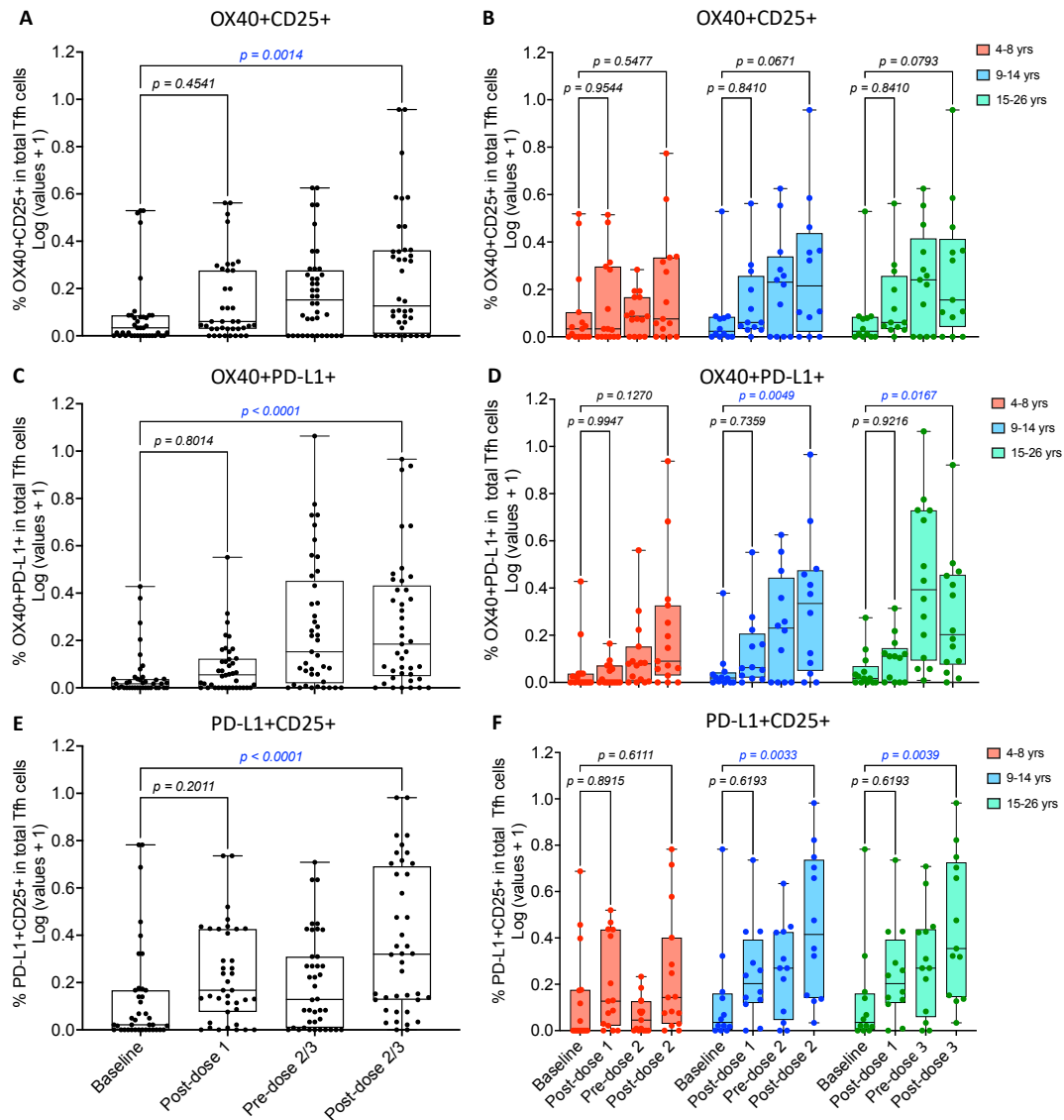


Figure 5.3. HPV 18 specific Tfh cell AIM responses after Gardasil 9 vaccination

Frozen PBMC from baseline, day 7 post-dose 1, pre- and day 7 post-dose 2 or 3 of Gardasil 9 vaccination were thawed and stimulated in culture for 18 hours using HPV 18 virus like particles. Stimulated cells were stained with activation induced marker (AIM) flow cytometry panel and data acquired on LSR Fortessa III. Gating was first performed on lymphocytes and single cells, then dead and CD14+ cells excluded in a dump channel. Total Tfh cells were identified as CD4+FoxP3-CD45RO+CXCR5+ and AIM frequencies identified as OX40+CD25+, OX40+PD-L1+ and PD-L1+CD25+. Data is presented comparing frequencies of OX40+CD25+, OX40+PD-L1+ and PD-L1+CD25+ Tfh cells in the pooled (**A, C & E**) and age-stratified (**B, D & F**) analysis at baseline and post dose 2 or 3 in the respective age groups as shown. One-way ANOVA followed by Dunnett's adjusted multiple comparison tests were performed for the pooled data and Two-way ANOVA followed by Tukey adjusted multiple comparison tests were performed for age-stratified data. The three age groups are shown in different colours. Each dot represents an individual. The box and whisker plots represent response distribution with the lower, central and upper lines denoting minimum, median and maximum values, respectively. Statistically significant p values ($p < 0.05$) are highlighted in blue.

Simple main effects ANOVA analysis showed that age had a significant effect on vaccine-induced Tfh cell AIM frequencies for both HPV types. The age effect was observed from the three AIM combinations for HPV 16 as follows: OX40+CD25+; $p = 0.0008$, OX40+PD-L1+; $p < 0.0001$ and PD-L1+CD25+; $p < 0.0001$) while for HPV 18, it was from two AIM combinations: OX40+PD-L1-; $p = 0.0098$ and PD-L1+CD25+; $p = 0.0081$. Multiple age comparisons per timepoint were therefore used to identify the sources of the age-related differences. These showed that the two older age groups had significantly higher Tfh cell AIM frequencies mainly at the timepoints just before and/or after the second or third vaccination doses as shown in the respective plots for HPV 16 (Figure 5.4A, C & E) and HPV 18 (Figure 5.4B, D & F).

Considering different vaccination schedules used in this study, the detected antigen specific Tfh cell AIM responses align with the B cell responses observed earlier where significant increases were mainly observed after the second or third vaccination doses. However, more age-related differences were observed in the Tfh cell responses than in B cell responses.

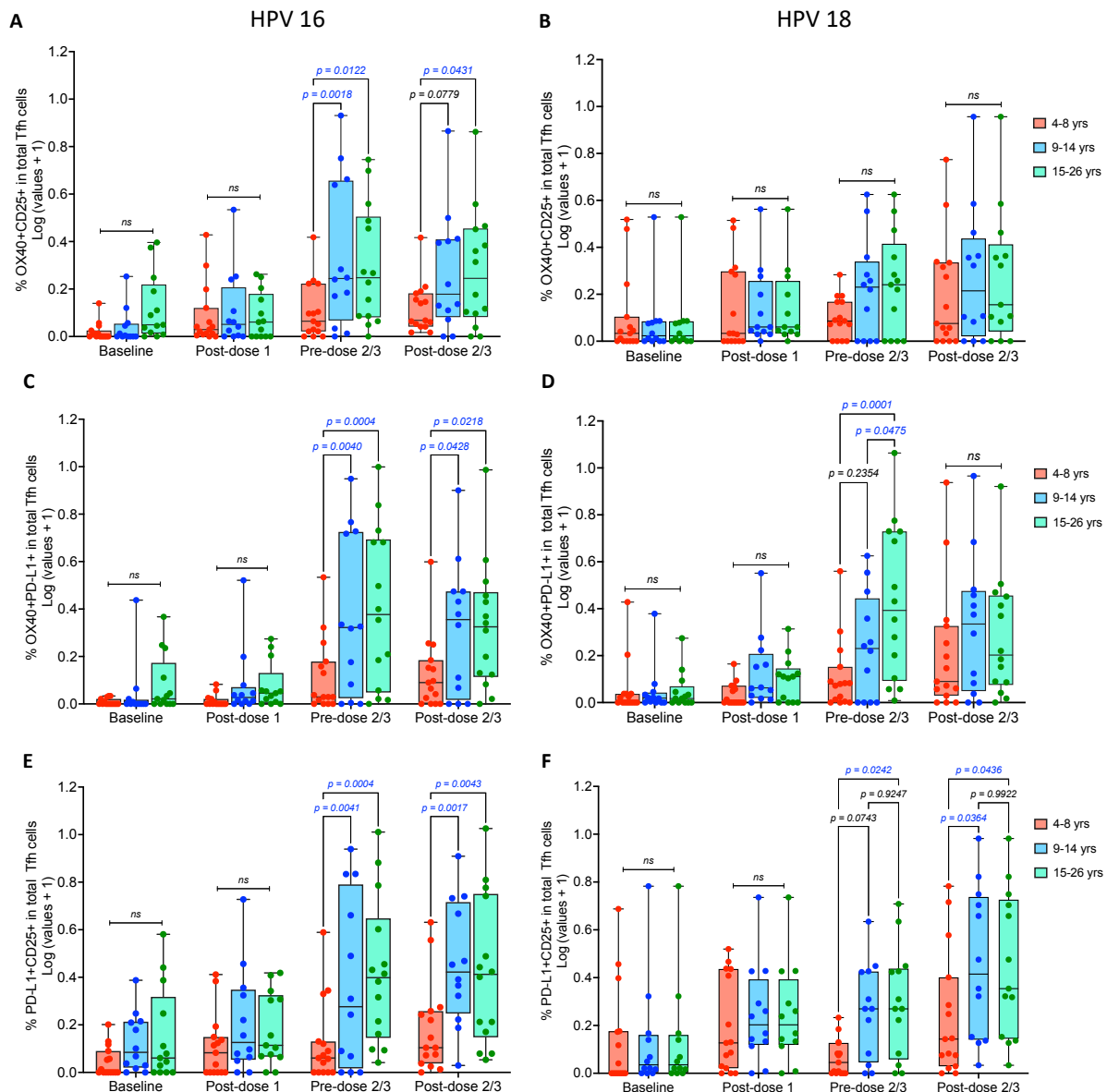


Figure 5.4. Impact of age on HPV 16 and HPV 18 specific Tfh cell responses after Gardasil 9 vaccination

Frozen PBMC from baseline, day 7 post-dose 1, pre- and day 7 post-dose 2 or 3 of Gardasil 9 vaccination were thawed and stimulated in culture for 18 hours using HPV 16 or HPV 18 virus like particles. Stimulated cells were stained with activation induced marker (AIM) flow cytometry panel and data was acquired on LSR Fortessa III. Gating was first done on lymphocytes and single cells, then dead and CD14+ cells excluded in a dump channel. Total Tfh cells were identified as CD4+FoxP3-CD45RO+CXCR5+ and AIM frequencies identified as OX40+CD25+ (**A & B**), OX40+PD-L1+ (**C & D**) or PD-L1+CD25+ (**E & F**). Two-way ANOVA followed by Tukey adjusted multiple comparison tests were performed for age-stratified data. The three age groups are shown in different colours. Each dot represents an individual. The box and whisker plots represent response distribution with the lower, central and upper lines denoting minimum, median and maximum values, respectively. Statistically significant p values ($p < 0.05$) are highlighted in blue.

5.2.2 Comparison of HPV 16 and HPV 18 specific Tfh cell AIM frequencies with plasma cell numbers

Pearson correlation analysis was performed to evaluate the relationship between vaccine-induced antigen specific plasma cells and Tfh cells where post-dose 2 or 3 matched data was available. Correlation was assessed in a total of 33 samples across the three age groups (4-8-year-olds = 13, 9-14-year-olds = 10 and 15-26-year-olds = 10). The correlation analysis was based on OX40+PD-L1+ AIM combination previously reported to be highly precise in identifying antigen specific Tfh cells. There was no significant correlation observed between Tfh cell frequencies and plasma cell numbers for both HPV 16 ($r = -0.0266$, $p = 0.8832$) and HPV 18 ($r = -0.0377$, $p = 0.8350$) (Figure 5.5A & B).

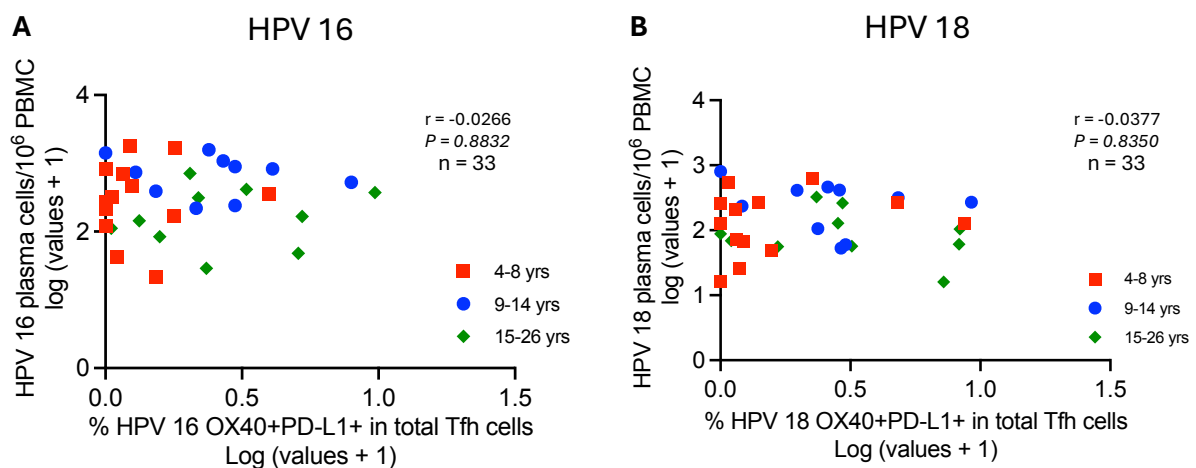


Figure 5.5. Correlation of HPV 16 (A) and HPV 18 (B) specific Tfh cell frequencies with plasma cell numbers

Pearson correlation analysis was performed to compare vaccine-induced HPV 16 (A) and HPV 18 (B) specific IgG plasma cells and frequencies of corresponding in vitro stimulated T follicular helper cells as shown. Analysis was performed on the pooled dataset. The age groups are shown in different colours.

5.2.3 Frequencies of total ex vivo activated Tfh cells after Gardasil 9 vaccination

After looking at the vaccine-induced in vitro stimulated Tfh cells using the AIM assay, overall vaccine-induced ex vivo stimulated Tfh cell frequencies were evaluated based on ICOS and PD-L1 expression. The gating strategy used to identify the three main Tfh cell subsets, Tfh1 (CXCR3+CCR6-), Tfh2 (CXCR3-CCR6-) and Tfh17 (CXCR3-CCR6+) in the total Tfh cell population (CD4+FoxP3-CD45RO+CXCR5+) and the activated (ICOS+PD-1++) frequencies in each subset is shown (Figure 5.6A & B). In the analyses for ex vivo activated Tfh cells, considerations were made for activated frequencies in the total Tfh cells pool as well as in the three subsets. Pooled and age-stratified analyses were performed as discussed earlier comparing baseline to post-dose 1 and post-dose 2 or 3. From the pooled analysis, there was no significant difference in total ex vivo activated Tfh cell frequencies between baseline and post-dose 1 although the post-dose 1 response tended to be higher (Table 5.4A, Figure 5.7A). The second and third vaccination doses caused a significant increase in the total ex vivo activated Tfh cell frequencies (median; 25th - 75th percentiles: baseline = 1.18%; 0.69 - 1.83%, post-dose 2 or 3 = 2.25%; 1.44 - 3.78%, $p < 0.0001$) (Table 5.4A, Figure 5.7A).

From the age stratified analysis, a significant increase in ex vivo activated Tfh cell frequency after the first vaccination dose was only observed in the 4-8-year-olds group (baseline = 1.66%; 1.18 - 2.13%, post-dose 1 = 2.24%; 1.62 - 2.81%, $p = 0.0091$) (Table 5.4B, Figure 5.7B). The second or third vaccination doses induced significant increases in ex vivo activated Tfh cell frequencies across the three age groups as follows: median; 25th - 75th percentiles: (post-dose 2 = 3.23%; 2.15 - 3.87%, $p = 0.0021$ for 4-8-year-olds, baseline = 1.17%; 0.71 - 1.36%, post-dose 2 = 3.27; 2.03 - 4.17%, $p < 0.0001$ for 9-14-year-olds and baseline = 0.68%; 0.16 - 0.95%, post-dose 3 = 1.41%; 0.95 - 1.68%, $p = 0.0066$ for 15-26-year-olds (Table 5.4B, Figure 5.7B).

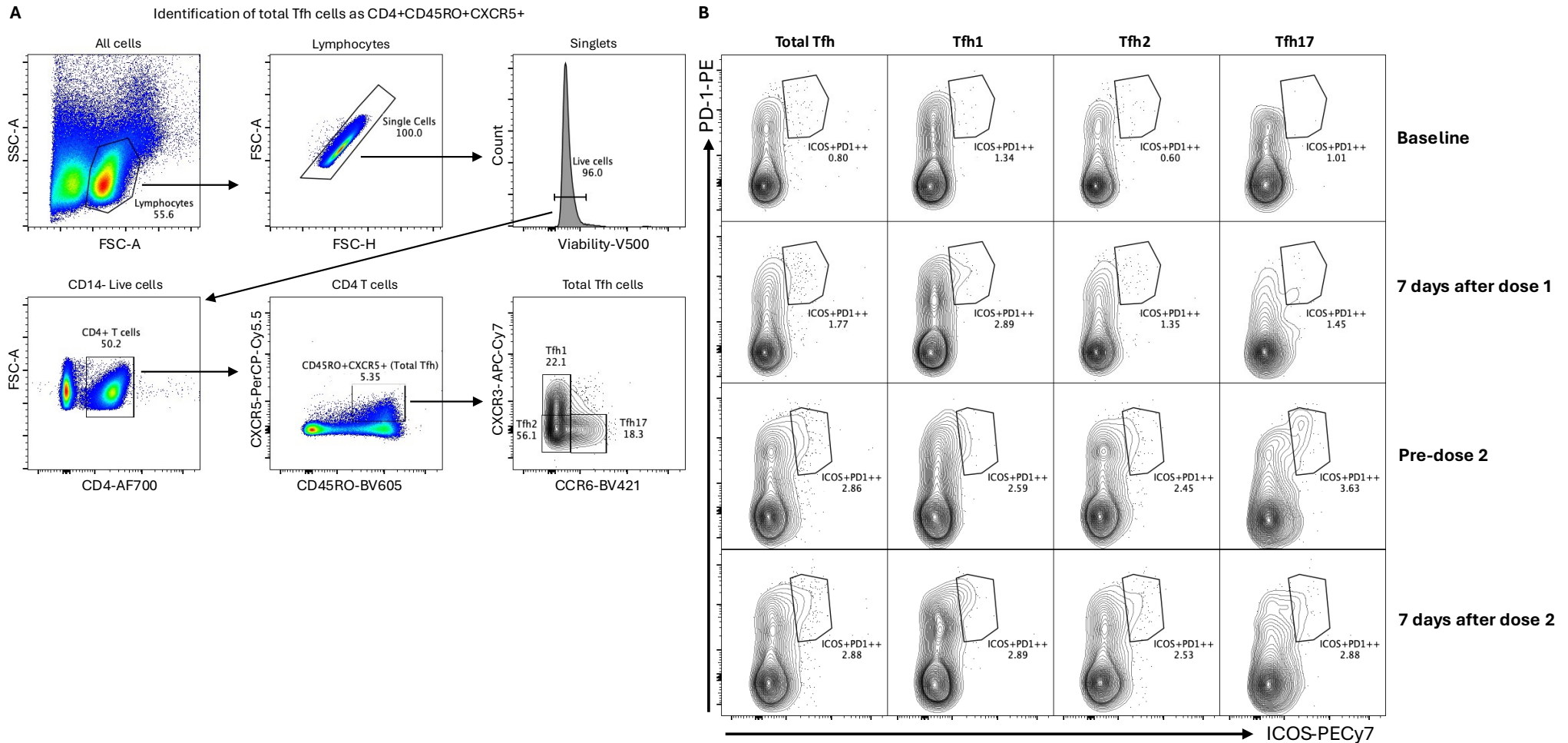


Figure 5.6. Gating strategy for identification of ex vivo activated Tfh cells

Frozen PBMC from baseline, day 7 post-dose 1, pre- and day 7 post-dose 2 of Gardasil 9 vaccination were thawed and stained with a Tfh cell ex vivo cytometry panel. Data was acquired on LSR Fortessa III. **A:** Gating was first done on lymphocytes and single cells then total Tfh cells were identified as CD4+CD45RO+CXCR5+. From the total Tfh cells, Tfh subsets were identified as Tfh1 (CXCR3+CCR6-), Tfh2 (CXCR3-CCR6-) and Tfh17 (CXCR3-CCR6+). **B:** Activated frequencies defined as ICOS+ PD-1++ were then identified from the total Tfh cells population and from each subset. The contour plots show examples of activated frequencies at the four targeted timepoints from one study participant in the 4-8-year-olds group.

Table 5.4. Frequencies of total ex vivo activated Tfh cells after Gardasil 9 vaccination

A: Total Tfh pooled

	All ages	4 to 26 years			
		n = 44	n = 44	n = 51	n = 51
	Sampling timepoint	Baseline	Post-dose 1	Pre-dose 2/3	Post-dose 2/3
% ICOS+PD-1++ in total Tfh cells	25% Percentile	0.69	0.80	0.88	1.44
	Median	1.18	1.41	1.36	2.25
	75% Percentile	1.83	2.27	1.91	3.78

B: Total Tfh age-stratified

	Age stratified	4 to 8 years; n = 18				9 to 14 years; n = 19				15 to 26 years; n = 16			
		n = 20	n = 20	n = 19	n = 19	n = 16	n = 16	n = 16	n = 16	n = 8	n = 8	n = 16	n = 16
	Sampling timepoint	Baseline	Post-dose 1	Pre-dose 2	Post-dose 2	Baseline	Post-dose 1	Pre-dose 2	Post-dose 2	Baseline	Post-dose 1	Pre-dose 3	Post-dose 3
% ICOS+PD-1++ in total Tfh cells	25% Percentile	1.18	1.62	1.39	2.15	0.71	0.65	0.92	2.03	0.16	0.19	0.66	0.95
	Median	1.66	2.24	1.91	3.23	1.17	0.99	1.56	3.27	0.68	0.65	0.90	1.41
	75% Percentile	2.13	2.81	2.61	3.87	1.36	1.54	1.80	4.17	0.95	1.04	1.07	1.68

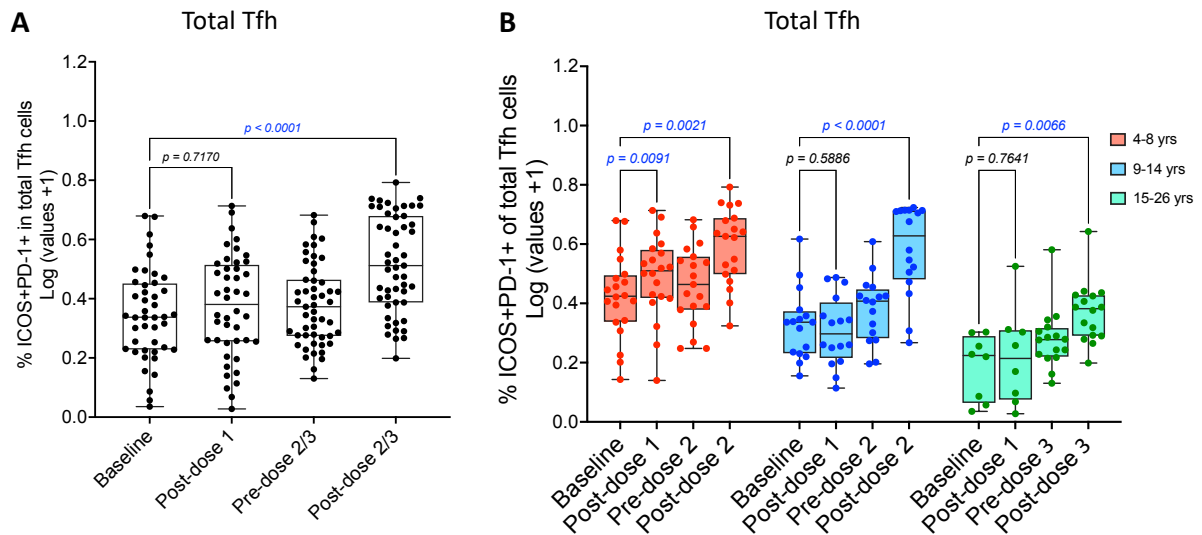


Figure 5.7. Frequencies of total ex vivo activated Tfh cells after Gardasil 9 vaccination

Frozen PBMC from baseline, day 7 post-dose 1, pre- and day 7 post-dose 2 or 3 of Gardasil 9 vaccination were thawed and analysed with an ex vivo flow cytometry antibody panel. Data was acquired on LSR Fortessa III. Cells were first gated on lymphocytes and single cells and dead cells excluded. Total Tfh cells were then gated as CD4+FoxP3-CD45RO+CXCR5+ and activated Tfh frequencies identified as ICOS+PD-1++. One-way ANOVA followed by Dunnett's adjusted multiple comparison tests were performed for the pooled data (A) and Two-way ANOVA followed by Tukey adjusted multiple comparison tests were performed for age-stratified data (B). The three age groups are shown in different colours. Each dot represents an individual. The box and whisker plots represent response distribution with the lower, central and upper lines denoting minimum, median and maximum values, respectively. Statistically significant p values ($p < 0.05$) are highlighted in blue.

After evaluating frequencies of total ex vivo activated Tfh cells, activation in the subsets was considered. Pooled analysis showed no significant differences between baseline and post-dose 1 across the three subsets although the post-dose 1 responses tended to be higher (Table 5.5A - C, Figure 5.8A, C & E). Following second or third doses, significant activation was observed in Tfh1 (median; 25th - 75th percentiles: baseline = 1.24%; 0.73 - 2.37%, post-dose 2 or 3 = 3.40%; 1.96 - 4.71%, $p < 0.0001$) and Tfh2 (baseline = 1.16%; 0.65 - 1.79%, post-dose 2 or 3 = 2.18%; 1.64 - 3.51%, $p < 0.0001$) and no significant increase was observed in Tfh17 (Table 5.5A - C, Figure 5.8A, C & E).

On the age-stratified analysis, significant activation after dose 1 was observed in Tfh2 subset only in the 4-8-year-olds (median; 25th - 75th percentiles: baseline = 1.54%; 1.06 -

2.69%, post-dose 1 = 2.50%; 1.67 - 3.12%, $p = 0.0008$) while in the older age groups, the post-dose 1 responses in all subsets were not significant but tended to be higher (Table 5.5D - F, Figure 5.8B, D & F).

Following the second and third doses, significant activation of Tfh1 and Tfh2 subsets was observed in the three age groups except in the youngest age group where Tfh1 activation was close to statistical significance as follows: 4-8-year-olds (median; 25th - 75th percentiles: Tfh1 baseline = 2.12; 1.23 - 3.27, post-dose 2 = 3.40; 2.48 - 4.29, $p = 0.0712$, Tfh2 baseline = 1.54; 1.06 - 2.69, post-dose 2 = 2.91%; 2.13 - 3.93%, $p = 0.0017$), 9-14-year-olds (Tfh1 baseline = 1.14%; 0.66 - 2.21%, post-dose 2 = 4.61%; 3.58 - 6.15%, $p < 0.0001$, Tfh2 baseline = 0.98%; 0.77 - 1.48%, post-dose 2 = 2.83%; 1.80 - 3.99%, $p = 0.0011$) and 15-26-year-olds (Tfh1 baseline = 0.67%; 0.00 - 0.80%, post-dose 3 = 2.07%; 1.33 - 3.24%, $p = 0.0093$ and Tfh2 baseline = 0.60%; 0.31 - 1.02%, post-dose 3 = 1.44%; 0.90 - 2.03%, $p = 0.0084$) (Table 5.5D - F, Figure 5.8B, D & F). Overall, there was no significant activation observed in the Tfh17 subset across all age groups although the frequencies tended to be increasing post-dose 1 and 2 in the younger age groups.

Table 5.5. Frequencies of ex vivo activated Tfh cell subsets after Gardasil 9 vaccination

A: Tfh1 pooled

		4 to 26 years			
	All ages	n = 44	n = 44	n = 51	n = 51
	Sampling timepoint	Baseline	Post-dose 1	Pre-dose 2/3	Post-dose 2/3
% ICOS+PD-1++ in Tfh1 cells	25% Percentile	0.73	1.02	0.98	1.96
	Median	1.24	1.59	1.50	3.40
	75% Percentile	2.37	2.89	3.28	4.72

B: Tfh2 pooled

	All ages	4 to 26 years			
		n = 44	n = 44	n = 51	n = 51
	Sampling timepoint	Baseline	Post-dose 1	Pre-dose 2/3	Post-dose 2/3
% ICOS+PD-1++ in Tfh2 cells	25% Percentile	0.65	0.82	0.77	1.64
	Median	1.16	1.58	1.18	2.18
	75% Percentile	1.79	2.45	1.89	3.51

C: Tfh17 pooled

	All ages	4 to 26 years			
		n = 44	n = 44	n = 51	n = 51
	Sampling timepoint	Baseline	Post-dose 1	Pre-dose 2/3	Post-dose 2/3
% ICOS+PD-1++ in Tfh17 cells	25% Percentile	0.53	0.47	0.72	0.63
	Median	0.86	1.09	1.21	1.29
	75% Percentile	1.79	1.71	1.52	2.27

Continued on next page

D: Tfh1 age-stratified

	Age stratified	4 to 8 years; n = 18				9 to 14 years; n = 19				15 to 26 years; n = 16			
		n = 20	n = 20	n = 19	n = 19	n = 16	n = 16	n = 16	n = 16	n = 8	n = 8	n = 16	n = 16
	Sampling timepoint	Baseline	Post-dose 1	Pre-dose 2	Post-dose 2	Baseline	Post-dose 1	Pre-dose 2	Post-dose 2	Baseline	Post-dose 1	Pre-dose 3	Post-dose 3
% ICOS+PD-1++ in Tfh1 cells	25% Percentile	1.23	1.59	1.50	2.48	0.66	0.56	1.09	3.58	0	0.06	0.66	1.33
	Median	2.12	2.72	2.11	3.40	1.14	1.17	1.85	4.61	0.67	0.81	0.96	2.07
	75% Percentile	3.27	4.14	3.43	4.29	2.21	1.69	3.58	6.15	0.80	1.39	1.34	3.24

E: Tfh2 age-stratified

	Age stratified	4 to 8 years; n = 18				9 to 14 years; n = 19				15 to 26 years; n = 16			
		n = 20	n = 20	n = 19	n = 19	n = 16	n = 16	n = 16	n = 16	n = 8	n = 8	n = 16	n = 16
	Sampling timepoint	Baseline	Post-dose 1	Pre-dose 2	Post-dose 2	Baseline	Post-dose 1	Pre-dose 2	Post-dose 2	Baseline	Post-dose 1	Pre-dose 3	Post-dose 3
% ICOS+PD-1++ in Tfh2 cells	25% Percentile	1.06	1.67	0.84	2.13	0.77	0.81	0.77	1.80	0.31	0.33	0.44	0.90
	Median	1.54	2.50	1.51	2.91	0.98	1.12	1.15	2.83	0.60	0.77	0.82	1.44
	75% Percentile	2.69	3.12	2.38	3.93	1.48	1.60	1.91	3.99	1.023	1.64	1.18	2.03

F: Tfh17 age-stratified

	Age stratified	4 to 8 years; n = 18				9 to 14 years; n = 19				15 to 26 years; n = 16			
		n = 20	n = 20	n = 19	n = 19	n = 16	n = 16	n = 16	n = 16	n = 8	n = 8	n = 16	n = 16
	Sampling timepoint	Baseline	Post-dose 1	Pre-dose 2	Post-dose 2	Baseline	Post-dose 1	Pre-dose 2	Post-dose 2	Baseline	Post-dose 1	Pre-dose 3	Post-dose 3
% ICOS+PD-1++ in Tfh17 cells	25% Percentile	0.79	0.82	1.09	1.17	0.00	0.40	0.72	0.59	0.08	0.10	0.51	0.39
	Median	1.19	1.49	1.35	2.15	0.55	0.75	1.25	1.87	0.62	0.50	0.83	0.67
	75% Percentile	2.44	1.76	2.19	2.93	1.57	1.95	1.5	2.82	0.98	1.00	1.18	1.43

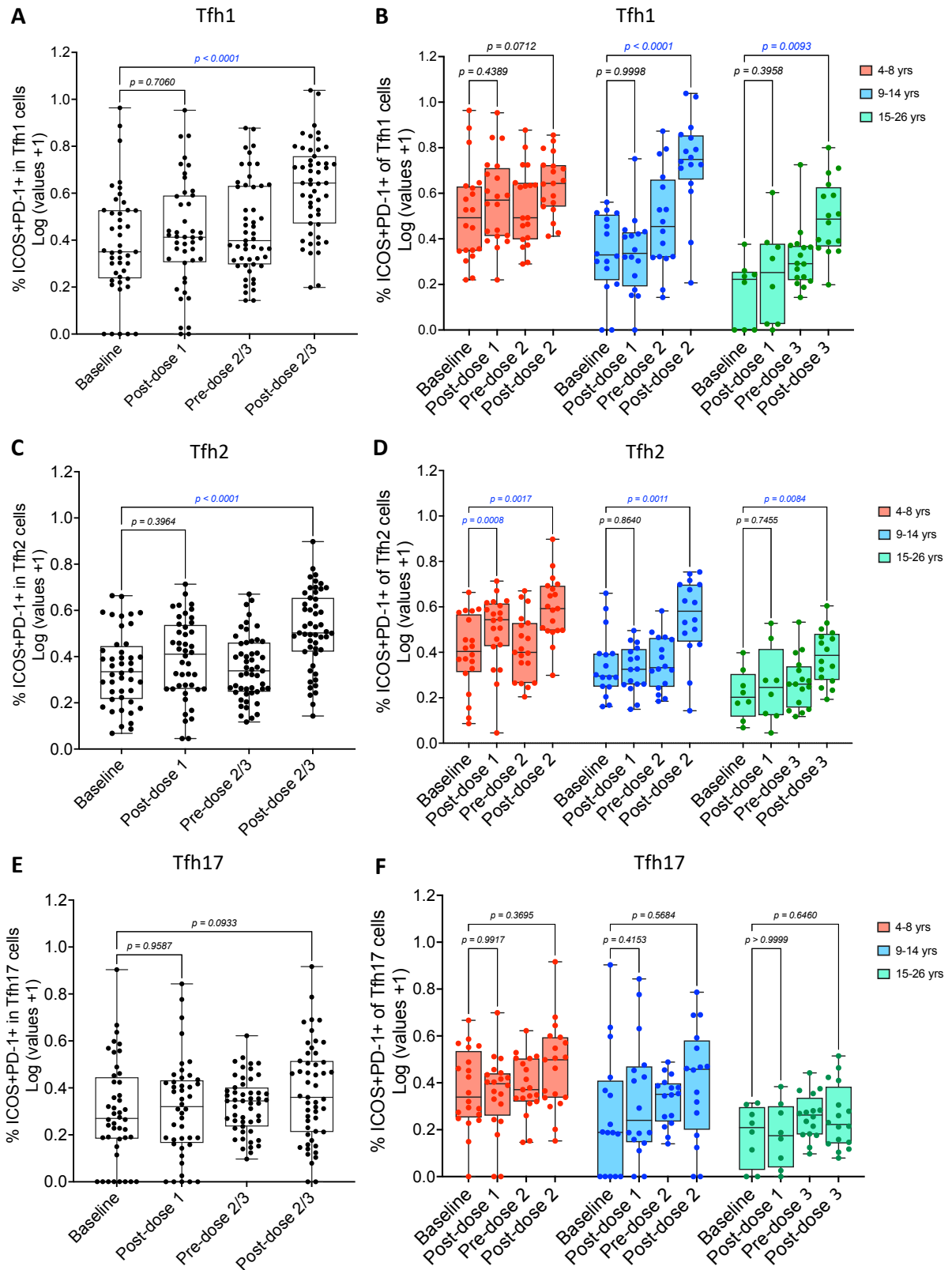


Figure 5.8. Frequencies of ex vivo activated Tfh cell subsets after Gardasil 9 vaccination

Figure legend on next page

Frozen PBMC from baseline, day 7 post-dose 1, pre- and day 7 post-dose 2 or 3 of Gardasil 9 vaccination were thawed and analysed using an ex vivo flow cytometry antibody panel. Cells were first gated on lymphocytes and single cells and dead cells excluded. Total Tfh cells were then gated as CD4+FoxP3-CD45RO+CXCR5+. From the total Tfh pool, Tfh subsets were identified as Tfh1 (CCR6+CXCR3+), Tfh2 (CCR6-CXCR3-) and Tfh17 (CCR6+CXCR3-). Activated frequencies were then identified as ICOS+PD-1++ in each subset. One-way ANOVA followed by Dunnett's adjusted multiple comparison tests were performed for the pooled data (**A, C & E**) and Two-way ANOVA followed by Tukey adjusted multiple comparison tests were performed for age-stratified data (**B, D & F**). The three age groups are shown in different colours. Each dot represents an individual. The box and whisker plots represent response distribution with the lower, central and upper lines denoting minimum, median and maximum values, respectively. Statistically significant p values ($p < 0.05$) are highlighted in blue.

Simple main effects ANOVA analysis showed a significant effect of age on vaccine-induced ex vivo Tfh cell activation ($p < 0.0002$). The source of age effect was evaluated by multiple comparisons per timepoint that showed overall increasing activation with decreasing age across the four timepoints (Figure 5.9). This trend was already observed before vaccination.

Further exploratory analyses were performed to evaluate changes in the total Tfh cell (CD4+CD45RO+CXCR5+) frequencies within the CD4+ T cells as well as the frequencies of the Tfh1, Tfh2 and Tfh17 subsets within the total Tfh cell (CD4+CD45RO+CXCR5+) population (Appendix 10).

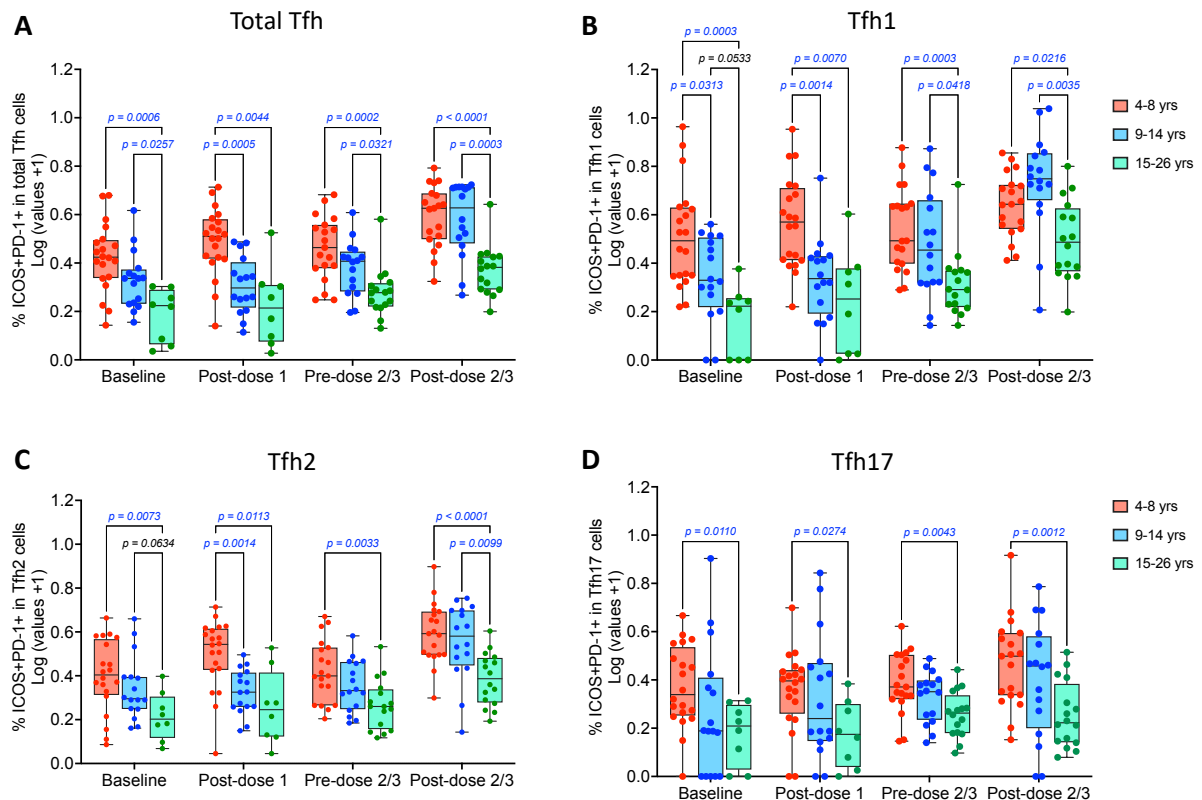


Figure 5.9. Comparisons of ex vivo Tfh cell activation in different age groups after Gardasil 9 vaccination

Frozen PBMC from baseline, day 7 post-dose 1, pre- and day 7 post-dose 2 or 3 of Gardasil 9 vaccination were thawed and analysed using an ex vivo flow cytometry antibody panel. Cells were first gated on lymphocytes and single cells and dead cells excluded. Total Tfh cells were then gated as CD4+FoxP3-CD45RO+CXCR5+. From the total Tfh pool, Tfh subsets were identified as Tfh1 (CCR6+CXCR3+), Tfh2 (CCR6-CXCR3-) and Tfh17 (CCR6+CXCR3-). Activated frequencies were then identified as ICOS+PD-1++ in total Tfh cells (**A**) and in each subset (**B, C & D**). Two-way ANOVA followed by Tukey adjusted multiple comparison tests were performed for age-stratified data. The three age groups are shown in different colours. Each dot represents an individual. The box and whisker plots represent response distribution with the lower, central and upper lines denoting minimum, median and maximum values, respectively. Statistically significant p values ($p < 0.05$) are highlighted in blue.

5.3 Discussion and future work

To address the current scarcity of data about Tfh cell responses generated by HPV vaccines, this is the first study to apply the AIM flow cytometry strategy and report that Gardasil 9 vaccine generates HPV type specific Tfh cell response. The strategy used in identification of HPV 16 and HPV 18 specific Tfh cells has been used in previous studies to identify other antigen specific T cell responses including cytomegalovirus, HIV, Ebola, *Mycobacterium tuberculosis*, Group A Streptococcus and tetanus.(Bowyer et al., 2018, Poloni et al., 2023, Reiss et al., 2017b, Barham et al., 2020) From these studies, the AIM assay proved to be more reliable than cytokine-based conventional approaches used to identify antigen specific T cells as some T cell subsets produce limited cytokine quantities. Additionally, due to heterogeneity in vaccine-induced immune responses following priming and booster vaccinations, cytokine-based methods could miss some antigen specific cells that may not secrete certain cytokines for long after vaccination.(Bowyer et al., 2018)

As the actual effectors, evaluation of cytokine responses gives a more direct measure for functionality of the identified cells. However, their secretion in limited quantities and subsequent decrease with the contracting immune response makes their characterisation challenging. The AIM assay therefore allows detection of a broader T cell specific response for comprehensive evaluation of vaccine immunogenicity even long after vaccination. Indeed, at 12 months after the first vaccination dose in the 4-8- and 9-14-year-olds and 9 months after the second dose in the 15-26-year-olds investigated in this study, HPV 16 and HPV 18 specific Tfh cells were detectable at considerably high levels. Notably, AIM markers can be upregulated on non-effector cells such as CD25 which is upregulated in Tregs upon stimulation. To maximise the specificity of the findings, FoxP3-based exclusion of Tregs was used.(Reiss et al., 2017a) This strategy is considered the most robust way to detect antigen specific T cells of interest using the AIM assay.(Reiss et al., 2017a)

Additionally, characterisation of ex vivo stimulated Tfh cells has been used to evaluate vaccine immunogenicity and is suggested to identify Tfh cell responses that contribute to

the affinity of vaccine induced antibody responses after influenza vaccination.(Bentebibel et al., 2016)

The overall profiles of in vitro and ex vivo activated Tfh cells were consistent with the profiles observed in plasma cell and memory B cell responses. As protein antigens, HPV vaccines are expected to induce T cell-dependent B cell activation through GC reaction leading to induction of Tfh cell responses.(Vinuesa and Chang, 2013)

During T cell-dependent immune activation after vaccine administration, the process of immune activation starts by the HPV VLP antigens being sensed by pattern recognition receptors on DCs surface causing them to mature, process and present the antigens on MHC II to naïve CD4 T cells.(Zepeda-Cervantes et al., 2020) Depending on the cytokine milieu, activated CD4 T cells polarise into different subsets including Tfh cells mainly found within the CD4 T cell memory compartment, reside principally in the lymph nodes and spleen and are also detectable in blood.(Zhu et al., 2010, Huber et al., 2020)

After the first vaccination dose, although there were no significant increases observed in activated Tfh cell frequencies except a few cases in the youngest age group, the frequencies tended to increase. The subsequent detection of higher frequencies before the second dose may indicate that the post-dose 1 timepoint may have been sub-optimal as it may be that at the seven days timepoint following primary vaccination the GCs had not fully formed to generate high Tfh cell frequencies that could be detected in circulation. This can be explained by the finding of higher Tfh frequencies at the timepoint before the second dose, which would mainly have been generated from the first dose after optimal GC formation. The GC formation is reported to occur between 5 to 14 days after immunization in mice, and although long-term GCs have been reported, the dynamics of GC-generated cells in circulation ought to be interpreted with caution.(Martínez-Riaño et al., 2023) It was also suggested that FDCs may continuously present persistent HPV VLP antigens to GC Tfh cells to promote continuous memory B cell reactivation as a potential explanation for long-term antibody titres generated by HPV vaccination.(Schiller and Lowy, 2018b) However, it is

not known how long the HPV VLP antigens persist to support continued immune activation after vaccination.

The induction of significant increase in Tfh cell responses at 7 days after the second or third vaccination doses indicate rapid recall response from the memory generated from the first dose and second doses in the respective dose schedules. The memory Tfh cells induced from primary antigen encounter are presumed to be available to rapidly reconstitute effector cells upon subsequent antigenic challenge during which they are expanded and can be identified earlier in circulation than after primary antigen challenge.(Hale and Ahmed, 2015)

Tfh cell responses have been reported to correlate with B cell numbers and antibody responses consistent with their role in B cell activation.(Huber et al., 2020, Baumjohann et al., 2013)

The HPV type specific Tfh cell responses reported here may play a critical role in the generation of highly potent and durable antibody responses following HPV vaccination. However, there was no direct correlation observed between antigen specific Tfh cell frequencies and plasma cells induced by vaccination post dose 2 or 3. While the lack of correlation may be as a result of different dynamics in the generation and appearance in circulation between the plasma cells and Tfh cells, or may alternatively reflect the modest sample size used, this finding may raise a question as to whether the maintenance of antibody protection from HPV vaccination is dependent on GC reaction. VLP multimeric antigens are believed to be highly potent with the ability to also induce T cell-independent response inducing IgM and IgG antibody response, but this has not been investigated after HPV vaccination.(López-Macías, 2012, Zepeda-Cervantes et al., 2020) In this process during primary antigen encounter, B cells are strongly activated via intensive crosslinking of the BCR and they process and present antigens to T cells enabling immune priming and subsequent rapid reactivation following antigen re-encounter.(Crisci et al., 2012)

Before this work, only two pilot studies had evaluated Tfh cell responses after HPV vaccination using an ex vivo flow cytometry assay based on ICOS+PD-1++

phenotype.(Matsui et al., 2015, Pasmans et al., 2022). One of these studies compared immunogenicity of Cervarix and Gardasil 9 in females aged 23 to 44 years by characterising a broad range of innate and adaptive cellular responses and reported no significant Tfh cell response in both vaccine groups.(Pasmans et al., 2022) This is inconsistent with the findings from this PhD work showing that Gardasil 9 vaccination induced Tfh cell responses that were detectable in both ex vivo and in vitro stimulated PBMC.

The second study compared activation of the three Tfh cell subsets (Tfh1, Tfh2 and Tfh17) after Cervarix and Gardasil vaccination of females aged 18 to 25 years and reported that both vaccines induced activation of mainly Tfh1 subset that peaked at 7 days after the first vaccination dose and there was minimal activation of Tfh cells at 7 days following the third dose.(Matsui et al., 2015) Additionally, the study reported an increasing trend of Tfh2 cells activation in both vaccine groups and a significant activation of Tfh17 in the Cervarix group after the first dose.

The finding on the vaccines inducing mainly Tfh1 and Tfh2 tending to be high are consistent with the results from this work. However, in the current study, such responses were observed more clearly and consistently after the second or third vaccination doses across the studied age groups, a time when the previous study did not detect much response. The absence of Tfh17 response following Gardasil vaccination is consistent with the findings presented here, which may be expected since Gardasil 9 and Gardasil vaccines are similarly produced and only differ in valency. In line with the results from this PhD work, the previous study did not find a correlation between vaccine-induced Tfh cell and antibody responses at one month post the third vaccination dose. Additionally, the findings of the exploratory analysis presented here showing no changes in frequencies of total Tfh cells within the CD4 T cell population as well as the Tfh subsets within the overall Tfh cell population, the previous study did not find changes in frequencies of the Tfh cell subsets in the CD4 T cell central memory compartment after Gardasil vaccination. Notably, the previous study

reported Tfh17 responses at various timepoints after Cervarix which may again be attributable to the highly potent ASO4 adjuvant inducing the proinflammatory cytokine IL-17.

While there are considerable consistencies in the findings from the current and previous study, notable discrepancies exist. Several factors may be attributable to the differences between the current and previous studies including prior HPV exposure which may impact on vaccine-induced immunity. These may arise from the different study populations used in the studies, with the previous studies being on only women while the current study involved both children and women. Some experimental differences also exist between the studies including different flow cytometry panels and gating strategies.

Overall, immunity is reported to decline with age, with frequencies of Tfh cells in circulation like other immune components, reported to decrease with increasing age in line with expected decreasing sizes of GCs but this is studied more in ages above the scope of the data presented here.(Linterman, 2023) This study reports a higher overall frequency of ex vivo activated Tfh cells based on ICOS+PD-1++ in the younger age groups which was existent before vaccination hence seems to be more age related than vaccine-induced. The ex vivo activation detected represents the total activated Tfh cells which may include some non- HPV specific CD4 T cell by-stander activation since ICOS and PD1 are not antigen specific activation markers. Without much data available on Tfh cell responses across the age spectrum, the findings in this study may indicate that the decline in Tfh cell activity possibly starts earlier than has been documented and may need further investigation in younger age groups.

In conclusion, this chapter provides evidence for HPV vaccines generating antigen specific Tfh cell response which may play a role in the generation of vaccine-induced antibody protection. Given the multimeric nature in the assembly of HPV vaccine antigens, it will be important to investigate the presence of and extend to which BCR cross-linking may be induced by HPV vaccines. Additionally, whether this cross-linking involves IgD or IgM or both and the influence this has on subsequent generation of antibody response needs to be

investigated. This will improve on understanding on whether the potency of HPV vaccines is as a result of synergy between T cell-dependent and T cell-independent pathways.

Another important aspect to be researched on is how long the HPV VLP antigen can persist in the lymphoid tissues to facilitate continued GC reaction after vaccination and how these impacts on vaccine-induced immunity.

6. SERUM IGG ANTIBODY RESPONSES AFTER HPV VACCINATION

This short chapter discusses serum IgG antibody titres induced by Gardasil 9 vaccination and how they correlate with the cellular responses presented in chapters 4 and 5.

A comprehensive body of evidence demonstrates that HPV vaccines are highly immunogenic, generating high antibody titres that are sustained for years and protect against HPV infections and HPV associated diseases (see introduction). Based on the evidence for long-term vaccine-induced antibody titres from observational and randomised studies (Barnabas Ruanne et al., 2022, Kreimer et al., 2020), WHO recommended a single dose HPV vaccination for girls aged 9 to 14 years as the primary target.(WHO, 2022) Alongside this, the need for continued research to provide more evidence on the sustainability of the antibody titres generated from single dose HPV vaccination was highlighted.

Given the critical role played by B cells and Tfh cells in the generation of long-term vaccine protection, evaluating the relationship between these cell responses with subsequent antibody responses after vaccination is critical in understanding the cellular mechanisms driving the vaccine immunogenicity. From the studies characterising B cell and Tfh cell responses following HPV vaccination, it is not clear what roles these cell populations play in the maintenance of the long-term antibody titres after completion of vaccination schedule.(Nicoli et al., 2020c, Miller et al., 2021, Matsui et al., 2015).

The trial of Gardasil 9 HPV vaccine in which this PhD research was nested provided an opportunity not only to evaluate the magnitude of vaccine-induced antibody titres, but also to explore the relationship between the antibody titres and vaccine-induced cellular immunity which may indicate their contribution to the vaccine protection.

6.1 Aims

- i) To determine geometric mean titres (GMTs) of HPV 16 and HPV 18 specific IgG antibodies generated by Gardasil 9 vaccination of 4-8-, 9-14- and 15-26-year-olds.
- ii) To evaluate the effect of age on the magnitude of vaccine-induced IgG antibody titres.
- iii) To evaluate the correlation between vaccine-induced HPV 16 and HPV 18 specific IgG GMTs and HPV 16 and HPV 18 specific plasma cell, memory B cell and Tfh cell responses.

6.2 Results

6.2.1 HPV 16 and HPV 18 antibody titres

The antibody responses presented here were measured at baseline (just before vaccination) and at 28 days after completion of the vaccination schedule of 2 doses in 4-14-year-olds and 3 doses in 15-26-year-olds as earlier outlined in the methods chapter 2. The antibody data presented here include only those samples with matched results for plasma cells and Tfh cells (group B) or memory B cells (group C) after the second or third vaccination doses. Based on HPV being a sexually transmitted infection, there was no significant HPV specific antibody response expected from the 4-8-year-olds before vaccination, hence baseline antibody response was not measured in this age group. Baseline data is therefore presented for the two older age groups and post-vaccination data for all three age groups.

At baseline, HPV 16 and HPV 18 specific antibodies were detected at very low levels in the 9-14- and 15-26-year-olds with no significant difference between the two age groups (Table 6.1, Figure 6.1). Following vaccination, a robust antibody response was observed across the three age groups (Table 6.1, Figure 6.1) The vaccine-induced GMTs were highest in the 4-8-year-olds, followed by 9-14-year-olds and lowest in the 15-26-year-olds. Significant differences were observed between post-vaccination GMTs in the 15-26-year-olds (HPV 16: 8066; 95% CI 6210 - 10477, HPV 18: 2694; 95% CI 2036 - 3566) compared to both 4-8-

year-olds (HPV 16: 16174; 95% CI 13163 - 19874, $p = 0.0002$, HPV 18: 4317; 95% CI 33558 - 5550, $p = 0.0026$) and 9-14-year-olds (HPV 16: 13475; 95% CI 9454 - 19203, $p = 0.0055$) (Table 6.1.A & B, Figure 6.1A & B).

Table 6.1. HPV 16 and HPV 18 specific antibody titres after Gardasil 9 vaccination

A: HPV 16

Age-stratified	9 to 14 years n = 37	15 to 26 years n = 31	4 to 8 years n = 38	9 to 14 years n = 37	15 to 26 years n = 31
Sampling timepoint	Baseline	Baseline	Post-dose 2	Post-dose 2	Post-dose 3
Lower 95% CI of GMTs	13	14	13163	9454	6210
HPV 16 specific GMTs (mMU/mL)	16	19	16174	13474	8066
Upper 95% CI of GMTs	18	26	19874	19203	10477

B: HPV18

Age-stratified	9 to 14 years n = 39	15 to 26 years n = 32	4 to 8 years n = 42	9 to 14 years n = 37	15 to 26 years n = 31
Sampling timepoint	Baseline	Baseline	Post-dose 2	Post-dose 2	Post-dose 3
Lower 95% CI of GMTs	44	51	3358	2462	2036
HPV 18 specific GMTs (mMU/mL)	48	58	4317	3250	2694
Upper 95% CI of GMTs	52	66	5550	4290	3566

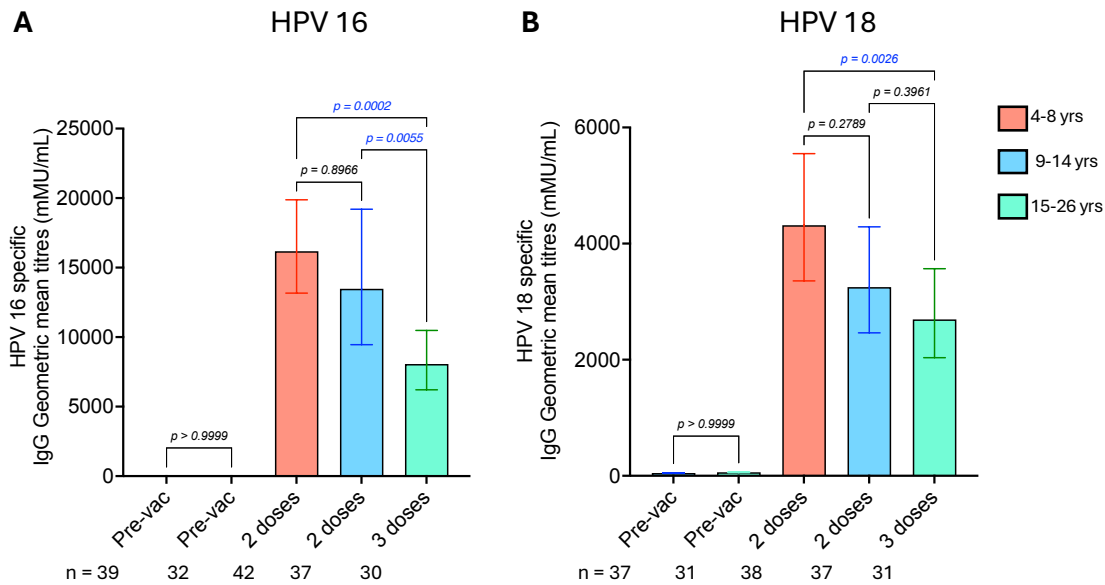


Figure 6.1. HPV 16 and HPV 18 specific antibody titres after Gardasil 9 vaccination

One way ANOVA was used to compare HPV 16 (A) and HPV 18 (B) specific IgG geometric mean titres between age groups at pre-vaccination (pre-vac) and after 2- or 3-dose vaccination schedules. The bar graphs represent geometric mean titres with 95% confidence intervals. Significant p values are shown in blue. The three age groups are shown in different colours. mMU/mL – milli-Merck units/millilitre

6.2.2 Correlations between plasma cells, memory B cells and Tfh cells with antibody titres

Pearson correlation analysis was performed between antibody titres and the cellular responses described in chapters 4 and 5.

This was performed on pooled datasets from the three age groups as they showed similar correlational distribution patterns by visual inspection. A strong positive correlation was observed between plasma cells and antibody titres (HPV 16; $r = 0.7016$, $p < 0.0001$, HPV 18; $r = 0.6184$, $p < 0.0001$) (Figure 6.2A & B). On the other hand, no significant correlation was observed between antibody titres and memory B cells (HPV 16; $r = -0.1496$, $p = 0.2948$, HPV 18; $r = -0.0031$, $p = 0.9826$) (Figure 6.2C & D), as well as Tfh cells (HPV 16; $r = -0.1291$, $p = 0.4743$, HPV 18; $r = -0.1537$, $p = 0.3930$) (Figure 6.2E & F).

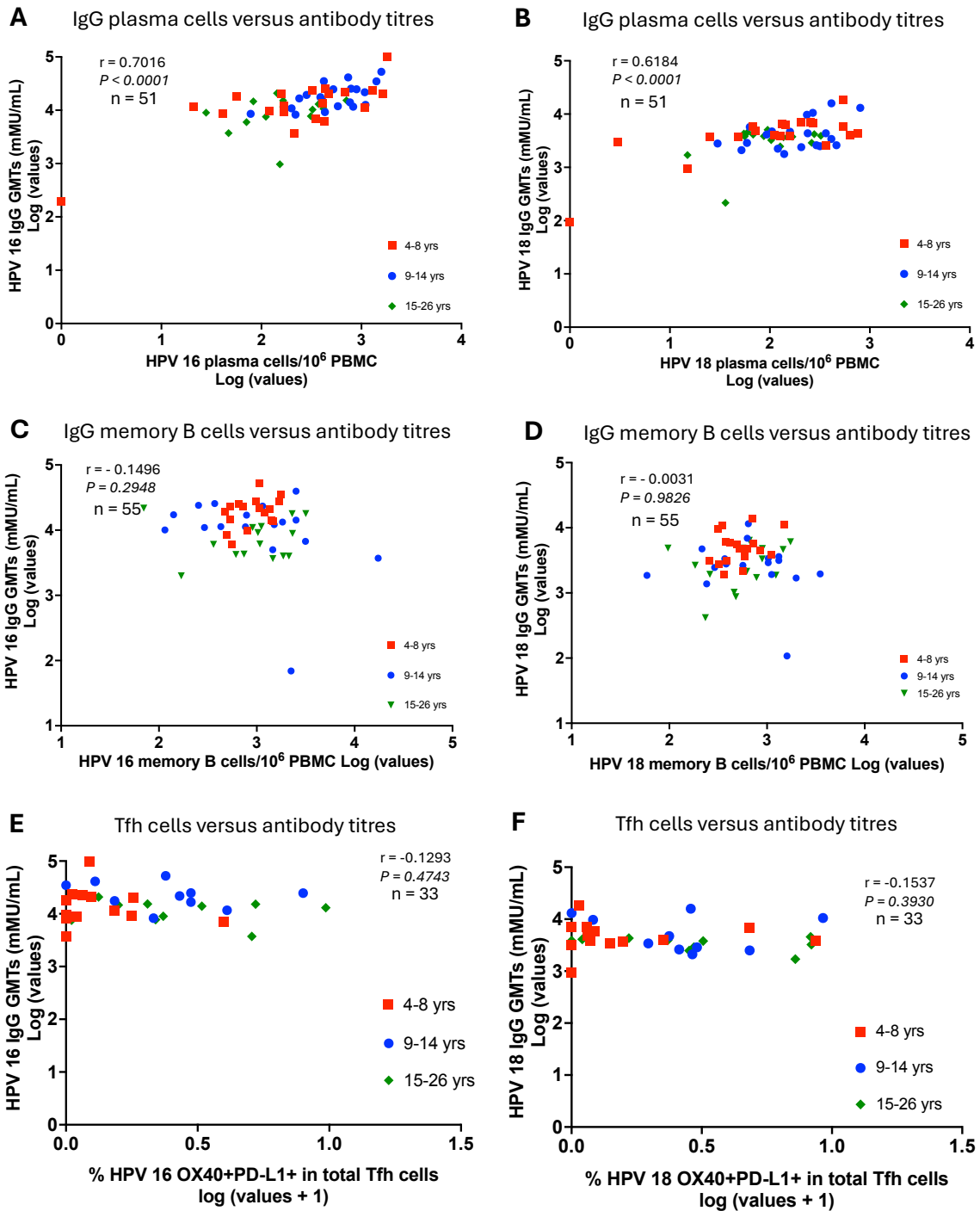


Figure 6.2. Comparisons between HPV 16 and HPV 18 specific IgG antibody titres with plasma cells, memory B cells and Tfh cells

Pearson correlation analysis was performed between HPV 16 and HPV 18 specific IgG geometric mean titres and IgG plasma cells (**A & B**), IgG memory B cells (**C & D**) and in vitro stimulated AIM OX40+PD-L1+Tfh cells (**E & F**). Plasma cells and Tfh cell frequencies were measured on the same samples at 7 days, memory B cells at 14 days and antibody titres at 28 days after completion of a two- or three-dose vaccination schedule. The 3 age groups are shown in different colours. AIM - activation induced-marker assay, GMTs - Geometric mean titres, r - Pearson correlation coefficient, p - p value

6.3 Discussion and future work

This chapter reports the induction of higher HPV 16 and HPV 18 GMTs in younger age groups than in older ones after Gardasil 9 vaccination consistent with previous studies of the same vaccine as well as other HPV vaccines.(Zhang et al., 2017, Restrepo et al., 2023) The immunogenicity of HPV vaccines in 4-8-year-olds is first reported in this study and the results indicate that the antibody titres are higher than in the ages for which the vaccine is currently recommended. This is again consistent with findings from a previous comparison of immunogenicity of the same vaccine in girls aged 9 to 12 years and 13 to 15 years showing induction of higher antibody titres in those aged 9 to 12 years, indicating the possibility of increasing immunogenicity even below these ages.(Restrepo et al., 2023)

This study also shows that vaccination dosing intervals as a key determinant of vaccine immunogenicity may need further optimisation. The longer vaccination dose intervals used in this study (0, 12 months for 4-14-year-olds and 0, 2, 12 months for 15-26-year-olds) induced higher antibody titres than the commonly used shorter intervals (0, 6 in 9-14-year-olds and 0, 2, 6 in 15-26-year-olds).(Gilca et al., 2019, Pinto et al., 2018, Bergman et al., 2019)

The only study to have compared vaccine-induced memory B cell and plasma cell responses to antibody titres shortly after HPV vaccination used a flow cytometry-based approach unlike ELISpot and FluoroSpot used in this PhD work.(Scherer et al., 2018) The study identified HPV 16 specific memory B cell and total plasma cell (blasmablast) responses and compared them with antibody titres induced by an initial three-dose schedule (0, 2, 6 months) and after a fourth booster dose of Gardasil vaccine at 24 months. The study reported an overall increasing trend of memory B cell response after the booster doses at 6- and 24-months booster doses, that inversely correlated with pre-vaccination antibody titres. The vaccination schedules evaluated in this PhD work were different from this study and given the different assays applied, and that the current work only compared post vaccination responses, the results between these studies are not directly comparable.

The robust plasma cell response reported here to correlate with corresponding high antibody titres is consistent with the role of plasma cells in antibody secretion. Following secondary or tertiary vaccination doses, in addition to proliferation of memory B cells from earlier vaccination doses, their differentiation into plasma cells contributes to the boost in plasma cell numbers which contributes to expanded antibody responses,(Stanley, 2010c) hence the positive correlation.

The absence of significant correlations between memory B cell numbers and antibody titres reported in this work although evaluated at short-term, aligns with previous studies suggesting these responses may be sustained independently since even at 4 to 6 years post-completion of three-dose vaccination schedule of Cervarix or Gardasil vaccines in females aged 12 to 20 years, no correlation was observed between memory B cell and antibody responses.(Nicoli et al., 2020a) Although it may be argued that memory B cell dynamics are different from plasma cells, if they (memory B cells) are key players in sustaining vaccine induced antibody titres, their numbers would at least be expected to positively correlate with these titres in the long-term term as has been observed from other vaccines such as smallpox, pertussis and measles.(Crotty et al., 2003, Buisman et al., 2009) Similar to this study, HBV antigen challenge of pre-vaccinated individuals induced a clear anamnestic antibody response indicative of memory B cell reactivation but there was no correlation observed between the Hepatitis B surface antigen (HBsAg) specific memory B cells and corresponding antibodies levels.(Ward et al., 2008) Additionally, observational studies on tetanus toxoid and diphtheria vaccination reported no positive correlation between antigen specific circulating memory B cells and antibody titres.(Leyendeckers et al., 1999, Amanna et al., 2007) Given that antibody titres after HPV vaccination are maintained at high levels presumed to neutralise new HPV infections before reactivation of immune memory, this may explain why the memory B cell responses do not correlate with antibody titres.(Schiller and Lowy, 2018b) Current longest follow up studies after HPV vaccination have been up to 12 years and it remains to be discovered if such antibodies will in the long-

term wane to levels where new infections may reactivate immune memory.(Kurosawa et al., 2022) It has been predicted that HPV-vaccine induced neutralising antibodies in young women may last above infection-induced levels for up to 20 years after a single vaccination dose of Cervarix and Gardasil although HPV 18 specific antibodies from Gardasil were predicted to wane to below infection-induced levels by the predicted 20 years.(Einstein et al., 2014) However, this remains to be confirmed in real life long-term studies, during which evaluation of the relationship between the antibody response and memory B cell response could be investigated to elucidate their role in the long-term protection.

There was no significant correlation observed between in vitro stimulated HPV specific Tfh cell response and the corresponding antibody response. This finding is consistent with results from a previous pilot study that compared ex vivo stimulated Tfh frequencies at 7 days with antibody responses at 30 days post-completion of three-dose vaccination schedule (0, 3, 6 months) with Cervarix or Gardasil vaccines and reported no significant correlation between these responses for either vaccine.(Matsui et al., 2015)

In conclusion, this research reports high HPV 16 and HPV 18 IgG antibody titres following Gardasil 9 vaccination and that the antibody titres positively correlated with plasma cells and did not have significant correlation with either memory B cells or Tfh cells. The vaccine-induced antibody titres increased with decreasing age as was observed for the B cell and Tfh cell responses.

The demonstration of highest vaccine immunogenicity in younger age groups than the currently targeted age groups highlight the need for investigating HPV vaccination in age groups below 9 years.

7. SINGLE CELL SORTING OF HPV 16 SPECIFIC MEMORY B CELLS AND B CELL REPERTOIRE MAPPING

7.1 Introduction

B cells recognize their specific antigens through membrane-bound receptors, BCRs which are unique to each cell and its progeny.(Janeway CA Jr, 2001b) A wide diversity of BCRs is required for recognition of the many antigens that an individual is constantly exposed to. This is achieved during the early stages of B cell development when the BCRs are formed through sequentially controlled random somatic changes of germline DNA involving recombination of the VDJ gene segments.(Janeway CA Jr, 2001b) Typical BCR is composed of two identical heavy chains (IGH) and two identical light chains which can be either kappa or lambda (IGK/L).(Dong et al., 2022) Both IGH and IGK/L consist of constant and variable regions.(Dong et al., 2022) The constant region determines the type of Ig isotype (whether IgG, IgM, IgA, IgE or IgD) produced from a B cell while the variable region has the sites for antigen recognition and binding. The IgG isotype is composed of four subclasses which occur in different concentrations in blood IgG1 (60-70%), IgG2 (20-30%), IgG3 (5-8%) and IgG4 (1-3%).(Hashira et al., 2000) IgG1 and IgG3 are described as potent triggers of effector mechanisms while IgG2 and IgG4 only induce subtle responses in certain cases.(Vidarsson et al., 2014) IgA, the major isotype secreted from mucosal surfaces is composed of two subclasses found in different frequencies in blood IgA1 (80%) and IgA2 (20%) which are associated with different mucosal immune functions.(Steffen et al., 2020)

The BCR is divided to two parts; the antibody binding fragment (Fab region) and the crystallizable fragment (Fc) that interacts with other components of the immune system including the complement and phagocytes to promote antigen removal. Figure 7.1 shows the BCR structure. The diverse range of BCRs expressed by all B cells in an individual gives their B cell repertoire.

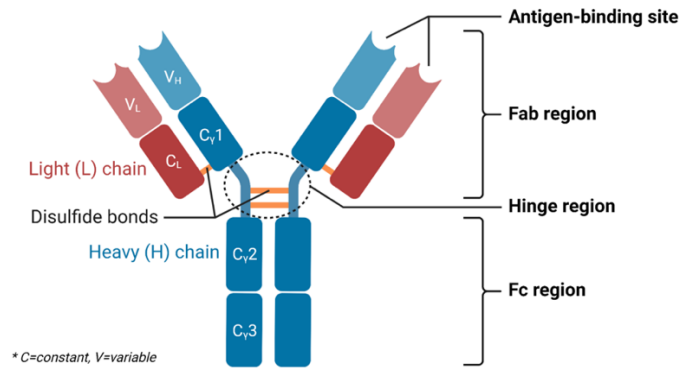


Figure 7.1. B cell receptor structure

(Biorender templates - Biorender.com)

B cell development in the bone marrow takes place through several stages from the stem cell, early pro-B cell, late pro-B cell, large pre-B cell, small pre-B cell, immature B cell and mature B cell during which the BCR is assembled as outlined. (Figure 7.2). The IGH chain is assembled from the V, D and J segments locus on the long arm of chromosome 14 while IGK/L are assembled from V and J segments locus on the short arm of chromosome 2 and 22 respectively. This process is regulated by recombination activating genes (RAGs 1/2) enzymes. The V, D and J sequences contain multiple open reading frames (44, 25 and 6 for V, D and J, respectively) used to encode for IGH. (Li et al., 2004) Since B cells cannot use all these segments at once, only one VDJ (containing one of V, D and J) segment is selected to form a particular exon for completion of BCR assembly. Coupling of the variable regions determining specific antigen recognition with relatively conserved framework regions leads to formation of complete IGH variable region.

There are three complementarity determining regions (CDRs) named CDR1, CDR2 and CDR3 that are coded within the IGH and IGK/L chains. The CDR regions form loops on the antigen binding sites. (Polonelli et al., 2008) Each of the IGH and IGK/L chains contains three of the CDRs making a total of two sets of 6 identical CDRs per BCR. Therefore, there are a total of 6 CDRs on each of the two antigen binding sites located on the two different polypeptide chains of a BCR and these can collectively encounter the antigen. IgA exist as a

dimer and IgM a pentamer while the other isotypes are monomers, hence multimeric isotypes have more than 12 CDRs which contribute to collective affinity of all antigen-binding sites resulting to increased avidity.(Janeway CA Jr, 2001a)

Most sequence variation in BCRs are found within the CDRs, causing them to be referred to as hypervariable regions. Within the variable domain, CDR1 and CDR2 are found in the V region of a polypeptide chain, and CDR3 contains some of V, all of D and J regions. CDR1 and CDR2 are generated from the germline while somatic recombination generates diversification in CDR3. It is this diversification that ultimately gives antibodies their specificity, and ability to recognize antigens.(Gabrielli et al., 2009) The overall diversity of BCRs generated during B cell development has been predicted to be more than 10^{18} BCRs.(Elhanati et al., 2015)

Interaction between the BCR and antigen is dependent on CDR3 amino acid residues and overall length. The location of amino acid residues in particular positions of a CDR loop define the conformations of the antigen binding loops.(Gabrielli et al., 2009, Chiu et al., 2019) Several studies have shown that the length of a given CDR can have a profound effect on its shape with differences of as little as one amino acid being able to change the overall structure significantly.(Chothia et al., 1989) The CDR3 amino acid length can be affected by SHM that predominantly takes place in this region and can subsequently affect the ability of the antibody to bind to their specific antigens. IGH CDR3 variability in length and amino acid content has been described to be sufficient for most antigen specificities while CDR1 and CDR2 were found to be much more cross-reactive.(Xu and Davis, 2000) Many studies on B cell repertoire mostly characterise CDR3 in detail owing to its key role in determining antigen specificity.

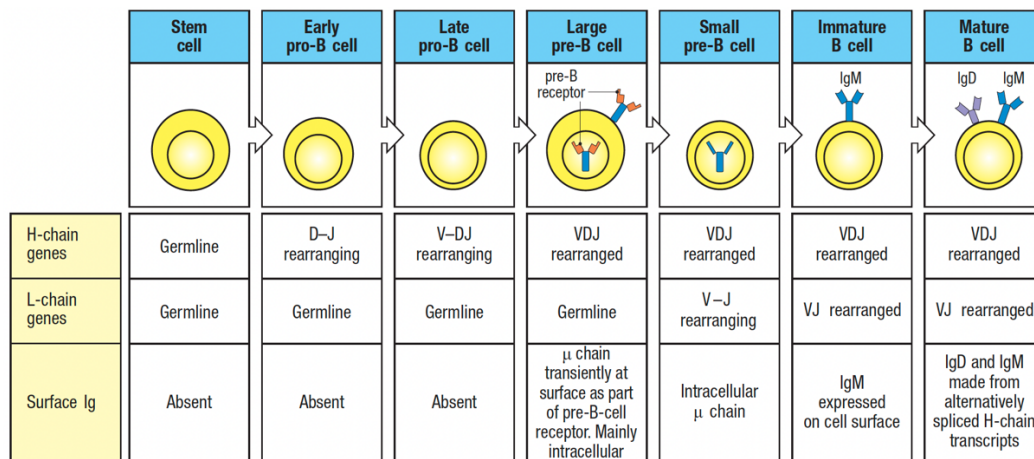


Figure 7.2. VDJ recombination during B cell development stages

The different stages of rearrangement of variable (V), diversity (D) and junctional (J) genes on the heavy (H) and light (L) chains during B cell development are shown.

(Janeway CA Jr, 2001a)

Random deletion or insertion of nucleotides in segment junctions may also contribute to the final BCR diversity.(Hoehn et al., 2016) After successful assembly of complete BCR, the mature naïve B cells leave the bone marrow to localise mainly in primary lymphoid follicles in lymph nodes, spleen and mucosa-associated lymphoid tissue.(Abramson et al., 2020) Upon encountering different antigens, B cell activation and differentiation leads to generation of subclones with specificity to each antigen.

Further BCR diversification takes place because of class-switch recombination and SHM in GCs.(Maul and Gearhart, 2010) SHM is a complex process tightly regulated and coordinated by the AID enzyme (Maul and Gearhart, 2010) While isotype switching causes changes in the IGH constant region facilitating production of multiple Igs with specific functions such as IgM, IgG1, IgG2, IgG3, IgG4, IgA1, IgA2, IgD, and IgE , the SHM process alters the BCR sequence on both constant and variable regions of IGH and IGK/L. It is estimated that SHM can cause increased mutation rate in the variable regions to approximately one mutation per B cell subclone in the relevant locus.(Victora and Nussenzweig, 2012b, Teng and Papavasiliou, 2007) SHM is critical for specificity and affinity maturation allowing the immune system to recognize and respond to different antigens appropriately. Antigens

activate B cell signalling pathways that induce antibody-mediated immunity of varying magnitudes, quality, and durability. Out of the billions of B cells in the immune repertoire, very small fractions, mainly memory B cells have affinity-matured for antigens that an individual has been exposed to.(Hoven et al., 1989, Hayakawa et al., 1987, Franz et al., 2011) The detectable frequency of such affinity matured B cells, even after a robust immune reaction, has been reported to be in the range of 0.01 to 0.1% of total B cells.(Hoven et al., 1989, Hayakawa et al., 1987, Franz et al., 2011)

Many factors determine the magnitude, quality and longevity of vaccine-induced antibody-mediated immunity ranging from the vaccine characteristics, host and environmental characteristics.(Zimmermann and Curtis, 2019) The mechanisms of vaccine action can be characterised from different levels of host immune activation.(Laszlofy et al., 2024) B cells, the direct source of antibodies, play an extremely important role in vaccine protection. Mechanisms of B cell immunity can be studied at different levels such as evaluating frequencies of activated B cells as discussed in chapter 4 of this work or at molecular single cell precision discussed in this chapter. Single cell sorting and repertoire mapping of antigen specific memory B cells has been used to broaden understanding of B cell memory to vaccine antigens or natural infections.(Zheng et al., 2022, Setliff et al., 2019)

Antigen specific B cell repertoire mapping involves isolation of B cells that specifically bind to a particular antigen and sequencing of their paired IGH and IGK/L chains. The sequence data is evaluated for molecular level changes that may be attributable to specificity for different antigens.(Zheng et al., 2022, Setliff et al., 2019)

To characterise HPV 16 specific B cell repertoire, this chapter first describes the optimisation, validation and application of a single cell sorting assay using fluorescently labelled HPV 16 pseudovirions as previously described.(Scherer et al., 2018) It then describes the B cell repertoire mapping of the singly sorted HPV 16 specific memory B cells using the Arm iPair technology (iRepertoire Inc.).

7.2 Aims

- i) To immunophenotypically identify and sort single HPV 16 specific memory B cells after Gardasil 9 vaccination.
- ii) To sequence the paired IGH and IGK/L chains on the BCRs of sorted HPV 16 specific memory B cells.
- iii) To evaluate IGH and IGK/L gene usage from HPV 16 specific memory B cells.

7.3 Results

7.3.1 Titration of HPV 16-AF488 and HPV 18-AF647 VLP

The protocol used here for identification and single cell sorting of HPV 16 specific memory B cells utilized a fluorescently labelled HPV 16 pseudovirions as previously described.(Scherer et al., 2014a, Scherer et al., 2018) The initial aim was to characterise both HPV 16 and HPV 18 specific memory B cells. The first optimisation steps involved titrating the fluorescently labelled pseudovirions (HPV 16-AF488 and HPV 18-AF647) on frozen PBMC samples collected at baseline and at 14 days after Gardasil 9 vaccination of one study participant in the 15-26-year-olds age group. The flow cytometry results were compared to ELISpot results measuring the same antigen specific memory B cell responses on the same sample (Figure 7.3A). Titrating the antigens in this sample allowed for optimisation of the assay on the actual samples to be analysed in the study. Additionally, testing the antigens on pre- and post-vaccination samples in the first instance allowed for assessment of their binding specificity since low frequencies of HPV 16 and HPV 18 specific memory B cells were observed at baseline and were expanded after vaccination (Figure 7.3A).

Three dilutions (1:40, 1:20 and 1:10) of the pseudovirions were tested based on previous studies using the same protocol. PBMC staining for identification of memory B cells was performed following the procedures described in chapter 2. The antibodies used in this memory B cell panel had been titrated in the plasma cell panel as earlier described in chapter 4 except the anti-human CD27-BV421 which was titrated separately for this panel.

A dump channel was used to exclude CD3+ T cells, CD14+ monocytes and dead cells. The staining/binding frequencies from titration of the two HPV types were assessed in the CD19+CD38-/lowCD27+ B memory B cell population (Figure 7.3B). The results showed minimal (0.01%) HPV 16 staining at baseline which did not change across the three dilutions used (Figure 7.3C). Post-vaccination, HPV 16 staining frequency (0.01%) at a dilution of 1:40 was similar to that observed at baseline and increased with the decreasing pseudovirion dilution to 0.03% at 1:20 and 0.04% at 1:10 (Figure 7.3D). HPV 18 binding frequencies across the three dilutions were higher (above 1.00% of total memory B cells) than expected from the ELISpot results with no clear expansion observed post-vaccination (Figure 7.3C & D). Further testing of lower HPV18-AF647 dilutions did not improve its binding specificity.

The frequencies of HPV 16 staining at baseline and their expansion post-vaccination were comparable to the ELISpot results. The variations observed could be attributable to different sensitivities of the assays. On the other hand, the HPV 18 staining was indicative of non-specific binding and was therefore excluded from the panel and subsequent analyses were performed for HPV 16.

A HPV specific memory B cells by ELISpot

Participant 1460Z	% of HPV specific cells in total IgG memory B cells	
HPV type	Baseline	Post-dose 3
HPV 16	0.03	0.06
HPV 18	0.01	0.03

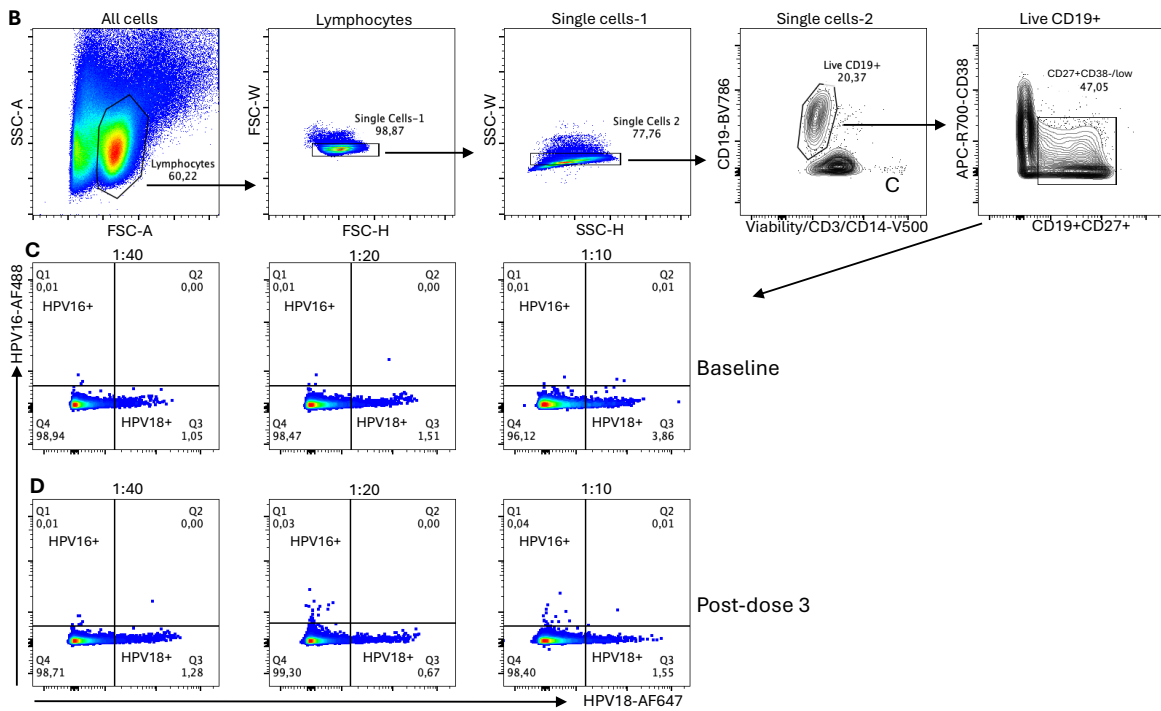


Figure 7.3. Titration of HPV 16-AF488 and HPV 18-AF647 VLP

PBMC were isolated from a study participant (1460Z) at baseline and at 14 days post-dose 3 of Gardasil 9. HPV 16 and HPV 18 specific and total IgG memory B cells (MBC) at these timepoints were enumerated by ELISpot. The antigen specific cells were expressed as percentages of total IgG (**A**). Some of the PBMC from the same timepoints were frozen and later stained with a B cell antibody panel containing three dilutions (1:40, 1:20 and 1:10) of HPV16-AF488 and HPV18-AF647 pseudovirions. Data was acquired on LSR Fortessa III. Gating was first performed for lymphocytes and single cells. CD3+ T cells, CD14+ monocytes and dead cells were then excluded in a dump channel and B cells identified as CD3-CD14-CD19+. Total MBC were identified as CD27+CD38+/low (**B**). HPV16+ and HPV18+ cells from each dilution were identified from the total memory B cells identified at baseline (**C**) and post-dose 3 (**D**) samples.

7.3.2 Confirmation of HPV 16+ memory B cell staining on fresh PBMC

The titration of HPV antigens was performed on frozen PBMC as the ideal sample for which the assay was being optimised. However, due to limited cell numbers from the study participants, although an expansion in HPV 16 staining was observed post-vaccination, there were few events in the antigen specific population. Further confirmation of the antigen specific staining using the complete panel was performed on freshly isolated PBMC from a donor who had received Gardasil 9 vaccine. An antigen dilution of 1:10 selected from the titration results was used in this experiment. Compared to the prior analysed frozen PBMC, more freshly isolated PBMC were available for staining allowing confident conclusions to be drawn from acquisition of more antigen specific events. Frequencies of IgG+IgM- and IgM+IgG- in the antigen specific population would be identified using the complete panel, hence, more antigen specific events allowed for identification of realistic frequencies for the fewer Ig events expected upon downstream gating from the total pool of antigen specific memory B cells.

The staining was performed (as described in chapter 2) on pre- and 13 days post-dose 3 PBMC samples. Flow cytometry gating for identification of HPV 16 specific frequencies in the total CD19+CD38-/lowCD27+ memory B cell population was performed as described for the frozen PBMC from which the IgG+IgM- and IgM+IgG- cell frequencies were identified.

The results showed almost no realistic detectable HPV 16+ memory B cells pre-dose 3 (Figure 7.4A) while post-dose 3, the frequency of HPV 16+ cells was expanded to 0.07% of the total CD19+CD38-/lowCD27+ memory B cell population (Figure 7.4B). Majority of the HPV 16+ cells were IgG+IgM- (64.55%) and IgM+IgG- cells were 20.91%. Within the HPV 16 specific memory B cell pool, a population of cells expressing neither IgG nor IgM was identified to be expanded by vaccination. Although not further characterised, these may represent IgA+ memory B cells which are of relevance and warrants further investigation given the primary mucosal route of HPV infection.

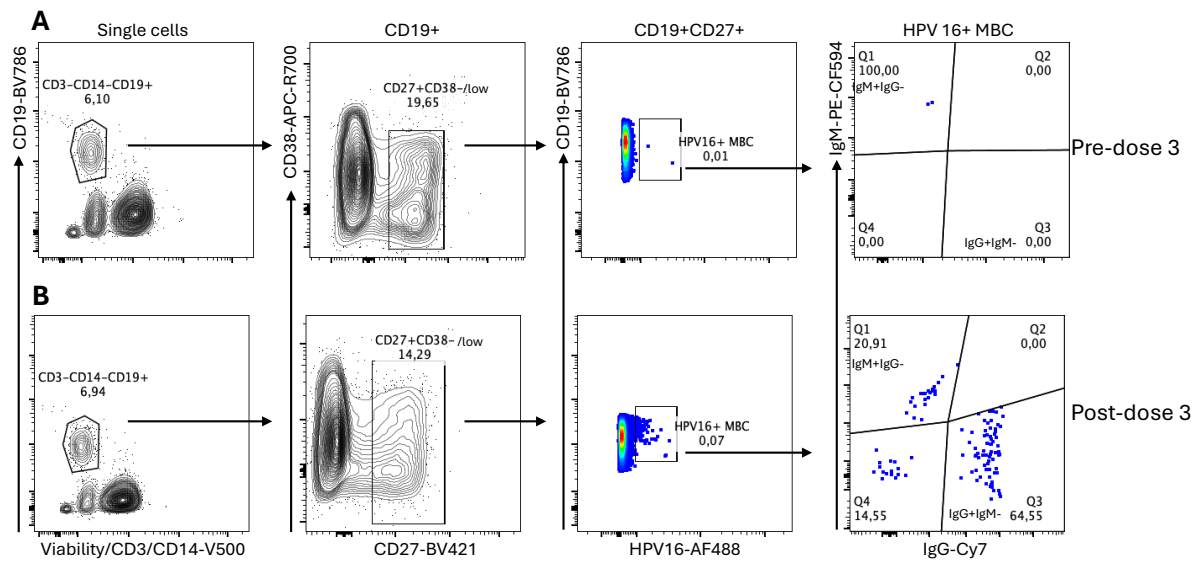


Figure 7.4. HPV 16+ memory B cell frequency on fresh PBMC before and after Gardasil 9 vaccination

Freshly isolated PBMC from a single donor just before (A) and 13 days after dose 3 (B) of Gardasil 9 was stained for identification of HPV 16 specific memory B cells (MBC) and data acquired on LSR Fortessa III. Gating was first done on lymphocytes and single cells. CD3+ T cells, CD14+ monocytes and dead cells were then excluded in a dump channel and B cells identified as CD3-CD14-CD19+. Total MBC were identified as CD27+CD38+/low from which the antigen specific cells were identified as HPV 16+. IgG+IgM- and IgM+IgG- cells were identified from the HPV 16+ population.

7.3.3 Confirmation of HPV 16+ memory B cells staining in young age groups

Following confirmation of HPV 16+ memory B cell staining on fresh PBMC, further testing was performed on frozen PBMC from one participant in the younger age group (9-14-year-olds). Identification of HPV 16+ memory B cells from baseline and post-dose 2 samples was performed as earlier described. The frequency of HPV 16+ cells at baseline and post-dose 2 were 0.06% and 0.15% of the total memory B cells, respectively (Figure 7.5A & B). About 91% of the antigen specific cells identified at baseline were IgM+IgG- and no IgG+IgM- cells were identified. On the other hand, the HPV 16+ cells identified post-vaccination were mainly comprised of IgG+IgM- (67.92%) and IgM+IgG- (22.64%) (Figure 7.5A & B).

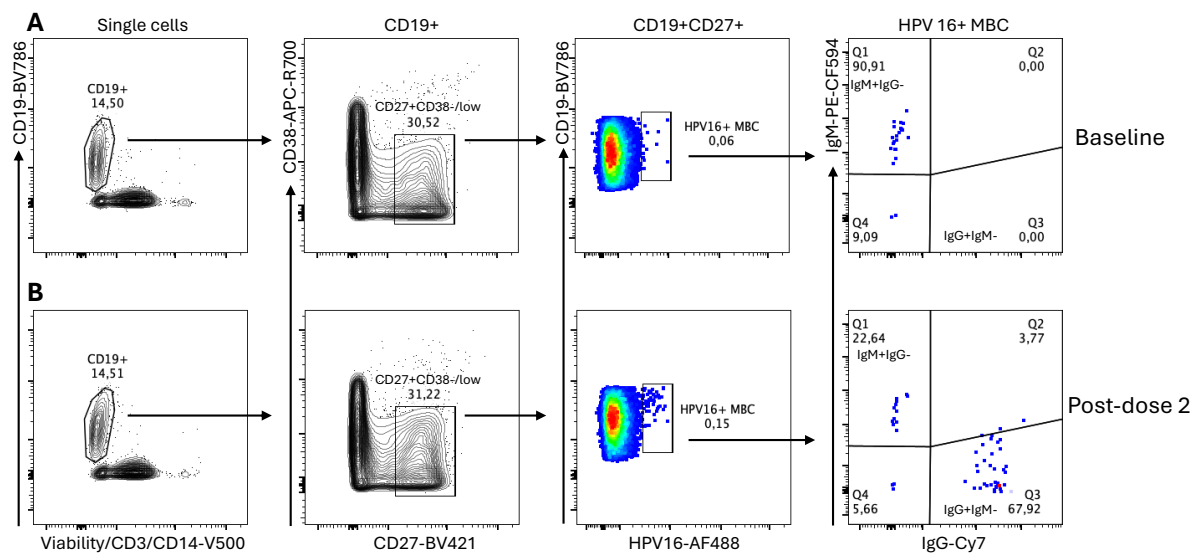


Figure 7.5. HPV 16+ frequencies before and after Gardasil 9 vaccination

Frozen PBMC isolated from one participant in the 9-14-year-olds group at baseline (**A**) and 14 days post-dose 2 (**B**) of Gardasil 9 was thawed and stained for identification of HPV 16 specific memory B cells (MBC). Data was acquired on LSR Fortessa III. Gating was first done on lymphocytes and single cells. CD3+ T cells, CD14+ monocytes and dead cells were then excluded in a dump channel and B cells identified as CD3-CD14-CD19+. Total MBC were identified as CD27+CD38+/low from which the antigen specific cells were identified as HPV 16+. IgG+IgM- and IgM+IgG- cells were identified from the HPV 16+ population.

Having successfully optimised the staining procedure for identification of HPV 16+ memory B cells, the next step was to optimise the FACS Melody cell sorting parameters to ensure healthy viable cells are sorted for subsequent sequencing analysis.

Important parameters to be considered for any cell sorting experiment include: sort nozzle size, flow rate, threshold rate and yield calculations. Substantial optimisation is critical for any sort experiment, especially index sorting into a plate that involve many steps where cells can be lost leading to low yields.(Higdon et al., 2019)

The FACS Melody used in this work has a standard sort nozzle size of 100 μm which was appropriate for sorting B cells. Appropriate flow rate determines the sample pressure which is crucial to minimise the impact of shear forces on the cells and increases viability. A low flow rate on adequately diluted cells balances the threshold and increases sorting efficiency. If cells are sorted to be analysed on a later time, they need to be frozen immediately to keep them viable. The sample dilution and flow rates needed be adjusted to allow a threshold of 1000 cells per second in the sorting experiments. However, yield estimations based on the very low frequencies of HPV 16+ memory B cells previously observed indicated that very large volume (10 to 15 mL) of stained PBMC would be required for a yield of a single complete plate of single antigen specific cells. This would require 1-3 hours to sort a single plate, a prolonged time during which many sorted cells may die and increase the risk of contamination from non-B cell subsets within PBMC. A two-step flow cytometry cell sorting approach was assessed; first bulk sorting of the total CD19+ B cells from which antigen specific memory B cells would be singly sorted in the second step. This approach resulted to longer overall sorting time and lower yields since more cells were lost at the two sorting steps.

To minimise the time required for single cell sorting, increase sort yield and allow for faster freezing of the sorted cells to maintain their integrity, B cell enrichment prior to single cell sorting of antigen specific memory B cells was considered as discussed next.

7.3.4 B cell enrichment using magnetic activated cell sorting and staining

B cells were thawed in complete culture medium at 37°C, counted and enriched for B cells by negative B cell selection on magnetic activated cell sorting (MACS) Kit II (Miltenyi Biotec, Inc.) following manufacturer's instructions. To isolate the B cells, non-B cells (T cells, NK cells, monocytes, dendritic cells, granulocytes, platelets, and erythroid cells) were labelled with a cocktail of biotinylated CD2, CD14, CD16, CD36, CD43 and CD235a (glycophorin A) antibodies. These cells were subsequently magnetically labelled with anti-Biotin microbeads. The unstained B cells were then obtained by magnetic depletion of the labelled non-B cells using MACS columns capable of separating materials 30 µm in size (Miltenyi Biotec). The B cells were washed through the columns into a sterile tube and counted to confirm sufficient cells were recovered for staining. The columns were removed from the magnetic field and the stained non-B cells washed into a separate tube. Enriched B cells, non-B cells and PBMC were washed and resuspended in PBS before staining using the dump channel and anti-CD19 antibody to identify live CD3-CD14-CD19+ B cell frequencies in the three samples. This would confirm the purity of isolated B cells as well as assess B cell loss in non-B cells. Following gating, the live CD3-CD14-CD19+ B cells were enriched from 13.8% in PBMC to 88.7% and only 0.88% was detected in the non-B cell depleted cells (Figure 7.6).

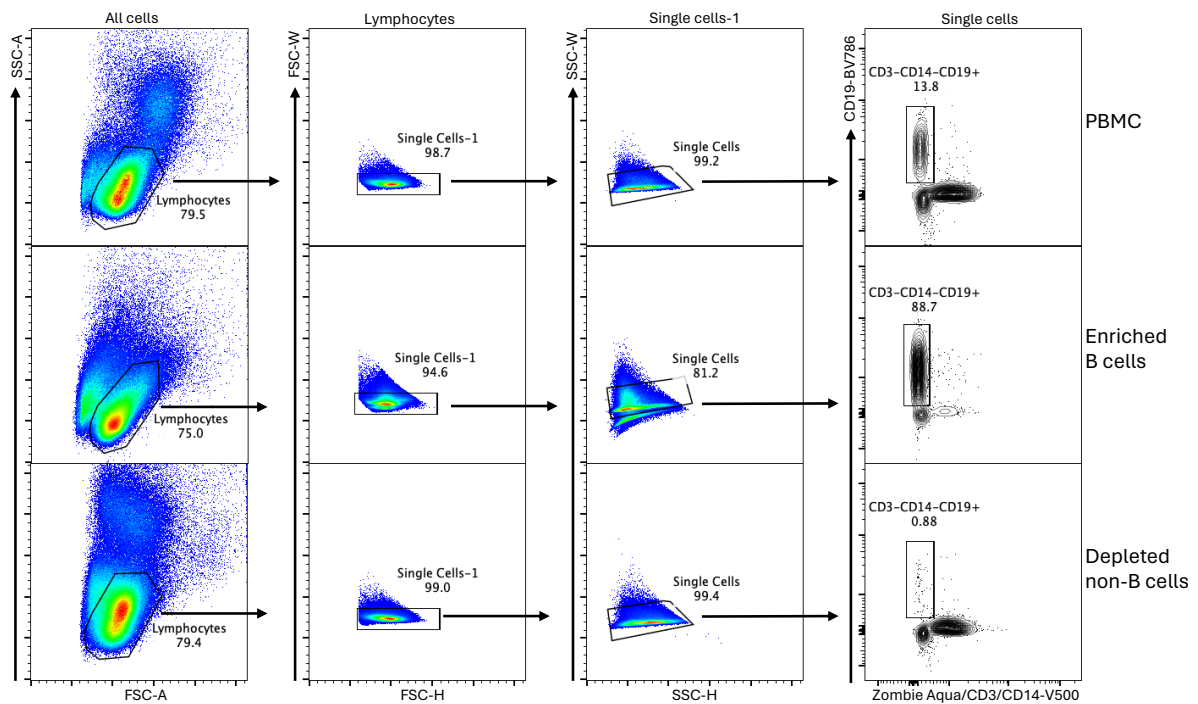


Figure 7.6. B cell frequencies after enrichment by magnetic activated cell sorting

B cells were isolated from fresh PBMC by magnetic activated cell sorting (MACS) negative selection. The enriched B cells and MACS-depleted non-B cells were stained alongside total PBMC to exclude CD3+ T cells, CD14+ monocytes and identify CD19+ B cells. Data was acquired on LSR Fortessa III and gating was first performed to identify lymphocytes and single cells from which live B cells were identified as CD3-CD14-CD19+.

7.3.5 Validation of single sorting on FACS Melody

Before applying the optimised B cell staining assay to sort antigen HPV 16+ memory B cells, single cell sorting on the FACS Melody (BD Biosciences) was validated by sorting a Raji B cell Lymphoma cell line into a 96-well iCapture plate (iRepertoire, Inc.), specially treated for dry capture of cells. For this, frozen Raji cells were thawed and stained for viability with Zombie Aqua-V500 dye. The live Raji cells were identified by acquisition on the FACS Melody cell sorter (Figure 7.7A) and singly sorted into a 96-well cell capture plate which was shipped for commercial validation testing at iRepertoire, Inc. The validation test performed uses iPair arm-PCR-amplification technology which applies primer mixes targeting the V-gene and C-gene sequences in the human BCR chains. PCR-amplification success is checked using an agarose gel and image. For successful single cell sorting, a particular

pattern of the expected band size (500/517 base pairs) from amplification of the targeted IGH and IGK/L chain sequences should be observed on the gel image (Figure 7.7B) in at least 80% of the amplified wells. Any deviance from that pattern may indicate issues with plating or problems with the cells themselves. The validation results from iRepertoire, Inc showed successful iPair amplification with 81.25% (78/96) of the tested wells showing expected band size (Figure 7.7C).

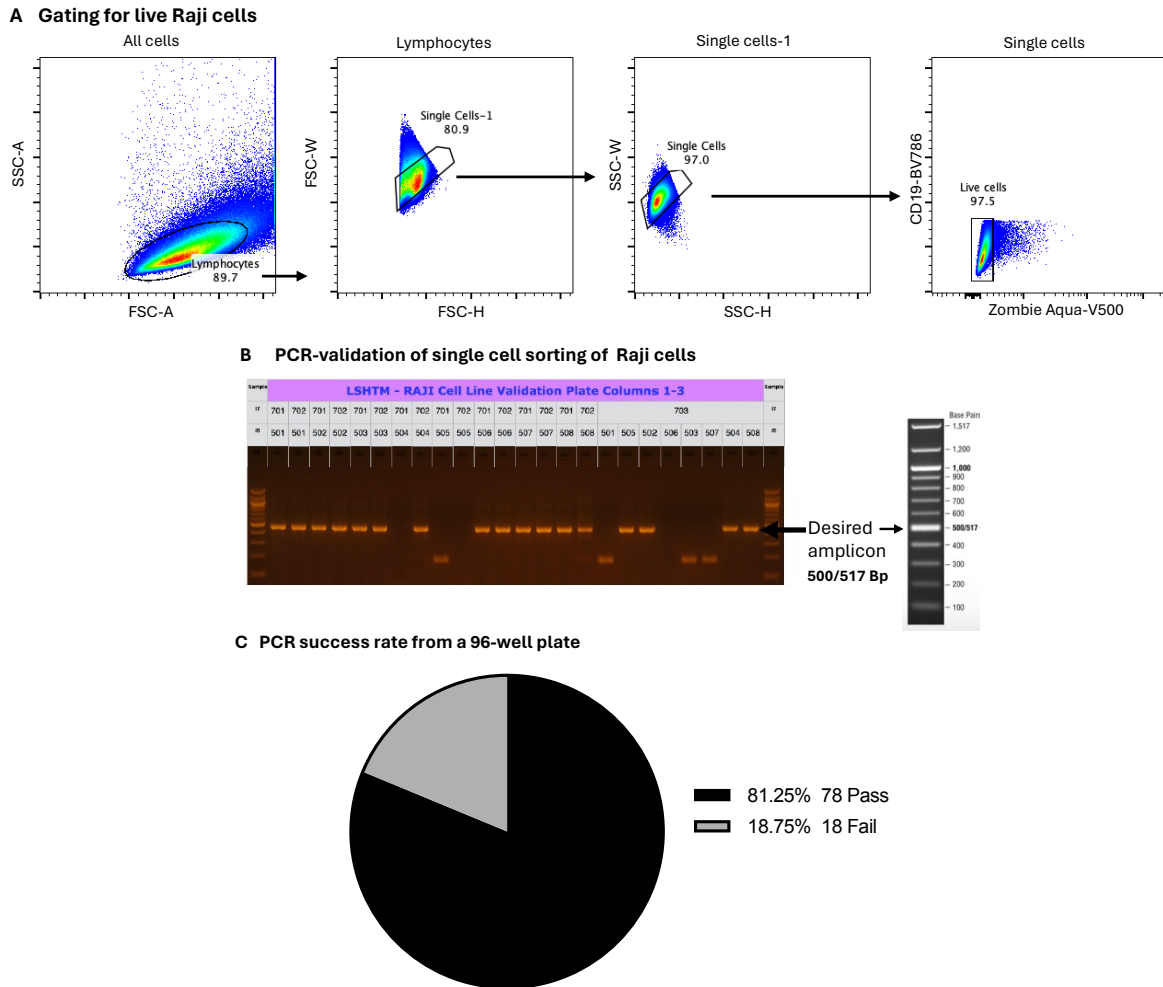


Figure 7.7. Validation of single cell sorting of Raji cell line by iPair arm-PCR-amplification

Frozen Raji cells were thawed and stained with viability dye. Data was acquired on FACS Melody. Single live Raji cells were identified from the lymphocytes single cell gate (A) and singly sorted into a 96-well cell capture plate. The single cell sorting validation testing was commercially performed by iRepertoire, Inc based on the success rate of a PCR amplification targeting paired heavy and light chain sequences on the BCR in each well. The PCR test is expected to yield about 500/517 base pairs amplicon as represented by results from one row of the 96-well plate tested (B). The PCR success rate is represented in a pie chart as a percentage of the total wells tested (C). (iRepertoire, Inc)

7.3.6 Single cell sorting of HPV 16+IgG+ memory B cells for B cell repertoire mapping

After successful validation of single cell sorting of Raji cell line, the protocol was applied to identify and sort HPV 16+ memory B cells from B cells isolated from frozen PBMC of a donor whose fresh PBMC had been stained for HPV 16+ memory B cells (fresh PBMC staining earlier shown in Figure 7.4).

It had been observed from the earlier experiments on fresh PBMC that this donor had mainly HPV 16+IgG+ memory B cells after a third dose of Gardasil 9. The staining panel was improved by replacing anti-CD38-APC-R700 antibody with anti-human IgD-R718. The fluorochromes APC-R700 and R718 are detectable on the same channel and gating on IgD negative cells would further refine identification of the memory B cell population by pre-excluding naïve B cells. The target antigen-specific memory B cell population was thus identified as CD27+IgD-HPV 16+ in the CD19+ subset after excluding dead cells and any residual CD3+ T cells and CD14+ monocytes. HPV 16+ memory B cells were identified post-dose 3 at a frequency of 0.08% in the total memory B cell pool (Figure 7.8A). The identified HPV 16+ cells were mainly IgG+IgM- (71.66%) while the frequency of IgM+IgG- in HPV 16+ cells was 8.02%. (Figure 7.8A)

The differences observed between the analysis of fresh and frozen PBMC from the same donor may be attributable to changes that were made in the antibody panel used. The analysis of fresh PBMC identified the memory B cell population based on CD38 and CD27 markers while the latter utilised CD38 and IgD. Both isolation of B cells before staining and use of IgD in identifying memory B cells could have led to better exclusion of contaminating non-memory B cells.

HPV 16+IgG+IgM- memory B cells were sorted into two 96-well plates, one at 75 and the other at 25 sort rates to assess the effect of flow rate on the subsequent analysis of the sorted cells. Sorted cells were kept on ice and quickly transferred to -80°C prior to shipping and sequencing using the arm-iPair technology by iRepertoire, Inc. The percentage cell sorting efficiency, calculated as the actual number of sorted HPV 16+IgG+ memory B cell divided by the number of total identified HPV 16+IgG+ memory B cells on the sort gate and multiplying by 100 was estimated to be 43%.

The sorting of only HPV 16+IgG+IgM- cells would allow assessment of the sorting purity since no other isotypes would be expected to be detected in the sequence data.

7.3.7 PCR-amplification of B cell heavy and light chains of HPV 16 specific memory B cells

The iPair technology uses a mixture of arm-iPair primers that flank V, D, J regions and a small sequence on the C region enough to infer Ig isotypes. For single B cell analysis, iPair captures the physically paired BCR heavy and light chains. Cells sorted from the control sample were tested in two 96-well plates sorted at different sort rates. This would allow for evaluation of the effect of sort rate on the quality of sorted cells and subsequent sequencing analysis. Arm-PCR using multiplex primers (iRepertoire, Inc.) was performed to amplify naturally paired IGH and IGK/L chains from each well and gel electrophoresis was used to verify the presence of expected amplicon size (Figure 7.8B). (See appendix 11 for complete gel image verification of both plates). The first plate, sorted at a sort rate of 75 had a PCR pass rate of 80.21% (71/96 wells) (Figure 7.8C) while the second one sorted at a sort rate of 25 had a PCR pass rate of 82.11% (73/95 wells) (Figure 7.8D). One well in plate 2 was reported to have been lost during shipment of the samples to the analysis lab. Overall PCR pass rate for both plates was 81.2% (155/191) (Figure 7.8E). These results were similar to those obtained from the sorter validation where single cells were sorted from Raji cell line and had a PCR pass rate of 81.25% (earlier shown in Figure 7.7).

The PCR step checks integrity of the sorted cells, hence, to ensure that reliable sequence data is generated downstream, the PCR pass rate is expected to be high (about 80%) as earlier indicated at the validation stage.

After PCR-confirmation of successfully sorted B cells, the paired IGH and IGK/L chains were sequenced from the wells that passed the PCR check as described next.

7.3.8 Sequencing of naturally paired B cell heavy and light chains

The successful PCR-verified amplicons were pooled and sequenced using Illumina MiSeq Reagent Nano Kit v2 (500-cycle) for mapping of the IGH and IGK/L repertoire as described previously.(Zhang et al., 2022, Niu et al., 2020) High quality sequences were generated with 91.2% of all reads having quality scores (Q) above 30 (91.2% \geq Q30), most of which were between Q35 and Q40 (Figure 7.9A). Q scores measure the likelihood of accurate base calling during the sequencing run and are a metric used to assess the quality of sequenced DNA sequences. A minimum of Q30 score which indicates 1:1000 chance of incorporating an inaccurate base (99.9% accuracy) is recommended from Illumina MiSeq DNA sequencing.(Illumina)

The sequence data was analysed using iPair Analyzer software which utilizes a pipeline optimised for filtering of the raw sequence data, sequence annotation by alignment to the international ImMunoGeneTics information system (IMGT) (<https://www.imgt.org/>) and computation of the various sequence components for downstream use and additional comparisons in other software. iPair Analyzer can be used to visualize data for each single cell position on the 96-well plate. A general view of the data on iPair Analyzer clearly shows IGH and IGK/L pairing in the analysed wells as shown for plates 1 and 2 analysed in this control experiment (Figure 7.9B & C).

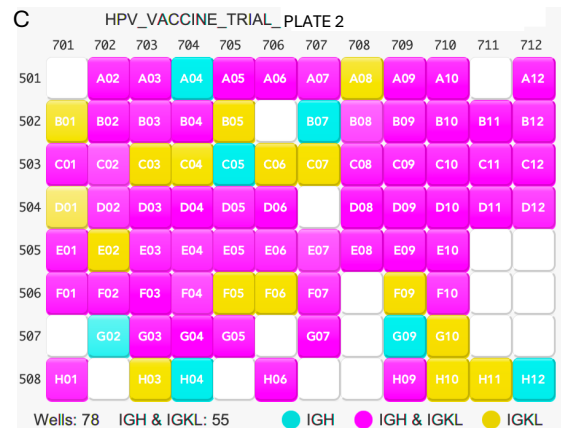
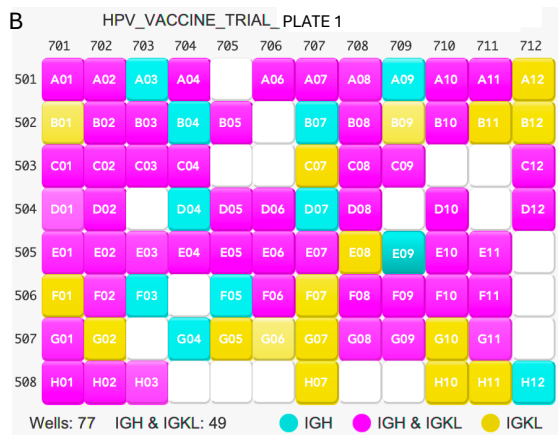
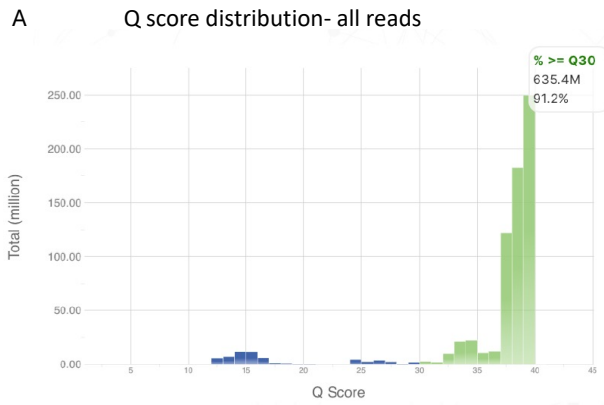


Figure 7.9. Sequence quality distribution, heavy (IGH) and light chain (IGK/L) pairing on plates 1 and 2

Wells containing paired or unpaired sequences are colour-coded and corresponding well counts shown below each plate. The non-coloured wells are those that had failed PCR amplification and were not sequenced.

The exported spread sheet contains sequence information on the various gene segments on the IGH and IGK/L chains as shown by results for 6 wells from plate 1 as an example (Table 7.1A & B).

Table 7.1. Examples of sequence data for IGH and IGK/L chains from iPair analyzer software

A IGH chain sequence

Well position	Copy number	V gene	J gene	C region (isotype)	CDR1 Peptide	CDR2 Peptide	CDR3 Peptide	CDR3 Nucleotide
A01	4600	IGHV3-21*01	IGHJ6*02	IGHG1-2	GFTFSSYT	ISSSSTDI	ARDDSRVVVAATPMYYFVGM DV	GCGAGAGATGATTTCGCGCGTAGTGGTGGTAGCTGCTACCCC GATGTACTACTACTTCGGTATGGACGTC
A02	1317	IGHV3-30*20	IGHJ6*02	IGHG1-2	GFSFSTYG	VSFDGSHK	ARDTQPNRHKTSRFLESTVGNYYNAMDV	GCGAGAGATACCCAACCGAACCGTCACAAGACGTCACGATTTT TGGAGTCGACAGTGGGCAACTACTACAACGCTATGGACGTC
A04	5839	IGHV3-66*01	IGHJ4*02	IGHG1-2	GFTVSTNY	LYSGGRT	TGVIIYESRGNFYFDY	ACTGGAGTGATTTATTATGAGAGTCGTGGTTATAATTATTTGA CTAC
A06	5029	IGHV1-2*02	IGHJ4*02	IGHG1-2	GYTFTGY	IDPHSGGT	ARPRVATILDY	GCGAGGCCCGTGTGGCTACAATCCTTGACTAC
A10	4781	IGHV4-30-2*06	IGHJ4*02	IGHG3-4	GGSISSGGYS	ISHTESA	ARVRHYDSSGYETLDY	GCCAGAGTCCGACACTATGATAGTAGTGGTTATGAGACACTT GACTAC
A11	5319	IGHV4-59*08	IGHJ4*02	IGHG1-2	GGSIGGFY	SYTIVST	ARGYGHIDS	GCGAGAGGCTATGGTCACATTGACTCC

B IGK/L chain sequence

Well position	Copy number	V gene	J gene	C region (K or L)	CDR1 Peptide	CDR2 Peptide	CDR3 Peptide	CDR3 Nucleotide
A01	133	IGKV3-15*01	IGKJ2*01	IGKC	QSVSSN	GVF	QQYNNWPYT	CAGCAGTATAATAACTGGCCGTACTACT
A02	3574	IGLV2-14*03	IGLJ2*01	IGLC	SSDIGRYNY	DVS	SSYTSSRTLTV	AGCTCATATACAAGCAGCAGAACTCTGGTC
A04	28	IGKV1-17*03	IGKJ4*01	IGKC	EGISNF	DAS	LQYHTYPPT	CTACAGTATCATACTTACCCTCCCACT
A06	234	IGKV1D-16*01	IGKJ5*01	IGKC	QGISSW	GAS	QQYNSYPHT	CAACAGTATAATAGTTACCCTCACACC
A10	236	IGKV1-39*01	IGKJ5*01	IGKC	QSIDIY	ASS	QQSLSFPLT	CAACAGAGTTTAAGTTTCCCTCTCACC
A11	299	IGKV3-20*01	IGKJ2*01	IGKC	QSVDSRY	GAS	EQYASSPNT	GAGCAGTATGCCAGCTCACCCAACACT

The column titles show the sequence annotations for various gene segments on the IGH (**A**) and IGK/L (**B**) chains from international ImMunoGeneTics information system (IMGT). Data is shown with copy numbers of identified variable (V) and junctional (J) gene variants, B cell receptor isotype inferred from the constant region (C), peptide/amino acid sequences of complementarity determining regions (CDR1, CDR2 and CDR3) and nucleotide sequence for CDR3 for cells analysed in plate 1 positions A01, A02, A04, A06, A10 and A11.

The sequence data from the two plates were analysed separately and as pooled. Preliminary analyses were performed to evaluate isotype identities, IGH-IGK/L pairing and to confirm the presence of only a single CDR3 sequence on each chain for each single cell. Firstly, the data was evaluated for isotype identity of each sequenced cell. The isotype is inferred from the sequenced constant region. The iPair technology identifies a short segment of the constant region on both heavy and light chains of sequenced B cell receptors. From this, it can identify and classify IgG subclasses into either IgG1-2 or IgG3-4 and can identify other isotypes as IgD, IgM, IgA and IgE as indicated in column 'C' of table 7.1A, as well as differentiate between IGK and IGL chains as indicated in column 'C' of table 7.1B.

The cells sorted for this control test were all phenotypically HPV 16+IgG+ as earlier described (Figure 7.8A), hence, isotype evaluation of the sequence data would allow for assessment of the sorting accuracy. From plate 1, 97.40% (75/77 wells) were IgG+ (IGHG) and only 2.60% (2/77 wells) were IgM+ (IGHM) (Figure 7.10A) and from plate 2, 98.72% (77/78 wells) were IgG+ (IGHG) and only 1.28% (1/78 wells) were IgD+ (IGHD) (Figure 7.10B). The overall isotype accuracy from the two plates was 98.06% (152/155 cells) (Figure 7.10C). Data from the 3 IgG- cells were excluded from subsequent analyses. Next, IGH-IGK/L pairing was evaluated on sequences confirmed to be IGHG. Majority of the wells contained paired IGH-IGK/L sequences as earlier observed in the plate view (Figure 7.9). Plate 1 had 62.67% (47/75) paired IGH-IGK/L, 22.67% (17/75) unpaired IGH and 14.67% (11/75) unpaired IGK/L chains and plate 2 had 71.43% (55/77) paired IGH-IGK/L, 20.78% (16/77) unpaired IGH and 7.79% (6/77) unpaired IGK/L chains (Figure 7.10A & B). Overall paired IGH-IGK/L, unpaired IGH and unpaired IGK/L chains for the two plates were 67.11% (102/152), 21.71% (33/152) and 11.18% (17/152), respectively (Figure 7.10C). The final preliminary check evaluated the presence of unique CDR3 segments on both paired and unpaired IGH and IGK/L sequences. This allowed for identification of wells that may have had multiple cells indicated by more than one unique CDR3 sequence in a well. Plate 1 had

92.00% (69/75 wells) single unique CDR3 sequences and 8.00% (6/75 wells) two unique CDR3 sequences of which 6.67% (5/75 wells) and 1.33% (1/75 wells) were from unpaired IGK/L and IGH chains, respectively (Figure 7.10A). Plate 2 had 93.51% (72/77 wells) single unique CDR3 sequences and 6.49% (5/77 wells) two unique CDR3 sequences of which 3.90% (3/77 wells) and 2.60% (2/77 wells) were from unpaired IGK/L and IGH chains, respectively (Figure 7.10B). Overall, both plates had a total of 92.76% (141/152 wells) single unique CDR3 sequences and 7.23% (11/152 wells) two unique CDR3 sequences of which 5.26% (8/152 wells) and 1.97% (3/152 wells) were from unpaired IGK/L and IGH chains, respectively (Figure 7.10C). There were no wells with more than two unique CDR3 sequences.

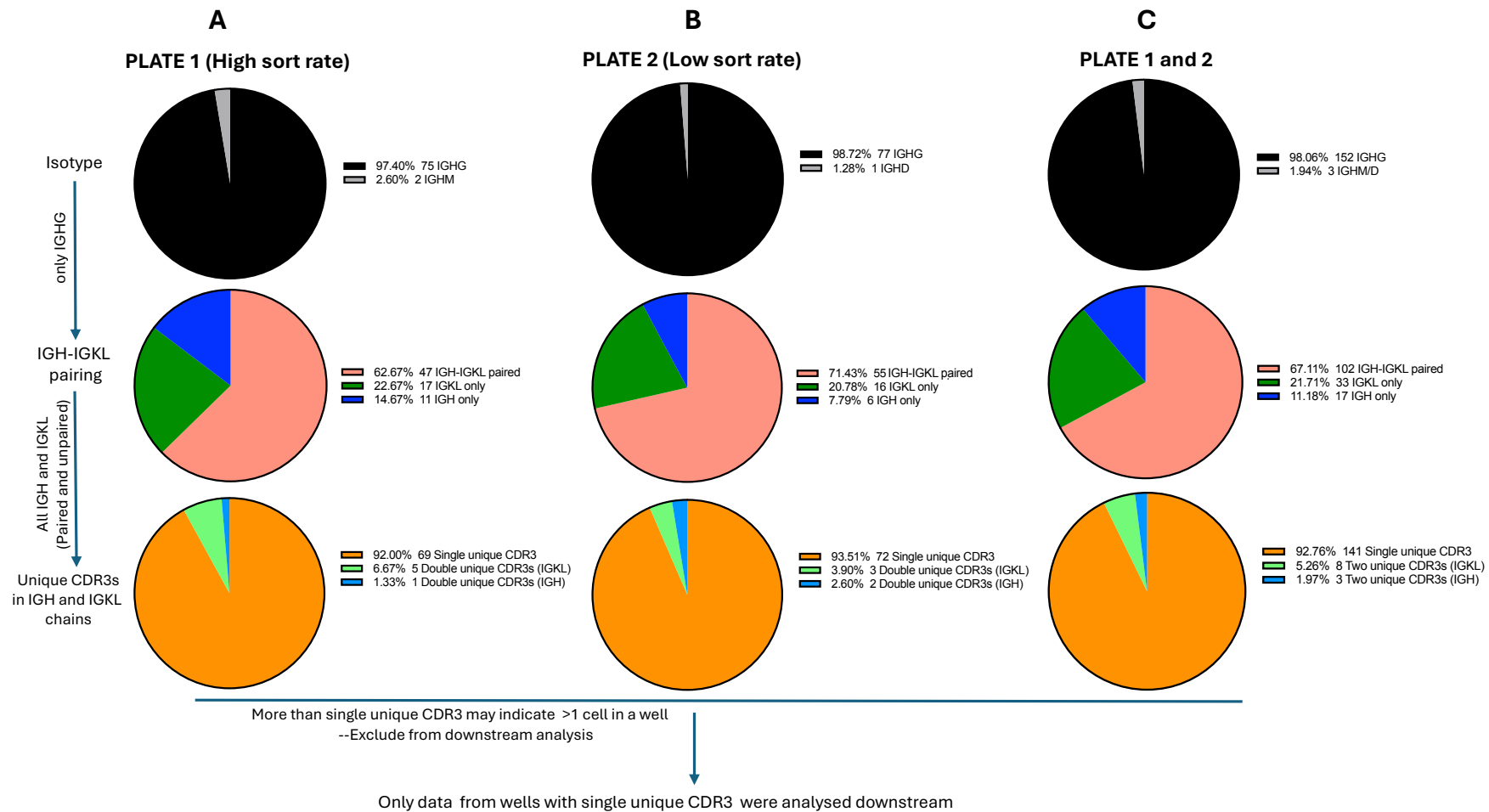


Figure 7.10. Confirmation of isotype, heavy-light (GH-IGK/L) chain pairing and unique CDR3s

Single cell sequence data of the B cell receptor from plate 1 (A) and plate 2 (B) as well as combined plate 1 and 2 (C) were evaluated for isotypes present, IGH-IGK/L pairing and utilization of unique CDR3s. Frequencies for each evaluated component are shown as percentages and total numbers.

7.3.9 Usage of germline IGHV, IGKV/LV, IGHJ, and IGKV/LJ gene variants and unique CDR3 amino acid length

The IGH and IGK/L sequences confirmed to contain a single unique CDR3 sequence were analysed for usage of specific IGHV, IGKV/LV, IGHJ and IGKJ/LJ gene variants and the distribution of the unique CDR3s length as previously described.(Zhang et al., 2022, Niu et al., 2020) There were no major differences observed in the sequence output between the two plates and the data were therefore combined in the analysis presented next.

A total of 36 IGHV variants were identified. IGHV3-23*01 was the most used at a frequency of 11.82% followed by IGHV3-30*01 (8.18) and IGHV1-2*02 (7.27%) (Figure 7.11A). About 79% of the total IGH sequences (cells) utilised 15 IGHV variants out of which the least used were shared by three cells.

A total of 39 IGK/L variants were identified out of which about half were IGK (53.22%) and half were IGL (46.78%). These frequencies were similar to findings from a previous study that used a similar approach to characterise HPV 16 specific memory B cells induced by a quadrivalent HPV vaccine although the previous study reported slightly higher IGL (53%) than IGK (47%).(Scherer et al., 2014b) The ratio of IGK:IGL is reported to be skewed in memory B cells of different individuals due to the complex selection process involving additional light chain rearrangements.(Berkowska et al., 2011) The repertoire data presented in this study was from one individual, thus not sufficient to draw firm conclusions. It is expected that analysis of the repertoire data from more samples will be more informative on the distribution of the IGK/L chains and the overall repertoire.

IGLV1-44*01 (8.87%) and IGLV2-14*01 (8.87%) were the most used followed by IGLV1-51*01 (8.06%), IGKV3-15*01 (7.26%) and IGKV3-20*01 (7.26%) (Figure 7.11B). About 76% of the total IGK/L sequences (cells) utilised 17 IGK/L variants out of which the least used were shared by at three cells.

All six junctional genes were utilised on both IGH and IGK/L chains with more than one variant for some of them (Figure 7.11C & D). On the IGH chain, IGHJ4*02 (52.73%) was the most used followed by IGHJ6*02 (20%) and IGHJ5*2 (8.18%) while on the IGK/L chain, IGLJ2*01 (22.13%) was most used followed by IGKJ4*01 (18.85%) and IGLJ3*02 (15.57%) (Figure 7.11C & D).

The overall lengths of identified unique CDR3s on the IGH chain (HCDR3s) ranged between 9 and 28 amino acids. The lengths of identified unique CDR3s on the IGK/L chain (K/LCDR3) ranged between 9 and 27 amino acids and had a similar distribution to HCDR3s (Figure 7.11E & F).

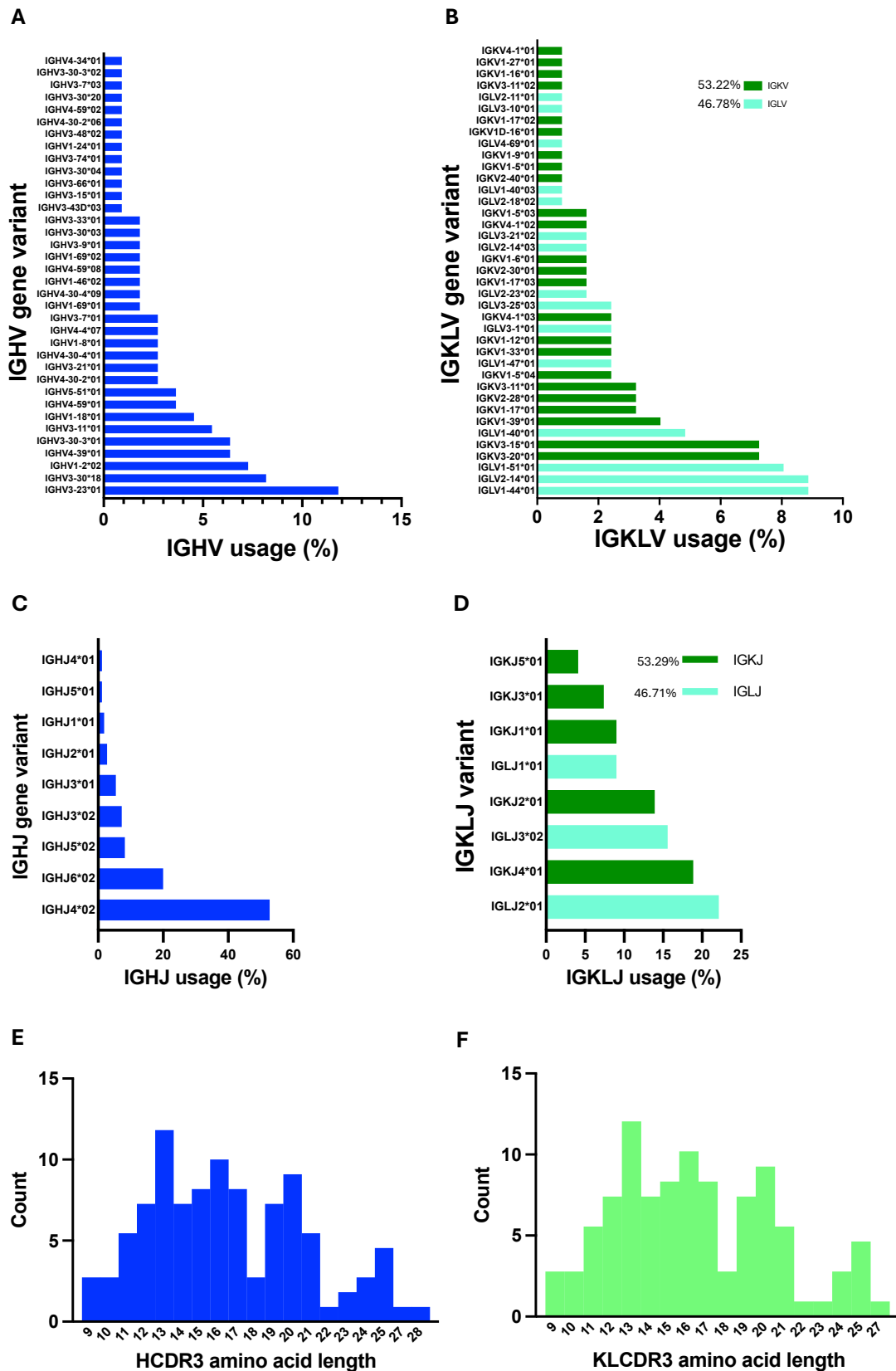


Figure 7.11. Usage of germline heavy and light chain gene variants and distribution of CDR3 amino acid length

Figure legend on next page

Distribution of the heavy chain variable (IGHV) **(A)**, junctional (IGHJ) **(C)** gene variants and complementarity determining (HCDR3) amino acid length **(E)** are shown in blue while the same results on the light chain IGKL **(B)**, IGKLJ **(D)** and amino acid length **(F)** are shown in green; IGK and IGL chains are indicated by dark and light green shades, respectively **(B and D)**.

7.3.10 Single cell sorting of HPV 16+ memory B cells from different study age groups

Following successful sorting of HPV 16 specific memory B cells from a control donor. The cell sorting assay was applied to sort HPV 16+ memory B cells from the three study age groups after 2 or 3 dose regimens earlier described. For each age group, B cells were first isolated from 8 individuals separately before pooling them in equal ratios for staining.

The control sample described earlier had IgG isotype frequency sufficiently high (71.66%) allowing for single cell sorting of only HPV 16+IgG+IgM- memory B cells. This was not the case with the study samples as they had substantial isotype heterogeneity in the HPV 16+ memory B cell population. In the post-vaccination antigen specific memory B cells, HPV 16+IgG+IgM- cells had the highest frequency across all age groups (Figure 7.12A-C). The 4-8-year-olds had the highest HPV 16+IgG+IgM- memory B cell frequency (57.82%) compared to the older age groups; 40.1% and 46.67% for 9-14- and 15-26-year-olds, respectively. This youngest group also had the lowest frequency of HPV 16+IgM+IgG- (17.69%) compared to 9-14-year-olds; HPV 16+IgM+IgG- (25.45%) and 15-26-year-olds; HPV 16+IgM+IgG- (26.67%) (Figure 7.12A-C). The trend observed for HPV 16+IgG+ memory B cells by age is consistent with what was observed from the ELISpot data evaluating the same population in chapter 4 although there were no significant differences across ages.

The total pool of HPV 16+ memory B cell population identified post-vaccination was sorted into microplates for repertoire mapping. This allowed for evaluation of isotype distribution from the sequence data.

B cells were isolated from frozen PBMC of 8 participants for each of three age groups (4-8- (A), 9-14- (B) and 15-26-year-olds(C)) and pooled in equal ratios before staining. Data was acquired on FACS Melody. Gating was first done on lymphocytes and single cells, then residual CD3+ T cells, CD14+ monocytes and dead cells excluded in a dump channel and B cells identified as CD3-CD14-CD19+. Total memory B cell were identified in CD3-CD14-CD19+ B cells as IgD-CD27+ from which the HPV 16+ population was identified from both baseline and post-vaccination timepoints. HPV 16+IgG+, HPV 16+IgG-IgM- and HPV 16+IgM+ memory B cell frequencies were then identified from HPV 16+ memory b cell after vaccination. The post-dose 2 or 3 HPV16+ memory B cells were index-sorted into microplates for subsequent sequencing of the B cell receptor.

To allow for comparison of HPV 16 specific and non-specific B cell repertoire, the baseline HPV 16- memory B cells were also sorted for repertoire mapping. This would allow for identification of any vaccine-induced changes attributable to HPV 16 specificity. The sorting of HPV 16- memory B cells was performed based on the gating shown (Figure 7.13).

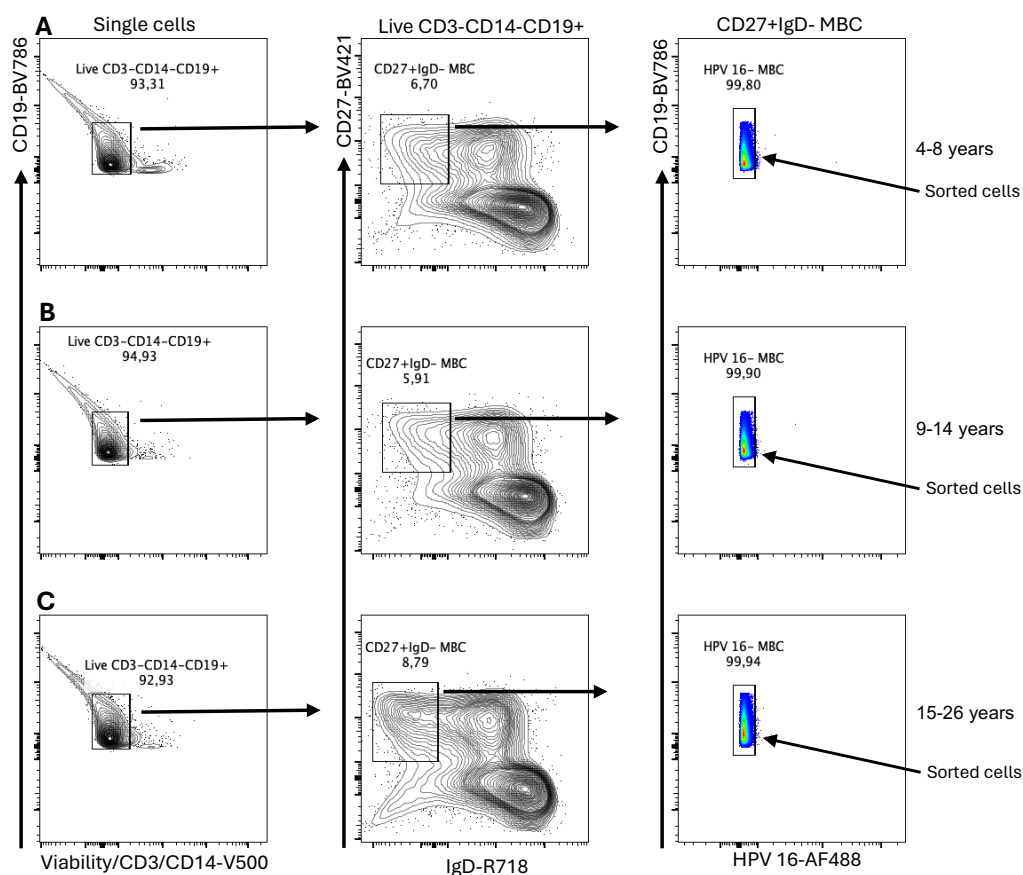


Figure 7.13. Identification of baseline HPV 16- memory B cells for single cell sorting

B cells were isolated from frozen PBMC of 8 participants for each of three age groups (4-8- (A), 9-14- (B) and 15-26-year-olds (C)) and pooled in equal numbers before staining. Data was acquired on FACS Melody. Gating was first done on lymphocytes and single cells, then residual CD3+ T cells, CD14+ monocytes and dead cells excluded in a dump channel and B cells identified as CD3-CD14-CD19+. Total memory B cells were identified in CD3-CD14-CD19+ B cells as IgD-CD27+ from which the HPV 16- MBC population was identified from the baseline pre-vaccination timepoint and index-sorted into microplates for subsequent sequencing repertoire mapping.

The singly sorted HPV 16+ memory B cells from the post-vaccination samples and the HPV 16- memory B cells from the pre-vaccination samples are being analysed for the BCR repertoire as earlier described. Comparison of the pre- and post-vaccination B cell repertoire may identify vaccine induced BCR characteristics of relevance to the vaccine immunogenicity.

To this level, the specificity of the identified memory B cells is based on flow cytometry antigen staining. These will be further confirmed for specificity and function by cloning and expression of monoclonal antibodies from the identified paired IGH and IGK/L chain sequences from HPV 16+ BCRs. This will be followed by evaluation of the ability of the expressed monoclonal antibodies to neutralise HPV 16.

7.4 Discussion and future work

B cell repertoire diversity is necessary to respond to a variety of antigens. Technological advancements incorporating sequencing and bioinformatics tools have enabled comprehensive characterization of BCRs to the level of their nucleotide sequence. This has the potential to improve understanding on the dynamics of B cell response and humoral immunity to guide development of better vaccines. (Trück et al., 2015, Galson et al., 2014)

This study reports successful flow cytometry-based identification and single cell sorting of HPV 16 specific memory B cells following HPV vaccination and subsequent mapping of the BCR repertoire. This work builds on previous studies conducted to characterise HPV specific memory B cells at single cell level. (Scherer et al., 2014a, Scherer et al., 2018, Scherer et al., 2016)

The frequencies of HPV 16 specific memory B cells identified by flow cytometry after two or three vaccination doses ranged between 0.01 to 0.08% of total memory B cell pool and were lower than those identified on the same samples by ELISpot (ranging from 0.46 to 0.68% of total IgG memory B cells) across the three age groups (in chapter 4). The difference was expected due to various assay-dependent characteristics including the higher sensitivity of ELISpot. Additionally, flow cytometry was performed on ex vivo stimulated PBMC and identified antigen specific cells as a percentage of the total memory B cell pool, and ELISpot on fresh in vitro stimulated PBMC and presented identified antigen specific cells as a percentage of the total IgG memory B cell pool. Therefore, enrichment of antigen specific memory B cells detected by both assays following vaccination was considered as an indication that the same population was being identified, given the assays are optimised for identification of the HPV specific memory B cell population. Additionally, results from both assays showed that the frequencies of identified HPV 16 specific memory B cell after vaccination tended to increase with decreasing age.

These results, though not directly comparable due to experimental and study design-related differences, are consistent with findings from two previous separate studies of Gardasil

vaccine that used the same PBMC samples. One of them used flow cytometry and the other one used ELISpot to evaluate the HPV specific memory B cell response at one month following two or three vaccination doses as per age-recommended vaccination schedule. The study using flow cytometry reported the frequency of vaccine-induced HPV 16+ memory B cells to be 0.2% of the total memory B cell population which was reported to be an order lower than findings from the ELISpot-generated results.(Scherer et al., 2014b, Smolen et al., 2012)

Phenotypically identified HPV 16+ memory B cells from the samples evaluated in this PhD work had highest frequencies of IgG+, followed by a population likely to be IgA+ and IgM+ cells across the three age groups. The sequence data of HPV 16+IgG+ BCR presented from a single donor identified about half of IGK (53%) and half of IGL (47%). These findings are consistent with earlier studies that identified isotype distribution of HPV 16 specific memory B cells to be pre-dominated by IgG+ (79%) followed by IgA+ (16%) and IgM+ (5%), of which approximately half were IGK (47.00%) and half were IGL (53%).(Scherer et al., 2014a, Scherer et al., 2016) The most reported variants used by HPV 16 specific memory B cells including IGHV3-23, IGHV3-30, IGHV3-30-3, IGHV1-18*01, IGHV3-21, IGHV3-11 and IGHV5-51 were also among those highly used by the HPV 16 specific memory B cells identified in this research work.(Zhang et al., 2022) Some IGHV variants identified in this study to be highly used (IGHV1-2, IGH4-39 and IGH4-59) were previously reported to be less used by HPV 16 monoclonal antibodies. However, these variants have also been reported at high frequencies in monoclonal antibodies for other viral antigens such as severe acute respiratory syndrome coronavirus (SARS) and HIV.(Zhang et al., 2022, Abu-Shmais et al., 2023)

Although this study identified a broader repertoire from HPV 16+ memory B cells than previously reported, the specificity and functionality of the sequenced BCRs warrants confirmation by cloning, expression and testing for viral neutralisation. While the approach used here was previously applied to selectively identify HPV 16 specific memory B cells, subsequent testing of monoclonal antibodies expressed from those cells, for viral

neutralisation and binding confirmed some of them to be non-specific.(Scherer et al., 2014b) Such non-specificity has also previously been reported from fluorescently labelled HIV-VLP antigen.(Hicar et al., 2010)

A previous study reported rapid expansion and contraction of certain B cell clones following vaccination, but these were qualitatively different between individuals and did not show relationship to vaccine type or efficacy.(Laserson et al., 2014) It is extensively reported that the B cell repertoire undergoes changes characterised by SHM and decreased diversity after vaccination and this was reported to correspond to the number of mutated plasma cells detected in circulation at the same time.(Wu et al., 2012, Wang et al., 2015, Galson et al., 2015) The sorting of B cells responding to a particular antigen, for repertoire mapping as done in this study provides more precise information on the evolution of immunity to the antigen. Additionally, where identifiable following different vaccination doses, antigen specific B cells can be sorted to evaluate the changes in B cell response between doses. In the current study, comparisons have been made only between baseline and post dose 2 or 3 in the different age groups because very low numbers of HPV 16 specific memory B cells were identified after dose and were not amenable to sorting.

Future comparison of HPV specific B cell repertoire between the first and subsequent doses will improve understanding on the evolution of antigen specificity following vaccination and the implication any identifiable differences may have on single dose serological protection. However, to be able to achieve feasible numbers of antigen specific memory B cells following the first vaccination dose, future studies may need to target a range of days during which they can identify these cells at their peak in circulation.

Repertoire mapping of antigen specific cells presents an important step in monoclonal antibody generation, availing rich useful molecular information that can be explored computationally for engineering effective monoclonals for disease control not only for HPV but also for other antigens.

8. FINAL DISCUSSION

8.1 Research aims and background

This research aimed to characterise plasma cells, memory B cells and Tfh cell responses generated by Gardasil 9 HPV vaccination and to evaluate the relationship of these cellular responses with subsequent corresponding antibody response, presumed to provide direct protection against HPV infection by viral neutralisation.(Wu et al., 2019a, Wu et al., 2019b, Mariz et al., 2021) Additionally, the effect of age and dose number on the vaccine-induced immune responses was evaluated.

Despite there being highly effective vaccines against HPV, global new cases and mortality rates from cervical cancer have been increasing yearly, disproportionately affecting low income countries where the HPV vaccination coverage is lowest.(Bray et al., 2024, Spayne and Hesketh, 2021) In the Gambia, where this study was conducted, cervical cancer is the leading cause of cancer deaths nationally.(Mali et al., 2023) A major barrier to achieving a good vaccination coverage in these countries has been the vaccine affordability and the capacity of health systems to an adolescent female population which calls for a global effort to explore strategies of increasing HPV vaccination coverage in these settings. The WHO recommendation of a single dose HPV vaccination in females aged 20 years and below is expected to reduce vaccination cost and the burden on health systems.(WHO, 2022) Additionally, the main trial in which this PhD work was nested aims to evaluate alternative HPV vaccination schedules as well as vaccination of children below the current age targeted for HPV vaccination which may provide an opportunity for easier vaccine delivery logistics and potentially reduce the number of girls who may otherwise miss vaccination at older ages. <https://clinicaltrials.gov/ct2/show/NCT03832049>

Most research on immunogenicity of HPV vaccines has focused on the magnitude and function of antibody responses including avidity, viral binding and neutralisation capacity.(Whitworth et al., 2024, Kjaer et al., 2020a) This is attributable to the fact that following induction of antibody responses after vaccination of HPV naïve individuals,

protection against HPV infections and associated diseases remain very high.(Kjaer et al., 2020a) Evidence from such studies has been critical in guiding HPV vaccination policies.

However, important gaps still exist on understanding of the cellular and molecular mechanisms driving such robust immunogenicity from sub-unit vaccines. Long-term vaccine protection is mediated by LLPCs and memory B cells generated from the GC reaction between cognate B cells and Tfh cells.(Ionescu and Urschel, 2019) Previous enumeration of adaptive cellular responses after HPV vaccination in different age cohorts has mainly been performed after completion of two- and three-dose vaccination schedules and the influence of these cell responses on serological vaccine immunogenicity is poorly understood.(Smolen et al., 2012, Matsui et al., 2015, Nicoli et al., 2022, Pasmans et al., 2022) Additionally, the potential immunological implications of single dose-vaccination as currently recommended cannot be inferred from findings in those studies. Therefore, continued research to understand the influence of adaptive cell responses on both short- and long-term serological protection by age and dose remains important.

8.2 Summary of results

To be able to objectively identify vaccine-induced cellular responses and address the research objectives appropriately, this research work started by developing the necessary assays encompassing a comprehensive optimisation process to confirm the assays sensitivity and specificity on pre- and post-vaccination samples using appropriate positive and negative controls. These assays are established as reliable for identification of vaccine-induced immune responses and are widely applied in research.(Robinson et al., 2023, Janetzki, 2015) Specifically, the ELISpot and flow cytometry approaches used in this study have previously been used successfully to selectively identify HPV specific responses after vaccination.(Scherer et al., 2014b, Nicoli et al., 2020c, Smolen et al., 2012) As such, their successful optimisation assured applicability in subsequent identification of the targeted cell responses.

The identification of overall higher numbers of IgG than IgM plasma cells following vaccination were expected in line with well demonstrated induction of predominantly protective IgG antibodies by not only HPV but also other vaccines including Tetanus, Haemophilus influenzae Type b, Pneumococcus and yellow fever.(Schauer et al., 2003, Frazer, 2007, Schnyder et al., 2024) The observation of IgM being significantly induced after the first vaccination dose and declining with subsequent doses while significant induction of IgG plasma cells was observed with the subsequent doses, is in line with expected dynamics of these isotypes following CSR.(Blanchard-Rohner et al., 2009) The first vaccination dose induces lower and delayed plasma cell numbers mainly from activation of naïve B cells compared to subsequent doses which rapidly reactivate memory B cells to differentiate to enhanced plasma cell numbers.(Wietschel et al., 2024). The numbers of plasma cell responses identified by dose in this study followed this trend.

Contextualizing this to the dynamics of documented antibody titres, a single HPV vaccination dose is reported to induce IgG antibody titres that are significantly lower than those from two or three doses, more or less a similar trend to what was observed for short-term plasma cells in this study. Importantly, such titres are similarly sustained without waning. At 10 years post-vaccination, HPV 16 and HPV 18 neutralising GMTs from a single dose of Gardasil vaccine were reported to be about about 2 times higher than those induced by natural infection. This may be interpreted to suggest that despite the low IgG plasma cells detected in circulation after the first vaccination, this dose is able to generate sufficient numbers of LLPCs in the secondary lymphoid organs to be able to sustain the observed long-term titres. The undertaking of this study on blood samples meant LLPCs could not be characterised since after their generation in the GCs, they home in the bone marrow.(Lightman et al., 2019)

More information about the phenotype expected of IgM and IgG plasma cells identified in this study by ELISpot was generated by the additional flow cytometry analysis.(Perez-Andres et al., 2010) It is recognized that the expression of survival markers such as CD138,

Blimp-1 and BCMA on plasma cells identifiable transiently in circulation is downregulated; and the markers are mainly applicable in identification of LLPCs in the bone marrow where they are upregulated.(Perez-Andres et al., 2010, Brynjolfsson et al., 2018) This may explain the low expression of CD138 initially observed in freshly isolated PBMC during the plasma cell assay optimisation in this study. Additionally, the CD138 expression has been described to be volatile and time-lag dependent following sample isolation. One study showed that CD138 expression from bone marrow plasma cells was sufficiently detected when samples were processed within 4 hours after isolation.(Dorwal et al., 2014) This further may explain the loss of CD138 expression on frozen PBMC.

The identified profiles of memory B cells being low following the first and higher after subsequent doses are in line with the expectation that, similar to plasma cells, the priming vaccine dose induces lower immunogenicity than subsequent booster doses. Following immune priming, booster vaccination doses reactivate memory B cells to proliferate and differentiate to plasma cells increasing the numbers of both cell populations.(Palm and Henry, 2019, Muecksch et al., 2022) Unlike plasma cells, memory B cells recirculate and are detectable in blood for years following infection or vaccination as an indicator of long-term protection.(Weill and Reynaud, 2016) Indeed, although this research looked at short-term immune responses after Gardasil 9 vaccination, HPV specific memory B cells have been detected in circulation at 4 to 6 years after Cervarix and Gardasil vaccination.(Nicoli et al., 2020a)

Based on biological plausibility, several proposals have been put forward to suggest LLPCs as the most likely source of long-term antibodies induced by HPV vaccination. Although there is no exact level of antibodies has been established to be a correlate of protection against HPV, the high levels maintained above those generated from natural infection have been suggested to be protective against the expected low doses of transmissible virus.(Scherer et al., 2014b) Additionally the mostly reported absence of an increase once antibody titres have attained the long-term plateau phase likely indicates little or no

contribution of memory B cells at that phase.(Schiller and Lowy, 2018b) This thought is further supported by the absence of a direct positive correlation between HPV specific memory B cells and antibody titres both in the short-term as observed in this study and in the long-term as previously reported.(Nicoli et al., 2020a) However, given the coordinated nature of the immune system, the contributions of both memory B cells and LLPCs to long-term protection is important and needs to be considered especially in evaluating immunogenicity of a single dose vaccination schedule expected to induce overall lower immunogenicity than multi-dose schedules.

The higher magnitudes of long-term antibody titres observed from multi-dose HPV vaccination indicate the early role of memory B cells in boosting LLPCs. Based on the age-dependent infection dynamics of HPV and that the vaccines are primarily recommended to be administered before sexual debut, it is possible that the role of memory B cells in long-term protection may be realized in future longer-term follow ups. Indeed, a 10-year follow up after Gardasil vaccination reported some decrease in plateau-phase antibody titres from the single dose group to levels induced by natural vaccination in unvaccinated individuals.(Joshi et al., 2023) This was followed by an increase when most-vaccinees were married and expected to be exposed to HPV. The increase in antibody response was suggested to be from memory B cell reactivation. Additionally, the proportion of individuals with detectable neutralising antibodies was lower for HPV 18 (49.1%) compared to HPV 16 (97.8%). It is noted that the study was not a single-dose randomised trial and that findings from ongoing single-dose randomised studies will provide more reliable data.

Memory B cell responses may be beneficial in sustaining long-term protection in low responders following a single dose vaccination in whom the antibody titres may wane in the coming years. The findings from this PhD work show that at 12 months, before the second vaccination dose in the young cohorts, the memory B cell numbers were very low and, should the antibody titres wane to warrant the recruitment of memory B cells, it remains to

be understood if such low numbers will be able to provide sufficient long-term protection against new infections.

The selective identification of HPV 16 specific memory B cells based on the antigen binding enabled further analysis to better understand the phenotype and molecular characteristics of the HPV specific repertoire. The identified diverse usage of IGH and IGK/L gene variants is consistent with findings from previous studies on HPV as well as other antigens.(Scherer et al., 2014b, Scherer et al., 2016, Scherer et al., 2018, Niu et al., 2020, Galson et al., 2015) HPV 16 monoclonal antibodies previously generated following B cell repertoire mapping have been shown to possess potent viral neutralisation capacity.(Scherer et al., 2014b) This approach has potential for application in future development of monoclonal antibodies for other antigens.

Given the requirement of Tfh cells help for B cells to differentiate to memory B cells and LLPCs, the identification of similar profiles of plasma cell, memory B cell and Tfh cell responses was relevant. While all evaluated responses were higher in the younger age groups, the lower AIM-based Tfh cell response observed in the youngest age group was exceptional and this difference remains to be understood. The AIM assay has not been used to compare T cell responses in different age groups, and whether the AIM markers used are expressed at different levels by age is not clear. Nevertheless, even these low Tfh cells increased by doses as observed for all other responses evaluated across the age groups.

The finding of HPV vaccine-induced antibody responses to increase with decreasing age was expected as previously documented from adolescent and adults cohorts.(Ellingson et al., 2023) The similar observation that the evaluated cell responses were also higher in younger age groups is consistent with their role in shaping subsequent serological response. The positive correlation between the antibody titres and plasma cells reflect their direct relationship while the absence of such correlation with the memory B cells and Tfh cells may

be as a result of different dynamics of their maintenance as previously reported.(Matsui et al., 2015, Nicoli et al., 2020b)

In conclusion the application of robustly optimised methods and analysis of a modest sample size ensured that vaccine-induced immune responses that were detectable in peripheral circulation at the targeted timepoints were confidently identified. Taken together, the integrated evaluation of both cellular and serological responses undertaken in this PhD work provides a broader understanding of HPV vaccine immunogenicity. The findings from this work add to the existent literature demonstrating higher immunogenicity of HPV vaccines in young age groups and longer vaccination dose intervals.

The head-to-head comparison of HPV vaccine-induced immunogenicity in the three age groups evaluated in this work has not been performed before. Consequently, the finding that the vaccine is more immunogenic in the 4-8-year-olds in whom HPV vaccination has not been tested before warrants consideration to explore vaccination of younger age targets than currently recommended.

8.3 Future work

Subsequent confirmation of the specificity and functionality of the sequenced BCRs will be determined by cloning and expression of monoclonal antibodies from the paired heavy and light chain sequences, and the monoclonal antibodies will be evaluated for viral neutralisation. Subsequently, the sorted post-vaccination HPV 16+ and pre-vaccination HPV 16- memory B cells from the youngest and oldest cohorts in this study have been sequenced and are being analysed to evaluate vaccine-specific enrichment of the repertoire. The specificity and function of cells identified from the different age groups will also be evaluated.

The potential of utilising repertoire data for disease control and prevention by generation of monoclonal antibodies support this research as an important contribution to the immunity and vaccinology field and could be advanced to investigate the use of monoclonal antibodies against HPV as well as other antigens. Monoclonal antibodies are being used to prevent

Respiratory Syncytial Virus (RSV) in infants with more research ongoing to explore their use in prevention of other infectious diseases such as Ebola, ZIKA, Dengue and flu.(Pantaleo et al., 2022) Studies are also ongoing to understand B cell repertoire changes during immunosenescence and to explore the use of monoclonals to rejuvenate immunity in old age.(Ross et al., 2024, 2006, Dunn-Walters and O'Hare, 2019)

In addition to the adaptive immune responses presented in this work, characterising innate immunity following HPV vaccination will provide a broader understanding on the early innate mechanisms driving the vaccine protection. Following completion of this PhD work, a planned exploratory study (funded by British Society of Immunology Career Enhancing Grants 2024) will start looking at early molecular signatures of HPV vaccine immunogenicity. It is expected that findings from that work will identify genes that are differentially expressed early on following vaccination, their associated signalling pathways and relationship with corresponding vaccine-induced adaptive responses. This may identify innate pathways that may be targeted in future vaccine development strategies.

Future studies to confirm the presence of HPV specific LLPCs in the bone marrow may play a major role in demonstrating the extent to which these are generated following different HPV vaccination schedules. This may answer the major question many studies are trying to answer on the longevity of HPV vaccine-induced antibody titres, especially from the single dose schedule.

In summary, this research has provided insights on the influence that early HPV vaccine-induced B cell and Tfh cell responses may have on the differences observed in subsequent antibody titres by age and dose. The study also highlights potential long-term implications of single dose vaccination that, should immunity in low responders wane, they may be at risk of being infected with HPV and developing cancer leading to deaths that may have otherwise been prevented with two doses.

Future work has been proposed to better understand immunological mechanisms underlying HPV vaccine protection as well as to take the B cell biology and vaccine immunology research forward.

REFERENCES

2006. Antibody Quality in Old Age. *Rejuvenation Research*, 9, 117-125.
- AARON, T. S. & FOOKSMAN, D. R. 2022. Dynamic organization of the bone marrow plasma cell niche. *The FEBS Journal*, 289, 4228-4239.
- ABRAMSON, J., AHMED, S. S., ALBA, M. A., ALI, Y. M., AMBRUS, J. L., ANDERSSON SVÄRD, A., ARINGER, M., ASSASSI, S., AUNG, T., AYZENBERG, I., BARKER, R. N., BAXTER, A. G., BETTERLE, C., BIRLEA, S. A., BJÖRKSTRÖM, N. K., BLAIR, P. A., BLÜML, S., BOSCH, X., BRODSKY, R. A., BRYCESON, Y. T., BURKETT, P. R., BUSSEL, J. B., CARICCHIO, R., CASCIOLA-ROSEN, L., CATUREGLI, P., CHAIGNE-DELALANDE, B., CHALAN, P., CHATENOU, L., COHEN, P. L., COOPER, M. A., COPPIETERS, K., CRYSTAL, R. G., CULTON, D. A., DAMATO, V., DAVIDSON, A., DELFINO, L., DELVES, P. J., DI DALMAZI, G., DIAMOND, B., DIAZ, L. A., FALK, R. J., FRITZLER, M. J., GALLUCCI, S., GANGAPUTRA, S., GELBMAN, B., GERSHWIN, M. E., GERY, I., GETTS, D. R., GOLD, R., GOLDFARB, Y., GONG, J., GORDON, S., GORONZY, J. J., GREER, J. M., GUAZZONE, V. A., GUILHERME, L., HAFLER, D. A., HAHN, B. H., HAMAD, A. R. A., HAMANO, H., HARRISON, L. C., HOMANN, D., HUSEBYE, E. S., JENNETTE, J. C., JONES, R. J., JORDAN, M. A., KALIL, J., KAWA, S., KAYA, Z., KELLER, C. W., KING, N. J. C., KITCHAROENSACKUL, M., KIYOSAWA, K., KÖNIGS, C., KRONENBERG, M., KUCHROO, V. K., LAURENCE, A., LEE, E.-J., LEHMANN, H. C., LERNMARK, Å., LINDBLADH, I., LIU, Z., LJUNGGREN, H.-G., LUNARDI, C., LUNDIN, K. E. A., LÜNEMANN, J. D., LUNN, M. P. T., LUSTIG, L., MACKAY, C. R., MACKAY, I. R., MALATTIA, C., MARTINEZ-POMARES, L., MARTINI, A., MAURI, C., MCCOMBE, P. A., MELCHERS, F., MIELI-VERGANI, G., MILLER, F. W., MILLER, S. D., MIZUI, M., et al. 2020. List of Contributors. In: ROSE, N. R. & MACKAY, I. R. (eds.) *The Autoimmune Diseases (Sixth Edition)*. Academic Press.
- ABU-SHMAIS, A. A., VUKOVICH, M. J., WASDIN, P. T., SURESH, Y. P., RUSH, S. A., GILLESPIE, R. A., SANKHALA, R. S., CHOE, M., JOYCE, M. G., KANEKIYO, M., MCLELLAN, J. S. & GEORGIEV, I. S. 2023. Convergent Sequence Features of Antiviral B Cells. *bioRxiv*, 2023.09.06.556442.
- ADAM, L., ROSENBAUM, P., BONDUELLE, O. & COMBADIÈRE, B. 2021. Strategies for Immunomonitoring after Vaccination and during Infection. *Vaccines (Basel)*, 9.
- AGEMATSU, K. 2000. Memory B cells and CD27. *Histol Histopathol*, 15, 573-6.
- AGEMATSU, K., HOKIBARA, S., NAGUMO, H. & KOMIYAMA, A. 2000. CD27: a memory B-cell marker. *Immunology Today*, 21, 204-206.
- AKHATOVA, A., AZIZAN, A., ATAGELDIYEVA, K., ASHIMKHANOVA, A., MARAT, A., IZTLEUOV, Y., SULEIMENOVA, A., SHAMKEEVA, S. & AIMAGAMBETOVA, G. 2022. Prophylactic Human Papillomavirus Vaccination: From the Origin to the Current State. *Vaccines (Basel)*, 10.
- ALLMAN, D., JAIN, A., DENT, A., MAILE, R. R., SELVAGGI, T., KEHRY, M. R. & STAUDT, L. M. 1996. BCL-6 expression during B-cell activation.
- ALLMAN, D. & PILLAI, S. 2008. Peripheral B cell subsets. *Curr Opin Immunol*, 20, 149-57.
- ALT, F. W., OLTZ, E. M., YOUNG, F., GORMAN, J., TACCIOLI, G. & CHEN, J. 1992. VDJ recombination. *Immunol Today*, 13, 306-14.
- AMADOR-MOLINA, A., HERNÁNDEZ-VALENCIA, J. F., LAMOYI, E., CONTRERAS-PAREDES, A. & LIZANO, M. 2013. Role of innate immunity against human papillomavirus (HPV) infections and effect of adjuvants in promoting specific immune response. *Viruses*, 5, 2624-42.
- AMANNA, I. J., CARLSON, N. E. & SLIFKA, M. K. 2007. Duration of humoral immunity to common viral and vaccine antigens. *N Engl J Med*, 357, 1903-15.

- AMANNA, I. J. & SLIFKA, M. K. 2010a. Mechanisms that determine plasma cell lifespan and the duration of humoral immunity. *Immunological Reviews*, 236, 125-138.
- AMANNA, I. J. & SLIFKA, M. K. 2010b. Mechanisms that determine plasma cell lifespan and the duration of humoral immunity. *Immunol Rev*, 236, 125-38.
- ARBYN, M. & XU, L. 2018. Efficacy and safety of prophylactic HPV vaccines. A Cochrane review of randomized trials. *Expert Rev Vaccines*, 17, 1085-1091.
- ARROYO, E. N. & PEPPER, M. 2020. B cells are sufficient to prime the dominant CD4+ Tfh response to Plasmodium infection. *J Exp Med*, 217.
- ARULRAJ, T., BINDER, S. C., ROBERT, P. A. & MEYER-HERMANN, M. 2021. Germinal Centre Shutdown. *Frontiers in Immunology*, 12.
- ASKONAS, B. A. 1975. Immunoglobulin formation in B lymphoid cells. *J Clin Pathol Suppl (Assoc Clin Pathol)*, 6, 8-12.
- AWASTHI, A. & KUCHROO, V. K. 2009. The yin and yang of follicular helper T cells. *Science*, 325, 953-955.
- AYRE, D. C., CHUTE, I. C., JOY, A. P., BARNETT, D. A., HOGAN, A. M., GRÜLL, M. P., PEÑA-CASTILLO, L., LANG, A. S., LEWIS, S. M. & CHRISTIAN, S. L. 2017. CD24 induces changes to the surface receptors of B cell microvesicles with variable effects on their RNA and protein cargo. *Scientific Reports*, 7, 8642.
- BACHMANN, M. F. & JENNINGS, G. T. 2010. Vaccine delivery: a matter of size, geometry, kinetics and molecular patterns. *Nat Rev Immunol*, 10, 787-96.
- BACHMANN, M. F., KÜNDIG, T., KALBERER, C. P., HENGARTNER, H. & ZINKERNAGEL, R. M. 1994. How many specific B cells are needed to protect against a virus? *Journal of immunology (Baltimore, Md.: 1950)*, 152, 4235-4241.
- BAH CAMARA, H., ANYANWU, M., WRIGHT, E. & KIMMITT, P. T. 2018. Human papilloma virus genotype distribution and risk factor analysis amongst reproductive-age women in urban Gambia. *J Med Microbiol*, 67, 1645-1654.
- BAISLEY, K., KEMP, T. J., KREIMER, A. R., BASU, P., CHANGALUCHA, J., HILDESHEIM, A., PORRAS, C., WHITWORTH, H., HERRERO, R., LACEY, C. J., SCHILLER, J. T., LUCAS, E., MUTANI, P., DILLNER, J., INDANGASI, J., MUWONGE, R., HAYES, R. J., PINTO, L. A. & WATSON-JONES, D. 2022. Comparing one dose of HPV vaccine in girls aged 9–14 years in Tanzania (DoRIS) with one dose of HPV vaccine in historical cohorts: an immunobridging analysis of a randomised controlled trial. *The Lancet Global Health*, 10, e1485-e1493.
- BAISLEY, K., KEMP, T. J., MUGO, N. R., WHITWORTH, H., ONONO, M. A., NJOROGE, B., INDANGASI, J., BUKUSI, E. A., PRABHU, P. R., MUTANI, P., GALLOWAY, D. A., MWANZALIME, D., KAPIGA, S., LACEY, C. J., HAYES, R. J., CHANGALUCHA, J., PINTO, L. A., BARNABAS, R. V. & WATSON-JONES, D. 2024. Comparing one dose of HPV vaccine in girls aged 9–14 years in Tanzania (DoRIS) with one dose in young women aged 15–20 years in Kenya (KEN SHE): an immunobridging analysis of randomised controlled trials. *The Lancet Global Health*, 12, e491-e499.
- BALLESTEROS-TATO, A., LEÓN, B., LUND, F. E. & RANDALL, T. D. 2013. CD4+ T helper cells use CD154–CD40 interactions to counteract T reg cell–mediated suppression of CD8+ T cell responses to influenza. *Journal of Experimental Medicine*, 210, 1591-1601.
- BALLESTEROS-TATO, A., RANDALL, T. D., LUND, F. E., SPOLSKI, R., LEONARD, W. J. & LEÓN, B. 2016. T Follicular Helper Cell Plasticity Shapes Pathogenic T Helper 2 Cell-Mediated Immunity to Inhaled House Dust Mite. *Immunity*, 44, 259-73.

- BALOGH, K. N., TEMPLETON, D. J. & CROSS, J. V. 2018. Macrophage Migration Inhibitory Factor protects cancer cells from immunogenic cell death and impairs anti-tumor immune responses. *PLoS One*, 13, e0197702.
- BANNARD, O., HORTON, R. M., ALLEN, C. D., AN, J., NAGASAWA, T. & CYSTER, J. G. 2013. Germinal center centroblasts transition to a centrocyte phenotype according to a timed program and depend on the dark zone for effective selection. *Immunity*, 39, 912-24.
- BARHAM, M. S., WHATNEY, W. E., KHAYUMBI, J., ONGALO, J., SASSER, L. E., CAMPBELL, A., FRANCZEK, M., KABONGO, M. M., OUMA, S. G., HAYARA, F. O., GANDHI, N. R. & DAY, C. L. 2020. Activation-Induced Marker Expression Identifies Mycobacterium tuberculosis–Specific CD4 T Cells in a Cytokine-Independent Manner in HIV-Infected Individuals with Latent Tuberculosis. *ImmunoHorizons*, 4, 573-584.
- BARNABAS RUANNE, V., BROWN ELIZABETH, R., ONONO MARICIANAH, A., BUKUSI ELIZABETH, A., NJOROGI, B., WINER RACHEL, L., GALLOWAY DENISE, A., PINDER LEEYA, F., DONNELL, D., WAKHUNGU, I., CONGO, O., BIWOTT, C., KIMANTHI, S., OLUOCH, L., HELLER KATE, B., LEINGANG, H., MORRISON, S., RECHKINA, E., CHERNE, S., SCHAAFSMA TORIN, T., MCCLELLAND, R. S., CELUM, C., BAETEN JARED, M. & MUGO, N. 2022. Efficacy of Single-Dose Human Papillomavirus Vaccination among Young African Women. *NEJM Evidence*, 1, EVIDoA2100056.
- BARNABAS, R. V., BROWN, E. R., ONONO, M. A., BUKUSI, E. A., NJOROGI, B., WINER, R. L., GALLOWAY, D. A., PINDER, L. F., DONNELL, D., WAKHUNGU, I., CONGO, O., BIWOTT, C., KIMANTHI, S., OLUOCH, L., HELLER, K. B., LEINGANG, H., MORRISON, S., RECHKINA, E., CHERNE, S., SCHAAFSMA, T. T., MCCLELLAND, R. S., CELUM, C., BAETEN, J. M. & MUGO, N. 2022. Efficacy of single-dose HPV vaccination among young African women. *NEJM Evid*, 1, EVIDoA2100056.
- BARRINGTON, R. A., SCHNEIDER, T. J., PITCHER, L. A., MEMPEL, T. R., MA, M., BARTENEVA, N. S. & CARROLL, M. C. 2009. Uncoupling CD21 and CD19 of the B-cell coreceptor. *Proc Natl Acad Sci U S A*, 106, 14490-5.
- BASHAW, A. A., LEGGATT, G. R., CHANDRA, J., TUONG, Z. K. & FRAZER, I. H. 2017. Modulation of antigen presenting cell functions during chronic HPV infection. *Papillomavirus Research*, 4, 58-65.
- BATTEN, M., RAMAMOORTHY, N., KLJAVIN, N. M., MA, C. S., COX, J. H., DENGLER, H. S., DANILENKO, D. M., CAPLAZI, P., WONG, M., FULCHER, D. A., COOK, M. C., KING, C., TANGYE, S. G., DE SAUVAGE, F. J. & GHILARDI, N. 2010. IL-27 supports germinal center function by enhancing IL-21 production and the function of T follicular helper cells. *J Exp Med*, 207, 2895-906.
- BAUMJOHANN, D., PREITE, S., REBOLDI, A., RONCHI, F., ANSEL, K. M., LANZAVECCHIA, A. & SALLUSTO, F. 2013. Persistent Antigen and Germinal Center B Cells Sustain T Follicular Helper Cell Responses and Phenotype. *Immunity*, 38, 596-605.
- BEACHLER, D. C., JENKINS, G., SAFAEIAN, M., KREIMER, A. R. & WENTZENSEN, N. 2016. Natural Acquired Immunity Against Subsequent Genital Human Papillomavirus Infection: A Systematic Review and Meta-analysis. *J Infect Dis*, 213, 1444-54.
- BENTEBIBEL, S.-E., KHURANA, S., SCHMITT, N., KURUP, P., MUELLER, C., OBERMOSER, G., PALUCKA, A. K., ALBRECHT, R. A., GARCIA-SASTRE, A., GOLDING, H. & UENO, H. 2016. ICOS+PD-1+CXCR3+ T follicular helper cells contribute to the generation of high-avidity antibodies following influenza vaccination. *Scientific Reports*, 6, 26494.
- BERE, A., TAYIB, S., KRIEK, J.-M., MASSON, L., JAUMDALLY, S. Z., BARNABAS, S. L., CARR, W. H., ALLAN, B., WILLIAMSON, A.-L., DENNY, L. & PASSMORE, J.-A. S. 2014. Altered phenotype and

- function of NK cells infiltrating Human Papillomavirus (HPV)-associated genital warts during HIV infection. *Clinical Immunology*, 150, 210-219.
- BERGMAN, H., BUCKLEY, B. S., VILLANUEVA, G., PETKOVIC, J., GARRITTY, C., LUTJE, V., RIVEROS-BALTA, A. X., LOW, N. & HENSCHKE, N. 2019. Comparison of different human papillomavirus (HPV) vaccine types and dose schedules for prevention of HPV-related disease in females and males. *Cochrane Database Syst Rev*, 2019.
- BERKOWSKA, M. A., DRIESSEN, G. J., BIKOS, V., GROSSERICHTER-WAGENER, C., STAMATOPOULOS, K., CERUTTI, A., HE, B., BIERMANN, K., LANGE, J. F., VAN DER BURG, M., VAN DONGEN, J. J. & VAN ZELM, M. C. 2011. Human memory B cells originate from three distinct germinal center-dependent and -independent maturation pathways. *Blood*, 118, 2150-8.
- BIERL, C., KAREM, K., POON, A. C., SWAN, D., TORTOLERO-LUNA, G., FOLLEN, M., WIDEROFF, L., UNGER, E. R. & REEVES, W. C. 2005. Correlates of cervical mucosal antibodies to human papillomavirus 16: results from a case control study. *Gynecol Oncol*, 99, S262-8.
- BIERNAT-SUDOLSKA, M., SZOSTEK, S., ROJEK-ZAKRZEWSKA, D., KLIMEK, M. & KOSZ-VNENCHAK, M. 2011. Concomitant infections with human papillomavirus and various mycoplasma and ureaplasma species in women with abnormal cervical cytology. *Adv Med Sci*, 56, 299-303.
- BIGOS, M. 2007. Separation index: an easy-to-use metric for evaluation of different configurations on the same flow cytometer. *Curr Protoc Cytom*, Chapter 1, Unit1.21.
- BLACK, A. P., ARDERN-JONES, M. R., KASPROWICZ, V., BOWNESS, P., JONES, L., BAILEY, A. S. & OGG, G. S. 2007. Human keratinocyte induction of rapid effector function in antigen-specific memory CD4+ and CD8+ T cells. *Eur J Immunol*, 37, 1485-93.
- BLANCHARD-ROHNER, G., PULICKAL, A. S., JOL-VAN DER ZIJDE, C. M., SNAPE, M. D. & POLLARD, A. J. 2009. Appearance of peripheral blood plasma cells and memory B cells in a primary and secondary immune response in humans. *Blood*, 114, 4998-5002.
- BONTKES, H. J., DE GRUIJL, T. D., WALBOOMERS, J. M., SCHILLER, J. T., DILLNER, J., HELMERHORST, T. J., VERHEIJEN, R. H., SCHEPER, R. J. & MEIJER, C. J. 1999. Immune responses against human papillomavirus (HPV) type 16 virus-like particles in a cohort study of women with cervical intraepithelial neoplasia. II. Systemic but not local IgA responses correlate with clearance of HPV-16. *J Gen Virol*, 80 (Pt 2), 409-417.
- BONTKES, H. J., DE GRUIJL, T. D., WALBOOMERS, J. M., VAN DEN MUYSENBERG, A. J., GUNTHER, A. W., SCHEPER, R. J., MEIJER, C. J. & KUMMER, J. A. 1997. Assessment of cytotoxic T-lymphocyte phenotype using the specific markers granzyme B and TIA-1 in cervical neoplastic lesions. *Br J Cancer*, 76, 1353-60.
- BORGHESI, L. & MILCAREK, C. 2006. From B cell to plasma cell: regulation of V(D)J recombination and antibody secretion. *Immunol Res*, 36, 27-32.
- BOSSLER, F., HOPPE-SEYLER, K. & HOPPE-SEYLER, F. 2019. PI3K/AKT/mTOR Signaling Regulates the Virus/Host Cell Crosstalk in HPV-Positive Cervical Cancer Cells. *Int J Mol Sci*, 20.
- BOULIANNE, B. & GOMMERMAN, J. L. 2016. Germinal Centers. In: RATCLIFFE, M. J. H. (ed.) *Encyclopedia of Immunobiology*. Oxford: Academic Press.
- BOUVET, J. P., BÉLEC, L., PIRÈS, R. & PILLOT, J. 1994. Immunoglobulin G antibodies in human vaginal secretions after parenteral vaccination. *Infect Immun*, 62, 3957-61.
- BOWYER, G., RAMPLING, T., POWLSON, J., MORTER, R., WRIGHT, D., HILL, A. V. S. & EWER, K. J. 2018. Activation-induced Markers Detect Vaccine-Specific CD4+ T Cell Responses Not Measured by Assays Conventionally Used in Clinical Trials. *Vaccines (Basel)*, 6.

- BRAY, F., LAVERSANNE, M., SUNG, H., FERLAY, J., SIEGEL, R. L., SOERJOMATARAM, I. & JEMAL, A. 2024. Global cancer statistics 2022: GLOBOCAN estimates of incidence and mortality worldwide for 36 cancers in 185 countries. *CA: A Cancer Journal for Clinicians*, 74, 229-263.
- BREITBURD, F., KIRNBAUER, R., HUBBERT, N. L., NONNENMACHER, B., TRIN-DINH-DESMARQUET, C., ORTH, G., SCHILLER, J. T. & LOWY, D. R. 1995. Immunization with viruslike particles from cottontail rabbit papillomavirus (CRPV) can protect against experimental CRPV infection. *J Virol*, 69, 3959-63.
- BREITFELD, D., OHL, L., KREMMER, E., ELLWART, J., SALLUSTO, F., LIPP, M. & FÖRSTER, R. 2000. Follicular B helper T cells express CXC chemokine receptor 5, localize to B cell follicles, and support immunoglobulin production. *J Exp Med*, 192, 1545-52.
- BRYNJOLFSSON, S. F., PERSSON BERG, L., OLSEN EKERHULT, T., RIMKUTE, I., WICK, M.-J., MÅRTENSSON, I.-L. & GRIMSHOLM, O. 2018. Long-Lived Plasma Cells in Mice and Men. *Frontiers in Immunology*, 9.
- BUISMAN, A. M., DE ROND, C. G., OZTÜRK, K., TEN HULSCHER, H. I. & VAN BINNENDIJK, R. S. 2009. Long-term presence of memory B-cells specific for different vaccine components. *Vaccine*, 28, 179-86.
- BÜRKLE, A., NIEDERMEIER, M., SCHMITT-GRÄFF, A., WIERDA, W. G., KEATING, M. J. & BURGER, J. A. 2007. Overexpression of the CXCR5 chemokine receptor, and its ligand, CXCL13 in B-cell chronic lymphocytic leukemia. *Blood*, 110, 3316-3325.
- CAMPONESCHI, A., KLÄSENER, K., SUNDELL, T., LUNDQVIST, C., MANNA, P. T., AYOUBZADEH, N., SUNDQVIST, M., THORARINSDOTTIR, K., GATTO, M., VISENTINI, M., ÖNNHEIM, K., ARANBURU, A., FORSMAN, H., EKWALL, O., FOGELSTRAND, L., GJERTSSON, I., RETH, M. & MÅRTENSSON, I.-L. 2022. Human CD38 regulates B cell antigen receptor dynamic organization in normal and malignant B cells. *Journal of Experimental Medicine*, 219.
- CAO, Y., LIU, C., GU, Z., ZHANG, Y., DUAN, Y., ZHANG, Y., ZHANG, H., TANG, K. & HUANG, B. 2017. Microparticles mediate human papillomavirus type 6 or 11 infection of human macrophages. *Cellular & Molecular Immunology*, 14, 395-397.
- CARROLL, M. C. & ISENMAN, D. E. 2012. Regulation of humoral immunity by complement. *Immunity*, 37, 199-207.
- CARTER, J. J., KOUTSKY, L. A., HUGHES, J. P., LEE, S. K., KUYPERS, J., KIVIAT, N. & GALLOWAY, D. A. 2000. Comparison of human papillomavirus types 16, 18, and 6 capsid antibody responses following incident infection. *J Infect Dis*, 181, 1911-9.
- CARTER, M. J., MITCHELL, R. M., MEYER SAUTEUR, P. M., KELLY, D. F. & TRÜCK, J. 2017a. The Antibody-Secreting Cell Response to Infection: Kinetics and Clinical Applications. *Frontiers in Immunology*, 8, 630-630.
- CARTER, M. J., MITCHELL, R. M., MEYER SAUTEUR, P. M., KELLY, D. F. & TRÜCK, J. 2017b. The Antibody-Secreting Cell Response to Infection: Kinetics and Clinical Applications. *Frontiers in Immunology*, 8.
- CESTA, M. F. 2006. Normal structure, function, and histology of the spleen. *Toxicol Pathol*, 34, 455-65.
- CHANG, E. Y., CHEN, C. H., JI, H., WANG, T. L., HUNG, K., LEE, B. P., HUANG, A. Y., KURMAN, R. J., PARDOLL, D. M. & WU, T. 2000. Antigen-specific cancer immunotherapy using a GM-CSF secreting allogeneic tumor cell-based vaccine. *Int J Cancer*, 86, 725-30.
- CHEN, H. T., BHANDoola, A., DIFILIPPANTONIO, M. J., ZHU, J., BROWN, M. J., TAI, X., ROGAKOU, E. P., BROTZ, T. M., BONNER, W. M., RIED, T. & NUSSENZWEIG, A. 2000. Response to RAG-mediated VDJ cleavage by NBS1 and gamma-H2AX. *Science*, 290, 1962-5.

- CHEN, H. Z., TSAI, S. Y. & LEONE, G. 2009. Emerging roles of E2Fs in cancer: an exit from cell cycle control. *Nat Rev Cancer*, 9, 785-97.
- CHEN, J. & ALT, F. W. 1993. Gene rearrangement and B-cell development. *Curr Opin Immunol*, 5, 194-200.
- CHEN, J. J. 2010. Genomic Instability Induced By Human Papillomavirus Oncogenes. *N Am J Med Sci (Boston)*, 3, 43-47.
- CHEN, L., MIZUNO, M. T., SINGHAL, M. C., HU, S. L., GALLOWAY, D. A., HELLSTRÖM, I. & HELLSTRÖM, K. E. 1992. Induction of cytotoxic T lymphocytes specific for a syngeneic tumor expressing the E6 oncoprotein of human papillomavirus type 16. *J Immunol*, 148, 2617-21.
- CHEN, L. P., THOMAS, E. K., HU, S. L., HELLSTRÖM, I. & HELLSTRÖM, K. E. 1991. Human papillomavirus type 16 nucleoprotein E7 is a tumor rejection antigen. *Proc Natl Acad Sci U S A*, 88, 110-4.
- CHEN, M. & WANG, J. 2010. Programmed cell death of dendritic cells in immune regulation. *Immunol Rev*, 236, 11-27.
- CHEN, Z., GAO, X. & YU, D. 2022. Longevity of vaccine protection: Immunological mechanism, assessment methods, and improving strategy. *VIEW*, 3, 20200103.
- CHITADZE, G., BHAT, J., LETTAU, M., JANSSEN, O. & KABELITZ, D. 2013. Generation of Soluble NKG2D Ligands: Proteolytic Cleavage, Exosome Secretion and Functional Implications. *Scandinavian Journal of Immunology*, 78, 120-129.
- CHIU, M. L., GOULET, D. R., TEPLYAKOV, A. & GILLILAND, G. L. 2019. Antibody Structure and Function: The Basis for Engineering Therapeutics. *Antibodies*, 8, 55.
- CHO, H. J., KIM, J. Y., LEE, Y., KIM, J. M., KIM, Y. B., CHUN, T. & OH, Y. K. 2010. Enhanced humoral and cellular immune responses after sublingual immunization against human papillomavirus 16 L1 protein with adjuvants. *Vaccine*, 28, 2598-606.
- CHOTHIA, C., LESK, A. M., TRAMONTANO, A., LEVITT, M., SMITH-GILL, S. J., AIR, G., SHERIFF, S., PADLAN, E. A., DAVIES, D., TULIP, W. R. & ET AL. 1989. Conformations of immunoglobulin hypervariable regions. *Nature*, 342, 877-83.
- CHTANOVA, T., TANGYE, S. G., NEWTON, R., FRANK, N., HODGE, M. R., ROLPH, M. S. & MACKAY, C. R. 2004. T follicular helper cells express a distinctive transcriptional profile, reflecting their role as non-Th1/Th2 effector cells that provide help for B cells. *The Journal of Immunology*, 173, 68-78.
- CINAMON, G., MATLOUBIAN, M., LESNESKI, M. J., XU, Y., LOW, C., LU, T., PROIA, R. L. & CYSTER, J. G. 2004. Sphingosine 1-phosphate receptor 1 promotes B cell localization in the splenic marginal zone. *Nat Immunol*, 5, 713-20.
- CLIFFORD, G. M., FRANCESCHI, S., KEISER, O., SCHÖNI-AFFOLTER, F., LISE, M., DEHLER, S., LEVI, F., MOUSAVI, M., BOUCHARDY, C., WOLFENSBERGER, A., DARLING, K. E., STAEHELIN, C., BERTISCH, B., KUENZLI, E., BERNASCONI, E., PAWLITA, M. & EGGER, M. 2016a. Immunodeficiency and the risk of cervical intraepithelial neoplasia 2/3 and cervical cancer: A nested case-control study in the Swiss HIV cohort study. *Int J Cancer*, 138, 1732-40.
- CLIFFORD, G. M., FRANCESCHI, S., KEISER, O., SCHÖNI-AFFOLTER, F., LISE, M., DEHLER, S., LEVI, F., MOUSAVI, M., BOUCHARDY, C., WOLFENSBERGER, A., DARLING, K. E., STAEHELIN, C., BERTISCH, B., KUENZLI, E., BERNASCONI, E., PAWLITA, M., EGGER, M. & STUDY, O. B. O. T. S. H. C. 2016b. Immunodeficiency and the risk of cervical intraepithelial neoplasia 2/3 and cervical cancer: A nested case-control study in the Swiss HIV cohort study. *International Journal of Cancer*, 138, 1732-1740.

- CLIFFORD, G. M., GALLUS, S., HERRERO, R., MUÑOZ, N., SNIJDERS, P. J. F., VACCARELLA, S., ANH, P. T. H., FERRECCIO, C., HIEU, N. T., MATOS, E., MOLANO, M., RAJKUMAR, R., RONCO, G., DE SANJOSÉ, S., SHIN, H. R., SUKVIKACH, S., THOMAS, J. O., TUNSAKUL, S., MEIJER, C. & FRANCESCHI, S. 2005. Worldwide distribution of human papillomavirus types in cytologically normal women in the International Agency for Research on Cancer HPV prevalence surveys: a pooled analysis. *The Lancet*, 366, 991-998.
- COLEMAN, N., BIRLEY, H. D., RENTON, A. M., HANNA, N. F., RYAIT, B. K., BYRNE, M., TAYLOR-ROBINSON, D. & STANLEY, M. A. 1994. Immunological events in regressing genital warts. *Am J Clin Pathol*, 102, 768-74.
- CONNOR, M. E. & STERN, P. L. 1990. Loss of MHC class-I expression in cervical carcinomas. *Int J Cancer*, 46, 1029-34.
- COOPER, M. D. & ALDER, M. N. 2006. The evolution of adaptive immune systems. *Cell*, 124, 815-22.
- COSTA, A. P., GIRALDO, P. C., COBUCCI, R. N., CONSOLARO, M. L., SOUZA, R. P., CANÁRIO, L. B., MACHADO, P. R., RANDALL MARTINS, R., VIEIRA BAPTISTA, P., JR, J. E. & GONÇALVES, A. K. 2020. Cross-Protective IgG and IgA Antibodies against Oncogenic and Non-Oncogenic HPV Genotypes. *Asian Pac J Cancer Prev*, 21, 2799-2804.
- COUREY-GHAOUZI, A. D., KLEBERG, L. & SUNDLING, C. 2022. Alternative B Cell Differentiation During Infection and Inflammation. *Front Immunol*, 13, 908034.
- COX, R. J., BROKSTAD, K. A., ZUCKERMAN, M. A., WOOD, J. M., HAAHEIM, L. R. & OXFORD, J. S. 1994. An early humoral immune response in peripheral blood following parenteral inactivated influenza vaccination. *Vaccine*, 12, 993-9.
- CRISCI, E., BÁRCENA, J. & MONTOYA, M. 2012. Virus-like particles: The new frontier of vaccines for animal viral infections. *Veterinary Immunology and Immunopathology*, 148, 211-225.
- CROTTY, S. 2011a. Follicular helper CD4 T cells (Tfh). *Annual review of immunology*, 29, 621-663.
- CROTTY, S. 2011b. Follicular Helper CD4 T Cells (TFH). *Annual Review of Immunology*, 29, 621-663.
- CROTTY, S. 2011c. Follicular helper CD4 T cells (TFH). *Annu Rev Immunol*, 29, 621-63.
- CROTTY, S. 2019. T Follicular Helper Cell Biology: A Decade of Discovery and Diseases. *Immunity*, 50, 1132-1148.
- CROTTY, S., FELGNER, P., DAVIES, H., GLIDEWELL, J., VILLARREAL, L. & AHMED, R. 2003. Cutting edge: long-term B cell memory in humans after smallpox vaccination. *J Immunol*, 171, 4969-73.
- CULLEN, A. P., REID, R., CAMPION, M. & LÖRINCZ, A. T. 1991. Analysis of the physical state of different human papillomavirus DNAs in intraepithelial and invasive cervical neoplasm. *J Virol*, 65, 606-12.
- CUMBERBATCH, M. & KIMBER, I. 1995. Tumour necrosis factor-alpha is required for accumulation of dendritic cells in draining lymph nodes and for optimal contact sensitization. *Immunology*, 84, 31-5.
- CUTRONA, G., DONO, M., PASTORINO, S., ULIVI, M., BURGIO, V. L., ZUPO, S., RONCELLA, S. & FERRARINI, M. 1997. The propensity to apoptosis of centrocytes and centroblasts correlates with elevated levels of intracellular myc protein. *Eur J Immunol*, 27, 234-8.
- DAN, J. M., LINDESTAM ARLEHAMN, C. S., WEISKOPF, D., DA SILVA ANTUNES, R., HAVENAR-DAUGHTON, C., REISS, S. M., BRIGGER, M., BOTHWELL, M., SETTE, A. & CROTTY, S. 2016. A Cytokine-Independent Approach To Identify Antigen-Specific Human Germinal Center T Follicular Helper Cells and Rare Antigen-Specific CD4+ T Cells in Blood. *J Immunol*, 197, 983-93.

- DAY, P. M., LOWY, D. R. & SCHILLER, J. T. 2003. Papillomaviruses infect cells via a clathrin-dependent pathway. *Virology*, 307, 1-11.
- DAY, P. M., LOWY, D. R. & SCHILLER, J. T. 2008. Heparan sulfate-independent cell binding and infection with furin-precleaved papillomavirus capsids. *J Virol*, 82, 12565-8.
- DE VINCENZO, R., CONTE, C., RICCI, C., SCAMBIA, G. & CAPELLI, G. 2014. Long-term efficacy and safety of human papillomavirus vaccination. *Int J Womens Health*, 6, 999-1010.
- DEENICK, E. K., CHAN, A., MA, C. S., GATTO, D., SCHWARTZBERG, P. L., BRINK, R. & TANGYE, S. G. 2010. Follicular helper T cell differentiation requires continuous antigen presentation that is independent of unique B cell signaling. *Immunity*, 33, 241-253.
- DIDIERLAURENT, A. M., MOREL, S., LOCKMAN, L., GIANNINI, S. L., BISTEAU, M., CARLSEN, H., KIELLAND, A., VOSTERS, O., VANDERHEYDE, N., SCHIAVETTI, F., LAROCQUE, D., VAN MECHELEN, M. & GARÇON, N. 2009. AS04, an aluminum salt- and TLR4 agonist-based adjuvant system, induces a transient localized innate immune response leading to enhanced adaptive immunity. *J Immunol*, 183, 6186-97.
- DIGIUSEPPE, S., BIENKOWSKA-HABA, M. & SAPP, M. 2016. Human Papillomavirus Entry: Hiding in a Bubble. *Journal of virology*, 90, 8032-8035.
- DILLON, S., SASAGAWA, T., CRAWFORD, A., PRESTIDGE, J., INDER, M. K., JERRAM, J., MERCER, A. A. & HIBMA, M. 2007. Resolution of cervical dysplasia is associated with T-cell proliferative responses to human papillomavirus type 16 E2. *J Gen Virol*, 88, 803-813.
- DING, H., CAI, J., MAO, M., FANG, Y., HUANG, Z., JIA, J., LI, T., XU, L., WANG, J., ZHOU, J., YANG, Q. & WANG, Z. 2014. Tumor-associated macrophages induce lymphangiogenesis in cervical cancer via interaction with tumor cells. *Apmis*, 122, 1059-69.
- DOBSON, S. R., MCNEIL, S., DIONNE, M., DAWAR, M., OGILVIE, G., KRAJDEN, M., SAUVAGEAU, C., SCHEIFELE, D. W., KOLLMANN, T. R., HALPERIN, S. A., LANGLEY, J. M., BETTINGER, J. A., SINGER, J., MONEY, D., MILLER, D., NAUS, M., MARRA, F. & YOUNG, E. 2013. Immunogenicity of 2 doses of HPV vaccine in younger adolescents vs 3 doses in young women: a randomized clinical trial. *Jama*, 309, 1793-802.
- DONG, Y., PI, X., BARTELS-BURGAHN, F., SALTUKOGLU, D., LIANG, Z., YANG, J., ALT, F. W., RETH, M. & WU, H. 2022. Structural principles of B cell antigen receptor assembly. *Nature*, 612, 156-161.
- DOORBAR, J. 2007. Papillomavirus life cycle organization and biomarker selection. *Dis Markers*, 23, 297-313.
- DOORBAR, J., QUINT, W., BANKS, L., BRAVO, I. G., STOLER, M., BROKER, T. R. & STANLEY, M. A. 2012. The biology and life-cycle of human papillomaviruses. *Vaccine*, 30 Suppl 5, F55-70.
- DORWAL, P., THAKUR, R. & RAWAT, S. 2014. CD138 expression in plasma cells is volatile and time-lag dependent. *The Egyptian Journal of Haematology*, 39, 258-259.
- DUARTE, J. H. 2016. Functional switching. *Nature Immunology*, 17, S12-S12.
- DUNN-WALTERS, D. K. & O'HARE, J. S. 2019. Older Human B Cells and Antibodies. *Handbook of Immunosenescence*, 785-819.
- DUY, C., YU, J. J., NAHAR, R., SWAMINATHAN, S., KWEON, S. M., POLO, J. M., VALLS, E., KLEMM, L., SHOJAEI, S., CERCHIETTI, L., SCHUH, W., JACK, H. M., HURTZ, C., RAMEZANI-RAD, P., HERZOG, S., JUMAA, H., KOEFFLER, H. P., DE ALBORAN, I. M., MELNICK, A. M., YE, B. H. & MUSCHEN, M. 2010. BCL6 is critical for the development of a diverse primary B cell repertoire. *J Exp Med*, 207, 1209-21.

- EDDAHRI, F., DENANGLAIRE, S., BUREAU, F., SPOLSKI, R., LEONARD, W. J., LEO, O. & ANDRIS, F. 2009. Interleukin-6/STAT3 signaling regulates the ability of naive T cells to acquire B-cell help capacities. *Blood, The Journal of the American Society of Hematology*, 113, 2426-2433.
- EGAWA, N., EGAWA, K., GRIFFIN, H. & DOORBAR, J. 2015. Human Papillomaviruses; Epithelial Tropisms, and the Development of Neoplasia. *Viruses*, 7, 3863-3890.
- EINSTEIN, M. H., BARON, M., LEVIN, M. J., CHATTERJEE, A., EDWARDS, R. P., ZEPP, F., CARLETTI, I., DESSY, F. J., TROFA, A. F., SCHUIND, A., DUBIN, G. & GROUP, H. P. V. S. 2009. Comparison of the immunogenicity and safety of Cervarix and Gardasil human papillomavirus (HPV) cervical cancer vaccines in healthy women aged 18-45 years. *Hum Vaccin*, 5, 705-19.
- EINSTEIN, M. H., TAKACS, P., CHATTERJEE, A., SPERLING, R. S., CHAKHTOURA, N., BLATTER, M. M., LALEZARI, J., DAVID, M. P., LIN, L., STRUYF, F. & DUBIN, G. 2014. Comparison of long-term immunogenicity and safety of human papillomavirus (HPV)-16/18 AS04-adjuvanted vaccine and HPV-6/11/16/18 vaccine in healthy women aged 18-45 years: end-of-study analysis of a Phase III randomized trial. *Hum Vaccin Immunother*, 10, 3435-45.
- ELGUETA, R., BENSON, M. J., DE VRIES, V. C., WASIUK, A., GUO, Y. & NOELLE, R. J. 2009. Molecular mechanism and function of CD40/CD40L engagement in the immune system. *Immunol Rev*, 229, 152-72.
- ELHANATI, Y., SETHNA, Z., MARCOU, Q., CALLAN, C. G., MORA, T. & WALCZAK, A. M. 2015. Inferring processes underlying B-cell repertoire diversity. *Philosophical Transactions of the Royal Society B: Biological Sciences*, 370, 20140243.
- ELLINGSON, M. K., SHEIKHA, H., NYHAN, K., OLIVEIRA, C. R. & NICCOLAI, L. M. 2023. Human papillomavirus vaccine effectiveness by age at vaccination: A systematic review. *Hum Vaccin Immunother*, 19, 2239085.
- ELLYARD, J. I., AVERY, D. T., PHAN, T. G., HARE, N. J., HODGKIN, P. D. & TANGYE, S. G. 2004. Antigen-selected, immunoglobulin-secreting cells persist in human spleen and bone marrow. *Blood*, 103, 3805-12.
- ENK, A. H., ANGELONI, V. L., UDEY, M. C. & KATZ, S. I. 1993. Inhibition of Langerhans cell antigen-presenting function by IL-10. A role for IL-10 in induction of tolerance. *J Immunol*, 151, 2390-8.
- ESSONE, P. N., KALSDORF, B., CHEGOU, N. N., LOXTON, A. G., KRIEL, M., PREYER, R., ERNST, M., WALZL, G. & LANGE, C. 2014. Bifunctional T-cell-derived cytokines for the diagnosis of tuberculosis and treatment monitoring. *Respiration*, 88, 251-61.
- EVANS, C., BAUER, S., GRUBERT, T., BRUCKER, C., BAUR, S., HEEG, K., WAGNER, H. & LIPFORD, G. B. 1996. HLA-A2-restricted peripheral blood cytolytic T lymphocyte response to HPV type 16 proteins E6 and E7 from patients with neoplastic cervical lesions. *Cancer Immunol Immunother*, 42, 151-60.
- EVANS, E. M., MAN, S., EVANS, A. S. & BORYSIEWICZ, L. K. 1997. Infiltration of cervical cancer tissue with human papillomavirus-specific cytotoxic T-lymphocytes. *Cancer Res*, 57, 2943-50.
- FAGARASAN, S. & HONJO, T. 2000. T-Independent immune response: new aspects of B cell biology. *Science*, 290, 89-92.
- FERRIS, D. G., SAMAKOSES, R., BLOCK, S. L., LAZCANO-PONCE, E., RESTREPO, J. A., MEHLSSEN, J., CHATTERJEE, A., IVERSEN, O. E., JOSHI, A., CHU, J. L., KRICK, A. L., SAAH, A. & DAS, R. 2017. 4-Valent Human Papillomavirus (4vHPV) Vaccine in Preadolescents and Adolescents After 10 Years. *Pediatrics*, 140.
- FIFE, K. H., WHEELER, C. M., KOUTSKY, L. A., BARR, E., BROWN, D. R., SCHIFF, M. A., KIVIAT, N. B., JANSEN, K. U., BARBER, H., SMITH, J. F., TADESSE, A., GIACOLETTI, K., SMITH, P. R., SUHR, G.

- & JOHNSON, D. A. 2004. Dose-ranging studies of the safety and immunogenicity of human papillomavirus Type 11 and Type 16 virus-like particle candidate vaccines in young healthy women. *Vaccine*, 22, 2943-52.
- FRANZ, B., MAY, K. F., JR., DRANOFF, G. & WUCHERPFENNIG, K. 2011. Ex vivo characterization and isolation of rare memory B cells with antigen tetramers. *Blood*, 118, 348-57.
- FRAZER, I. 2007. Correlating immunity with protection for HPV infection. *Int J Infect Dis*, 11 Suppl 2, S10-6.
- FRISCH, S. M. & FRANCIS, H. 1994. Disruption of epithelial cell-matrix interactions induces apoptosis. *J Cell Biol*, 124, 619-26.
- FRÖLICH, D., GIESECKE, C., MEI, H. E., REITER, K., DARIDON, C., LIPSKY, P. E. & DÖRNER, T. 2010. Secondary immunization generates clonally related antigen-specific plasma cells and memory B cells. *J Immunol*, 185, 3103-10.
- GABRIELLI, E., PERICOLINI, E., CENCI, E., ORTELLI, F., MAGLIANI, W., CIOCIOLA, T., BISTONI, F., CONTI, S., VECCHIARELLI, A. & POLONELLI, L. 2009. Antibody complementarity-determining regions (CDRs): a bridge between adaptive and innate immunity. *PLoS One*, 4, e8187.
- GALSON, J. D., POLLARD, A. J., TRÜCK, J. & KELLY, D. F. 2014. Studying the antibody repertoire after vaccination: practical applications. *Trends Immunol*, 35, 319-31.
- GALSON, J. D., TRÜCK, J., FOWLER, A., CLUTTERBUCK, E. A., MÜNZ, M., CERUNDOLO, V., REINHARD, C., VAN DER MOST, R., POLLARD, A. J., LUNTER, G. & KELLY, D. F. 2015. Analysis of B Cell Repertoire Dynamics Following Hepatitis B Vaccination in Humans, and Enrichment of Vaccine-specific Antibody Sequences. *EBioMedicine*, 2, 2070-9.
- GARCIA-IGLESIAS, T., DEL TORO-ARREOLA, A., ALBARRAN-SOMOZA, B., DEL TORO-ARREOLA, S., SANCHEZ-HERNANDEZ, P. E., RAMIREZ-DUEÑAS, M. G., BALDERAS-PEÑA, L. M., BRAVO-CUELLAR, A., ORTIZ-LAZARENO, P. C. & DANERI-NAVARRO, A. 2009. Low NKp30, NKp46 and NKG2D expression and reduced cytotoxic activity on NK cells in cervical cancer and precursor lesions. *BMC Cancer*, 9, 186.
- GARRAUD, O., BORHIS, G., BADR, G., DEGRELLE, S., POZZETTO, B., COGNASSE, F. & RICHARD, Y. 2012. Revisiting the B-cell compartment in mouse and humans: more than one B-cell subset exists in the marginal zone and beyond. *BMC Immunol*, 13, 63.
- GARZETTI, G. G., CIAVATTINI, A., GOTERI, G., DE NICTOLIS, M., MENSIO, S., MUZZIOLI, M. & FABRIS, N. 1995. HPV DNA positivity and natural killer cell activity in the clinical outcome of mild cervical dysplasia: integration between virus and immune system. *Gynecol Obstet Invest*, 39, 130-5.
- GEISBERGER, R., LAMERS, M. & ACHATZ, G. 2006. The riddle of the dual expression of IgM and IgD. *Immunology*, 118, 429-37.
- GHEBRE, R. G., GROVER, S., XU, M. J., CHUANG, L. T. & SIMONDS, H. 2017. Cervical cancer control in HIV-infected women: Past, present and future. *Gynecol Oncol Rep*, 21, 101-108.
- GILCA, V., SAUVAGEAU, C., PANICKER, G., DE SERRES, G., SCHILLER, J., OUAKKI, M. & UNGER, E. R. 2019. Long intervals between two doses of HPV vaccines and magnitude of the immune response: a post hoc analysis of two clinical trials. *Hum Vaccin Immunother*, 15, 1980-1985.
- GIROGLOU, T., FLORIN, L., SCHÄFER, F., STREECK, R. E. & SAPP, M. 2001. Human papillomavirus infection requires cell surface heparan sulfate. *J Virol*, 75, 1565-70.
- GIULIANO, A. R., JOURA, E. A., GARLAND, S. M., HUH, W. K., IVERSEN, O.-E., KJAER, S. K., FERENCZY, A., KURMAN, R. J., RONNETT, B. M., STOLER, M. H., BAUTISTA, O. M., MOELLER, E., RITTER, M., SHIELDS, C. & LUXEMBOURG, A. 2019a. Nine-valent HPV vaccine efficacy against related

- diseases and definitive therapy: comparison with historic placebo population. *Gynecologic Oncology*, 154, 110-117.
- GIULIANO, A. R., JOURA, E. A., GARLAND, S. M., HUH, W. K., IVERSEN, O. E., KJAER, S. K., FERENCZY, A., KURMAN, R. J., RONNETT, B. M., STOLER, M. H., BAUTISTA, O. M., MOELLER, E., RITTER, M., SHIELDS, C. & LUXEMBOURG, A. 2019b. Nine-valent HPV vaccine efficacy against related diseases and definitive therapy: comparison with historic placebo population. *Gynecol Oncol*, 154, 110-117.
- GIULIANO, A. R., LEE, J. H., FULP, W., VILLA, L. L., LAZCANO, E., PAPENFUSS, M. R., ABRAHAMSEN, M., SALMERON, J., ANIC, G. M., ROLLISON, D. E. & SMITH, D. 2011. Incidence and clearance of genital human papillomavirus infection in men (HIM): a cohort study. *Lancet*, 377, 932-40.
- GIULIANO, A. R., VISCIDI, R., TORRES, B. N., INGLES, D. J., SUDENGA, S. L., VILLA, L. L., BAGGIO, M. L., ABRAHAMSEN, M., QUITERIO, M., SALMERON, J. & LAZCANO-PONCE, E. 2015. Seroconversion Following Anal and Genital HPV Infection in Men: The HIM Study. *Papillomavirus research (Amsterdam, Netherlands)*, 1, 109-115.
- GLEW, S. S., DUGGAN-KEEN, M., CABRERA, T. & STERN, P. L. 1992. HLA Class II Antigen Expression in Human Papillomavirus-associated Cervical Cancer¹. *Cancer Research*, 52, 4009-4016.
- GOENKA, R., BARNETT, L. G., SILVER, J. S., O'NEILL, P. J., HUNTER, C. A., CANCRO, M. P. & LAUFER, T. M. 2011. Cutting edge: dendritic cell-restricted antigen presentation initiates the follicular helper T cell program but cannot complete ultimate effector differentiation. *The Journal of Immunology*, 187, 1091-1095.
- GONÇALVES, A. K., GIRALDO, P. C., FARIAS, K. J., MACHADO, P. R., COSTA, A. P., DE SOUZA, L. C., CRISPIM, J. C., ELEUTÉRIO, J., JR. & WITKIN, S. S. 2016. Characterization of Immunoglobulin A/G Responses During 3 Doses of the Human Papillomavirus-16/18 ASO4-Adjuvanted Vaccine. *Sex Transm Dis*, 43, 335-9.
- GORDON, S. & PLÜDDEMANN, A. 2017. Tissue macrophages: heterogeneity and functions. *BMC Biology*, 15, 53.
- GORDON, S. R., MAUTE, R. L., DULKEN, B. W., HUTTER, G., GEORGE, B. M., MCCRACKEN, M. N., GUPTA, R., TSAI, J. M., SINHA, R., COREY, D., RING, A. M., CONNOLLY, A. J. & WEISSMAN, I. L. 2017. PD-1 expression by tumour-associated macrophages inhibits phagocytosis and tumour immunity. *Nature*, 545, 495-499.
- GRAHAM, S. V. 2010. Human papillomavirus: gene expression, regulation and prospects for novel diagnostic methods and antiviral therapies. *Future Microbiol*, 5, 1493-506.
- GRAHAM, S. V. 2017. Keratinocyte Differentiation-Dependent Human Papillomavirus Gene Regulation. *Viruses* [Online], 9.
- GRANATO, A., CHEN, Y. & WESEMANN, D. R. 2015. Primary immunoglobulin repertoire development: time and space matter. *Curr Opin Immunol*, 33, 126-31.
- GRAY, D., SIEPMANN, K., VAN ESSEN, D., POUDRIER, J., WYKES, M., JAINANDUNSING, S., BERGTHORSDOTTIR, S. & DULLFORCE, P. 1996. B-T Lymphocyte Interactions in the Generation and Survival of Memory Cells. *Immunological Reviews*, 150, 45-61.
- GROUP, F. I. I. S., DILLNER, J., KJAER, S. K., WHEELER, C. M., SIGURDSSON, K., IVERSEN, O. E., HERNANDEZ-AVILA, M., PEREZ, G., BROWN, D. R., KOUTSKY, L. A., TAY, E. H., GARCIA, P., AULT, K. A., GARLAND, S. M., LEODOLTER, S., OLSSON, S. E., TANG, G. W., FERRIS, D. G., PAAVONEN, J., LEHTINEN, M., STEBEN, M., BOSCH, F. X., JOURA, E. A., MAJEWSKI, S., MUNOZ, N., MYERS, E. R., VILLA, L. L., TADDEO, F. J., ROBERTS, C., TADESSE, A., BRYAN, J. T., MAANSSON, R., LU, S., VUOCOLO, S., HESLEY, T. M., BARR, E. & HAUPT, R. 2010. Four year efficacy of prophylactic human papillomavirus quadrivalent vaccine against low grade

cervical, vulvar, and vaginal intraepithelial neoplasia and anogenital warts: randomised controlled trial. *BMJ*, 341, c3493.

- GROUP, F. I. S. 2007. Quadrivalent vaccine against human papillomavirus to prevent high-grade cervical lesions. *The New England journal of medicine*, 356, 1915-1927.
- GUEVARA, A., CABELLO, R., WOELBER, L., MOREIRA, E. D., JOURA, E., REICH, O., SHIELDS, C., ELLISON, M. C., JOSHI, A. & LUXEMBOURG, A. 2017. Antibody persistence and evidence of immune memory at 5 years following administration of the 9-valent HPV vaccine. *Vaccine*, 35, 5050-5057.
- HAAS, K. M., POE, J. C., STEEBER, D. A. & TEDDER, T. F. 2005. B-1a and B-1b cells exhibit distinct developmental requirements and have unique functional roles in innate and adaptive immunity to *S. pneumoniae*. *Immunity*, 23, 7-18.
- HAGENSEE, M. E., KOUTSKY, L. A., LEE, S. K., GRUBERT, T., KUYPERS, J., KIVIAT, N. B. & GALLOWAY, D. A. 2000. Detection of cervical antibodies to human papillomavirus type 16 (HPV-16) capsid antigens in relation to detection of HPV-16 DNA and cervical lesions. *J Infect Dis*, 181, 1234-9.
- HALE, J. S. & AHMED, R. 2015. Memory T Follicular Helper CD4 T Cells. *Frontiers in Immunology*, 6.
- HALLILEY, J. L., TIPTON, C. M., LIESVELD, J., ROSENBERG, A. F., DARCE, J., GREGORETTI, I. V., POPOVA, L., KAMINISKI, D., FUCILE, C. F., ALBIZUA, I., KYU, S., CHIANG, K. Y., BRADLEY, K. T., BURACK, R., SLIFKA, M., HAMMARLUND, E., WU, H., ZHAO, L., WALSH, E. E., FALSEY, A. R., RANDALL, T. D., CHEUNG, W. C., SANZ, I. & LEE, F. E. 2015. Long-Lived Plasma Cells Are Contained within the CD19(-)CD38(hi)CD138(+) Subset in Human Bone Marrow. *Immunity*, 43, 132-45.
- HANDISURYA, A., DAY, P. M., THOMPSON, C. D., BONELLI, M., LOWY, D. R. & SCHILLER, J. T. 2014. Strain-specific properties and T cells regulate the susceptibility to papilloma induction by *Mus musculus* papillomavirus 1. *PLoS Pathog*, 10, e1004314.
- HAO, Y., YUAN, J. L., ABUDULA, A., HASIMU, A., KADEER, N. & GUO, X. 2014. TLR9 expression in uterine cervical lesions of Uyghur women correlate with cervical cancer progression and selective silencing of human papillomavirus 16 E6 and E7 oncoproteins in vitro. *Asian Pac J Cancer Prev*, 15, 5867-72.
- HARDER, T., WICHMANN, O., KLUG, S. J., VAN DER SANDE, M. A. B. & WIESE-POSSELT, M. 2018. Efficacy, effectiveness and safety of vaccination against human papillomavirus in males: a systematic review. *BMC Med*, 16, 110.
- HARDY, R. R. & HAYAKAWA, K. 2001. B Cell Development Pathways. *Annual Review of Immunology*, 19, 595-621.
- HASHIRA, S., OKITSU-NEGISHI, S. & YOSHINO, K. 2000. Placental transfer of IgG subclasses in a Japanese population. *Pediatrics International*, 42, 337-342.
- HAYAKAWA, K., ISHII, R., YAMASAKI, K., KISHIMOTO, T. & HARDY, R. R. 1987. Isolation of high-affinity memory B cells: phycoerythrin as a probe for antigen-binding cells. *Proc Natl Acad Sci U S A*, 84, 1379-83.
- HAYNES, N. M., ALLEN, C. D., LESLEY, R., ANSEL, K. M., KILLEEN, N. & CYSTER, J. G. 2007. Role of CXCR5 and CCR7 in follicular Th cell positioning and appearance of a programmed cell death gene-1high germinal center-associated subpopulation. *The Journal of Immunology*, 179, 5099-5108.
- HEBEIS, B. J., KLENOVSEK, K., ROHWER, P., RITTER, U., SCHNEIDER, A., MACH, M. & WINKLER, T. H. 2004. Activation of virus-specific memory B cells in the absence of T cell help. *J Exp Med*, 199, 593-602.

- HENTGES, F. 1994. B lymphocyte ontogeny and immunoglobulin production. *Clin Exp Immunol*, 97 Suppl 1, 3-9.
- HERNÁNDEZ-ÁVILA, M., TORRES-IBARRA, L., STANLEY, M., SALMERÓN, J., CRUZ-VALDEZ, A., MUÑOZ, N., HERRERO, R., VILLASEÑOR-RUÍZ, I. F. & LAZCANO-PONCE, E. 2016. Evaluation of the immunogenicity of the quadrivalent HPV vaccine using 2 versus 3 doses at month 21: An epidemiological surveillance mechanism for alternate vaccination schemes. *Human vaccines & immunotherapeutics*, 12, 30-38.
- HERRIN, D. M., COATES, E. E., COSTNER, P. J., KEMP, T. J., NASON, M. C., SAHARIA, K. K., PAN, Y., SARWAR, U. N., HOLMAN, L., YAMSHCHIKOV, G., KOUP, R. A., PANG, Y. Y. S., SEDER, R. A., SCHILLER, J. T., GRAHAM, B. S., PINTO, L. A. & LEDGERWOOD, J. E. 2014. Comparison of adaptive and innate immune responses induced by licensed vaccines for Human Papillomavirus. *Human vaccines & immunotherapeutics*, 10, 3446-3454.
- HICAR, M. D., KALAMS, S. A., SPEARMAN, P. W. & CROWE, J. E., JR. 2010. Emerging studies of human HIV-specific antibody repertoires. *Vaccine*, 28 Suppl 2, B18-23.
- HIGDON, L. E., CAIN, C. J., COLDEN, M. A. & MALTZMAN, J. S. 2019. Optimization of single-cell plate sorting for high throughput sequencing applications. *J Immunol Methods*, 466, 17-23.
- HOEHN, K. B., FOWLER, A., LUNTER, G. & PYBUS, O. G. 2016. The Diversity and Molecular Evolution of B-Cell Receptors during Infection. *Molecular Biology and Evolution*, 33, 1147-1157.
- HOES, J., PASMANS, H., SCHURINK-VAN 'T KLOOSTER, T. M., VAN DER KLIS, F. R. M., DONKEN, R., BERKHOF, J. & DE MELKER, H. E. 2022. Review of long-term immunogenicity following HPV vaccination: Gaps in current knowledge. *Hum Vaccin Immunother*, 18, 1908059.
- HOPMAN, A. H., THEELEN, W., HOMMELBERG, P. P., KAMPS, M. A., HERRINGTON, C. S., MORRISON, L. E., SPEEL, E. J., SMEDTS, F. & RAMAEKERS, F. C. 2006. Genomic integration of oncogenic HPV and gain of the human telomerase gene TERC at 3q26 are strongly associated events in the progression of uterine cervical dysplasia to invasive cancer. *J Pathol*, 210, 412-9.
- HORVATH, C. A., BOULET, G. A., RENOUX, V. M., DELVENNE, P. O. & BOGERS, J. P. 2010. Mechanisms of cell entry by human papillomaviruses: an overview. *Virology*, 7, 11.
- HOULIHAN, C. F., LARKE, N. L., WATSON-JONES, D., SMITH-MCCUNE, K. K., SHIBOSKI, S., GRAVITT, P. E., SMITH, J. S., KUHN, L., WANG, C. & HAYES, R. 2012. Human papillomavirus infection and increased risk of HIV acquisition. A systematic review and meta-analysis. *AIDS (London, England)*, 26, 2211-2222.
- HOVEN, M. Y., DE LEIJ, L., KEIJ, J. F. & THE, T. H. 1989. Detection and isolation of antigen-specific B cells by the fluorescence activated cell sorter (FACS). *J Immunol Methods*, 117, 275-84.
- HSU, H.-C., YANG, P., WANG, J., WU, Q., MYERS, R., CHEN, J., YI, J., GUENTERT, T., TOUSSON, A. & STANUS, A. L. 2008. Interleukin 17-producing T helper cells and interleukin 17 orchestrate autoreactive germinal center development in autoimmune BXD2 mice. *Nature immunology*, 9, 166-175.
- HUBER, J. E., AHLFELD, J., SCHECK, M. K., ZAUCHA, M., WITTER, K., LEHMANN, L., KARIMZADEH, H., PRITSCH, M., HOELSCHER, M., VON SONNENBURG, F., DICK, A., BARBA-SPAETH, G., KRUG, A. B., ROTHENFUSSE, S. & BAUMJOHANN, D. 2020. Dynamic changes in circulating T follicular helper cell composition predict neutralising antibody responses after yellow fever vaccination. *Clin Transl Immunology*, 9, e1129.
- HUO, Z., BISSETT, S. L., GIEMZA, R., BEDDOWS, S., OESER, C. & LEWIS, D. J. 2012. Systemic and mucosal immune responses to sublingual or intramuscular human papilloma virus antigens in healthy female volunteers. *PLoS One*, 7, e33736.

- HWANG, J.-R., BYEON, Y., KIM, D. & PARK, S.-G. 2020. Recent insights of T cell receptor-mediated signaling pathways for T cell activation and development. *Experimental & Molecular Medicine*, 52, 750-761.
- HYLAND, L., SANGSTER, M., SEALY, R. & COLECLOUGH, C. 1994. Respiratory virus infection of mice provokes a permanent humoral immune response. *Journal of virology*, 68, 6083-6086.
- ILLUMINA. *Understanding Illumina Quality Scores* [Online]. Available: https://www.illumina.com/content/dam/illumina-marketing/documents/products/technotes/technote_understanding_quality_scores.pdf [Accessed May to July 2024].
- INGLIS, S., SHAW, A. & KOENIG, S. 2006. Chapter 11: HPV vaccines: commercial research & development. *Vaccine*, 24 Suppl 3, S3/99-105.
- IONESCU, L. & URSCHEL, S. 2019. Memory B Cells and Long-lived Plasma Cells. *Transplantation*, 103, 890-898.
- IVERSEN, O. E., MIRANDA, M. J., ULIED, A., SOERDAL, T., LAZARUS, E., CHOKEPHAIBULKIT, K., BLOCK, S. L., SKRIVANEK, A., NUR AZURAH, A. G., FONG, S. M., DVORAK, V., KIM, K. H., CESTERO, R. M., BERKOVITCH, M., CEYHAN, M., ELLISON, M. C., RITTER, M. A., YUAN, S. S., DINUBILE, M. J., SAAH, A. J. & LUXEMBOURG, A. 2016. Immunogenicity of the 9-Valent HPV Vaccine Using 2-Dose Regimens in Girls and Boys vs a 3-Dose Regimen in Women. *Jama*, 316, 2411-2421.
- JAFFE, E. S., HARRIS, N. L., STEIN, H. & ISAACSON, P. G. 2008. Classification of lymphoid neoplasms: the microscope as a tool for disease discovery. *Blood*, 112, 4384-99.
- JAKOB, T. & UDEY, M. C. 1998. Regulation of E-cadherin-mediated adhesion in Langerhans cell-like dendritic cells by inflammatory mediators that mobilize Langerhans cells in vivo. *J Immunol*, 160, 4067-73.
- JANETZKI, S. 2015. Immune monitoring technology primer: the enzyme-linked immunospot (Elispot) and Fluorospot assay. *Journal for Immunotherapy of Cancer*, 3, 30.
- JANEWAY CA JR, T. P., WALPORT M, ET AL. 2001a. The Immune System in Health and Disease. 5th edition. New York: Garland Science; 2001. T-cell receptor gene rearrangement. *Immunobiology*. New York and London: Garland Science.
- JANEWAY CA JR, T. P., WALPORT M, ET AL. 2001b. *Immunobiology: The Immune System in Health and Disease. 5th edition*, New York, Garland Science.
- JERNE, N. K. 1955. THE NATURAL-SELECTION THEORY OF ANTIBODY FORMATION. *Proceedings of the National Academy of Sciences*, 41, 849.
- JOAG, V. R., MCKINNON, L. R., LIU, J., KIDANE, S. T., YUDIN, M. H., NYANGA, B., KIMWAKI, S., BESEL, K. E., OBILA, J. O., HUIBNER, S., OYUGI, J. O., ARTHOS, J., ANZALA, O., KIMANI, J., OSTROWSKI, M. A., KAUL, R. & TORONTO, H. I. V. R. G. 2016. Identification of preferential CD4+ T-cell targets for HIV infection in the cervix. *Mucosal Immunology*, 9, 1-12.
- JOHNSON, K. M., KINES, R. C., ROBERTS, J. N., LOWY, D. R., SCHILLER, J. T. & DAY, P. M. 2009. Role of heparan sulfate in attachment to and infection of the murine female genital tract by human papillomavirus. *J Virol*, 83, 2067-74.
- JOHNSTON, R. J., POHOLEK, A. C., DITORO, D., YUSUF, I., ETO, D., BARNETT, B., DENT, A. L., CRAFT, J. & CROTTY, S. 2009. Bcl6 and Blimp-1 are reciprocal and antagonistic regulators of T follicular helper cell differentiation. *Science*, 325, 1006-1010.
- JORGE ISMAEL, C.-S., ANA ROSA MUÑOZ, D., MARÍA LILIA, D.-L., JUAN JOSÉ DE LA, C.-L. & JULIETA, L.-H. 2017. B Lymphocyte as a Target of Bacterial Infections. In: GHEORGHITA, I. (ed.) *Lymphocyte Updates*. Rijeka: IntechOpen.

- JOSHI, S., ANANTHARAMAN, D., MUWONGE, R., BHATLA, N., PANICKER, G., BUTT, J., RANI REDDY POLI, U., MALVI, S. G., ESMY, P. O., LUCAS, E., VERMA, Y., SHAH, A., ZOMAWIA, E., PIMPLE, S., JAYANT, K., HINGMIRE, S., CHIWATE, A., DIVATE, U., VASHIST, S., MISHRA, G., JADHAV, R., SIDDIQI, M., SANKARAN, S., PILLAI RAMESHWARI AMMAL KANNAN, T., KARTHA, P., SHASTRI, S. S., SAUVAGET, C., RADHAKRISHNA PILLAI, M., WATERBOER, T., MÜLLER, M., SEHR, P., UNGER, E. R., SANKARANARAYANAN, R. & BASU, P. 2023. Evaluation of immune response to single dose of quadrivalent HPV vaccine at 10-year post-vaccination. *Vaccine*, 41, 236-245.
- JOURA, E. A., GIULIANO, A. R., IVERSEN, O.-E., BOUCHARD, C., MAO, C., MEHLSSEN, J., MOREIRA, E. D., JR., NGAN, Y., PETERSEN, L. K., LAZCANO-PONCE, E., PITISUTTITHUM, P., RESTREPO, J. A., STUART, G., WOELBER, L., YANG, Y. C., CUZICK, J., GARLAND, S. M., HUH, W., KJAER, S. K., BAUTISTA, O. M., CHAN, I. S. F., CHEN, J., GESSER, R., MOELLER, E., RITTER, M., VUOCOLO, S., LUXEMBOURG, A. & BROAD SPECTRUM, H. P. V. V. S. 2015. A 9-valent HPV vaccine against infection and intraepithelial neoplasia in women. *The New England journal of medicine*, 372, 711-723.
- JOYCE, J. G., TUNG, J. S., PRZYSIECKI, C. T., COOK, J. C., LEHMAN, E. D., SANDS, J. A., JANSEN, K. U. & KELLER, P. M. 1999. The L1 major capsid protein of human papillomavirus type 11 recombinant virus-like particles interacts with heparin and cell-surface glycosaminoglycans on human keratinocytes. *J Biol Chem*, 274, 5810-22.
- KAJITANI, N., SATSUKA, A., KAWATE, A. & SAKAI, H. 2012. Productive Lifecycle of Human Papillomaviruses that Depends Upon Squamous Epithelial Differentiation. *Front Microbiol*, 3, 152.
- KAMOLRATANAKUL, S. & PITISUTTITHUM, P. 2021. Human Papillomavirus Vaccine Efficacy and Effectiveness against Cancer. *Vaccines (Basel)*, 9.
- KÄMPER, N., DAY, P. M., NOWAK, T., SELINKA, H. C., FLORIN, L., BOLSCHER, J., HILBIG, L., SCHILLER, J. T. & SAPP, M. 2006. A membrane-destabilizing peptide in capsid protein L2 is required for egress of papillomavirus genomes from endosomes. *J Virol*, 80, 759-68.
- KANTOR, A. B., STALL, A. M., ADAMS, S., HERZENBERG, L. A. & HERZENBERG, L. A. 1992. Differential development of progenitor activity for three B-cell lineages. *Proc Natl Acad Sci U S A*, 89, 3320-4.
- KASUKAWA, H., HOWLEY, P. M. & BENSON, J. D. 1998. A fifteen-amino-acid peptide inhibits human papillomavirus E1-E2 interaction and human papillomavirus DNA replication in vitro. *J Virol*, 72, 8166-73.
- KAWABE, T., NAKA, T., YOSHIDA, K., TANAKA, T., FUJIWARA, H., SUEMATSU, S., YOSHIDA, N., KISHIMOTO, T. & KIKUTANI, H. 1994. The immune responses in CD40-deficient mice: impaired immunoglobulin class switching and germinal center formation. *Immunity*, 1, 167-78.
- KE, F., BENET, Z. L., SHELYAKIN, P., BRITANOVA, O. V., GUPTA, N., DENT, A. L., MOORE, B. B. & GRIGOROVA, I. L. 2024. Targeted checkpoint control of B cells undergoing positive selection in germinal centers by follicular regulatory T cells. *Proceedings of the National Academy of Sciences*, 121, e2304020121.
- KEMP, T. J., GARCÍA-PIÑERES, A., FALK, R. T., PONCELET, S., DESSY, F., GIANNINI, S. L., RODRIGUEZ, A. C., PORRAS, C., HERRERO, R., HILDESHEIM, A. & PINTO, L. A. 2008. Evaluation of systemic and mucosal anti-HPV16 and anti-HPV18 antibody responses from vaccinated women. *Vaccine*, 26, 3608-16.
- KHALLOUF, H., GRABOWSKA, A. K. & RIEMER, A. B. 2014. Therapeutic Vaccine Strategies against Human Papillomavirus. *Vaccines (Basel)*, 2, 422-62.

- KHODADADI, L., CHENG, Q., RADBRUCH, A. & HIEPE, F. 2019. The Maintenance of Memory Plasma Cells. *Front Immunol*, 10, 721.
- KIM, C. H., LIM, H. W., KIM, J. R., ROTT, L., HILLSAMER, P. & BUTCHER, E. C. 2004. Unique gene expression program of human germinal center T helper cells. *Blood*, 104, 1952-1960.
- KINDT, N., DESCAMPS, G., LECHIEN, J. R., REMMELINK, M., COLET, J. M., WATTIEZ, R., BERCHEM, G., JOURNE, F. & SAUSSEZ, S. 2019. Involvement of HPV Infection in the Release of Macrophage Migration Inhibitory Factor in Head and Neck Squamous Cell Carcinoma. *J Clin Med*, 8.
- KINES, R. C. & SCHILLER, J. T. 2022. Harnessing Human Papillomavirus' Natural Tropism to Target Tumors. *Viruses*, 14, 1656.
- KINES, R. C., THOMPSON, C. D., LOWY, D. R., SCHILLER, J. T. & DAY, P. M. 2009. The initial steps leading to papillomavirus infection occur on the basement membrane prior to cell surface binding. *Proc Natl Acad Sci U S A*, 106, 20458-63.
- KIRNBAUER, R., BOOY, F., CHENG, N., LOWY, D. R. & SCHILLER, J. T. 1992. Papillomavirus L1 major capsid protein self-assembles into virus-like particles that are highly immunogenic. *Proc Natl Acad Sci U S A*, 89, 12180-4.
- KITAMURA, T., QIAN, B. Z. & POLLARD, J. W. 2015. Immune cell promotion of metastasis. *Nat Rev Immunol*, 15, 73-86.
- KITANO, M., MORIYAMA, S., ANDO, Y., HIKIDA, M., MORI, Y., KUROSAKI, T. & OKADA, T. 2011. Bcl6 protein expression shapes pre-germinal center B cell dynamics and follicular helper T cell heterogeneity. *Immunity*, 34, 961-72.
- KJAER, S. K., NYGÅRD, M., SUNDSTRÖM, K., DILLNER, J., TRYGGVADOTTIR, L., MUNK, C., BERGER, S., ENERLY, E., HORTLUND, M., ÁGÚSTSSON, Á. I., BJELKENKRANTZ, K., FRIDRICH, K., GUÐMUNDSDÓTTIR, I., SØRBYE, S. W., BAUTISTA, O., GROUP, T., LUXEMBOURG, A., MARSHALL, J. B., RADLEY, D., YANG, Y. S., BADSHAH, C. & SAAH, A. 2020a. Final analysis of a 14-year long-term follow-up study of the effectiveness and immunogenicity of the quadrivalent human papillomavirus vaccine in women from four nordic countries. *eClinicalMedicine*, 23.
- KJAER, S. K., NYGÅRD, M., SUNDSTRÖM, K., DILLNER, J., TRYGGVADOTTIR, L., MUNK, C., BERGER, S., ENERLY, E., HORTLUND, M., ÁGÚSTSSON, Á. I., BJELKENKRANTZ, K., FRIDRICH, K., GUÐMUNDSDÓTTIR, I., SØRBYE, S. W., BAUTISTA, O., GROUP, T., LUXEMBOURG, A., MARSHALL, J. B., RADLEY, D., YANG, Y. S., BADSHAH, C. & SAAH, A. 2020b. Final analysis of a 14-year long-term follow-up study of the effectiveness and immunogenicity of the quadrivalent human papillomavirus vaccine in women from four nordic countries. *EClinicalMedicine*, 23, 100401-100401.
- KLEIN, C., SAMWEL, K., KAHESA, C., MWAISELAGE, J., WEST, J. T., WOOD, C. & ANGELETTI, P. C. 2020. Mycoplasma Co-Infection Is Associated with Cervical Cancer Risk. *Cancers (Basel)*, 12.
- KLEIN, U. & DALLA-FAVERA, R. 2008a. Germinal centres: role in B-cell physiology and malignancy. *Nature Rev. Immunol.*, 8.
- KLEIN, U. & DALLA-FAVERA, R. 2008b. Germinal centres: role in B-cell physiology and malignancy. *Nature Reviews Immunology*, 8, 22-33.
- KOUTSKY, L. A., AULT, K. A., WHEELER, C. M., BROWN, D. R., BARR, E., ALVAREZ, F. B., CHIACCHIERINI, L. M., JANSEN, K. U. & PROOF OF PRINCIPLE STUDY, I. 2002. A controlled trial of a human papillomavirus type 16 vaccine. *N Engl J Med*, 347, 1645-51.
- KREIMER, A. R., SAMPSON, J. N., PORRAS, C., SCHILLER, J. T., KEMP, T., HERRERO, R., WAGNER, S., BOLAND, J., SCHUSSLER, J., LOWY, D. R., CHANOCK, S., ROBERSON, D., SIERRA, M. S., TSANG, S. H., SCHIFFMAN, M., RODRIGUEZ, A. C., CORTES, B., GAIL, M. H., HILDESHEIM, A.,

- GONZALEZ, P. & PINTO, L. A. 2020. Evaluation of Durability of a Single Dose of the Bivalent HPV Vaccine: The CVT Trial. *J Natl Cancer Inst*, 112, 1038-1046.
- KREIMER, A. R., STRUYF, F., DEL ROSARIO-RAYMUNDO, M. R., HILDESHEIM, A., SKINNER, S. R., WACHOLDER, S., GARLAND, S. M., HERRERO, R., DAVID, M. P., WHEELER, C. M., GONZÁLEZ, P., JIMÉNEZ, S., LOWY, D. R., PINTO, L. A., PORRAS, C., RODRIGUEZ, A. C., SAFAEIAN, M., SCHIFFMAN, M., SCHILLER, J. T., SCHUSSLER, J., SHERMAN, M. E., BOSCH, F. X., CASTELLSAGUE, X., CHATTERJEE, A., CHOW, S. N., DESCAMPS, D., DIAZ-MITOMA, F., DUBIN, G., GERMAR, M. J., HARPER, D. M., LEWIS, D. J., LIMSON, G., NAUD, P., PETERS, K., POPPE, W. A., RAMJATTAN, B., ROMANOWSKI, B., SALMERON, J., SCHWARZ, T. F., TEIXEIRA, J. C. & TJALMA, W. A. 2015. Efficacy of fewer than three doses of an HPV-16/18 AS04-adjuvanted vaccine: combined analysis of data from the Costa Rica Vaccine and PATRICIA Trials. *Lancet Oncol*, 16, 775-86.
- KROEGER, D. R., RUDULIER, C. D. & BRETSCHER, P. A. 2013. Antigen Presenting B Cells Facilitate CD4 T Cell Cooperation Resulting in Enhanced Generation of Effector and Memory CD4 T Cells. *PLOS ONE*, 8, e77346.
- KUNKEL, E. J. & BUTCHER, E. C. 2003. Plasma-cell homing. *Nat Rev Immunol*, 3, 822-9.
- KUROSAWA, M., SEKINE, M., YAMAGUCHI, M., KUDO, R., HANLEY, S. J. B., HARA, M., ADACHI, S., UEDA, Y., MIYAGI, E., IKEDA, S., YAGI, A. & ENOMOTO, T. 2022. Long-Term Effects of Human Papillomavirus Vaccination in Clinical Trials and Real-World Data: A Systematic Review. *Vaccines (Basel)*, 10.
- LAPPIN, M. B., KIMBER, I. & NORVAL, M. 1996. The role of dendritic cells in cutaneous immunity. *Arch Dermatol Res*, 288, 109-21.
- LASERSON, U., VIGNEAULT, F., GADALA-MARIA, D., YAARI, G., UDUMAN, M., VANDER HEIDEN, J. A., KELTON, W., TAEK JUNG, S., LIU, Y., LASERSON, J., CHARI, R., LEE, J. H., BACHELET, I., HICKEY, B., LIEBERMAN-AIDEN, E., HANCZARUK, B., SIMEN, B. B., EGHOLM, M., KOLLER, D., GEORGIU, G., KLEINSTEIN, S. H. & CHURCH, G. M. 2014. High-resolution antibody dynamics of vaccine-induced immune responses. *Proc Natl Acad Sci U S A*, 111, 4928-33.
- LASZLOFY, C., FAZEKAS, G., BARATH, Z. & VAJO, Z. 2024. Evaluation of Vaccine Immunogenicity—Correlates to Real-World Protection: Influenza. *Viruses*, 16, 441.
- LEBIEN, T. W. & TEDDER, T. F. 2008a. B lymphocytes: how they develop and function. *Blood*, 112, 1570-1580.
- LEBIEN, T. W. & TEDDER, T. F. 2008b. B lymphocytes: how they develop and function. *Blood*, 112, 1570-80.
- LEBRE, M. C., VAN DER AAR, A. M., VAN BAARSEN, L., VAN CAPEL, T. M., SCHUITEMAKER, J. H., KAPSENBERG, M. L. & DE JONG, E. C. 2007. Human keratinocytes express functional Toll-like receptor 3, 4, 5, and 9. *J Invest Dermatol*, 127, 331-41.
- LECHLER, T. & FUCHS, E. 2005. Asymmetric cell divisions promote stratification and differentiation of mammalian skin. *Nature*, 437, 275-80.
- LEE, J. H., SUTTON, H. J., COTTRELL, C. A., PHUNG, I., OZOROWSKI, G., SEWALL, L. M., NEDELLEC, R., NAKAO, C., SILVA, M., RICHEY, S. T., TORRES, J. L., LEE, W.-H., GEORGESON, E., KUBITZ, M., HODGES, S., MULLEN, T.-M., ADACHI, Y., CIRELLI, K. M., KAUR, A., ALLERS, C., FAHLBERG, M., GRASPERGE, B. F., DUFOUR, J. P., SCHIRO, F., AYE, P. P., KALYUZHNIY, O., LIGUORI, A., CARNATHAN, D. G., SILVESTRI, G., SHEN, X., MONTEFIORI, D. C., VEAZEY, R. S., WARD, A. B., HANGARTNER, L., BURTON, D. R., IRVINE, D. J., SCHIEF, W. R. & CROTTY, S. 2022. Long-primed germinal centres with enduring affinity maturation and clonal migration. *Nature*, 609, 998-1004.

- LEE, S. K., RIGBY, R. J., ZOTOS, D., TSAI, L. M., KAWAMOTO, S., MARSHALL, J. L., RAMISCAL, R. R., CHAN, T. D., GATTO, D., BRINK, R., YU, D., FAGARASAN, S., TARLINTON, D. M., CUNNINGHAM, A. F. & VINUESA, C. G. 2011. B cell priming for extrafollicular antibody responses requires Bcl-6 expression by T cells. *J Exp Med*, 208, 1377-88.
- LENZ, P., THOMPSON, C. D., DAY, P. M., BACOT, S. M., LOWY, D. R. & SCHILLER, J. T. 2003. Interaction of papillomavirus virus-like particles with human myeloid antigen-presenting cells. *Clin Immunol*, 106, 231-7.
- LESTER, S. N. & LI, K. 2014. Toll-like receptors in antiviral innate immunity. *J Mol Biol*, 426, 1246-64.
- LEUNG, T. F., LIU, A. P., LIM, F. S., THOLLOT, F., OH, H. M., LEE, B. W., ROMBO, L., TAN, N. C., ROUZIER, R., FRIEL, D., DE MUYNCK, B., DE SIMONI, S., SURYAKIRAN, P., HEZAREH, M., FOLSCHWEILLER, N., THOMAS, F. & STRUYF, F. 2015. Comparative immunogenicity and safety of human papillomavirus (HPV)-16/18 AS04-adjuvanted vaccine and HPV-6/11/16/18 vaccine administered according to 2- and 3-dose schedules in girls aged 9-14 years: Results to month 12 from a randomized trial. *Hum Vaccin Immunother*, 11, 1689-702.
- LEYENDECKERS, H., ODENDAHL, M., LÖHNDORF, A., IRSCH, J., SPANGFORT, M., MILTENYI, S., HUNZELMANN, N., ASSENMACHER, M., RADBRUCH, A. & SCHMITZ, J. 1999. Correlation analysis between frequencies of circulating antigen-specific IgG-bearing memory B cells and serum titers of antigen-specific IgG. *Eur J Immunol*, 29, 1406-17.
- LI, A., RUE, M., ZHOU, J., WANG, H., GOLDWASSER, M. A., NEUBERG, D., DALTON, V., ZUCKERMAN, D., LYONS, C., SILVERMAN, L. B., SALLAN, S. E. & GRIBBEN, J. G. 2004. Utilization of Ig heavy chain variable, diversity, and joining gene segments in children with B-lineage acute lymphoblastic leukemia: implications for the mechanisms of VDJ recombination and for pathogenesis. *Blood*, 103, 4602-4609.
- LIGHTMAN, S. M., UTLEY, A. & LEE, K. P. 2019. Survival of Long-Lived Plasma Cells (LLPC): Piecing Together the Puzzle. *Frontiers in Immunology*, 10.
- LINDQUIST, R. L., NIESNER, R. A. & HAUSER, A. E. 2019. In the Right Place, at the Right Time: Spatiotemporal Conditions Determining Plasma Cell Survival and Function. *Front Immunol*, 10, 788.
- LINK, A., ZABEL, F., SCHNETZLER, Y., TITZ, A., BROMBACHER, F. & BACHMANN, M. F. 2012. Innate immunity mediates follicular transport of particulate but not soluble protein antigen. *J Immunol*, 188, 3724-33.
- LINTERMAN, M. A. 2023. Age-dependent changes in T follicular helper cells shape the humoral immune response to vaccination. *Seminars in Immunology*, 69, 101801.
- LIU, Y. J., JOHNSON, G. D., GORDON, J. & MACLENNAN, I. C. 1992. Germinal centres in T-cell-dependent antibody responses. *Immunol Today*, 13, 17-21.
- LONGWORTH, M. S. & LAIMINS, L. A. 2004. Pathogenesis of human papillomaviruses in differentiating epithelia. *Microbiol Mol Biol Rev*, 68, 362-72.
- LOPEZ, T. V., CANCIO, C., CRUZ-TALONIA, F., RUIZ, B., SAPP, M. & ROCHA-ZAVALA, L. 2008. Binding of human papillomavirus type 16 to heparan sulfate is inhibited by mucosal antibodies from patients with low-grade squamous intraepithelial lesions but not from cervical cancer patients. *FEMS Immunol Med Microbiol*, 54, 167-76.
- LÓPEZ-MACÍAS, C. 2012. Virus-like particle (VLP)-based vaccines for pandemic influenza: performance of a VLP vaccine during the 2009 influenza pandemic. *Human vaccines & immunotherapeutics*, 8, 411-414.
- LUCAS, A. H., MOULTON, K. D., TANG, V. R. & REASON, D. C. 2001. Combinatorial library cloning of human antibodies to *Streptococcus pneumoniae* capsular polysaccharides: variable region

primary structures and evidence for somatic mutation of Fab fragments specific for capsular serotypes 6B, 14, and 23F. *Infection and immunity*, 69, 853-864.

- LUGEMWA, F. N. & ESKO, J. D. 1991. Estradiol beta-D-xyloside, an efficient primer for heparan sulfate biosynthesis. *Journal of Biological Chemistry*, 266, 6674-6677.
- LUNING PRAK, E. T., MONESTIER, M. & EISENBERG, R. A. 2011. B cell receptor editing in tolerance and autoimmunity. *Ann N Y Acad Sci*, 1217, 96-121.
- MAHAJAN, V. S., MATTOO, H., SUN, N., VISWANADHAM, V., YUEN, G. J., ALLARD-CHAMARD, H., AHMAD, M., MURPHY, S. J. H., CARIAPPA, A., TUNCAY, Y. & PILLAI, S. 2021. B1a and B2 cells are characterized by distinct CpG modification states at DNMT3A-maintained enhancers. *Nature Communications*, 12, 2208.
- MAK, T. W. & SAUNDERS, M. E. 2006. 9 - The Humoral Response: B Cell Development and Activation. In: MAK, T. W. & SAUNDERS, M. E. (eds.) *The Immune Response*. Burlington: Academic Press.
- MALEJCZYK, J., MAJEWSKI, S., JABLONSKA, S., ROGOZINSKI, T. T. & ORTH, G. 1989. Abrogated NK-cell lysis of human papillomavirus (HPV)-16-bearing keratinocytes in patients with pre-cancerous and cancerous HPV-induced anogenital lesions. *Int J Cancer*, 43, 209-14.
- MALI, M. E., SANYANG, O., HARRIS, K. L., SORENSEN, J., BITTAYE, M., NELLERMOE, J., PRICE, R. R. & SUTHERLAND, E. K. 2023. Capacity assessment and spatial analysis of cervical cancer services in The Gambia. *BMC Women's Health*, 23, 660.
- MANGINO, M., ROEDERER, M., BEDDALL, M. H., NESTLE, F. O. & SPECTOR, T. D. 2017. Innate and adaptive immune traits are differentially affected by genetic and environmental factors. *Nature Communications*, 8, 13850.
- MANGSBO, S. M., HAVERVALL, S., LAURÉN, I., LINDSAY, R., JERNBOM FALK, A., MARKING, U., LORD, M., BUGGERT, M., DÖNNES, P., CHRISTOFFERSSON, G., NILSSON, P., HOBER, S., PHILLIPSON, M., KLINGSTRÖM, J. & THÅLIN, C. 2021. An evaluation of a FluoroSpot assay as a diagnostic tool to determine SARS-CoV-2 specific T cell responses. *PLoS One*, 16, e0258041.
- MANICKAM, A. & SIVANANDHAM, M. 2011. Mycobacterium bovis BCG and purified protein derivative-induced reduction in the CD80 expression and the antigen up-take function of dendritic cells from patients with cervical cancer. *Eur J Obstet Gynecol Reprod Biol*, 159, 413-7.
- MANJGALADZE, K., TEVDORASHVILI, G., MUZASHVILI, T., GACHECHILADZE, M. & BURKADZE, G. 2019. TLR9 EXPRESSION, LANGERHANS CELL DENSITY AND LYMPHOCYTIC INFILTRATION IN PROGRESSING CERVICAL INTRAEPITHELIAL NEOPLASIA. *Georgian Med News*, 126-130.
- MANUCK, S. B., COHEN, S., RABIN, B. S., MULDOON, M. F. & BACHEN, E. A. 1991. Individual Differences in Cellular Immune Response to Stress. *Psychological Science*, 2, 111-115.
- MANZ, R. A., THIEL, A. & RADBRUCH, A. 1997. Lifetime of plasma cells in the bone marrow. *Nature*, 388, 133-4.
- MARIZ, F. C., GRAY, P., BENDER, N., ERIKSSON, T., KANN, H., APTER, D., PAAVONEN, J., PAJUNEN, E., PRAGER, K. M., SEHR, P., SURCEL, H.-M., WATERBOER, T., MÜLLER, M., PAWLITA, M. & LEHTINEN, M. 2021. Sustainability of neutralising antibodies induced by bivalent or quadrivalent HPV vaccines and correlation with efficacy: a combined follow-up analysis of data from two randomised, double-blind, multicentre, phase 3 trials. *The Lancet Infectious Diseases*, 21, 1458-1468.
- MARTIN, F. & KEARNEY, J. F. 2002. Marginal-zone B cells. *Nature Reviews Immunology*, 2, 323-335.
- MARTIN, F., OLIVER, A. M. & KEARNEY, J. F. 2001. Marginal zone and B1 B cells unite in the early response against T-independent blood-borne particulate antigens. *Immunity*, 14, 617-29.

- MARTÍNEZ GÓMEZ, J. M., PERIASAMY, P., DUTERTRE, C.-A., IRVING, A. T., NG, J. H. J., CRAMERI, G., BAKER, M. L., GINHOUX, F., WANG, L.-F. & ALONSO, S. 2016. Phenotypic and functional characterization of the major lymphocyte populations in the fruit-eating bat *Pteropus alecto*. *Scientific Reports*, 6, 37796.
- MARTÍNEZ-RIAÑO, A., WANG, S., BOEING, S., MINOUGHAN, S., CASAL, A., SPILLANE, K. M., LUDEWIG, B. & TOLAR, P. 2023. Long-term retention of antigens in germinal centers is controlled by the spatial organization of the follicular dendritic cell network. *Nat Immunol*, 24, 1281-1294.
- MASSAD, L. S., XIE, X., BURK, R., KELLER, M. J., MINKOFF, H., D'SOUZA, G., WATTS, D. H., PALEFSKY, J., YOUNG, M., LEVINE, A. M., COHEN, M. & STRICKLER, H. D. 2014. Long-term cumulative detection of human papillomavirus among HIV seropositive women. *Aids*, 28, 2601-8.
- MASTELIC-GAVILLET, B., BALINT, K., BOUDOUSQUIE, C., GANNON, P. O. & KANDALAFT, L. E. 2019. Personalized Dendritic Cell Vaccines-Recent Breakthroughs and Encouraging Clinical Results. *Front Immunol*, 10, 766.
- MATSUI, K., ADELSBERGER, J. W., KEMP, T. J., BASELER, M. W., LEDGERWOOD, J. E. & PINTO, L. A. 2015. Circulating CXCR5(+)CD4(+) T Follicular-Like Helper Cell and Memory B Cell Responses to Human Papillomavirus Vaccines. *PLoS One*, 10, e0137195.
- MATTHEWS, K., LEONG, C. M., BAXTER, L., INGLIS, E., YUN, K., BÄCKSTRÖM, B. T., DOORBAR, J. & HIBMA, M. 2003. Depletion of Langerhans cells in human papillomavirus type 16-infected skin is associated with E6-mediated down regulation of E-cadherin. *J Virol*, 77, 8378-85.
- MATZ, H. C., MCINTIRE, K. M. & ELLEBEDY, A. H. 2023a. 'Persistent germinal center responses: slow-growing trees bear the best fruits'. *Curr Opin Immunol*, 83, 102332.
- MATZ, H. C., MCINTIRE, K. M. & ELLEBEDY, A. H. 2023b. 'Persistent germinal center responses: slow-growing trees bear the best fruits'. *Current Opinion in Immunology*, 83, 102332.
- MAUL, R. W. & GEARHART, P. J. 2010. AID and somatic hypermutation. *Adv Immunol*, 105, 159-91.
- MBULAWA, Z. Z. A., WILLIAMSON, A. L., STEWART, D., PASSMORE, J. S., DENNY, L., ALLAN, B. & MARAIS, D. J. 2008. Association of serum and mucosal neutralizing antibodies to human papillomavirus type 16 (HPV-16) with HPV-16 infection and cervical disease. *J Gen Virol*, 89, 910-914.
- MCHEYZER-WILLIAMS, M. G., MCLEAN, M. J., LALOR, P. A. & NOSSAL, G. J. 1993. Antigen-driven B cell differentiation in vivo. *J Exp Med*, 178, 295-307.
- MEMAR, O. M., ARANY, I. & TYRING, S. K. 1995. Skin-associated lymphoid tissue in human immunodeficiency virus-1, human papillomavirus, and herpes simplex virus infections. *J Invest Dermatol*, 105, 99s-104s.
- MESHER, D., SOLDAN, K., LEHTINEN, M., BEDDOWS, S., BRISSON, M., BROTHERTON, J. M., CHOW, E. P., CUMMINGS, T., DROLET, M., FAIRLEY, C. K., GARLAND, S. M., KAHN, J. A., KAVANAGH, K., MARKOWITZ, L., POLLOCK, K. G., SÖDERLUND-STRAND, A., SONNENBERG, P., TABRIZI, S. N., TANTON, C., UNGER, E. & THOMAS, S. L. 2016. Population-Level Effects of Human Papillomavirus Vaccination Programs on Infections with Nonvaccine Genotypes. *Emerg Infect Dis*, 22, 1732-40.
- MESIN, L., ERSCHING, J. & VICTORA, G. D. 2016. Germinal Center B Cell Dynamics. *Immunity*, 45, 471-482.
- MILLER, C. N., KEMP, T. J., ABRAHAMSEN, M., ISAACS-SORIANO, K., DUNHAM, K., SIRAK, B., PAN, Y., LAZCANO-PONCE, E., SALMERON, J., PINTO, L. A. & GIULIANO, A. R. 2021. Increases in HPV-16/18 antibody avidity and HPV-specific memory B-cell response in mid-adult aged men post-dose three of the quadrivalent HPV vaccine. *Vaccine*, 39, 5295-5301.

- MILLER, J. J., 3RD 1964. AN AUTORADIOGRAPHIC STUDY OF PLASMA CELL AND LYMPHOCYTE SURVIVAL IN RAT POPLITEAL LYMPH NODES. *J Immunol*, 92, 673-81.
- MILLER, L. S. & MODLIN, R. L. 2007. Human keratinocyte Toll-like receptors promote distinct immune responses. *J Invest Dermatol*, 127, 262-3.
- MINOR, P. D. 2015. Live attenuated vaccines: Historical successes and current challenges. *Virology*, 479-480, 379-92.
- MISHRA, D., SINGH, S. & NARAYAN, G. 2016. Role of B Cell Development Marker CD10 in Cancer Progression and Prognosis. *Mol Biol Int*, 2016, 4328697.
- MITCHELL, R. A., LIAO, H., CHESNEY, J., FINGERLE-ROWSON, G., BAUGH, J., DAVID, J. & BUCALA, R. 2002. Macrophage migration inhibitory factor (MIF) sustains macrophage proinflammatory function by inhibiting p53: regulatory role in the innate immune response. *Proc Natl Acad Sci U S A*, 99, 345-50.
- MOEINZADEH, M., KHEIRKHAH, B., AMINI, K. & POURYASIN, A. 2020. Classification and identification of human papillomavirus based on its prevalence and development of cervical lesion among Iranian women. *Bioimpacts*, 10, 235-242.
- MOND, J. J., VOS, Q., LEES, A. & SNAPPER, C. M. 1995. T cell independent antigens. *Curr Opin Immunol*, 7, 349-54.
- MONGINI, P. K., JACKSON, A. E., TOLANI, S., FATTAH, R. J. & INMAN, J. K. 2003. Role of complement-binding CD21/CD19/CD81 in enhancing human B cell protection from Fas-mediated apoptosis. *J Immunol*, 171, 5244-54.
- MONTECINO-RODRIGUEZ, E. & DORSHKIND, K. 2016. B-1 B Cell Development. In: RATCLIFFE, M. J. H. (ed.) *Encyclopedia of Immunobiology*. Oxford: Academic Press.
- MOTA, F., RAYMENT, N., CHONG, S., SINGER, A. & CHAIN, B. 1999. The antigen-presenting environment in normal and human papillomavirus (HPV)-related premalignant cervical epithelium. *Clin Exp Immunol*, 116, 33-40.
- MUECKSCH, F., WANG, Z., CHO, A., GAEBLER, C., BEN TANFOUS, T., DASILVA, J., BEDNARSKI, E., RAMOS, V., ZONG, S., JOHNSON, B., RASPE, R., SCHAEFER-BABAJEW, D., SHIMELIOVICH, I., DAGA, M., YAO, K.-H., SCHMIDT, F., MILLARD, K. G., TURROJA, M., JANKOVIC, M., OLIVEIRA, T. Y., GAZUMYAN, A., CASKEY, M., HATZIOANNOU, T., BIENIASZ, P. D. & NUSSENZWEIG, M. C. 2022. Increased memory B cell potency and breadth after a SARS-CoV-2 mRNA boost. *Nature*, 607, 128-134.
- MUGO, N., ANSAH, N. A., MARINO, D., SAAH, A. & GARNER, E. I. O. 2015. Evaluation of safety and immunogenicity of a quadrivalent human papillomavirus vaccine in healthy females between 9 and 26 years of age in Sub-Saharan Africa. *Human vaccines & immunotherapeutics*, 11, 1323-1330.
- MUÑOZ, N., MANALASTAS, R., JR., PITISUTTITHUM, P., TRESUKOSOL, D., MONSONEGO, J., AULT, K., CLAVEL, C., LUNA, J., MYERS, E., HOOD, S., BAUTISTA, O., BRYAN, J., TADDEO, F. J., ESSER, M. T., VUOCOLO, S., HAUPT, R. M., BARR, E. & SAAH, A. 2009. Safety, immunogenicity, and efficacy of quadrivalent human papillomavirus (types 6, 11, 16, 18) recombinant vaccine in women aged 24-45 years: a randomised, double-blind trial. *Lancet (London, England)*, 373, 1949-1957.
- NAKAGAWA, M., STITES, D. P., FARHAT, S., SISLER, J. R., MOSS, B., KONG, F., MOSCICKI, A. B. & PALEFSKY, J. M. 1997. Cytotoxic T lymphocyte responses to E6 and E7 proteins of human papillomavirus type 16: relationship to cervical intraepithelial neoplasia. *J Infect Dis*, 175, 927-31.

- NAKAGAWA, M., STITES, D. P., PALEFSKY, J. M., KNEASS, Z. & MOSCICKI, A. B. 1999. CD4-positive and CD8-positive cytotoxic T lymphocytes contribute to human papillomavirus type 16 E6 and E7 responses. *Clin Diagn Lab Immunol*, 6, 494-8.
- NAKAGAWA, M., STITES, D. P., PATEL, S., FARHAT, S., SCOTT, M., HILLS, N. K., PALEFSKY, J. M. & MOSCICKI, A. B. 2000. Persistence of human papillomavirus type 16 infection is associated with lack of cytotoxic T lymphocyte response to the E6 antigens. *J Infect Dis*, 182, 595-8.
- NARDELLI-HAEFLIGER, D., LURATI, F., WIRTHNER, D., SPERTINI, F., SCHILLER, J. T., LOWY, D. R., PONCI, F. & DE GRANDI, P. 2005. Immune responses induced by lower airway mucosal immunisation with a human papillomavirus type 16 virus-like particle vaccine. *Vaccine*, 23, 3634-41.
- NARDELLI-HAEFLIGER, D., WIRTHNER, D., SCHILLER, J. T., LOWY, D. R., HILDESHEIM, A., PONCI, F. & DE GRANDI, P. 2003. Specific antibody levels at the cervix during the menstrual cycle of women vaccinated with human papillomavirus 16 virus-like particles. *J Natl Cancer Inst*, 95, 1128-37.
- NARISAWA-SAITO, M. & KIYONO, T. 2007. Basic mechanisms of high-risk human papillomavirus-induced carcinogenesis: Roles of E6 and E7 proteins. *Cancer Science*, 98, 1505-1511.
- NAUD, P. S., ROTELI-MARTINS, C. M., DE CARVALHO, N. S., TEIXEIRA, J. C., DE BORBA, P. C., SANCHEZ, N., ZAHAF, T., CATTEAU, G., GEERAERTS, B. & DESCAMPS, D. 2014. Sustained efficacy, immunogenicity, and safety of the HPV-16/18 AS04-adjuvanted vaccine. *Human Vaccines & Immunotherapeutics*, 10, 2147-2162.
- NEJO, Y. T., OLALEYE, D. O. & ODAIBO, G. N. 2018. Prevalence and Risk Factors for Genital Human Papillomavirus Infections Among Women in Southwest Nigeria. *Archives of basic and applied medicine*, 6, 105-112.
- NGUYEN, D. C., DUAN, M., ALI, M., LEY, A., SANZ, I. & LEE, F. E. 2021. Plasma cell survival: The intrinsic drivers, migratory signals, and extrinsic regulators. *Immunol Rev*, 303, 138-153.
- NGUYEN, D. C., HENTENAAR, I. T., MORRISON-PORTER, A., SOLANO, D., HADDAD, N. S., CASTRILLON, C., LAMOTHE, P. A., ANDREWS, J., ROBERTS, D., LONIAL, S., SANZ, I. & LEE, F. E.-H. 2024. The Majority of SARS-CoV-2 Plasma Cells are Excluded from the Bone Marrow Long-Lived Compartment 33 Months after mRNA Vaccination. *medRxiv*, 2024.03.02.24303242.
- NGUYEN, D. C., JOYNER, C. J., SANZ, I. & LEE, F. E.-H. 2019. Factors Affecting Early Antibody Secreting Cell Maturation Into Long-Lived Plasma Cells. *Frontiers in Immunology*, 10.
- NICOLI, F., MANTELLI, B., GALLERANI, E., TELATIN, V., BONAZZI, I., MARCONI, P., GAVIOLI, R., GABRIELLI, L., LAZZAROTTO, T., BARZON, L., PALÙ, G., CAPUTO & ANTONELLA 2020a. HPV-Specific Systemic Antibody Responses and Memory B Cells are Independently Maintained up to 6 Years and in a Vaccine-Specific Manner Following Immunization with Cervarix and Gardasil in Adolescent and Young Adult Women in Vaccination Programs in Italy. *Vaccines*, 8, 26.
- NICOLI, F., MANTELLI, B., GALLERANI, E., TELATIN, V., BONAZZI, I., MARCONI, P., GAVIOLI, R., GABRIELLI, L., LAZZAROTTO, T., BARZON, L., PALÙ, G. & CAPUTO, A. 2020b. HPV-Specific Systemic Antibody Responses and Memory B Cells are Independently Maintained up to 6 Years and in a Vaccine-Specific Manner Following Immunization with Cervarix and Gardasil in Adolescent and Young Adult Women in Vaccination Programs in Italy. *Vaccines*, 8, 26.
- NICOLI, F., MANTELLI, B., GALLERANI, E., TELATIN, V., BONAZZI, I., MARCONI, P., GAVIOLI, R., GABRIELLI, L., LAZZAROTTO, T., BARZON, L., PALÙ, G. & CAPUTO, A. A. 2020c. HPV-Specific Systemic Antibody Responses and Memory B Cells are Independently Maintained up to 6 Years and in a Vaccine-Specific Manner Following Immunization with Cervarix and Gardasil in Adolescent and Young Adult Women in Vaccination Programs in Italy. *Vaccines (Basel)*, 8.

- NICOLI, F., MANTELLI, B., GALLERANI, E., TELATIN, V., SQUARZON, L., MASIERO, S., GAVIOLI, R., PALÙ, G., BARZON, L. & CAPUTO, A. 2022. Effects of the age of vaccination on the humoral responses to a human papillomavirus vaccine. *npj Vaccines*, 7, 37.
- NIU, X., LI, S., LI, P., PAN, W., WANG, Q., FENG, Y., MO, X., YAN, Q., YE, X., LUO, J., QU, L., WEBER, D., BYRNE-STEEL, M. L., WANG, Z., YU, F., LI, F., MYERS, R. M., LOTZE, M. T., ZHONG, N., HAN, J. & CHEN, L. 2020. Longitudinal Analysis of T and B Cell Receptor Repertoire Transcripts Reveal Dynamic Immune Response in COVID-19 Patients. *Front Immunol*, 11, 582010.
- NOMA, I. H. Y., SHINOBU-MESQUITA, C. S., SUEHIRO, T. T., MORELLI, F., DE SOUZA, M. V. F., DAMKE, E., DA SILVA, V. R. S. & CONSOLARO, M. E. L. 2021. Association of High-Risk Human Papillomavirus and Ureaplasma parvum Co-Infections with Increased Risk of Low-Grade Squamous Intraepithelial Cervical Lesions. *Asian Pac J Cancer Prev*, 22, 1239-1246.
- NURIEVA, R. I. 2008. Generation of T follicular helper cells is mediated by interleukin-21 but independent of T helper 1, 2, or 17 cell lineages. *Immunity*, 29.
- NURIEVA, R. I., CHUNG, Y., HWANG, D., YANG, X. O., KANG, H. S., MA, L., WANG, Y.-H., WATOWICH, S. S., JETTEN, A. M. & TIAN, Q. 2008. Generation of T follicular helper cells is mediated by interleukin-21 but independent of T helper 1, 2, or 17 cell lineages. *Immunity*, 29, 138-149.
- NURIEVA, R. I., CHUNG, Y., MARTINEZ, G. J., YANG, X. O., TANAKA, S., MATSKEVITCH, T. D., WANG, Y.-H. & DONG, C. 2009. Bcl6 mediates the development of T follicular helper cells. *Science*, 325, 1001-1005.
- NUTT, S. L., HODGKIN, P. D., TARLINTON, D. M. & CORCORAN, L. M. 2015a. The generation of antibody-secreting plasma cells. *Nature Reviews Immunology*, 15, 160-171.
- NUTT, S. L., HODGKIN, P. D., TARLINTON, D. M. & CORCORAN, L. M. 2015b. The generation of antibody-secreting plasma cells. *Nat Rev Immunol*, 15, 160-71.
- OLSSON, S.-E., KJAER, S. K., SIGURDSSON, K., IVERSEN, O.-E., HERNANDEZ-AVILA, M., WHEELER, C. M., PEREZ, G., BROWN, D. R., KOUTSKY, L. A., TAY, E. H., GARCÍA, P., AULT, K. A., GARLAND, S. M., LEODOLTER, S., TANG, G. W. K., FERRIS, D. G., PAAVONEN, J., LEHTINEN, M., STEBEN, M., BOSCH, F. X., DILLNER, J., JOURA, E. A., MAJEWSKI, S., MUÑOZ, N., MYERS, E. R., VILLA, L. L., TADDEO, F. J., ROBERTS, C., TADESSE, A., BRYAN, J., MAANSSON, R., VUOCOLO, S., HESLEY, T. M., SAAH, A., BARR, E. & HAUPT, R. M. 2009. Evaluation of quadrivalent HPV 6/11/16/18 vaccine efficacy against cervical and anogenital disease in subjects with serological evidence of prior vaccine type HPV infection. *Human vaccines*, 5, 696-704.
- OLSSON, S. E., RESTREPO, J. A., REINA, J. C., PITISUTTITHUM, P., ULIED, A., VARMAN, M., VAN DAMME, P., MOREIRA, E. D., JR., FERRIS, D., BLOCK, S., BAUTISTA, O., GALLAGHER, N., MCCAULEY, J. & LUXEMBOURG, A. 2020. Long-term immunogenicity, effectiveness, and safety of nine-valent human papillomavirus vaccine in girls and boys 9 to 15 years of age: Interim analysis after 8 years of follow-up. *Papillomavirus Res*, 10, 100203.
- OSMOND, D. G. 1986. Population dynamics of bone marrow B lymphocytes. *Immunol Rev*, 93, 103-24.
- OSMOND, D. G., PARK, Y. H. & JACOBSEN, K. B Cell Precursors in Bone Marrow: In Vivo Proliferation, Localization, Stimulation by Activated Macrophages and Implications for Oncogenesis. In: POTTER, M. & MELCHERS, F., eds. Mechanisms in B-Cell Neoplasia 1988, 1988// 1988 Berlin, Heidelberg. Springer Berlin Heidelberg, 2-10.
- OZBUN, M. A. 2002. Human papillomavirus type 31b infection of human keratinocytes and the onset of early transcription. *J Virol*, 76, 11291-300.
- OZBUN, M. A. 2019. Extracellular events impacting human papillomavirus infections: Epithelial wounding to cell signaling involved in virus entry. *Papillomavirus Research*, 7, 188-192.

- PAAVONEN, J., JENKINS, D., BOSCH, F. X., NAUD, P., SALMERÓN, J., WHEELER, C. M., CHOW, S.-N., APTER, D. L., KITCHENER, H. C., CASTELLSAGUE, X., DE CARVALHO, N. S., SKINNER, S. R., HARPER, D. M., HEDRICK, J. A., JAISAMRARN, U., LIMSON, G. A. M., DIONNE, M., QUINT, W., SPIESSENS, B., PEETERS, P., STRUYF, F., WIETING, S. L., LEHTINEN, M. O. & DUBIN, G. 2007. Efficacy of a prophylactic adjuvanted bivalent L1 virus-like-particle vaccine against infection with human papillomavirus types 16 and 18 in young women: an interim analysis of a phase III double-blind, randomised controlled trial. *The Lancet*, 369, 2161-2170.
- PALM, A.-K. E. & HENRY, C. 2019. Remembrance of Things Past: Long-Term B Cell Memory After Infection and Vaccination. *Frontiers in Immunology*, 10.
- PANTALEO, G., CORREIA, B., FENWICK, C., JOO, V. S. & PEREZ, L. 2022. Antibodies to combat viral infections: development strategies and progress. *Nature Reviews Drug Discovery*, 21, 676-696.
- PARK, J. S., KIM, E. J., KWON, H. J., HWANG, E. S., NAMKOONG, S. E. & UM, S. J. 2000. Inactivation of interferon regulatory factor-1 tumor suppressor protein by HPV E7 oncoprotein. Implication for the E7-mediated immune evasion mechanism in cervical carcinogenesis. *J Biol Chem*, 275, 6764-9.
- PASMANS, H., BERKOWSKA, M. A., DIKS, A. M., DE MOOIJ, B., GROENLAND, R. J., DE ROND, L., NICOLAIE, M. A., VAN DER BURG, S. H., VAN DONGEN, J. J. M., VAN DER KLIS, F. R. M. & BUISMAN, A.-M. 2022. Characterization of the early cellular immune response induced by HPV vaccines. *Frontiers in Immunology*, 13.
- PASSMORE, J. A., MARAIS, D. J., SAMPSON, C., ALLAN, B., PARKER, N., MILNER, M., DENNY, L. & WILLIAMSON, A. L. 2007. Cervicovaginal, oral, and serum IgG and IgA responses to human papillomavirus type 16 in women with cervical intraepithelial neoplasia. *J Med Virol*, 79, 1375-80.
- PATTYN, J., VAN KEER, S., TJALMA, W., MATHEEUSSEN, V., VAN DAMME, P. & VORSTERS, A. 2019a. Infection and vaccine-induced HPV-specific antibodies in cervicovaginal secretions. A review of the literature. *Papillomavirus Res*, 8, 100185.
- PATTYN, J., VAN KEER, S., TJALMA, W., MATHEEUSSEN, V., VAN DAMME, P. & VORSTERS, A. 2019b. Infection and vaccine-induced HPV-specific antibodies in cervicovaginal secretions. A review of the literature. *Papillomavirus research (Amsterdam, Netherlands)*, 8, 100185-100185.
- PAUL, S. & LAL, G. 2017. The Molecular Mechanism of Natural Killer Cells Function and Its Importance in Cancer Immunotherapy. *Front Immunol*, 8, 1124.
- PAVLASOVA, G. & MRAZ, M. 2020. The regulation and function of CD20: an "enigma" of B-cell biology and targeted therapy. *Haematologica*, 105, 1494-1506.
- PEREZ-ANDRES, M., PAIVA, B., NIETO, W. G., CARAUX, A., SCHMITZ, A., ALMEIDA, J., VOGT, R. F., JR., MARTI, G. E., RAWSTRON, A. C., VAN ZELM, M. C., VAN DONGEN, J. J., JOHNSEN, H. E., KLEIN, B. & ORFAO, A. 2010. Human peripheral blood B-cell compartments: a crossroad in B-cell traffic. *Cytometry B Clin Cytom*, 78 Suppl 1, S47-60.
- PERREAU, M., SAVOYE, A. L., DE CRIGNIS, E., CORPATAUX, J. M., CUBAS, R., HADDAD, E. K., DE LEVAL, L., GRAZIOSI, C. & PANTALEO, G. 2013. Follicular helper T cells serve as the major CD4 T cell compartment for HIV-1 infection, replication, and production. *J Exp Med*, 210, 143-56.
- PERRIN-COCON, L. A., VILLIERS, C. L., SALAMERO, J., GABERT, F. & MARCHE, P. N. 2004. B cell receptors and complement receptors target the antigen to distinct intracellular compartments. *J Immunol*, 172, 3564-72.
- PETÄJÄ, T., PEDERSEN, C., PODER, A., STRAUSS, G., CATTEAU, G., THOMAS, F., LEHTINEN, M. & DESCAMPS, D. 2011. Long-term persistence of systemic and mucosal immune response to

- HPV-16/18 AS04-adjuvanted vaccine in preteen/adolescent girls and young women. *Int J Cancer*, 129, 2147-57.
- PINNA, D., CORTI, D., JARROSSAY, D., SALLUSTO, F. & LANZAVECCHIA, A. 2009. Clonal dissection of the human memory B-cell repertoire following infection and vaccination. *European Journal of Immunology*, 39, 1260-1270.
- PINTO, L. A., CASTLE, P. E., RODEN, R. B., HARRO, C. D., LOWY, D. R., SCHILLER, J. T., WALLACE, D., WILLIAMS, M., KOPP, W., FRAZER, I. H., BERZOFOSKY, J. A. & HILDESHEIM, A. 2005. HPV-16 L1 VLP vaccine elicits a broad-spectrum of cytokine responses in whole blood. *Vaccine*, 23, 3555-64.
- PINTO, L. A., DILLNER, J., BEDDOWS, S. & UNGER, E. R. 2018. Immunogenicity of HPV prophylactic vaccines: Serology assays and their use in HPV vaccine evaluation and development. *Vaccine*, 36, 4792-4799.
- PINTO, L. A., EDWARDS, J., CASTLE, P. E., HARRO, C. D., LOWY, D. R., SCHILLER, J. T., WALLACE, D., KOPP, W., ADELSBERGER, J. W., BASELER, M. W., BERZOFOSKY, J. A. & HILDESHEIM, A. 2003. Cellular immune responses to human papillomavirus (HPV)-16 L1 in healthy volunteers immunized with recombinant HPV-16 L1 virus-like particles. *J Infect Dis*, 188, 327-38.
- PINTO, L. A., VISCIDI, R., HARRO, C. D., KEMP, T. J., GARCIA-PINERES, A. J., TRIVETT, M., DEMUTH, F., LOWY, D. R., SCHILLER, J. T., BERZOFOSKY, J. A. & HILDESHEIM, A. 2006. Cellular immune responses to HPV-18, -31, and -53 in healthy volunteers immunized with recombinant HPV-16 L1 virus-like particles. *Virology*, 353, 451-62.
- PIRAMI, L., GIACHÈ, V. & BECCIOLINI, A. 1997. Analysis of HPV16, 18, 31, and 35 DNA in pre-invasive and invasive lesions of the uterine cervix. *J Clin Pathol*, 50, 600-4.
- POHOLEK, A. C., HANSEN, K., HERNANDEZ, S. G., ETO, D., CHANDELE, A., WEINSTEIN, J. S., DONG, X., ODEGARD, J. M., KAECH, S. M. & DENT, A. L. 2010. In vivo regulation of Bcl6 and T follicular helper cell development. *The Journal of immunology*, 185, 313-326.
- POLLARD, A. J. & BIJKER, E. M. 2021. A guide to vaccinology: from basic principles to new developments. *Nature Reviews Immunology*, 21, 83-100.
- POLONELLI, L., PONTÓN, J., ELGUEZABAL, N., MORAGUES, M. D., CASOLI, C., PILOTTI, E., RONZI, P., DOBROFF, A. S., RODRIGUES, E. G., JULIANO, M. A., MAFFEI, D. L., MAGLIANI, W., CONTI, S. & TRAVASSOS, L. R. 2008. Antibody complementarity-determining regions (CDRs) can display differential antimicrobial, antiviral and antitumor activities. *PLoS One*, 3, e2371.
- POLONI, C., SCHONHOFER, C., IVISON, S., LEVINGS, M. K., STEINER, T. S. & COOK, L. 2023. T-cell activation-induced marker assays in health and disease. *Immunol Cell Biol*, 101, 491-503.
- PONE, E. J., HERNANDEZ-DAVIES, J. E., JAN, S., SILZEL, E., FELGNER, P. L. & DAVIES, D. H. 2022. Multimericity Amplifies the Synergy of BCR and TLR4 for B Cell Activation and Antibody Class Switching. *Front Immunol*, 13, 882502.
- POPI, A. F., LONGO-MAUGÉRI, I. M. & MARIANO, M. 2016. An Overview of B-1 Cells as Antigen-Presenting Cells. *Front Immunol*, 7, 138.
- PORRAS, C., TSANG, S. H., HERRERO, R., GUILLÉN, D., DARRAGH, T. M., STOLER, M. H., HILDESHEIM, A., WAGNER, S., BOLAND, J., LOWY, D. R., SCHILLER, J. T., SCHIFFMAN, M., SCHUSSLER, J., GAIL, M. H., QUINT, W., OCAMPO, R., MORALES, J., RODRÍGUEZ, A. C., HU, S., SAMPSON, J. N. & KREIMER, A. R. 2020. Efficacy of the bivalent HPV vaccine against HPV 16/18-associated precancer: long-term follow-up results from the Costa Rica Vaccine Trial. *Lancet Oncol*, 21, 1643-1652.
- POULSON, N. D. & LECHLER, T. 2012. Asymmetric cell divisions in the epidermis. *Int Rev Cell Mol Biol*, 295, 199-232.

- PRAGER, I. & WATZL, C. 2019. Mechanisms of natural killer cell-mediated cellular cytotoxicity. *J Leukoc Biol*, 105, 1319-1329.
- PUTHANAKIT, T., HUANG, L. M., CHIU, C. H., TANG, R. B., SCHWARZ, T. F., ESPOSITO, S., FRENETTE, L., GIAQUINTO, C., MCNEIL, S., RHEAULT, P., DURANDO, P., HORN, M., KLAR, M., PONCELET, S., DE SIMONI, S., FRIEL, D., DE MUYNCK, B., SURYAKIRAN, P. V., HEZAREH, M., DESCAMPS, D., THOMAS, F. & STRUYF, F. 2016. Randomized Open Trial Comparing 2-Dose Regimens of the Human Papillomavirus 16/18 AS04-Adjuvanted Vaccine in Girls Aged 9-14 Years Versus a 3-Dose Regimen in Women Aged 15-25 Years. *J Infect Dis*, 214, 525-36.
- PYEON, D., PEARCE, S. M., LANK, S. M., AHLQUIST, P. & LAMBERT, P. F. 2009. Establishment of Human Papillomavirus Infection Requires Cell Cycle Progression. *PLOS Pathogens*, 5, e1000318.
- RASHEED, A. U., RAHN, H. P., SALLUSTO, F., LIPP, M. & MÜLLER, G. 2006. Follicular B helper T cell activity is confined to CXCR5hiICOShi CD4 T cells and is independent of CD57 expression. *European journal of immunology*, 36, 1892-1903.
- REDDY, S. T., REHOR, A., SCHMOEKEL, H. G., HUBBELL, J. A. & SWARTZ, M. A. 2006. In vivo targeting of dendritic cells in lymph nodes with poly(propylene sulfide) nanoparticles. *J Control Release*, 112, 26-34.
- REISS, S., BAXTER, A. E., CIRELLI, K. M., DAN, J. M., MOROU, A., DAIGNEAULT, A., BRASSARD, N., SILVESTRI, G., ROUTY, J.-P., HAVENAR-DAUGHTON, C., CROTTY, S. & KAUFMANN, D. E. 2017a. Comparative analysis of activation induced marker (AIM) assays for sensitive identification of antigen-specific CD4 T cells. *PLoS one*, 12, e0186998-e0186998.
- REISS, S., BAXTER, A. E., CIRELLI, K. M., DAN, J. M., MOROU, A., DAIGNEAULT, A., BRASSARD, N., SILVESTRI, G., ROUTY, J. P., HAVENAR-DAUGHTON, C., CROTTY, S. & KAUFMANN, D. E. 2017b. Comparative analysis of activation induced marker (AIM) assays for sensitive identification of antigen-specific CD4 T cells. *PLoS One*, 12, e0186998.
- RESTREPO, J., HERRERA, T., SAMAKOSES, R., REINA, J. C., PITISUTTITHUM, P., ULIED, A., BEKKER, L.-G., MOREIRA, E. D., JR, OLSSON, S.-E., BLOCK, S. L., HAMMES, L. S., LAGINHA, F., FERENCZY, A., KURMAN, R., RONNETT, B. M., STOLER, M., BAUTISTA, O., GALLAGHER, N. E., SALITURO, G., YE, M. & LUXEMBOURG, A. 2023. Ten-Year Follow-up of 9-Valent Human Papillomavirus Vaccine: Immunogenicity, Effectiveness, and Safety. *Pediatrics*, 152.
- REUSSER, N. M., DOWNING, C., GUIDRY, J. & TYRING, S. K. 2015. HPV Carcinomas in Immunocompromised Patients. *Journal of clinical medicine*, 4, 260-281.
- RICHARDS, R. M., LOWY, D. R., SCHILLER, J. T. & DAY, P. M. 2006. Cleavage of the papillomavirus minor capsid protein, L2, at a furin consensus site is necessary for infection. *Proc Natl Acad Sci U S A*, 103, 1522-7.
- RICHMOND, J. M. & HARRIS, J. E. 2014. Immunology and skin in health and disease. *Cold Spring Harbor perspectives in medicine*, 4, a015339.
- ROBERTS, C., GREEN, T., HESS, E., MATYS, K., BROWN, M. J., HAUPT, R. M., LUXEMBOURG, A., VUOCOLO, S., SAAH, A. & ANTONELLO, J. 2014. Development of a human papillomavirus competitive luminex immunoassay for 9 HPV types. *Hum Vaccin Immunother*, 10, 2168-74.
- ROBERTS, J. N., BUCK, C. B., THOMPSON, C. D., KINES, R., BERNARDO, M., CHOYKE, P. L., LOWY, D. R. & SCHILLER, J. T. 2007. Genital transmission of HPV in a mouse model is potentiated by nonoxynol-9 and inhibited by carrageenan. *Nat Med*, 13, 857-61.
- ROBINSON, J. P., OSTAFE, R., IYENGAR, S. N., RAJWA, B. & FISCHER, R. 2023. Flow Cytometry: The Next Revolution. *Cells*, 12.

- RODRIGUEZ-PINTO, D., SARAVIA, N. G. & MCMAHON-PRATT, D. 2014. CD4 T cell activation by B cells in human Leishmania (Viannia) infection. *BMC Infectious Diseases*, 14, 108.
- ROMERO-RAMÍREZ, H., MORALES-GUADARRAMA, M. T., PELAYO, R., LÓPEZ-SANTIAGO, R. & SANTOS-ARGUMEDO, L. 2015. CD38 expression in early B-cell precursors contributes to extracellular signal-regulated kinase-mediated apoptosis. *Immunology*, 144, 271-81.
- RONCO, L. V., KARPOVA, A. Y., VIDAL, M. & HOWLEY, P. M. 1998. Human papillomavirus 16 E6 oncoprotein binds to interferon regulatory factor-3 and inhibits its transcriptional activity. *Genes Dev*, 12, 2061-72.
- ROSS, J. B., MYERS, L. M., NOH, J. J., COLLINS, M. M., CARMODY, A. B., MESSER, R. J., DHUEY, E., HASENKRUG, K. J. & WEISSMAN, I. L. 2024. Depleting myeloid-biased haematopoietic stem cells rejuvenates aged immunity. *Nature*, 628, 162-170.
- ROTH, D. B. 2014. V(D)J Recombination: Mechanism, Errors, and Fidelity. *Microbiol Spectr*, 2.
- ROTHSTEIN, T. L., GRIFFIN, D. O., HOLODICK, N. E., QUACH, T. D. & KAKU, H. 2013. Human B-1 cells take the stage. *Ann N Y Acad Sci*, 1285, 97-114.
- ROURA, E., CASTELLSAGUÉ, X., PAWLITA, M., TRAVIER, N., WATERBOER, T., MARGALL, N., BOSCH, F. X., DE SANJOSÉ, S., DILLNER, J., GRAM, I. T., TJØNNELAND, A., MUNK, C., PALA, V., PALLI, D., KHAW, K. T., BARNABAS, R. V., OVERVAD, K., CLAVEL-CHAPELON, F., BOUTRON-RUAULT, M. C., FAGHERAZZI, G., KAAKS, R., LUKANOVA, A., STEFFEN, A., TRICHOPOULOU, A., TRICHOPOULOS, D., KLINAKI, E., TUMINO, R., SACERDOTE, C., PANICO, S., BUENO-DE-MESQUITA, H. B., PEETERS, P. H., LUND, E., WEIDERPASS, E., REDONDO, M. L., SÁNCHEZ, M. J., TORMO, M. J., BARRICARTE, A., LARRAÑAGA, N., EKSTRÖM, J., HORTLUND, M., LINDQUIST, D., WAREHAM, N., TRAVIS, R. C., RINALDI, S., TOMMASINO, M., FRANCESCHI, S. & RIBOLI, E. 2014. Smoking as a major risk factor for cervical cancer and pre-cancer: results from the EPIC cohort. *Int J Cancer*, 135, 453-66.
- ROY, V., JUNG, W., LINDE, C., COATES, E., LEDGERWOOD, J., COSTNER, P., YAMSHCHIKOV, G., STREECK, H., JUELIG, B., LAUFFENBURGER, D. A. & ALTER, G. 2023. Differences in HPV-specific antibody Fc-effector functions following Gardasil® and Cervarix® vaccination. *npj Vaccines*, 8, 39.
- SACCUCCI, M., FRANCO, E. L., DING, L., BERNSTEIN, D. I., BROWN, D. & KAHN, J. A. 2018. Non-Vaccine-Type Human Papillomavirus Prevalence After Vaccine Introduction: No Evidence for Type Replacement but Evidence for Cross-Protection. *Sex Transm Dis*, 45, 260-265.
- SAFAEIAN, M., CASTELLSAGUÉ, X., HILDESHEIM, A., WACHOLDER, S., SCHIFFMAN, M. H., BOZONNAT, M. C., BARIL, L. & ROSILLON, D. 2018. Risk of HPV-16/18 Infections and Associated Cervical Abnormalities in Women Seropositive for Naturally Acquired Antibodies: Pooled Analysis Based on Control Arms of Two Large Clinical Trials. *J Infect Dis*, 218, 84-94.
- SAFAEIAN, M., PORRAS, C., PAN, Y., KREIMER, A., SCHILLER, J. T., GONZALEZ, P., LOWY, D. R., WACHOLDER, S., SCHIFFMAN, M., RODRIGUEZ, A. C., HERRERO, R., KEMP, T., SHELTON, G., QUINT, W., VAN DOORN, L. J., HILDESHEIM, A. & PINTO, L. A. 2013. Durable antibody responses following one dose of the bivalent human papillomavirus L1 virus-like particle vaccine in the Costa Rica Vaccine Trial. *Cancer Prev Res (Phila)*, 6, 1242-50.
- SAGAERT, X. & DE WOLF-PEETERS, C. 2003. Classification of B-cells according to their differentiation status, their micro-anatomical localisation and their developmental lineage. *Immunol Lett*, 90, 179-86.
- SAGE, P. T., ALVAREZ, D., GODEC, J., VON ANDRIAN, U. H. & SHARPE, A. H. 2014. Circulating T follicular regulatory and helper cells have memory-like properties. *J Clin Invest*, 124, 5191-204.

- SALLUSTO, F., LANZAVECCHIA, A., ARAKI, K. & AHMED, R. 2010. From vaccines to memory and back. *Immunity*, 33, 451-463.
- SANZ, I., WEI, C., JENKS, S. A., CASHMAN, K. S., TIPTON, C., WOODRUFF, M. C., HOM, J. & LEE, F. E. 2019. Challenges and Opportunities for Consistent Classification of Human B Cell and Plasma Cell Populations. *Front Immunol*, 10, 2458.
- SASAGAWA, T., INOUE, M., LEHTINEN, M., ZHANG, W., GSCHMEISSNER, S. E., HAJIBAGHERI, M. A., FINCH, J. & CRAWFORD, L. 1996. Serological responses to human papillomavirus type 6 and 16 virus-like particles in patients with cervical neoplastic lesions. *Clinical and diagnostic laboratory immunology*, 3, 403-410.
- SASAGAWA, T., YAMAZAKI, H., DONG, Y. Z., SATAKE, S., TATENO, M. & INOUE, M. 1998. Immunoglobulin-A and -G responses against virus-like particles (VLP) of human papillomavirus type 16 in women with cervical cancer and cervical intra-epithelial lesions. *Int J Cancer*, 75, 529-35.
- SATHE A, C. J. Updated 2021 December. *Biochemistry, Immunoglobulin M.*, Treasure Island (FL): StatPearls Publishing.
- SCHAUER, U., STEMBERG, F., RIEGER, C. H., BÜTTNER, W., BORTE, M., SCHUBERT, S., MÖLLERS, H., RIEDEL, F., HERZ, U., RENZ, H. & HERZOG, W. 2003. Levels of antibodies specific to tetanus toxoid, Haemophilus influenzae type b, and pneumococcal capsular polysaccharide in healthy children and adults. *Clin Diagn Lab Immunol*, 10, 202-7.
- SCHERER, E. M., SMITH, R. A., CARTER, J. J., WIPF, G. C., GALLEGRO, D. F., STERN, M., WALD, A. & GALLOWAY, D. A. 2018. Analysis of Memory B-Cell Responses Reveals Suboptimal Dosing Schedule of a Licensed Vaccine. *J Infect Dis*, 217, 572-580.
- SCHERER, E. M., SMITH, R. A., GALLEGRO, D. F., CARTER, J. J., WIPF, G. C., HOYOS, M., STERN, M., THURSTON, T., TRINKLEIN, N. D., WALD, A. & GALLOWAY, D. A. 2016. A Single Human Papillomavirus Vaccine Dose Improves B Cell Memory in Previously Infected Subjects. *EBioMedicine*, 10, 55-64.
- SCHERER, E. M., SMITH, R. A., SIMONICH, C. A., NIYONZIMA, N., CARTER, J. J. & GALLOWAY, D. A. 2014a. Characteristics of memory B cells elicited by a highly efficacious HPV vaccine in subjects with no pre-existing immunity. *PLoS Pathog*, 10, e1004461.
- SCHERER, E. M., SMITH, R. A., SIMONICH, C. A., NIYONZIMA, N., CARTER, J. J. & GALLOWAY, D. A. 2014b. Characteristics of Memory B Cells Elicited by a Highly Efficacious HPV Vaccine in Subjects with No Pre-existing Immunity. *PLOS Pathogens*, 10, e1004461.
- SCHERPENISSE, M., MOLLERS, M., SCHEPP, R. M., MEIJER, C. J., DE MELKER, H. E., BERBERS, G. A. & VAN DER KLIS, F. R. 2013a. Detection of systemic and mucosal HPV-specific IgG and IgA antibodies in adolescent girls one and two years after HPV vaccination. *Hum Vaccin Immunother*, 9, 314-21.
- SCHERPENISSE, M., SCHEPP, R. M., MOLLERS, M., MEIJER, C. J., BERBERS, G. A. & VAN DER KLIS, F. R. 2013b. Characteristics of HPV-specific antibody responses induced by infection and vaccination: cross-reactivity, neutralizing activity, avidity and IgG subclasses. *PLoS One*, 8, e74797.
- SCHILLER, J. & LOWY, D. 2018a. Explanations for the high potency of HPV prophylactic vaccines. *Vaccine*, 36, 4768-4773.
- SCHILLER, J. & LOWY, D. 2018b. Explanations for the high potency of HPV prophylactic vaccines. *Vaccine*, 36, 4768-4773.
- SCHILLER, J. T., DAY, P. M. & KINES, R. C. 2010. Current understanding of the mechanism of HPV infection. *Gynecol Oncol*, 118, S12-7.

- SCHILLER, J. T. & LOWY, D. R. 2012. Understanding and learning from the success of prophylactic human papillomavirus vaccines. *Nat Rev Microbiol*, 10, 681-92.
- SCHILLER, J. T. & MÜLLER, M. 2015. Next generation prophylactic human papillomavirus vaccines. *Lancet Oncol*, 16, e217-25.
- SCHMITT, N. & UENO, H. 2013. Human T follicular helper cells: development and subsets. *Adv Exp Med Biol*, 785, 87-94.
- SCHNYDER, J. L., DE JONG, H. K., BACHE, B. E., SCHAUMBURG, F. & GROBUSCH, M. P. 2024. Long-term immunity following yellow fever vaccination: a systematic review and meta-analysis. *The Lancet Global Health*, 12, e445-e456.
- SCHOLZEN, A., NAHRENDORF, W., LANGHORNE, J. & SAUERWEIN, R. W. 2014. Expansion of IgG+ B-Cells during Mitogen Stimulation for Memory B-Cell ELISpot Analysis Is Influenced by Size and Composition of the B-Cell Pool. *PLOS ONE*, 9, e102885.
- SCHULZ, A. R., FIEBIG, L., HIRSELAND, H., DIEKMANN, L.-M., REINKE, S., HARDT, S., NIEDOBITEK, A. & MEI, H. E. 2023. SARS-CoV-2 specific plasma cells acquire long-lived phenotypes in human bone marrow. *eBioMedicine*, 95.
- SCHWARZ, T. F., KOCKEN, M., PETÄJÄ, T., EINSTEIN, M. H., SPACZYNSKI, M., LOUWERS, J. A., PEDERSEN, C., LEVIN, M., ZAHAF, T., PONCELET, S., HARDT, K., DESCAMPS, D. & DUBIN, G. 2010. Correlation between levels of human papillomavirus (HPV)-16 and 18 antibodies in serum and cervicovaginal secretions in girls and women vaccinated with the HPV-16/18 AS04-adjuvanted vaccine. *Hum Vaccin*, 6, 1054-61.
- SCOTT, M., NAKAGAWA, M. & MOSCICKI, A. B. 2001. Cell-mediated immune response to human papillomavirus infection. *Clinical and diagnostic laboratory immunology*, 8, 209-220.
- SELINKA, H. C., FLORIN, L., PATEL, H. D., FREITAG, K., SCHMIDTKE, M., MAKAROV, V. A. & SAPP, M. 2007. Inhibition of transfer to secondary receptors by heparan sulfate-binding drug or antibody induces noninfectious uptake of human papillomavirus. *J Virol*, 81, 10970-80.
- SELINKA, H. C., GIROGLOU, T. & SAPP, M. 2002. Analysis of the infectious entry pathway of human papillomavirus type 33 pseudovirions. *Virology*, 299, 279-287.
- SERESINI, S., ORIGONI, M., CAPUTO, L., LILLO, F., LONGHI, R., VANTINI, S., PAGANONI, A. M. & PROTTI, M. P. 2010. CD4+ T cells against human papillomavirus-18 E7 in patients with high-grade cervical lesions associate with the absence of the virus in the cervix. *Immunology*, 131, 89-98.
- SERESINI, S., ORIGONI, M., LILLO, F., CAPUTO, L., PAGANONI, A. M., VANTINI, S., LONGHI, R., TACCAGNI, G., FERRARI, A., DOGLIONI, C., SECCHI, P. & PROTTI, M. P. 2007. IFN-gamma produced by human papilloma virus-18 E6-specific CD4+ T cells predicts the clinical outcome after surgery in patients with high-grade cervical lesions. *J Immunol*, 179, 7176-83.
- SETLIFF, I., SHIAKOLAS, A. R., PILEWSKI, K. A., MURJI, A. A., MAPENGO, R. E., JANOWSKA, K., RICHARDSON, S., OOSTHUYSEN, C., RAJU, N., RONSARD, L., KANEKIYO, M., QIN, J. S., KRAMER, K. J., GREENPLATE, A. R., MCDONNELL, W. J., GRAHAM, B. S., CONNORS, M., LINGWOOD, D., ACHARYA, P., MORRIS, L. & GEORGIEV, I. S. 2019. High-Throughput Mapping of B Cell Receptor Sequences to Antigen Specificity. *Cell*, 179, 1636-1646.e15.
- SHAFTI-KERAMAT, S., HANDISURYA, A., KRIEHLBER, E., MENEGUZZI, G., SLUPETZKY, K. & KIRNBAUER, R. 2003. Different heparan sulfate proteoglycans serve as cellular receptors for human papillomaviruses. *J Virol*, 77, 13125-35.
- SHAH, H. B., SMITH, K., WREN, J. D., WEBB, C. F., BALLARD, J. D., BOURN, R. L., JAMES, J. A. & LANG, M. L. 2019. Insights From Analysis of Human Antigen-Specific Memory B Cell Repertoires. *Frontiers in Immunology*, 9.

- SHATTOCK, A. J., JOHNSON, H. C., SIM, S. Y., CARTER, A., LAMBACH, P., HUTUBESSY, R. C. W., THOMPSON, K. M., BADIZADEGAN, K., LAMBERT, B., FERRARI, M. J., JIT, M., FU, H., SILAL, S. P., HOUNSELL, R. A., WHITE, R. G., MOSSER, J. F., GAYTHORPE, K. A. M., TROTTER, C. L., LINDSTRAND, A., O'BRIEN, K. L. & BAR-ZEEV, N. 2024. Contribution of vaccination to improved survival and health: modelling 50 years of the Expanded Programme on Immunization. *The Lancet*, 403, 2307-2316.
- SHINNAKASU, R. & KUROSAKI, T. 2017. Regulation of memory B and plasma cell differentiation. *Current Opinion in Immunology*, 45, 126-131.
- SIEGRIST, C.-A. 2008. Chapter 2 - Vaccine immunology. In: PLOTKIN, S. A., ORENSTEIN, W. A. & OFFIT, P. A. (eds.) *Vaccines (Fifth Edition)*. Edinburgh: W.B. Saunders.
- SLIFKA, M. K. & AHMED, R. 1996. Limiting dilution analysis of virus-specific memory B cells by an ELISPOT assay. *J Immunol Methods*, 199, 37-46.
- SLIFKA, M. K., ANTIA, R., WHITMIRE, J. K. & AHMED, R. 1998a. Humoral Immunity Due to Long-Lived Plasma Cells. *Immunity*, 8, 363-372.
- SLIFKA, M. K., ANTIA, R., WHITMIRE, J. K. & AHMED, R. 1998b. Humoral immunity due to long-lived plasma cells. *Immunity*, 8, 363-72.
- SLIFKA, M. K., MATLOUBIAN, M. & AHMED, R. 1995. Bone marrow is a major site of long-term antibody production after acute viral infection. *Journal of virology*, 69, 1895-1902.
- SMITH, K. G., LIGHT, A., NOSSAL, G. & TARLINTON, D. M. 1997. The extent of affinity maturation differs between the memory and antibody-forming cell compartments in the primary immune response. *The EMBO journal*, 16, 2996-3006.
- SMOLEN, K. K., GELINAS, L., FRANZEN, L., DOBSON, S., DAWAR, M., OGILVIE, G., KRAJDEN, M., FORTUNO, E. S. & KOLLMANN, T. R. 2012. Age of recipient and number of doses differentially impact human B and T cell immune memory responses to HPV vaccination. *Vaccine*, 30, 3572-3579.
- SOW, P. S., WATSON-JONES, D., KIVIAT, N., CHANGALUCHA, J., MBAYE, K. D., BROWN, J., BOUSSO, K., KAVISHE, B., ANDREASEN, A., TOURE, M., KAPIGA, S., MAYAUD, P., HAYES, R., LEBACQ, M., HERAZEH, M., THOMAS, F. & DESCAMPS, D. 2013. Safety and immunogenicity of human papillomavirus-16/18 AS04-adjuvanted vaccine: a randomized trial in 10-25-year-old HIV-Seronegative African girls and young women. *The Journal of infectious diseases*, 207, 1753-1763.
- SPAYNE, J. & HESKETH, T. 2021. Estimate of global human papillomavirus vaccination coverage: analysis of country-level indicators. *BMJ Open*, 11, e052016.
- STADNYK, A. W. 1994. Cytokine production by epithelial cells. *Faseb j*, 8, 1041-7.
- STANLEY, M. 2010a. HPV - immune response to infection and vaccination. *Infectious agents and cancer*, 5, 19-19.
- STANLEY, M. 2010b. HPV - immune response to infection and vaccination. *Infect Agent Cancer*, 5, 19.
- STANLEY, M. 2010c. Potential mechanisms for HPV vaccine-induced long-term protection. *Gynecol Oncol*, 118, S2-7.
- STANLEY, M. 2010d. Potential mechanisms for HPV vaccine-induced long-term protection. *Gynecologic Oncology*, 118, S2-S7.
- STANLEY, M. A. 2009. Immune responses to human papilloma viruses. *Indian J Med Res*, 130, 266-76.
- STANLEY, M. A. & STERLING, J. C. 2014. Host responses to infection with human papillomavirus. *Curr Probl Dermatol*, 45, 58-74.

- STAVNEZER, J. & SCHRADER, C. E. 2014. IgH chain class switch recombination: mechanism and regulation. *J Immunol*, 193, 5370-8.
- STEFFEN, U., KOELEMAN, C. A., SOKOLOVA, M. V., BANG, H., KLEYER, A., RECH, J., UNTERWEGER, H., SCHICHT, M., GARREIS, F., HAHN, J., ANDES, F. T., HARTMANN, F., HAHN, M., MAHAJAN, A., PAULSEN, F., HOFFMANN, M., LOCHNIT, G., MUÑOZ, L. E., WUHRER, M., FALCK, D., HERRMANN, M. & SCHETT, G. 2020. IgA subclasses have different effector functions associated with distinct glycosylation profiles. *Nature Communications*, 11, 120.
- STEIN, K., HUMMEL, M., KORBUJHN, P., FOSS, H. D., ANAGNOSTOPOULOS, I., MARAFIOTI, T. & STEIN, H. 1999. Monocytoid B cells are distinct from splenic marginal zone cells and commonly derive from unmutated naive B cells and less frequently from postgerminal center B cells by polyclonal transformation. *Blood*, 94, 2800-8.
- STEINBACH, A. & RIEMER, A. B. 2018. Immune evasion mechanisms of human papillomavirus: An update. *Int J Cancer*, 142, 224-229.
- STELZLE, D., TANAKA, L. F., LEE, K. K., IBRAHIM KHALIL, A., BAUSSANO, I., SHAH, A. S. V., MCALLISTER, D. A., GOTTLIEB, S. L., KLUG, S. J., WINKLER, A. S., BRAY, F., BAGGALEY, R., CLIFFORD, G. M., BROUTET, N. & DALAL, S. 2021. Estimates of the global burden of cervical cancer associated with HIV. *The Lancet Global Health*, 9, e161-e169.
- STENTELLA, P., FREGA, A., CICCARONE, M., CIPRIANO, L., TINARI, A., TZANTZOGLOU, S. & PACHÌ, A. 1998. HPV and intraepithelial neoplasia recurrent lesions of the lower genital tract: assessment of the immune system. *Eur J Gynaecol Oncol*, 19, 466-9.
- STERLING, J. C., SKEPPER, J. N. & STANLEY, M. A. 1993. Immunoelectron microscopical localization of human papillomavirus type 16 L1 and E4 proteins in cervical keratinocytes cultured in vivo. *J Invest Dermatol*, 100, 154-8.
- STRICKLER, H. D., BURK, R. D., FAZZARI, M., ANASTOS, K., MINKOFF, H., MASSAD, L. S., HALL, C., BACON, M., LEVINE, A. M., WATTS, D. H., SILVERBERG, M. J., XUE, X., SCHLECHT, N. F., MELNICK, S. & PALEFSKY, J. M. 2005. Natural history and possible reactivation of human papillomavirus in human immunodeficiency virus-positive women. *J Natl Cancer Inst*, 97, 577-86.
- SURVILADZE, Z., DZIDUSZKO, A. & OZBUN, M. A. 2012. Essential Roles for Soluble Virion-Associated Heparan Sulfonated Proteoglycans and Growth Factors in Human Papillomavirus Infections. *PLOS Pathogens*, 8, e1002519.
- SYEDA, M. Z., HONG, T., HUANG, C., HUANG, W. & MU, Q. 2024. B cell memory: from generation to reactivation: a multipronged defense wall against pathogens. *Cell Death Discovery*, 10, 117.
- SZAKAL, A. K., KOSCO, M. H. & TEW, J. G. 1989. Microanatomy of Lymphoid Tissue During Humoral Immune Responses: Structure Function Relationships. *Annual Review of Immunology*, 7, 91-109.
- TAILLARDET, M., HAFFAR, G., MONDIÈRE, P., ASENSIO, M. J., GHEIT, H., BURDIN, N., DEFRANCE, T. & GENESTIER, L. 2009. The thymus-independent immunity conferred by a pneumococcal polysaccharide is mediated by long-lived plasma cells. *Blood*, 114, 4432-40.
- TANG, A., AMAGAI, M., GRANGER, L. G., STANLEY, J. R. & UDEY, M. C. 1993. Adhesion of epidermal Langerhans cells to keratinocytes mediated by E-cadherin. *Nature*, 361, 82-5.
- TANGYE, S. G. 2011. Staying alive: regulation of plasma cell survival. *Trends Immunol*, 32, 595-602.
- TANTENGO, O. A. G., NAKURA, Y., YOSHIMURA, M., NISHIUMI, F., LLAMAS-CLARK, E. F. & YANAGIHARA, I. 2022. Co-infection of human papillomavirus and other sexually transmitted bacteria in cervical cancer patients in the Philippines. *Gynecologic Oncology Reports*, 40, 100943.

- TAY, S. K., JENKINS, D., MADDOX, P., CAMPION, M. & SINGER, A. 1987a. Subpopulations of Langerhans' cells in cervical neoplasia. *Br J Obstet Gynaecol*, 94, 10-5.
- TAY, S. K., JENKINS, D., MADDOX, P., HOGG, N. & SINGER, A. 1987b. Tissue macrophage response in human papillomavirus infection and cervical intraepithelial neoplasia. *Br J Obstet Gynaecol*, 94, 1094-7.
- TEDDER, T. F. & SCHLOSSMAN, S. F. 1988. Phosphorylation of the B1 (CD20) molecule by normal and malignant human B lymphocytes. *J Biol Chem*, 263, 10009-15.
- TEHRANI, Z. R., HABIBZADEH, P., FLINKO, R., CHEN, H., ABBASI, A., YARED, J. A., CIUPE, S. M., LEWIS, G. K. & SAJADI, M. M. 2024. Deficient Generation of Spike-Specific Long-Lived Plasma Cells in the Bone Marrow After Severe Acute Respiratory Syndrome Coronavirus 2 Infection. *The Journal of Infectious Diseases*.
- TEIJARO, J. R. 2016. Type I interferons in viral control and immune regulation. *Curr Opin Virol*, 16, 31-40.
- TENG, G. & PAPAVALIOU, F. N. 2007. Immunoglobulin Somatic Hypermutation. *Annual Review of Genetics*, 41, 107-120.
- THYAGARAJAN, R., ARUNKUMAR, N. & SONG, W. 2003. Polyvalent antigens stabilize B cell antigen receptor surface signaling microdomains. *J Immunol*, 170, 6099-106.
- TOFT, L., TOLSTRUP, M., MÜLLER, M., SEHR, P., BONDE, J., STORGAARD, M., ØSTERGAARD, L. & SØGAARD, O. S. 2014. Comparison of the immunogenicity of Cervarix® and Gardasil® human papillomavirus vaccines for oncogenic non-vaccine serotypes HPV-31, HPV-33, and HPV-45 in HIV-infected adults. *Hum Vaccin Immunother*, 10, 1147-54.
- TOKOYODA, K., ZEHENTMEIER, S., CHANG, H. D. & RADBRUCH, A. 2009. Organization and maintenance of immunological memory by stroma niches. *Eur J Immunol*, 39, 2095-9.
- TONEGAWA, S. 1983. Somatic generation of antibody diversity. *Nature*, 302, 575-81.
- TORRES, L. M., CABRERA, T., CONCHA, A., OLIVA, M. R., RUIZ-CABELLO, F. & GARRIDO, F. 1993. HLA class I expression and HPV-16 sequences in premalignant and malignant lesions of the cervix. *Tissue Antigens*, 41, 65-71.
- TRÜCK, J., RAMASAMY, M. N., GALSON, J. D., RANCE, R., PARKHILL, J., LUNTER, G., POLLARD, A. J. & KELLY, D. F. 2015. Identification of antigen-specific B cell receptor sequences using public repertoire analysis. *J Immunol*, 194, 252-261.
- TURNER, J. S., MARTHI, M., BENET, Z. L. & GRIGOROVA, I. 2017. Transiently antigen-primed B cells return to naive-like state in absence of T-cell help. *Nature Communications*, 8, 15072.
- ULBRICHT, C., CAO, Y., NIESNER, R. A. & HAUSER, A. E. 2023. In good times and in bad: How plasma cells resolve stress for a life-long union with the bone marrow. *Front Immunol*, 14, 1112922.
- VALE, A. M., KEARNEY, J. F., NOBREGA, A. & SCHROEDER, H. W. 2015. Chapter 7 - Development and Function of B Cell Subsets. In: ALT, F. W., HONJO, T., RADBRUCH, A. & RETH, M. (eds.) *Molecular Biology of B Cells (Second Edition)*. London: Academic Press.
- VAMBUTAS, A., BONAGURA, V. R. & STEINBERG, B. M. 2000. Altered expression of TAP-1 and major histocompatibility complex class I in laryngeal papillomatosis: correlation of TAP-1 with disease. *Clin Diagn Lab Immunol*, 7, 79-85.
- VAN ROOIJEN, N. 1990. Direct intrafollicular differentiation of memory B cells into plasma cells. *Immunol Today*, 11, 154-7.
- VANDEPAPELIERE, P., BARRASSO, R., MEIJER, C. J., WALBOOMERS, J. M., WETTENDORFF, M., STANBERRY, L. R. & LACEY, C. J. 2005. Randomized controlled trial of an adjuvanted human

- papillomavirus (HPV) type 6 L2E7 vaccine: infection of external anogenital warts with multiple HPV types and failure of therapeutic vaccination. *J Infect Dis*, 192, 2099-107.
- VAQUER, S., JORDÁ, J., LÓPEZ DE LA OSA, E., ALVAREZ DE LOS HEROS, J., LÓPEZ-GARCÍA, N. & ALVAREZ DE MON, M. 1990. Clinical implications of natural killer (NK) cytotoxicity in patients with squamous cell carcinoma of the uterine cervix. *Gynecol Oncol*, 36, 90-2.
- VELOUNIAS, R. L. & TULL, T. J. 2022. Human B-cell subset identification and changes in inflammatory diseases. *Clin Exp Immunol*, 210, 201-216.
- VENERI, D., ORTOLANI, R., FRANCHINI, M., TRIDENTE, G., PIZZOLO, G. & VELLA, A. 2009. Expression of CD27 and CD23 on peripheral blood B lymphocytes in humans of different ages. *Blood Transfus*, 7, 29-34.
- VERESS, G., KÓNYA, J., CSIKY-MÉSZÁROS, T., CZEGLÉDY, J. & GERGELY, L. 1994. Human papillomavirus DNA and anti-HPV secretory IgA antibodies in cytologically normal cervical specimens. *J Med Virol*, 43, 201-7.
- VIAC, J., SOLER, C., CHARDONNET, Y., EUVRARD, S. & SCHMITT, D. 1993. Expression of immune associated surface antigens of keratinocytes in human papillomavirus-derived lesions. *Immunobiology*, 188, 392-402.
- VICTORA, G. D. & NUSSENZWEIG, M. C. 2012a. Germinal centers. *Annu Rev Immunol*, 30, 429-57.
- VICTORA, G. D. & NUSSENZWEIG, M. C. 2012b. Germinal Centers. *Annual Review of Immunology*, 30, 429-457.
- VIDARSSON, G., DEKKERS, G. & RISPENS, T. 2014. IgG subclasses and allotypes: from structure to effector functions. *Front Immunol*, 5, 520.
- VIEIRA, P. & RAJEWSKY, K. 1988. The half-lives of serum immunoglobulins in adult mice. *European journal of immunology*, 18, 313-316.
- VILLA, A., PATTON, L. L., GIULIANO, A. R., ESTRICH, C. G., PAHLKE, S. C., O'BRIEN, K. K., LIPMAN, R. D. & ARAUJO, M. W. B. 2020. Summary of the evidence on the safety, efficacy, and effectiveness of human papillomavirus vaccines: Umbrella review of systematic reviews. *The Journal of the American Dental Association*, 151, 245-254.e24.
- VILLA, L. L., AULT, K. A., GIULIANO, A. R., COSTA, R. L. R., PETTA, C. A., ANDRADE, R. P., BROWN, D. R., FERENCZY, A., HARPER, D. M., KOUTSKY, L. A., KURMAN, R. J., LEHTINEN, M., MALM, C., OLSSON, S.-E., RONNETT, B. M., SKJELDESTAD, F. E., STEINWALL, M., STOLER, M. H., WHEELER, C. M., TADDEO, F. J., YU, J., LUPINACCI, L., RAILKAR, R., MARCHESE, R., ESSER, M. T., BRYAN, J., JANSEN, K. U., SINGS, H. L., TAMMS, G. M., SAAH, A. J. & BARR, E. 2006a. Immunologic responses following administration of a vaccine targeting human papillomavirus Types 6, 11, 16, and 18. *Vaccine*, 24, 5571-5583.
- VILLA, L. L., COSTA, R. L., PETTA, C. A., ANDRADE, R. P., AULT, K. A., GIULIANO, A. R., WHEELER, C. M., KOUTSKY, L. A., MALM, C., LEHTINEN, M., SKJELDESTAD, F. E., OLSSON, S. E., STEINWALL, M., BROWN, D. R., KURMAN, R. J., RONNETT, B. M., STOLER, M. H., FERENCZY, A., HARPER, D. M., TAMMS, G. M., YU, J., LUPINACCI, L., RAILKAR, R., TADDEO, F. J., JANSEN, K. U., ESSER, M. T., SINGS, H. L., SAAH, A. J. & BARR, E. 2005. Prophylactic quadrivalent human papillomavirus (types 6, 11, 16, and 18) L1 virus-like particle vaccine in young women: a randomised double-blind placebo-controlled multicentre phase II efficacy trial. *Lancet Oncol*, 6, 271-8.
- VILLA, L. L., COSTA, R. L., PETTA, C. A., ANDRADE, R. P., PAAVONEN, J., IVERSEN, O. E., OLSSON, S. E., HOYE, J., STEINWALL, M., RIIS-JOHANNESSEN, G., ANDERSSON-ELLSTROM, A., ELFGREN, K., KROGH, G., LEHTINEN, M., MALM, C., TAMMS, G. M., GIACOLETTI, K., LUPINACCI, L., RAILKAR, R., TADDEO, F. J., BRYAN, J., ESSER, M. T., SINGS, H. L., SAAH, A. J. & BARR, E. 2006b. High sustained efficacy of a prophylactic quadrivalent human papillomavirus types

- 6/11/16/18 L1 virus-like particle vaccine through 5 years of follow-up. *Br J Cancer*, 95, 1459-66.
- VINUESA, C. G. & CHANG, P. P. 2013. Innate B cell helpers reveal novel types of antibody responses. *Nat Immunol*, 14, 119-26.
- WALBOOMERS, J. M., JACOBS, M. V., MANOS, M. M., BOSCH, F. X., KUMMER, J. A., SHAH, K. V., SNIJDERS, P. J., PETO, J., MEIJER, C. J. & MUNOZ, N. 1999. Human papillomavirus is a necessary cause of invasive cervical cancer worldwide. *J Pathol*, 189, 12-9.
- WALL, S. R., SCHERF, C. F., MORISON, L., HART, K. W., WEST, B., EKPO, G., FIANDER, A. N., MAN, S., GELDER, C. M., WALRAVEN, G. & BORYSIEWICZ, L. K. 2005. Cervical human papillomavirus infection and squamous intraepithelial lesions in rural Gambia, West Africa: viral sequence analysis and epidemiology. *Br J Cancer*, 93, 1068-76.
- WANG, B., AMERIO, P. & SAUDER, D. N. 1999. Role of cytokines in epidermal Langerhans cell migration. *J Leukoc Biol*, 66, 33-9.
- WANG, B., LI, X., LIU, L. & WANG, M. 2020. β -Catenin: oncogenic role and therapeutic target in cervical cancer. *Biol Res*, 53, 33.
- WANG, C., LIU, Y., CAVANAGH, M. M., LE SAUX, S., QI, Q., ROSKIN, K. M., LOONEY, T. J., LEE, J. Y., DIXIT, V., DEKKER, C. L., SWAN, G. E., GORONZY, J. J. & BOYD, S. D. 2015. B-cell repertoire responses to varicella-zoster vaccination in human identical twins. *Proc Natl Acad Sci U S A*, 112, 500-5.
- WANG, C., WRIGHT, T. C., DENNY, L. & KUHN, L. 2011. Rapid rise in detection of human papillomavirus (HPV) infection soon after incident HIV infection among South African women. *J Infect Dis*, 203, 479-86.
- WANG, H., LEAVITT, L., RAMASWAMY, R. & RAPRAEGER, A. C. 2010. Interaction of syndecan and $\alpha 6 \beta 4$ integrin cytoplasmic domains: regulation of ErbB2-mediated integrin activation. *Journal of Biological Chemistry*, 285, 13569-13579.
- WARD, S. M., PHALORA, P., BRADSHAW, D., LEYENDECKERS, H. & KLENERMAN, P. 2008. Direct ex vivo evaluation of long-lived protective antiviral memory B cell responses against hepatitis B virus. *J Infect Dis*, 198, 813-7.
- WATSON-JONES, D., CHANGALUCHA, J., WHITWORTH, H., PINTO, L., MUTANI, P., INDANGASI, J., KEMP, T., HASHIM, R., KAMALA, B., WIGGINS, R., SONGORO, T., CONNOR, N., MBWANJI, G., PAVON, M. A., LOWE, B., MMBANDO, D., KAPIGA, S., MAYAUD, P., DE SANJOSÉ, S., DILLNER, J., HAYES, R. J., LACEY, C. J. & BAISLEY, K. 2022. Immunogenicity and safety of one-dose human papillomavirus vaccine compared with two or three doses in Tanzanian girls (DoRIS): an open-label, randomised, non-inferiority trial. *Lancet Glob Health*, 10, e1473-e1484.
- WATZL, C. 2014. How to trigger a killer: modulation of natural killer cell reactivity on many levels. *Adv Immunol*, 124, 137-70.
- WEI, C., JUNG, J. & SANZ, I. 2011. OMIP-003: phenotypic analysis of human memory B cells. *Cytometry A*, 79, 894-6.
- WEILL, J.-C. & REYNAUD, C.-A. 2016. Human B Cell Subsets. In: RATCLIFFE, M. J. H. (ed.) *Encyclopedia of Immunobiology*. Oxford: Academic Press.
- WELLER, S., FAILI, A., GARCIA, C., BRAUN, M. C., LE DEIST, F. F., DE SAINT BASILE, G. G., HERMINE, O., FISCHER, A., REYNAUD, C. A. & WEILL, J. C. 2001. CD40-CD40L independent Ig gene hypermutation suggests a second B cell diversification pathway in humans. *Proc Natl Acad Sci U S A*, 98, 1166-70.
- WHITWORTH, H. S., GALLAGHER, K. E., HOWARD, N., MOUNIER-JACK, S., MBWANJI, G., KREIMER, A. R., BASU, P., KELLY, H., DROLET, M., BRISSON, M. & WATSON-JONES, D. 2020. Efficacy and B cell and Tfh cell responses after HPV vaccination, effect of age and dose number. E. Kiamba 2024

immunogenicity of a single dose of human papillomavirus vaccine compared to no vaccination or standard three and two-dose vaccination regimens: A systematic review of evidence from clinical trials. *Vaccine*, 38, 1302-1314.

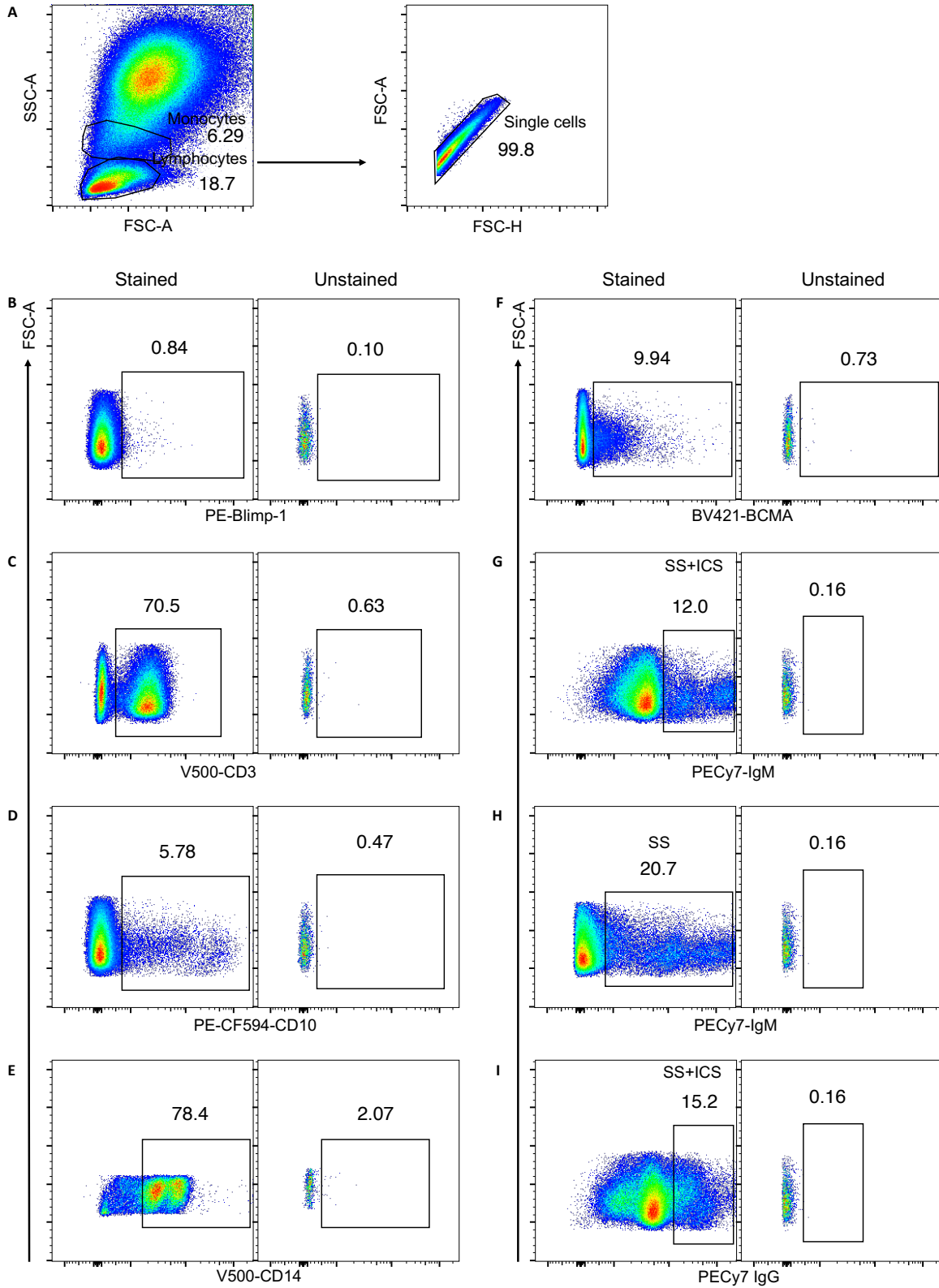
- WHITWORTH, H. S., MOUNIER-JACK, S., CHOI, E. M., GALLAGHER, K. E., HOWARD, N., KELLY, H., MBWANJI, G., KREIMER, A. R., BASU, P., BARNABAS, R., DROLET, M., BRISSON, M. & WATSON-JONES, D. 2024. Efficacy and immunogenicity of a single dose of human papillomavirus vaccine compared to multidose vaccination regimens or no vaccination: An updated systematic review of evidence from clinical trials. *Vaccine: X*, 19, 100486.
- WHO 2017a. HPV_vaccine_information_sheet_1217.
- WHO 2017b. Human papillomavirus vaccines: WHO position paper, May 2017-Recommendations. *Vaccine*, 35, 5753-5755.
- WHO. 2022. *WHO updates recommendations on HPV vaccination schedule* [Online]. Available: <https://www.who.int/news/item/20-12-2022-who-updates-recommendations-on-HPV-vaccination-schedule> [Accessed 06 February 2023].
- WHO 2023. Human Papillomavirus and Related Diseases, Summary Report 2023. ©ICO/IARC Information Centre on HPV and Cancer (HPV Information Centre)
- WIETSCHER, K. A., FECHTNER, K., ANTILEO, E., ABDURRAHMAN, G., DRECHSLER, C. A., MAKUVISE, M. K., ROSE, R., VOS, M., KRUMBHOLZ, A., MICHALIK, S., WEISS, S., ULM, L., FRANIKOWSKI, P., FICKENSCHER, H., BRÖKER, B. M., RAAFAT, D. & HOLTFRETER, S. 2024. Non-cross-reactive epitopes dominate the humoral immune response to COVID-19 vaccination – kinetics of plasma antibodies, plasmablasts and memory B cells. *Frontiers in Immunology*, 15.
- WILLIAMS, G. M. & NOSSAL, G. J. 1966. Ontogeny of the immune response. I. The development of the follicular antigen-trapping mechanism. *J. Exp. Med.*, 124.
- WOO, Y. L., STERLING, J., DAMAY, I., COLEMAN, N., CRAWFORD, R., VAN DER BURG, S. H. & STANLEY, M. 2008. Characterising the local immune responses in cervical intraepithelial neoplasia: a cross-sectional and longitudinal analysis. *BJOG*, 115, 1616-21; discussion 1621-2.
- WOODWORTH, C. D., LICHTI, U., SIMPSON, S., EVANS, C. H. & DIPAOLO, J. A. 1992. Leukoregulin and gamma-interferon inhibit human papillomavirus type 16 gene transcription in human papillomavirus-immortalized human cervical cells. *Cancer Res*, 52, 456-63.
- WOODWORTH, C. D., NOTARIO, V. & DIPAOLO, J. A. 1990. Transforming growth factors beta 1 and 2 transcriptionally regulate human papillomavirus (HPV) type 16 early gene expression in HPV-immortalized human genital epithelial cells. *J Virol*, 64, 4767-75.
- WOODWORTH, C. D. & SIMPSON, S. 1993. Comparative lymphokine secretion by cultured normal human cervical keratinocytes, papillomavirus-immortalized, and carcinoma cell lines. *Am J Pathol*, 142, 1544-55.
- WU, X., MA, X., LI, Y., XU, Y., ZHENG, N., XU, S., NAWAZ, W. & WU, Z. 2019a. Induction of neutralizing antibodies by human papillomavirus vaccine generated in mammalian cells. *Antibody Therapeutics*, 2, 45-53.
- WU, X., MA, X., LI, Y., XU, Y., ZHENG, N., XU, S., NAWAZ, W. & WU, Z. 2019b. Induction of neutralizing antibodies by human papillomavirus vaccine generated in mammalian cells. *Antib Ther*, 2, 45-53.
- WU, Y.-C. B., KIPLING, D. & DUNN-WALTERS, D. K. 2012. Age-related changes in human peripheral blood IGH repertoire following vaccination. *Frontiers in immunology*, 3, 26564.
- XU, J. L. & DAVIS, M. M. 2000. Diversity in the CDR3 Region of VH Is Sufficient for Most Antibody Specificities. *Immunity*, 13, 37-45.

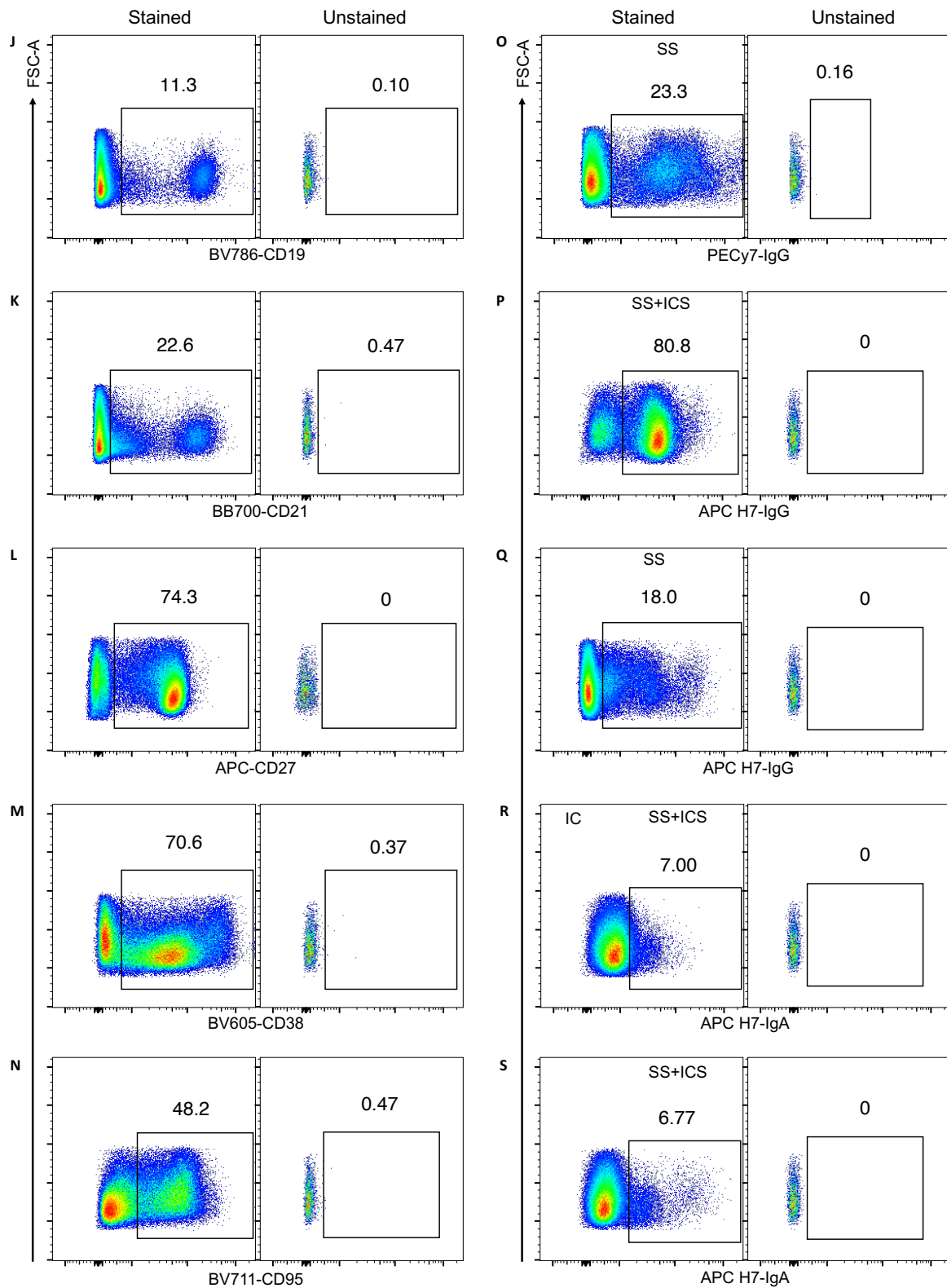
- YANG, K., PUEL, A., ZHANG, S., EIDENSCHENK, C., KU, C. L., CASROUGE, A., PICARD, C., VON BERNUTH, H., SENECHAL, B., PLANCOULAIN, S., AL-HAJJAR, S., AL-GHONAIUM, A., MARODI, L., DAVIDSON, D., SPEERT, D., ROIFMAN, C., GARTY, B. Z., OZINSKY, A., BARRAT, F. J., COFFMAN, R. L., MILLER, R. L., LI, X., LEBON, P., RODRIGUEZ-GALLEGO, C., CHAPEL, H., GEISSMANN, F., JOUANGUY, E. & CASANOVA, J. L. 2005. Human TLR-7-, -8-, and -9-mediated induction of IFN-alpha/beta and -lambda is IRAK-4 dependent and redundant for protective immunity to viruses. *Immunity*, 23, 465-78.
- YANG, Y. 2015. Cancer immunotherapy: harnessing the immune system to battle cancer. *J Clin Invest*, 125, 3335-7.
- YOON, C.-S., KIM, K.-D., PARK, S.-N. & CHEONG, S.-W. 2001. $\alpha 6$ integrin is the main receptor of human papillomavirus type 16 VLP. *Biochemical and biophysical research communications*, 283, 668-673.
- YOSHIDA, T., MEI, H., DÖRNER, T., HIEPE, F., RADBRUCH, A., FILLATREAU, S. & HOYER, B. F. 2010. Memory B and memory plasma cells. *Immunological Reviews*, 237, 117-139.
- YOUNG, N. A. & AL-SALEEM, T. 2008. CHAPTER 24 - Lymph Nodes: Cytomorphology and Flow Cytometry. In: BIBBO, M. & WILBUR, D. (eds.) *Comprehensive Cytopathology (Third Edition)*. Edinburgh: W.B. Saunders.
- YU, X., TSIBANE, T., MCGRAW, P. A., HOUSE, F. S., KEEFER, C. J., HICAR, M. D., TUMPEY, T. M., PAPPAS, C., PERRONE, L. A., MARTINEZ, O., STEVENS, J., WILSON, I. A., AGUILAR, P. V., ALTSCHULER, E. L., BASLER, C. F. & CROWE, J. E., JR. 2008. Neutralizing antibodies derived from the B cells of 1918 influenza pandemic survivors. *Nature*, 455, 532-6.
- ZARETSKY, A. G., TAYLOR, J. J., KING, I. L., MARSHALL, F. A., MOHRS, M. & PEARCE, E. J. 2009. T follicular helper cells differentiate from Th2 cells in response to helminth antigens. *Journal of Experimental Medicine*, 206, 991-999.
- ZEHEMTEI, S., ROTH, K., CSERESNYES, Z., SERCAN, Ö., HORN, K., NIESNER, R. A., CHANG, H. D., RADBRUCH, A. & HAUSER, A. E. 2014. Static and dynamic components synergize to form a stable survival niche for bone marrow plasma cells. *Eur J Immunol*, 44, 2306-17.
- ZEPEDA-CERVANTES, J., RAMÍREZ-JARQUÍN, J. O. & VACA, L. 2020. Interaction Between Virus-Like Particles (VLPs) and Pattern Recognition Receptors (PRRs) From Dendritic Cells (DCs): Toward Better Engineering of VLPs. *Frontiers in Immunology*, 11.
- ZHANG, Y., YAN, Q., LUO, K., HE, P., HOU, R., ZHAO, X., WANG, Q., YI, H., LIANG, H., DENG, Y., HU, F., LI, F., LIU, X., FENG, Y., LI, P., QU, L., CHEN, Z., PAN-HAMMARSTRÖM, Q., FENG, L., NIU, X. & CHEN, L. 2022. Analysis of B Cell Receptor Repertoires Reveals Key Signatures of the Systemic B Cell Response after SARS-CoV-2 Infection. *Journal of Virology*, 96, e01600-21.
- ZHANG, Z., ZHANG, J., XIA, N. & ZHAO, Q. 2017. Expanded strain coverage for a highly successful public health tool: Prophylactic 9-valent human papillomavirus vaccine. *Hum Vaccin Immunother*, 13, 2280-2291.
- ZHENG, B., YANG, Y., CHEN, L., WU, M. & ZHOU, S. 2022. B-cell receptor repertoire sequencing: Deeper digging into the mechanisms and clinical aspects of immune-mediated diseases. *iScience*, 25, 105002.
- ZHOU, C., TUONG, Z. K. & FRAZER, I. H. 2019a. Papillomavirus Immune Evasion Strategies Target the Infected Cell and the Local Immune System. *Frontiers in oncology*, 9, 682-682.
- ZHOU, C., TUONG, Z. K. & FRAZER, I. H. 2019b. Papillomavirus Immune Evasion Strategies Target the Infected Cell and the Local Immune System. *Front Oncol*, 9, 682.
- ZHU, F. C., ZHONG, G. H., HUANG, W. J., CHU, K., ZHANG, L., BI, Z. F., ZHU, K. X., CHEN, Q., ZHENG, T. Q., ZHANG, M. L., LIU, S., XU, J. B., PAN, H. X., SUN, G., ZHENG, F. Z., ZHANG, Q. F., YI, X. M.,

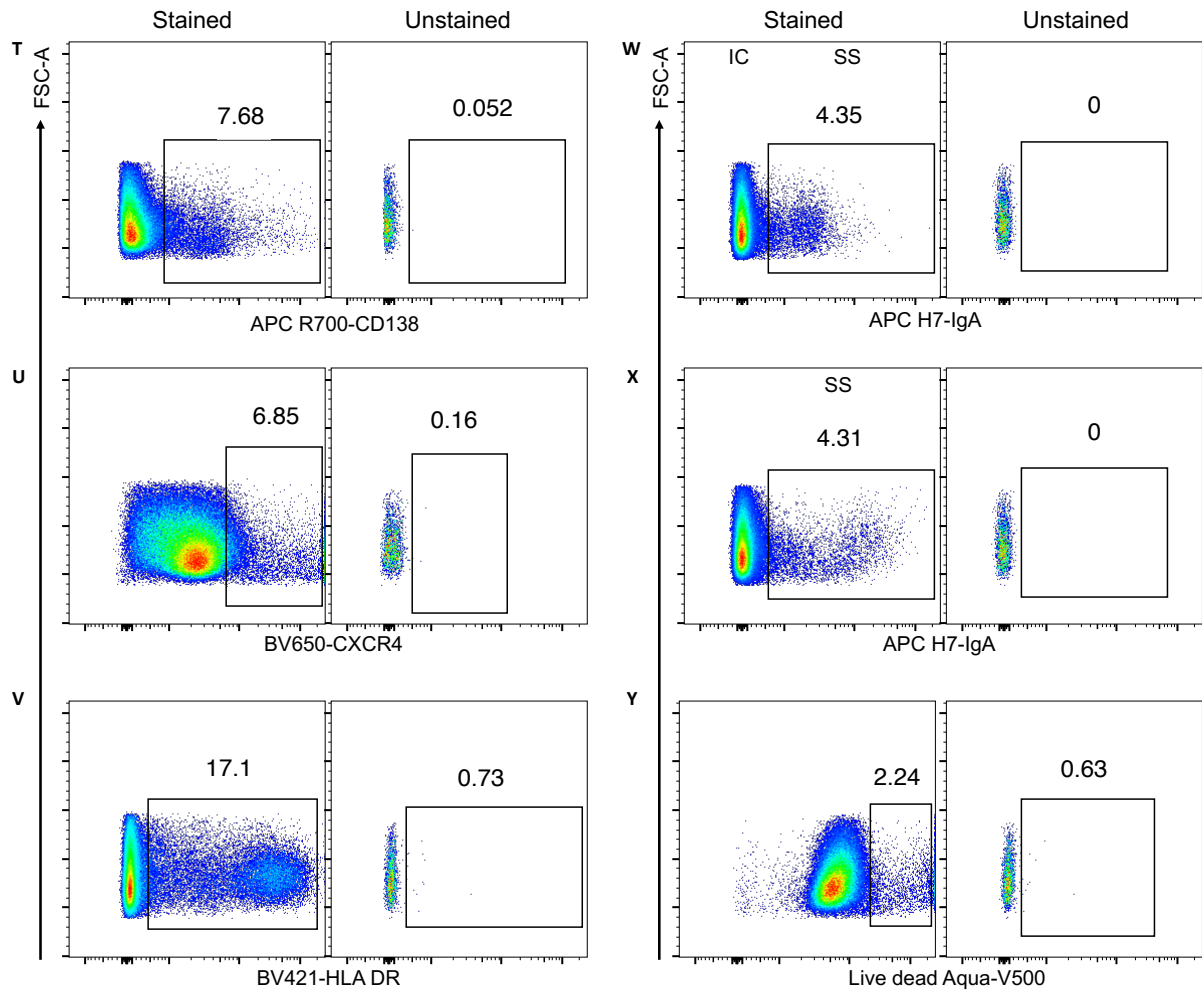
- ZHUANG, S. J., HUANG, S. J., PAN, H. R., SU, Y. Y., WU, T., ZHANG, J. & XIA, N. S. 2023. Head-to-head immunogenicity comparison of an Escherichia coli-produced 9-valent human papillomavirus vaccine and Gardasil 9 in women aged 18-26 years in China: a randomised blinded clinical trial. *Lancet Infect Dis*, 23, 1313-1322.
- ZHU, J., YAMANE, H. & PAUL, W. E. 2010. Differentiation of effector CD4 T cell populations (*). *Annu Rev Immunol*, 28, 445-89.
- ZIMMERMANN, P. & CURTIS, N. 2019. Factors That Influence the Immune Response to Vaccination. *Clin Microbiol Rev*, 32.
- ZUR HAUSEN, H. 1996. Papillomavirus infections--a major cause of human cancers. *Biochim Biophys Acta*, 1288, F55-78.
- ZUR HAUSEN, H. 2002. Papillomaviruses and cancer: from basic studies to clinical application. *Nat Rev Cancer*, 2, 342-50.

APPENDICES

Appendix 1. Preliminary testing of antibodies in the plasma cell panel at manufacturer's recommended dilutions

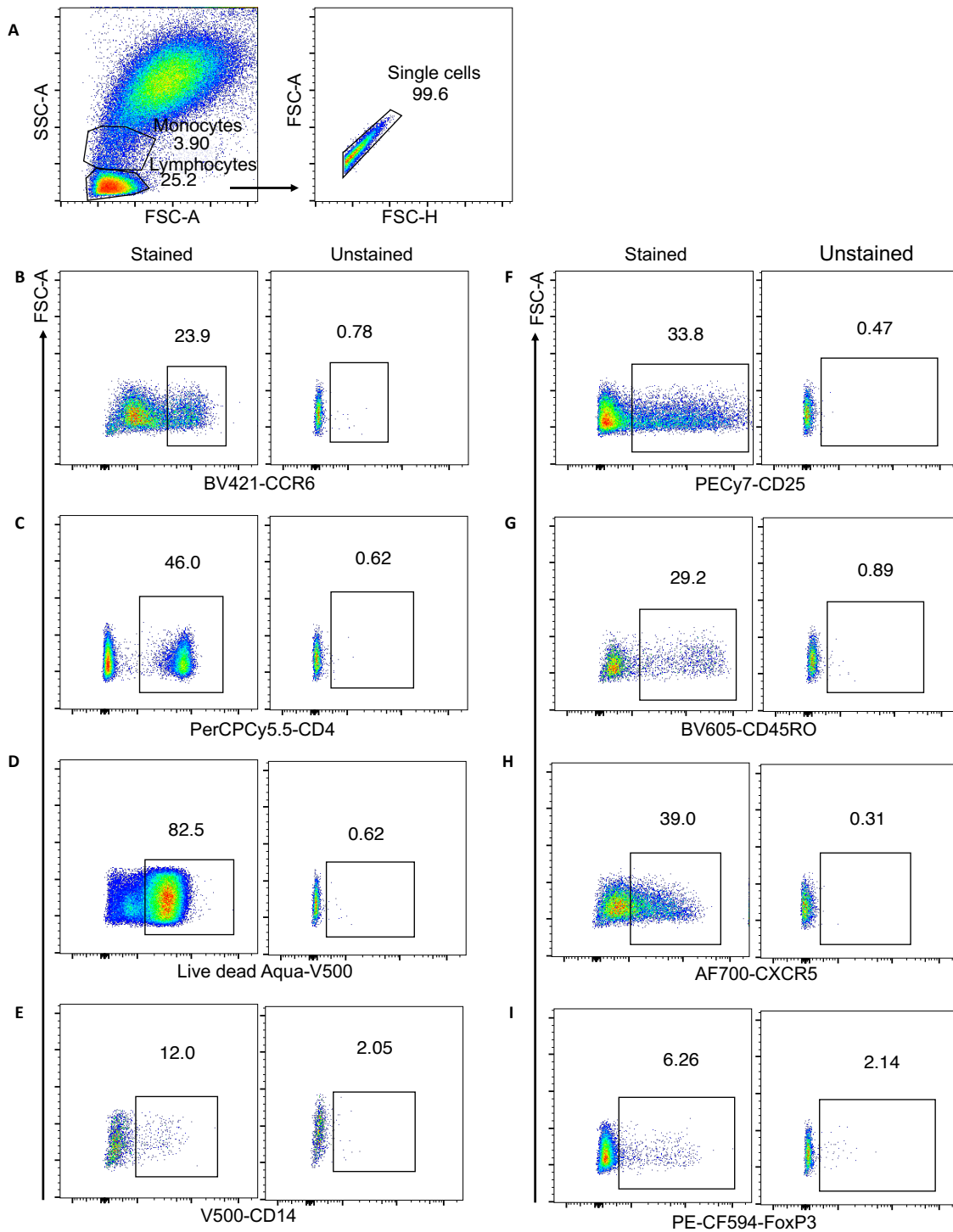


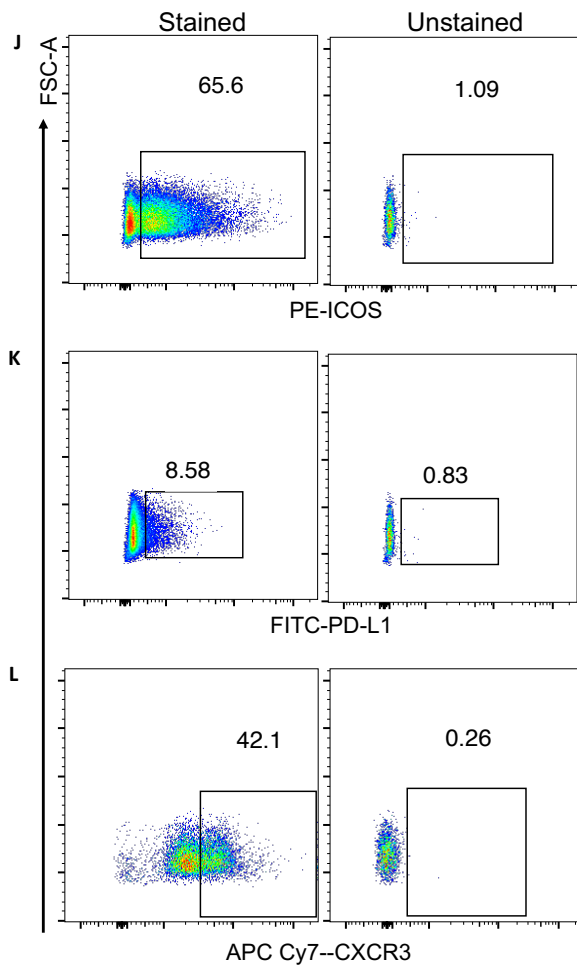




Whole blood was single colour stained for fifteen markers or Zombie Aqua viability dye at the manufacturer's recommended dilutions using the B cell staining procedure to be used in the final complete panel. Cells were first gated on lymphocytes or monocytes (in case of CD14) **(A)** and then single cells. From the single cells, positive and negative populations were defined for each marker on stained cells using unstained cells as control **(B-Y)**. Surface staining (SS) only or both surface and intracellular staining (SS+ICS) were tested for immunoglobulin markers IgG, IgM and IgA. To define IgA staining, the respective SS and ICS of IgA isotype control (IC) is also shown.

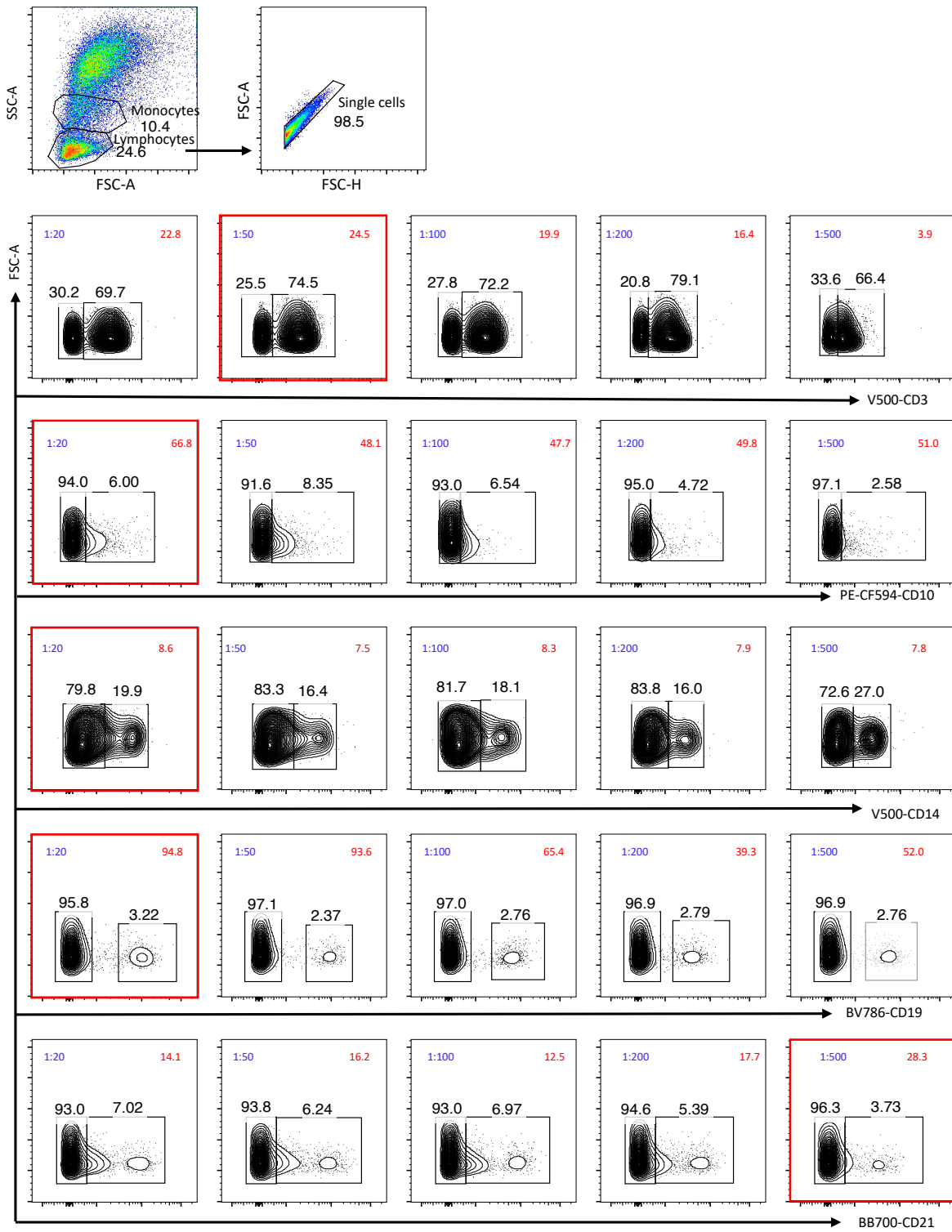
Appendix 2. Preliminary testing of antibodies in the Tfh cell AIM panel at manufacturers' recommended dilutions

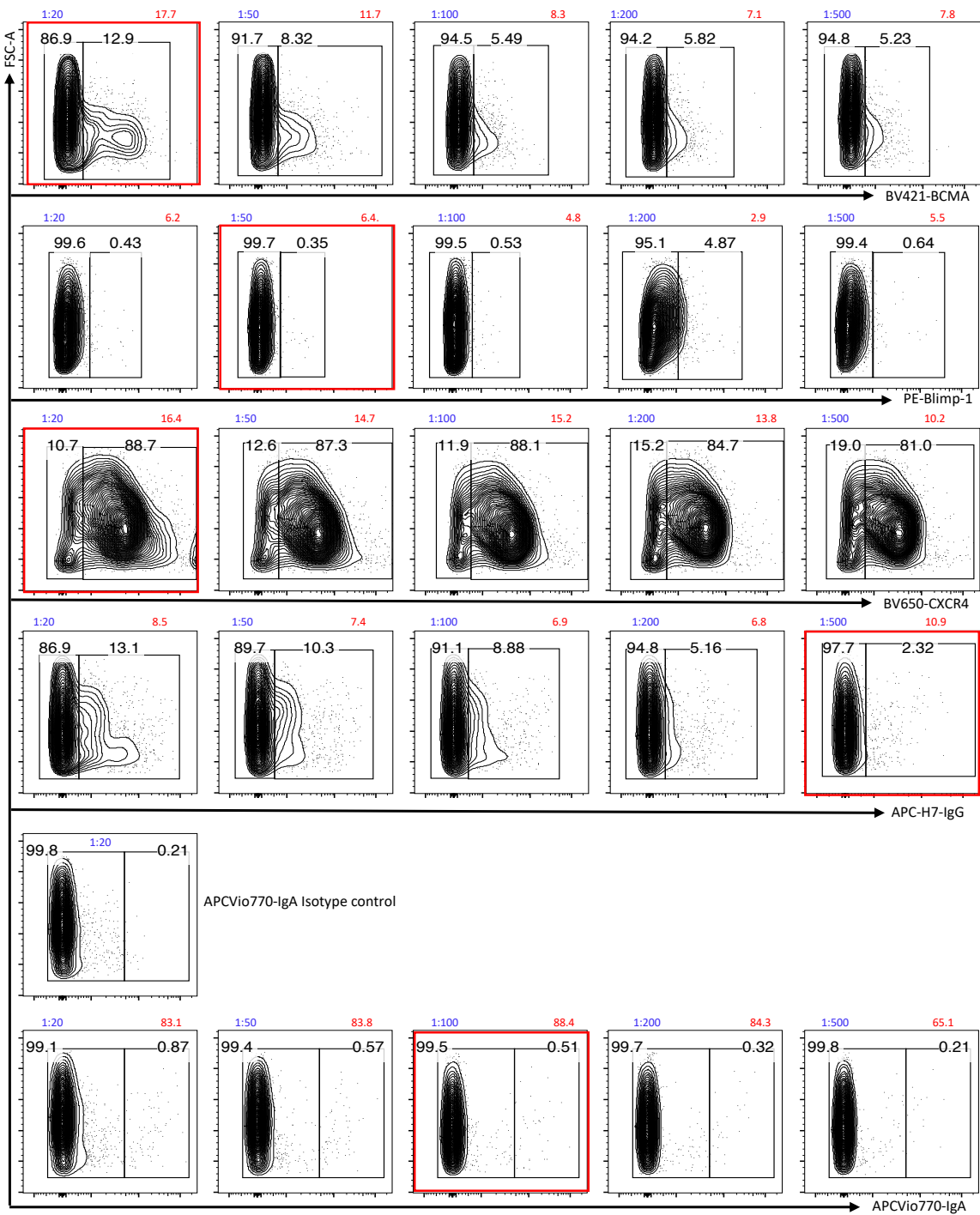


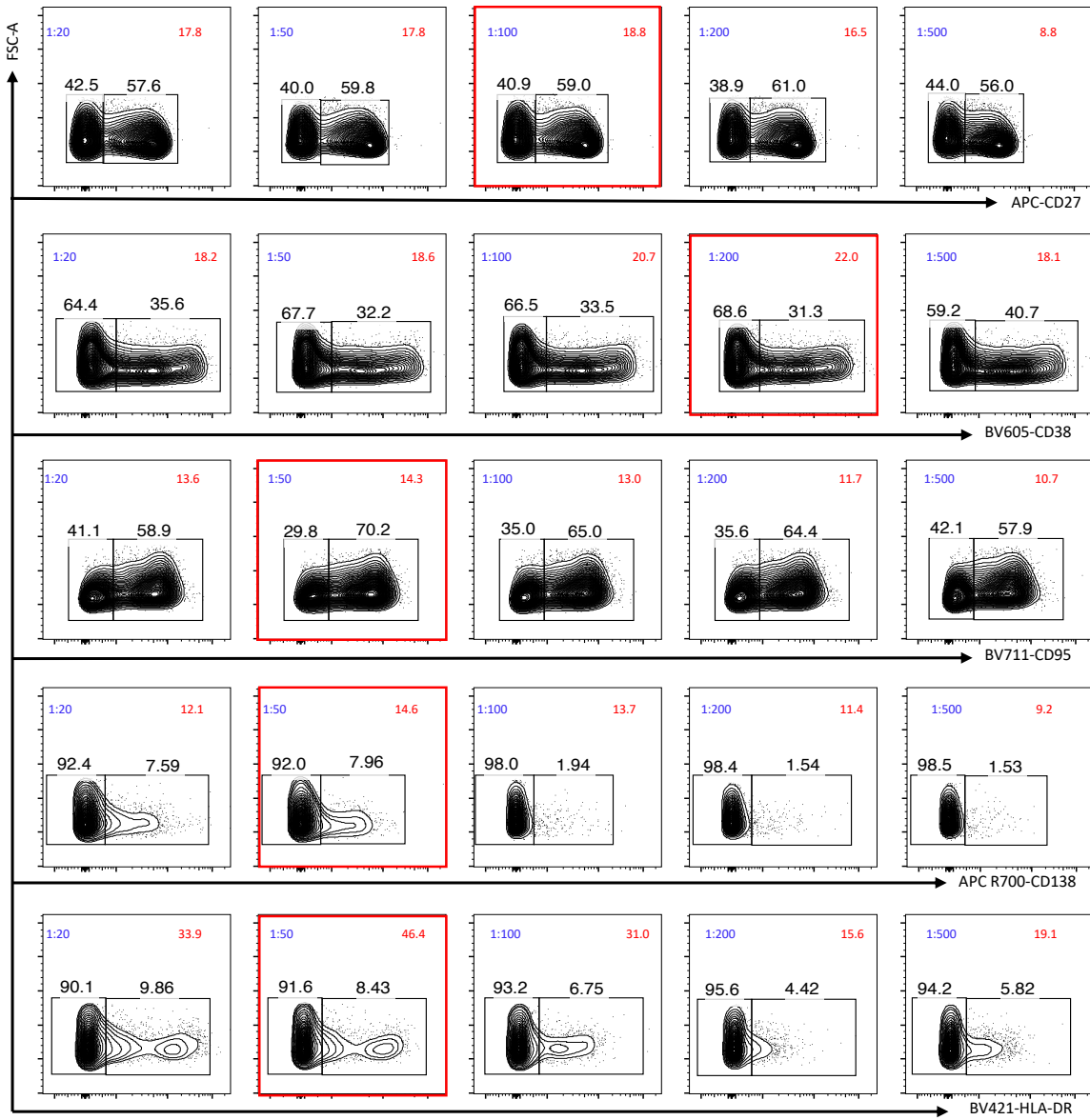


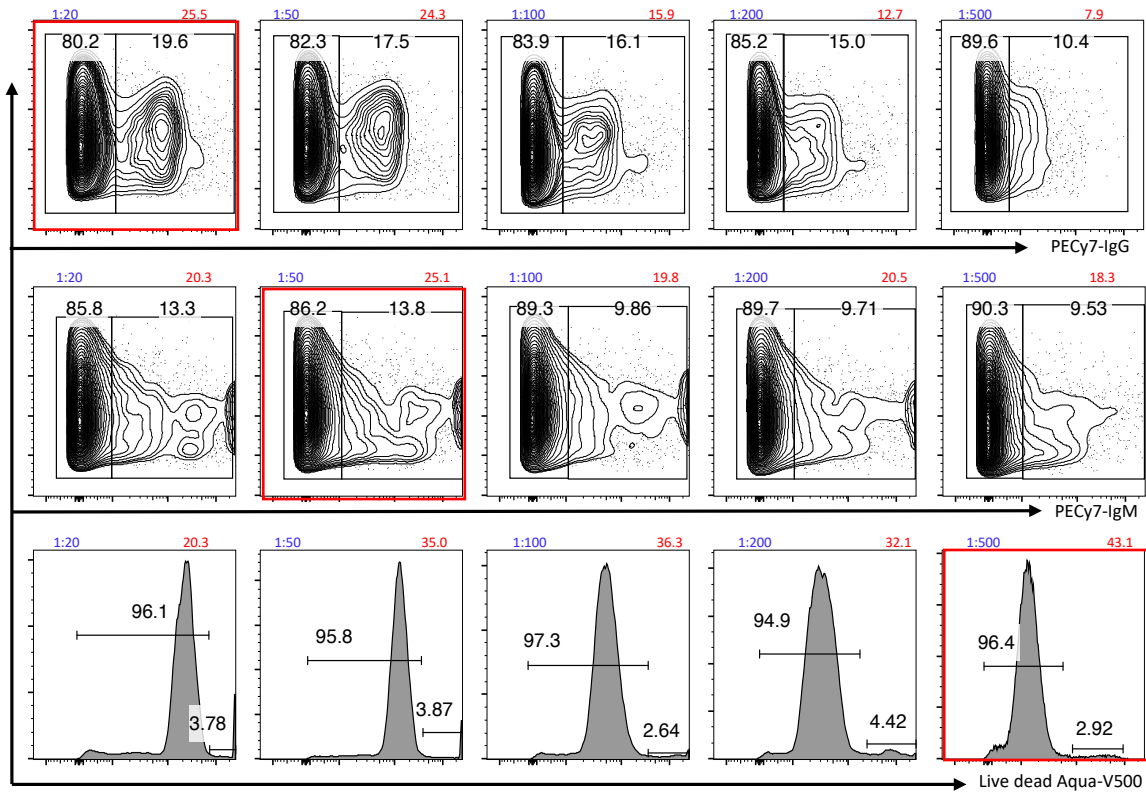
Human whole blood was single colour stained for eleven markers and Zombie Aqua viability dye at the manufacturer's recommended dilutions using the Tfh AIM staining procedure for protocol and antibody testing. Cells were first gated on lymphocytes or monocytes (in case of CD14) (A). From the single cells, positive and negative populations were defined for each marker/dye on stained cells using unstained cells as a control (B-L).

Appendix 3. Antibody titration for initial plasma cell panel



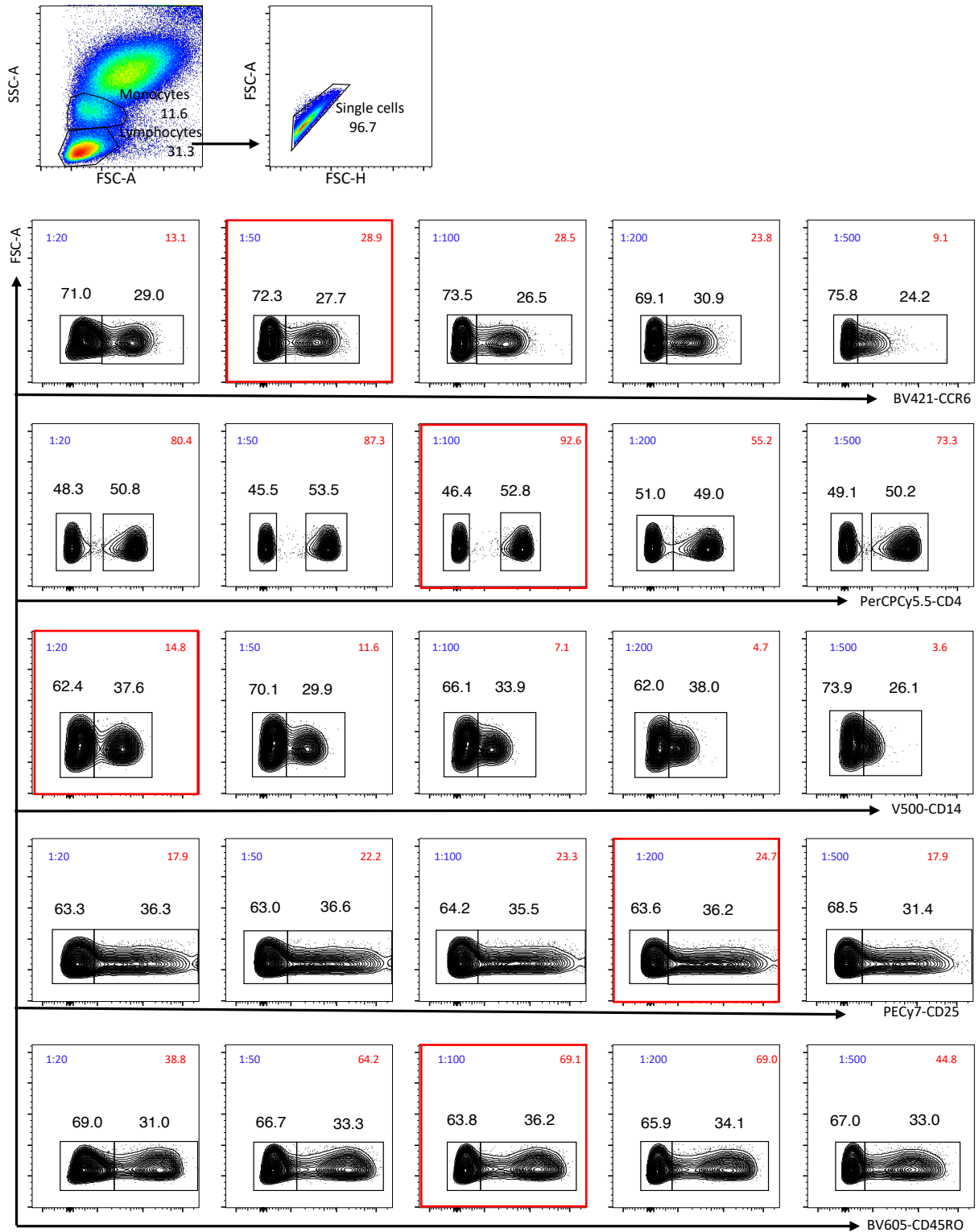


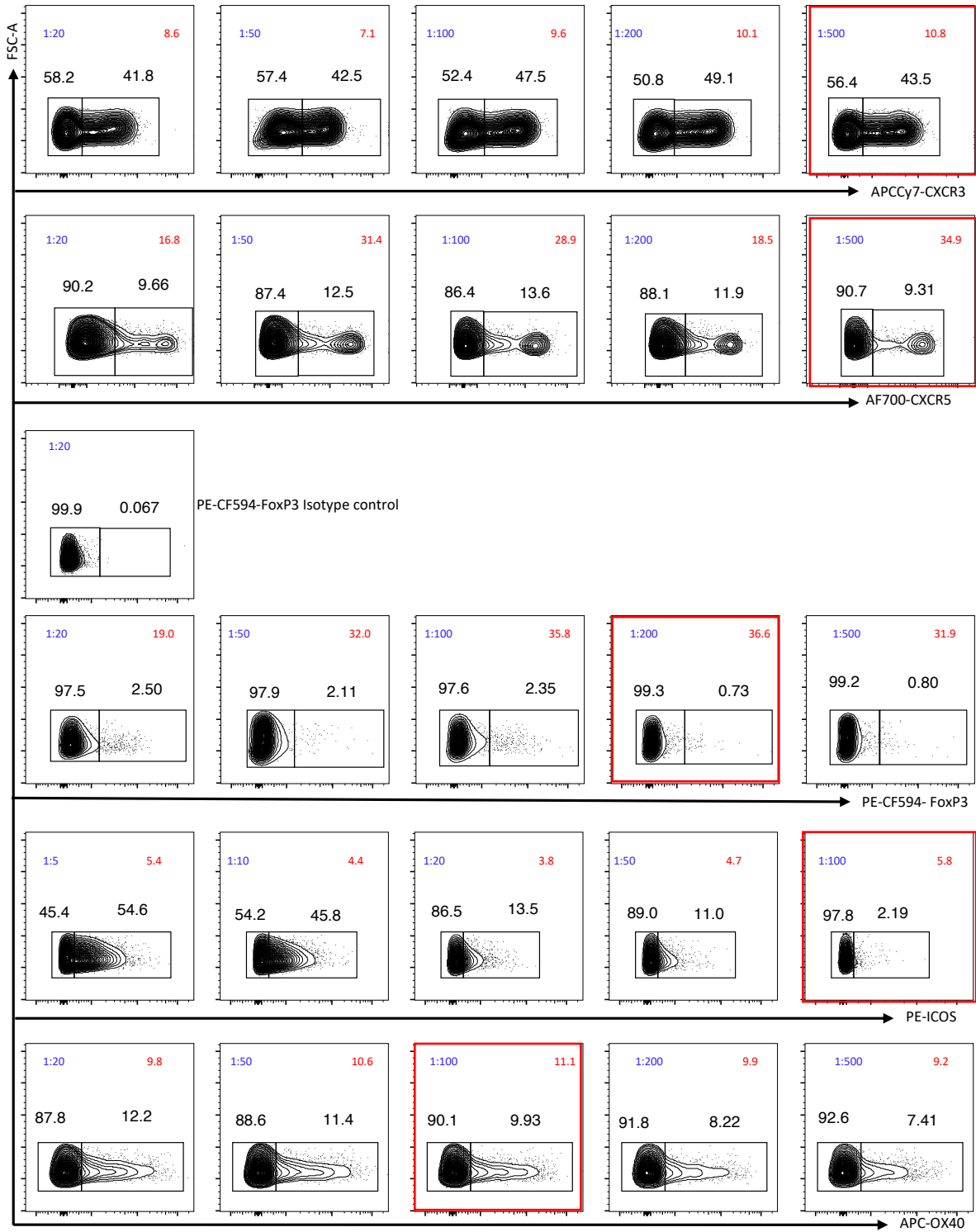


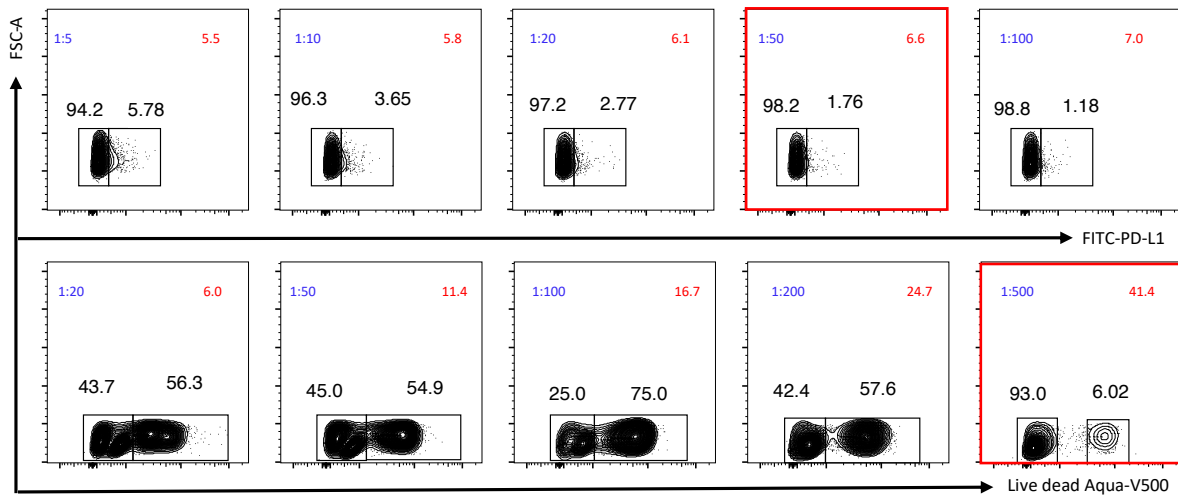


Each antibody was titrated in single colour-stained whole blood using five dilutions starting from manufacturer's recommendation using the B cell panel staining protocol. Cells were first gated on lymphocytes and single cells. From the single cells, positive and negative populations were defined for each marker and SI values were calculated for each dilution. Black numbers indicate frequencies (%) of positive and negative populations, respectively; purple numbers indicate antibody dilutions, red numbers indicate SI values and red show the gating for optimal dilution.

Appendix 4. Antibody titration for initial Tfh cell AIM panel

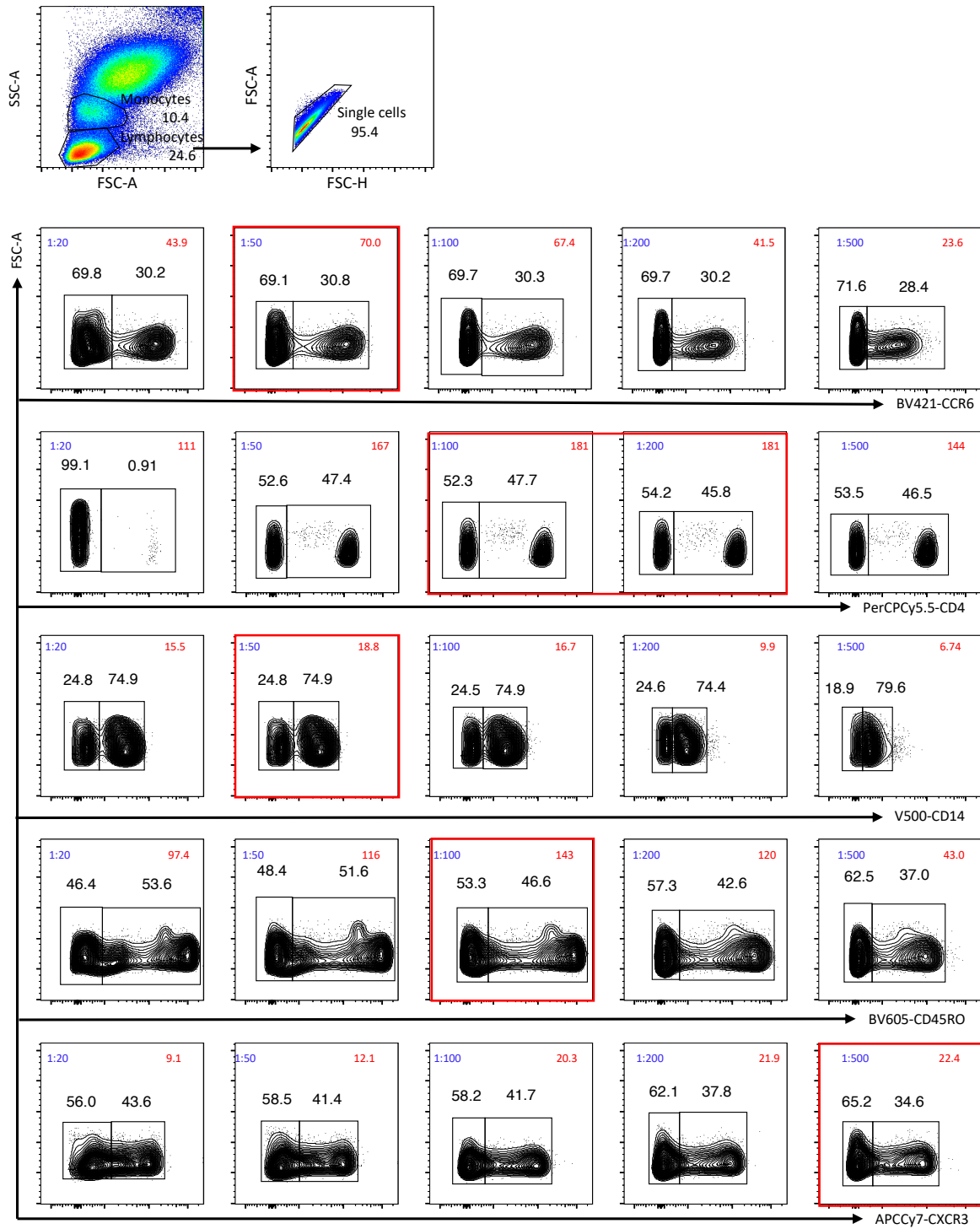


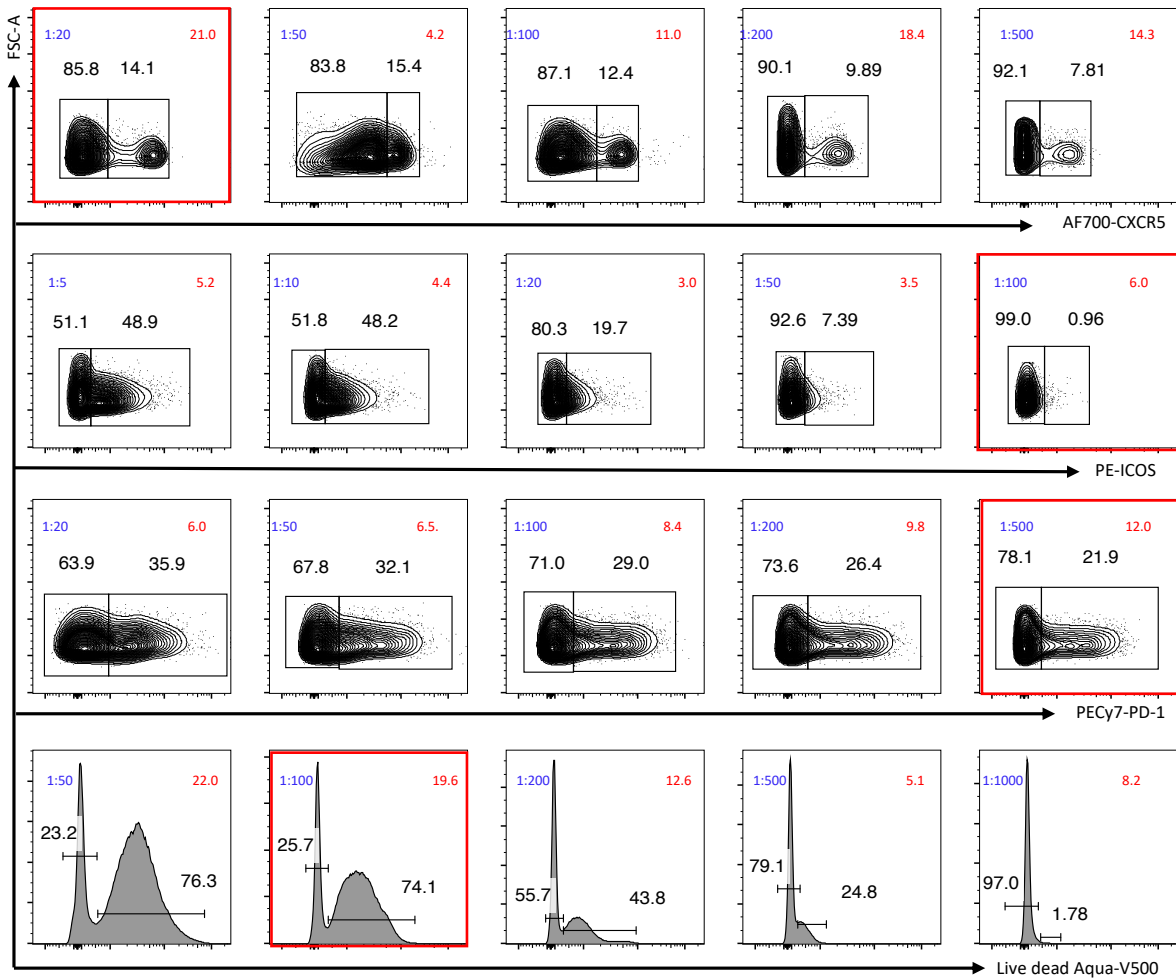




Each antibody was titrated in single colour-stained whole blood using five dilutions starting from manufacturer's recommendation using the Tfh AIM panel staining protocol. Cells were first gated on lymphocytes and single cells. From the single cells, positive and negative populations were defined for each marker and SI values were calculated for each dilution. FoxP3-PECF594 isotope control is shown. Black numbers indicate frequencies (%) of positive and negative populations, respectively; purple numbers indicate antibody dilutions, red numbers indicate SI values and red boxes show the gating for optimal dilutions.

Appendix 5. Antibody titration for initial Tfh cell ex vivo panel





Each antibody was titrated in single colour-stained whole blood using five dilutions starting from manufacturer's recommendation using the Tfh ex-vivo panel staining protocol. Cells were first gated on lymphocytes and single cells. From the single cells, positive and negative populations were defined for each marker and SI values were calculated for each dilution. Black numbers indicate frequencies (%) of positive and negative populations, respectively; purple numbers indicate antibody dilutions, red numbers indicate SI values and red boxes show the gating for optimal dilutions.

Appendix 6. Antibody titration for re-designed plasma cell panel

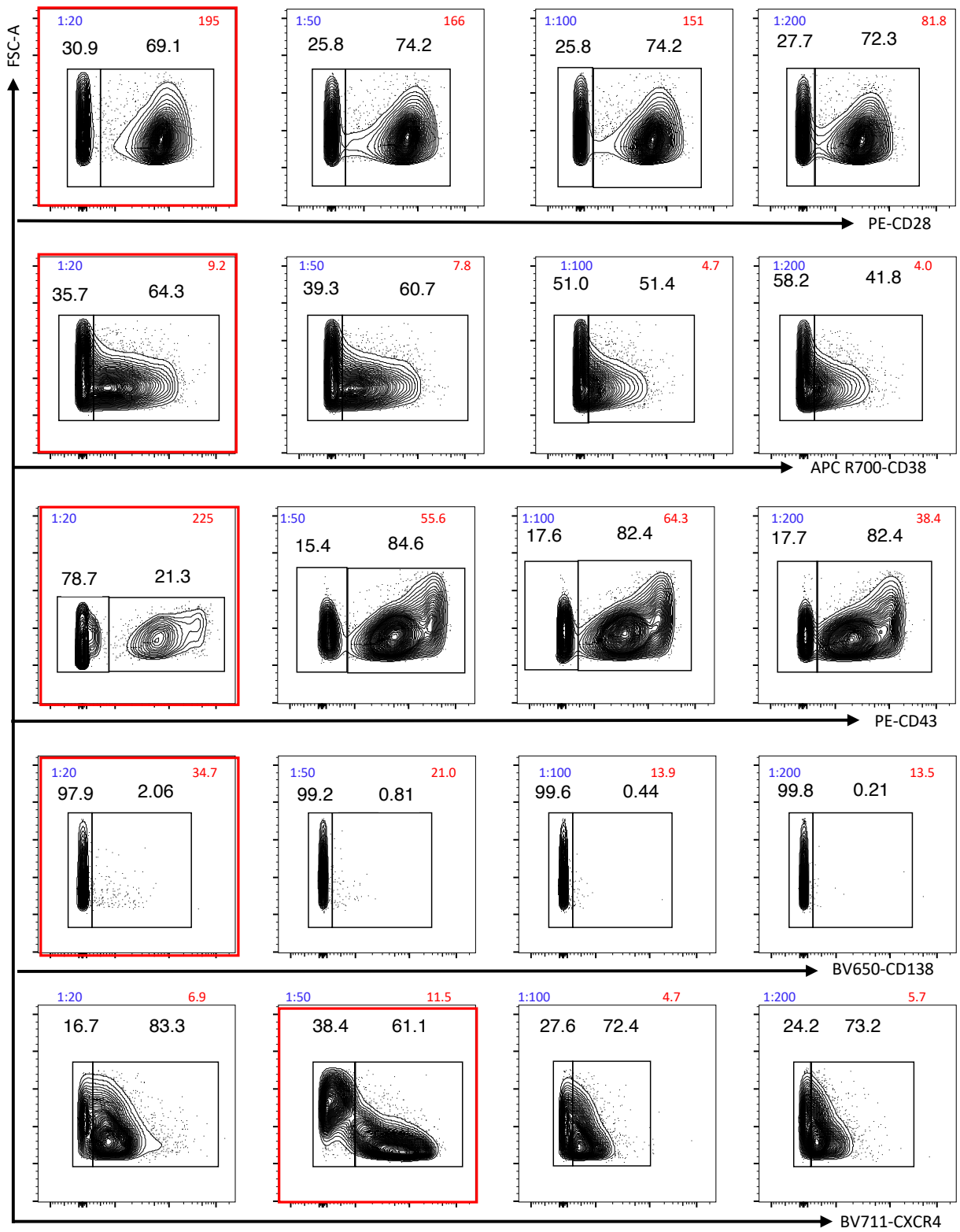
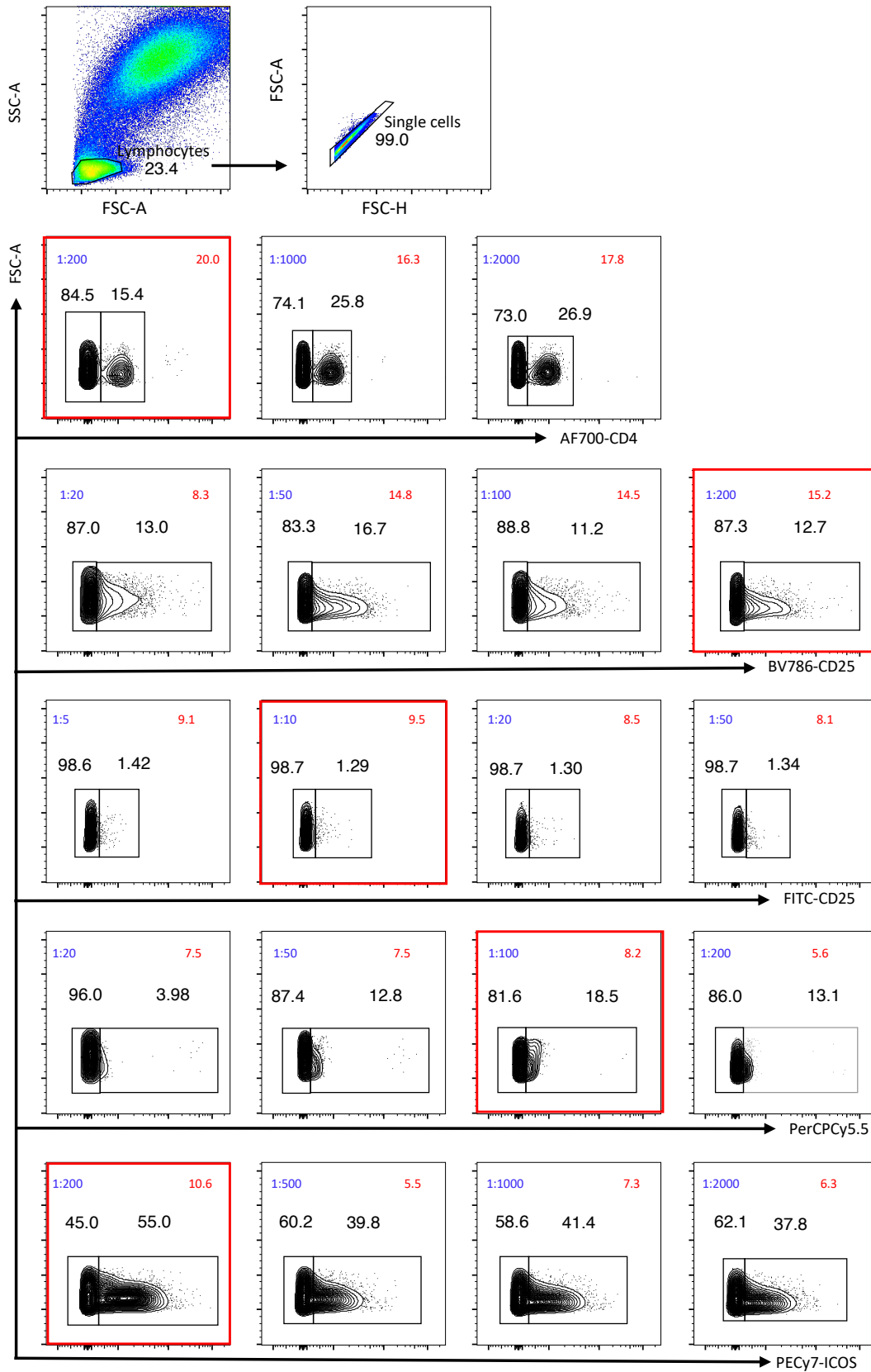
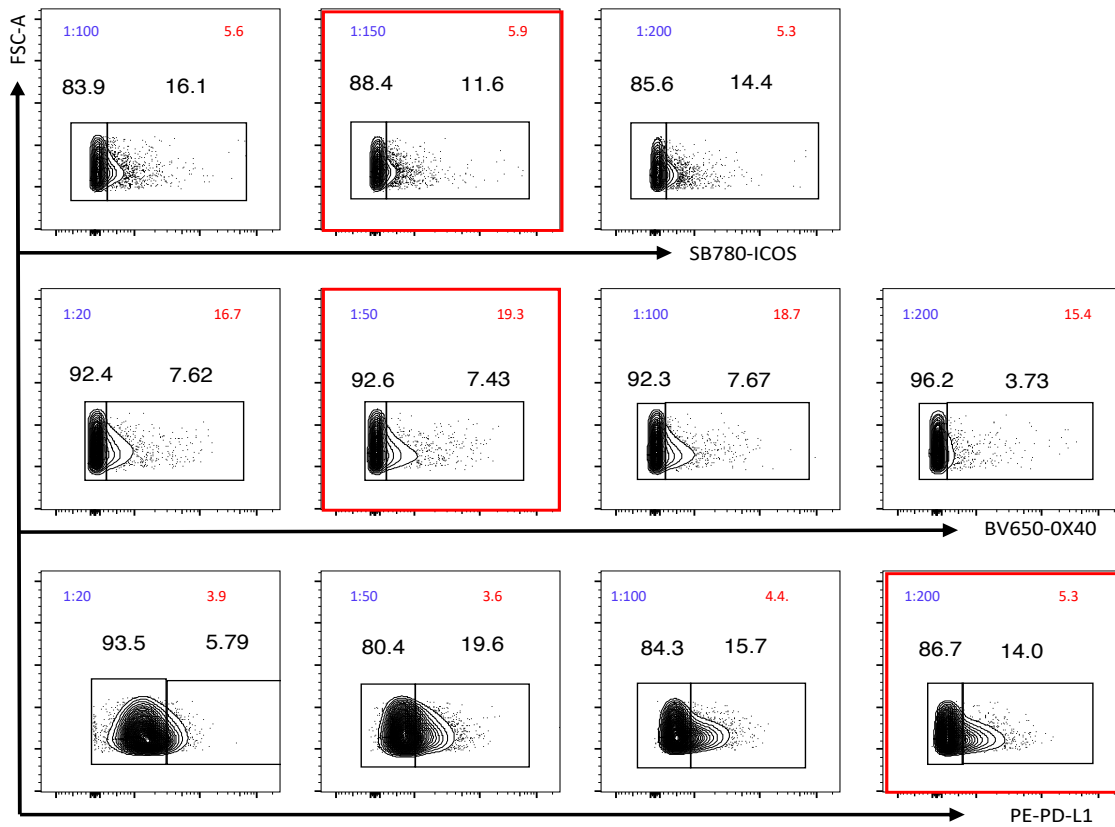


Figure legend on next page

Each antibody was titrated in single colour-stained whole blood using five dilutions starting from manufacturers's recommendation using the B cell panel staining protocol. Cells were first gated on lymphocytes and single cells. From the single cells, positive and negative populations were defined for each marker and SI values were calculated for each dilution. Black numbers indicate frequencies (%) of positive and negative populations, respectively; purple numbers indicate antibody dilutions, red numbers indicate SI values and red boxes show the gating for optimal dilutions.

Appendix 7. Antibody titration for re-designed Tfh cell AIM panel





Each antibody was titrated in single colour-stained whole blood using five dilutions starting from manufacturer's recommendation using the Tfh AIM panel staining protocol. Cells were first gated on lymphocytes and single cells. From the single cells, positive and negative populations were defined for each marker and SI values were calculated for each dilution. Black numbers indicate frequencies (%) of positive and negative populations, respectively; purple numbers indicate antibody dilutions, red numbers indicate SI values and red boxes show the gating for optimal dilutions.

Appendix 8: Antibody titration for re-designed Tfh cell ex vivo panel

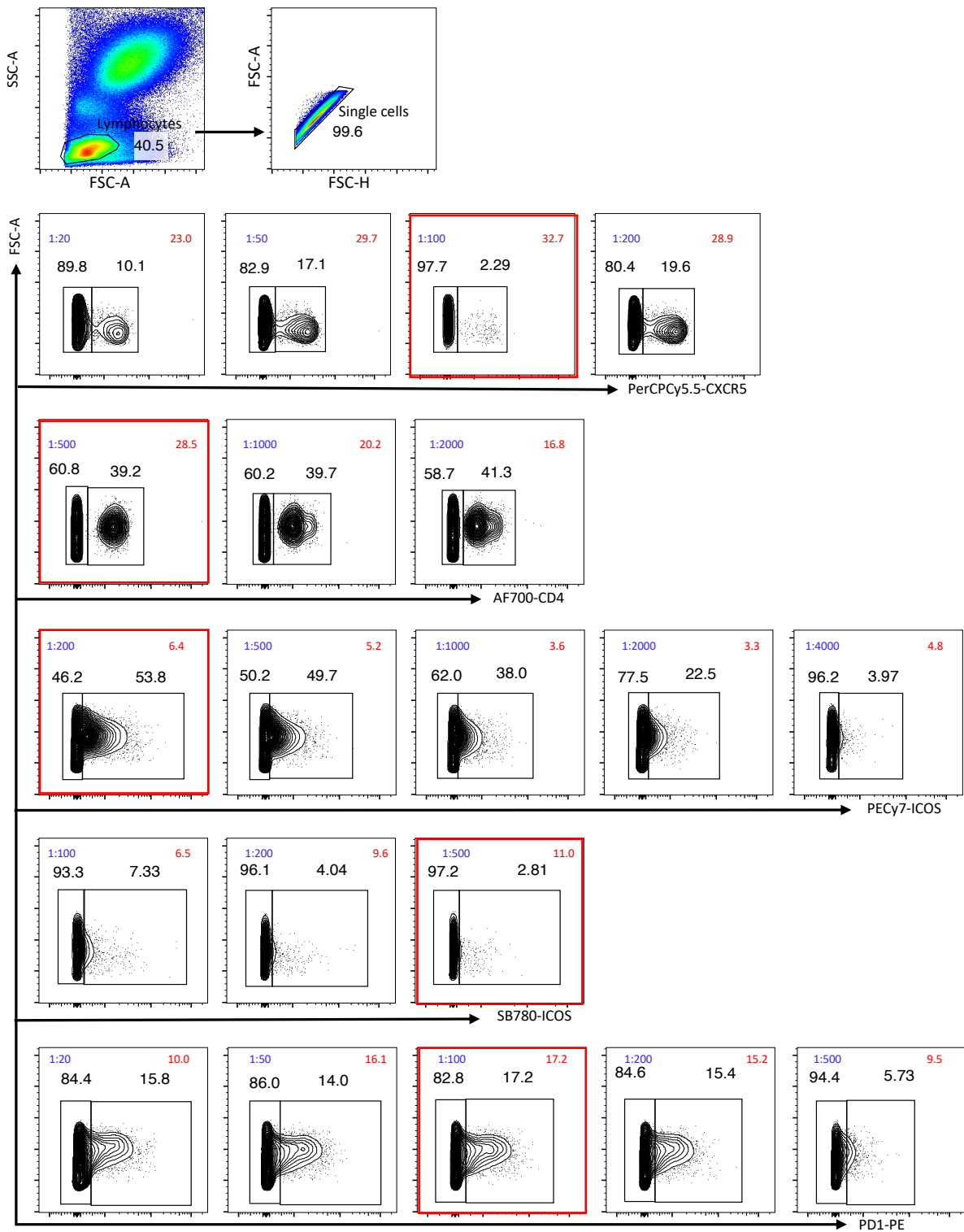


Figure legend on next page

Each antibody was titrated in single colour-stained whole blood using five dilutions starting from manufacturer's recommendation using the Tfh ex-vivo panel staining protocol. Cells were first gated on lymphocytes and single cells. From the single cells, positive and negative populations were defined for each marker and SI values were calculated for each dilution. Black numbers indicate frequencies (%) of positive and negative populations, respectively; purple numbers indicate antibody dilutions, red numbers indicate SI values and red boxes show the gating for optimal dilutions.

Appendix 9. Tfh cell responses in negative and positive controls used in the AIM

assay

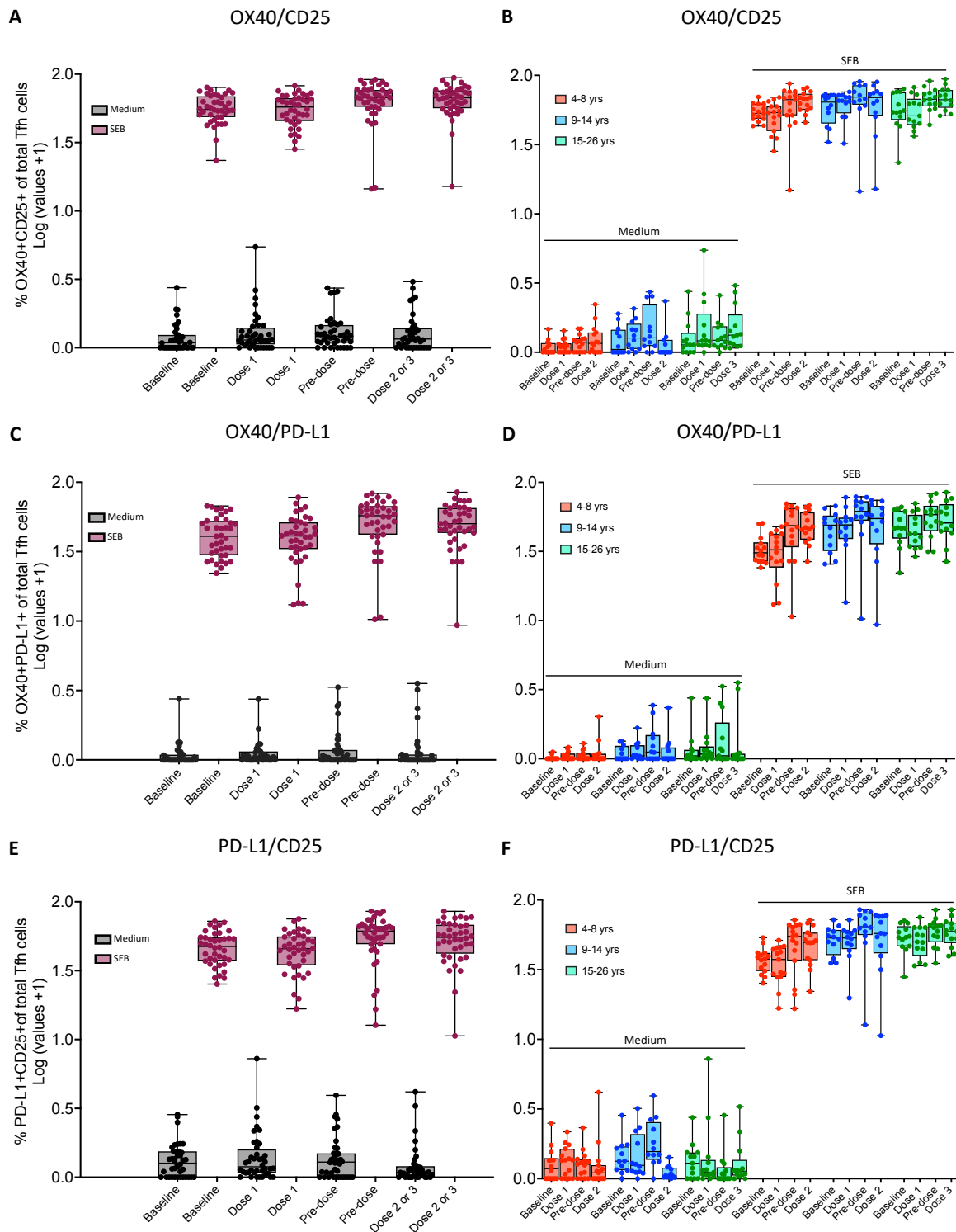
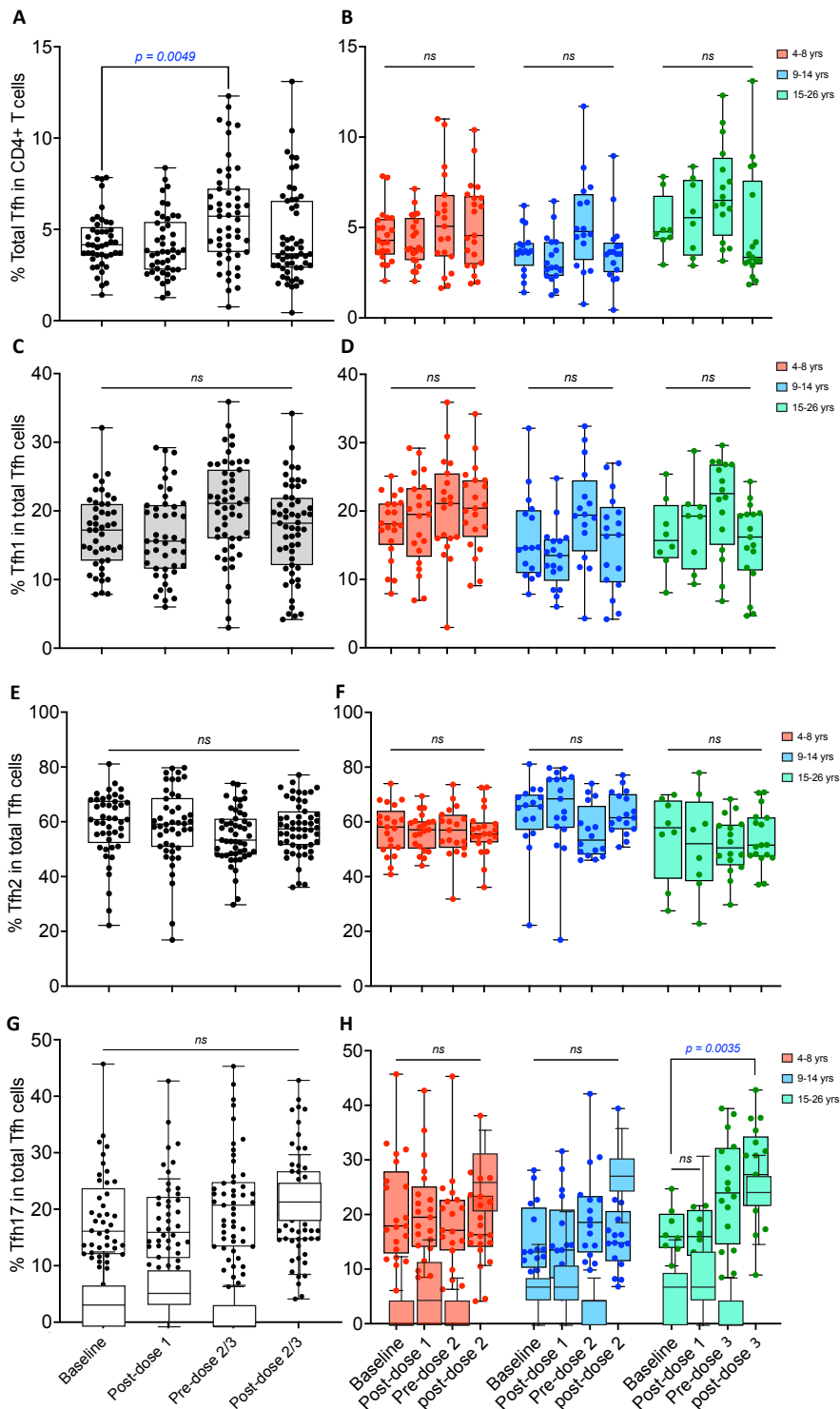


Figure legend on next page

Frozen PBMC from baseline, day 7 post-dose 1 and day 7 post-dose 2 or 3 of Gardasil 9 vaccination were thawed and stimulated in culture for 18 hours using $\mu\text{g/mL}$ of SEB as a positive control or cultured in medium without stimulation as a negative control to define background response for the AIM Tfh cell assay. Stimulated cells were stained with the AIM flow cytometry panel in a similar manner to the antigen specific tests. Gating was first done on lymphocytes and single cells, then dead and CD14+ cells excluded in a dump channel. Total Tfh cells were identified as CD4+FoxP3-CD45RO+CXCR5+ and AIM frequencies identified as OX40+CD25+, OX40+PD-L1+ and PD-L1+CD25+. All points are plotted on the box and whisker plots to show Log_{10} (% frequencies + 1) of OX40+CD25+, OX40+PD-L1+ and PD-L1+CD25+ Tfh in the pooled (**A, C & E**) and age stratified analyses (**B, D & F**) of both negative and positive controls. The three age groups are shown in different colours.

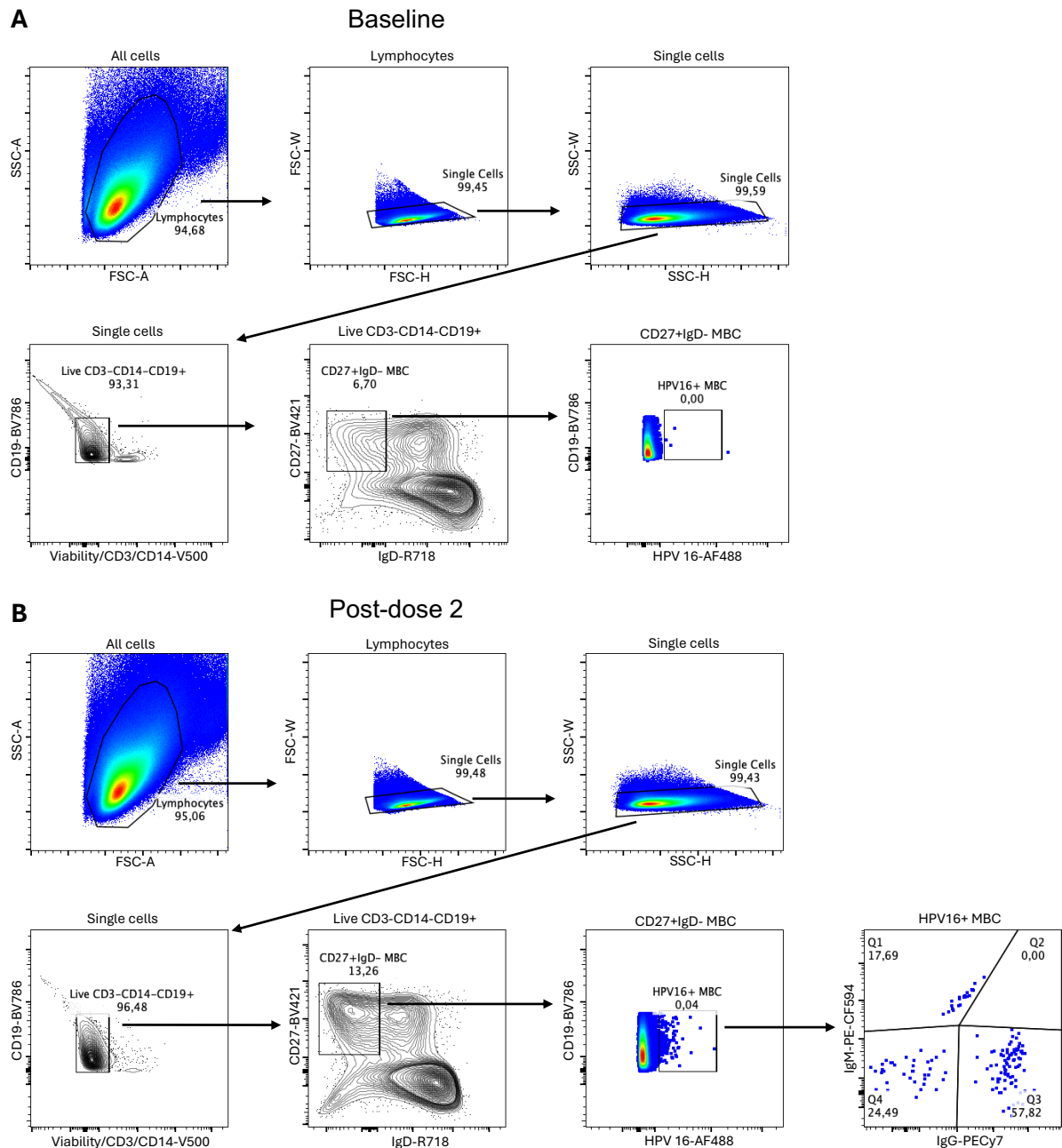
Appendix 10. Total Tfh cell frequencies after Gardasil 9 vaccination



Frozen PBMC from baseline, day 7 post-dose 1 and day 7 post-dose 2 or 3 of Gardasil 9 vaccination were thawed and analysed using an ex vivo flow cytometry antibody panel. Cells were first gated on lymphocytes and single cells and dead cells excluded. Total Tfh cells were then gated as CD4+FoxP3-CD45RO+CXCR5+. All points are plotted on the box and whisker plots to show frequencies of the total Tfh pool in CD4 T cells (**A & B**) as well as frequencies of the Tfh subsets Tfh1 (**C & D**), Tfh2 (**E & F**) and Tfh17 (**G & H**) in the total Tfh pool. Data is presented for both pooled (**A, C, E & G**) and age stratified (**B, D, F & H**) analyses.

B cell and Tfh cell responses after HPV vaccination, effect of age and dose number. E. Kiamba 2024

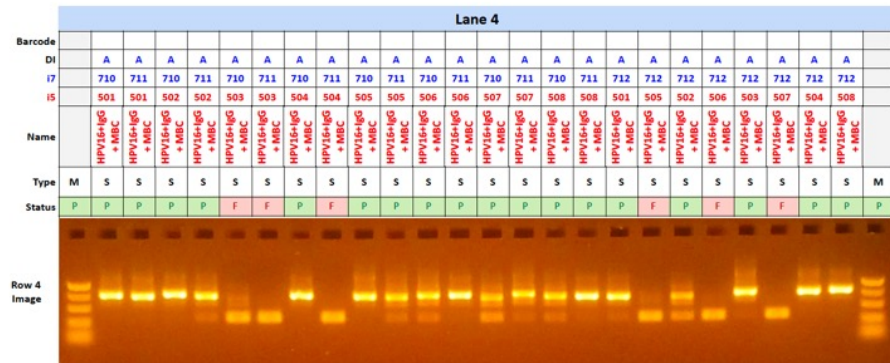
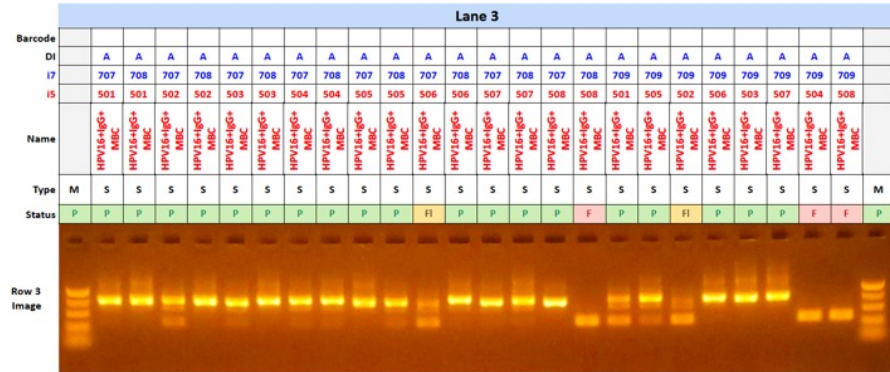
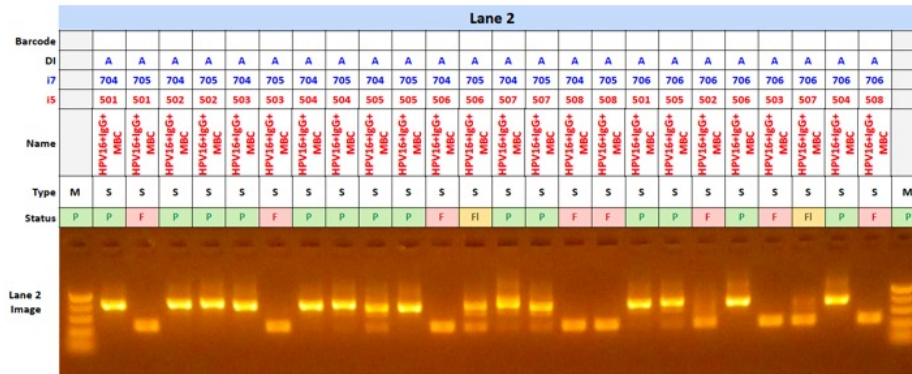
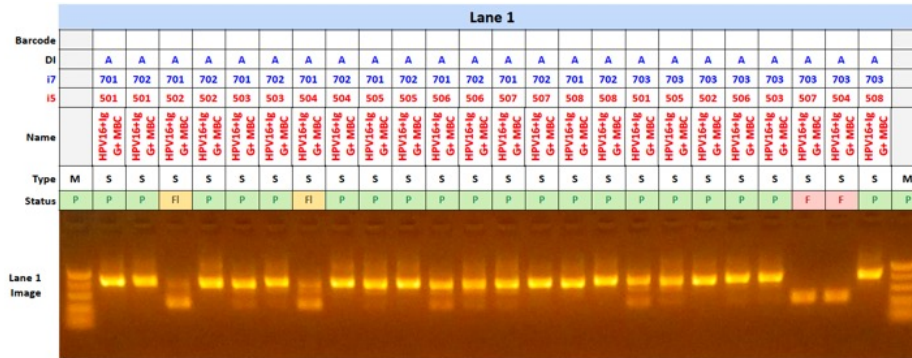
Appendix 11. Gating strategy for identification of HPV 16+IgG+, HPV 16+IgG-IgM- and HPV 16+IgM+ memory B cell for single cell sorting.



B cells were isolated from frozen PBMC of 8 participants aged 4-8 years and pooled in equal numbers before staining. Gating was first done on lymphocytes and single cells, then residual CD3+ T cells, CD14+ monocytes and dead cells excluded in a dump channel and B cells identified as CD3-CD14-CD19+. Total MBC were identified in CD3-CD14-CD19+ B cells as IgD-CD27+ from which the HPV 16+ population was identified from both baseline and post-vaccination timepoints. HPV 16+IgG+, HPV 16+IgG-IgM- and HPV 16+IgM+ frequencies were then identified from HPV 16+ MBC after vaccination. The post-vaccination HPV16+ MBC were singly sorted into microplates for subsequent sequencing of the B cell receptor.

Appendix 12. Gel image for PCR amplification of B cell receptor; A - plate 1, B - plate 2

A Plate 1 gel image



Continued on next page

Appendix 13. The Gambia Government/MRC Joint ethical approval

The Gambia Government/MRC Joint

ETHICS COMMITTEE

C/o MRC Unit: The Gambia @ LSHTM, Fajara
P.O. Box 273, Banjul
The Gambia, West Africa
Fax: +220 – 4495919 or 4496513
Tel: +220 – 4495442-6 Ext. 2308
Email: ethics@mrc.gm

25 June 2018

Dr Ed Clarke
Vaccines and Immunity Theme
MRCG at LSHTM
Fajara

Dear Dr Clarke

SCC 1597v2.1, A randomized, observer-blind, non-inferiority trial to evaluate alternative human papillomavirus (HPV) vaccination schedules in females in West Africa

Thank you for submitting your response letter dated 18 June 2018 addressing the issues raised by The Gambia Government/MRC Joint Ethics Committee at its meeting held on 2 June 2018.

Your application has now received full ethical approval.

With best wishes

Yours sincerely



Mr Malamin Sonko
Chairman, Gambia Government/MRC Joint Ethics Committee

Documents submitted for review:

- Response letter – 18 June 2018
- SCC approval letter – 18 May 2018
- SCC application form, V2.1 – 10 May 2018
- Protocol, V1.2 – 18 June 2018
- ICD (parent of 4 to 14 year old, V1.2 – 18 June 2018
- ICD (parent of 4 to 14 year old_sub-study), V1.2 – 18 June 2018
- ICD (parent of 15 to 17 year old), V1.2 – 18 June 2018
- ICD (parent of 15 to 17 year old_sub-study), V1.2 – 18 June 2018
- ICD (18 to 26 year old participant), V1.2 – 18 June 2018
- ICD (18 to 26 year old participant_sub-study), V1.2 – 18 June 2018
- Assent (11 to 17 year old participant), V1.2 – 18 June 2018
- AoU (4 to 14 years_parent), V1.1 – 18 June 2018

The Gambia Government/MRC Joint Ethics Committee:

Mr Malamin Sonko, Chairman
Prof Ousman Nyan, Scientific Advisor
Ms Naffie Jobe, Secretary
Dr Roddie Cole
Dr Ahmadou Lamin Samateh
Mrs Tulai Jawara-Ceesay

Prof. Umberto D'Alessandro
Dr Mamady Cham
Dr Ramatoulie Njie
Dr Jane Achan
Prof Martin Antonio

Continued on next page

- AoU (15 to 17 years_parent), V1.1 – 18 June 2018
- AoU (participant), V1.1 – 18 June 2018
- ID Card, V1.0 – 18 March 2018
- Contact details, V1.0 – 18 March 2018
- Summary of Product Characteristics_Gardasil – 19 March 2018
- Schedule Reminders, V1.0 – 21 April 2018
- CVs: Margaret Anne Stanley; Simon A. Beddows; Mark Jit; Heidi J. Larson

Appendix 14. London School of Hygiene and Tropical Medicine Ethical approval

London School of Hygiene & Tropical Medicine
 Keppel Street, London WC1E 7HT
 United Kingdom
 Switchboard: +44 (0)20 7636 8636
www.lshtm.ac.uk



Observational / Interventions Research Ethics Committee

Dr Ed Clarke
 Principal Investigator, Vaccines and Immunity Theme
 Other
 LSHTM

7 September 2018

Dear Dr Clarke

Study Title: A randomized, observer-blind, non-inferiority trial to evaluate alternative human papillomavirus (HPV) vaccination schedules in females in West Africa (The HANDS HPV Vaccine Trial).

LSHTM Ethics Ref: 16076

Thank you for your application for the above research project which has now been considered by the Interventions Committee via Chair's Action.

Confirmation of ethical opinion

On behalf of the Committee, I am pleased to confirm a favourable ethical opinion for the above research on the basis described in the application form, protocol and supporting documentation, subject to the conditions specified below.

Conditions of the favourable opinion

Approval is dependent on local ethical approval having been received, where relevant.

Approved documents

The final list of documents reviewed and approved is as follows:

Document Type	File Name	Date	Version
Safety Information	Summary of Product Characteristics_Gardasil_19Mar2018	01/03/2017	latest update
Investigator CV	Margaret Stanley CV	31/12/2017	1.0
Advertisements	SCC1597_HP V Vaccine Trial_ID Card_V1.0_18Mar2018	18/03/2018	1.0
Sponsor Letter	180410 - 2018-MUG-100_Sponsor Confirmation_Clarke	10/04/2018	1.0
Advertisements	SCC1597_HP V Vaccine Trial_Schedule Reminder_V1.0_21Apr2018	21/04/2018	1.0
Local Approval	SCC 1597v2.1_Clarke_Approved_18May18_final	18/05/2018	1.0
Other	Ed Clarke_GCP certificate_24May2018	24/05/2018	1.0
Protocol / Proposal	SCC1597_HP V Vaccine Trial_Protocol_V1.2_18Jun2018_FINAL SIGNED	18/06/2018	1.2
Information Sheet	SCC1597_HP V Vaccine Trial_Assent_11 to 17 year old participant_V1.2_18Jun2018	18/06/2018	1.2
Information Sheet	SCC1597_HP V Vaccine Trial_ICD_18 to 26 year old participant_sub-study_V1.2_18Jun2018	18/06/2018	1.2
Information Sheet	SCC1597_HP V Vaccine Trial_ICD_18 to 26 year old participant_V1.2_18Jun2018	18/06/2018	1.2
Information Sheet	SCC1597_HP V Vaccine Trial_ICD_parent of 4 to 14 year old_sub-study_V1.2_18Jun2018	18/06/2018	1.2
Information Sheet	SCC1597_HP V Vaccine Trial_ICD_parent of 4 to 14 year old_V1.2_18Jun2018	18/06/2018	1.2
Information Sheet	SCC1597_HP V Vaccine Trial_ICD_parent of 15 to 17 year old_V1.2_18Jun2018	18/06/2018	1.2
Information Sheet	SCC1597_HP V Vaccine Trial_ICD_parent of 15 to 17 year old_sub-study_V1.2_18Jun2018	18/06/2018	1.2
Information	SCC1597_HP V Vaccine Trial_AoU Participant_V1.1_18Jun2018	18/06/2018	1.1

Continued on next page

Information Sheet	SCC1597_HPVP Vaccine Trial_AoU_4 to 14 years_parent_V1.1_18Jun2018	18/06/2018	1.1
Information Sheet	SCC1597_HPVP Vaccine Trial_AoU_15 to 17 years_parent_V1.1_18Jun2018	18/06/2018	1.1
Local Approval	SCC 1597v2.1_Clarke (Approve)_final	25/06/2018	1.0
Investigator CV	Mark Jit CV	01/08/2018	1.0
Investigator CV	Heidi Larson CV	01/08/2018	1.0
Investigator CV	180812 - Ed Clarke CV_12Aug2018	12/08/2018	1.0
Advertisements	SCC 1597 HPV Vaccine Trial_Contact details_V1.0_18Mar2018	18/08/2018	1.0

After ethical review

The Chief Investigator (CI) or delegate is responsible for informing the ethics committee of any subsequent changes to the application. These must be submitted to the committee for review using an Amendment form. Amendments must not be initiated before receipt of written favourable opinion from the committee.

The CI or delegate is also required to notify the ethics committee of any protocol violations and/or Suspected Unexpected Serious Adverse Reactions (SUSARs) which occur during the project by submitting a Serious Adverse Event form.

An annual report should be submitted to the committee using an Annual Report form on the anniversary of the approval of the study during the lifetime of the study.

At the end of the study, the CI or delegate must notify the committee using the End of Study form.

All aforementioned forms are available on the ethics online applications website and can only be submitted to the committee via the website at: <http://leo.lshtm.ac.uk>.

Further information is available at: www.lshtm.ac.uk/ethics.

Yours sincerely,



Professor John DH Porter
Chair

ethics@lshtm.ac.uk
<http://www.lshtm.ac.uk/ethics/>

Improving health worldwide